

Axiomata sive Leges Motus

Lex I.

omnes per se movere in flatu suo
directum, nisi quatenus a
movere.

per se movere in motibus suis
curvantibus et in gravitatis inf
secundo probetur ut
motus omni quatenus
intra et Conclat
venientes in flatu
suo.

Lex II.

omni motus proportionis
habet lineam rectam
sive motum quem
generabit, sive si
impulsa fuerit. Et tunc motus
in eum in generatorem dicitur
obliquus, motus sive vel coefficientem
et obliquus obliquus adjuvitur et
mirationem componitur.

Lex III.

contrariam semper et equalen
tiam actiones in se mutuo per
vias dirigi
premit vel trahit alterum
trahitur. Siquis lapidem digito
et lapide. Si equus lapidem p
am et equus equaliter in la
eodem relaxandi se conati
m, ac lapidem versat equus
et quantum premit et pro
in corpus aliud impingit.
mutaverit, idem quoque versat
actionem in partem contras
versivam mutuo) fuerit. Hoc

A. Menzel

Modelling and Computation
of Geometrically Nonlinear
Anisotropic Inelasticity

Axiomata sive Leges Motus

Lex I.

omnes percurrere in flatu suo
in directionem, nisi quatenus a
mutare.

percurrant in motibus suis
lucidantibus et in gravitatibus nisi
secundo profectus est
non nisi quatenus
normam et Conclaves
reulares in flatu
suo.

Lex II.

omnes motus profectus
sunt lineam rectam
ma motum quem
generabilis, sine
interessa fuerit. Et hinc motus
in curva in generabilibus debet
aliter, motus sive vel coefficientem
et oblique oblique adiacentibus et
minutionem componitur.

Lex III.

contrarium semper et aequaliter
sunt actiones in se mutuo pro
vires dirigi
premit vel trahit alterum
valentur. Siquis lapidem digitis
a lapide. Si sequit lapidem p
am et sequit aequaliter in la
eodem relaxandi se conati
on, ac lapidem trahit equum
et quantum premit et pro,
in corpus aliud impingent
mutaverit, idem quoque trahit
actionem in partem contras
trahentis mutuo) subit. Hoc

A. Menzel

Modelling and Computation
of Geometrically Nonlinear
Anisotropic Inelasticity

Andreas Menzel

Modelling and Computation of Geometrically Nonlinear Anisotropic Inelasticity

key words anisotropy, structural tensors, fictitious configurations, plasticity, continuum damage, finite deformations, finite elements

abstract Based on the framework of continuum mechanics two different concepts to formulate phenomenological anisotropic inelasticity are developed in a thermodynamically consistent manner. On the one hand, special emphasis is placed on the incorporation of structural tensors while on the other hand, fictitious configurations are introduced. Substantial parts of this work deal with the numerical treatment of the presented theory within the finite element method.

zusammenfassung Basierend auf dem Rahmen der Kontinuumsmechanik werden zwei unterschiedliche Konzepte zur Formulierung phenomenologischer anisotroper Inelastizität thermodynamisch konsistent entwickelt. Einerseits wird die Berücksichtigung von Strukturtenoren betont, andererseits werden fiktive Konfigurationen eingeführt. Wesentliche Anteile dieser Arbeit sind der numerischen Umsetzung der dargestellten Theorie mit Hilfe der Finiten Element Methode gewidmet.

Die Deutsche Bibliothek – CIP–Einheitsaufnahme

Menzel, Andreas:

Modelling and computation of geometrically nonlinear anisotropic inelasticity / Andreas Menzel. – Kaiserslautern: Univ.–Bibliothek, 2002

(UKL–LTM–Reports: T;[20]02,01)

Zugl.: Kaiserslautern, Univ., Diss., 2002

ISSN 1610–4641

ISBN 3–925178–86–4

URL http://kluedo.ub.uni-kl.de/MV/Listen/dissertation_de.html

publisher Chair of Applied Mechanics
Department of Mechanical and Process Engineering
University of Kaiserslautern
P.O. Box 3049
D–67653 Kaiserslautern, Germany
FON + 631 205 2124
FAX + 631 205 2128
URL <http://mechnik.mv.uni-kl.de>

print University of Kaiserslautern, ZBT, Foto–Repro–Druck

© by A. Menzel 2002

This work is subject to copyright. All rights are reserved, whether the whole or part of the material is concerned, specifically the rights of translation, reprinting, reuse of illustrations, recitation, broadcasting, reproduction on microfilm or in any other way, and storage in data banks. Duplication of this publication or parts thereof is permitted in connection with reviews or scholarly analysis. Permission for use must always be obtained from the author.

printed in Germany

Modelling and Computation of Geometrically Nonlinear Anisotropic Inelasticity

vom Fachbereich Maschinenbau und
Verfahrenstechnik der Universität Kaiserslautern
zur Verleihung des akademischen Grades
Doktor-Ingenieur (Dr.-Ing.)
genehmigte Dissertation

von
Dipl.-Ing. Andreas Menzel
aus Hannover

Hauptreferent:	Prof. Dr.-Ing. P. Steinmann
Korreferenten:	Prof. Dr. rer. nat. B. Svendsen Prof. Dr. K. Runesson
Vorsitzender:	Prof. Dr.-Ing. R. Renz
Dekan:	Prof. Dipl.-Ing. Dr. tech. H.-J. Bart

Tag der Einreichung:	22. November 2001
Tag der mündl. Prüfung:	22. Februar 2002

Kaiserslautern, Februar 2002

Preface

But I must speak again about crystals, shapes, colours. There are crystals as huge as the colonnade of a cathedral, soft as mould, prickly as thorns; pure, azure, green, like nothing else in the world, fiery, black; mathematically exact, complete, like constructions by crazy, capricious scientists, or reminiscent of the liver, the heart . . . There are crystal grottos, monstrous bubbles of minerals, architecture and engineering art . . . Even in human life there is a hidden force towards crystallisation. Egypt crystallises in pyramids and obelisks, Greece in columns; the middle ages in vials; London in grimy cubes . . . Like secret mathematical flashes of lightning the countless laws of construction penetrate the matter. To equal nature it is necessary to be mathematically and geometrically exact. Number and phantasy, law and abundance – these are the living, creative strengths of nature; not to sit under a green tree but to create crystals and to form ideas, that is what it means to become one with nature!

Karel Čapek [1890 – 1938]
after his visit of the mineral
collection of the British Museum

The work presented in this thesis has been carried out between the period 1997–2001 at the Chair of Applied Mechanics at the University of Kaiserslautern.

First of all, I want to thank Professor Paul Steinmann for his never ending enthusiasm and guidance which I have received during these years. He was the person who frequently protected myself from several painstaking hours of speculation within one enlightening second. I owe a great deal to our discussions and enjoyed the freedom to set up this thesis.

Special acknowledgements are dedicated to Professor Bob Svendsen and Professor Kenneth Runesson for serving as assessors. Stimulating discussions during the period of this work, their openness and acceptance of myself as young learner in the field of Solid Mechanics were a great encouragement.

As my roots go back to Hannover, I would like to record my gratitude to Professor Erwin Stein who introduced me to the subject of Computational Mechanics.

My fellow colleagues at the Chair of Applied Mechanics at the University of Kaiserslautern are sincerely thanked for providing such a pleasant working atmosphere. Always remember the driving force “*What is new – compared to my papers of the seventies?*”, G.A.M. [EMMC2, 02/1998].

Most of all, I thank my family and especially Simone for their love, support, patience and infinite tolerance and understanding.

Kaiserslautern in Februar 2002

Andreas Menzel

Contents

Preface	I
Nomenclature	VII
Introduction	1
1 Concepts of the formulation of anisotropy	9
1.1 Principles of objectivity	9
1.2 Some essentials of groups and classes	12
1.3 Constitutive functions	17
1.3.1 Anisotropic tensor functions	19
1.3.2 Isotropic tensor functions	20
1.3.3 Curvilinear anisotropy	21
1.3.4 Fictitious configurations	21
1.3.5 Anisotropic linear elasticity	22
2 Anisotropic hyper-elasticity based on structural tensors	25
2.1 Kinematics	26
2.2 General hyper-elasticity	28
2.2.1 General spatial and material stress relation	30
2.2.1.1 Derivation of the general spatial stress relation	30
2.2.1.2 Derivation of the general material stress relation	30
2.2.2 General spatial and material tangent operator	31
2.2.2.1 Derivation of the general spatial and material tangent operator	31
2.3 Representation of anisotropy	31
2.3.1 Anisotropic spatial and material stress relation	31
2.3.1.1 Derivation of the anisotropic spatial stress relation	32
2.3.1.2 Derivation of the anisotropic material stress relation	32
2.3.1.3 Derivation of the anisotropic spatial and material stress relation via invariants	32
2.3.2 Anisotropic spatial and material tangent operator	34
2.3.2.1 Derivation of the anisotropic spatial tangent operator	35
2.3.2.2 Derivation of the anisotropic material tangent operator	36

2.3.2.3	Derivation of the anisotropic spatial and material tangent operator via invariants	36
2.4	Examples	38
2.4.1	Analytical example within orthotropic symmetry	39
2.4.2	Numerical example within transversely isotropic symmetry	41
2.4.2.1	Simple shear	41
2.4.2.2	Cook's problem	42
3	Anisotropic elasto–plasticity based on structural tensors	45
3.1	Kinematics	46
3.2	Free Helmholtz energy density	46
3.3	Coleman–Noll entropy principle	48
3.3.1	Derivation of the anisotropic stress relation via invariants	50
3.3.2	Derivation of the anisotropic tangent operator via invariants	52
3.3.3	Thermodynamic forces	53
3.4	Non–standard dissipative materials	53
3.5	Reduction to isotropy	56
3.6	Relation to Eshelbian mechanics	57
3.7	Numerical time integration	59
3.8	Prototype model	61
3.8.1	Free Helmholtz energy density	61
3.8.2	Inelastic potentials	64
3.9	Numerical examples	66
3.9.1	Simple shear	67
3.9.2	Strip with a hole	71
4	Anisotropic hyper–elasticity based on a fictitious configuration	85
4.1	The concept of a fictitious configuration	85
4.1.1	Kinematics of the fictitious configuration	86
4.1.2	Energy metric tensors	87
4.1.3	Hyper–elasticity	88
4.2	Relations between structural tensors and the fictitious configuration	89
4.2.1	Review of orthotropic hyper–elasticity based on structural tensors	89
4.2.2	Incorporation of structural tensors into the fictitious linear tangent map	90
4.2.3	Two arbitrary fibres	91
4.2.4	Two equivalent fibres	92
4.2.5	Two orthogonal fibres	93
4.2.6	Transverse isotropy	93
4.2.7	Isotropy	94
4.2.8	Spectral representation	94
4.3	Numerical examples	95
4.3.1	Simple shear	96
4.3.2	Cook's problem	97

5	Anisotropic damage based on a fictitious configuration	101
5.1	Coleman–Noll entropy principle	102
5.2	Generalised standard dissipative materials	103
5.3	Numerical time integration	105
5.4	Numerical examples	108
5.4.1	Simple shear	109
5.4.1.1	Quasi isotropic damage	109
5.4.1.2	Anisotropic damage	109
5.4.2	Cracked plate under mode 3 loading	111
6	Anisotropic damage coupled to multiplicative elasto–plasticity based on fictitious configurations	117
6.1	Kinematical framework of fictitious configurations	118
6.2	Construction of the free Helmholtz energy density	119
6.3	Coleman–Noll entropy principle	120
6.4	Non–standard dissipative materials	122
6.4.1	Construction of the damage potential	122
6.4.2	Construction of the hardening potential	122
6.4.3	Construction of the plastic potential	122
6.4.3.1	Prototype model	124
6.5	Numerical time integration	125
6.6	Numerical examples	128
6.6.1	Simple shear	128
6.6.1.1	Anisotropic elasto–plasticity	128
6.6.1.2	Anisotropic elasto–plasticity coupled to quasi isotropic damage	130
6.6.1.3	Anisotropic elasto–plasticity coupled to anisotropic damage	133
6.6.1.4	Numerical aspects	133
6.6.2	Stamping of a sheet	136
6.6.2.1	Numerical aspects	142
A	Notation	151
A.1	Useful abbreviations	151
A.2	Denomination of spaces	153
A.3	Denomination of functions	153
B	Some comments on isotropic tensor functions	155
B.1	Characteristic polynomial	155
B.2	Useful relations between different types of invariants	156
B.3	Tensor–valued isotropic tensor functions of second order	157
B.4	First and second derivatives of the basic invariants	157
B.4.1	Alternative proof of the spatial anisotropic stress relation: Application to hyper–elasticity	159
B.5	First and second derivatives of the basic invariants	160
B.5.1	Alternative proof of the spatial anisotropic stress relation: Application to multiplicative elasto–plasticity	161

C Hyper-elastic constitutive functions	163
C.1 Isotropy	163
C.2 Transversal isotropy	165
C.3 Some remarks on homogenisation concepts	166
D Visualisation of anisotropy	167
D.1 A scalar-valued anisotropy measure	167
D.2 Stereo-graphic projection	167
D.3 The acoustic tensor	168
E Numerical aspects	169
E.1 Some Runge-Kutta schemes	169
E.2 Numerical approximation of Jacobians	170
Bibliography	173
Curriculum Vitae	185

Nomenclature

8 c 357 8xup ZEUs!

id 21V18 Pt 7 gallisc 3I4002a I7 ? V 3I GpU 4a 2g,
39, 49 ? mz 7IFi16 3400712g pp 34 udir9jem I3349
bubu WEg!

Muff I9 exi; sc i6 enu 070 zIm 40I9 absI2c spü, 43
asti siv I3999 idle 48, I9 037 pem 8 pho 36. IOI2
sabi FR26a FlisCh 26 : iwo - I8447 g7 gg !

Glent 3I, glent I4 Po

Arno Schmidt [1914 – 1979]

In this work, a tensor notation in the spirit of Marsden and Hughes [MH94] is applied since the point of view that “*Even for a simple body, tensor analysis on manifolds clarifies the basic theory. For instance, using manifold ideas we can see clearly how to formulate the pull-back and push-forward ...*” is adopted [MH94, Chap. 1, Box 2.1]. In addition to standard conventions, we introduce the symbol \natural to indicate mixed-variant tensors. Therefore the spatial identity, with the Kronecker delta δ_{ij} in terms of Cartesian coordinates, will read \mathbf{g}^\natural in the sequel. The scalar product and the tensor product of vectors – say $\mathbf{v}_1^\natural, \mathbf{v}_2^\flat, \mathbf{v}_3^\natural$ – are written in standard fashion, namely $\mathbf{v}_1^\natural \cdot \mathbf{v}_2^\flat = \mathbf{v}_2^\flat \cdot \mathbf{v}_1^\natural$ and $[\mathbf{v}_1^\natural \otimes \mathbf{v}_3^\natural] \cdot \mathbf{v}_2^\flat = [\mathbf{v}_3^\natural \cdot \mathbf{v}_2^\flat] \mathbf{v}_1^\natural$ whereby each \cdot indicates one contraction. Moreover, the trace operation for second order tensors is consequently determined by e.g. $\text{tr}(\mathbf{g}^\flat \cdot [\mathbf{b}^\natural]^\flat) = \mathbf{g}^\flat : \mathbf{b}^\natural$, compare Appendix A for a reiteration on the transposition operator.

To give an example, we highlight the celebrated Truesdell or rather Murnaghan formula for the Kirchhoff stress tensor within an isotropic setting which allows the following representations

$$\begin{aligned} \text{general tensor notation:} \quad \boldsymbol{\tau}^\natural &= 2 \mathbf{g}^\natural \cdot \partial_{\mathbf{b}^\flat} \psi_0^\flat \cdot \mathbf{b}^\natural \\ \text{general components:} \quad \tau^{ij} &= 2 g^{ik} \partial_{b^{kl}} \psi_0^\flat b^{lj} = \mathbf{g}^i \cdot \boldsymbol{\tau}^\natural \cdot \mathbf{g}^j \\ \text{Cartesian components:} \quad \tau_{ij} &= 2 \delta_{ik} \partial_{b_{kl}} \psi_0^\flat b_{lj} = \mathbf{e}_i \cdot \boldsymbol{\tau} \cdot \mathbf{e}_j \end{aligned}$$

whereby the summation convention is implied and the free Helmholtz energy density ψ_0^\flat represents an isotropic scalar-valued tensor function. Predominantly, we deal with body tensor fields and do not strictly distinguish the denomination of these objects from space tensor fields, see Lodge [Lod74, Chaps. 2 & 11] for a detailed outline.

Standard notations are used as much as possible, casually under the common contradiction in understanding small bold symbols as vectors (\mathbf{n}), capital bold symbols as second order material tensors (\mathbf{N}) and small bold symbols as spatial second order tensors (\mathbf{n}). Fourth order spatial and material tensors are depicted differently from second order fields (\mathbf{n}, \mathbf{N}). For notational simplicity, we abuse notation and denote functions and their values by the same symbol. The subsequent list summarises symbols which are frequently used in this work (without asserting completeness)*.

*The applied denomination of spaces is given in Appendix A.2 and thus not highlighted here.

B	body
\mathcal{M}	material body manifold
t	time
\mathbf{X}, \mathbf{x}	placement of a material point at time t_0 and t
$\mathcal{B}_0, T\mathcal{B}_0, T^*\mathcal{B}_0$	compatible material configuration and tangent, co-tangent (dual) space
$\mathcal{B}_t, T\mathcal{B}_t, T^*\mathcal{B}_t$	compatible spatial configuration and tangent, co-tangent (dual) space
φ, Φ	direct and inverse motion (material and spatial diffeomorphism)
$\mathbf{F}^\sharp, \mathbf{f}^\sharp$	linear tangent map of φ and Φ
$\mathfrak{S}, \mathfrak{I}$	stress functions
\mathbb{G}	symmetry group
Q^\sharp	orthogonal transformation
rot \mathbf{R}^\sharp , ref \mathbf{R}^\sharp	rotations and reflections
Θ^i, θ^i	material and spatial convected coordinates
$\mathbf{G}_i, \mathbf{G}^i$	material contra- and co-variant base vectors
$\mathbf{g}_i, \mathbf{g}^i$	spatial contra- and co-variant base vectors
$\mathbf{G}^\sharp, \mathbf{G}^b, \mathbf{G}^\sharp$	material metric tensors and mixed-variant second order identity
$\mathbf{g}^\sharp, \mathbf{g}^b, \mathbf{g}^\sharp$	spatial metric tensors and mixed-variant second order identity
$\mathbf{U}^\sharp, \mathbf{V}^\sharp, \mathbf{R}^\sharp$	right, left stretch tensors and rotational part of \mathbf{F}^\sharp
$\mathbf{u}^\sharp, \mathbf{v}^\sharp, \mathbf{r}^\sharp$	left, right stretch tensors and rotational part of \mathbf{f}^\sharp
$\mathbf{C}^b, \mathbf{B}^\sharp$	material right Cauchy-Green tensor and inverse field
$\mathbf{b}^\sharp, \mathbf{c}^b$	spatial Finger tensor and inverse field
$\mathbf{e}^b, \mathbf{E}^b$	spatial Almansi and material Green-Lagrange strain tensor
$\mathbf{l}^\sharp, \mathbf{L}^\sharp$	spatial velocity gradient and pull-back in \mathcal{B}_0
$\mathbf{A}_{1,\dots,n}^\sharp, \mathbf{a}_{1,\dots,n}^\sharp$	material and spatial tensor series
$[\mathbf{M}^\sharp]^\sharp, [\mathbf{m}^\sharp]^\sharp$	material and spatial Mandel stress
$\mathbf{S}^\sharp, \boldsymbol{\tau}^\sharp$	material second Piola-Kirchhoff and spatial Kirchhoff stress
$\mathbf{E}^\sharp, \mathbf{e}^\sharp$	material and spatial elastic tangent operator
\mathbf{q}^\sharp	spatial acoustic tensor
$\mathcal{B}_p, T\mathcal{B}_p, T^*\mathcal{B}_p$	incompatible intermediate configuration and tangent, co-tangent (dual) space
$\mathbf{F}_p^\sharp, \mathbf{f}_p^\sharp$	direct and inverse inelastic linear tangent map
$\mathbf{F}_e^\sharp, \mathbf{f}_e^\sharp$	direct and inverse elastic linear tangent map
$\widehat{\mathbf{G}}^\sharp, \widehat{\mathbf{G}}^b, \widehat{\mathbf{G}}^\sharp$	metric tensors and mixed-variant second order identity in \mathcal{B}_p
$\mathbf{C}_p^b, \mathbf{B}_p^\sharp$	inelastic right Cauchy-Green tensor and inverse field
$\widehat{\mathbf{C}}_e^b, \widehat{\mathbf{B}}_e^\sharp$	elastic right Cauchy-Green tensor and inverse field
$\widehat{\mathbf{b}}_p^\sharp, \widehat{\mathbf{c}}_p^b$	inelastic Finger tensor and inverse field
$\mathbf{b}_e^\sharp, \mathbf{c}_e^b$	elastic Finger tensor and inverse field
$\mathbf{l}_p^\sharp, \mathbf{l}_e^\sharp$	inelastic and elastic velocity gradient
$\widehat{\mathbf{L}}_p^\sharp, \widehat{\mathbf{L}}_e^\sharp$	inelastic and elastic velocity gradient, pull-back in \mathcal{B}_p
$\mathbf{L}_p^\sharp, \mathbf{L}_e^\sharp$	inelastic and elastic velocity gradient, pull-back in \mathcal{B}_0
$\widehat{\mathbf{D}}_p^b, \widehat{\mathbf{W}}_p^b$	symmetric and skew-symmetric representation of $\widehat{\mathbf{L}}_p^\sharp$

$\widehat{\mathbf{A}}_{1,\dots,n}^\sharp$	tensor series in \mathcal{B}_p
κ	proportional hardening variable
$[\widehat{\mathbf{M}}^\sharp]^\dagger$	Mandel stress in \mathcal{B}_p
$\widehat{\mathbf{S}}^\sharp$	second Piola–Kirchhoff stress in \mathcal{B}_p
$\mathbf{Y}^b, \widehat{\mathbf{Y}}^b, \mathbf{y}^b$	thermodynamic force conjugate to $\mathbf{B}_p^\sharp, \widehat{\mathbf{G}}^\sharp, \mathbf{b}_e^\sharp$
$\mathbf{Z}_i^b, \widehat{\mathbf{Z}}_i^b, \mathbf{z}_i^b$	thermodynamic force conjugate to $\mathbf{A}_i^\sharp, \widehat{\mathbf{A}}_i^\sharp, \mathbf{a}_i^\sharp$
h	thermodynamics force conjugate to κ
\mathbb{A}	admissible domain
$[\boldsymbol{\pi}_e^\sharp]^\dagger$	elastic inverse motion first Piola–Kirchhoff stress
$[\widehat{\boldsymbol{\sigma}}_e^\sharp]^\dagger, [\widehat{\boldsymbol{\Sigma}}_e^\sharp]^\dagger, [\boldsymbol{\Sigma}_e^\sharp]^\dagger$	elastic inverse motion Cauchy stress in $\mathcal{B}_t, \mathcal{B}_p, \mathcal{B}_0$
$\bar{\mathcal{B}}, T\bar{\mathcal{B}}, T^*\bar{\mathcal{B}}$	incompatible fictitious configuration and tangent, co-tangent (dual) space
$\bar{\mathbf{F}}^\sharp, \bar{\mathbf{f}}^\sharp$	direct and inverse fictitious linear tangent maps
$\bar{\mathbf{G}}_i, \bar{\mathbf{G}}^i$	fictitious contra- and co-variant base vectors in $\bar{\mathcal{B}}$
$\bar{\mathbf{C}}^b, \bar{\mathbf{B}}^\sharp$	fictitious right Cauchy–Green tensor and inverse field
$\bar{\mathbf{E}}^b$	fictitious Green–Lagrange strain tensor
$\bar{\mathbf{A}}^\sharp, \mathbf{A}^\sharp$	anisotropy/damage metric in $\bar{\mathcal{B}}, \mathcal{B}_0$
$\bar{\mathbf{S}}^\sharp$	fictitious second Piola–Kirchhoff stress
$\bar{\mathbf{Z}}^b, \mathbf{Z}^b$	thermodynamic force conjugate to $\bar{\mathbf{A}}^\sharp, \mathbf{A}^\sharp$
$\widetilde{\mathcal{B}}, T\widetilde{\mathcal{B}}, T^*\widetilde{\mathcal{B}}$	incompatible fictitious configuration and tangent, co-tangent (dual) space
$\widetilde{\mathbf{F}}^\sharp, \widetilde{\mathbf{f}}^\sharp$	direct and inverse fictitious linear tangent map
$\widetilde{\mathbf{F}}_e^\sharp, \widetilde{\mathbf{f}}_e^\sharp$	direct and inverse elastic fictitious linear tangent map
$\widetilde{\mathbf{g}}_i, \widetilde{\mathbf{g}}^i$	fictitious contra- and co-variant base vectors in $\widetilde{\mathcal{B}}$
$\widetilde{\mathbf{p}}^b, \bar{\mathbf{P}}^b, \widehat{\mathbf{P}}^b$	inelastic metric in $\widetilde{\mathcal{B}}$, pull-back in $\bar{\mathcal{B}}$ and \mathcal{B}_p
$\widetilde{\mathbf{E}}_e^b, \widehat{\mathbf{E}}_e^b$	elastic Green–Lagrange strain tensor in $\widetilde{\mathcal{B}}$ and \mathcal{B}_p
$\widehat{\mathbf{A}}^\sharp$	anisotropy/damage metric in \mathcal{B}_p
$\widetilde{\boldsymbol{\tau}}^\sharp$	fictitious Kirchhoff stress
ψ_0, Φ	free Helmholtz energy density and inelastic potential
$\mathcal{W}_0, \mathcal{D}_0$	stress power and dissipation
$[\bullet]^{[\circ]} I_q$	basic invariants wrt a set of second order fields and appropriate metric tensors
$[\bullet]^{[\circ]} J_{1,2,3}$	principal invariants wrt a second order field and appropriate metric tensor
$[\bullet]^{[\circ]} H_{1,2,3}$	Haigh–Westergaard coordinates wrt a second order field and appr. metric tensor
$\vartheta^{1,2}$	spherical coordinates wrt a unit-vector
$\delta([\bullet], [\circ])$	anisotropy measure ($\delta([\bullet], [\circ]) > 0$ if $[\bullet]$ and $[\circ]$ do not commute)
D_t, L_t, L_t^P	material time derivative and Lie-derivatives wrt $\mathcal{B}_t, \mathcal{B}_p$
$\bullet^{0,p,t}, \bar{\bullet}, \widetilde{\bullet}$	functions wrt $\mathcal{B}_0, \mathcal{B}_p, \mathcal{B}_t, \bar{\mathcal{B}}, \widetilde{\mathcal{B}}$
$[\widehat{\bullet}], [\bar{\bullet}], [\widetilde{\bullet}]$	fields wrt $\mathcal{B}_p, \bar{\mathcal{B}}, \widetilde{\mathcal{B}}$
$[\bullet]^\sharp, [\bullet]^\sharp, [\bullet]^b$	mixed-variant, contra-variant and co-variant
$[\bullet]_*, [\bullet]^*$	push-forward and pull-back under the action of the diffeomorphism $[\bullet]$
$[\bullet]_\star, [\bullet]^\star$	push-forward and pull-back under the action of the linear tangent map $[\bullet]$

Introduction



have discovered that writing a book is a nonlinear problem, the solution of which requires many iterations. Since the present form of this work varied very little in the last few iterations, I present it with the hope that it provides an approximate solution to the problem at hand.

John Tinsley Oden
Finite Elements of Nonlinear Continua, 1972

The title of this work is in a way misleading; however any possible title would displease at least someone. For mathematicians, the idea of anisotropy reflects e.g. group theoretical settings. Material scientist and physicists probably have atomistic models, micro-structures, grains, etc. in mind and might like to completely omit the terminology of anisotropy since it is obvious that almost all inelastic processes are anisotropic. Finally, engineers, who have to accomplish failure and lifetime predictions, possibly expect experimental results, strange material behaviour and some curve-fitting procedures. I hope that “*Modelling and Computation of Geometrically Nonlinear Anisotropic Inelasticity*” allures at last some readers from these communities.

The modelling of anisotropic material behaviour on different scales has been an active research subject in the last decades and is of cardinal importance in material and engineering science. Since almost all materials are anisotropic, due to their natural occurrence or as a consequence of manufacturing procedures and deformation histories, it is clear that various applications are found in the branches of material science and mechanics. Typical examples are detected in the context of texture (development) and crystalline and poly-crystalline materials, see e.g. the recent monographs by Kocks et al. [KTW00], Phillips [Phi01], Nembach [Nem97] or the contributions in Teodosiu [Teo97]. Another wide field of applications for anisotropic material behaviour is provided by fibre reinforced plastics and composites which are a very broad and important class of engineering materials – conventionally polymer, metal and ceramic composites. For a general survey, we refer to Hull and Clyne [HC96] and Spencer [Spe72] – see also references cited therein. Moreover, it is clear that geo-materials, like soil and rock, and biological materials, namely materials with growth, show overall anisotropic characteristics. For instance, the modelling of wood and muscles or teeth and bones in consideration of their interaction with orthopaedic implants is of major interest, see the overview article by Taber [Tab95] and for an introduction to correlated finite element settings, we refer to Huiskes and Chao [HC83]. Conceptually speaking for a wide class of bodies, what we observe as phenomenological anisotropy on the macro-scale is attached to a specific structure on the micro-scale which might allow representation via tensorial fields within the framework of continuum mechanics. Typical applications are e.g. continua with voids, spin, rotational degrees of freedom, etc. – see Capriz [Cap89] for a general overview and Svendsen [Sve01a].

In this work, a phenomenological framework (for simple materials) is developed, that is the thermomechanical response of each particle in the body of interest allows to be determined from the history of the overall motion and temperature at this particular material point. The entire state and state functions are represented by constitutive functionals which account for the knowledge of the history of independent variables including internal variables which are not accessible to direct observation. Thereby, constitutive theories of continuous solid materials with respect to convected coordinates (related to body fields – attached to particles to which the history of the material is referred)

result usually in simpler formulations compared to approaches with respect to bases which are fixed in space (space fields – attached to places). Nevertheless, for specific applications like e.g. typical finite elements settings, it incidentally turns out to be convenient to choose a specific coordinate system that coincides with the (body) convected coordinates in the considered particle at time t , e.g. orthogonal or even Cartesian coordinates. For conceptual clarity, but without loss of generality, we restrict ourselves to the rate-independent and isothermal case.

One possible approach to model anisotropy – within the framework of continuum mechanics and a phenomenological hyper-elastic setting – is based on the incorporation of additional tensorial arguments into the free Helmholtz energy density. A typical application is for instance the introduction of symmetric second order tensors which define preferred orientations of the material; for a detailed outline see e.g. the contributions by Spencer [Spe84], Qiu and Pence [QP97] or Menzel and Steinmann [MS01h] among many other authors and special emphasis on applications within finite element settings is placed by Weiss et al. [WMG96], Almeida and Spilker [AS98] – see also references cited in these works. Then, the set up of isotropic or anisotropic tensor functions together with general representation theorems and the correlated sets of invariants and generators is a natural consequence and allows the modelling of anisotropic materials. For extensive background information and a general overview, we refer to the monographs by Green and Adkins [GA70], Smith [Smi94], the early work of Pipkin and Rivlin [PR59] and the contributions in Boehler [Boe87]. Furthermore, recall that anisotropy is incorporated as soon as the assumed free Helmholtz energy density is additionally defined by further non-spherical arguments or components on top of an appropriate kinematic tensor field, compare Marsden and Hughes [MH94, Chap. 3, Prop. 5.7] for isotropic behaviour and the applications in Park and Youn [PY98]. Throughout this work, we choose symmetric second order tensors to represent the type of anisotropy. Indeed, more complex theories are possible incorporating constitutive anisotropy tensors of higher order, compare e.g. Zhang and Rychlewsky [ZR90] or Zheng and Spencer [ZS93]. In this context, Betten [Bet82a] generated the set of irreducible invariants of a fourth order tensor and, in view of the coupling to a second order tensor like e.g. stress or strain, additionally the corresponding simultaneous invariants.

Nevertheless, a remaining task is to account for anisotropy within a phenomenological approach of inelastic processes – for instance elasto-plastic behaviour. In this context, a powerful framework is provided by the theory of generalised standard dissipative materials as proposed by Halphen and Nguyen [HN75], see also Maugin [Mau99, Chap. 7] or Antman [Ant95, Chap. XV] and references cited in these monographs for a general overview. Conceptually speaking, the set of variables included in the free Helmholtz energy density is enlarged by additional arguments. These arguments are treated as internal variables and allow to account for e.g. plastic deformations and possibly for induced anisotropy. For an outline of anisotropic plasticity see e.g. the recent contributions by v.d. Giessen [vdG89], Steinmann et al. [SMS96], Miehe [Mie98a], Papadopoulos and Lu [PL01], Svendsen [Sve01b], Resse et al. [RRW01], Tsakmakis [Tsa00] or Menzel and Steinmann [MS01d, MS01a] among others.

The appropriate choice of the physical nature of internal variables describing the anisotropic state of a material and their tensorial representation is since long under discussion, compare Leckie and Onat [LO81] for special emphasis on damage mechanics. An alternative framework to model anisotropic material behaviour is provided by the introduction of fictitious mappings which allows to shift some of the characteristics of additional internal variables to the properties of the chosen transformation. It is clear that these approaches monitor reduced representations of general anisotropy. Nevertheless, as a main advantage, one has the opportunity to base the modelling of anisotropic material behaviour on standard isotropic constitutive equations. The idea of undamaged microscopic fictitious configurations (similar to the effective space of the classical isotropic $[1 - D]$ damage theory) which are attached to macroscopic configurations was originally established for the formulation of anisotropic failure criteria of inelastic processes like creep and damage, see Betten [Bet82b] and Murakami [Mur88] or Betten [Bet76], Karafillis and Boyce [KB93] and Oller et al. [OBMO95] with application to plasticity. Recently Park and Voyiadjis [PV98] discussed in detail the underlying kinematics with application to damage. Likewise, the concept of a fictitious, undeformed configuration has been advocated by Steinmann and Carol [SC98] and was further elaborated in Menzel and Steinmann [MS01c, MS01f, MS01e, MS01b]. Thereby, as the fundamental assumption, the storage of strain energy due to either nominal or effective strains is measured by either the damage or the energy metric based on the hypothesis of strain en-

ergy equivalence between microscopic and macroscopic configurations, compare e.g. Sidoroff [Sid81].

Besides the formulation of the initial elastic anisotropic state of the material, the incorporation of yield criteria and appropriate flow rules that account for anisotropy are of cardinal importance. In analogy to the free Helmholtz energy density, the introduction of further arguments into inelastic potentials – in addition and coupled to the appropriate thermodynamic driving forces – and the application of representation theorems give a powerful tool at hand, compare e.g. Smith [Smi62], Boehler and Sawczuk [BS76, BS77], Litewka and Sawczuk [LS81] and Betten [Bet85]. For an overview and applications on anisotropic yield criteria, we refer to Desai and Siriwardane [DS84, Chap. 12]. Thereby, it is obvious that the general type of evolution equations results in a modification of the underlying symmetry group of the material which is often denoted as deformation induced anisotropy. In this direction, the evolution of anisotropic continuum damage within the small strain case has been highlighted in, e.g., Chaboche [Cha93] or Carol et al. [CRW01]. General surveys on anisotropic damage and creep theory are summarised by Murakami [Mur87], Lemaitre and Chaboche [LC98, Chap. 7] and Betten [Bet91] among others. Special emphasis on the incorporation of structural tensors in the context of continuum damage mechanics has been placed by e.g. Matzenmiller and Sackman [MS94], Betten et al. [BSZ98] and Menzel and Steinmann [MS99]. A classical yield criterion for anisotropic metals is represented by the celebrated Hill-type plasticity [Hil50, Chap. XI] which is defined via a quadratic form in terms of stress (the conjugate thermodynamic force) and a fourth order tensor (that accounts for the incorporated type of plastic anisotropy – similar to the tangent operator in anisotropic linear elasticity). Furthermore, recall that plastic anisotropy enters the modelling of the material as soon as kinematic hardening is incorporated since the flow direction generally does not commute with the conjugate internal variable that accounts for plastic deformations in this case, compare Haupt [Hau00, Sect. 11.3], Diegele et al. [DJT00], Svendsen [Sve98, SAKS98] and Ekh et al. [ER01, EMRS02] among others. Until now, the concept of plastic spin is not settled extensively harmonised in the computational mechanics community. Likewise, we do not adopt this approach in the sequel, but refer to the discussion in Dafalias [Daf98], the contribution by Paulun and Peçherski [PR92] and, for special emphasis on additional initial anisotropy, to Cleja-Tigoiu [CT00] – see also references cited therein.

A fundamental part of any formulation in computational inelasticity is the numerical (time-) integration of the corresponding rate equations. If possible, families of radial-return algorithms or exponential integration schemes are applied, see e.g. Simo [Sim98] and Weber and Anand [WA90] for an overview on applications within elasto-plasticity. However, for a general anisotropic setting, no exponential-type integrator of the governing evolution equations is conveniently available which is obviously due to the non-coaxiality of the internal variables and their correlated flow directions. In this case, Runge-Kutta methods allow advantageous integration procedures, see e.g. the textbook by Ascher and Petzold [AP98], Lambert [Lam91] and Hairer et al. [HNW93, Chap. II] for a general outline. Typically higher order implicit multi stage methods are adopted which allow the setup of two different schemes, namely that only the actual configuration is demanded to stay in the elastic domain or, on the contrary, that all intermediate stages are additionally constrained to satisfy this condition. For a survey on the integration of rate equations in the context of higher order Runge-Kutta schemes, we refer to Hackl [Hac98], Hackl and Schmidt-Baldassari [HSB01], Diebels et al. [DEE98], Kirchner and Kollmann [KK99] and Menzel and Steinmann [MS01f].

Goals of this study and modus operandi

The modelling of anisotropy is naturally related to group theoretical settings, the crystal classes, representation theorems and specific formats within linear elasticity. Since these subjects are of fundamental importance and permanently present (between the lines) throughout this work but are otherwise well-established in the literature, we reiterate briefly some of the basic essentials in the separate Chapter 1 which completes this introduction.

The formulation of large strain hyper-elasticity is usually based on the right Cauchy-Green tensor within the Lagrangian setting or alternatively on the Finger tensor with respect to an Eulerian framework. As a usual drawback, at least in the field of computational mechanics, the spatial outline

was essentially restricted to isotropy. Thus, we develop a modular formulation for anisotropic hyperelasticity in Chapter 2 which accounts for additional tensorial arguments and allows a direct setup in terms of spatial fields. The derivation is strictly based on the general representation theorem of isotropic tensor functions and the fundamental covariance relation of the free Helmholtz energy density.


On this basis, the generated anisotropic framework is enlarged to the formulation of dissipative processes in a thermodynamically consistent manner, namely anisotropic multiplicative elasto–plasticity with respect to non–standard dissipative materials, Chapter 3. Thereby, the covariant character is additionally applied to the incorporated inelastic potentials. In particular, we account for initially elastic, plastic and deformation induced anisotropy. The setup of different types of evolution equations and the corresponding algorithmic treatment is displayed in detail.

The main objective of Chapter 4 is to clarify the relation between two strategies to formulate constitutive equations for hyper–elastic orthotropic materials at large strains. In particular, the classical Lagrangian approach with respect to the incorporation of structural tensors is compared to the framework of a fictitious isotropic configuration which defines an anisotropic reference configuration via the correlated linear tangent map. Thereby, the principle of strain energy equivalence or rather covariance with respect to the fictitious configuration and the standard reference configuration is adopted and the free Helmholtz energy density allows to be computed via push–forward operations within the nominal setting. Thereby, anisotropy comes into the picture if the obtained anisotropy metric is non–spherical which is apparently determined by the fictitious mapping. This approach results in a reduced but nevertheless physically motivated set of invariants which are related to the invariants defined by structural tensors. As a main conceptual advantage, standard isotropic constitutive equations can be applied and moreover, the numerical treatment within a finite element setting becomes cheaper since we deal with a reduced set of invariants.

To capture the anisotropic nature of damage, one has to introduce at least a second order internal variable. In this context, the goal of Chapter 5 consists in extending the framework based on a fictitious isotropic configuration to geometrically non–linear, anisotropic, tensorial second order continuum damage. Referring to the framework of standard dissipative materials, associated evolution equations are constructed which substantially affect the anisotropic nature of the damage formulation. Specifically, the categories of quasi isotropic and anisotropic damage evolution are classified. The numerical integration of the obtained system of ordinary differential equations is discussed whereby two different schemes and higher order methods are taken into account.

Finally, Chapter 6 generalises the concept of a fictitious configuration, namely a framework for continuum damage mechanics coupled to multiplicative elasto–plasticity is developed whereby it turns out to be convenient to introduce two different fictitious configurations. Specifically, in addition to the intermediate configuration of multiplicative elasto–plasticity, we account for two microscopic configurations of Lagrangian and Eulerian type which characterise the so–called fictitious undamaged material. This kinematical framework enables us to apply two well–established postulates based on the standard terminology in nonlinear continuum mechanics. Concerning the free Helmholtz energy density, the postulate of strain energy equivalence is adopted and in view of the plastic dissipation potential, the concept of effective stress is a natural outcome of the underlying kinematical assumptions. Moreover, we focus on the integration technique for the class of obtained evolution equations.

Einleitung

 In den letzten zwei Monaten habe ich mich viel mit eigenen mathematischen Spekulationen beschäftigt, die mir viel Zeit gekostet, ohne daß ich eigentlich mein erstes Ziel bisher erreicht hätte. Immer wurde ich von den vielfach sich kreuzenden Aufsichten von einer Richtung in eine andere gelockt, mitunter auch von Irrlichtern, wie dies bei mathematischen Spekulationen nichts Seltenes ist.

Carl Friedrich Gauß [1777 – 1855]
Brief an W. Weber, Göttingen, 21.05.1843

Der Titel dieser Arbeit mag in gewisser Weise irreführend sein; allerdings könnte kein Titel allen potenziellen Lesergruppen gerecht werden. Für Mathematiker steht Anisotropie sicherlich in engem Zusammenhang mit gruppentheoretischen Aspekten. Materialwissenschaftler und Physiker haben wahrscheinlich atomistische Vorgehensweisen, Mikrostrukturen, Körner, etc. vor Augen und ließen eventuell die Bezeichnung Anisotropie am liebsten gänzlich weg, da offensichtlich nahezu sämtliche inelastischen Prozesse anisotrop verlaufen. Ingenieure, die Versagens – und Lebensdauervorhersagen zu verantworten haben, erwarten unter Umständen experimentelle Ergebnisse, merkwürdiges Materialverhalten und Kurvenanpassungen. Ich hoffe, daß *“Modelling and Computation of Geometrically Nonlinear Anisotropic Inelasticity”* zumindest einige Leser dieser Bereiche anspricht.

Die Modellierung anisotropen Materialverhaltens auf unterschiedlichen Skalen ist ein seit einigen Jahrzehnten aktiv verfolgtes Forschungsgebiet und von großer Bedeutung in den Material- und Ingenieurwissenschaften. Da nahezu alle Materialien anisotrop sind, aufgrund ihrer natürlichen Erscheinungsform oder als Folge von Herstellungs- und Deformationsprozessen, existiert offensichtlich eine Vielzahl von Anwendungen in den Werkstoffwissenschaften und in der Mechanik. Typische Beispiele findet man in Zusammenhang mit Textur (-bildung) und kristallinem sowie poly-kristallinem Material, siehe z.B. die aktuellen Monographien von Kocks et al. [KTW00], Phillips [Phi01], Nembach [Nem97] oder die Beiträge in Teodosiu [Teo97]. Ein weiteres Anwendungsfeld anisotropen Materialverhaltens stellen faserverstärkte Kunststoffe sowie Verbundwerkstoffe dar, die eine große und wichtige Klasse von Ingenieurmaterialien sind – üblicherweise Polymer, Metal und Keramik Verbundwerkstoffe. Für einen allgemeinen Überblick verweisen wir auf Hull und Clyne [HC96] und Spencer [Spe72] – siehe auch die dort zitierte Literatur. Des weiteren ist offensichtlich, daß Geomaterialien, wie z.B. Boden und Fels, und Biomaterialien, d.h. Materialien die wachsen, allgemein anisotrope Eigenschaften aufweisen. So ist z.B. die Modellierung von Holz und Muskelgewebe oder von Zähnen und Knochen unter Berücksichtigung mit der Interaktion mit Implantaten von zunehmender Bedeutung, siehe den Überblickartikel von Taber [Tab95] und in Hinblick auf eine Einführung in die Umsetzungen der Finiten Element Methode im Rahmen der Biomechanik verweisen wir auf Huiskes and Chao [HC83]. Konzeptionell betrachtet werden die Eigenschaften von vielen Materialien, die wir phänomenologisch auf der Makro-Skala beobachten, von einer speziellen Struktur auf der Mikro-Skala bestimmt, welche in der Kontinuumsmechanik mit Hilfe von tensoriellen Feldern modelliert werden können. Typische Beispiele sind Kontinua mit Fehlstellen, Spin, rotatorischen Freiheitsgraden, etc. – siehe Capriz [Cap89] für einen allgemeinen Überblick und Svendsen [Sve01a].

In dieser Arbeit wird ein phänomenologischer Rahmen (für einfache Materialien) entwickelt, d.h. die thermomechanischen Eigenschaften eines jeden Partikels des betrachteten Körpers seien durch die

Deformationsgeschichte und Temperatur an diesem einen materiellen Punkt bestimmbar. Der Zustand sowie die Zustandsfunktionen werden mittels konstitutiver Funktionale repräsentiert, die der Kenntnis der Geschichte unabhängiger Variablen sowie interner Variablen, welche der direkten Beobachtung nicht zugänglich sind, Rechnung tragen. Dabei ist es grundsätzlich vorzuziehen, für Formulierungen kontinuierlicher Festkörper allgemeine konvektive Koordinaten (Körper Felder – bzgl. eines Partikels, auf den sich ebenfalls die Kenntnis der Deformationsgeschichte bezieht) an Stelle von raumfesten Koordinaten (Raum Felder – bzgl. eines Ortes) zu verwenden. Nichtsdestotrotz kann es bei speziellen Anwendungen, wie z.B. typische Finite Element Algorithmen, vorteilhaft sein, für die konvektiven Koordinaten in einem betrachteten Partikel zum Zeitpunkt t ein spezielles Koordinatensystem zu wählen, z.B. ein orthogonales oder Kartesisches. Der Übersichtlichkeit halber, aber ohne Beschränkung der Allgemeinheit, modellieren wir ausschließlich ratenunabhängiges und isothermes Verhalten.

Eine mögliche Vorgehensweise der Modellierung anisotropen Materialverhaltens – im Rahmen der Kontinuumsmechanik und phänomenologischer Hyper-Elastizität – basiert auf der Einführung ergänzender tensorieller Argumente in die freie Helmholtz Energiedichte. Als typisches Beispiel sei die Berücksichtigung von symmetrischen Tensoren zweiter Stufe genannt, die bevorzugte Faserorientierungen des Materials definieren; detaillierte Ausführungen sind z.B. in den Beiträgen von Spencer [Spe84], Qiu und Pence [QP97] oder Menzel und Steinmann [MS01h] enthalten und die Umsetzung im Rahmen der Finiten Element Methode wird speziell von Weiss et al. [WMG96], Almeida und Spilker [AS98] betont – siehe auch die dort zitierte Literatur. Basierend auf den allgemeinen Darstellungstheoremen isotroper und anisotroper Tensorfunktionen, definieren die zugrundeliegenden Invarianten und Generatoren konstitutive Gleichungen, welche die Modellierung von Anisotropie gestatten. Für eine umfassende Darstellung der Grundlagen und einen allgemeinen Überblick sei auf die Monographien von Green und Adkins [GA70], Smith [Smi94], die frühzeitige Arbeit von Pipkin und Rivlin [PR59] sowie die Beiträge in Boehler [Boe87] verwiesen. Des weiteren sei daran erinnert, daß Anisotropie bereits modelliert wird, wenn die angenommene freie Helmholtz Energiedichte neben dem existentiellen kinematischen Feld weitere tensorielle, nicht-sphärische Argumente oder ergänzende Komponenten enthält, vergleiche Marsden und Hughes [MH94, Kap. 3, Prop. 5.7] für Isotropie sowie die Anwendung in Park und Youn [PY98]. In dieser Arbeit sollen stets symmetrische Tensoren zweiter Stufe gewählt werden, um Anisotropie zu erfassen. Allerdings sei darauf hingewiesen, daß weitaus komplexere Theorien möglich sind, die z.B. auf Tensoren höherer Stufe basieren, welche den entsprechenden Typ von Anisotropie charakterisieren, vergleiche Zhang und Rychlewsky [ZR90] oder Zheng und Spencer [ZS93]. In diesem Zusammenhang ermittelte Betten [Bet82a] den Satz nicht reduzierbarer Invarianten eines Tensors vierter Stufe und in Hinblick auf die Kopplung mit einem zweistufigen Tensor wie z.B. dem Spannung- oder Verzerrungsfeld die zugehörigen Simultaninvarianten.

Nichtsdestotrotz verbleibt die Aufgabe, Anisotropie im Rahmen eines phänomenologischen Ansatzes für inelastische Prozesse umzusetzen – z.B. für elasto-plastisches Verhalten. In diesem Zusammenhang stellt die Theorie generalisierter standard dissipativer Materialien einen leistungsfähigen Rahmen zur Verfügung, siehe Halphen und Nguyen [HN75], Maugin [Mau99, Kap. 7] oder Antman [Ant95, Kap. XV] sowie die dort zitierte Literatur für einen allgemeinen Überblick. Hierbei wird die Liste der Argumente der freien Helmholtz Energiedichte um Felder erweitert, welche interne Variablen repräsentieren und plastische Deformationen sowie möglicherweise deformationsinduzierte Anisotropie darstellen können. Aktuelle Formulierungen anisotroper Plastizität sind z.B. in v.d. Giessen [vdG89], Steinmann et al. [SMS96], Miehe [Mie98a], Papadopoulos und Lu [PL01], Svendsen [Sve01b], Resse et al. [RRW01], Tsakmakis [Tsa00] oder Menzel und Steinmann [MS01d, MS01a] enthalten.

Die adäquate Wahl der physikalischen Eigenschaften interner Variablen, welche Anisotropie modellieren sollen, sowie ihre tensorielle Darstellungsform sind seit langem Gegenstand intensiver Diskussionen, vergleiche Leckie und Onat [LO81] mit spezieller Ausrichtung auf Schädigungsmechanik. Eine alternative Vorgehensweise stellt die Einführung fiktiver Abbildungen dar, die wesentliche Eigenschaften der Anisotropie beinhalten sollen. Einerseits kann ein solcher Rahmen lediglich eine reduzierte Darstellung allgemeiner Anisotropie liefern. Andererseits ist es möglich, mit Hilfe von standard isotropen Stoffgesetzen anisotropes Materialverhalten zu modellieren, was ein wesentlicher Vorteil dieser Methode ist. Die Vorstellung einer ungeschädigten, mikroskopischen Konfiguration (ähnlich der effektiven Konfiguration der klassischen, isotropen $[1 - D]$ Schädigungstheorie), die mit der makroskopischen Konfiguration in Relation steht, wurde ursprünglich für anisotrope Versagenkriterien wie Krie-

chen und Schädigung verwendet, siehe Betten [Bet82b] und Murakami [Mur88] oder Betten [Bet76], Karafillis und Boyce [KB93] und Oller et al. [OBMO95] mit Anwendung auf Plastizität. Kürzlich diskutierten Park und Voyiadjis [PV98] ausführlich die zugrundeliegende Kinematik in Hinblick auf Kontinuumschädigung. Desgleichen wurde von Steinmann and Carol [SC98] eine fiktive, undeformierte Konfiguration eingeführt und in Menzel und Steinmann [MS01c, MS01f, MS01e, MS01b] weiter entwickelt. Als fundamentale Grundlage wird hierbei die gespeicherte Verzerrungsenergie in nominellen und fiktiven Verzerrungen in Bezug auf eine Schädigungs- bzw. Energiemetrik gemessen, was der Hypothese der Verzerrungsenergie Äquivalenz entspricht, vergleiche z.B. Sidoroff [Sid81].

Neben der Formulierung der anfänglich elastischen, anisotropen Ausgangskonfiguration ist die Berücksichtigung von Fließkriterien und Fließfunktionen, die ebenfalls Anisotropie modellieren, entscheidend. In Analogie zur freien Helmholtz Energiedichte stellt die Einführung zusätzlicher Argumente in die inelastischen Potenziale – als Ergänzung und gekoppelt mit den zutreffenden thermodynamischen, treibenden Kräften – sowie die Anwendung von Darstellungstheoremen einen leistungsfähigen Rahmen zur Verfügung, vergleiche z.B. Smith [Smi62], Boehler und Sawczuk [BS76, BS77], Litewka und Sawczuk [LS81] und Betten [Bet85]. Für einen Überblick und Anwendungen anisotroper Fließkriterien verweisen wir auf Desai und Siriwardane [DS84, Kap. 12]. Dabei ist es offensichtlich, daß die allgemeine Form anisotroper Evolutionsgleichungen zu einer Veränderung der Symmetriegruppe des Materials führt, was oft als deformationsinduzierte Anisotropie bezeichnet wird. In dieser Richtung wurde die Evolution anisotroper Kontinuumschädigung für kleine Verzerrungen z.B. von Chaboche [Cha93] oder Carol et al. [CRW01] untersucht. Allgemeine Übersichten zu anisotroper Schädigung sowie anisotropen Kriechens sind in Murakami [Mur87], Lemaitre und Chaboche [LC98, Kap. 7] und Betten [Bet91] zusammengefaßt. Der Einführung von Strukturtenoren in Zusammenhang mit der Kontinuumschädigungsmechanik wird besondere Aufmerksamkeit in den Arbeiten von Matzenmiller und Sackman [MS94], Betten et al. [BSZ98] und Menzel und Steinmann [MS99] gewidmet. Ein klassisches Fließkriterium für anisotrope Metalle stellt die viel beachtete Hill-Plastizität dar [Hil50, Kap. XI], welche über eine quadratische Form bezüglich der Spannungen (die konjugierte thermodynamische Kraft) und einen vierstufigen Tensor (welcher – ähnlich dem Tangentenoperator anisotroper, linearer Elastizität – Anisotropie berücksichtigt) definiert ist. Des weiteren sei daran erinnert, daß plastische Anisotropie bereits in der Modellierung enthalten ist, sobald kinematische Verfestigung Berücksichtigung findet, da in diesem Fall die Fließrichtung im allgemeinen nicht mehr mit den konjugierten internen Variablen, welche die Plastizität beschreiben, kommutiert, vergleiche Haupt [Hau00, Abs. 11.3], Diegele et al. [DJT00], Svendsen [Sve98, SAKS98] und Ekh et al. [ER01, EMRS02] unter anderen. Bis heute wurde das Konzept eines plastischen Spins im Bereich der computerorientierten Mechanik unterschiedlich verwendet. Gleichermaßen übernehmen wir diese Theorie im Folgenden nicht, sondern verweisen vielmehr auf die Diskussion in Dafalias [Daf98], den Beitrag von Paulun und Pęcherski [PR92] sowie, in Hinblick auf die Berücksichtigung anfänglicher Anisotropie, auf Cleja-Țigoiu [CT00] – siehe auch die in diesen Arbeiten zitierte Literatur.

Ein wesentlicher Anteil jeglicher numerisch umzusetzender Formulierung von Inelastizität besteht in der (Zeit-) Integration der zugrundeliegenden Ratengleichungen. Soweit möglich, finden zumeist Radial-Return Algorithmen oder exponentielle Vorgehensweisen Anwendung, siehe z.B. Simo [Sim98] und Weber und Anand [WA90] für eine Übersicht und Beispiele im Rahmen elasto-plastischen Materialverhaltens. Im allgemeinen anisotropen Fall lassen sich derartige Exponential-Integratoren nicht mehr komfortabel umsetzen, denn die internen Variablen sind dann offensichtlich nicht koaxial zu ihrer Fließrichtung. In diesem Fall erlauben Runge-Kutta Methoden vorteilhafte Integrationsalgorithmen, siehe z.B. das Lehrbuch von Ascher und Petzold [AP98], Lambert [Lam91] und Hairer et al. [HNW93, Kap. II] für eine allgemeine Übersicht. Typischer Weise können implizite mehrstufige Verfahren höherer Ordnung eingesetzt werden, die prinzipiell zwei unterschiedliche Vorgehensweisen erlauben. Entweder wird lediglich vom aktuellen Zustand gefordert, daß er sich im zulässigen elastischen Gebiet befinden soll, oder alle weiteren Zwischenzustände sollen ebenfalls dieser Bedingung genügen. Für einen Überblick zur Integration der Ratengleichungen in Zusammenhang mit Runge-Kutta Methoden höherer Ordnung verweisen wir auf Hackl [Hac98], Hackl und Schmidt-Baldassari [HSB01], Diebels et al. [DEE98], Kirchner und Kollmann [KK99] und Menzel und Steinmann [MS01f].

Zielsetzung dieser Arbeit und modus operandi

Die Modellierung anisotropen Materialverhaltens ist natürlicher Weise mit der Gruppentheorie, den Kristallklassen, Darstellungstheoremen und speziellen Formen linearer Elastizität verbunden. Da diese Themenbereiche von fundamentaler Wichtigkeit sind und stets (zwischen den Zeilen) in dieser Arbeit auftauchen, allerdings in der Literatur ausführlich abgehandelt wurden, fassen wir lediglich einige wesentliche Grundlagen in dem separaten Kapitel 1 zusammen, das diese Einleitung abrundet.

Hyper-Elastizität bei großen Verzerrungen ist gewöhnlich mit dem rechten Cauchy-Green Tensor materiell formuliert oder basiert auf dem räumlichen Finger Tensor. Im Bereich der numerischen Mechanik besteht ein Nachteil der ansonsten vorteilhaften, direkten räumlichen Vorgehensweise in der Beschränkung auf Isotropie. Daher wird in Kapitel 2 eine Formulierung anisotroper Hyper-Elastizität entwickelt, die zusätzliche tensorielle Argumente berücksichtigt und eine direkte Beschreibung in räumlichen Feldern erlaubt. Die Herleitung beruht auf dem allgemeinen Darstellungstheorem isotroper Tensorfunktionen und der fundamentalen Kovarianz der freien Helmholtz Energiedichte.

Auf dieser Basis kann der entwickelte Rahmen für dissipative Prozesse thermodynamisch konsistent erweitert werden, z.B. auf anisotrope multiplikative Elasto-Plastizität unter Verwendung nicht-standard dissipativer Materialien, Kapitel 3. Dabei soll die Kovarianz Eigenschaft zusätzlich für die inelastischen Potentiale gelten. Im Einzelnen berücksichtigen wir anfängliche elastische, plastische sowie deformationsinduzierte Anisotropie. Die Umsetzung unterschiedlicher Evolutionsgleichungen und deren algorithmische Handhabung werden detailliert ausgeführt.


Das Hauptziel des Kapitels 4 besteht in der Gegenüberstellung zweier unterschiedlicher Vorgehensweisen, konstitutive Gleichungen für hyper-elastische Orthotropie bei großen Verzerrungen zu formulieren. Im Einzelnen wird die klassische materielle Strukturtenso-Formulierung mit der Einführung einer fiktiven Konfiguration, welche eine anisotrope Ausgangskonfiguration über lineare Tangentialabbildungen definiert, verglichen. Das Konzept der Verzerrungsenergie-Äquivalenz bzw. die fundamentale Kovarianz bezüglich der fiktiven Konfiguration und der standardmäßigen Referenzkonfiguration wird angewendet und die freie Helmholtz Energiedichte kann nun mit Hilfe von push-forward Operationen nominell formuliert werden. Anisotropie ist berücksichtigt, sobald die entsprechende Anisotropie Metrik nicht sphärisch ist, was ausschließlich die fiktive Abbildung bestimmt. Diese Vorgehensweise führt zu einem reduzierten aber physikalisch motivierten Satz von Invarianten, welcher mittels der Invarianten, die durch Strukturtenso-oren definiert sind, dargestellt werden kann. Ein Hauptvorteil dieser Methode besteht in der Verwendung standard isotroper Stoffgesetze und der effizienten numerischen Umsetzung im Rahmen der Finiten Element Methode, welche bei weitem nicht so aufwendig ist wie die vorherige Vorgehensweise, da ein reduzierter Satz von Invarianten vorliegt.

Zur Erfassung der anisotropen Eigenschaften von Schädigungsprozessen ist es notwendig, eine zumindest zweistufige interne Variable einzuführen. In diesem Zusammenhang besteht das Ziel des Kapitels 5 darin, das Konzept einer fiktiven isotropen Konfiguration auf geometrisch nichtlineare, tensoriell zweistufige, anisotrope Schädigung zu erweitern. Basierend auf der Theorie standard dissipativer Materialien werden assoziierte Evolutionsgleichungen entwickelt, welche die anisotropen Schädigungseigenschaften wesentlich beeinflussen. Im Einzelnen gilt es, die Kategorien quasi isotroper und anisotroper Schädigung zu klassifizieren. Die numerische Umsetzung des so erhaltenen Systems gewöhnlicher Differentialgleichungen wird ausführlich behandelt, wobei zwei unterschiedliche Vorgehensweisen sowie Verfahren höherer Ordnung Anwendung finden.

Abschließend wird in Kapitel 6 das Konzept einer fiktiven Konfiguration generalisiert, und zwar auf die Kopplung von Kontinuumsschädigung mit multiplikativer Elasto-Plastizität, wobei es vorteilhaft ist, zwei unterschiedliche fiktive Konfigurationen einzuführen. Genau genommen berücksichtigen wir ergänzend zur Zwischenkonfiguration multiplikativer Elasto-Plastizität zwei mikroskopische Konfigurationen vom Lagrange sowie Euler Typ, welche das sogenannte fiktive, ungeschädigte Material charakterisieren sollen. Dieses kinematische Gerüst erlaubt uns, zwei etablierte Postulate im Rahmen der nichtlinearen Kontinuumsmechanik anzuwenden. Bezogen auf die freie Helmholtz Energiedichte findet das Postulat der Verzerrungsenergie-Äquivalenz Anwendung und für das plastische Potenzial ergibt sich direkt aus den kinematischen Annahmen das Konzept effektiver Spannungen. Des Weiteren wird die Integration der entwickelten Klasse von Evolutionsgleichungen ausführlich diskutiert.

Chapter 1

Concepts of the formulation of anisotropy

 From the days of Voigt, who introduced the term ‘tensor’, some kind of tensor calculus has always been the best instrument for dealing with the properties of anisotropic media.

J.A. Schouten
Tensor Analysis for Physicists, 1951

The contents of the subsequent Chapter is independent of the rest of this work. The readers who would like to start directly with the modelling of anisotropic materials should skip this Chapter. In fact, a brief review on common strategies to incorporate anisotropy into constitutive equations is given and, hopefully, a sufficient number of representative examples is included since – being an engineer – I personally learn a lot from examples. For the sake of maximal congruence with the literature, the applied notation in this Chapter is fairly standard and does not explicitly distinguish between co-, contra- and mixed-variant fields. Conventional details are highlighted in Appendix A.

1.1 Principles of objectivity

Preliminary, we focus on material objectivity, namely the fundamental principle of material frame indifference (as represented by superposed spatial rigid body motions) and the appropriate definition of the symmetry class which characterises the body of interest. Both concepts are well-established and documented in several standard monographs on continuum mechanics, see e.g. Eringen [Eri62, Arts. 27 & 44], Truesdell and Noll [TN92, Sect. C.I], Antman [Ant95, Sects. XII.11 & 13], Šilhavý [Šil97, Chap. 6, Sects. 9.3 & 9.4] or Murdoch [Mur00] and the contributions by Svendsen and Bertram [SB99] and Ericksen [Eri00]. Please note that these relations are specific cases of general covariance which is thoroughly highlighted in Chapter 2.

Distance preserving transformations: Let $\mathbf{X}_{1,2} \in \mathbb{E}^3$ characterise two points at time $t_{1,2} \in \mathbb{R}$. Now, consider a mapping of these points onto $\mathbf{X}'_{1,2} \in \mathbb{E}^3$ at time $t'_{1,2} \in \mathbb{R}$. We require an observer to measure identical distances between the particles $\mathbf{X}_{1,2}$ and $\mathbf{X}'_{1,2}$ which is guaranteed under the time-dependent transformation

$$\mathbf{X}'_2 - \mathbf{X}'_1 = \mathbf{Q}(t) \cdot [\mathbf{X}_2 - \mathbf{X}_1] \implies \|\mathbf{X}'_2 - \mathbf{X}'_1\| = \|\mathbf{X}_2 - \mathbf{X}_1\| \quad (1.1)$$

with $\mathbf{X}'_2 - \mathbf{X}'_1, \mathbf{X}_2 - \mathbf{X}_1 \in \mathbb{V}^3$ for any orientation preserving function $\mathbf{Q}(\bullet) \in C^\infty : \mathbb{R} \rightarrow \mathbb{O}_+^3$. Recall that this transformation is related to the concept of superposed rigid body motions (active version). Alternatively, Eq.(1.1) can be written as

$$\mathbf{X}'_2 = \mathbf{Q}(t) \cdot \mathbf{X}_2 + \mathbf{c}(t) \quad \text{with} \quad \mathbf{c}(t) = \mathbf{X}'_1 - \mathbf{Q}(t) \cdot \mathbf{X}_1 \in C^\infty : \mathbb{R} \rightarrow \mathbb{V}^3 \quad (1.2)$$

associated with the shift in time scale $\delta = t'_2 - t_2 \doteq t'_1 - t_1 \in \mathbb{R}$ which possibly vanishes, without loss of generality. Likewise, Eq.(1.2) allows to characterise two different observers (being related via an orthogonal transformation $\mathbf{Q}(\bullet) \in C^\infty : \mathbb{R} \rightarrow \mathbb{O}^3$), one monitoring $\mathbf{X}_{1,2}$ and the other accounting for $\mathbf{X}'_{1,2}$, but both obviously observing the identical incident. This interpretation is established as the change of (Euclidian) observer, frame or coordinate system, respectively (passive version).

Principle of indifference with respect to superposed rigid body motions (active version): We consider an admissible but otherwise arbitrary motion of the body of interest denoted by $\varphi(\mathbf{X}, t) : \mathbb{R}^3 \times \mathbb{R} \rightarrow \mathbb{R}^3$ incorporating the position field $\mathbf{X} \in \mathbb{R}^3$ which allows identification with points, or at least distances between points, in \mathbb{E}^3 . The previous discussion on distance preserving transformations indicates two classical principles on material objectivity with respect to the physical properties of the body of interest. On the one hand, the Hooke–Poisson–Cauchy representation characterises invariance of a constitutive equation under superposed spatial rigid body motions ($\mathbf{Q}(\bullet) \in C^\infty : \mathbb{R} \rightarrow \mathbb{O}_+^3 \subset \mathbb{O}^3$, active version) while on the other hand, the Zaremba–Jaumann format allows an arbitrary change of observer ($\mathbf{Q}(\bullet) \in C^\infty : \mathbb{R} \rightarrow \mathbb{O}^3$, passive version). The “classical” conclusion is that the second framework is generally more restrictive compared to the first since improper orthogonal transformations are additionally included; i.e. a response function which satisfies the Zaremba–Jaumann form fulfils equally the Hooke–Poisson–Cauchy restriction – but not the opposite way round, compare Truesdell and Noll [TN92, Sect. 19A]. However, each format represents a principle on its own (say rigid body motion– and Euclidian frame–indifference) which both have to be satisfied, then imply additionally form–invariance and, finally, elaborate material objectivity, see Svendsen and Bertram [SB99] for a detailed outline. Now, adopting the Hooke–Poisson–Cauchy approach, Eq.(1.2)₁ is related to an Euclidian transformation (in the language of differential geometry, we deal with a spatial orientation preserving isometry)

$$\boxed{\varphi'(\mathbf{X}, t') = \mathbf{Q}(t) \cdot \varphi(\mathbf{X}, t) + \mathbf{c}(t) \implies \mathbf{F}'(\mathbf{X}, t') = \mathbf{Q}(t) \cdot \mathbf{F}(\mathbf{X}, t)} \quad (1.3)$$

which, conceptually speaking, represents a superposed spatial rigid body motion and includes the functions $\mathbf{c}(\bullet) \in C^\infty : \mathbb{R} \rightarrow \mathbb{R}^3$, $\mathbf{Q}(\bullet) \in C^\infty : \mathbb{R} \rightarrow \mathbb{O}_+^3$. Moreover, the applied abbreviations $\mathbf{F}'(\mathbf{X}, t') = \partial_{\mathbf{X}} \varphi'(\mathbf{X}, t') \in \mathbb{L}_+^3$ and $\mathbf{F}(\mathbf{X}, t) = \partial_{\mathbf{X}} \varphi(\mathbf{X}, t) \in \mathbb{L}_+^3$, respectively, represent the corresponding linear tangent maps. Next, based on the assumption of a simple elastic stress function solely defined in terms of $\mathbf{F}(\mathbf{X}, t)$, namely $\mathfrak{S}(\mathbf{X}, t) \doteq \mathfrak{S}(\mathbf{F}(\mathbf{X}, t); \mathbf{X})$ whereby $\mathfrak{S}(\mathbf{X}, t)$ is expected to be a one–point tensor, we define the stress vector $[\mathfrak{S}(\mathbf{X}, t) \cdot \mathbf{N}]$, for arbitrary $\mathbf{N} \in \mathbb{U}^2$, which results under the motion as determined by Eq.(1.3) in

$$\boxed{\mathfrak{S}'(\mathbf{X}, t') \cdot \mathbf{N}' = \mathbf{Q}(t) \cdot [\mathfrak{S}(\mathbf{X}, t) \cdot \mathbf{N}] \implies \mathfrak{S}'(\mathbf{X}, t') = \mathbf{Q}(t) \cdot \mathfrak{S}(\mathbf{X}, t) \cdot \mathbf{Q}^t(t)} \quad (1.4)$$

with $\mathfrak{S}'(\mathbf{X}, t') = \mathfrak{S}(\mathbf{F}'(\mathbf{X}, t'); \mathbf{X}) = \mathfrak{S}(\mathbf{Q}(t) \cdot \mathbf{F}(\mathbf{X}, t); \mathbf{X})$ and $\mathbf{N}' = \mathbf{Q}(t) \cdot \mathbf{N}$. Note that Eq.(1.4)₂ defines an objective tensor function. Next, applying the right polar decomposition theorem $\mathbf{F}(\mathbf{X}, t) = \mathbf{R}(\mathbf{X}, t) \cdot \mathbf{U}(\mathbf{X}, t)$, $\mathbf{F}'(\mathbf{X}, t') = \mathbf{R}'(\mathbf{X}, t') \cdot \mathbf{U}'(\mathbf{X}, t') = \mathbf{Q}(t) \cdot \mathbf{R}(\mathbf{X}, t) \cdot \mathbf{U}(\mathbf{X}, t) \implies \mathbf{U}'(\mathbf{X}, t') = \mathbf{U}(\mathbf{X}, t)$ with $\mathbf{R}, \mathbf{R}' \in \mathbb{O}_+^3$ and $\mathbf{U}, \mathbf{U}' \in \mathbb{S}_+^3$, and taking into account the specific case $\mathbf{Q}(t) \doteq \mathbf{R}^t(\mathbf{X}, t)$, we end up with the reduced format [†]

$$\boxed{\mathfrak{S}(\mathbf{X}, t) \doteq \mathfrak{S}(\mathbf{F}(\mathbf{X}, t); \mathbf{X}) = \mathbf{R}(\mathbf{X}, t) \cdot \mathfrak{S}(\mathbf{U}(\mathbf{X}, t); \mathbf{X}) \cdot \mathbf{R}^t(\mathbf{X}, t)}, \quad (1.5)$$

[†] In this Section we adopt the ansatz $\mathbf{Q}(t) \doteq \mathbf{R}^t(\mathbf{X}, t) \implies \mathbf{F}'(\mathbf{X}, t) = \mathbf{U}(\mathbf{X}, t)$ which is well–established in the literature, see e.g. the monographs by Truesdell and Noll [TN92, Sect. 29], Ogden [Ogd97, Sect. 4.2], Antman [Ant95, Sect. XII.11], Haupt [Hau00, Sect. 7.2.2]. A criticism of this approach with respect to the strain energy density, compare Section 1.3, as e.g. highlighted by Truesdell and Noll [TN92, Sect. 84] or Green and Adkins [GA70, Sects. 1.3 & 8.3] among many other authors has been emphasised in Rivlin and Smith [RS87], see also Rivlin [Riv91] and Truesdell [Tru66, Chap.IV, Sect. 37]. However, as mentioned above, the stretch of $\mathbf{F}'(\mathbf{X}, t)$ equals the stretch of $\mathbf{F}(\mathbf{X}, t)$ and therefore an elegant derivation can be based on the argument $\mathbf{U}(\mathbf{X}) = \sqrt{\mathbf{F}^t(\mathbf{X}, t) \cdot \mathbf{F}(\mathbf{X}, t)} = \sqrt{[\mathbf{F}'(\mathbf{X}, t')]^t \cdot \mathbf{F}'(\mathbf{X}, t')}$ which is satisfied for any $\mathbf{Q}(t) \in \mathbb{O}^3$ including $\mathbf{Q}(t) = \mathbf{R}^t(\mathbf{X}, t)$. Finally, the fundamental covariance principle enables us to give a clear representation of the problem at hand, see Section 2.2.

compare Truesdell and Noll [TN92, p. 66, footnote 1]. Thus, the simple elastic stress function $\mathfrak{S}(\mathbf{X}, t)$ is defined in terms of the stretch tensor $\mathbf{U}(\mathbf{X}, t)$ and does not incorporate the rotation $\mathbf{R}(\mathbf{X}, t)$. Note that Eq.(1.5) is objective which is easily verified by inserting this function into Eq.(1.4)₂. Furthermore, various representations of stress functions can be applied. One likely candidate is

$$\begin{aligned}\mathfrak{S}(\mathbf{F}(\mathbf{X}, t); \mathbf{X}) &= \mathbf{F}(\mathbf{X}, t) \cdot \mathbf{U}^{-1}(\mathbf{X}, t) \cdot \mathfrak{S}(\mathbf{U}(\mathbf{X}, t); \mathbf{X}) \cdot \mathbf{U}^{-1}(\mathbf{X}, t) \cdot \mathbf{F}^t(\mathbf{X}, t) \\ &\doteq \mathbf{F}(\mathbf{X}, t) \cdot \mathfrak{S}(\mathbf{U}(\mathbf{X}, t); \mathbf{X}) \cdot \mathbf{F}^t(\mathbf{X}, t).\end{aligned}\quad (1.6)$$

Among several possible arguments, the introduction of $\mathfrak{S}(\mathbf{U}(\mathbf{X}, t); \mathbf{X}) \implies \mathbf{S}(\mathbf{C}(\mathbf{X}, t); \mathbf{X})$ with $\mathbf{C}(\mathbf{X}, t) = \mathbf{U}^t(\mathbf{X}, t) \cdot \mathbf{U}(\mathbf{X}, t) = \mathbf{F}^t(\mathbf{X}, t) \cdot \mathbf{F}(\mathbf{X}, t) = \mathbf{F}^t(\mathbf{X}, t) \cdot \mathbf{Q}^t(t) \cdot \mathbf{Q}(t) \cdot \mathbf{F}(\mathbf{X}, t) = [\mathbf{F}'(\mathbf{X}, t')]^t \cdot \mathbf{F}'(\mathbf{X}, t') = \mathbf{C}'(\mathbf{X}, t') \in \mathbb{S}_+^3$ is obviously a natural outcome.

Material symmetry (active version)[‡]: Consider two different events; first let $\varphi(\mathbf{X}, t)$ correspond to an admissible motion, second assume the homogeneous body of interest to be primarily mapped by a transformation that incorporates $\mathbf{Q} \in \mathbb{O}^3$ and subsequently be deformed via $\varphi(\mathbf{X}, t)$. Conceptually speaking, we deal with a preceding Euclidian transformation and consequently focus on the inverse non-linear deformation map $\Phi(\mathbf{x}, t) : \mathbb{R}^3 \times \mathbb{R} \rightarrow \mathbb{R}^3$, similar to Eq.(1.3), which allowed interpretation as a superposed spatial rigid body motion (in the language of differential geometry, we deal now with a material isometry)

$$\boxed{\Phi'(\mathbf{x}, t') = \mathbf{Q} \cdot \Phi(\mathbf{x}, t) + \mathbf{c} \implies \mathbf{f}'(\mathbf{x}, t') = \mathbf{Q} \cdot \mathbf{f}(\mathbf{x}, t)} \quad (1.7)$$

Again the abbreviations $\mathbf{f}'(\mathbf{x}, t') = \partial_{\mathbf{x}} \Phi'(\mathbf{x}, t') \in \mathbb{L}_{\text{inv}}^3$ and $\mathbf{f}(\mathbf{x}, t) = \partial_{\mathbf{x}} \Phi(\mathbf{x}, t) \in \mathbb{L}_+^3$, respectively, represent the corresponding linear tangent maps and $\mathbf{c} \in \mathbb{R}^3$. Obviously, by inversion, the correlated deformation gradient of the direct motion reads $\mathbf{F}'(\mathbf{X}, t') = \mathbf{F}(\mathbf{X}, t) \cdot \mathbf{Q}^t \in \mathbb{L}_{\text{inv}}^3$. The previously introduced simple elastic stress function then renders

$$\mathfrak{S}(\mathbf{X}, t) = \mathfrak{S}(\mathbf{F}(\mathbf{X}, t); \mathbf{X}) \quad \text{and} \quad \mathfrak{S}'(\mathbf{X}, t') = \mathfrak{S}(\mathbf{F}'(\mathbf{X}, t'); \mathbf{X}) = \mathfrak{S}(\mathbf{F}(\mathbf{X}, t) \cdot \mathbf{Q}^t; \mathbf{X}). \quad (1.8)$$

For any admissible but otherwise arbitrary deformation gradient $\mathbf{F}(\mathbf{X}, t) \in \mathbb{L}_+^3$, the fixed transformation \mathbf{Q}^t is called symmetry transformation if the relation $\mathfrak{S}(\mathbf{X}, t) = \mathfrak{S}'(\mathbf{X}, t')$ is satisfied. In this case, conceptually speaking, the above stress function remains unchanged under the action of $\mathbf{Q}^t \in \mathbb{G} \subset \mathbb{O}^3$, whereby \mathbb{G} is called symmetry group. In particular, the material represented by the constitutive stress equation (1.8) is denoted as isotropic if $\mathbb{G} = \mathbb{O}^3$ (holohedral isotropic) and as hemitropic if $\mathbb{G} = \mathbb{O}_+^3$ (hemihedral isotropic) but otherwise classified as anisotropic (not hemihedral isotropic). Moreover, since the choice of $\mathbf{F}(\mathbf{X}, t)$ is arbitrary, Eq.(1.8) holds without loss of generality for $\mathbf{Q} \cdot \mathbf{F}(\mathbf{X}, t) \in \mathbb{L}_{\text{inv}}^3$ as well and under consideration of Eq.(1.4) we obtain

$$\boxed{\mathfrak{S}(\mathbf{Q} \cdot \mathbf{F}(\mathbf{X}, t) \cdot \mathbf{Q}^t; \mathbf{X}) \doteq \mathfrak{S}(\mathbf{Q} \cdot \mathbf{F}(\mathbf{X}, t); \mathbf{X}) = \mathbf{Q} \cdot \mathfrak{S}(\mathbf{F}(\mathbf{X}, t); \mathbf{X}) \cdot \mathbf{Q}^t} \quad (1.9)$$

for $\mathbf{Q} \in \mathbb{G}$. Note that Eq. (1.9) defines an isotropic tensor function if $\mathbb{G} = \mathbb{O}^3$ and an hemitropic tensor function if $\mathbb{G} = \mathbb{O}_+^3$, respectively [§]. For this case, we apply the left polar decomposition $\mathbf{F}(\mathbf{X}, t) = \mathbf{V}(\mathbf{X}, t) \cdot \mathbf{R}(\mathbf{X}, t)$, with $\mathbf{V} \in \mathbb{S}_+^3$, and assume $\mathbf{R}(\mathbf{X}, t) \doteq \mathbf{Q}$ which results in $\mathfrak{S}(\mathbf{F}(\mathbf{X}, t)) = \mathfrak{S}(\mathbf{V}(\mathbf{X}, t))$, compare footnote † on page 10. Thus the simple elastic stress function is defined in terms of the left stretch tensor $\mathbf{V}(\mathbf{X}, t)$ and does not account for the rotation $\mathbf{R}(\mathbf{X}, t)$. Another likely ingredient for the stress function among several possible is in analogy to $\mathbf{C}(\mathbf{X}, t)$, the introduction of $\mathbf{b}(\mathbf{X}, t)$ with $\mathbf{b}(\mathbf{X}, t) = \mathbf{V}(\mathbf{X}, t) \cdot \mathbf{V}^t(\mathbf{X}, t) = \mathbf{F}(\mathbf{X}, t) \cdot \mathbf{F}^t(\mathbf{X}, t) = \mathbf{F}(\mathbf{X}, t) \cdot \mathbf{Q}^t \cdot \mathbf{Q} \cdot \mathbf{F}^t(\mathbf{X}, t) = \mathbf{F}'(\mathbf{X}, t') \cdot [\mathbf{F}'(\mathbf{X}, t')]^t = \mathbf{b}'(\mathbf{X}, t') \in \mathbb{S}_+^3$.

[‡]In the sequel we restrict ourselves to material symmetry and do not focus on the concept of physical symmetry, see Zheng and Boehler [ZB94] and references cited therein.

[§] Since any orthogonal tensor is either proper orthogonal or the negative of a proper orthogonal tensor it is straightforward to show that a hemitropic tensor function of even order is isotropic, e.g. $[-\mathbf{Q}] \cdot \mathbf{T} \cdot [-\mathbf{Q}]^t = \mathbf{Q} \cdot \mathbf{T} \cdot \mathbf{Q}^t \forall \mathbf{T} \in \mathbb{L}^3$. However, there are several applications in continuum physics that deal with tensorial fields of odd order, see e.g. Ericksen [Eri00] for a discussion on the related invariance groups.

Summarising, we can obtain the restriction to objective stress functions after superposing spatial rigid body motions. It turns out that these functions are not affected by the rotation of the deformation gradient. One possible argument is $\mathbf{C}(\mathbf{X}, t)$, which here remains invariant under the action of $\mathbf{Q}(t)$ whereby $\mathbf{b}'(\mathbf{X}, t) = \mathbf{F}'(\mathbf{X}, t) \cdot [\mathbf{F}'(\mathbf{X}, t)]^t = \mathbf{Q}(t) \cdot \mathbf{b}(\mathbf{X}, t) \cdot \mathbf{Q}(t)^t$ transforms objectively. Contrary, in the case of a preceding material orthogonal transformation, $\mathbf{C}'(\mathbf{X}, t) = [\mathbf{F}'(\mathbf{X}, t)]^t \cdot \mathbf{F}'(\mathbf{X}, t) = \mathbf{Q} \cdot \mathbf{C}(\mathbf{X}, t) \cdot \mathbf{Q}^t$ transforms objectively and $\mathbf{b}(\mathbf{X}, t)$ remains invariant, which restricts the simple elastic stress function to isotropy (if no other ingredients beside $\mathbf{b}(\mathbf{X}, t)$ are involved).

1.2 Some essentials of groups and classes

The structure of space can be defined via relations between points which goes back to Euclid. Any transformation, or rather mapping, of a point onto another point which does not change the structure of space is called automorphism, compare Section 1.1. For instance, recognising the wings of a butterfly to be essentially identical is one-to-one with stating that the corresponding reflection of each wing, with respect to the appropriate plane, is an automorphism. In the language of mathematics, automorphisms form a group, say \mathbb{G} ; see e.g. Alperin and Bell [AB95] for a general review or Cornwell [Cor69, Chap. 1] and Smith [Smi94, Chap. II] in view of an outline on group theory in the present context.

Let $\{\mathbf{G}_1, \mathbf{G}_2, \mathbf{G}_3, \dots, \mathbf{G}_g\}$ be the elements of the group \mathbb{G} . Then the following relations must hold

$$\left. \begin{array}{l} \text{(i)} \quad \mathbf{G}_k \in \mathbb{G} \quad \text{with} \quad \mathbf{G}_k = \mathbf{G}_i \circ \mathbf{G}_j \\ \text{(ii)} \quad \mathbf{I} \in \mathbb{G} \quad \text{with} \quad \mathbf{G}_i = \mathbf{I} \circ \mathbf{G}_i = \mathbf{G}_i \circ \mathbf{I} \\ \text{(iii)} \quad \mathbf{G}_i^{-1} \in \mathbb{G} \quad \text{with} \quad \mathbf{I} = \mathbf{G}_i \circ \mathbf{G}_i^{-1} = \mathbf{G}_i^{-1} \circ \mathbf{G}_i \end{array} \right\} \forall \mathbf{G}_i, \mathbf{G}_j \in \mathbb{G} \quad (1.10)$$

whereby \circ represents an associative combination $\mathbf{G}_i \circ [\mathbf{G}_j \circ \mathbf{G}_k] = [\mathbf{G}_i \circ \mathbf{G}_j] \circ \mathbf{G}_k$; concerning matrices, \circ usually characterises multiplication. The group \mathbb{G} is called Abelian if \circ is additionally commutative, $\mathbf{G}_i \circ \mathbf{G}_j = \mathbf{G}_j \circ \mathbf{G}_i$, and finite if its order g is finite. As a typical example, the set of integers $\{\dots, -n, \dots, -1, 1, \dots, n, \dots\}$ forms an infinite Abelian group whereby \circ complies to addition.

A set of elements of \mathbb{G} forms a subgroup ${}^{\text{sub}}\mathbb{G}$ if conditions (1.10) are fulfilled and is denoted as proper subgroup for $1 < {}^{\text{sub}}g < g$ and otherwise as improper. A set of elements of \mathbb{G} , say ${}^{\text{gen}}\mathbb{G}$, is a system of generators of \mathbb{G} if any $\mathbf{G}_i \in \mathbb{G}$ can be constructed as a combination of the elements of ${}^{\text{gen}}\mathbb{G}$ and the inverse elements of ${}^{\text{gen}}\mathbb{G}$.

Example 1.1 A group is a point group if at least one point remains unchanged under the action of all elements of the group which are rotations and reflections, respectively. A typical and simple example (e.g. the molecules CHCl_3 or CH_3CCl_3), among the infinite number of subgroups of the orthogonal group, is given by

$$C_{3v} = \{\mathbf{I}, \text{rot } \mathbf{R}(\frac{2\pi}{3} \mathbf{n}), \text{rot } \mathbf{R}(\frac{4\pi}{3} \mathbf{n}), \text{ref } \mathbf{R}(\mathbf{m}_1), \text{ref } \mathbf{R}(\mathbf{m}_2), \text{ref } \mathbf{R}(\mathbf{m}_3)\}. \quad (1.11)$$

We thereby have agreed to an isomorphic relation between the symmetry transformations and a faithful matrix representation since $\text{rot } \mathbf{R}(\theta[\bullet])$ and $\text{ref } \mathbf{R}([\bullet])$ are assumed to denote rotations and reflections – compare Eq.(2.19) – with respect to an orthonormal frame $\mathbf{e}_{1,2,3}$ for $\mathbf{n} \doteq \mathbf{e}_3$, $\mathbf{m}_1 \doteq \mathbf{e}_1$, $\mathbf{m}_2 \doteq \text{rot } \mathbf{R}(-\pi/6 \mathbf{n}) \cdot \mathbf{e}_1$ and $\mathbf{m}_3 \doteq \text{rot } \mathbf{R}(\pi/6 \mathbf{n}) \cdot \mathbf{e}_1$, respectively. Consequently, the associative combination \circ can be replaced by the symbol \cdot , which indicates ordinary tensor multiplication. Moreover, we have chosen the classical Schönflies notation to indicate the considered group; see any standard textbook on crystallography, e.g. Juretschke [Jur74]. The corresponding multiplication table reads

C_{3v}	\mathbf{I}	$\text{rot } \mathbf{R}(\frac{2\pi}{3} \mathbf{n})$	$\text{rot } \mathbf{R}(\frac{4\pi}{3} \mathbf{n})$	$\text{ref } \mathbf{R}(\mathbf{m}_1)$	$\text{ref } \mathbf{R}(\mathbf{m}_2)$	$\text{ref } \mathbf{R}(\mathbf{m}_3)$
\mathbf{I}	\mathbf{I}	$\text{rot } \mathbf{R}(\frac{2\pi}{3} \mathbf{n})$	$\text{rot } \mathbf{R}(\frac{4\pi}{3} \mathbf{n})$	$\text{ref } \mathbf{R}(\mathbf{m}_1)$	$\text{ref } \mathbf{R}(\mathbf{m}_2)$	$\text{ref } \mathbf{R}(\mathbf{m}_3)$
$\text{rot } \mathbf{R}(\frac{2\pi}{3} \mathbf{n})$	$\text{rot } \mathbf{R}(\frac{2\pi}{3} \mathbf{n})$	$\text{rot } \mathbf{R}(\frac{4\pi}{3} \mathbf{n})$	\mathbf{I}	$\text{ref } \mathbf{R}(\mathbf{m}_3)$	$\text{ref } \mathbf{R}(\mathbf{m}_1)$	$\text{ref } \mathbf{R}(\mathbf{m}_3)$
$\text{rot } \mathbf{R}(\frac{4\pi}{3} \mathbf{n})$	$\text{rot } \mathbf{R}(\frac{4\pi}{3} \mathbf{n})$	\mathbf{I}	$\text{rot } \mathbf{R}(\frac{2\pi}{3} \mathbf{n})$	$\text{ref } \mathbf{R}(\mathbf{m}_2)$	$\text{ref } \mathbf{R}(\mathbf{m}_3)$	$\text{ref } \mathbf{R}(\mathbf{m}_1)$
$\text{ref } \mathbf{R}(\mathbf{m}_1)$	$\text{ref } \mathbf{R}(\mathbf{m}_1)$	$\text{ref } \mathbf{R}(\mathbf{m}_2)$	$\text{ref } \mathbf{R}(\mathbf{m}_3)$	\mathbf{I}	$\text{rot } \mathbf{R}(\frac{2\pi}{3} \mathbf{n})$	$\text{rot } \mathbf{R}(\frac{4\pi}{3} \mathbf{n})$
$\text{ref } \mathbf{R}(\mathbf{m}_2)$	$\text{ref } \mathbf{R}(\mathbf{m}_2)$	$\text{ref } \mathbf{R}(\mathbf{m}_3)$	$\text{ref } \mathbf{R}(\mathbf{m}_1)$	$\text{rot } \mathbf{R}(\frac{4\pi}{3} \mathbf{n})$	\mathbf{I}	$\text{rot } \mathbf{R}(\frac{2\pi}{3} \mathbf{n})$
$\text{ref } \mathbf{R}(\mathbf{m}_3)$	$\text{ref } \mathbf{R}(\mathbf{m}_2)$	$\text{ref } \mathbf{R}(\mathbf{m}_1)$	$\text{ref } \mathbf{R}(\mathbf{m}_2)$	$\text{rot } \mathbf{R}(\frac{2\pi}{3} \mathbf{n})$	$\text{rot } \mathbf{R}(\frac{4\pi}{3} \mathbf{n})$	\mathbf{I}

and highlights the non-Abelian character. Applying this table, one easily verifies the relations

$$\begin{aligned} \text{rot } \mathbf{R}^3 \left(\frac{2\pi}{3} \mathbf{n} \right) &= \mathbf{I}, & \text{rot } \mathbf{R}^2 \left(\frac{2\pi}{3} \mathbf{n} \right) \cdot \text{ref } \mathbf{R}(\mathbf{m}_1) &= \text{ref } \mathbf{R}(\mathbf{m}_2), \\ \text{rot } \mathbf{R}^{-1} \left(\frac{2\pi}{3} \mathbf{n} \right) &= \text{rot } \mathbf{R} \left(\frac{4\pi}{3} \mathbf{n} \right), & \text{rot } \mathbf{R} \left(\frac{2\pi}{3} \mathbf{n} \right) \cdot \text{ref } \mathbf{R}(\mathbf{m}_1) &= \text{ref } \mathbf{R}(\mathbf{m}_3) \end{aligned} \quad (1.13)$$

and thus the set of generators reads

$$\text{gen } C_{3v} = \{ \text{rot } \mathbf{R} \left(\frac{2\pi}{3} \mathbf{n} \right), \text{ref } \mathbf{R}(\mathbf{m}_1) \}. \quad (1.14)$$

Moreover, we have four proper subgroups of C_{3v} , e.g. $C_3 = \{ \mathbf{I}, \text{rot } \mathbf{R} \left(\frac{2\pi}{3} \mathbf{n} \right), \text{rot } \mathbf{R} \left(\frac{4\pi}{3} \mathbf{n} \right) \}$ with the cyclic properties $\text{rot } \mathbf{R}^2 \left(\frac{2\pi}{3} \mathbf{n} \right) = \text{rot } \mathbf{R} \left(\frac{4\pi}{3} \mathbf{n} \right)$ and $\text{rot } \mathbf{R}^3 \left(\frac{2\pi}{3} \mathbf{n} \right) = \mathbf{I}$ and consequently $\text{gen } C_3 = \{ \text{rot } \mathbf{R} \left(\frac{2\pi}{3} \mathbf{n} \right) \}$.

Next, leaving the abstract representation of point groups behind, recall that these symmetries are permanently present in daily life, see e.g. Weyl [Wey52] for a survey on applications of symmetry. In this context, Figure 1.1 highlights point symmetries in a typical artwork by M.C. Escher and of an Ethiopian vegetable (okra). A likely candidate to find such symmetries in music is “Die Kunst der

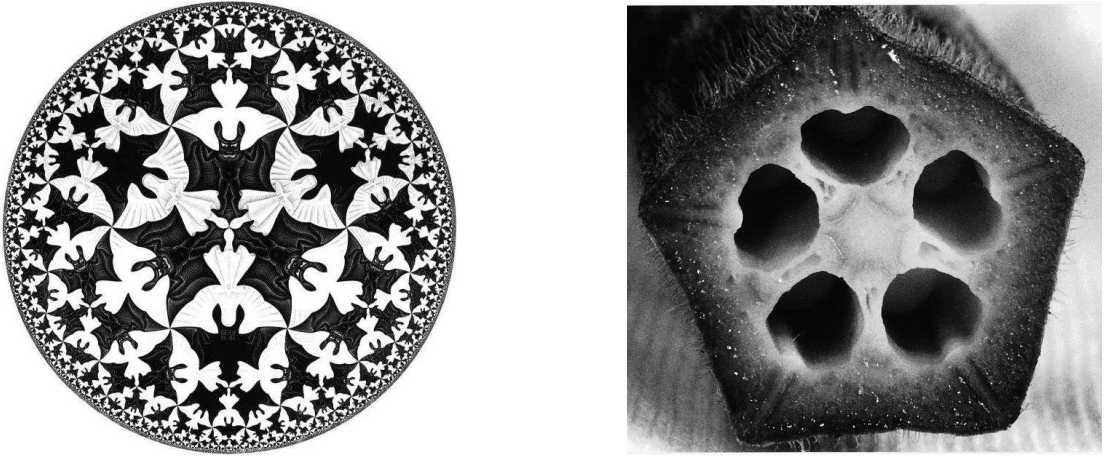


Figure 1.1: Point groups: C_{3v} (M.C. Escher: “Circle Limit IV”, taken from S. Singh: *Fermat’s Last Theorem*, Fourth Estate, 1997) and C_{5v} (okra).

Fuge” by J.S. Bach [Bac56]. Figures 1.2 and 1.3 give only two examples of such symmetries (reflections). Impressively, the complete “polyphone Satz” in *Contrapunctus 12* and *13* is based on a horizontal reflection plane.

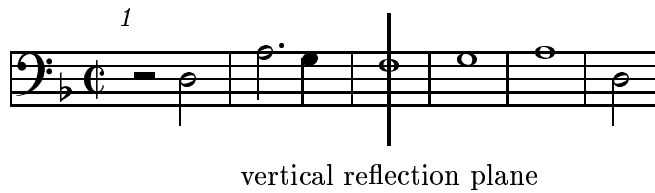


Figure 1.2: J.S. Bach: “Die Kunst der Fuge”, vertical reflection in *Contrapunctus 18*.

An element \mathbf{A} is conjugate to an element \mathbf{B} with respect to, say, \mathbf{G} if the relation

$$\boxed{\mathbf{A} = \mathbf{G} \circ \mathbf{B} \circ \mathbf{G}^{-1}} \quad (1.15)$$

holds. Likewise, \mathbf{B} is obviously conjugate to \mathbf{A} ; $\mathbf{B} = \mathbf{G}^{-1} \circ \mathbf{A} \circ [\mathbf{G}^{-1}]^{-1}$. Now let \mathbf{G} run through all elements of the group \mathbb{G} . With this procedure, we construct the class of elements conjugate to \mathbf{B} .

Example 1.2 In view of the previously discussed symmetry group C_{3v} , we compute

$$\begin{aligned} \{ [\mathbf{I}, \text{rot } \mathbf{R} \left(\frac{2\pi}{3} \mathbf{n} \right), \dots] \cdot \mathbf{I} \cdot [\mathbf{I}, \text{rot } \mathbf{R} \left(\frac{2\pi}{3} \mathbf{n} \right), \dots]^{-1} \} &= \{ \mathbf{I} \} \\ \{ [\mathbf{I}, \text{rot } \mathbf{R} \left(\frac{2\pi}{3} \mathbf{n} \right), \dots] \cdot \text{rot } \mathbf{R} \left(\frac{2\pi}{3} \mathbf{n}, \frac{4\pi}{3} \mathbf{n} \right) \cdot [\mathbf{I}, \text{rot } \mathbf{R} \left(\frac{2\pi}{3} \mathbf{n} \right), \dots]^{-1} \} &= \{ \text{rot } \mathbf{R} \left(\frac{2\pi}{3} \mathbf{n}, \frac{4\pi}{3} \mathbf{n} \right) \} \\ \{ [\mathbf{I}, \text{rot } \mathbf{R} \left(\frac{2\pi}{3} \mathbf{n} \right), \dots] \cdot \text{ref } \mathbf{R}(\mathbf{m}_{1,2,3}) \cdot [\mathbf{I}, \text{rot } \mathbf{R} \left(\frac{2\pi}{3} \mathbf{n} \right), \dots]^{-1} \} &= \{ \text{ref } \mathbf{R}(\mathbf{m}_{1,2,3}) \} \end{aligned} \quad (1.16)$$

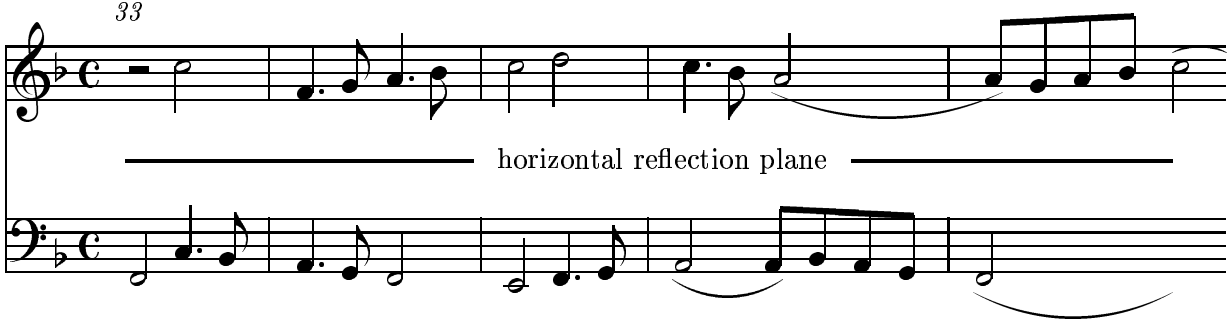


Figure 1.3: J.S. Bach: “Die Kunst der Fuge”, horizontal reflection in Contrapunctus 5.

and thus obtain the three classes which separately collect the identity, rotations and reflections

$$C_{3v} = \{I\} + \{\text{rot } \mathbf{R}(\frac{2\pi}{3} \mathbf{n}), \text{rot } \mathbf{R}(\frac{4\pi}{3} \mathbf{n})\} + \{\text{ref } \mathbf{R}(\mathbf{m}_1), \text{ref } \mathbf{R}(\mathbf{m}_2), \text{ref } \mathbf{R}(\mathbf{m}_3)\}. \quad (1.17)$$

Paying attention to the type of transformation as given in Eq.(1.2), we see that in addition to those transformation associated with elements of point groups, a vector (translation) is additionally incorporated. A set of such symmetry operations, which includes the primitive case of pure translations is called space group if conditions (1.10) are satisfied. The usual abbreviated notation in view of Eq.(1.7) reads as

$$\boxed{\mathbf{X}' = \mathbf{Q} \cdot \mathbf{X} + \mathbf{c} \doteq \{\mathbf{Q}|\mathbf{c}\} \mathbf{X}}, \quad (1.18)$$

and allows usual operations like inversion, etc.

$$\{\mathbf{Q}|\mathbf{c}\}^{-1} \{\mathbf{Q}|\mathbf{c}\} \mathbf{X} = \{I|\mathbf{0}\} \mathbf{X} = \mathbf{X} \implies \{\mathbf{Q}|\mathbf{c}\}^{-1} = \{\mathbf{Q}^{-1} | -\mathbf{Q}^{-1} \cdot \mathbf{c}\}, \quad (1.19)$$

see e.g. Sands [San95, Chap. 4] for more background information. Next, with emphasis on applications in material science, we focus on crystals which generally allow interpretation as arrangements of atoms in patterns that are periodically repeated in the three-dimensional space. Choosing any arbitrary point in such a pattern and identifying all other points that are translatory identical to the chosen one, we obtain a set of lattice points. With this set at hand, the points can be connected by parallelepipeds which define the unit cell of the underlying structure[¶]. The space of a unit cell is spanned by three non-coplanar vectors, namely the lattice vectors. In the following, this basis is denoted as \mathbf{a}_i characterising the set

$$\mathbf{t}_n = \sum_{i=1}^3 n^i \mathbf{a}_i \quad (1.20)$$

with $n^{1,2,3}$ obviously being integers, see e.g. Šilhavý [Šil97, Sect. 1.5]. Next, based on Eq.(1.18), the construction of the conjugate element to a primitive lattice translation with respect to a symmetry operation of the underlying group, say $\{\mathbf{Q}|\mathbf{c}\}$, yields

$$\begin{aligned} \{\mathbf{Q}|\mathbf{c}\} \{I|\mathbf{t}_n\} \{\mathbf{Q}|\mathbf{c}\}^{-1} &= \{\mathbf{Q}|\mathbf{c}\} \{I|\mathbf{t}_n\} \{\mathbf{Q}^{-1} | -\mathbf{Q}^{-1} \cdot \mathbf{c}\} \\ &= \{\mathbf{Q}|\mathbf{c}\} \{\mathbf{Q}^{-1} | \mathbf{t}_n - \mathbf{Q}^{-1} \cdot \mathbf{c}\} \\ &= \{I|\mathbf{Q} \cdot \mathbf{t}_n\} \end{aligned} \quad (1.21)$$

which is nothing but a primitive lattice translation characterising the periodicity, compare Eq.(1.15). Recall that this operation has to be an element of the corresponding symmetry group and thus the relation

$$\mathbf{Q} \cdot \mathbf{t}_n = [\mathbf{Q}^i_j \mathbf{a}_i \otimes \mathbf{a}^j] \cdot [n^k \mathbf{a}_k] = Q^i_j n^j \mathbf{a}_i = m^i \mathbf{a}_i = \mathbf{t}_m \quad (1.22)$$

must be fulfilled. Therefore, the coefficients Q^i_j are forced to be integers since n^k and m^i are integers. Consequently, the trace of the symmetry operation $\text{tr}(\mathbf{Q})$, must also be an integer. In this context, we consider the characteristic polynomial

$${}^Q \lambda^3 - \text{tr}(\mathbf{Q}) {}^Q \lambda^2 + \frac{1}{2} [\text{tr}^2(\mathbf{Q}) - \text{tr}(\mathbf{Q}^2)] {}^Q \lambda - \det(\mathbf{Q}) = 0 \quad (1.23)$$

[¶]Generally, unit cells or even primitive cells may have a much more involved geometry compared to the crystalline case, see e.g. the artwork of M.C. Escher for graphical representations.

with $\text{tr}(\mathbf{Q}) = \mathcal{Q}\lambda_1 + \mathcal{Q}\lambda_2 + \mathcal{Q}\lambda_3$, $\text{tr}(\mathbf{Q}^2) = \mathcal{Q}\lambda_1^2 + \mathcal{Q}\lambda_2^2 + \mathcal{Q}\lambda_3^2$, $\det(\mathbf{Q}) = \mathcal{Q}\lambda_1 \mathcal{Q}\lambda_2 \mathcal{Q}\lambda_3$ and $\mathcal{Q}\lambda_{1,2,3}$ characterising the eigenvalues of \mathbf{Q} . Making use of the orthogonality, $\det(\mathbf{Q}) = \pm 1$ for the proper and improper case, one easily verifies that $\mathcal{Q}\lambda_1 = \pm 1$ satisfies Eq.(1.23) if $\mathcal{Q}\lambda_2 \mathcal{Q}\lambda_3 = \pm 1$ or $\mathcal{Q}\lambda_2 \mathcal{Q}\lambda_3 = \mp 1$. In accordance with the area preserving restriction $\mathcal{Q}\lambda_1 \mathcal{Q}\lambda_2 \mathcal{Q}\lambda_3 = \pm 1$ we obtained two complex conjugate eigenvalues $\mathcal{Q}\lambda_{2,3}$ lying on the unit circle, compare e.g. Smith [Smi71b] or Arnold [Arn95, Sect. 28.2]. Denoting the corresponding angle by $\theta \in (0, 2\pi]$, we end up with

$$\text{tr}(\mathbf{Q}) = \pm 1 + 2 \cos(\theta) \implies \theta = \{n^{-1}2\pi \mid n = 1, 2, 3, 4, 6\}, \quad (1.24)$$

see e.g. Sands [San93, Sect. 3–4] for a geometrical proof. Note that a symmetry operation which does not satisfy this severe restriction is not allowed in any lattice structure, which is in strong contrast to molecules where almost all point groups are allowed. To give an example, the group C_{5v} , visualised in Figure 1.1, is especially excluded.

A crystal class collects space groups that incorporate identical point groups. It turns out that only 32 crystallographic finite point groups exist, see e.g. Schouten [Sch89, Sect. VII.5], Sternberg [Ste94, Chap. 1] for a graphical visualisation of these groups, Cornwell [Cor69, App. 3] where the appropriate space groups within each class are additionally highlighted or any other standard textbook on crystallography. Furthermore, when taking electromagnetic effects into account, we refer to Kiral and Eringen [KE90, Chap. 3] for a detailed outline on the 90 crystallographic magnetic finite point groups. Nevertheless, we have only 14 space-filling infinite lattice types, namely the Bravais lattices,

$$\begin{aligned} \Gamma_t &: \text{any non-coplanar combination of } \mathbf{a}_{1,2,3} \\ \Gamma_m &: \mathbf{a}_3 \perp \mathbf{a}_{1,2} \\ \Gamma_m^b &: \mathbf{a}_1 = \alpha \mathbf{e}_1 + \beta \mathbf{e}_2 & \mathbf{a}_2 = \alpha \mathbf{e}_1 - \beta \mathbf{e}_2 & \mathbf{a}_3 = \gamma \mathbf{e}_1 + \delta \mathbf{e}_3 \\ \Gamma_o &: \mathbf{a}_1 = \alpha \mathbf{e}_1 & \mathbf{a}_2 = \beta \mathbf{e}_2 & \mathbf{a}_3 = \gamma \mathbf{e}_3 \\ \Gamma_o^b &: \mathbf{a}_1 = \alpha \mathbf{e}_1 + \beta \mathbf{e}_2 & \mathbf{a}_2 = \alpha \mathbf{e}_1 - \beta \mathbf{e}_2 & \mathbf{a}_3 = \gamma \mathbf{e}_3 \\ \Gamma_o^v &: \mathbf{a}_1 = \alpha \mathbf{e}_1 + \beta \mathbf{e}_2 + \gamma \mathbf{e}_3 & \mathbf{a}_2 = \alpha \mathbf{e}_1 + \beta \mathbf{e}_2 - \gamma \mathbf{e}_3 & \mathbf{a}_3 = \alpha \mathbf{e}_1 - \beta \mathbf{e}_2 - \gamma \mathbf{e}_3 \\ \Gamma_o^f &: \mathbf{a}_1 = \alpha \mathbf{e}_1 + \beta \mathbf{e}_2 & \mathbf{a}_2 = \beta \mathbf{e}_2 + \gamma \mathbf{e}_3 & \mathbf{a}_3 = \alpha \mathbf{e}_1 + \gamma \mathbf{e}_3 \\ \Gamma_q &: \mathbf{a}_1 = \alpha \mathbf{e}_1 & \mathbf{a}_2 = \alpha \mathbf{e}_2 & \mathbf{a}_3 = \beta \mathbf{e}_3 \\ \Gamma_q^v &: \mathbf{a}_1 = \alpha \mathbf{e}_1 + \alpha \mathbf{e}_2 + \beta \mathbf{e}_3 & \mathbf{a}_2 = \alpha \mathbf{e}_1 + \alpha \mathbf{e}_2 - \beta \mathbf{e}_3 & \mathbf{a}_3 = \alpha \mathbf{e}_1 - \alpha \mathbf{e}_2 + \beta \mathbf{e}_3 \\ \Gamma_c &: \mathbf{a}_1 = \alpha \mathbf{e}_1 & \mathbf{a}_2 = \alpha \mathbf{e}_2 & \mathbf{a}_3 = \alpha \mathbf{e}_3 \\ \Gamma_c^v &: \mathbf{a}_1 = \frac{\alpha}{2} \mathbf{e}_1 + \frac{\alpha}{2} \mathbf{e}_2 + \frac{\alpha}{2} \mathbf{e}_3 & \mathbf{a}_2 = \frac{\alpha}{2} \mathbf{e}_1 + \frac{\alpha}{2} \mathbf{e}_2 - \frac{\alpha}{2} \mathbf{e}_3 & \mathbf{a}_3 = \frac{\alpha}{2} \mathbf{e}_1 - \frac{\alpha}{2} \mathbf{e}_2 - \frac{\alpha}{2} \mathbf{e}_3 \\ \Gamma_c^f &: \mathbf{a}_1 = \frac{\alpha}{2} \mathbf{e}_1 + \frac{\alpha}{2} \mathbf{e}_2 & \mathbf{a}_2 = \frac{\alpha}{2} \mathbf{e}_2 + \frac{\alpha}{2} \mathbf{e}_3 & \mathbf{a}_3 = \frac{\alpha}{2} \mathbf{e}_1 + \frac{\alpha}{2} \mathbf{e}_3 \\ \Gamma_{rh} &: \mathbf{a}_1 = \alpha \mathbf{e}_1 + \beta \mathbf{e}_3 & \mathbf{a}_2 = \frac{\sqrt{3}\alpha}{2} \mathbf{e}_1 - \frac{\alpha}{2} \mathbf{e}_2 + \beta \mathbf{e}_3 & \mathbf{a}_3 = \frac{-\sqrt{3}\alpha}{2} \mathbf{e}_1 - \frac{\alpha}{2} \mathbf{e}_2 + \beta \mathbf{e}_3 \\ \Gamma_h &: \mathbf{a}_1 = \gamma \mathbf{e}_3 & \mathbf{a}_2 = \alpha \mathbf{e}_1 & \mathbf{a}_3 = \frac{-\alpha}{2} \mathbf{e}_1 - \frac{\sqrt{3}\alpha}{2} \mathbf{e}_2 \end{aligned} \quad (1.25)$$

with $\alpha, \beta, \gamma, \delta \in \mathbb{R}_+$, see e.g. Sands [San93, Chap. 3]. There are seven symmetry systems which collect Bravais lattices associated with the order of their principal axis

$$\begin{aligned} & \text{triclinic } (\Gamma_t) & \text{cubic } (\Gamma_c, \Gamma_c^v, \Gamma_c^f) \\ & \text{monoclinic } (\Gamma_m, \Gamma_m^b) & \text{rhombohedral } (\Gamma_{rh}) \\ & \text{orthorhombic } (\Gamma_o, \Gamma_o^b, \Gamma_o^v, \Gamma_o^f) & \text{hexagonal } (\Gamma_h) \\ & \text{tetragonal } (\Gamma_q, \Gamma_q^v) \end{aligned} \quad (1.26)$$

whereby the triclinic (C_i, C_1), monoclinic (C_{2h}, C_2, C_s), rhombohedral – or trigonal – ($D_{3d}, C_3, C_{3v}, D_3, S_6$), tetragonal ($D_{4h}, D_{2d}, S_4, C_4, C_{4h}, D_4, C_{4v}$) and hexagonal ($D_{6h}, C_3, C_{3v}, D_3, S_6, D_{3h}, D_{3h}$,

C_6, C_{6h}, C_{6v}, D_6) systems incorporate a single principal axis of order 1, 2, 3, 4, 6, respectively. Contrary, three mutually orthogonal rotation axis of order 2 are described within an orthorhombic symmetry (D_{2h}, C_{2v}, D_2) and, finally, a cubic system incorporates four rotation axis of order 3 with orientations towards the vertices of a regular tetrahedron.

Remark 1.1 *The orthogonal group has an infinite number of subgroups associated with non-crystalline solids. We specifically deal with isotropic, transversely isotropic, icosahedral or non-crystal dihedral symmetries. These systems are usually characterised in Schönflies – or Hermann–Mauguin symbols, see any standard textbook on crystallography, e.g. Juretschke [Jur74]). A special role is due to the state between a crystal and a liquid with a quasi-periodic lattice structure, called quasi-crystal. Interestingly, an infinite number of symmetry groups is observed for these materials – including classes that are not embodied in the 32 crystallographic finite point groups, see e.g. Levine and Steinhardt [LS84] or Bruhns et al. [BXM99] where special emphasis on the construction of appropriate yield functions is placed.*

As advocated by Smith and Rivlin [SR58] the symmetry operation according to the 32 crystallographic finite point groups allows for a matrix representation, which is essentially based on the previously mentioned homomorphic relation between the symmetry operations of interest and matrix operations. It turns out that a set of 15 square matrices is obtained. The corresponding coefficients read as

$$\begin{aligned}
 I^{ij} &= \text{Diag}(1 \ 1 \ 1) & \bar{I}^{ij} &= \text{Diag}(-1 \ -1 \ -1) \\
 R_1^{ij} &= \text{Diag}(-1 \ 1 \ 1) & R_2^{ij} &= \text{Diag}(1 \ -1 \ 1) & R_3^{ij} &= \text{Diag}(1 \ 1 \ -1) \\
 D_1^{ij} &= \text{Diag}(1 \ -1 \ -1) & D_2^{ij} &= \text{Diag}(-1 \ 1 \ -1) & D_3^{ij} &= \text{Diag}(-1 \ -1 \ 1) \\
 T_1^{ij} &= \begin{bmatrix} 1 & 0 & 0 \\ 0 & 0 & 1 \\ 0 & 1 & 0 \end{bmatrix} & T_2^{ij} &= \begin{bmatrix} 0 & 0 & 1 \\ 0 & 1 & 0 \\ 1 & 0 & 0 \end{bmatrix} & T_3^{ij} &= \begin{bmatrix} 0 & 1 & 0 \\ 1 & 0 & 0 \\ 0 & 0 & 1 \end{bmatrix} \\
 M_1^{ij} &= \begin{bmatrix} 0 & 1 & 0 \\ 0 & 0 & 1 \\ 1 & 0 & 0 \end{bmatrix} & M_2^{ij} &= \begin{bmatrix} 0 & 0 & 1 \\ 1 & 0 & 0 \\ 0 & 1 & 0 \end{bmatrix} \\
 S_1^{ij} &= \begin{bmatrix} -\frac{1}{2} & \frac{\sqrt{3}}{2} & 0 \\ -\frac{\sqrt{3}}{2} & -\frac{1}{2} & 0 \\ 0 & 0 & 1 \end{bmatrix} & S_2^{ij} &= \begin{bmatrix} -\frac{1}{2} & -\frac{\sqrt{3}}{2} & 0 \\ \frac{\sqrt{3}}{2} & \frac{1}{2} & 0 \\ 0 & 0 & 1 \end{bmatrix}
 \end{aligned} \tag{1.27}$$

whereby \mathbf{I} denotes the second order identity and $\bar{\mathbf{I}}$ central inversion. Moreover, let $\mathbf{n}_{1,2,3}$ be unit-vectors co-linear to $\mathbf{a}_{1,2,3}$. Then the abbreviated notations $\mathbf{R}_{1,2,3}$ characterise reflections with respect to planes defined by the normal vectors $\mathbf{n}_{1,2,3}$, respectively. Similarly $\mathbf{D}_{1,2,3}$ represent rotations with axis $\mathbf{n}_{1,2,3}$ and angle $\theta = \pi$. The operation associated with $\mathbf{T}_{i=1,2,3}$ corresponds to a reflection in the plane through \mathbf{n}_i bisecting the other axis $\mathbf{n}_{j,k}$, $j = 1, 2, 3 \wedge \neq i$, $k = 1, 2, 3 \wedge \neq i \wedge \neq j$. The rotations \mathbf{M}_i share the same axis $[\mathbf{n}_1 + \mathbf{n}_2 + \mathbf{n}_3]/\sqrt{3}$ and incorporate the angles $\theta_i = \frac{2}{3}i\pi$. Finally, $\mathbf{S}_{1,2}$ are rotations with identical angles compared to $\mathbf{M}_{1,2}$ but with respect to the rotation axis \mathbf{n}_3 . For a comprehensive Table of the 32 crystalline finite point groups including the operations highlighted in (1.27) we refer to Rivlin [Riv66] and Şuhubi [Şuh75, Sect. 2.10].

Summarising, a crystal is represented by repeating a unit cell numerous times with respect to three non-planar translations. The admissible space groups are defined by the 32 crystallographic point groups and the 14 Bravais lattices, at least in the non-magnetic case. In addition, we have further symmetry elements, which are actually combinations of rotations of reflections and translatory symmetry, and that are skew axis and glide planes. Thereby, the operation due to a skew axis is characterised by a rotation and a translation with respect to the axis of the rotation. The coupling of a reflection and a translation is established as a glide plane operation. Finally, by combining these symmetry transformations and the 32 crystallographic point groups, one ends up with 230 admissible infinite space groups, see e.g. Sands [San93, App. 1] for a comprehensive table.

Example 1.3 Once more “Die Kunst der Fuge” by J.S. Bach [Bac56] is a likely candidate to find applications for space groups. The trivial case is given by one-dimensional translation where the rotational part boils down to the identity. In the language of music, this specific symmetry is nothing else but the concept of rhythm, compare Figure 1.4 for an image of this idea.

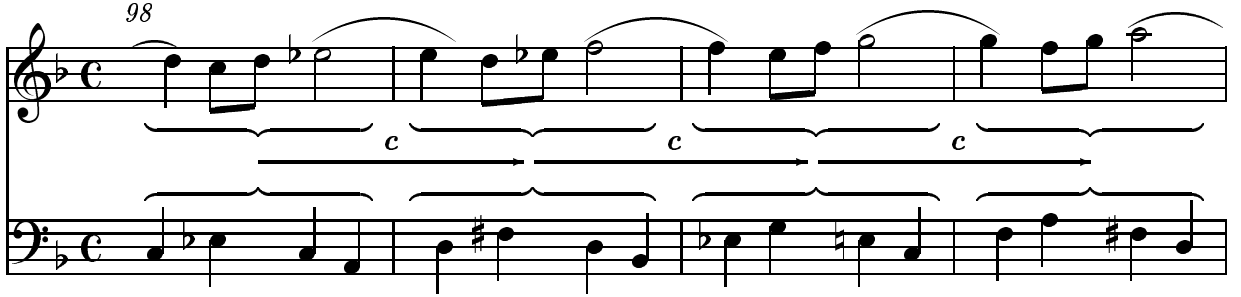


Figure 1.4: J.S. Bach: “Die Kunst der Fuge”, the concept of rhythm in Contrapunctus 4.

1.3 Constitutive functions

In the sequel, we adopt the framework that the stress tensor is derivable from a scalar-valued function $\psi_0 \in \mathbb{R}$ (established as strain energy density) in terms of the right Cauchy–Green tensor $\mathbf{C}(\mathbf{X}, t)$ which is invariant with respect to specific symmetry transformations represented by $\mathbb{G} = \{\mathbf{G}_{1,\dots,g}; \mathbf{X}\}$. Moreover, let ψ_0 be defined by a set of real quantities $I_{1,\dots,n}(\mathbf{C}(\mathbf{X}, t); \mathbf{X})$ which is consequently claimed to remain invariant under the action of $\mathbf{G}_{1,\dots,g}$. The set $I_{1,\dots,n}(\mathbf{C}(\mathbf{X}, t); \mathbf{X})$ is called functional basis if $I_{1,\dots,n}(\mathbf{C}(\mathbf{X}, t); \mathbf{X}) = c_{1,\dots,n}$ has one, but only one set of solutions $\mathbf{C} = \mathbf{G}_{1,\dots,g} \star \mathbf{C}$ whereby the notation \star represents the linear operator and $c_{1,\dots,n}$ denotes an admissible set of constants. For this case, the strain energy density is obviously defined by the functional basis $I_{1,\dots,n}(\mathbf{C}(\mathbf{X}, t); \mathbf{X})$.

Next, without loss of generality, we additionally represent the right Cauchy–Green tensor in terms of the components $C_{ij}(\mathbf{X}, t) = \mathbf{e}_i \cdot \mathbf{C}(\mathbf{X}, t) \cdot \mathbf{e}_j \in \mathbb{R}^6$, whereby $\mathbf{e}_i \in \mathbb{R}^3$ define a, e.g., Cartesian frame, and obtain

$$\boxed{\begin{aligned} \psi_0 &\doteq \psi_0(\mathbf{C}(\mathbf{X}, t); \mathbf{X}) = \psi_0(I_{1,\dots,n}(\mathbf{C}(\mathbf{X}, t); \mathbf{X})) \\ &\doteq \psi_0(C_{ij}(\mathbf{X}, t); \mathbf{X}) = \psi_0(I_{1,\dots,n}(C_{ij}(\mathbf{X}, t); \mathbf{X})) \end{aligned}} \quad (1.28)$$

Alternatively, the strain energy function allows notation in the format of a series expansion relative to the second order identity $\mathbf{I} \in \mathbb{S}_+^3$, namely

$$\begin{aligned} \psi_0(\mathbf{C}(\mathbf{X}, t); \mathbf{X}) &= \psi_0(\mathbf{C}; \mathbf{X}) \Big|_{\mathbf{C}=\mathbf{I}} \\ &+ \partial_{\mathbf{C}} \psi_0(\mathbf{C}; \mathbf{X}) \Big|_{\mathbf{C}=\mathbf{I}} : [\mathbf{C} - \mathbf{I}] \\ &+ \frac{1}{2!} \partial_{\mathbf{C} \otimes \mathbf{C}}^2 \psi_0(\mathbf{C}; \mathbf{X}) \Big|_{\mathbf{C}=\mathbf{I}} :: [[\mathbf{C} - \mathbf{I}] \otimes [\mathbf{C} - \mathbf{I}]] \\ &+ \frac{1}{3!} \partial_{\mathbf{C} \otimes \mathbf{C} \otimes \mathbf{C}}^3 \psi_0(\mathbf{C}; \mathbf{X}) \Big|_{\mathbf{C}=\mathbf{I}} ::: [[\mathbf{C} - \mathbf{I}] \otimes [\mathbf{C} - \mathbf{I}] \otimes [\mathbf{C} - \mathbf{I}]] \\ &+ \dots \quad , \end{aligned} \quad (1.29)$$

by agreeing to the common request $\psi_0(\mathbf{C}(\mathbf{X}, t); \mathbf{X})|_{\mathbf{C}=\mathbf{I}} = 0$.

The overall constitutive equation for the stress tensor reads as

$$\boxed{\mathbf{S}(\mathbf{C}(\mathbf{X}, t); \mathbf{X}) \doteq 2 \partial_{\mathbf{C}} \psi_0(\mathbf{C}(\mathbf{X}, t); \mathbf{X}) = \sum_{i=1}^n 2 \partial_{I_i} \psi_0(\mathbf{C}(\mathbf{X}, t); \mathbf{X}) \boldsymbol{\Xi}_i(\mathbf{C}(\mathbf{X}, t); \mathbf{X})} \quad (1.30)$$

with $\mathbf{S}(\mathbf{C}(\mathbf{X}, t); \mathbf{X}) \in \mathbb{S}^3$, $\boldsymbol{\Xi}_i(\mathbf{C}(\mathbf{X}, t); \mathbf{X}) = \partial_{\mathbf{C}} I_i(\mathbf{C}(\mathbf{X}, t); \mathbf{X}) \in \mathbb{S}^3$. Note that $\boldsymbol{\Xi}_i(\mathbf{C}(\mathbf{X}, t); \mathbf{X})$ are obviously independent of $\psi_0(\mathbf{C}(\mathbf{X}, t); \mathbf{X})$ but rather defined by the corresponding symmetry type of

the material, $\mathbf{G}_{1,\dots,g\star} \Xi_i(\mathbf{C}(\mathbf{X}, t); \mathbf{X}) = \Xi_i(\mathbf{G}_{1,\dots,g\star} \mathbf{C}(\mathbf{X}, t); \mathbf{X})$. In view of the series expansion as given in Eq.(1.29) we obtain

$$\begin{aligned} \mathbf{S}(\mathbf{C}(\mathbf{X}, t); \mathbf{X}) &= 2 \quad \partial_{\mathbf{C}} \psi_0(\mathbf{C}; \mathbf{X}) \Big|_{\mathbf{C}=\mathbf{I}} \\ &+ \frac{4}{2!} \quad \partial_{\mathbf{C} \otimes \mathbf{C}}^2 \psi_0(\mathbf{C}; \mathbf{X}) \Big|_{\mathbf{C}=\mathbf{I}} : [\mathbf{C} - \mathbf{I}] \\ &+ \frac{6}{3!} \quad \partial_{\mathbf{C} \otimes \mathbf{C} \otimes \mathbf{C}}^3 \psi_0(\mathbf{C}; \mathbf{X}) \Big|_{\mathbf{C}=\mathbf{I}} :: \left[[\mathbf{C} - \mathbf{I}] \otimes [\mathbf{C} - \mathbf{I}] \right] \\ &+ \frac{8}{4!} \quad \partial_{\mathbf{C} \otimes \mathbf{C} \otimes \mathbf{C} \otimes \mathbf{C}}^4 \psi_0(\mathbf{C}; \mathbf{X}) \Big|_{\mathbf{C}=\mathbf{I}} ::: \left[[\mathbf{C} - \mathbf{I}] \otimes [\mathbf{C} - \mathbf{I}] \otimes [\mathbf{C} - \mathbf{I}] \right] \\ &+ \quad \dots \quad . \end{aligned} \tag{1.31}$$

In order to satisfy the physically reasonable restriction $\mathbf{S}(\mathbf{C}(\mathbf{X}, t); \mathbf{X}) \Big|_{\mathbf{C}=\mathbf{I}} = \mathbf{0}$, one observes the constraint $\partial_{\mathbf{C}} \psi_0(\mathbf{C}(\mathbf{X}, t); \mathbf{X}) \Big|_{\mathbf{C}=\mathbf{I}} = \mathbf{0}$.

Moreover, the general format of the Hessian of the strain energy density with respect to $\mathbf{C}(\mathbf{X}, t)$ reads as

$$\begin{aligned} \mathbf{E}(\mathbf{C}(\mathbf{X}, t); \mathbf{X}) &= 4 \partial_{\mathbf{C} \otimes \mathbf{C}}^2 \psi_0(\mathbf{C}(\mathbf{X}, t); \mathbf{X}) \\ &= \sum_{i=1}^n 4 \quad \partial_{I_i} \psi_0(\mathbf{C}(\mathbf{X}, t); \mathbf{X}) \Xi_i(\mathbf{C}(\mathbf{X}, t); \mathbf{X}) \\ &+ \sum_{i,j=1}^n 4 \quad \partial_{I_i I_j}^2 \psi_0(\mathbf{C}(\mathbf{X}, t); \mathbf{X}) \Xi_i(\mathbf{C}(\mathbf{X}, t); \mathbf{X}) \otimes \Xi_j(\mathbf{C}(\mathbf{X}, t); \mathbf{X}) \end{aligned} \tag{1.32}$$

with $\mathbf{E}(\mathbf{C}(\mathbf{X}, t); \mathbf{X}) \in \mathbb{S}^{3 \times 3}$ and apparently $\Xi_i(\mathbf{C}(\mathbf{X}, t); \mathbf{X}) = \partial_{\mathbf{C} \otimes \mathbf{C}}^2 I_i(\mathbf{C}(\mathbf{X}, t); \mathbf{X}) \in \mathbb{S}^{3 \times 3}$, $\mathbf{G}_{1,\dots,g\star} \Xi_i(\mathbf{C}(\mathbf{X}, t); \mathbf{X}) = \Xi_i(\mathbf{G}_{1,\dots,g\star} \mathbf{C}(\mathbf{X}, t); \mathbf{X})$. Application of the series expansion naturally yields

$$\begin{aligned} \mathbf{E}(\mathbf{C}(\mathbf{X}, t); \mathbf{X}) &= \frac{8}{2!} \quad \partial_{\mathbf{C} \otimes \mathbf{C}}^2 \psi_0(\mathbf{C}; \mathbf{X}) \Big|_{\mathbf{C}=\mathbf{I}} \\ &+ \frac{12}{3!} \quad \partial_{\mathbf{C} \otimes \mathbf{C} \otimes \mathbf{C}}^3 \psi_0(\mathbf{C}; \mathbf{X}) \Big|_{\mathbf{C}=\mathbf{I}} : [\mathbf{C} - \mathbf{I}] \\ &+ \frac{16}{4!} \quad \partial_{\mathbf{C} \otimes \mathbf{C} \otimes \mathbf{C} \otimes \mathbf{C}}^4 \psi_0(\mathbf{C}; \mathbf{X}) \Big|_{\mathbf{C}=\mathbf{I}} :: \left[[\mathbf{C} - \mathbf{I}] \otimes [\mathbf{C} - \mathbf{I}] \right] \\ &+ \frac{20}{5!} \quad \partial_{\mathbf{C} \otimes \mathbf{C} \otimes \mathbf{C} \otimes \mathbf{C} \otimes \mathbf{C}}^5 \psi_0(\mathbf{C}; \mathbf{X}) \Big|_{\mathbf{C}=\mathbf{I}} ::: \left[[\mathbf{C} - \mathbf{I}] \otimes [\mathbf{C} - \mathbf{I}] \otimes [\mathbf{C} - \mathbf{I}] \right] \\ &+ \quad \dots \quad . \end{aligned} \tag{1.33}$$

However, if we assume a linear constitutive equation in the spirit that the stress tensor is computed by a linear map of an appropriate strain measure, we obtain Hooke's law

$$\begin{aligned} \mathbf{E}^{\text{lin}}(\mathbf{C}(\mathbf{X}, t); \mathbf{X}) &\doteq 4 \partial_{\mathbf{C} \otimes \mathbf{C}}^2 \psi_0(\mathbf{C}; \mathbf{X}) \Big|_{\mathbf{C}=\mathbf{I}}, \\ \mathbf{S}^{\text{lin}}(\mathbf{C}(\mathbf{X}, t); \mathbf{X}) &\doteq \frac{1}{2} \mathbf{E}^{\text{lin}} : [\mathbf{C} - \mathbf{I}], \\ \psi_0^{\text{lin}}(\mathbf{C}(\mathbf{X}, t); \mathbf{X}) &\doteq \frac{1}{4} \mathbf{E}^{\text{lin}} :: \left[[\mathbf{C} - \mathbf{I}] \otimes [\mathbf{C} - \mathbf{I}] \right]. \end{aligned} \tag{1.34}$$

Summarising, the nature of tensor functions with respect to Eqs.(1.28,1.30) and the, say elasticity tensor \mathbf{E} in Eq.(1.32) – that is the nature of tensor functions of zero, second and fourth order – is characterised via

$$\left. \begin{aligned} \psi_0(\mathbf{C}(\mathbf{X}, t), [\bullet](\mathbf{X}, t); \mathbf{X}) &= \psi_0(\mathbf{G}_{i\star} \mathbf{C}(\mathbf{X}, t), \mathbf{G}_{i\star} [\bullet](\mathbf{X}, t); \mathbf{X}) \\ \mathbf{G}_{i\star} \mathbf{S}(\mathbf{C}(\mathbf{X}, t), [\bullet](\mathbf{X}, t); \mathbf{X}) &= \mathbf{S}(\mathbf{G}_{i\star} \mathbf{C}(\mathbf{X}, t), \mathbf{G}_{i\star} [\bullet](\mathbf{X}, t); \mathbf{X}) \\ \mathbf{G}_{i\star} \mathbf{E}(\mathbf{C}(\mathbf{X}, t), [\bullet](\mathbf{X}, t); \mathbf{X}) &= \mathbf{E}(\mathbf{G}_{i\star} \mathbf{C}(\mathbf{X}, t), \mathbf{G}_{i\star} [\bullet](\mathbf{X}, t); \mathbf{X}) \end{aligned} \right\} \forall \mathbf{G}_i \in \mathbb{G} \tag{1.35}$$

whereby the abbreviation $[\bullet](\mathbf{X}, t)$ characterises an additional set of appropriate arguments. If we choose $\psi_0(\mathbf{C}(\mathbf{X}, t), [\bullet](\mathbf{X}, t); \mathbf{X})$ to be a polynomial in (the components of) $\mathbf{C}(\mathbf{X}, t)$ and $[\bullet](\mathbf{X}, t)$,

then it is noted that the functional basis $I_{1,\dots,n}(\mathbf{C}(\mathbf{X}, t), [\bullet](\mathbf{X}, t); \mathbf{X})$ itself turns out to be a polynomial function and is thus called polynomial basis or rather integrity basis. As a disadvantage, polynomial functions contain, in general, more elements than non-polynomial approaches [TN92, “We see no sign that nature loves a polynomial, . . .”; footnote 1 on page 61]. Therefore, an integrity basis usually leads to less compact settings compared to a non-polynomial approach even if the integrity basis is irreducible, i.e. none of its elements can be expressed in terms of a single-valued function of the remaining arguments of the set. However, in the case that the underlying group of transformations is finite the scalar-valued integrity basis also forms a (typically reducible) functional basis since any scalar invariant, whether polynomial or not, may be expressed as a single-valued function of the elements of the integrity basis, see e.g. Pipkin and Wineman [PW63, WP64]. Furthermore, please note that even an irreducible functional basis is often not unique and most of all that for an anisotropic constitutive equation, the constraint of the existence of a potential ψ_0 , which defines the constitutive equation for the stress tensor, is a restriction compared to a general tensor-valued tensor function for the stress measure.

There exists a large body of literature on the classical theory of invariants, see e.g. Weyl [Wey87], Gurevich [Gur64] or Olver [Olv99]. For an overview in the present context, we refer to Truesdell and Noll [TN92, Chap. B], Spencer [Spe71], Rivlin [Riv80] and the contributions in Boehler [Boe87]. Nevertheless, with emphasis on much more advanced functions – compared to the simple cases considered in this work – the computation of irreducible sets of invariants $I_{1,\dots,n}(\mathbf{C}(\mathbf{X}, t), [\bullet](\mathbf{X}, t); \mathbf{X})$ (commonly realized with the aid of group representation theory), or alternatively the complete elimination of syzygies, is still a crucial issue under discussion.

1.3.1 Anisotropic tensor functions

Anisotropic tensor functions with respect to Eqs.(1.35) are identified by a symmetry group \mathbb{G} that does not include the complete proper orthogonal group \mathbb{O}_+^3 . Representations of anisotropic tensor functions for the polynomial case are well-developed, see e.g. Smith and Rivlin [SR57, SR58] and Liu [Liu82]. A clear Table summarising the corresponding set of invariants for all 32 crystallographic finite point groups with respect to one tensorial argument of second order is included, e.g., in the contributions by Rivlin [Riv66] or Gairola [Gai79] and many other references. The development of irreducible representations for anisotropic non-polynomial tensor functions is discussed by, e.g., Boehler [Boe79] and Zheng [Zhe93b].

Example 1.4 *A coherent case of symmetry is a transversely isotropic material, which is of major interest in engineering applications. We generally have five different types of transversal isotropy, $T_{1,\dots,5}$, see e.g. Smith [Smi94, Sect. 8.10]. Within the subsequent example, the group $T_1 = \{\mathbf{I}, \bar{\mathbf{I}}, {}^{\text{rot}}\mathbf{R}_3(\theta \mathbf{e}_3), \theta \in [0, 2\pi)\}$ is discussed which is essentially defined by the rotation axis $\mathbf{e}_3 \in \mathbb{R}^3$. We follow the works by Ericksen and Rivlin [ER54] and Pipkin and Rivlin [PR59] and thus apply index-notation as introduced in Eq.(1.28). The transformation relations for the identity and central inversion are obvious and for the rotational operation with respect to $\boldsymbol{\theta}_3 \doteq \theta \mathbf{e}_3$, we obtain*

$$\begin{aligned} {}^{\text{rot}}\mathbf{C}(\mathbf{X}, \boldsymbol{\theta}_3, t) &\doteq {}^{\text{rot}}\mathbf{R}_3^t(\boldsymbol{\theta}_3) \cdot \mathbf{C}(\mathbf{X}, t) \cdot {}^{\text{rot}}\mathbf{R}_3(\boldsymbol{\theta}_3) \\ {}^{\text{rot}}C_{ij}(\mathbf{X}, \boldsymbol{\theta}_3, t) &\doteq {}^{\text{rot}}R_3^k{}_i(\boldsymbol{\theta}_3) C_{kl}(\mathbf{X}, t) {}^{\text{rot}}R_3^l{}_j(\boldsymbol{\theta}_3) \end{aligned} \quad \text{with } {}^{\text{rot}}R_3^m{}_n = \begin{bmatrix} \cos(\theta) & \sin(\theta) & 0 \\ -\sin(\theta) & \cos(\theta) & 0 \\ 0 & 0 & 1 \end{bmatrix} \quad (1.36)$$

which results in

$${}^{\text{rot}}C_{ij} = \begin{bmatrix} c^2 C_{11} + s^2 C_{22} + 2 s c C_{12} & s c [C_{22} - C_{11}] + [c^2 - s^2] C_{12} & s C_{23} + c C_{13} \\ & s^2 C_{11} + c^2 C_{22} - 2 s c C_{12} & c C_{23} - s C_{13} \\ \text{sym} & & C_{33} \end{bmatrix} \quad (1.37)$$

whereby the abbreviated notations $c \doteq \cos(\theta)$ and $s \doteq \sin(\theta)$ have been applied. The corresponding invariance requirement for a scalar-valued anisotropic tensor function is characterised by the constraint of complete independence of the rotation angle θ . Thus, for the free energy density, we obtain

$$\begin{aligned} \psi_0(\mathbf{C}(\mathbf{X}, t); \mathbf{X}) &= \psi_0({}^{\text{rot}}\mathbf{C}(\mathbf{X}, \boldsymbol{\theta}_3, t); \mathbf{X}) = \psi_0(\mathbf{C}(\mathbf{X}, t), \boldsymbol{\theta}_3; \mathbf{X}) \\ \implies \partial_\theta \psi_0(\mathbf{X}, \boldsymbol{\theta}_3, t); \mathbf{X}) &= \partial_{{}^{\text{rot}}\mathbf{C}} \psi_0 : \partial_{{}^{\text{rot}}\mathbf{R}_3} {}^{\text{rot}}\mathbf{C} : \partial_\theta {}^{\text{rot}}\mathbf{R}_3 \doteq 0. \end{aligned} \quad (1.38)$$

Next, some straightforward computations and the application of index notation yield

$$\begin{aligned}
\partial_\theta \psi_0 &= \partial_{\text{rot } C_{ij}} \psi_0 [\delta_i^l C_{kn} \text{rot } R_3^n_j + \text{rot } R_3^m_i C_{mk} \delta_j^l] \partial_\theta \text{rot } R_3^k_l \\
&= [\partial_{\text{rot } C_{ij}} \psi_0 \partial_\theta \text{rot } R_3^k_l C_{kn} \text{rot } R_3^n_j + \partial_{\text{rot } C_{il}} \psi_0 \text{rot } R_3^m_i C_{mk} \delta_j^l] \partial_\theta \text{rot } R_3^k_l \\
&= 2 [\partial_{\text{rot } C_{22}} \psi_0 - \partial_{\text{rot } C_{11}} \psi_0] \text{rot } C_{12} + \partial_{\text{rot } C_{12}} \psi_0 [\text{rot } C_{11} - \text{rot } C_{22}] \\
&+ \partial_{\text{rot } C_{23}} \psi_0 \text{rot } C_{13} - \partial_{\text{rot } C_{13}} \psi_0 \text{rot } C_{23} = 0
\end{aligned} \tag{1.39}$$

since the non-vanishing parts of the derivatives $\partial_\theta \text{rot } R_3^i_j$ result in $\partial_\theta \text{rot } R_3^1_1 = \partial_\theta \text{rot } R_3^2_2 = \text{rot } R_3^2_1$ and $\partial_\theta \text{rot } R_3^1_2 = -\partial_\theta \text{rot } R_3^2_1 = \text{rot } R_3^1_1$, respectively. The differential equation (1.39) remains invariant under any replacement as defined in Eq.(1.36). Apparently, Eq.(1.39) is satisfied for the following polynomial basis

$$I_{1,\dots,5} = \{C_{11} + C_{22}, C_{11} C_{22} - C_{12}^2, C_{33}, C_{13}^2 + C_{23}^2, \det(C_{ij})\} \tag{1.40}$$

which is easily proved by setting $C_{ij} \mapsto \text{rot } C_{ij}$ and employing these invariants into Eq.(1.39) with $\det(C_{ij}) = C_{11} C_{22} C_{33} + 2 C_{12} C_{23} C_{13} - C_{11} C_{23}^2 - C_{22} C_{13}^2 - C_{33} C_{12}^2$ being obvious.

1.3.2 Isotropic tensor functions

The nature of isotropic tensor functions in the present context is naturally pictured by Eq.(1.35) whereby the symmetry group coincides with the full orthogonal group $\mathbb{G} \doteq \mathbb{O}^3$ (holohedral isotropic) or with the complete proper orthogonal group $\mathbb{G} \doteq \mathbb{O}_+^3$ (hemihedral isotropic; the distinction becoming relevant if the list of fields includes quantities of odd order, compare footnote § on page 11). The underlying painstaking analysis to end up with general irreducible representations of isotropic tensor functions has been developed over several decades, see Spencer [Spe71] for the polynomial case and Wang [Wan70], Smith [Smi71a], Boehler [Boe77] and Zheng [Zhe93a] for emphasis on non-polynomial settings.

Example 1.5 The introduction of structural tensors that characterise the anisotropy of the modelled material is widely used, see Zhang and Rychlewsky [ZR90] and Zheng and Spencer [ZS93] for general surveys. In this context, let the set of additional structural tensors be represented by $\mathbf{A}_{1,\dots,n}(\mathbf{X}, t)$ which enters the list of arguments in the free energy density

$$\psi_0 = \psi_0(\mathbf{C}(\mathbf{X}, t), [\bullet](\mathbf{X}, t), \mathbf{A}_{1,\dots,n}(\mathbf{X}, t); \mathbf{X}). \tag{1.41}$$

Next, in analogy to Example 1.4, we consider the case of transversal isotropy. Following the approach by Boehler [Boe79] with respect to the scalar-valued case, the representation for the isotropic tensor function (1.41) is a representation for ψ_0 considered as a transversely isotropic tensor function of $\mathbf{C}(\mathbf{X}, t)$ and $[\bullet](\mathbf{X}, t)$, respectively, since $\mathbf{G}_{1,\dots,g} \mathbf{A}_{1,\dots,n}(\mathbf{X}, t) = \mathbf{A}_{1,\dots,n}(\mathbf{X}, t)$ whereby $\mathbf{G}_{1,\dots,g}$ characterise appropriate symmetry transformations. The simplest case is obtained by neglecting the additional variables $[\bullet](\mathbf{X}, t)$, assuming $\mathbf{A}_3(\mathbf{X}) \doteq \mathbf{a}_3(\mathbf{X}) \otimes \mathbf{a}_3(\mathbf{X})$ with $\mathbf{a}_3(\mathbf{X}) \in \mathbb{R}^3$ (in analogy to Example 1.4) and setting $\mathbf{A}_{1,2,4,\dots,n}(\mathbf{X}, t) = \mathbf{0}$. Interestingly, the correlated functional basis and the integrity basis are identical for this specific case, namely

$$I_{1,\dots,5} = \{\mathbf{C} : \mathbf{I}, \mathbf{C}^2 : \mathbf{I}, \mathbf{C}^3 : \mathbf{I}, \mathbf{C} : \mathbf{A}_3, \mathbf{C}^2 : \mathbf{A}_3\}. \tag{1.42}$$

It is a straightforward exercise to exchange the invariants $I_{2,3}$ for the invariants obtained via the characteristic polynomial as highlighted in Eq.(1.23), that is $\frac{1}{2}[\mathbf{C} : \mathbf{I} - \mathbf{C}^2 : \mathbf{I}] \mapsto I_2$ and $\det(\mathbf{C}) \mapsto I_3$. Next, switching to index notation and choosing $\mathbf{a}_3(\mathbf{X}) \doteq \mathbf{e}_3$, we obtain

$$\begin{aligned}
I_{1,\dots,5} &= \{C_{11} + C_{22} + C_{33}, C_{11} C_{22} + C_{22} C_{33} + C_{11} C_{33} - C_{12}^2 - C_{23}^2 - C_{13}^2, \\
&\det(C_{ij}), C_{33}, C_{13}^2 + C_{23}^2 + C_{33}^2\}.
\end{aligned} \tag{1.43}$$

Now the relation between this set, say $^{\text{iso}}I_{1,\dots,5}$ and the invariants $^{\text{tra}}I_{1,\dots,5}$ in Eq.(1.40) becomes clear since

$$\begin{aligned}
^{\text{tra}}I_1 &= ^{\text{iso}}I_1 - ^{\text{iso}}I_4, & ^{\text{tra}}I_2 &= ^{\text{iso}}I_2 - ^{\text{iso}}I_1 ^{\text{iso}}I_4 + ^{\text{iso}}I_5, \\
^{\text{tra}}I_3 &= ^{\text{iso}}I_4, & ^{\text{tra}}I_4 &= ^{\text{iso}}I_5 - ^{\text{iso}}I_4^2, & ^{\text{tra}}I_5 &= ^{\text{iso}}I_3.
\end{aligned} \tag{1.44}$$

1.3.3 Curvilinear anisotropy

So far, we did not account for any constraints on the homogeneity of the body of interest since the orientations that define the underlying anisotropy are generally allowed to differ at each material point \mathbf{X} . The concept of curvilinear anisotropy provides a simplification of the overall approach. Conceptually speaking, in addition to a material curvilinear system of coordinates $\Theta^i(\mathbf{X})$ we incorporate another set of material curvilinear coordinates $\Theta'^i(\mathbf{X})$ into the free energy density which later on allows to model anisotropic behaviour. This approach was advocated by Adkins [Adk55], see also Green and Adkins [GA70, Sect. 1.16], Truesdell and Noll [TN92, Sect. 34], Şuhubi [Şuh75, Sect. 2.10.4] and for applications with special emphasis on elastic liquids, we refer to Lodge [Lod64, Chaps. 9 & 12].

In this context, we introduce the two-point tensor field

$$\mathbf{F}'^t(\mathbf{X}) \doteq \partial_{\mathbf{X}}\Theta^i(\mathbf{X}) \otimes \partial_{\Theta'^i}\mathbf{X} \doteq \partial_{\mathbf{X}}\Theta^i(\mathbf{X}) \otimes \mathbf{a}_i(\mathbf{X}) \quad (1.45)$$

whereby the vectors $\mathbf{a}_i(\mathbf{X}) = \partial_{\Theta'^i}\mathbf{X} \in \mathbb{R}^3$ are obviously co-linear to a natural basis at \mathbf{X} . With these relations at hand, the transformed right Cauchy–Green tensor enters the free energy density which now accounts for curvilinear anisotropy, i.e.

$$\mathbf{C}'(\mathbf{X}, t) = \mathbf{f}'^t(\mathbf{X})_* \mathbf{C}(\mathbf{X}, t) \implies \psi'_0 \doteq \psi'_0(\mathbf{C}'(\mathbf{X}, t); \mathbf{X}) = \psi'_0(I_{1, \dots, n}(\mathbf{C}'(\mathbf{X}, t); \mathbf{X}); \mathbf{X}) \quad (1.46)$$

incorporating the abbreviation $\mathbf{f}'(\mathbf{X}) = [\mathbf{F}'(\mathbf{X})]^{-1}$. If we assume the basis $\mathbf{a}_i(\mathbf{X})$ to be orthogonal, then the corresponding constitutive equation for the stress tensor results in

$$\mathbf{S}(\mathbf{C}(\mathbf{X}, t); \mathbf{X}) = 2 \mathbf{F}'^t(\mathbf{X}) \cdot \mathbf{a}_{\text{Diag}}^{-1}(\mathbf{X}) \cdot \partial_{\mathbf{C}'}\psi'_0(\mathbf{C}'(\mathbf{X}, t); \mathbf{X}) \cdot \mathbf{a}_{\text{Diag}}^{-1}(\mathbf{X}) \cdot \mathbf{F}'(\mathbf{X}) \quad (1.47)$$

with $\mathbf{a}_{\text{Diag}}(\mathbf{X}) \doteq \sqrt{\mathbf{a}_i(\mathbf{X}) \cdot \mathbf{a}_i(\mathbf{X})} \mathbf{a}_i(\mathbf{X}) \otimes \mathbf{a}_i(\mathbf{X})$.

Example 1.6 *In the present context of curvilinear anisotropy, a transversely isotropic material is characterised by symmetries with respect to the normal and the tangent plane to the surface $\Theta'^3(\mathbf{X}) \doteq \text{const}$. The strain energy density thus has to remain invariant under the coordinate transformations $\Theta'^3 = \pm \Theta'^3$ and $\Theta'^{1,2} = \Theta'^{1,2}(\Theta'^{1,2})$ with $\Theta'^i(\mathbf{X})$ representing another set of orthogonal curvilinear coordinates. Based on Eq.(1.43) the underlying set of invariants reads as $I_{1, \dots, 5} = \{I_1, I_2, I_3, C'_{33}, C'^2_{13} + C'^2_{23} + C'^2_{33}\}$.*

1.3.4 Fictitious configurations

The concept of the introduction of fictitious configurations has originally been established within the modelling of inelasticity, see e.g. Betten [Bet82b] and Murkami [Mur88]. Thereby, likely (standard) constitutive equations can be applied to compute the fictitious symmetric stress measure $\bar{\mathbf{S}}(\bar{\mathbf{C}}(\mathbf{X}, t), [\bullet](\mathbf{X}, t); \mathbf{X}) \in \mathbb{S}^3$ in terms of arguments that refer to the fictitious configuration. Then an anisotropy map $\bar{\boldsymbol{\alpha}}([\bar{\circ}](\mathbf{X}, t); \mathbf{X}) : \bar{\mathbf{S}} \rightarrow \mathbf{S}$ is introduced, which depends on a set of variables $[\bar{\circ}](\mathbf{X}, t)$ with respect to the fictitious configuration and maps the fictitious stress field to the nominal stress tensor of interest (note that in general \mathbf{S} could be non-symmetric). A typical example of this approach is characterised via a fourth order tensor $\bar{\mathbf{A}}([\bar{\circ}](\mathbf{X}, t); \mathbf{X}) \in \mathbb{L}^{3 \times 3}$ i.e. the mapping

$$\mathbf{S}(\mathbf{C}(\mathbf{X}, t), [\bullet](\mathbf{X}, t); \mathbf{X}) \doteq \bar{\mathbf{A}}([\bar{\circ}](\mathbf{X}, t); \mathbf{X}) : \bar{\mathbf{S}}(\bar{\mathbf{C}}(\mathbf{X}, t), [\bar{\bullet}](\mathbf{X}, t); \mathbf{X}) \quad (1.48)$$

Example 1.7 *For the sake of simplicity we do not incorporate any additional arguments $[\bullet](\mathbf{X}, t)$. Furthermore, let the fourth order tensor $\bar{\mathbf{A}}([\bar{\circ}](\mathbf{X}, t); \mathbf{X})$ remain constant with respect to each material point and be defined by a second order tensor $([\bar{\circ}](\mathbf{X}, t) \doteq) \bar{\mathbf{A}}(\mathbf{X}) \doteq \text{const}|_{\mathbf{X}} \in \mathbb{L}^3$ via*

$$\begin{aligned} \mathbf{S}(\mathbf{C}(\mathbf{X}, t); \mathbf{X}) &\doteq \bar{\mathbf{A}}(\bar{\mathbf{A}}(\mathbf{X})) : \bar{\mathbf{S}}(\bar{\mathbf{C}}(\mathbf{X}, t); \mathbf{X}) \doteq [\bar{\mathbf{A}}(\mathbf{X}) \otimes \bar{\mathbf{A}}(\mathbf{X})] : \bar{\mathbf{S}}(\bar{\mathbf{C}}(\mathbf{X}, t); \mathbf{X}) \\ &= \bar{\mathbf{A}}(\mathbf{X})_* \bar{\mathbf{S}}(\bar{\mathbf{C}}(\mathbf{X}, t); \mathbf{X}) = \bar{\mathbf{A}}(\mathbf{X}) \cdot \bar{\mathbf{S}}(\bar{\mathbf{C}}(\mathbf{X}, t); \mathbf{X}) \cdot \bar{\mathbf{A}}^t(\mathbf{X}) \end{aligned} \quad (1.49)$$

and $\bar{\mathbf{S}}(\bar{\mathbf{C}}(\mathbf{X}, t); \mathbf{X}), \mathbf{S}(\mathbf{C}(\mathbf{X}, t); \mathbf{X}) \in \mathbb{S}^3$ being obvious. In this context $\bar{\mathbf{A}}(\mathbf{X})$ allows interpretation as a linear tangent map that determines a stress-free, affinely pre-deformed reference configuration. The specific choice $\bar{\mathbf{A}}(\mathbf{X}) \equiv \delta \mathbf{I} + \alpha \mathbf{a}(\mathbf{X}) \otimes \mathbf{a}(\mathbf{X})$, with $\mathbf{a}(\mathbf{X}) \in \mathbb{R}^3$, $\delta \in \mathbb{R}_+$, $\alpha \in \mathbb{R}_{\text{inv}} : \alpha > -\delta$, results in a transversal isotropic setting if the constitutive equation for $\bar{\mathbf{S}}(\bar{\mathbf{C}}(\mathbf{X}, t); \mathbf{X})$ represents isotropy.

1.3.5 Anisotropic linear elasticity

The modelling of linear elastic anisotropic materials is extensively harmonised. Under the broad amount of literature on linear elasticity, the monograph by Love [Lov44, Sect. 109] is of outstanding sustainability. For a recent review on anisotropic linear elasticity, we refer to Cowin and Mehrabadi [CM95]. One of the nice things in linear anisotropic elasticity is the opportunity to picture the modelling with simple linear elastic springs and rigid balls (atoms). In this direction, Figure 1.5 monitors

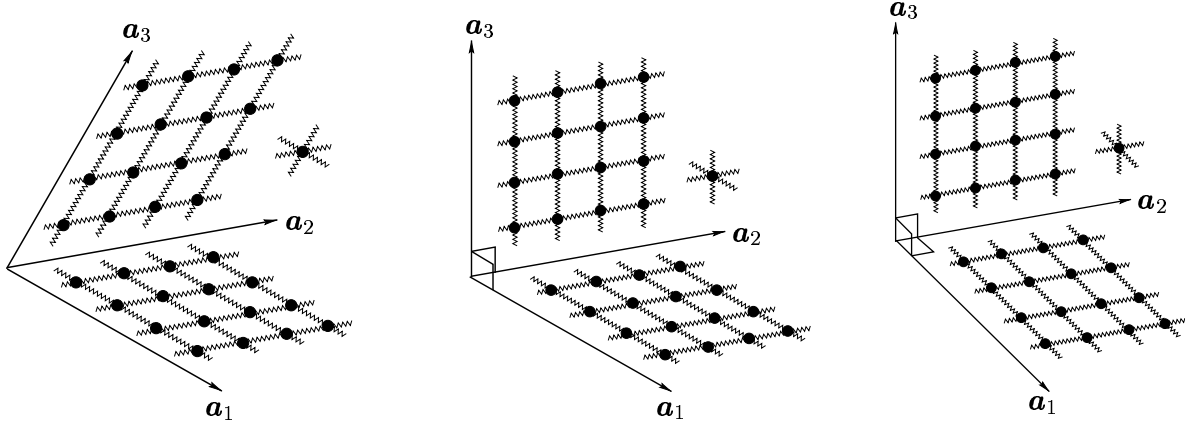


Figure 1.5: Spring–ball–model for linear anisotropic elasticity: General anisotropy, monoclinic symmetry and orthotropy.

a basic representation of general anisotropy or rather the triclinic class, monoclinic symmetry and orthotropy. Apparently, for the general case, none of the lattice vectors \mathbf{a}_i are pairwise orthogonal and the springs in each direction have different properties. The symmetry group is completely defined by the identity and central inversion, $\mathbb{G} = \{ \mathbf{I}, \bar{\mathbf{I}} \}$ and the elasticity tensor \mathbf{E}^{lin} in Eq.(1.34) is generally determined by 21 independent constitutive parameters. The monoclinic material is characterised by the requirement that the elastic constants do not change under reflection with respect to a plane. In Figure 1.5 this plane is defined by the lattice vectors \mathbf{a}_1 and \mathbf{a}_2 , respectively. Thus the underlying symmetry group reads $\mathbb{G} = \{ \mathbf{I}, \bar{\mathbf{I}}, \mathbf{R}_3 \}$ and the fourth order tensor \mathbf{E}^{lin} possesses “only” 13 independent elastic constants. Typically, an orthotropic material obeys two orthogonal reflection planes which are defined in Figure 1.5 by the lattice vectors $\mathbf{a}_{1,2}$ and $\mathbf{a}_{2,3}$, respectively. This additional condition – on top of the monoclinic symmetry – results in a set of nine material parameters and the appropriate transformation group reads $\mathbb{G} = \{ \mathbf{I}, \bar{\mathbf{I}}, \mathbf{R}_1, \mathbf{R}_3 \}$.

A delightful representation of Hooke’s law in anisotropic linear elasticity is provided by the introduction of Kelvin modes, or rather the application of the spectral decomposition theorem to the elasticity tensor, see Kelvin [Tho56], Podio–Guidugli [PG00, Sect. 16], Nemat–Nasser and Hori [NNH93, Sect. 15.6], Elata and Rubin [ER94], Sutcliffe [Sut92], Xiao [Xia97], Martins [Mar99] and Pericak–Spector et al. [PSSS99]. For a general overview we refer to Rychlewski [Ryc95] and Mehrabadi and Cowin [MC90]. Furthermore, correlated graphical visualisations are highlighted in Böhlke and Brüggemann [BB01]. In this context, the (symmetric) stress tensor is represented in the six–dimensional Cartesian space. The appropriate basis is denoted by $\mathbf{E}_{1,\dots,6}$ and the tensorial elements are constructed in terms of the base vectors $\mathbf{e}_{1,2,3}$ defining the three–dimensional Cartesian space, to be specific

$$\begin{aligned}
 \mathbf{E}_1 &= \mathbf{e}_1 \otimes \mathbf{e}_1, & \mathbf{E}_4 &= \sqrt{2} [\mathbf{e}_1 \otimes \mathbf{e}_2]^{\text{sym}}, \\
 \mathbf{E}_2 &= \mathbf{e}_2 \otimes \mathbf{e}_2, & \mathbf{E}_5 &= \sqrt{2} [\mathbf{e}_2 \otimes \mathbf{e}_3]^{\text{sym}}, \\
 \mathbf{E}_3 &= \mathbf{e}_3 \otimes \mathbf{e}_3, & \mathbf{E}_6 &= \sqrt{2} [\mathbf{e}_1 \otimes \mathbf{e}_3]^{\text{sym}},
 \end{aligned} \tag{1.50}$$

with $\mathbf{E}_i : \mathbf{E}_j = \delta_{ij}$ being obvious. Consequently, the elasticity tensor allows representation as

$$\boxed{\mathbf{E}^{\text{lin}} = \sum_{i,j=1}^6 \text{voi} \mathbf{E}_{ij}^{\text{lin}} \mathbf{E}_i \otimes \mathbf{E}_j} \tag{1.51}$$

whereby the coefficients $\text{voi} \mathbf{E}_{ij}^{\text{lin}}$ refer to Voigt's notation. Alternatively, we consider the eigenvalue problem $\mathbf{E}^{\text{lin}} : \mathbf{N} = {}^E \lambda \mathbf{N}$ of the elasticity tensor. The eigenvalues ${}^E \lambda_{1,\dots,6}$ of \mathbf{E}^{lin} are defined via the underlying characteristic polynomial

$$\det(\mathbf{E}^{\text{lin}} - {}^E \lambda \text{sym} \mathbf{I}) = 0 \implies {}^E \lambda^6 - J_1 {}^E \lambda^5 + J_2 {}^E \lambda^4 - J_3 {}^E \lambda^3 + J_4 {}^E \lambda^2 - J_5 {}^E \lambda + J_6 = 0 \quad (1.52)$$

and the appropriate spectral decomposition reads as

$$\mathbf{E}^{\text{lin}} = \sum_{i=1}^6 {}^E \lambda_i \mathbf{N}_i \quad \text{with} \quad \text{sym} \mathbf{I} = \sum_{i=1}^6 \mathbf{N}_i \quad \text{and} \quad \mathbf{N}_i = \prod_{j=1 \setminus i}^6 \frac{\mathbf{E}^{\text{lin}} - {}^E \lambda_j \text{sym} \mathbf{I}}{{}^E \lambda_i - {}^E \lambda_j} \quad (1.53)$$

whereby the abbreviated notation $\mathbf{N}_i \doteq \mathbf{N}_i \otimes \mathbf{N}_i$ has been introduced. These fourth order tensors allow interpretation as projection operators and represent the celebrated Kelvin modes. For a detailed outline on the incorporated fourth order identity tensors see Appendix A. Furthermore, note that the application of Serrin's formula in Eq.(1.53)₃ assumes distinct eigenvalues. Applications of these concepts to the modelling of anisotropic inelasticity are given by, e.g., Schreyer [Sch95], Biegler and Mehrabadi [BM95] and Qi and Bertram [QB99] for continuum damage mechanics, Arramon et al. [AMMC00] pay attention to plasticity and Mahnen [Mah02] places special emphasis on the formulation of creep.

Example 1.8 *For comparative reasons, we consider once more the case of a transversely isotropic material determined by the rotation axis \mathbf{e}_3 , now within linear elasticity. The corresponding representation with respect to Eq.(1.51) is well-established and reads as*

$$\text{voi} \mathbf{E}_{ij}^{\text{lin}} \equiv \begin{bmatrix} \lambda + 2\mu_T & \lambda & \lambda + \alpha & 0 & 0 & 0 \\ \lambda & \lambda + 2\mu_T & \lambda + \alpha & 0 & 0 & 0 \\ \lambda + \alpha & \lambda + \alpha & \lambda + 2\alpha + 4\mu_L - 2\mu_T + \beta & 0 & 0 & 0 \\ 0 & 0 & 0 & \mu_T & 0 & 0 \\ 0 & 0 & 0 & 0 & \mu_L & 0 \\ 0 & 0 & 0 & 0 & 0 & \mu_L \end{bmatrix} \quad (1.54)$$

whereby the constants $\lambda, \mu_T, \mu_L, \alpha, \beta$ denote the set of material parameters, compare Spencer [Spe84].

An overview on the computation of the elasticity tensor via eigentensors, i.e. the determination by Kelvin modes, is given by Mehrabadi and Cowin [MC90, Table 3]. In the sequel, we reiterate the outline highlighted in Cowin and Yang [CY97, App. A] for transverse isotropy with rotation axis \mathbf{e}_3 . Based on Eqs.(1.52, 1.53), the corresponding eigenvalues of \mathbf{E}^{lin} read

$${}^E \lambda_{1,2} = \frac{1}{2} \left[\text{voi} \mathbf{E}_{11}^{\text{lin}} + \text{voi} \mathbf{E}_{12}^{\text{lin}} + \text{voi} \mathbf{E}_{33}^{\text{lin}} \pm \left[\left(\text{voi} \mathbf{E}_{11}^{\text{lin}} + \text{voi} \mathbf{E}_{12}^{\text{lin}} - \text{voi} \mathbf{E}_{33}^{\text{lin}} \right)^2 + 8 \left(\text{voi} \mathbf{E}_{13}^{\text{lin}} \right)^2 \right]^{1/2} \right], \quad (1.55)$$

$${}^E \lambda_3 = \text{voi} \mathbf{E}_{11}^{\text{lin}} - \text{voi} \mathbf{E}_{12}^{\text{lin}}, \quad {}^E \lambda_{4,5} = 2 \text{voi} \mathbf{E}_{44}^{\text{lin}}, \quad {}^E \lambda_6 = 2 \text{voi} \mathbf{E}_{66}^{\text{lin}}.$$


The second order tensors \mathbf{N}_i that define the appropriate projection operators $\mathbf{N}_i = \mathbf{N}_i \otimes \mathbf{N}_i$ allow representation in terms of the basis in Eq.(1.50), namely

$$\begin{aligned} \mathbf{N}_1 &= \frac{1}{2} [\cos(\vartheta) + \sin(\vartheta)] [\mathbf{E}_1 + \mathbf{E}_2] + \frac{1}{\sqrt{2}} [\cos(\vartheta) - \sin(\vartheta)] \mathbf{E}_3, \\ \mathbf{N}_2 &= \frac{1}{2} [\sin(\vartheta) - \cos(\vartheta)] [\mathbf{E}_1 + \mathbf{E}_2] + \frac{1}{\sqrt{2}} [\cos(\vartheta) + \sin(\vartheta)] \mathbf{E}_3, \\ \mathbf{N}_3 &= \frac{1}{\sqrt{2}} [\mathbf{E}_1 - \mathbf{E}_2], \quad \mathbf{N}_4 = \frac{1}{\sqrt{2}} \mathbf{E}_4, \quad \mathbf{N}_5 = \frac{1}{\sqrt{2}} \mathbf{E}_5, \quad \mathbf{N}_6 = \frac{1}{\sqrt{2}} \mathbf{E}_6, \end{aligned} \quad (1.56)$$

whereby ϑ is determined via $\tan(2\vartheta) = \left[\text{voi} \mathbf{E}_{11}^{\text{lin}} + \text{voi} \mathbf{E}_{12}^{\text{lin}} - \text{voi} \mathbf{E}_{33}^{\text{lin}} \right] / \left[2\sqrt{2} \text{voi} \mathbf{E}_{13}^{\text{lin}} \right]$.

Chapter 2

Anisotropic hyper– elasticity based on structural tensors

 It is an important characteristic of scientific theory that it aims at eliminating irrelevant subjective aspects from a field of human experience. In doing so it creates a possibility to focus on the important observations. The covariance principle in physics is a very typical example of this objectivation procedure which aims at an elimination of the subjective feature of the space-time frame of reference in the formulation of physical relations.

E.J. Post

Formal Structure of Electromagnetics, 1962

In this Chapter we consider a modification of the free Helmholtz energy density compared to the isotropic case with special emphasis on the Eulerian setting. For the sake of clarity we restrict ourselves to non-dissipative materials and focus on the extension to multiplicative elasto-plasticity in Chapter 3.

The main objective is to derive an anisotropic spatial framework in terms of the Finger tensor $\mathbf{b}^\sharp = \mathbf{F}^\sharp \cdot \mathbf{G}^\sharp \cdot [\mathbf{F}^\sharp]^\dagger$ which is often applied in computational mechanics but usually restricts the formulation to isotropy. Here, we present an anisotropic version of the established formula $\boldsymbol{\tau}^\sharp = 2 \mathbf{g}^\sharp \cdot \partial_{\mathbf{b}^\sharp} \psi_0^\sharp \cdot \mathbf{b}^\sharp$, highlighted in Truesdell and Noll [TN92, Eq.(85.15)] which was already given by Murnaghan [Mur37] in terms of $\det^{-1}(\mathbf{b}^\sharp) \operatorname{cof}(\mathbf{b}^\sharp)$; see in addition the contribution by Richter [Ric52] where emphasis is placed on a geometric approach. For the anisotropic setting, it turns out that after the introduction of an additional tensor series of symmetric second order tensors into the free Helmholtz energy density $\psi_0^\sharp(\mathbf{g}^\sharp, \mathbf{b}^\sharp, \mathbf{a}_{1,\dots,n}^\sharp; \mathbf{X})$, the representations (of the stress tensors and tangent operators) referring to the formulations in terms of \mathbf{g}^\sharp or \mathbf{b}^\sharp and $\mathbf{a}_{1,\dots,n}^\sharp$, decompose into a specific additive structure. As a by-product, we observe an analogous format within the Lagrangian framework.

The Chapter is organised as follows: We first summarise basic essentials of non-linear continuum mechanics in Section 2.1 and introduce some of the notations used in the sequel. Further notational comments are given in Appendix A. To set the stage, Section 2.2 reiterates an established representation of anisotropic hyper-elasticity in terms of the spatial co-variant metric tensor or the right Cauchy-Green tensor, respectively. Next, the concept of the anisotropic approach is highlighted in Section 2.3. As the main contribution of this Chapter, we deduce representations of the spatial and material stress tensors and tangent operators in terms of $\mathbf{b}^\sharp, \mathbf{a}_{1,\dots,n}^\sharp$ or $\mathbf{G}^\sharp, \mathbf{A}_{1,\dots,n}^\sharp$, respectively. Thereby, as one possible proof, the representation theorem of isotropic tensor functions is the essential point of departure. An alternative proof is given in Appendix B.4.1. Finally, Section 2.4 highlights an analytical example of orthotropic hyper-elastic material and a numerical setting taking transversal isotropy into account.

2.1 Kinematics

In this Section we give a rather brief survey on essentials of non-linear continuum mechanics. For detailed overviews we refer e.g. to the monographs by Murnaghan [Mur51], Green and Zerna [GZ92], Eringen [Eri62] and to Svendsen and Tsakmakis [ST94] – among many other contributions.

A collection of material points represented by a connected differential (body) manifold \mathcal{M} of finite dimension defines the material body B of interest. Embedding material points into a vector space $(\mathcal{M}, t) \mapsto \mathbf{x}(t) \in \mathbb{V}^3$, $(\mathcal{M}, t_0) \mapsto \mathbf{X} \in \mathbb{V}^3$ is called a placement, whereby $t \in \mathbb{R}$ characterises the time. The placement of B at time t defines the corresponding configuration. In this context, let the stress free reference configuration of B be embedded into the Euclidian space denoted by $(B, t_0) \mapsto \mathcal{B}(t_0) = \mathcal{B}_0 \subset \mathbb{E}^3$ and the corresponding spatial complement by $(B, t) \mapsto \mathcal{B}(t) = \mathcal{B}_t \subset \mathbb{E}^3$. The direct non-linear motion $\varphi(\mathbf{X}, t) : \mathcal{B}_0 \times \mathbb{R} \rightarrow \mathcal{B}_t$ maps material points \mathbf{X} in \mathcal{B}_0 onto spatial points $\mathbf{x} = \varphi(\mathbf{X}, t)$ in \mathcal{B}_t . Thereby, the local chart or rather the tangent $(T\mathcal{B}_t, T\mathcal{B}_0)$ – and co-tangent spaces $(T^*\mathcal{B}_t, T^*\mathcal{B}_0)$ are spanned by line elements which are identified as natural and dual base vectors and take the following format

$$\begin{aligned} \mathbf{g}_i &= \partial_{\theta^i} \mathbf{x} \in \mathbb{R}^3 : T^*\mathcal{B}_t \rightarrow \mathbb{R}, & \mathbf{g}^i &= \partial_{\mathbf{x}} \theta^i \in \mathbb{R}^3 : T\mathcal{B}_t \rightarrow \mathbb{R}, \\ \mathbf{G}_i &= \partial_{\Theta^i} \mathbf{X} \in \mathbb{R}^3 : T^*\mathcal{B}_0 \rightarrow \mathbb{R}, & \mathbf{G}^i &= \partial_{\mathbf{X}} \Theta^i \in \mathbb{R}^3 : T\mathcal{B}_0 \rightarrow \mathbb{R} \end{aligned} \quad (2.1)$$

in terms of convected coordinates $\theta^i(\mathbf{x}, t) = \Theta^i(\mathbf{X}) \circ \Phi(\mathbf{x}, t)$ and $\Theta^i(\mathbf{X}) = \theta^i(\mathbf{x}, t) \circ \varphi(\mathbf{X}, t)$ whereby, for the sake of notational simplicity, the inverse non-linear motion $\Phi(\mathbf{x}, t) = \varphi^{-1} : \mathcal{B}_t \times \mathbb{R} \rightarrow \mathcal{B}_0$ has been introduced (and we naturally identify $T^{**}\mathcal{B}_t \doteq T\mathcal{B}_t$ and $T^{**}\mathcal{B}_0 \doteq T\mathcal{B}_0$, respectively). Please note that the natural base vectors \mathbf{g}_i and \mathbf{G}_i in Eq.(2.1) define contra-variant body fields that allow interpretation as tangent vectors while the dual base vectors \mathbf{g}^i and \mathbf{G}^i denote co-variant body fields which are characterised as normals to the surfaces $\theta^i(\mathbf{x}, t) = \text{const}$ and $\Theta^i(\mathbf{X}) = \text{const}$, respectively. Moreover, contra-variant body vectors constitute fields that are dedicated to determine properties of continuous bodies in a manner of being generally independent of any specific choice of a body coordinate system, $\theta^i(\mathbf{x}, t)$ in the configuration \mathcal{B}_t or $\Theta^i(\mathbf{X})$ in the configuration \mathcal{B}_0 , respectively. A typical example for a contra-variant space vector is a “displacement” field, e.g. $d\mathbf{X}(\mathbf{X}, t) \in \mathbb{R}^3 : T^*\mathcal{B}_0 \rightarrow \mathbb{R}$ whereby the corresponding components represent differences of the coordinates of two neighbouring points in \mathcal{B}_0 and, for the sake of simplicity, explicit notational accentuation of the contra-variant character has been neglected. The correlated material time derivative is naturally a contra-variant space field which is obtained if the distinct points refer to the same particle but at different times ^{||}.

The corresponding spatial and material body metric tensor fields follow straightforward

$$\begin{aligned} \mathbf{g}^b &= g_{ij} \mathbf{g}^i \otimes \mathbf{g}^j \in \mathbb{S}_+^3 : T\mathcal{B}_t \times T\mathcal{B}_t \rightarrow \mathbb{R}, & g_{ij} &= \mathbf{g}_i \cdot \mathbf{g}_j, \\ \mathbf{g}^\sharp &= g^{ij} \mathbf{g}_i \otimes \mathbf{g}_j \in \mathbb{S}_+^3 : T^*\mathcal{B}_t \times T^*\mathcal{B}_t \rightarrow \mathbb{R}, & g^{ij} &= \mathbf{g}^i \cdot \mathbf{g}^j, \\ \mathbf{G}^b &= G_{ij} \mathbf{G}^i \otimes \mathbf{G}^j \in \mathbb{S}_+^3 : T\mathcal{B}_0 \times T\mathcal{B}_0 \rightarrow \mathbb{R}, & G_{ij} &= \mathbf{G}_i \cdot \mathbf{G}_j, \\ \mathbf{G}^\sharp &= G^{ij} \mathbf{G}_i \otimes \mathbf{G}_j \in \mathbb{S}_+^3 : T^*\mathcal{B}_0 \times T^*\mathcal{B}_0 \rightarrow \mathbb{R}, & G^{ij} &= \mathbf{G}^i \cdot \mathbf{G}^j \end{aligned} \quad (2.2)$$

^{||}Referring to the engineering and physics community we deal with contra- and co-variant vectors in the sequel, despite the fact that strictly speaking what we call co-variant vectors arise as linear maps or rather one-forms, see e.g. Dodson and Poston [DP91, Chap. III]. It turns out to be useful to introduce fields directly as contra- or co-variant, referring to contra- or co-variant base vectors, respectively, even though general tensors naturally allow representation within any admissible base system when identifying the (finite) space of base vectors with it's dual space via a metric. Moreover, we usually do not thoroughly distinguish between the notation of body fields (including Cartesian frames in the case of rigid motions) and space fields (including Cartesian frames), see Lodge [Lod64, Chap. 12], [Lod74, Chaps. 2 & 11] for a detailed outline. Nevertheless, recall that in general one can construct a body coordinate system that uniquely corresponds to a space coordinate system at time t . Furthermore a Cartesian frame in a point at time t can be introduced and from then on used within a curvilinear coordinate system. For a detailed discussion on the introduction of the space displacement fields in the Eulerian setting $\text{dis} \mathbf{u}(\mathbf{x}, t) = \mathbf{x} - \text{shi} \mathbf{i}^\sharp \cdot \Phi(\mathbf{x}, t)$ or the Lagrangian format $\text{dis} \mathbf{U}(\mathbf{X}, t) = \text{shi} \mathbf{I}^\sharp \cdot \varphi(\mathbf{X}, t) - \mathbf{X}$, whereby $\text{shi} \mathbf{i}^\sharp$ and $\text{shi} \mathbf{I}^\sharp$ denote shifters, we refer to Truesdell and Toupin [TT60, Sect. 18], Eringen [Eri62, Art. 5] and Marsden and Hughes [MH94, Sect. 1.3]. Nevertheless, the incorporation of the displacement field usually complicates almost all terms where it has been considered and is thus preferably avoided in this work.

with $\mathbf{g}^\sharp = \det^{-1}(\mathbf{g}^b) \text{cof}(\mathbf{g}^b)$, $\mathbf{G}^\sharp = \det^{-1}(\mathbf{G}^b) \text{cof}(\mathbf{G}^b)$ (compare Appendix B.1) and the (body) manifold \mathcal{M} apparently allows interpretation as Euclidian manifold whose metric depends on time. While Cartesian vectors have unique magnitude and direction in space, the base vectors as defined in Eq.(2.1) have only unique direction with respect to the body. Their magnitude depends on the body metric tensors which are generally subjected to time. Due to the nature of these fields, body vectors at different points can not be added which is obviously in contrast to Cartesian vectors. Even contra- and co-variant fields at one point can not be connected by any additive composition since they represent geometrically different object – with all zero fields being the only exception.

Complementing Eq.(2.2), we apply in the sequel mixed-variant spatial and material identity-tensors in terms of the natural and dual base vectors, i.e.

$$\mathbf{g}^\sharp = \mathbf{g}_i \otimes \mathbf{g}^i \in \mathbb{L}_+^3 : T^*\mathcal{B}_t \times T\mathcal{B}_t \rightarrow \mathbb{R} \quad \text{and} \quad \mathbf{G}^\sharp = \mathbf{G}_i \otimes \mathbf{G}^i \in \mathbb{L}_+^3 : T^*\mathcal{B}_0 \times T\mathcal{B}_0 \rightarrow \mathbb{R} \quad (2.3)$$

which reflects the nature of general tensor analysis where neither contra- nor co-variant identity-tensors exist. Accordingly, the corresponding linear tangent map with respect to the direct motion $\varphi(\mathbf{X}, t)$ is a mixed-variant two-point tensor (motion or rather deformation gradient)

$$\mathbf{F}^\sharp = \partial_{\mathbf{X}}\varphi = \partial_{\theta^i}\varphi \otimes \partial_{\mathbf{X}}\theta^i = \partial_{\theta^i}\varphi \otimes \partial_{\mathbf{X}}[\Theta^i \circ \Phi] = \mathbf{g}_i \otimes \mathbf{G}^i \in \mathbb{L}_+^3 : T\mathcal{B}_0 \rightarrow T\mathcal{B}_t \quad (2.4)$$

which transforms tangent vectors to material curves into tangent vectors to spatial curves. The inverse motion or rather deformation gradient is consequently introduced as

$$\mathbf{f}^\sharp = \partial_{\mathbf{x}}\Phi = \partial_{\Theta^i}\Phi \otimes \partial_{\mathbf{x}}\Theta^i = \partial_{\Theta^i}\Phi \otimes \partial_{\mathbf{x}}[\theta^i \circ \varphi] = \mathbf{G}_i \otimes \mathbf{g}^i \in \mathbb{L}_+^3 : T\mathcal{B}_t \rightarrow T\mathcal{B}_0 \quad (2.5)$$

in terms of the inverse non-linear deformation map $\Phi(\mathbf{x}, t)$. In the following, we make use of four types of kinematic tensors in terms of \mathbf{F}^\sharp and \mathbf{f}^\sharp , denoted by \mathbf{b}^\sharp (Finger tensor), $\mathbf{c}^b = \det^{-1}(\mathbf{b}^\sharp) \text{cof}(\mathbf{b}^\sharp)$, \mathbf{C}^b (right Cauchy-Green tensor) and $\mathbf{B}^\sharp = \det^{-1}(\mathbf{C}^b) \text{cof}(\mathbf{C}^b)$ which are defined via **

$$\begin{aligned} \mathbf{c}^b &= \Phi^* \mathbf{G}^b = \mathbf{f}^\sharp \star \mathbf{G}^b = [\mathbf{f}^\sharp]^\dagger \cdot \mathbf{G}^b \cdot \mathbf{f}^\sharp = G_{ij} \mathbf{g}^i \otimes \mathbf{g}^j \in \mathbb{S}_+^3 : T\mathcal{B}_t \times T\mathcal{B}_t \rightarrow \mathbb{R}, \\ \mathbf{b}^\sharp &= \varphi_* \mathbf{G}^\sharp = \mathbf{F}^\sharp \star \mathbf{G}^\sharp = \mathbf{F}^\sharp \cdot \mathbf{G}^\sharp \cdot [\mathbf{F}^\sharp]^\dagger = G^{ij} \mathbf{g}_i \otimes \mathbf{g}_j \in \mathbb{S}_+^3 : T^*\mathcal{B}_t \times T^*\mathcal{B}_t \rightarrow \mathbb{R}, \\ \mathbf{C}^b &= \varphi^* \mathbf{g}^b = \mathbf{F}^\sharp \star \mathbf{g}^b = [\mathbf{F}^\sharp]^\dagger \cdot \mathbf{g}^b \cdot \mathbf{F}^\sharp = g_{ij} \mathbf{G}^i \otimes \mathbf{G}^j \in \mathbb{S}_+^3 : T\mathcal{B}_0 \times T\mathcal{B}_0 \rightarrow \mathbb{R}, \\ \mathbf{B}^\sharp &= \Phi_* \mathbf{g}^\sharp = \mathbf{f}^\sharp \star \mathbf{g}^\sharp = \mathbf{f}^\sharp \cdot \mathbf{g}^\sharp \cdot [\mathbf{f}^\sharp]^\dagger = g^{ij} \mathbf{G}_i \otimes \mathbf{G}_j \in \mathbb{S}_+^3 : T^*\mathcal{B}_0 \times T^*\mathcal{B}_0 \rightarrow \mathbb{R}, \end{aligned} \quad (2.6)$$

see Appendix A.3 for notational details. With these metric tensors at hand, generalised strain measures can be constructed. Since strain means change of metric with configuration, one obtains the following differences ($n \in \mathbb{R}_+$)

$$\begin{aligned} n \mathbf{e}_{(n)}^b &= \mathbf{g}^b - [\mathbf{c}^b]^{n/2} = [g_{ij} - [G_{ij}]^{n/2}] \mathbf{g}^i \otimes \mathbf{g}^j \in \mathbb{S}^3 : T\mathcal{B}_t \times T\mathcal{B}_t \rightarrow \mathbb{R}, \\ n \mathbf{k}_{(n)}^\sharp &= [\mathbf{b}^\sharp]^{n/2} - \mathbf{g}^\sharp = [[G^{ij}]^{n/2} - g^{ij}] \mathbf{g}_i \otimes \mathbf{g}_j \in \mathbb{S}^3 : T^*\mathcal{B}_t \times T^*\mathcal{B}_t \rightarrow \mathbb{R}, \\ n \mathbf{E}_{(n)}^b &= [\mathbf{C}^b]^{n/2} - \mathbf{G}^b = [[g_{ij}]^{n/2} - G_{ij}] \mathbf{G}^i \otimes \mathbf{G}^j \in \mathbb{S}^3 : T\mathcal{B}_0 \times T\mathcal{B}_0 \rightarrow \mathbb{R}, \\ n \mathbf{K}_{(n)}^\sharp &= \mathbf{G}^\sharp - [\mathbf{B}^\sharp]^{n/2} = [G^{ij} - [g^{ij}]^{n/2}] \mathbf{G}_i \otimes \mathbf{G}_j \in \mathbb{S}^3 : T^*\mathcal{B}_0 \times T^*\mathcal{B}_0 \rightarrow \mathbb{R}. \end{aligned} \quad (2.7)$$

** When applying a geometrically strict framework, the transposed of a tensor field is commonly defined in a manner such that the field and it's transposed have identical transformation properties, i.e. they map identical spaces to identical spaces. On the contrary, the associated dual field maps the corresponding dual spaces. As a specific application, we consider the mixed-variant two-point tensor \mathbf{F}^\sharp and denote it's dual by $[\mathbf{F}^\sharp]^D$ which is consequently defined as

$$[\mathbf{F}^\sharp]^D : T^*\mathcal{B}_t \rightarrow T^*\mathcal{B}_0 \quad \text{with} \quad [\mathbf{F}^\sharp]^D \cdot \mathbf{v}^b = \mathbf{v}^b \cdot \mathbf{F}^\sharp \quad \forall \mathbf{v}^b : T\mathcal{B}_t \rightarrow \mathbb{R} \quad (**.1)$$

and the usual denomination of the transposed, abbreviated by $[\mathbf{F}^\sharp]^{\text{tra}}$, reads

$$[\mathbf{F}^\sharp]^{\text{tra}} : T\mathcal{B}_t \rightarrow T\mathcal{B}_0 \quad \text{with} \quad [\mathbf{F}^\sharp]^{\text{tra}} = \mathbf{G}^\sharp \cdot [\mathbf{F}^\sharp]^D \cdot \mathbf{g}^b, \quad (**.2)$$

whereby the identification of the transposed with the dual field holds since we map finite-dimensional vector spaces. Based on this, the definition of e.g. the right Cauchy-Green tensor results in $\mathbf{C}^b = [\mathbf{F}^\sharp]^{\text{tra}} \cdot \mathbf{F}^\sharp : T\mathcal{B}_0 \times T^*\mathcal{B}_0 \rightarrow \mathbb{R}$ with $\mathbf{C}^b = \mathbf{G}^b \cdot \mathbf{C}^b = [\mathbf{F}^\sharp]^D \cdot \mathbf{g}^b \cdot \mathbf{F}^\sharp = \varphi^* \mathbf{g}^b$ and the Finger tensor reads $\mathbf{b}^\sharp = \mathbf{F}^\sharp \cdot [\mathbf{F}^\sharp]^{\text{tra}} : T\mathcal{B}_t \times T^*\mathcal{B}_t \rightarrow \mathbb{R}$ with $\mathbf{b}^\sharp = \mathbf{b}^\sharp \cdot \mathbf{g}^\sharp = \mathbf{F}^\sharp \cdot \mathbf{G}^\sharp \cdot [\mathbf{F}^\sharp]^D = \varphi_* \mathbf{G}^\sharp$. For more background informations see e.g. Dodson and Poston [DP91, Chaps. II–IV], Ogden [Ogd97, Sect. 1.4.3], Marsden and Hughes [MH94, Sects. 1.3 & 1.4] or Lodge [Lod74, Sect. 2.5]. In this work however, we simplify notation and thus indicate the dual of a mixed-variant field as the transposed, e.g. $[\mathbf{F}^\sharp]^D \mapsto [\mathbf{F}^\sharp]^\dagger$.

Apparently, $n = 2$ results in the definition of the Almansi and Green–Lagrange strain tensors which are respectively denoted by \mathbf{e}^b and $\mathbf{E}^b = \boldsymbol{\varphi}^* \mathbf{e}^b$ in the sequel (likewise the relation $\mathbf{K}^\sharp = \boldsymbol{\Phi}_* \mathbf{k}^\sharp$ for $n = 2$ is obvious) and the specific choice $n = 0$ is associated with the definition of logarithmic Hencky-type strain measures ^{††}

$$\begin{aligned} \mathbf{e}_{(0)}^b &= -\frac{1}{2} \ln(\mathbf{c}^b) \in \mathbb{S}^3 : T\mathcal{B}_t \times T\mathcal{B}_t \rightarrow \mathbb{R}, & \mathbf{k}_{(0)}^\sharp &= \frac{1}{2} \ln(\mathbf{b}^\sharp) \in \mathbb{S}^3 : T^*\mathcal{B}_t \times T^*\mathcal{B}_t \rightarrow \mathbb{R}, \\ \mathbf{E}_{(0)}^b &= \frac{1}{2} \ln(\mathbf{C}^b) \in \mathbb{S}^3 : T\mathcal{B}_0 \times T\mathcal{B}_0 \rightarrow \mathbb{R}, & \mathbf{K}_{(0)}^\sharp &= -\frac{1}{2} \ln(\mathbf{B}^\sharp) \in \mathbb{S}^3 : T^*\mathcal{B}_0 \times T^*\mathcal{B}_0 \rightarrow \mathbb{R}. \end{aligned} \quad (2.8)$$

It is clear that these different strain measures are qualitatively similar – namely equal to first order in \mathcal{B}_t or \mathcal{B}_0 , respectively – only for the specific case when we deal with almost small strains, i.e. $\mathbf{c}^b \rightarrow \mathbf{g}^b$, $\mathbf{C}^b \rightarrow \mathbf{G}^b$, $\mathbf{b}^\sharp \rightarrow \mathbf{g}^\sharp$ and $\mathbf{B}^\sharp \rightarrow \mathbf{G}^\sharp$ (then appropriate strain rates are identical but the corresponding rates of their conjugate thermodynamic forces (stresses) generally differ from each other).

2.2 General hyper-elasticity

Consider the scalar-valued isotropic tensor function (free Helmholtz energy per unit volume) of the format

$$\psi_0 = \psi_0(\mathbf{g}^b, \mathbf{F}^\sharp, \mathbf{G}^\sharp, \mathbf{A}_{1,\dots,n}^\sharp; \mathbf{X}) \in \mathbb{R}, \quad (2.9)$$

whereby the spatial co-variant metric allows to account for a set of general non-linear coordinates and an additional tensor series of n symmetric, second (at least even) order tensors is incorporated

$$\mathbf{a}_{1,\dots,n}^\sharp \in \mathbb{S}^3 : [T^*\mathcal{B}_t \times T^*\mathcal{B}_t]_{1,\dots,n} \rightarrow \mathbb{R}, \quad \mathbf{A}_{1,\dots,n}^\sharp \in \mathbb{S}^3 : [T^*\mathcal{B}_0 \times T^*\mathcal{B}_0]_{1,\dots,n} \rightarrow \mathbb{R} \quad (2.10)$$

that fulfils usual push-forward and pull-back relations

$$\mathbf{a}_i^\sharp = \boldsymbol{\varphi}_* \mathbf{A}_i^\sharp = \mathbf{F}^\sharp \cdot \mathbf{A}_i^\sharp \cdot [\mathbf{F}^\sharp]^\mathfrak{t} = [\mathbf{a}_i^\sharp]^\mathfrak{t} \quad \text{and} \quad \mathbf{A}_i^\sharp = \boldsymbol{\Phi}_* \mathbf{a}_i^\sharp = \mathbf{f}^\sharp \cdot \mathbf{a}_i^\sharp \cdot [\mathbf{f}^\sharp]^\mathfrak{t} = [\mathbf{A}_i^\sharp]^\mathfrak{t}. \quad (2.11)$$

They allow the description of anisotropic characteristics if there is at least one non-spherical element \mathbf{A}_i^\sharp incorporated. Here, we refer to the case of an arbitrary number of elements \mathbf{a}_i^\sharp , \mathbf{A}_i^\sharp as “general” anisotropy despite the fact that “even more general” formulations have been proposed, which are e.g. not based on isotropic scalar-valued tensor functions or incorporate higher order structural tensors, etc.

In the following, we apply the essential covariance relation of the free energy density ψ_0 as given in Eq.(2.9). For a general survey on this principle in the present context we refer to Marsden and

^{††} It is common practice to introduce generalised strain measures in terms of sufficiently smooth monotone functions $f_i \in \mathbb{R}$ of the squared principal stretches $\lambda_i \in \mathbb{R}_+$ – say the eigenvalues of \mathbf{C}^b or \mathbf{b}^\sharp , namely $\lambda_i = \mathbf{c}^b \lambda_i = \mathbf{b}^\sharp \lambda_i$ – with $f_i(\lambda_i)|_{\lambda_i=1} = 0$, $\partial_{\lambda_i} f_i(\lambda_i)|_{\lambda_i=1} = 1$ for $i = 1, 2, 3$; compare Sections B.1 & B.2. In this direction, we obtain ($n \in \mathbb{R}_+$, $m \in \mathbb{R}_0$)

$$\begin{aligned} \mathbf{e}_{(n)}^b \lambda_i &= \mathbf{K}_{(n)}^\sharp \lambda_i = \frac{1}{n} \left[1 - \lambda_i^{-\frac{n}{2}} \right], & \mathbf{e}_{(0)}^b \lambda_i &= \mathbf{K}_{(0)}^\sharp \lambda_i = -\frac{1}{2} \ln(\lambda_i^{-1}), & \partial_{\lambda_i} \mathbf{e}_{(m)}^b, \mathbf{K}_{(m)}^\sharp \lambda_i &= \frac{1}{2} \lambda_i^{-\frac{m+2}{2}}, \\ \mathbf{k}_{(n)}^\sharp \lambda_i &= \mathbf{E}_{(n)}^b \lambda_i = \frac{1}{n} \left[\lambda_i^{\frac{n}{2}} - 1 \right], & \mathbf{k}_{(0)}^\sharp \lambda_i &= \mathbf{E}_{(0)}^b \lambda_i = \frac{1}{2} \ln(\lambda_i), & \partial_{\lambda_i} \mathbf{k}_{(m)}^\sharp, \mathbf{E}_{(m)}^b \lambda_i &= \frac{1}{2} \lambda_i^{\frac{m-2}{2}} \end{aligned} \quad (\dagger\dagger.1)$$

and in addition, it is straightforward to show that the relations

$$\begin{aligned} \mathbf{e}_{(m)}^b \cdot \mathbf{g}^\sharp &= [\mathbf{c}^b]_{\frac{m}{2}} \cdot \mathbf{k}_{(m)}^\sharp \iff \mathbf{k}_{(m)}^\sharp \cdot \mathbf{g}^b = [\mathbf{b}^\sharp]_{\frac{m}{2}} \cdot \mathbf{e}_{(m)}^b, \\ \mathbf{E}_{(m)}^b \cdot \mathbf{G}^\sharp &= [\mathbf{C}^b]_{\frac{m}{2}} \cdot \mathbf{K}_{(m)}^\sharp \iff \mathbf{K}_{(m)}^\sharp \cdot \mathbf{G}^b = [\mathbf{B}^\sharp]_{\frac{m}{2}} \cdot \mathbf{E}_{(m)}^b \end{aligned} \quad (\dagger\dagger.2)$$

as well as

$$\boldsymbol{\varphi}^* \mathbf{e}_{(m)}^b = \mathbf{C}^b \cdot \mathbf{K}_{(m)}^\sharp \cdot \mathbf{G}^b, \quad \boldsymbol{\Phi}_* \mathbf{k}_{(m)}^\sharp = \mathbf{B}^\sharp \cdot \mathbf{E}_{(m)}^b \cdot \mathbf{G}^\sharp, \quad \boldsymbol{\Phi}^* \mathbf{E}_{(m)}^b = \mathbf{c}^b \cdot \mathbf{k}_{(m)}^\sharp \cdot \mathbf{g}^b, \quad \boldsymbol{\varphi}_* \mathbf{K}_{(m)}^\sharp = \mathbf{b}^\sharp \cdot \mathbf{e}_{(m)}^b \cdot \mathbf{g}^\sharp \quad (\dagger\dagger.3)$$

hold without loss of generality (recall that the full length notation of an exponentiated field allows representation as, e.g., $[\mathbf{b}^\sharp]_{\frac{m}{2}} \equiv \mathbf{g}^\sharp \cdot [\mathbf{g}^b \cdot \mathbf{b}^\sharp]_{\frac{m}{2}} = \lambda_i^{\frac{m}{2}} \mathbf{g}_i \otimes \mathbf{g}_i$). For a detailed overview on generalised strain measures we refer the reader to Truesdell and Toupin [TT60, Sect. 33(A)], Truesdell [Tru66, Sects. 15 & 16], Seth [Set64], Hill [Hil68, Hil70] and Ogden [Ogd97, Sects. 2.2.7, 3.5 & 6.1]. Recently, Papadopoulos and Lu [PL98, PL01] applied generalised strain measures to an isotropic and anisotropic plasticity formulation in strain space (based on the framework of a St. Venant–Kirchhoff-type material, compare Sections 1.3, 1.3.5 & C.1) and Miehe and Lambrecht [ML01] placed special emphasis on hyper-elasticity.

Hughes [MH94, Chap. 2 & 3] and Simo and Marsden [SM84]. Special emphasis on anisotropic hyper-elasticity is placed in Menzel and Steinmann [MS01h] or Lu and Papadopoulos [LP00].

In this direction, let $\Psi(\mathbf{x}, t) : \mathcal{B}_t \times \mathbb{R} \rightarrow \mathcal{B}_\tau$ and $\omega(\mathbf{X}, t) : \mathcal{B}_0 \times \mathbb{R} \rightarrow \mathcal{B}_\tau$ represent arbitrary spatial and material diffeomorphisms with $\psi \doteq \Psi^{-1}$ and $\Omega \doteq \omega^{-1}$ respectively. The fundamental spatial covariance relation is then given as

$$\psi_0(\mathbf{g}^b, \mathbf{F}^\sharp, \mathbf{G}^\sharp, \mathbf{A}_{1,\dots,n}^\sharp; \mathbf{X}) \doteq \psi_0(\psi^* \mathbf{g}^b, \Psi_* \mathbf{F}^\sharp, \mathbf{G}^\sharp, \mathbf{A}_{1,\dots,n}^\sharp; \mathbf{X}). \quad (2.12)$$

Furthermore, Eq.(2.12) boils down to the principle of indifference with respect to superposed spatial rigid body motions (Hooke–Poisson–Cauchy form) if $\Psi(\mathbf{x}, t)$ denotes a regular, orientation–preserving spatial isometry

$$\psi_0 = \psi_0(\mathbf{q}^\sharp \cdot \mathbf{g}^b \cdot [\mathbf{q}^\sharp]^\dagger, \mathbf{q}^\sharp \cdot \mathbf{F}^\sharp, \mathbf{G}^\sharp, \mathbf{A}_{1,\dots,n}^\sharp; \mathbf{X}) = \psi_0(\mathbf{g}^b, \mathbf{q}^\sharp \cdot \mathbf{F}^\sharp, \mathbf{G}^\sharp, \mathbf{A}_{1,\dots,n}^\sharp; \mathbf{X}) \quad \forall \mathbf{q}^\sharp \in \mathbb{O}_+^3 \quad (2.13)$$

whereby \mathbf{q}^\sharp corresponds to the correlated linear tangent map which (by definition of an isometry) preserves the metric, i.e. $\mathbf{q}^\sharp \cdot \mathbf{g}^b \cdot [\mathbf{q}^\sharp]^\dagger = \mathbf{g}^b$; compare Marsden and Hughes [MH94, Chap. 3.2, Axiom 2.9] and e.g. Guggenheimer [Gug77, Chap. 11] for more background information. The specific choice $\Psi(\mathbf{x}, t) \doteq \Phi(\mathbf{x}, t) : \mathcal{B}_t \times \mathbb{R} \rightarrow \mathcal{B}_0$ results in the well–known conclusion that \mathbf{F}^\sharp enters the free Helmholtz energy density ψ_0 via \mathbf{C}^b with respect to the material setting,

$$\begin{aligned} \psi_0 &= \psi_0(\mathbf{g}^b, \mathbf{F}^\sharp, \mathbf{G}^\sharp, \mathbf{A}_{1,\dots,n}^\sharp; \mathbf{X}) \doteq \psi_0(\varphi^* \mathbf{g}^b, \Phi_* \mathbf{F}^\sharp, \mathbf{G}^\sharp, \mathbf{A}_{1,\dots,n}^\sharp; \mathbf{X}) \\ &= \psi_0^0(\mathbf{C}^b, \mathbf{G}^\sharp, \mathbf{G}^\sharp, \mathbf{A}_{1,\dots,n}^\sharp; \mathbf{X}) = \psi_0^0(\mathbf{C}^b, \mathbf{G}^\sharp, \mathbf{A}_{1,\dots,n}^\sharp; \mathbf{X}) \end{aligned} \quad (2.14)$$

and the mixed–variant identity $\mathbf{G}^\sharp = \Phi_* \mathbf{F}^\sharp$ being naturally redundant. Next, superposing a material diffeomorphism on the finding of Eq.(2.14), that is ψ_0^0 , we consequently obtain

$$\psi_0^0(\mathbf{C}^b, \mathbf{G}^\sharp, \mathbf{A}_{1,\dots,n}^\sharp; \mathbf{X}) \doteq \psi_0^0(\Omega^* \mathbf{C}^b, \omega_* \mathbf{G}^\sharp, \omega_* \mathbf{A}_{1,\dots,n}^\sharp; \mathbf{X}). \quad (2.15)$$

Similar to Eq.(2.14), the embodied option $\omega(\mathbf{X}, t) \doteq \varphi(\mathbf{X}, t) : \mathcal{B}_0 \times \mathbb{R} \rightarrow \mathcal{B}_t$ results in the spatial format of the free Helmholtz energy density

$$\psi_0 = \psi_0^0(\mathbf{C}^b, \mathbf{G}^\sharp, \mathbf{A}_{1,\dots,n}^\sharp; \mathbf{X}) \doteq \psi_0^0(\Phi^* \mathbf{C}^b, \varphi_* \mathbf{G}^\sharp, \varphi_* \mathbf{A}_{1,\dots,n}^\sharp; \mathbf{X}) = \psi_0^t(\mathbf{g}^b, \mathbf{b}^\sharp, \mathbf{a}_{1,\dots,n}^\sharp; \mathbf{X}) \quad (2.16)$$

which we will frequently apply in this work. Finally, when choosing the special case that $\omega(\mathbf{X}, t)$ coincides with a material isometry, we end up with the definition of a scalar–valued isotropic tensor function

$$\psi_0^0 \doteq \psi_0^0(\mathbf{Q}^\sharp \cdot \mathbf{C}^b \cdot [\mathbf{Q}^\sharp]^\dagger, \mathbf{Q}^\sharp \cdot \mathbf{G}^\sharp \cdot [\mathbf{Q}^\sharp]^\dagger, \mathbf{Q}^\sharp \cdot \mathbf{A}_{1,\dots,n}^\sharp \cdot [\mathbf{Q}^\sharp]^\dagger; \mathbf{X}) \quad \forall \mathbf{Q}^\sharp \in \mathbb{O}^3 \quad (2.17)$$

whereby \mathbf{Q}^\sharp represents the underlying linear tangent map which (by definition of an isometry) obviously preserves the metric, i.e. $\mathbf{Q}^\sharp \cdot \mathbf{G}^\sharp \cdot [\mathbf{Q}^\sharp]^\dagger = \mathbf{G}^\sharp$, compare Eq.(2.13). The correlated material symmetry group \mathbb{G} of the considered material is a sub–group of the orthogonal group \mathbb{O}^3 and defined by a set of elements $\mathbf{R}_{1,\dots,m}^\sharp$ via

$$\mathbb{G} = \left\{ \mathbf{R}_i^\sharp \in \mathbb{O}^3 \mid \mathbf{R}_{1,\dots,m}^\sharp \star \mathbf{A}_{1,\dots,n}^\sharp = \mathbf{R}_{1,\dots,m}^\sharp \cdot \mathbf{A}_{1,\dots,n}^\sharp \cdot [\mathbf{R}_{1,\dots,m}^\sharp]^\dagger \doteq \mathbf{A}_{1,\dots,n}^\sharp \right\}. \quad (2.18)$$

In order to specify the nature of the elements $\mathbf{R}_{1,\dots,m}^\sharp$ of the symmetry group, let $\mathbf{e}'_i, \mathbf{e}_i, \mathbf{e}^i \in \mathbb{R}^3$ in \mathcal{B}_0 denote frames (whereby each of them is assumed to be orthonormal at the material point \mathbf{X}) and $\mathbf{n}^\sharp, \mathbf{n}^b \in \mathbb{U}^2$ represent a unit–vector in \mathcal{B}_0 . Then, due to the nature of the orthogonal group, any element of \mathbb{G} allows representation as $\mathbf{R}^\sharp = \mathbf{e}'_i \otimes \mathbf{e}^i$, that are reflections ${}^{\text{ref}}\mathbf{R}^\sharp$ and rotations ${}^{\text{rot}}\mathbf{R}^\sharp$ which we construct via

$${}^{\text{ref}}\mathbf{R}^\sharp(\mathbf{n}^\sharp, \mathbf{n}^b) = \mathbf{G}^\sharp - 2 \mathbf{n}^\sharp \otimes \mathbf{n}^b \in \mathbb{O}^3 \quad \text{and} \quad {}^{\text{rot}}\mathbf{R}^\sharp(\theta \mathbf{n}^\sharp) = \exp(-\theta \boldsymbol{\varepsilon}^\sharp \cdot \mathbf{n}^\sharp) \in \mathbb{O}_+^3 \quad (2.19)$$

whereby $\boldsymbol{\varepsilon}^\sharp$ denotes a mixed–variant representation of the third order alternating permutation tensor in \mathcal{B}_0 and $\theta \in \mathbb{R} : (0, 2\pi]$. Please note that the central inversion mapping ($-\mathbf{G}^\sharp \doteq -\mathbf{e}_i \otimes \mathbf{e}^i$) is obtained by the reflection ${}^{\text{ref}}\mathbf{R}^\sharp(\mathbf{n}^\sharp, \mathbf{n}^b)$ if \mathbf{n}^\sharp is co–linear to $\mathbf{e}_1 + \mathbf{e}_2 + \mathbf{e}_3$ and that the identity (\mathbf{G}^\sharp) is included for any rotation with $\theta = 2\pi$.

2.2.1 General spatial and material stress relation

Within the standard argumentation of rational thermodynamics, the free Helmholtz energy density defines the stress tensors $\boldsymbol{\tau}^\sharp$ (Kirchhoff stress) and \boldsymbol{S}^\sharp (second Piola–Kirchhoff stress) as

$$\boxed{\begin{aligned} \boldsymbol{\tau}^\sharp &= 2 \partial_{\boldsymbol{g}^b} \psi_0^t(\boldsymbol{g}^b, \boldsymbol{b}^\sharp, \boldsymbol{a}_{1,\dots,n}^\sharp; \boldsymbol{X}) \in \mathbb{S}^3 : T^* \mathcal{B}_t \times T^* \mathcal{B}_t \rightarrow \mathbb{R}, \\ \boldsymbol{S}^\sharp &= 2 \partial_{\boldsymbol{C}^b} \psi_0^0(\boldsymbol{C}^b, \boldsymbol{G}^\sharp, \boldsymbol{A}_{1,\dots,n}^\sharp; \boldsymbol{X}) \in \mathbb{S}^3 : T^* \mathcal{B}_0 \times T^* \mathcal{B}_0 \rightarrow \mathbb{R}. \end{aligned}} \quad (2.20)$$

2.2.1.1 Derivation of the general spatial stress relation

The isothermal Clausius–Duhem inequality in local form for a purely elastic process reduces to an equality which reads within the spatial setting as

$$\mathcal{D}_0^t = [\boldsymbol{m}^\natural]^t : \boldsymbol{l}^\natural - D_t \psi_0^t(\boldsymbol{g}^b, \boldsymbol{b}^\sharp, \boldsymbol{a}_{1,\dots,n}^\sharp; \boldsymbol{X}) = 0, \quad (2.21)$$

whereby $[\boldsymbol{m}^\natural]^t = \boldsymbol{g}^b \cdot \boldsymbol{\tau}^\sharp \in \mathbb{L}^3 : T\mathcal{B}_t \times T^*\mathcal{B}_t \rightarrow \mathbb{R}$ denotes a mixed-variant spatial stress tensor of Mandel-type – or rather a mixed-variant representation of the Kirchhoff stress $\boldsymbol{\tau}^\sharp$, $D_t[\bullet] = \partial_t([\bullet](\boldsymbol{X}, t))$ characterises the material time derivative (holding \boldsymbol{X} fixed) and $\boldsymbol{l}^\natural = D_t \boldsymbol{F}^\natural \cdot \boldsymbol{f}^\natural \in \mathbb{L}^3 : T^*\mathcal{B}_t \times T\mathcal{B}_t \rightarrow \mathbb{R}$ defines the spatial gradient of the physical velocity, see e.g. Truesdell and Noll [TN92, Chap. D II a]. The stress power \mathcal{W}_0 can alternatively be written in the format

$$\mathcal{W}_0^t = [\boldsymbol{m}^\natural]^t : \boldsymbol{l}^\natural = [\boldsymbol{m}^\natural \cdot \boldsymbol{g}^\sharp]^t : [\boldsymbol{g}^b \cdot \boldsymbol{l}^\natural] = \boldsymbol{\tau}^\sharp : [\boldsymbol{g}^b \cdot \boldsymbol{l}^\natural]^{\text{sym}} = \frac{1}{2} \boldsymbol{\tau}^\sharp : L_t \boldsymbol{g}^b. \quad (2.22)$$

Thereby the notation $L_t[\bullet] = \varphi_*(D_t(\Phi_*([\bullet]^\sharp(\boldsymbol{x}, t))))$ represents the Lie derivative (here with respect to a contra-variant field), which is known as the Oldroyd rate $L_t \boldsymbol{\tau}^\sharp = D_t \boldsymbol{\tau}^\sharp - 2[\boldsymbol{l}^\natural \cdot \boldsymbol{\tau}^\sharp]^{\text{sym}}$ when applied to the Kirchhoff stress. Now, computing the material time derivative $D_t \psi_0^t$, one obtains

$$D_t \psi_0^t = \partial_{\boldsymbol{g}^b} \psi_0^t : L_t \boldsymbol{g}^b = 2 \partial_{\boldsymbol{g}^b} \psi_0^t : [\boldsymbol{g}^b \cdot \boldsymbol{l}^\natural]^{\text{sym}} = 2[\boldsymbol{g}^b \cdot \partial_{\boldsymbol{g}^b} \psi_0^t] : \boldsymbol{l}^\natural, \quad (2.23)$$

whereby the application of the Lie-derivative $L_t \boldsymbol{g}^b$ stems from the push-forward of the material time derivative $D_t \boldsymbol{C}^b$. Moreover, it is obvious that Eqs.(2.21) and (2.23) define the mixed-variant Kirchhoff stress tensor as

$$\boxed{[\boldsymbol{m}^\natural]^t = 2 \boldsymbol{g}^b \cdot \partial_{\boldsymbol{g}^b} \psi_0^t} \quad (2.24)$$

which results in the well-known Doyle–Ericksen formula $\boldsymbol{\tau}^\sharp = 2 \partial_{\boldsymbol{g}^b} \psi_0^t$ in view of Eq.(2.22).

2.2.1.2 Derivation of the general material stress relation

The material format of Eq.(2.24) can be derived by standard push-forward and pull-back operations or via

$$\mathcal{D}_0^0 = [\boldsymbol{M}^\natural]^t : \boldsymbol{L}^\natural - D_t \psi_0^0(\boldsymbol{C}^b, \boldsymbol{G}^\sharp, \boldsymbol{A}_{1,\dots,n}^\sharp; \boldsymbol{X}) = 0 \quad (2.25)$$

whereby $[\boldsymbol{M}^\natural]^t = \boldsymbol{C}^b \cdot \boldsymbol{S}^\sharp \in \mathbb{L}^3 : T\mathcal{B}_0 \times T^*\mathcal{B}_0 \rightarrow \mathbb{R}$ denotes the Mandel stress tensor and $\boldsymbol{L}^\natural = \boldsymbol{f}^\natural \cdot D_t \boldsymbol{F}^\natural \in \mathbb{L}^3 : T^*\mathcal{B}_0 \times T\mathcal{B}_0 \rightarrow \mathbb{R}$ represents the mixed-variant pull-back of the physical velocity gradient. Now, taking the relation

$$\mathcal{W}_0^0 = [\boldsymbol{M}^\natural]^t : \boldsymbol{L}^\natural = [\boldsymbol{M}^\natural \cdot \boldsymbol{B}^\sharp]^t : [\boldsymbol{C}^b \cdot \boldsymbol{L}^\natural] = \boldsymbol{S}^\sharp : [\boldsymbol{C}^b \cdot \boldsymbol{L}^\natural]^{\text{sym}} = 1/2 \boldsymbol{S}^\sharp : D_t \boldsymbol{C}^b \quad (2.26)$$

and $D_t \psi_0^0 = \partial_{\boldsymbol{C}^b} \psi_0^0 : D_t \boldsymbol{C}^b$ into account, the material hyper-elastic law reads

$$\boxed{[\boldsymbol{M}^\natural]^t = 2 \boldsymbol{C}^b \cdot \partial_{\boldsymbol{C}^b} \psi_0^0} \quad (2.27)$$

incorporating the usual format of the second Piola–Kirchhoff stress tensor, $\boldsymbol{S}^\sharp = 2 \partial_{\boldsymbol{C}^b} \psi_0^0$.

2.2.2 General spatial and material tangent operator

It is straightforward to show that the spatial and material tangent operators \mathbf{e}^\sharp and \mathbf{E}^\sharp are Hessians of the free Helmholtz energy density for a non-dissipative isothermal hyper-elastic setting. Here, the appropriate time derivatives of the elements of the additional tensor series vanish – $L_t \mathbf{a}_{1,\dots,n}^\sharp \doteq \mathbf{0}_{1,\dots,n}$ and $D_t \mathbf{A}_{1,\dots,n}^\sharp \doteq \mathbf{0}_{1,\dots,n}$ – thus the typical format reads

$$\boxed{\begin{aligned} \mathbf{e}^\sharp &= 4 \quad \partial_{\mathbf{g}^b \otimes \mathbf{g}^b}^2 \psi_0^t(\mathbf{g}^b, \mathbf{b}^\sharp, \mathbf{a}_{1,\dots,n}^\sharp; \mathbf{X}) \in \mathbb{S}^{3 \times 3} : T^* \mathcal{B}_t \times T^* \mathcal{B}_t \times T^* \mathcal{B}_t \times T^* \mathcal{B}_t \rightarrow \mathbb{R}, \\ \mathbf{E}^\sharp &= 4 \quad \partial_{\mathbf{C}^b \otimes \mathbf{C}^b}^2 \psi_0^0(\mathbf{C}^b, \mathbf{G}^\sharp, \mathbf{A}_{1,\dots,n}^\sharp; \mathbf{X}) \in \mathbb{S}^{3 \times 3} : T^* \mathcal{B}_0 \times T^* \mathcal{B}_0 \times T^* \mathcal{B}_0 \times T^* \mathcal{B}_0 \rightarrow \mathbb{R}. \end{aligned}} \quad (2.28)$$

2.2.2.1 Derivation of the general spatial and material tangent operator

For completeness, we give an outline of the derivation of the tangent operators which appear in the relations $L_t \boldsymbol{\tau}^\sharp = \frac{1}{2} \mathbf{e}^\sharp : L_t \mathbf{g}^b$ and $D_t \mathbf{S}^\sharp = \frac{1}{2} \mathbf{E}^\sharp : D_t \mathbf{C}^b$. The material version reads

$$D_t \mathbf{S}^\sharp = \partial_{\mathbf{C}^b} [2 \partial_{\mathbf{C}^b} \psi_0^0] : D_t \mathbf{C}^b = 2 \partial_{\mathbf{C}^b \otimes \mathbf{C}^b}^2 \psi_0^0 : D_t \mathbf{C}^b \quad (2.29)$$

which proves Eq.(2.28)₂. Standard transformations like

$$D_t \mathbf{S}^\sharp = \boldsymbol{\Phi}_* L_t \boldsymbol{\tau}^\sharp = \mathbf{f}^\sharp \cdot L_t \boldsymbol{\tau}^\sharp \cdot [\mathbf{f}^\sharp]^\dagger, \quad D_t \mathbf{C}^b = \boldsymbol{\varphi}^* L_t \mathbf{g}^b = [\mathbf{F}^\sharp]^\dagger \cdot L_t \mathbf{g}^b \cdot \mathbf{F}^\sharp \quad (2.30)$$

and

$$\begin{aligned} \partial_{\mathbf{C}^b} \psi_0^0 &= \partial_{\mathbf{g}^b} \psi_0^t : \partial_{\mathbf{C}^b} \mathbf{g}^b = \mathbf{f}^\sharp \cdot \partial_{\mathbf{g}^b} \psi_0^t \cdot [\mathbf{f}^\sharp]^\dagger, \\ \partial_{\mathbf{C}^b \otimes \mathbf{C}^b}^2 \psi_0^0 &= \partial_{\mathbf{g}^b} \left[\mathbf{f}^\sharp \cdot \partial_{\mathbf{g}^b} \psi_0^t \cdot [\mathbf{f}^\sharp]^\dagger \right] : \partial_{\mathbf{C}^b} \mathbf{g}^b \\ &= [\mathbf{f}^\sharp \overline{\otimes} \mathbf{f}^\sharp] : \partial_{\mathbf{g}^b \otimes \mathbf{g}^b}^2 \psi_0^t : \left[[\mathbf{f}^\sharp]^\dagger \overline{\otimes} [\mathbf{f}^\sharp]^\dagger \right] \end{aligned} \quad (2.31)$$

finally yield the spatial tangent operator \mathbf{e}^\sharp in Eq.(2.28)₁, see Appendix A for notational details.

2.3 Representation of anisotropy

As previously mentioned, anisotropy possibly enters the formulation if at least one non-spherical tensor \mathbf{A}_i^\sharp is employed to the free Helmholtz energy density. Without loss of generality, Eqs.(2.20) and (2.28) define the stress tensors and tangent operators but we additionally seek an analogous expression in terms of $\mathbf{b}^\sharp, \mathbf{a}_{1,\dots,n}^\sharp$ or $\mathbf{G}^\sharp, \mathbf{A}_{1,\dots,n}^\sharp$.

2.3.1 Anisotropic spatial and material stress relation

As the main thrust of this Chapter, we make the

Proposition 2.1 *Within the anisotropic framework based on the free Helmholtz energy density $\psi_0 = \psi_0^t(\mathbf{g}^b, \mathbf{b}^\sharp, \mathbf{a}_{1,\dots,n}^\sharp; \mathbf{X}) = \psi_0^0(\mathbf{C}^b, \mathbf{G}^\sharp, \mathbf{A}_{1,\dots,n}^\sharp; \mathbf{X})$, the stress tensor can alternatively be formulated in terms of $\mathbf{b}^\sharp, \mathbf{a}_{1,\dots,n}^\sharp$ or $\mathbf{G}^\sharp, \mathbf{A}_{1,\dots,n}^\sharp$ instead of \mathbf{g}^b or \mathbf{C}^b . The formal structure is similar to the established equation for the isotropic Kirchhoff stress tensor $\boldsymbol{\tau}^\sharp = 2 \mathbf{g}^\sharp \cdot \partial_{\mathbf{b}^\sharp} \psi_0^t \cdot \mathbf{b}^\sharp$ since the anisotropic formulation results in a specific additive decomposition into derivatives in terms of \mathbf{b}^\sharp and $\mathbf{a}_{1,\dots,n}^\sharp$ or \mathbf{G}^\sharp and $\mathbf{A}_{1,\dots,n}^\sharp$, respectively. Anticipating the result, we will end up with*

$$\boxed{\begin{aligned} \boldsymbol{\tau}^\sharp &= 2 \quad \mathbf{g}^\sharp \cdot \partial_{\mathbf{b}^\sharp} \psi_0^t \cdot \mathbf{b}^\sharp + 2 \sum_{i=1}^n \mathbf{g}^\sharp \cdot \partial_{\mathbf{a}_i^\sharp} \psi_0^t \cdot \mathbf{a}_i^\sharp = [\boldsymbol{\tau}^\sharp]^\dagger, \\ \mathbf{S}^\sharp &= 2 \quad \mathbf{B}^\sharp \cdot \partial_{\mathbf{G}^\sharp} \psi_0^0 \cdot \mathbf{G}^\sharp + 2 \sum_{i=1}^n \mathbf{B}^\sharp \cdot \partial_{\mathbf{A}_i^\sharp} \psi_0^0 \cdot \mathbf{A}_i^\sharp = [\mathbf{S}^\sharp]^\dagger. \end{aligned}} \quad (2.32)$$

The corresponding proof can be based on the general representation theorem of isotropic scalar-valued tensor functions. Thereby, one has to express every obtained stress generator based on \mathbf{g}^b or \mathbf{C}^b in terms of sums of generators based on \mathbf{b}^\sharp and $\mathbf{a}_{1,\dots,n}^\sharp$ or \mathbf{G}^\sharp and $\mathbf{A}_{1,\dots,n}^\sharp$, respectively.

2.3.1.1 Derivation of the anisotropic spatial stress relation

The local form of the isothermal Clausius–Duhem inequality within the anisotropic spatial setting for a non-dissipative process ($L_t \mathbf{a}_{1,\dots,n}^\sharp \doteq \mathbf{0}_{1,\dots,n}$ and $D_t \mathbf{A}_{1,\dots,n}^\sharp \doteq \mathbf{0}_{1,\dots,n}$) with $D_t \mathbf{b}^\sharp = 2[\mathbf{l}^\sharp \cdot \mathbf{b}^\sharp]^{\text{sym}}$ and $D_t \mathbf{a}_i^\sharp = 2[\mathbf{l}^\sharp \cdot \mathbf{a}_i^\sharp]^{\text{sym}}$ boils down to

$$\begin{aligned}
\mathcal{D}_0^t &= [\mathbf{m}^\sharp]^t : \mathbf{l}^\sharp - D_t \psi_0^t(\mathbf{g}^b, \mathbf{b}^\sharp, \mathbf{a}_{1,\dots,n}^\sharp; \mathbf{X}) \\
&= [\mathbf{m}^\sharp]^t : \mathbf{l}^\sharp - \partial_{\mathbf{b}^\sharp} \psi_0^t : D_t \mathbf{b}^\sharp - \sum_{i=1}^n \partial_{\mathbf{a}_i^\sharp} \psi_0^t : D_t \mathbf{a}_i^\sharp \\
&= [\mathbf{m}^\sharp]^t : \mathbf{l}^\sharp - 2 \partial_{\mathbf{b}^\sharp} \psi_0^t : [\mathbf{l}^\sharp \cdot \mathbf{b}^\sharp]^{\text{sym}} - 2 \sum_{i=1}^n \partial_{\mathbf{a}_i^\sharp} \psi_0^t : [\mathbf{l}^\sharp \cdot \mathbf{a}_i^\sharp]^{\text{sym}} \\
&= [\mathbf{m}^\sharp]^t : \mathbf{l}^\sharp - 2 \partial_{\mathbf{b}^\sharp} \psi_0^t : [\mathbf{l}^\sharp \cdot \mathbf{b}^\sharp] - 2 \sum_{i=1}^n \partial_{\mathbf{a}_i^\sharp} \psi_0^t : [\mathbf{l}^\sharp \cdot \mathbf{a}_i^\sharp] \\
&= 0,
\end{aligned} \tag{2.33}$$

whereby symmetry relations have been taken into account. Thus, following the standard argumentation of rational thermodynamics, a definition of the mixed-variant Kirchhoff stress tensor can be constructed as

$$[\mathbf{m}^\sharp]^t = 2 \partial_{\mathbf{b}^\sharp} \psi_0^t \cdot \mathbf{b}^\sharp + 2 \sum_{i=1}^n \partial_{\mathbf{a}_i^\sharp} \psi_0^t \cdot \mathbf{a}_i^\sharp. \tag{2.34}$$

The fact that the (material) elements of the tensor series $\mathbf{A}_{1,\dots,n}^\sharp$ are assumed to stay constant during the deformation process suggests the terminology material or rather deformation induced anisotropy.

2.3.1.2 Derivation of the anisotropic material stress relation

The material format of Eq.(2.34) can be obtained by standard pull-back operations and reads

$$[\mathbf{M}^\sharp]^t = 2 \partial_{\mathbf{G}^\sharp} \psi_0^0 \cdot \mathbf{G}^\sharp + 2 \sum_{i=1}^n \partial_{\mathbf{A}_i^\sharp} \psi_0^0 \cdot \mathbf{A}_i^\sharp. \tag{2.35}$$

2.3.1.3 Derivation of the anisotropic spatial and material stress relation via invariants

Next, we take the general representation theorem of isotropic tensor functions into account (an alternative proof is given in Appendix B.4.1) in order to prove the symmetry (or in other words the commutativity) of the introduced Kirchhoff stress tensor $\boldsymbol{\tau}^\sharp = \mathbf{m}^\sharp \cdot \mathbf{g}^\sharp = \mathbf{g}^\sharp \cdot [\mathbf{m}^\sharp]^t$ or the introduced second Piola–Kirchhoff stress tensor $\mathbf{S}^\sharp = \mathbf{M}^\sharp \cdot \mathbf{B}^\sharp = \mathbf{B}^\sharp \cdot [\mathbf{M}^\sharp]^t$, respectively, within the anisotropic framework highlighted in Eqs.(2.9, 2.34, 2.35). The corresponding set of invariants, e.g. $g^b b^\sharp I_{(i),(ii),(iii)}$, $g^b a_i^\sharp I_{(iv),(v),(vi)}$ for the free Helmholtz energy density in spatial quantities with respect to \mathcal{B}_t is summarised in Table 2.1 whereby $i, j \in [1, \dots, n]$ take all possible choices, compare e.g. Boehler [Boe77] and references cited therein. The correlated derivatives of these invariants with respect to \mathbf{g}^b , \mathbf{b}^\sharp and \mathbf{a}_i^\sharp (or \mathbf{C}^b , \mathbf{G}^\sharp and \mathbf{A}_i^\sharp , respectively) are highlighted in Appendix B. We focus on the spatial representation in Eqs.(2.20) and (2.32) in the sequel and end up with the alternative expressions

$$\begin{aligned}
\boldsymbol{\tau}^\sharp &= 2 \sum_{q=(i)}^{(vi)} \partial_{I_q} \psi_0^t \partial_{\mathbf{g}^b} I_q = [\boldsymbol{\tau}^\sharp]^t, \\
\boldsymbol{\tau}^\sharp &= 2 \sum_{q=(i)}^{(vi)} \partial_{I_q} \psi_0^t \mathbf{g}^\sharp \cdot \partial_{\mathbf{b}^\sharp} I_q \cdot \mathbf{b}^\sharp + 2 \sum_{q=(i)}^{(vi)} \sum_{s=1}^n \partial_{I_q} \psi_0^t \mathbf{g}^\sharp \cdot \partial_{\mathbf{a}_s^\sharp} I_q \cdot \mathbf{a}_s^\sharp = [\boldsymbol{\tau}^\sharp]^t.
\end{aligned} \tag{2.36}$$

Table 2.1: Complete set of invariants $\psi_0(I_{(i),\dots,(vi)}; \mathbf{X})$ with respect to \mathcal{B}_t and \mathcal{B}_0 for all possible choices of $i, j \in [1, \dots, n]$.

(i)	$\mathbf{g}^b : \mathbf{b}^\# =$	$\mathbf{C}^b : \mathbf{G}^\#$
(ii)	$[\mathbf{g}^b \cdot \mathbf{b}^\# \cdot \mathbf{g}^b] : \mathbf{b}^\# =$	$[\mathbf{C}^b \cdot \mathbf{G}^\# \cdot \mathbf{C}^b] : \mathbf{G}^\#$
(iii)	$[\mathbf{g}^b \cdot [\mathbf{b}^\# \cdot \mathbf{g}^b]^2] : \mathbf{b}^\# =$	$[\mathbf{C}^b \cdot [\mathbf{G}^\# \cdot \mathbf{C}^b]^2] : \mathbf{G}^\#$
(iv)	$\mathbf{g}^b : \mathbf{a}_i^\# =$	$\mathbf{C}^b : \mathbf{A}_i^\#$
(v)	$[\mathbf{g}^b \cdot \mathbf{b}^\# \cdot \mathbf{g}^b] : \mathbf{a}_i^\# =$	$[\mathbf{C}^b \cdot \mathbf{G}^\# \cdot \mathbf{C}^b] : \mathbf{A}_i^\#$
(vi)	$[\mathbf{g}^b \cdot \mathbf{a}_j^\# \cdot \mathbf{c}^b] : \mathbf{a}_i^\# =$	$[\mathbf{C}^b \cdot \mathbf{A}_j^\# \cdot \mathbf{G}^b] : \mathbf{A}_i^\#$

In this context, Proposition 2.1 for the anisotropic stress relation (Eq.(2.32)) is one-to-one with

$$\begin{aligned}
 \partial_{\mathbf{g}^b} I_q &= \mathbf{g}^\# \cdot \partial_{\mathbf{b}^\#} I_q \cdot \mathbf{b}^\# + \sum_{s=1}^n \mathbf{g}^\# \cdot \partial_{\mathbf{a}_s^\#} I_q \cdot \mathbf{a}_s^\# \\
 &= \mathbf{b}^\# \cdot \partial_{\mathbf{b}^\#} I_q \cdot \mathbf{g}^\# + \sum_{s=1}^n \mathbf{a}_s^\# \cdot \partial_{\mathbf{a}_s^\#} I_q \cdot \mathbf{g}^\#, \\
 \partial_{\mathbf{C}^b} I_q &= \mathbf{B}^\# \cdot \partial_{\mathbf{G}^\#} I_q \cdot \mathbf{G}^\# + \sum_{s=1}^n \mathbf{B}^\# \cdot \partial_{\mathbf{A}_s^\#} I_q \cdot \mathbf{A}_s^\# \\
 &= \mathbf{G}^\# \cdot \partial_{\mathbf{G}^\#} I_q \cdot \mathbf{B}^\# + \sum_{s=1}^n \mathbf{A}_s^\# \cdot \partial_{\mathbf{A}_s^\#} I_q \cdot \mathbf{B}^\#.
 \end{aligned} \tag{2.37}$$

Emphasis is placed here on the spatial setting and we verify Proposition 2.1 in the form of Eq.(2.37)₁. After some lengthy but straightforward algebra which is based essentially on the generators in Appendix B, we obtain

$$\begin{aligned}
 (i) \quad \partial_{\mathbf{g}^b} I_{(i)} &\doteq \mathbf{g}^\# \cdot \partial_{\mathbf{b}^\#} I_{(i)} \cdot \mathbf{b}^\# + \sum_{s=1}^n \mathbf{g}^\# \cdot \partial_{\mathbf{a}_s^\#} I_{(i)} \cdot \mathbf{a}_s^\# \\
 &= \mathbf{g}^\# \cdot \mathbf{g}^b \cdot \mathbf{b}^\# + \mathbf{0} = \mathbf{b}^\# \\
 (ii) \quad \partial_{\mathbf{g}^b} I_{(ii)} &\doteq \mathbf{g}^\# \cdot \partial_{\mathbf{b}^\#} I_{(ii)} \cdot \mathbf{b}^\# + \sum_{s=1}^n \mathbf{g}^\# \cdot \partial_{\mathbf{a}_s^\#} I_{(ii)} \cdot \mathbf{a}_s^\# \\
 &= 2 \mathbf{g}^\# \cdot \mathbf{g}^b \cdot \mathbf{b}^\# \cdot \mathbf{g}^b \cdot \mathbf{b}^\# + \mathbf{0} = 2 \mathbf{b}^\# \cdot \mathbf{g}^b \cdot \mathbf{b}^\# \\
 (iii) \quad \partial_{\mathbf{g}^b} I_{(iii)} &\doteq \mathbf{g}^\# \cdot \partial_{\mathbf{b}^\#} I_{(iii)} \cdot \mathbf{b}^\# + \sum_{s=1}^n \mathbf{g}^\# \cdot \partial_{\mathbf{a}_s^\#} I_{(iii)} \cdot \mathbf{a}_s^\# \\
 &= 3 \mathbf{g}^\# \cdot \mathbf{g}^b \cdot [\mathbf{b}^\# \cdot \mathbf{g}^b]^2 \cdot \mathbf{b}^\# = 3 \mathbf{b}^\# \cdot [\mathbf{g}^b \cdot \mathbf{b}^\#]^2 \\
 (iv) \quad \partial_{\mathbf{g}^b} I_{(iv)} &\doteq \mathbf{g}^\# \cdot \partial_{\mathbf{b}^\#} I_{(iv)} \cdot \mathbf{b}^\# + \sum_{s=1}^n \mathbf{g}^\# \cdot \partial_{\mathbf{a}_s^\#} I_{(iv)} \cdot \mathbf{a}_s^\# \\
 &= \mathbf{0} + \mathbf{g}^\# \cdot \mathbf{g}^b \cdot \mathbf{a}_i^\# = \mathbf{a}_i^\#
 \end{aligned}$$

$$\begin{aligned}
(v) \quad \partial_{\mathbf{g}^b} I_{(v)} &\doteq \mathbf{g}^\sharp \cdot \partial_{\mathbf{b}^\sharp} I_{(v)} \cdot \mathbf{b}^\sharp + \sum_{s=1}^n \mathbf{g}^\sharp \cdot \partial_{\mathbf{a}_s^\sharp} I_{(v)} \cdot \mathbf{a}_s^\sharp \\
&= \mathbf{g}^\sharp \cdot \mathbf{g}^b \cdot \mathbf{a}_i^\sharp \cdot \mathbf{g}^b \cdot \mathbf{b}^\sharp + \mathbf{g}^\sharp \cdot \mathbf{g}^b \cdot \mathbf{b}^\sharp \cdot \mathbf{g}^b \cdot \mathbf{a}_i^\sharp \\
&= 2 [\mathbf{b}^\sharp \cdot \mathbf{g}^b \cdot \mathbf{a}_i^\sharp]^{\text{sym}}
\end{aligned}$$

$$\begin{aligned}
(vi) \quad \partial_{\mathbf{g}^b} I_{(vi)} &\doteq \mathbf{g}^\sharp \cdot \partial_{\mathbf{b}^\sharp} I_{(vi)} \cdot \mathbf{b}^\sharp + \sum_{s=1}^n \mathbf{g}^\sharp \cdot \partial_{\mathbf{a}_s^\sharp} I_{(vi)} \cdot \mathbf{a}_s^\sharp \\
&= -\mathbf{g}^\sharp \cdot \mathbf{c}^b \cdot [\mathbf{a}_{i,j}^\sharp \cdot \mathbf{g}^b]_2^{\text{sym}} \\
&\quad + \mathbf{g}^\sharp \cdot [\mathbf{g}^b \cdot \mathbf{a}_j^\sharp \cdot \mathbf{c}^b]^{\text{sym}} \cdot \mathbf{a}_i^\sharp + \mathbf{g}^\sharp \cdot [\mathbf{g}^b \cdot \mathbf{a}_i^\sharp \cdot \mathbf{c}^b]^{\text{sym}} \cdot \mathbf{a}_j^\sharp \\
&= [\mathbf{a}_{i,j}^\sharp \cdot \mathbf{c}^b]_2^{\text{sym}}
\end{aligned}$$

which proves Proposition 2.1, the outline of the transposed version – Eq.(2.37)₂ – being obvious (note that the sum over all contributions in Eq.(2.36)₂ results in a symmetric Kirchhoff stress while single contributions are non-symmetric in general). Moreover, the derivation within the anisotropic material framework is straightforward and thus not highlighted here.

Remark 2.1 *Apparently, an isotropic setting is obtained if the additional tensor series are neglected, $\mathbf{A}_{1,\dots,n}^\sharp \doteq \mathbf{0}_{1,\dots,n}$, which results in*

$$\boxed{
\begin{aligned}
\boldsymbol{\tau}^\sharp &= 2 \mathbf{g}^\sharp \cdot \partial_{\mathbf{b}^\sharp} \psi_0^t(\mathbf{g}^b, \mathbf{b}^\sharp; \mathbf{X}) \cdot \mathbf{b}^\sharp = [\boldsymbol{\tau}^\sharp]^t, \\
\mathbf{S}^\sharp &= 2 \mathbf{B}^\sharp \cdot \partial_{\mathbf{G}^\sharp} \psi_0^0(\mathbf{C}^b, \mathbf{G}^\sharp; \mathbf{X}) \cdot \mathbf{G}^\sharp = [\mathbf{S}^\sharp]^t,
\end{aligned}
} \quad (2.38)$$

whereby the spatial format is well-established in the literature, see Truesdell and Noll [TN92, Eq.(85.15)] or Murnaghan [Mur37] for a corresponding outline in terms of \mathbf{c}^b , i.e. $\boldsymbol{\tau}^\sharp = -2 \mathbf{g}^\sharp \cdot \mathbf{c}^b \cdot \partial_{\mathbf{c}^b} \psi_0^t$. Furthermore, note that the specific choice of spherical elements $\mathbf{A}_{1,\dots,n}^\sharp \propto \mathbf{G}^\sharp$ or the incorporation of scalar-valued fields instead of second order tensors, results similarly in an isotropic constitutive equation.

2.3.2 Anisotropic spatial and material tangent operator

On the basis for the developed stress relation, the spatial and material tangent operator within a non-dissipative anisotropic setting can be derived in terms of \mathbf{b}^\sharp and $\mathbf{a}_{1,\dots,n}^\sharp$ or \mathbf{G}^\sharp and $\mathbf{A}_{1,\dots,n}^\sharp$, respectively. Anticipating the result, a specific additive structure is again obtained, i.e.

$$\boxed{
\begin{aligned}
\mathbf{e}^\sharp &= 4 \quad [\mathbf{b}^\sharp \overline{\otimes} \mathbf{g}^\sharp] : \partial_{\mathbf{b}^\sharp \otimes \mathbf{b}^\sharp}^2 \psi_0^t : [\mathbf{g}^\sharp \overline{\otimes} \mathbf{b}^\sharp] \\
&\quad + 4 \sum_{s=1}^n [\mathbf{a}_s^\sharp \overline{\otimes} \mathbf{g}^\sharp] : \partial_{\mathbf{a}_s^\sharp \otimes \mathbf{b}^\sharp}^2 \psi_0^t : [\mathbf{g}^\sharp \overline{\otimes} \mathbf{b}^\sharp] \\
&\quad + 4 \sum_{s=1}^n [\mathbf{b}^\sharp \overline{\otimes} \mathbf{g}^\sharp] : \partial_{\mathbf{b}^\sharp \otimes \mathbf{a}_s^\sharp}^2 \psi_0^t : [\mathbf{g}^\sharp \overline{\otimes} \mathbf{a}_s^\sharp] \\
&\quad + 4 \sum_{s,t=1}^n [\mathbf{a}_s^\sharp \overline{\otimes} \mathbf{g}^\sharp] : \partial_{\mathbf{a}_s^\sharp \otimes \mathbf{a}_t^\sharp}^2 \psi_0^t : [\mathbf{g}^\sharp \overline{\otimes} \mathbf{a}_t^\sharp], \\
\mathbf{E}^\sharp &= 4 \quad [\mathbf{G}^\sharp \overline{\otimes} \mathbf{B}^\sharp] : \partial_{\mathbf{G}^\sharp \otimes \mathbf{G}^\sharp}^2 \psi_0^0 : [\mathbf{B}^\sharp \overline{\otimes} \mathbf{G}^\sharp] \\
&\quad + 4 \sum_{s=1}^n [\mathbf{A}_s^\sharp \overline{\otimes} \mathbf{B}^\sharp] : \partial_{\mathbf{A}_s^\sharp \otimes \mathbf{G}^\sharp}^2 \psi_0^0 : [\mathbf{B}^\sharp \overline{\otimes} \mathbf{G}^\sharp] \\
&\quad + 4 \sum_{s=1}^n [\mathbf{G}^\sharp \overline{\otimes} \mathbf{B}^\sharp] : \partial_{\mathbf{G}^\sharp \otimes \mathbf{A}_s^\sharp}^2 \psi_0^0 : [\mathbf{B}^\sharp \overline{\otimes} \mathbf{A}_s^\sharp] \\
&\quad + 4 \sum_{s,t=1}^n [\mathbf{A}_s^\sharp \overline{\otimes} \mathbf{B}^\sharp] : \partial_{\mathbf{A}_s^\sharp \otimes \mathbf{A}_t^\sharp}^2 \psi_0^0 : [\mathbf{B}^\sharp \overline{\otimes} \mathbf{A}_t^\sharp].
\end{aligned}
} \quad (2.39)$$

2.3.2.1 Derivation of the anisotropic spatial tangent operator

The derivation of the spatial tangent operator within a non-dissipative ($L_t \mathbf{a}_{1,\dots,n}^\# \doteq \mathbf{0}_{1,\dots,n}$ and $D_t \mathbf{A}_{1,\dots,n}^\# \doteq \mathbf{0}_{1,\dots,n}$) anisotropic setting is based essentially on Eq.(2.32). In addition, the relations $\boldsymbol{\tau}^\# = \mathbf{g}^\# \cdot [\mathbf{m}^\#]^\dagger$ and $D_t \mathbf{b}^\# = 2 [\mathbf{l}^\# \cdot \mathbf{b}^\#]^{\text{sym}}$, $D_t \mathbf{a}_i^\# = 2 [\mathbf{l}^\# \cdot \mathbf{a}_i^\#]^{\text{sym}}$ are taken into account. In this context, the material time derivative of the Kirchhoff stress tensor

$$D_t \boldsymbol{\tau}^\# = 2 \partial_{\mathbf{b}^\#} \boldsymbol{\tau}^\# : [\mathbf{l}^\# \cdot \mathbf{b}^\#]^{\text{sym}} + 2 \sum_{s=1}^n \partial_{\mathbf{a}_s^\#} \boldsymbol{\tau}^\# : [\mathbf{l}^\# \cdot \mathbf{a}_s^\#]^{\text{sym}} \quad (2.40)$$

takes the following format by incorporating Eq.(2.32)

$$\begin{aligned} D_t \boldsymbol{\tau}^\# &= 2 \quad \partial_{\mathbf{b}^\#} [\mathbf{b}^\# \cdot \partial_{\mathbf{b}^\#} \psi_0^t \cdot \mathbf{g}^\#] : [\mathbf{l}^\# \cdot \mathbf{b}^\#] \quad + \quad \partial_{\mathbf{b}^\#} [\mathbf{g}^\# \cdot \partial_{\mathbf{b}^\#} \psi_0^t \cdot \mathbf{b}^\#] : [\mathbf{l}^\# \cdot \mathbf{b}^\#]^\dagger \\ &+ 2 \sum_{s=1}^n \partial_{\mathbf{a}_s^\#} [\mathbf{b}^\# \cdot \partial_{\mathbf{b}^\#} \psi_0^t \cdot \mathbf{g}^\#] : [\mathbf{l}^\# \cdot \mathbf{a}_s^\#] \quad + \quad \partial_{\mathbf{a}_s^\#} [\mathbf{g}^\# \cdot \partial_{\mathbf{b}^\#} \psi_0^t \cdot \mathbf{b}^\#] : [\mathbf{l}^\# \cdot \mathbf{a}_s^\#]^\dagger \\ &+ 2 \sum_{s=1}^n \partial_{\mathbf{b}^\#} [\mathbf{a}_s^\# \cdot \partial_{\mathbf{a}_s^\#} \psi_0^t \cdot \mathbf{g}^\#] : [\mathbf{l}^\# \cdot \mathbf{b}^\#] \quad + \quad \partial_{\mathbf{b}^\#} [\mathbf{g}^\# \cdot \partial_{\mathbf{a}_s^\#} \psi_0^t \cdot \mathbf{a}_s^\#] : [\mathbf{l}^\# \cdot \mathbf{b}^\#]^\dagger \\ &+ 2 \sum_{s,t=1}^n \partial_{\mathbf{a}_t^\#} [\mathbf{a}_s^\# \cdot \partial_{\mathbf{a}_s^\#} \psi_0^t \cdot \mathbf{g}^\#] : [\mathbf{l}^\# \cdot \mathbf{a}_t^\#] \quad + \quad \partial_{\mathbf{a}_t^\#} [\mathbf{g}^\# \cdot \partial_{\mathbf{a}_s^\#} \psi_0^t \cdot \mathbf{a}_s^\#] : [\mathbf{l}^\# \cdot \mathbf{a}_t^\#]^\dagger \\ &= 2 \quad [\mathbf{b}^\# \overline{\otimes} \mathbf{g}^\#] : \partial_{\mathbf{b}^\# \otimes \mathbf{b}^\#}^2 \psi_0^t : [\mathbf{l}^\# \cdot \mathbf{b}^\#] \quad + \quad [\mathbf{l}^\# \cdot \mathbf{b}^\#]^\dagger : \partial_{\mathbf{b}^\# \otimes \mathbf{b}^\#}^2 \psi_0^t : [\mathbf{g}^\# \overline{\otimes} \mathbf{b}^\#] \quad (2.41) \\ &+ 2 \sum_{s=1}^n [\mathbf{b}^\# \overline{\otimes} \mathbf{g}^\#] : \partial_{\mathbf{b}^\# \otimes \mathbf{a}_s^\#}^2 \psi_0^t : [\mathbf{l}^\# \cdot \mathbf{a}_s^\#] \quad + \quad [\mathbf{l}^\# \cdot \mathbf{a}_s^\#]^\dagger : \partial_{\mathbf{a}_s^\# \otimes \mathbf{b}^\#}^2 \psi_0^t : [\mathbf{g}^\# \overline{\otimes} \mathbf{b}^\#] \\ &+ 2 \sum_{s=1}^n [\mathbf{a}_s^\# \overline{\otimes} \mathbf{g}^\#] : \partial_{\mathbf{a}_s^\# \otimes \mathbf{b}^\#}^2 \psi_0^t : [\mathbf{l}^\# \cdot \mathbf{b}^\#] \quad + \quad [\mathbf{l}^\# \cdot \mathbf{b}^\#]^\dagger : \partial_{\mathbf{b}^\# \otimes \mathbf{a}_s^\#}^2 \psi_0^t : [\mathbf{g}^\# \overline{\otimes} \mathbf{a}_s^\#] \\ &+ 2 \sum_{s,t=1}^n [\mathbf{a}_s^\# \overline{\otimes} \mathbf{g}^\#] : \partial_{\mathbf{a}_s^\# \otimes \mathbf{a}_t^\#}^2 \psi_0^t : [\mathbf{l}^\# \cdot \mathbf{a}_t^\#] \quad + \quad [\mathbf{l}^\# \cdot \mathbf{a}_t^\#]^\dagger : \partial_{\mathbf{a}_t^\# \otimes \mathbf{a}_s^\#}^2 \psi_0^t : [\mathbf{g}^\# \overline{\otimes} \mathbf{a}_s^\#] \\ &+ 2 \quad [\mathbf{l}^\# \cdot \boldsymbol{\tau}^\#]^{\text{sym}}. \end{aligned}$$

Now, computing the Lie derivative of the Kirchhoff stress tensor, i.e. $L_t \boldsymbol{\tau}^\# = D_t \boldsymbol{\tau}^\# - 2 [\mathbf{l}^\# \cdot \boldsymbol{\tau}^\#]^{\text{sym}}$ (keeping the specific non-dissipative case in mind), in order to construct the spatial tangent operator $\mathbf{e}^\#$ and thereby proving Eq.(2.39)₁, we end up with

$$\begin{aligned} L_t \boldsymbol{\tau}^\# &= 2 \quad [\mathbf{b}^\# \overline{\otimes} \mathbf{g}^\#] : \partial_{\mathbf{b}^\# \otimes \mathbf{b}^\#}^2 \psi_0^t : [\mathbf{l}^\# \cdot \mathbf{g}^\# \cdot \mathbf{g}^\# \cdot \mathbf{b}^\#] \\ &+ 2 \quad [\mathbf{b}^\# \cdot [\mathbf{l}^\#]^\dagger \cdot \mathbf{g}^\# \cdot \mathbf{g}^\#] : \partial_{\mathbf{b}^\# \otimes \mathbf{b}^\#}^2 \psi_0^t : [\mathbf{g}^\# \overline{\otimes} \mathbf{b}^\#] \\ &+ 2 \sum_{s=1}^n [\mathbf{a}_s^\# \cdot [\mathbf{l}^\#]^\dagger \cdot \mathbf{g}^\# \cdot \mathbf{g}^\#] : \partial_{\mathbf{a}_s^\# \otimes \mathbf{b}^\#}^2 \psi_0^t : [\mathbf{g}^\# \overline{\otimes} \mathbf{b}^\#] \\ &+ 2 \sum_{s=1}^n [\mathbf{b}^\# \overline{\otimes} \mathbf{g}^\#] : \partial_{\mathbf{b}^\# \otimes \mathbf{a}_s^\#}^2 \psi_0^t : [\mathbf{l}^\# \cdot \mathbf{g}^\# \cdot \mathbf{g}^\# \cdot \mathbf{a}_s^\#] \\ &+ 2 \sum_{s=1}^n [\mathbf{a}_s^\# \overline{\otimes} \mathbf{g}^\#] : \partial_{\mathbf{a}_s^\# \otimes \mathbf{b}^\#}^2 \psi_0^t : [\mathbf{l}^\# \cdot \mathbf{g}^\# \cdot \mathbf{g}^\# \cdot \mathbf{b}^\#] \\ &+ 2 \sum_{s=1}^n [\mathbf{b}^\# \cdot [\mathbf{l}^\#]^\dagger \cdot \mathbf{g}^\# \cdot \mathbf{g}^\#] : \partial_{\mathbf{b}^\# \otimes \mathbf{a}_s^\#}^2 \psi_0^t : [\mathbf{g}^\# \overline{\otimes} \mathbf{a}_s^\#] \\ &+ 2 \sum_{s,t=1}^n [\mathbf{a}_s^\# \overline{\otimes} \mathbf{g}^\#] : \partial_{\mathbf{a}_s^\# \otimes \mathbf{a}_t^\#}^2 \psi_0^t : [\mathbf{l}^\# \cdot \mathbf{g}^\# \cdot \mathbf{g}^\# \cdot \mathbf{a}_t^\#] \quad (2.42) \\ &+ 2 \sum_{s,t=1}^n [\mathbf{a}_s^\# \cdot [\mathbf{l}^\#]^\dagger \cdot \mathbf{g}^\# \cdot \mathbf{g}^\#] : \partial_{\mathbf{a}_s^\# \otimes \mathbf{a}_t^\#}^2 \psi_0^t : [\mathbf{g}^\# \overline{\otimes} \mathbf{a}_t^\#] \\ &= [4 \quad [\mathbf{b}^\# \overline{\otimes} \mathbf{g}^\#] : \partial_{\mathbf{b}^\# \otimes \mathbf{b}^\#}^2 \psi_0^t : [\mathbf{g}^\# \overline{\otimes} \mathbf{b}^\#] \\ &+ 4 \sum_{s=1}^n [\mathbf{a}_s^\# \overline{\otimes} \mathbf{g}^\#] : \partial_{\mathbf{a}_s^\# \otimes \mathbf{b}^\#}^2 \psi_0^t : [\mathbf{g}^\# \overline{\otimes} \mathbf{b}^\#] \end{aligned}$$

$$\begin{aligned}
& + 4 \sum_{s=1}^n \left[\mathbf{b}^\# \overline{\otimes} \mathbf{g}^\# \right] : \partial_{\mathbf{b}^\# \otimes \mathbf{a}_s^\#}^2 \psi_0^t : \left[\mathbf{g}^\# \overline{\otimes} \mathbf{a}_s^\# \right] \\
& + 4 \sum_{s,t=1}^n \left[\mathbf{a}_s^\# \overline{\otimes} \mathbf{g}^\# \right] : \partial_{\mathbf{a}_s^\# \otimes \mathbf{a}_t^\#}^2 \psi_0^t : \left[\mathbf{g}^\# \overline{\otimes} \mathbf{a}_t^\# \right] : \left[\mathbf{g}^b \cdot \mathbf{l}^\natural \right]^{\text{sym}} \doteq \frac{1}{2} \mathbf{e}^\# : \mathbb{L}_t \mathbf{g}^b.
\end{aligned}$$

2.3.2.2 Derivation of the anisotropic material tangent operator

The derivation of the material tangent operator $\mathbf{E}^\#$ is again a straightforward exercise in terms of standard push-forward operations, namely

$$\begin{aligned}
\mathbb{L}_t \boldsymbol{\tau}^\# &= \boldsymbol{\varphi}_* \text{D}_t \mathbf{S}^\# = \mathbf{F}^\natural \cdot \text{D}_t \mathbf{S}^\# \cdot [\mathbf{F}^\natural]^\natural, & \mathbf{g}^\# &= \boldsymbol{\varphi}_* \mathbf{B}^\# = \mathbf{F}^\natural \cdot \mathbf{B}^\# \cdot [\mathbf{F}^\natural]^\natural, \\
\mathbb{L}_t \mathbf{g}^b &= \boldsymbol{\Phi}^* \text{D}_t \mathbf{C}^b = [\mathbf{f}^\natural]^\natural \cdot \text{D}_t \mathbf{C}^b \cdot \mathbf{f}^\natural, & \mathbf{b}^\# &= \boldsymbol{\varphi}_* \mathbf{G}^\# = \mathbf{F}^\natural \cdot \mathbf{G}^\# \cdot [\mathbf{F}^\natural]^\natural, \\
& & \mathbf{a}_i^\# &= \boldsymbol{\varphi}_* \mathbf{A}_i^\# = \mathbf{F}^\natural \cdot \mathbf{A}_i^\# \cdot [\mathbf{F}^\natural]^\natural
\end{aligned} \tag{2.43}$$

and

$$\begin{aligned}
\partial_{\mathbf{b}^\# \otimes \mathbf{b}^\#}^2 \psi_0^t &= \boldsymbol{\varphi}_* \partial_{\mathbf{G}^\# \otimes \mathbf{G}^\#}^2 \psi_0^0 = \left[[\mathbf{f}^\natural]^\natural \overline{\otimes} [\mathbf{f}^\natural]^\natural \right] : \partial_{\mathbf{G}^\# \otimes \mathbf{G}^\#}^2 \psi_0^0 : [\mathbf{f}^\natural \overline{\otimes} \mathbf{f}^\natural], \\
\partial_{\mathbf{b}^\# \otimes \mathbf{a}_i^\#}^2 \psi_0^t &= \boldsymbol{\varphi}_* \partial_{\mathbf{G}^\# \otimes \mathbf{A}_i^\#}^2 \psi_0^0 = \left[[\mathbf{f}^\natural]^\natural \overline{\otimes} [\mathbf{f}^\natural]^\natural \right] : \partial_{\mathbf{G}^\# \otimes \mathbf{A}_i^\#}^2 \psi_0^0 : [\mathbf{f}^\natural \overline{\otimes} \mathbf{f}^\natural], \\
\partial_{\mathbf{a}_i^\# \otimes \mathbf{b}^\#}^2 \psi_0^t &= \boldsymbol{\varphi}_* \partial_{\mathbf{A}_i^\# \otimes \mathbf{G}^\#}^2 \psi_0^0 = \left[[\mathbf{f}^\natural]^\natural \overline{\otimes} [\mathbf{f}^\natural]^\natural \right] : \partial_{\mathbf{A}_i^\# \otimes \mathbf{G}^\#}^2 \psi_0^0 : [\mathbf{f}^\natural \overline{\otimes} \mathbf{f}^\natural], \\
\partial_{\mathbf{a}_i^\# \otimes \mathbf{a}_j^\#}^2 \psi_0^t &= \boldsymbol{\varphi}_* \partial_{\mathbf{A}_i^\# \otimes \mathbf{A}_j^\#}^2 \psi_0^0 = \left[[\mathbf{f}^\natural]^\natural \overline{\otimes} [\mathbf{f}^\natural]^\natural \right] : \partial_{\mathbf{A}_i^\# \otimes \mathbf{A}_j^\#}^2 \psi_0^0 : [\mathbf{f}^\natural \overline{\otimes} \mathbf{f}^\natural].
\end{aligned} \tag{2.44}$$

With these transformations at hand, applying some algebra finally yields Eq.(2.39)₂.

2.3.2.3 Derivation of the anisotropic spatial and material tangent operator via invariants

In the sequel, we focus on the spatial setting with respect to a representation in terms of invariants similar to the contributions of the stress tensors in Eq.(2.37). Two different families of derivatives are obviously incorporated which can easily be seen in the usual spatial format in terms of the spatial metric tensor

$$\mathbf{e}^\# = 4 \partial_{\mathbf{g}^b \otimes \mathbf{g}^b}^2 \psi_0^t = 4 \sum_{q=(i)}^{(vi)} \partial_{I_q} \psi_0^t \partial_{\mathbf{g}^b \otimes \mathbf{g}^b}^2 I_q + 4 \sum_{q,r=(i)}^{(vi)} \partial_{I_q I_r}^2 \psi_0^t \partial_{\mathbf{g}^b} I_q \otimes \partial_{\mathbf{g}^b} I_r, \tag{2.45}$$

compare Appendix B. The second type of contributions in Eq.(2.45) incorporates dyadic products of the stress generators. Thus, with Eqs.(2.37)₁ at hand, the equations

$$\begin{aligned}
\partial_{\mathbf{g}^b} I_q \otimes \partial_{\mathbf{g}^b} I_r &= \left[\mathbf{g}^\# \cdot \partial_{\mathbf{b}^\#} I_q \cdot \mathbf{b}^\# \right] \otimes \left[\mathbf{g}^\# \cdot \partial_{\mathbf{b}^\#} I_r \cdot \mathbf{b}^\# \right] \\
&+ \left[\mathbf{g}^\# \cdot \partial_{\mathbf{b}^\#} I_q \cdot \mathbf{b}^\# \right] \otimes \left[\sum_{s=1}^n \mathbf{g}^\# \cdot \partial_{\mathbf{a}_s^\#} I_r \cdot \mathbf{a}_s^\# \right] \\
&+ \left[\sum_{s=1}^n \mathbf{g}^\# \cdot \partial_{\mathbf{a}_s^\#} I_q \cdot \mathbf{a}_s^\# \right] \otimes \left[\mathbf{g}^\# \cdot \partial_{\mathbf{b}^\#} I_r \cdot \mathbf{b}^\# \right] \\
&+ \left[\sum_{s=1}^n \mathbf{g}^\# \cdot \partial_{\mathbf{a}_s^\#} I_q \cdot \mathbf{a}_s^\# \right] \otimes \left[\sum_{t=1}^n \mathbf{g}^\# \cdot \partial_{\mathbf{a}_t^\#} I_r \cdot \mathbf{a}_t^\# \right] \\
&= \left[\mathbf{b}^\# \overline{\otimes} \mathbf{g}^\# \right] : \left[\partial_{\mathbf{b}^\#} I_q \otimes \partial_{\mathbf{b}^\#} I_r \right] : \left[\mathbf{g}^\# \overline{\otimes} \mathbf{b}^\# \right], \\
&+ \sum_{s=1}^n \left[\mathbf{b}^\# \overline{\otimes} \mathbf{g}^\# \right] : \left[\partial_{\mathbf{b}^\#} I_q \otimes \partial_{\mathbf{a}_s^\#} I_r \right] : \left[\mathbf{g}^\# \overline{\otimes} \mathbf{a}_s^\# \right] \\
&+ \sum_{s=1}^n \left[\mathbf{a}_s^\# \overline{\otimes} \mathbf{g}^\# \right] : \left[\partial_{\mathbf{a}_s^\#} I_q \otimes \partial_{\mathbf{b}^\#} I_r \right] : \left[\mathbf{g}^\# \overline{\otimes} \mathbf{b}^\# \right] \\
&+ \sum_{s,t=1}^n \left[\mathbf{a}_s^\# \overline{\otimes} \mathbf{g}^\# \right] : \left[\partial_{\mathbf{a}_s^\#} I_q \otimes \partial_{\mathbf{a}_t^\#} I_r \right] : \left[\mathbf{g}^\# \overline{\otimes} \mathbf{a}_t^\# \right]
\end{aligned} \tag{2.46}$$

hold. Next, the corresponding relation due to the first contribution in Eq.(2.45) is verified via the representation theorem. Therefore, in view of the spatial setting, the derivatives of the stress generators with respect to \mathbf{g}^b , \mathbf{b}^\sharp and $\mathbf{a}_{1,\dots,n}^\sharp$ have to be computed which are given in Appendix B. Now, the relation for the second derivatives of the invariants reads as

$$\begin{aligned}
 \partial_{\mathbf{g}^b \otimes \mathbf{g}^b}^2 I_q &= [\mathbf{b}^\sharp \overline{\otimes} \mathbf{g}^\sharp] : \partial_{\mathbf{b}^\sharp \otimes \mathbf{b}^\sharp}^2 I_q : [\mathbf{g}^\sharp \overline{\otimes} \mathbf{b}^\sharp] \\
 &+ \sum_{s=1}^n [\mathbf{b}^\sharp \overline{\otimes} \mathbf{g}^\sharp] : \partial_{\mathbf{b}^\sharp \otimes \mathbf{a}_s^\sharp}^2 I_q : [\mathbf{g}^\sharp \overline{\otimes} \mathbf{a}_s^\sharp] \\
 &+ \sum_{s=1}^n [\mathbf{a}_s^\sharp \overline{\otimes} \mathbf{g}^\sharp] : \partial_{\mathbf{a}_s^\sharp \otimes \mathbf{b}^\sharp}^2 I_q : [\mathbf{g}^\sharp \overline{\otimes} \mathbf{b}^\sharp] \\
 &+ \sum_{s,t=1}^n [\mathbf{a}_s^\sharp \overline{\otimes} \mathbf{g}^\sharp] : \partial_{\mathbf{a}_s^\sharp \otimes \mathbf{a}_t^\sharp}^2 I_q : [\mathbf{g}^\sharp \overline{\otimes} \mathbf{a}_t^\sharp]
 \end{aligned} \tag{2.47}$$

and can be verified after some lengthy algebra:

$$\begin{aligned}
 (ii) \quad \partial_{\mathbf{g}^b \otimes \mathbf{g}^b}^2 I_{(ii)} &\doteq [\mathbf{b}^\sharp \overline{\otimes} \mathbf{g}^\sharp] : \partial_{\mathbf{b}^\sharp \otimes \mathbf{b}^\sharp}^2 I_{(ii)} : [\mathbf{g}^\sharp \overline{\otimes} \mathbf{b}^\sharp] \\
 &+ \sum_{s=1}^n [\mathbf{b}^\sharp \overline{\otimes} \mathbf{g}^\sharp] : \partial_{\mathbf{b}^\sharp \otimes \mathbf{a}_s^\sharp}^2 I_{(ii)} : [\mathbf{g}^\sharp \overline{\otimes} \mathbf{a}_s^\sharp] \\
 &+ \sum_{s=1}^n [\mathbf{a}_s^\sharp \overline{\otimes} \mathbf{g}^\sharp] : \partial_{\mathbf{a}_s^\sharp \otimes \mathbf{b}^\sharp}^2 I_{(ii)} : [\mathbf{g}^\sharp \overline{\otimes} \mathbf{b}^\sharp] \\
 &+ \sum_{s,t=1}^n [\mathbf{a}_s^\sharp \overline{\otimes} \mathbf{g}^\sharp] : \partial_{\mathbf{a}_s^\sharp \otimes \mathbf{a}_t^\sharp}^2 I_{(ii)} : [\mathbf{g}^\sharp \overline{\otimes} \mathbf{a}_t^\sharp] \\
 &= [\mathbf{b}^\sharp \overline{\otimes} \mathbf{g}^\sharp] : [\mathbf{g}^b \overline{\otimes} \mathbf{g}^b + \mathbf{g}^b \underline{\otimes} \mathbf{g}^b] : [\mathbf{g}^\sharp \overline{\otimes} \mathbf{b}^\sharp] + \mathbf{0} + \mathbf{0} + \mathbf{0} \\
 &= [\mathbf{b}^\sharp \overline{\otimes} \mathbf{b}^\sharp + \mathbf{b}^\sharp \underline{\otimes} \mathbf{b}^\sharp]
 \end{aligned}$$

$$\begin{aligned}
 (iii) \quad \partial_{\mathbf{g}^b \otimes \mathbf{g}^b}^2 I_{(iii)} &\doteq [\mathbf{b}^\sharp \overline{\otimes} \mathbf{g}^\sharp] : \partial_{\mathbf{b}^\sharp \otimes \mathbf{b}^\sharp}^2 I_{(iii)} : [\mathbf{g}^\sharp \overline{\otimes} \mathbf{b}^\sharp] \\
 &+ \sum_{s=1}^n [\mathbf{b}^\sharp \overline{\otimes} \mathbf{g}^\sharp] : \partial_{\mathbf{b}^\sharp \otimes \mathbf{a}_s^\sharp}^2 I_{(iii)} : [\mathbf{g}^\sharp \overline{\otimes} \mathbf{a}_s^\sharp] \\
 &+ \sum_{s=1}^n [\mathbf{a}_s^\sharp \overline{\otimes} \mathbf{g}^\sharp] : \partial_{\mathbf{a}_s^\sharp \otimes \mathbf{b}^\sharp}^2 I_{(iii)} : [\mathbf{g}^\sharp \overline{\otimes} \mathbf{b}^\sharp] \\
 &+ \sum_{s,t=1}^n [\mathbf{a}_s^\sharp \overline{\otimes} \mathbf{g}^\sharp] : \partial_{\mathbf{a}_s^\sharp \otimes \mathbf{a}_t^\sharp}^2 I_{(iii)} : [\mathbf{g}^\sharp \overline{\otimes} \mathbf{a}_t^\sharp] \\
 &= 3 [\mathbf{b}^\sharp \overline{\otimes} \mathbf{g}^\sharp] : \left[\mathbf{g}^b \overline{\otimes} [\mathbf{g}^b \cdot \mathbf{b}^\sharp \cdot \mathbf{g}^b] + \mathbf{g}^b \underline{\otimes} [\mathbf{g}^b \cdot \mathbf{b}^\sharp \cdot \mathbf{g}^b] \right]^{\text{SYM}} : [\mathbf{g}^\sharp \overline{\otimes} \mathbf{b}^\sharp] \\
 &+ \mathbf{0} + \mathbf{0} + \mathbf{0} \\
 &= 3 \left[\mathbf{b}^\sharp \overline{\otimes} [\mathbf{b}^\sharp \cdot \mathbf{g}^b \cdot \mathbf{b}^\sharp] + \mathbf{b}^\sharp \underline{\otimes} [\mathbf{b}^\sharp \cdot \mathbf{g}^b \cdot \mathbf{b}^\sharp] \right]^{\text{SYM}}
 \end{aligned}$$

$$\begin{aligned}
 (v) \quad \partial_{\mathbf{g}^b \otimes \mathbf{g}^b}^2 I_{(v)} &\doteq [\mathbf{b}^\sharp \overline{\otimes} \mathbf{g}^\sharp] : \partial_{\mathbf{b}^\sharp \otimes \mathbf{b}^\sharp}^2 I_{(v)} : [\mathbf{g}^\sharp \overline{\otimes} \mathbf{b}^\sharp] \\
 &+ \sum_{s=1}^n [\mathbf{b}^\sharp \overline{\otimes} \mathbf{g}^\sharp] : \partial_{\mathbf{b}^\sharp \otimes \mathbf{a}_s^\sharp}^2 I_{(v)} : [\mathbf{g}^\sharp \overline{\otimes} \mathbf{a}_s^\sharp] \\
 &+ \sum_{s=1}^n [\mathbf{a}_s^\sharp \overline{\otimes} \mathbf{g}^\sharp] : \partial_{\mathbf{a}_s^\sharp \otimes \mathbf{b}^\sharp}^2 I_{(v)} : [\mathbf{g}^\sharp \overline{\otimes} \mathbf{b}^\sharp]
 \end{aligned}$$

$$\begin{aligned}
& + \sum_{s,t=1}^n [\mathbf{a}_s^\# \overline{\otimes} \mathbf{g}^\#] : \partial_{\mathbf{a}_s^\# \otimes \mathbf{a}_t^\#}^2 I(v) : [\mathbf{g}^\# \overline{\otimes} \mathbf{a}_t^\#] \\
& = \mathbf{0} + \frac{1}{2} [\mathbf{b}^\# \overline{\otimes} \mathbf{g}^\#] : [\mathbf{g}^b \overline{\otimes} \mathbf{g}^b + \mathbf{g}^b \underline{\otimes} \mathbf{g}^b] : [\mathbf{g}^\# \overline{\otimes} \mathbf{a}_i^\#] \\
& + \frac{1}{2} [\mathbf{a}_i^\# \overline{\otimes} \mathbf{g}^\#] : [\mathbf{g}^b \overline{\otimes} \mathbf{g}^b + \mathbf{g}^b \underline{\otimes} \mathbf{g}^b] : [\mathbf{g}^\# \overline{\otimes} \mathbf{b}^\#] + \mathbf{0} \\
& = [\mathbf{b}^\# \overline{\otimes} \mathbf{a}_i^\# + \mathbf{b}^\# \underline{\otimes} \mathbf{a}_i^\#]^{\text{SYM}}
\end{aligned}$$

(vi)

$$\begin{aligned}
\partial_{\mathbf{g}^b \otimes \mathbf{g}^b}^2 I(v_i) & \doteq [\mathbf{b}^\# \overline{\otimes} \mathbf{g}^\#] : \partial_{\mathbf{b}^\# \otimes \mathbf{b}^\#}^2 I(v_i) : [\mathbf{g}^\# \overline{\otimes} \mathbf{b}^\#] \\
& + \sum_{s=1}^n [\mathbf{b}^\# \overline{\otimes} \mathbf{g}^\#] : \partial_{\mathbf{b}^\# \otimes \mathbf{a}_s^\#}^2 I(v_i) : [\mathbf{g}^\# \overline{\otimes} \mathbf{a}_s^\#] \\
& + \sum_{s=1}^n [\mathbf{a}_s^\# \overline{\otimes} \mathbf{g}^\#] : \partial_{\mathbf{a}_s^\# \otimes \mathbf{b}^\#}^2 I(v_i) : [\mathbf{g}^\# \overline{\otimes} \mathbf{b}^\#] \\
& + \sum_{s,t=1}^n [\mathbf{a}_s^\# \overline{\otimes} \mathbf{g}^\#] : \partial_{\mathbf{a}_s^\# \otimes \mathbf{a}_t^\#}^2 I(v_i) : [\mathbf{g}^\# \overline{\otimes} \mathbf{a}_t^\#] \\
& = [\mathbf{b}^\# \overline{\otimes} \mathbf{g}^\#] : [\mathbf{c}^b \overline{\otimes} [\mathbf{c}^b \cdot \mathbf{a}_j^\# \cdot \mathbf{g}^b \cdot \mathbf{a}_i^\# \cdot \mathbf{c}^b]^{\text{sym}} \\
& \quad + \mathbf{c}^b \underline{\otimes} [\mathbf{c}^b \cdot \mathbf{a}_j^\# \cdot \mathbf{g}^b \cdot \mathbf{a}_i^\# \cdot \mathbf{c}^b]^{\text{sym}}]^{\text{SYM}} : [\mathbf{g}^\# \overline{\otimes} \mathbf{b}^\#] \\
& - \frac{1}{2} [\mathbf{b}^\# \overline{\otimes} \mathbf{g}^\#] : [\mathbf{c}^b \overline{\otimes} [\mathbf{c}^b \cdot \mathbf{a}_j^\# \cdot \mathbf{g}^b] + \mathbf{c}^b \underline{\otimes} [\mathbf{c}^b \cdot \mathbf{a}_j^\# \cdot \mathbf{g}^b]]^{\text{SYM}} : [\mathbf{g}^\# \overline{\otimes} \mathbf{a}_i^\#] \\
& - \frac{1}{2} [\mathbf{b}^\# \overline{\otimes} \mathbf{g}^\#] : [\mathbf{c}^b \overline{\otimes} [\mathbf{c}^b \cdot \mathbf{a}_i^\# \cdot \mathbf{g}^b] + \mathbf{c}^b \underline{\otimes} [\mathbf{c}^b \cdot \mathbf{a}_i^\# \cdot \mathbf{g}^b]]^{\text{SYM}} : [\mathbf{g}^\# \overline{\otimes} \mathbf{a}_j^\#] \\
& - \frac{1}{2} [\mathbf{a}_i^\# \overline{\otimes} \mathbf{g}^\#] : [\mathbf{c}^b \overline{\otimes} [\mathbf{g}^b \cdot \mathbf{a}_j^\# \cdot \mathbf{c}^b] + \mathbf{c}^b \underline{\otimes} [\mathbf{g}^b \cdot \mathbf{a}_j^\# \cdot \mathbf{c}^b]]^{\text{SYM}} : [\mathbf{g}^\# \overline{\otimes} \mathbf{b}^\#] \\
& - \frac{1}{2} [\mathbf{a}_j^\# \overline{\otimes} \mathbf{g}^\#] : [\mathbf{c}^b \overline{\otimes} [\mathbf{g}^b \cdot \mathbf{a}_i^\# \cdot \mathbf{c}^b] + \mathbf{c}^b \underline{\otimes} [\mathbf{g}^b \cdot \mathbf{a}_i^\# \cdot \mathbf{c}^b]]^{\text{SYM}} : [\mathbf{g}^\# \overline{\otimes} \mathbf{b}^\#] \\
& + \frac{1}{2} [\mathbf{a}_i^\# \overline{\otimes} \mathbf{g}^\#] : [\mathbf{g}^b \overline{\otimes} \mathbf{c}^b + \mathbf{g}^b \underline{\otimes} \mathbf{c}^b]^{\text{SYM}} : [\mathbf{g}^\# \overline{\otimes} \mathbf{a}_j^\#] \\
& + \frac{1}{2} [\mathbf{a}_j^\# \overline{\otimes} \mathbf{g}^\#] : [\mathbf{g}^b \overline{\otimes} \mathbf{c}^b + \mathbf{g}^b \underline{\otimes} \mathbf{c}^b]^{\text{SYM}} : [\mathbf{g}^\# \overline{\otimes} \mathbf{a}_i^\#] \\
& = \mathbf{0}
\end{aligned}$$

which proves essentially the spatial setting of Eq.(2.39). The outline of the material version is straightforward and thus not highlighted here.

Remark 2.2 In analogy to Remark 2.1, the specific isotropic case for $\mathbf{A}_{1,\dots,n}^\# \doteq \mathbf{0}_{1,\dots,n}$ yields

$$\boxed{
\begin{aligned}
\mathbf{e}^\# & = 4 [\mathbf{b}^\# \overline{\otimes} \mathbf{g}^\#] : \partial_{\mathbf{b}^\# \otimes \mathbf{b}^\#}^2 \psi_0^t(\mathbf{g}^b, \mathbf{b}^\#; \mathbf{X}) : [\mathbf{g}^\# \overline{\otimes} \mathbf{b}^\#], \\
\mathbf{E}^\# & = 4 [\mathbf{G}^\# \overline{\otimes} \mathbf{B}^\#] : \partial_{\mathbf{G}^\# \otimes \mathbf{G}^\#}^2 \psi_0^0(\mathbf{C}^b, \mathbf{G}^\#; \mathbf{X}) : [\mathbf{B}^\# \overline{\otimes} \mathbf{G}^\#].
\end{aligned}
} \quad (2.48)$$

For the proof of the spatial representation in the isotropic case, see Miehe [Mie94, A1]. Again, the introduction of exclusively spherical elements in the additional tensor series, $\mathbf{A}_{1,\dots,n}^\# \propto \mathbf{G}^\#$ or the incorporation of scalar-valued fields instead of tensorial quantities results in tangent operators which characterise an isotropic setting.

2.4 Examples

In the sequel, we consider two simple applications of an anisotropic material. On the one hand, orthotropic symmetry is incorporated via two ($n = 2$) constant (in \mathcal{B}_0) rank one structural tensors

$\mathbf{A}_{1,2}^\# \doteq A_{1,2}^\# \mathbf{N}^\# \otimes A_{1,2}^\# \mathbf{N}^\#$ with $A_{1,2}^\# \mathbf{N}^\# \in \mathbb{U}^2 : T^* \mathcal{B}_0 \rightarrow \mathbb{R}$. We thereby highlight ‘‘analytical’’ expressions of interest like the stress field and the corresponding tangent operator in detail. On the other hand, numerical examples incorporating transversely isotropic symmetry ($n = 1$, $\mathbf{A}_1^\# \doteq \text{const}$ in \mathcal{B}_0) are discussed within the homogeneous deformation in simple shear and a general, inhomogeneous finite element setting.

2.4.1 Analytical example within orthotropic symmetry

The considered spatial orthotropic setting is defined by two rank one structural tensors $\mathbf{a}_{1,2}^\# = \boldsymbol{\varphi}_* \mathbf{A}_{1,2}^\#$, compare Eq.(2.11). For the sake of generality, we assume $A_1^\# \mathbf{N}^\# \cdot \mathbf{G}^b \cdot A_2^\# \mathbf{N}^\# = \text{const} \neq 0$. In this context the free Helmholtz energy density $\psi_0^t = \psi_0^t(\mathbf{g}^b, \mathbf{b}^\#, \mathbf{a}_{1,2}^\#; \mathbf{X}) = \psi_0^t(I_{1,\dots,8}; \mathbf{X})$ is determined via the following set of eight invariants

$$\begin{aligned} g^b b^\# I_1 &= \mathbf{g}^b : \mathbf{b}^\#, & g^b b^\# I_2 &= [\mathbf{g}^b \cdot \mathbf{b}^\# \cdot \mathbf{g}^b] : \mathbf{b}^\#, & g^b b^\# I_3 &= [\mathbf{g}^b \cdot [\mathbf{b}^\# \cdot \mathbf{g}^b]^2] : \mathbf{b}^\#, \\ g^b a_{1,2}^\# I_4 &= \mathbf{g}^b : \mathbf{a}_1^\#, & g^b a_{1,2}^\# I_5 &= [\mathbf{g}^b \cdot \mathbf{b}^\# \cdot \mathbf{g}^b] : \mathbf{a}_1^\#, & & \\ g^b a_{1,2}^\# I_6 &= \mathbf{g}^b : \mathbf{a}_2^\#, & g^b a_{1,2}^\# I_7 &= [\mathbf{g}^b \cdot \mathbf{b}^\# \cdot \mathbf{g}^b] : \mathbf{a}_2^\#, & g^b a_{1,2}^\# I_8 &= [\mathbf{g}^b \cdot \mathbf{a}_1^\# \cdot \mathbf{c}^b] : \mathbf{a}_2^\#. \end{aligned} \quad (2.49)$$

The Kirchhoff stress tensor turns out to decompose additively into an isotropic and anisotropic contribution $\boldsymbol{\tau}^\# = \text{iso} \boldsymbol{\tau}^\# + \text{ani} \boldsymbol{\tau}^\#$ $\ddagger\ddagger$. Consequently, with emphasis on the derivatives of the free Helmholtz energy density, these particular contributions read

$$\begin{aligned} \text{iso} \boldsymbol{\tau}^\# &= 2 \sum_{q=1}^3 \partial_{I_q} \psi_0^t \mathbf{g}^\# \cdot \partial_{\mathbf{b}^\#} I_q \cdot \mathbf{b}^\# = 2 \sum_{q=1}^3 q \partial_{I_q} \psi_0^t \mathbf{b}^\# \cdot [\mathbf{g}^\# \cdot \mathbf{b}^\#]^{[q-1]}, \\ \text{ani} \boldsymbol{\tau}^\# &= 2 \sum_{q=4}^8 \left[\partial_{I_q} \psi_0^t \mathbf{g}^\# \cdot \partial_{\mathbf{b}^\#} I_q \cdot \mathbf{b}^\# + \sum_{s=1}^2 \partial_{I_q} \psi_0^t \mathbf{g}^\# \cdot \partial_{\mathbf{a}_s^\#} I_q \cdot \mathbf{a}_s^\# \right]. \end{aligned} \quad (2.50)$$

Next, the invariants $g^b a_{1,2}^\# I_{4,\dots,8}$ as given in Eq.(2.49) are incorporated which results in

$$\begin{aligned} \text{ani} \boldsymbol{\tau}^\# &= 2 \partial_{I_4} \psi_0^t \mathbf{a}_1^\# + 4 \partial_{I_5} \psi_0^t [\mathbf{b}^\# \cdot \mathbf{g}^b \cdot \mathbf{a}_1^\#]^{\text{sym}} \\ &+ 2 \partial_{I_6} \psi_0^t \mathbf{a}_2^\# + 4 \partial_{I_7} \psi_0^t [\mathbf{b}^\# \cdot \mathbf{g}^b \cdot \mathbf{a}_2^\#]^{\text{sym}} \\ &+ 2 \partial_{I_8} \psi_0^t [\mathbf{a}_1^\# \cdot \mathbf{g}^b \cdot \mathbf{a}_2^\#]^{\text{sym}}. \end{aligned} \quad (2.51)$$

Based on this, we now focus on the outline of the isotropic and the anisotropic contribution of the spatial tangent operator ($\mathbf{e}^\# = \text{iso} \mathbf{e}^\# + \text{ani} \mathbf{e}^\#$) defined by

$$\begin{aligned} \text{iso} \mathbf{e}^\# &= 4 \sum_{q=1}^3 \partial_{I_q} \psi_0^t [\mathbf{b}^\# \overline{\otimes} \mathbf{g}^\#] : [\partial_{\mathbf{b}^\# \otimes \mathbf{b}^\#}^2 I_q] : [\mathbf{g}^\# \overline{\otimes} \mathbf{b}^\#] \\ &+ 4 \sum_{q=1}^3 \sum_{s=1}^2 \partial_{I_q} \psi_0^t [\mathbf{b}^\# \overline{\otimes} \mathbf{g}^\#] : [\partial_{\mathbf{b}^\# \otimes \mathbf{a}_s^\#}^2 I_q] : [\mathbf{g}^\# \overline{\otimes} \mathbf{a}_s^\#] \\ &+ 4 \sum_{q=1}^3 \sum_{s=1}^2 \partial_{I_q} \psi_0^t [\mathbf{a}_s^\# \overline{\otimes} \mathbf{g}^\#] : [\partial_{\mathbf{a}_s^\# \otimes \mathbf{b}^\#}^2 I_q] : [\mathbf{g}^\# \overline{\otimes} \mathbf{b}^\#] \\ &+ 4 \sum_{q=1}^3 \sum_{s,t=1}^2 \partial_{I_q} \psi_0^t [\mathbf{a}_s^\# \overline{\otimes} \mathbf{g}^\#] : [\partial_{\mathbf{a}_s^\# \otimes \mathbf{a}_t^\#}^2 I_q] : [\mathbf{g}^\# \overline{\otimes} \mathbf{a}_t^\#] \\ &+ 4 \sum_{q,r=1}^3 \partial_{I_q I_r}^2 \psi_0^t [\mathbf{b}^\# \overline{\otimes} \mathbf{g}^\#] : [\partial_{\mathbf{b}^\#} I_q \otimes \partial_{\mathbf{b}^\#} I_r] : [\mathbf{g}^\# \overline{\otimes} \mathbf{b}^\#] \\ &+ 4 \sum_{q,r=1}^3 \sum_{s=1}^2 \partial_{I_q I_r}^2 \psi_0^t [\mathbf{b}^\# \overline{\otimes} \mathbf{g}^\#] : [\partial_{\mathbf{b}^\#} I_q \otimes \partial_{\mathbf{a}_s^\#} I_r] : [\mathbf{g}^\# \overline{\otimes} \mathbf{a}_s^\#] \\ &+ 4 \sum_{q,r=1}^3 \sum_{s=1}^2 \partial_{I_q I_r}^2 \psi_0^t [\mathbf{a}_s^\# \overline{\otimes} \mathbf{g}^\#] : [\partial_{\mathbf{a}_s^\#} I_q \otimes \partial_{\mathbf{b}^\#} I_r] : [\mathbf{g}^\# \overline{\otimes} \mathbf{b}^\#] \\ &+ 4 \sum_{q,r=1}^3 \sum_{s,t=1}^2 \partial_{I_q I_r}^2 \psi_0^t [\mathbf{a}_s^\# \overline{\otimes} \mathbf{g}^\#] : [\partial_{\mathbf{a}_s^\#} I_q \otimes \partial_{\mathbf{a}_t^\#} I_r] : [\mathbf{g}^\# \overline{\otimes} \mathbf{a}_t^\#], \end{aligned} \quad (2.52)$$

$\ddagger\ddagger$ Please note that the spatial stress field $\text{iso} \boldsymbol{\tau}^\#$ does not represent an isotropic constitutive equation if the invariants $g^b b^\# I_{1,2,3}$ and $g^b a_{1,2}^\# I_{4,\dots,8}$ are coupled within the chosen free Helmholtz energy density.

and

$$\begin{aligned}
\text{ani } \mathbf{e}^\# &= 4 \sum_{q=4}^8 \partial_{I_q} \psi_0^t \quad [\mathbf{b}^\# \overline{\otimes} \mathbf{g}^\#] : [\partial_{\mathbf{b}^\# \otimes \mathbf{b}^\#}^2 I_q] : [\mathbf{g}^\# \overline{\otimes} \mathbf{b}^\#] \\
&+ 4 \sum_{q=4}^8 \sum_{s=1}^2 \partial_{I_q} \psi_0^t \quad [\mathbf{b}^\# \overline{\otimes} \mathbf{g}^\#] : [\partial_{\mathbf{b}^\# \otimes \mathbf{a}_s^\#}^2 I_q] : [\mathbf{g}^\# \overline{\otimes} \mathbf{a}_s^\#] \\
&+ 4 \sum_{q=4}^8 \sum_{s=1}^2 \partial_{I_q} \psi_0^t \quad [\mathbf{a}_s^\# \overline{\otimes} \mathbf{g}^\#] : [\partial_{\mathbf{a}_s^\# \otimes \mathbf{b}^\#}^2 I_q] : [\mathbf{g}^\# \overline{\otimes} \mathbf{b}^\#] \\
&+ 4 \sum_{q=4}^8 \sum_{s,t=1}^2 \partial_{I_q} \psi_0^t \quad [\mathbf{a}_s^\# \overline{\otimes} \mathbf{g}^\#] : [\partial_{\mathbf{a}_s^\# \otimes \mathbf{a}_t^\#}^2 I_q] : [\mathbf{g}^\# \overline{\otimes} \mathbf{a}_t^\#] \\
&+ 8 \sum_{q=4}^8 \sum_{r=1}^3 \partial_{I_q I_r}^2 \psi_0^t \quad [\mathbf{b}^\# \overline{\otimes} \mathbf{g}^\#] : [\partial_{\mathbf{b}^\#} I_q \otimes \partial_{\mathbf{b}^\#} I_r]^{\text{SYM}} : [\mathbf{g}^\# \overline{\otimes} \mathbf{b}^\#] \\
&+ 8 \sum_{q=4}^8 \sum_{r=1}^3 \sum_{s=1}^2 \partial_{I_q I_r}^2 \psi_0^t \quad [\mathbf{b}^\# \overline{\otimes} \mathbf{g}^\#] : [\partial_{\mathbf{b}^\#} I_q \otimes \partial_{\mathbf{a}_s^\#} I_r]^{\text{SYM}} : [\mathbf{g}^\# \overline{\otimes} \mathbf{a}_s^\#] \\
&+ 8 \sum_{q=4}^8 \sum_{r=1}^3 \sum_{s=1}^2 \partial_{I_q I_r}^2 \psi_0^t \quad [\mathbf{a}_s^\# \overline{\otimes} \mathbf{g}^\#] : [\partial_{\mathbf{a}_s^\#} I_q \otimes \partial_{\mathbf{b}^\#} I_r]^{\text{SYM}} : [\mathbf{g}^\# \overline{\otimes} \mathbf{b}^\#] \\
&+ 8 \sum_{q=4}^8 \sum_{r=1}^3 \sum_{s,t=1}^2 \partial_{I_q I_r}^2 \psi_0^t \quad [\mathbf{a}_s^\# \overline{\otimes} \mathbf{g}^\#] : [\partial_{\mathbf{a}_s^\#} I_q \otimes \partial_{\mathbf{a}_t^\#} I_r]^{\text{SYM}} : [\mathbf{g}^\# \overline{\otimes} \mathbf{a}_t^\#] \\
&+ 4 \sum_{q,r=4}^8 \partial_{I_q I_r}^2 \psi_0^t \quad [\mathbf{b}^\# \overline{\otimes} \mathbf{g}^\#] : [\partial_{\mathbf{b}^\#} I_q \otimes \partial_{\mathbf{b}^\#} I_r] : [\mathbf{g}^\# \overline{\otimes} \mathbf{b}^\#] \\
&+ 4 \sum_{q,r=4}^8 \sum_{s=1}^2 \partial_{I_q I_r}^2 \psi_0^t \quad [\mathbf{b}^\# \overline{\otimes} \mathbf{g}^\#] : [\partial_{\mathbf{b}^\#} I_q \otimes \partial_{\mathbf{a}_s^\#} I_r] : [\mathbf{g}^\# \overline{\otimes} \mathbf{a}_s^\#] \\
&+ 4 \sum_{q,r=4}^8 \sum_{s=1}^2 \partial_{I_q I_r}^2 \psi_0^t \quad [\mathbf{a}_s^\# \overline{\otimes} \mathbf{g}^\#] : [\partial_{\mathbf{a}_s^\#} I_q \otimes \partial_{\mathbf{b}^\#} I_r] : [\mathbf{g}^\# \overline{\otimes} \mathbf{b}^\#] \\
&+ 4 \sum_{q,r=4}^8 \sum_{s,t=1}^2 \partial_{I_q I_r}^2 \psi_0^t \quad [\mathbf{a}_s^\# \overline{\otimes} \mathbf{g}^\#] : [\partial_{\mathbf{a}_s^\#} I_q \otimes \partial_{\mathbf{a}_t^\#} I_r] : [\mathbf{g}^\# \overline{\otimes} \mathbf{a}_t^\#].
\end{aligned} \tag{2.53}$$

Finally, after some tedious but straightforward computations, we end up with

$$\begin{aligned}
\text{ani } \mathbf{e}^\# &= 4 \partial_{I_5} \psi_0^t [\mathbf{b}^\# \overline{\otimes} \mathbf{a}_1^\# + \mathbf{b}^\# \underline{\otimes} \mathbf{a}_1^\#]^{\text{SYM}} \\
&+ 4 \partial_{I_7} \psi_0^t [\mathbf{b}^\# \overline{\otimes} \mathbf{a}_2^\# + \mathbf{b}^\# \underline{\otimes} \mathbf{a}_2^\#]^{\text{SYM}} + 8 \partial_{I_1 I_4}^2 \psi_0^t [\mathbf{b}^\# \otimes \mathbf{a}_1^\#]^{\text{SYM}} \\
&+ 16 \partial_{I_1 I_5}^2 \psi_0^t \left[\mathbf{b}^\# \otimes [\mathbf{b}^\# \cdot \mathbf{g}^\# \cdot \mathbf{a}_1^\#]^{\text{sym}} \right]^{\text{SYM}} + 8 \partial_{I_1 I_6}^2 \psi_0^t [\mathbf{b}^\# \otimes \mathbf{a}_2^\#]^{\text{SYM}} \\
&+ 16 \partial_{I_1 I_7}^2 \psi_0^t \left[\mathbf{b}^\# \otimes [\mathbf{b}^\# \cdot \mathbf{g}^\# \cdot \mathbf{a}_2^\#]^{\text{sym}} \right]^{\text{SYM}} \\
&+ 8 \partial_{I_1 I_8}^2 \psi_0^t \left[\mathbf{b}^\# \otimes [\mathbf{a}_1^\# \cdot \mathbf{c}^\# \cdot \mathbf{a}_2^\#]^{\text{sym}} \right]^{\text{SYM}} \\
&+ 8 \partial_{I_2 I_4}^2 \psi_0^t \left[[\mathbf{b}^\# \cdot \mathbf{g}^\# \cdot \mathbf{b}^\#] \otimes \mathbf{a}_1^\# \right]^{\text{SYM}} \\
&+ 8 \partial_{I_2 I_5}^2 \psi_0^t \left[[\mathbf{b}^\# \cdot \mathbf{g}^\# \cdot \mathbf{b}^\#] \otimes [\mathbf{b}^\# \cdot \mathbf{g}^\# \cdot \mathbf{a}_1^\#]^{\text{sym}} \right]^{\text{SYM}} \\
&+ 8 \partial_{I_2 I_6}^2 \psi_0^t \left[[\mathbf{b}^\# \cdot \mathbf{g}^\# \cdot \mathbf{b}^\#] \otimes \mathbf{a}_2^\# \right]^{\text{SYM}} \\
&+ 8 \partial_{I_2 I_7}^2 \psi_0^t \left[[\mathbf{b}^\# \cdot \mathbf{g}^\# \cdot \mathbf{b}^\#] \otimes [\mathbf{b}^\# \cdot \mathbf{g}^\# \cdot \mathbf{a}_2^\#]^{\text{sym}} \right]^{\text{SYM}} \\
&+ 16 \partial_{I_2 I_8}^2 \psi_0^t \left[[\mathbf{b}^\# \cdot \mathbf{g}^\# \cdot \mathbf{b}^\#] \otimes [\mathbf{a}_1^\# \cdot \mathbf{c}^\# \cdot \mathbf{a}_2^\#]^{\text{sym}} \right]^{\text{SYM}} \\
&+ 24 \partial_{I_3 I_4}^2 \psi_0^t \left[[\mathbf{b}^\# \cdot [\mathbf{g}^\# \cdot \mathbf{b}^\#]^2] \otimes \mathbf{a}_1^\# \right]^{\text{SYM}} \\
&+ 48 \partial_{I_3 I_5}^2 \psi_0^t \left[[\mathbf{b}^\# \cdot [\mathbf{g}^\# \cdot \mathbf{b}^\#]^2] \otimes [\mathbf{b}^\# \cdot \mathbf{g}^\# \cdot \mathbf{a}_1^\#]^{\text{sym}} \right]^{\text{SYM}} \\
&+ 24 \partial_{I_3 I_6}^2 \psi_0^t \left[[\mathbf{b}^\# \cdot [\mathbf{g}^\# \cdot \mathbf{b}^\#]^2] \otimes \mathbf{a}_2^\# \right]^{\text{SYM}} \\
&+ 48 \partial_{I_3 I_7}^2 \psi_0^t \left[[\mathbf{b}^\# \cdot [\mathbf{g}^\# \cdot \mathbf{b}^\#]^2] \otimes [\mathbf{b}^\# \cdot \mathbf{g}^\# \cdot \mathbf{a}_2^\#]^{\text{sym}} \right]^{\text{SYM}}
\end{aligned} \tag{2.54}$$

$$\begin{aligned}
& + 48 \partial_{I_3 I_8}^2 \psi_0^t \left[\left[\mathbf{b}^\# \cdot [\mathbf{g}^b \cdot \mathbf{b}^\#]^2 \right] \otimes [\mathbf{a}_1^\# \cdot \mathbf{c}^b \cdot \mathbf{a}_2^\#]^{\text{sym}} \right]^{\text{SYM}} \\
& + 4 \partial_{I_4 I_4}^2 \psi_0^t [\mathbf{a}_1^\# \otimes \mathbf{a}_1^\#] + 32 \partial_{I_4 I_5}^2 \psi_0^t \left[\mathbf{a}_1^\# \otimes [\mathbf{b}^\# \cdot \mathbf{g}^b \cdot \mathbf{a}_1^\#]^{\text{sym}} \right]^{\text{SYM}} \\
& + 16 \partial_{I_4 I_6}^2 \psi_0^t [\mathbf{a}_1^\# \otimes \mathbf{a}_2^\#]^{\text{SYM}} + 32 \partial_{I_4 I_7}^2 \psi_0^t \left[\mathbf{a}_1^\# \otimes [\mathbf{b}^\# \cdot \mathbf{g}^b \cdot \mathbf{a}_2^\#]^{\text{sym}} \right]^{\text{SYM}} \\
& + 16 \partial_{I_4 I_8}^2 \psi_0^t \left[\mathbf{a}_1^\# \otimes [\mathbf{a}_1^\# \cdot \mathbf{c}^b \cdot \mathbf{a}_2^\#]^{\text{sym}} \right]^{\text{SYM}} \\
& + 32 \partial_{I_5 I_5}^2 \psi_0^t \left[[\mathbf{b}^\# \cdot \mathbf{g}^b \cdot \mathbf{a}_1^\#]^{\text{sym}} \otimes [\mathbf{b}^\# \cdot \mathbf{g}^b \cdot \mathbf{a}_1^\#]^{\text{sym}} \right] \\
& + 32 \partial_{I_5 I_2}^2 \psi_0^t \left[[\mathbf{b}^\# \cdot \mathbf{g}^b \cdot \mathbf{a}_1^\#]^{\text{sym}} \otimes \mathbf{a}_2^\# \right]^{\text{SYM}} \\
& + 64 \partial_{I_5 I_7}^2 \psi_0^t \left[[\mathbf{b}^\# \cdot \mathbf{g}^b \cdot \mathbf{a}_1^\#]^{\text{sym}} \otimes [\mathbf{b}^\# \cdot \mathbf{g}^b \cdot \mathbf{a}_2^\#]^{\text{sym}} \right]^{\text{SYM}} \\
& + 32 \partial_{I_5 I_8}^2 \psi_0^t \left[[\mathbf{b}^\# \cdot \mathbf{g}^b \cdot \mathbf{a}_1^\#]^{\text{sym}} \otimes [\mathbf{a}_1^\# \cdot \mathbf{c}^b \cdot \mathbf{a}_2^\#]^{\text{sym}} \right]^{\text{SYM}} \\
& + 4 \partial_{I_6 I_6}^2 \psi_0^t [\mathbf{a}_2^\# \otimes \mathbf{a}_2^\#] + 32 \partial_{I_6 I_7}^2 \psi_0^t \left[\mathbf{a}_2^\# \otimes [\mathbf{b}^\# \cdot \mathbf{g}^b \cdot \mathbf{a}_2^\#]^{\text{sym}} \right]^{\text{SYM}} \\
& + 16 \partial_{I_6 I_8}^2 \psi_0^t \left[\mathbf{a}_2^\# \otimes [\mathbf{a}_1^\# \cdot \mathbf{c}^b \cdot \mathbf{a}_2^\#]^{\text{sym}} \right]^{\text{SYM}} \\
& + 16 \partial_{I_7 I_7}^2 \psi_0^t \left[[\mathbf{b}^\# \cdot \mathbf{g}^b \cdot \mathbf{a}_2^\#]^{\text{sym}} \otimes [\mathbf{b}^\# \cdot \mathbf{g}^b \cdot \mathbf{a}_2^\#]^{\text{sym}} \right]^{\text{SYM}} \\
& + 32 \partial_{I_7 I_8}^2 \psi_0^t \left[[\mathbf{b}^\# \cdot \mathbf{g}^b \cdot \mathbf{a}_2^\#]^{\text{sym}} \otimes [\mathbf{a}_1^\# \cdot \mathbf{c}^b \cdot \mathbf{a}_2^\#]^{\text{sym}} \right]^{\text{SYM}} \\
& + 4 \partial_{I_8 I_8}^2 \psi_0^t \left[[\mathbf{a}_1^\# \cdot \mathbf{c}^b \cdot \mathbf{a}_2^\#]^{\text{sym}} \otimes [\mathbf{a}_1^\# \cdot \mathbf{c}^b \cdot \mathbf{a}_2^\#]^{\text{sym}} \right].
\end{aligned}$$

Again, the outline for the material setting is straightforward and thus not highlighted here.

2.4.2 Numerical example within transversely isotropic symmetry

In the sequel we adopt a Mooney–Rivlin term for the isotropic part of the free Helmholtz energy density $\text{iso}\psi_0^t$ as the essential constitutive function and an additional anisotropic exponential contribution $\text{ani}\psi_0^t$ which accounts for transversal isotropy

$$\psi_0^t(\mathbf{g}^b, \mathbf{b}^\#, \mathbf{a}_1^\#; \mathbf{X}) \doteq \text{iso}\psi_0^t(g^b b^\# I_{1,2,3}; \mathbf{X}) + \text{ani}\psi_0^t(g^b b^\# I_{1,2,3}, g^b a_{1,2}^\# I_{4,5}; \mathbf{X}) \quad (2.55)$$

compare Eq.(2.49). Both representations are reiterated in detail in Appendices C.1 and C.2 and the set of chosen material parameters reads as

$$\begin{aligned}
c_1 &= 80, & c_2 &= 200, & \lambda^p &= 10, \\
\alpha &= 1, & \beta &= 1, & \delta &= 0.75, \\
\epsilon &= 0.5, & \eta &= 1, & n &= 1.25, \\
N_1^\# \vartheta^1 &= 36.86^\circ, & N_1^\# \vartheta^2 &= 76.69^\circ,
\end{aligned} \quad (2.56)$$

whereby the spherical coordinates $N_1^\# \vartheta^{1,2}$ define the orientation of the unit–vector that determines the incorporated structural tensor, compare Appendix D.2. For further investigations on the numerical treatment of anisotropic hyper–elastic materials at finite strains within a structural tensor setting, especially for the transversely isotropic case with application to compressible and incompressible materials, we refer to the contributions by Weiss et al. [WMG96] and Bonet and Burton [BB98].

2.4.2.1 Simple shear

We discuss a homogeneous deformation in simple shear which is determined by $\mathbf{F} = \mathbf{I} + \gamma \mathbf{e}_1 \otimes \mathbf{e}^2$ when referring to a Cartesian frame with $\mathbf{I} = \delta_j^i \mathbf{e}_i \otimes \mathbf{e}^j$ and the scalar γ characterises the shear number.

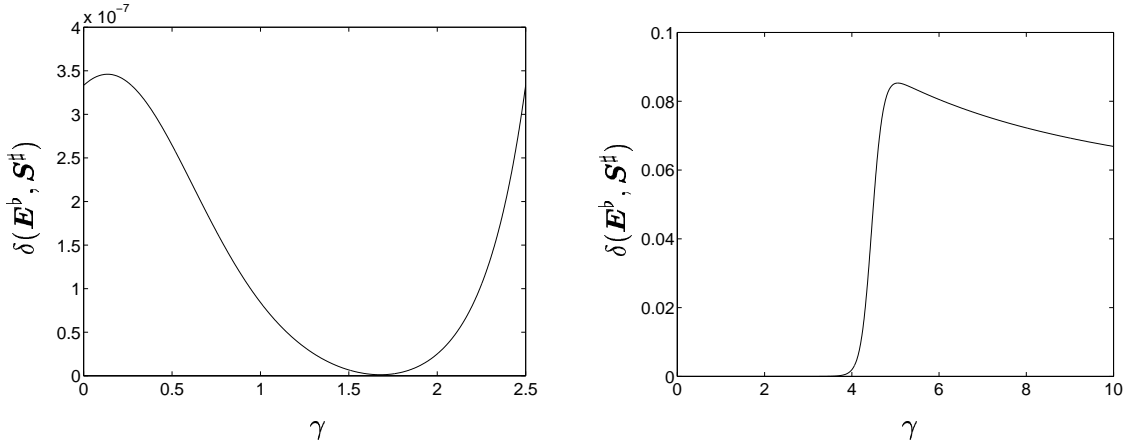


Figure 2.1: Simple shear: Anisotropy measure $\delta(\mathbf{E}^b, \mathbf{S}^\sharp)$ for $\gamma \in [0.0, 2.5]$ (left) and $\gamma \in [0.0, 10.0]$ (right).

As a typical indicator for anisotropy, the non-coaxiality of strain and stress fields is highlighted in Figure 2.1 by monitoring the anisotropy measure $\delta(\mathbf{E}^b, \mathbf{S}^\sharp)$, compare Appendix D.1. Obviously, it turns out that the degree of anisotropy shows a strong dependence on the shear number γ . Moreover, the determinant of the acoustic tensor at $\gamma = 3.5$ is highlighted in Figure 2.2 with respect to the spherical coordinates which characterise the propagation direction ($\mathbf{n}^b \doteq \mathbf{n}^b(n^b, \vartheta^{1,2})$), see Appendix D.3 for a reminder on the underlying theory. We observe a striking difference when comparing the introduced anisotropic setting ($\alpha = 1$) to an isotropic material ($\alpha = 0$).

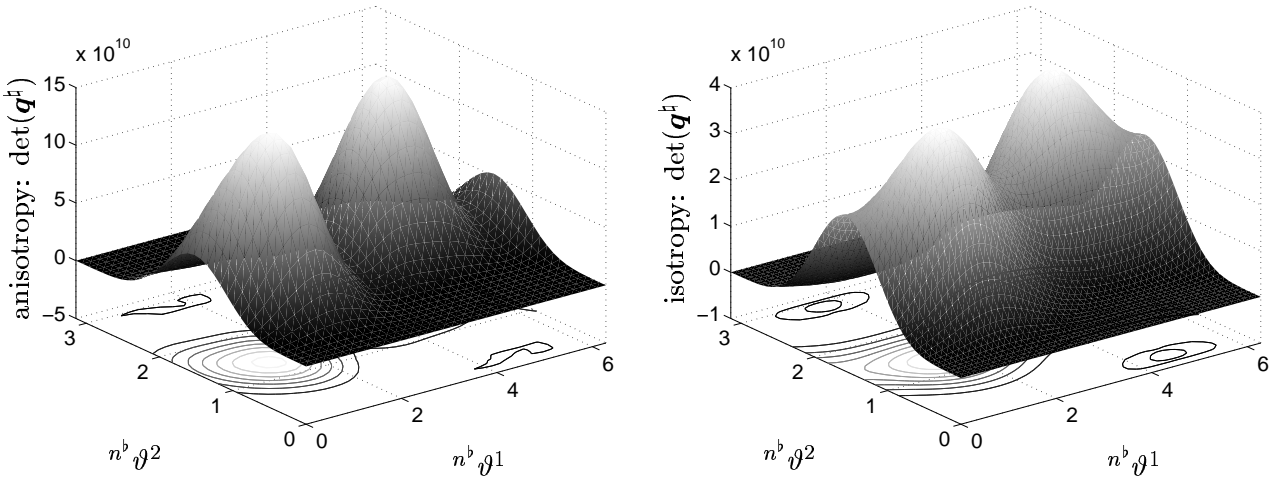


Figure 2.2: Simple shear: Determinant of the acoustic tensor \mathbf{q}^\sharp at $\gamma = 3.5$; anisotropic setting with $\alpha = 1$ (left) and isotropic setting with $\alpha = 0$ (right).

2.4.2.2 Cook's problem

Within the subsequent finite element example, we investigate a three-dimensional version of the classical two-dimensional Cook's membrane problem. The standard discretisation in the $\mathbf{e}_{1,2}$ plane is thus expanded into the \mathbf{e}_3 direction (when referring to a Cartesian frame). Geometry, as well as the boundary and loading conditions, are visualised in Figure 2.3 whereby we chose the following parameters: $L = 48$, $H_1 = 44$, $H_2 = 16$, $T = 4$. The discretisation consists of $16 \times 16 \times 4$ eight node bricks (Q1E9), whereby we invoke enhanced elements as advocated by Simo and Armero [SA92]. Furthermore, the conservative force \mathbf{F} is considered as the resultant of a continuous shear stress with respect to the undeformed configuration. Concerning the numerical implementation, a Lagrangian parametrisation in terms of spatial fields is chosen throughout this work. For the sake of brevity, we make no

further comments on the applied non-linear finite element setting but refer the reader to the books by Oden [Ode72] and Hughes [Hug00] for more background information.

Since the incorporated direction which characterises the transversely isotropic symmetry of the modelled material does not lie in the $\mathbf{e}_{1,2}$ plane, we consequently observe a severe out-of-plane deformation. Figures 2.3 and 2.4 show different views on the deformed mesh at $\|\mathbf{F}\| = 4.5 \times 10^3$. Moreover, we study the displacement of the mid point node at the top corner of the specimen, ${}^{\text{top}}\mathbf{u}$, see Figure 2.5. In order to compare these results to an isotropic setting, we simply set $\alpha \doteq 0$. Figure

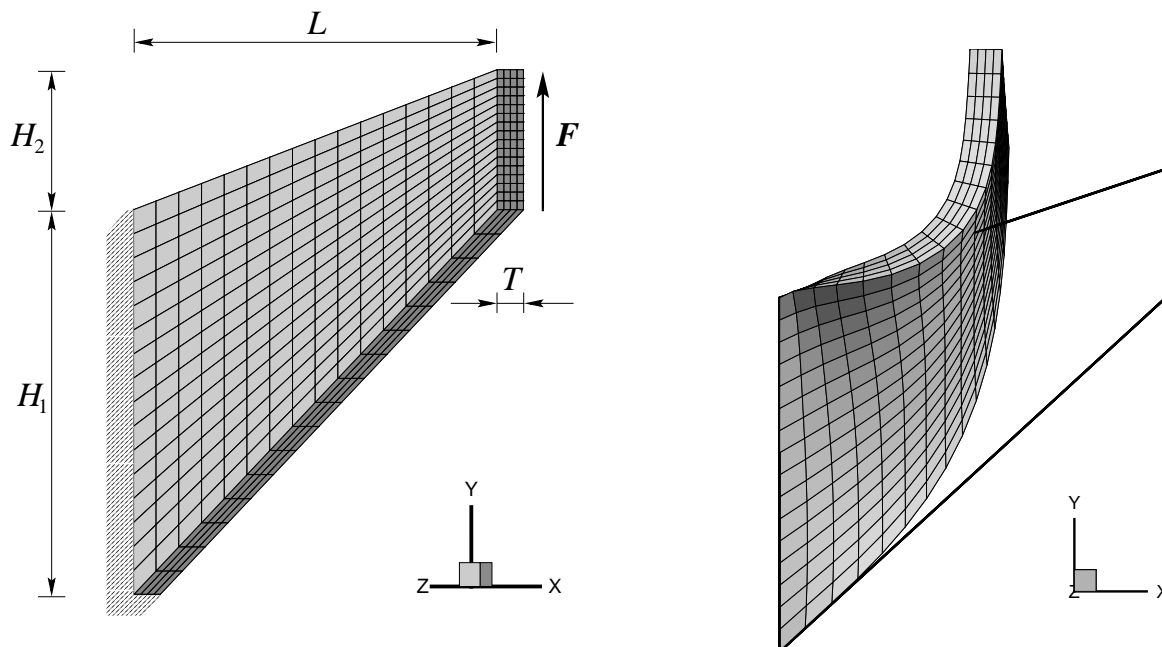


Figure 2.3: Cook's problem: Anisotropic (Q1E9); geometry, boundary and loading conditions, discretisation with $16 \times 16 \times 4$ eight node bricks (left) and deformed mesh at $\|\mathbf{F}\| = 4.5 \times 10^3$ (right).

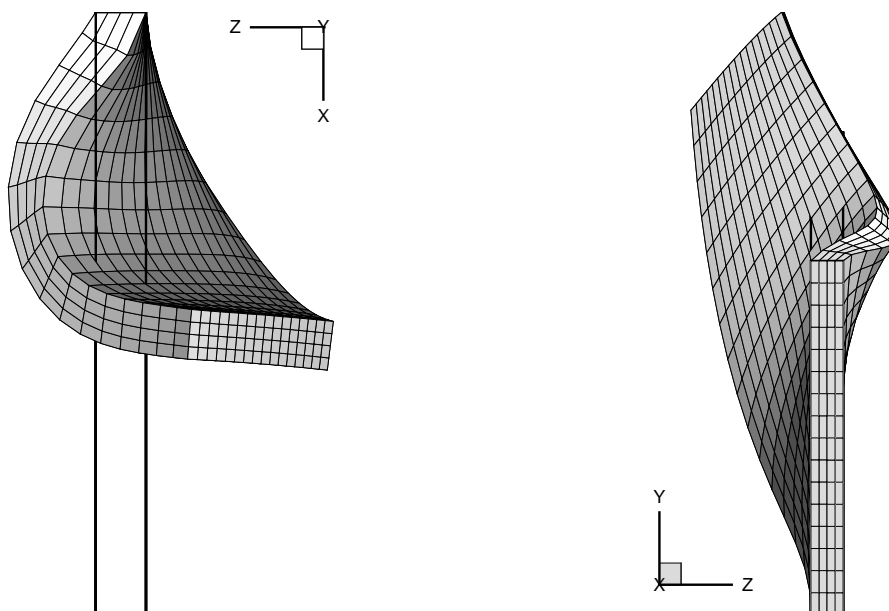


Figure 2.4: Cook's problem: Anisotropic (Q1E9); different views on the def. mesh at $\|\mathbf{F}\| = 4.5 \times 10^3$.

2.6 monitors the obtained displacement curves whereby an anisotropic setting based on standard trilinear eight node bricks (Q1) is additionally highlighted which shows a stiffer behaviour compared to the previous computation with enhanced elements (Q1E9). Finally, the convergence of these three different settings is summarised in Table 2.2 whereby the residual norm of the underlying Newton iteration steps are tabulated for the load step $\|\mathbf{F}\| : [0, 1000]$.

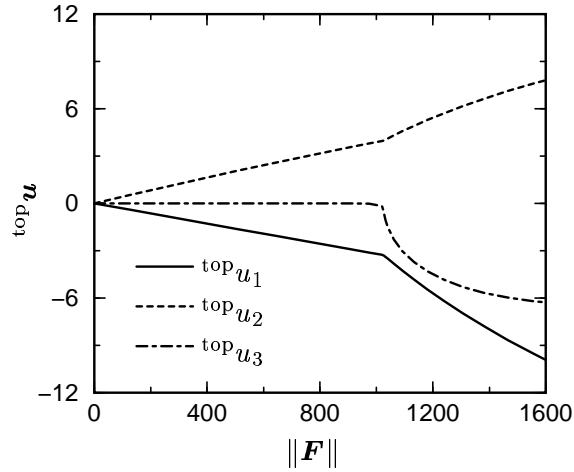


Figure 2.5: Cook's problem: Anisotropic (Q1E9); load–displacement curve of the mid point node at the top corner.

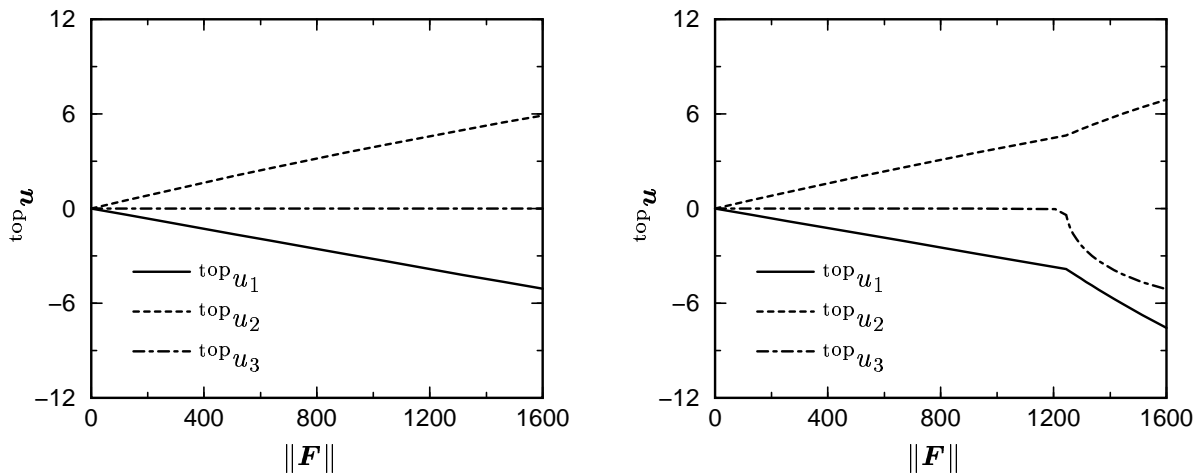



Figure 2.6: Cook's problem: Load–displacement curve of the mid point node at the top corner; isotropic setting (Q1E9, left) and anisotropic setting (Q1, right).

Table 2.2: Cook's problem: Residual norm for the load step $\|\mathbf{F}\| : [0, 1000]$.

Q1E9, anisotropic		Q1E9, isotropic		Q1, anisotropic	
no.	$\ \mathbf{R}\ $	no.	$\ \mathbf{R}\ $	no.	$\ \mathbf{R}\ $
1	$9.86979 E + 02$	1	$9.79760 E + 02$	1	$9.19998 E + 02$
2	$3.63984 E + 00$	2	$3.62822 E + 00$	2	$3.10966 E + 00$
3	$1.53097 E + 00$	3	$1.08340 E - 03$	3	$1.52990 E - 02$
4	$5.65937 E - 01$	4	$8.49209 E - 11$	4	$3.63277 E - 05$
5	$2.24507 E - 01$			5	$9.62855 E - 11$
6	$1.40378 E - 02$				
7	$1.73148 E - 04$				
8	$7.68584 E - 09$				

Chapter 3

Anisotropic elasto– plasticity based on structural tensors

f conditions which uniquely determine their effect possess certain symmetries, then the effect will exhibit the same symmetry. Thus Archimedes concluded a priori that equal weights balance in scales of equal arms. . . . As far as I see, all a priori statements in physics have their origin in symmetry.

Hermann Weyl [1885 – 1955]
Symmetry, 1952

In this Chapter, we develop a modular formulation of anisotropic elasto–plasticity and thereby adopt the framework of an un–stressed intermediate configuration and non–standard dissipative materials. For an overview on the general, almost isotropic, theory of elasto–plasticity, we refer to the textbooks by Lubliner [Lub90] and Maugin [Mau92], the survey by Naghdi [Nag90] and for a detailed outline on the algorithmic treatment, to Simo [Sim98]; see also references cited in these works. Here, we enlarge the set of arguments included in the free Helmholtz energy density by additional symmetric second order tensors. These fields are treated as internal variables and allow to account for deformation induced anisotropy. As an interesting side aspect, we set up two classes of evolution equations – one type results in a preservation of the material symmetry group while application of the other type of evolution equation ends up with a change of the symmetry properties of the material. Furthermore, and in analogy to the free Helmholtz energy density, additional symmetric tensorial arguments of second order are incorporated into the plastic potential. Thereby, the representation theorem of isotropic tensor functions is a powerful tool to derive reasonable flow rules. Usually, no exponential–type integrator of the governing evolution equations is conveniently available since the second order internal variables and their flow directions do not commute in general. However, standard Runge–Kutta–type integrators can be applied and as a demonstration of the developed methodology, a simple rate–independent prototype model is discussed within a homogeneous deformation and a finite element setting.

The Chapter is organised as follows: Sections 3.1 and 3.2 reiterate essentials of the kinematics on multiplicative elasto–plasticity and the fundamental covariance relation in analogy to Chapter 2. On this basis, the Coleman–Noll entropy principle is applied and, as a key constitutive equation, the expansion of the celebrated isotropic Truesdell or rather Murnaghan formula to anisotropic multiplicative elasto–plasticity is highlighted in Section 3.3. Then we adopt the framework of non–standard dissipative materials and introduce inelastic potentials within a Lemaitre–type model, whereby the setup of appropriate evolution equations is a natural outcome, Section 3.4. The numerical treatment of the obtained ordinary differential equations is reiterated in Section 3.7. With this formulation at hand, we set up a prototype model, Section 3.8, that accounts for different couplings of anisotropic elasticity to anisotropic plasticity along with the incorporation of deformation induced anisotropy. Finally, the numerical examples in Section 3.9 underline the applicability of the proposed formulation.

3.1 Kinematics

Adopting the framework of multiplicative elasto–plasticity, a stress–free and generally incompatible intermediate configuration \mathcal{B}_p is introduced, see e.g. Mandel [Man74] or Haupt [Hau00, Sect. 1.10] and e.g. Wang and Bloom [WB74], Svendsen [Sve98] or Bertram [Ber98] for an alternative derivation. In this context, let $T\mathcal{B}_p$ and $T^*\mathcal{B}_p$ represent the correlated tangent and dual space (with the natural identification $T^{**}\mathcal{B}_p \doteq T\mathcal{B}_p$) and let the additional metric tensors and the mixed–variant identity be denoted by

$$\widehat{\mathbf{G}}^b \in \mathbb{S}_+^3 : T\mathcal{B}_p \times T\mathcal{B}_p \rightarrow \mathbb{R}, \quad \widehat{\mathbf{G}}^\sharp \in \mathbb{S}_+^3 : T^*\mathcal{B}_p \times T^*\mathcal{B}_p \rightarrow \mathbb{R}, \quad \widehat{\mathbf{G}}^\sharp \in \mathbb{L}_+^3 : T^*\mathcal{B}_p \times T\mathcal{B}_p \rightarrow \mathbb{R} \quad (3.1)$$

with $\widehat{\mathbf{G}}^\sharp = \det^{-1}(\widehat{\mathbf{G}}^b) \text{cof}(\widehat{\mathbf{G}}^b)$. Based on the underlying non–singular linear tangent maps

$$\begin{aligned} \mathbf{F}_p^\sharp \in \mathbb{L}_+^3 : T\mathcal{B}_0 &\rightarrow T\mathcal{B}_p, & \mathbf{F}_e^\sharp \in \mathbb{L}_+^3 : T\mathcal{B}_p &\rightarrow T\mathcal{B}_t, & \mathbf{F}^\sharp &= \mathbf{F}_e^\sharp \cdot \mathbf{F}_p^\sharp, \\ \mathbf{f}_e^\sharp \in \mathbb{L}_+^3 : T\mathcal{B}_t &\rightarrow T\mathcal{B}_p, & \mathbf{f}_p^\sharp \in \mathbb{L}_+^3 : T\mathcal{B}_p &\rightarrow T\mathcal{B}_0, & \mathbf{f}^\sharp &= \mathbf{f}_p^\sharp \cdot \mathbf{f}_e^\sharp, \end{aligned} \quad (3.2)$$

additional kinematic tensors within all three configurations appear, namely

$$\begin{aligned} \mathbf{c}_e^b &= \mathbf{f}_e^{\sharp*} \widehat{\mathbf{G}}^b \in \mathbb{S}_+^3 : T\mathcal{B}_t \times T\mathcal{B}_t \rightarrow \mathbb{R}, & \mathbf{b}_e^\sharp &= \mathbf{F}_{e*}^\sharp \widehat{\mathbf{G}}^\sharp \in \mathbb{S}_+^3 : T^*\mathcal{B}_t \times T^*\mathcal{B}_t \rightarrow \mathbb{R}, \\ \widehat{\mathbf{c}}_p^b &= \mathbf{f}_p^{\sharp*} \mathbf{G}^b \in \mathbb{S}_+^3 : T\mathcal{B}_p \times T\mathcal{B}_p \rightarrow \mathbb{R}, & \widehat{\mathbf{b}}_p^\sharp &= \mathbf{F}_{p*}^\sharp \mathbf{G}^\sharp \in \mathbb{S}_+^3 : T^*\mathcal{B}_p \times T^*\mathcal{B}_p \rightarrow \mathbb{R}, \\ \widehat{\mathbf{C}}_e^b &= \mathbf{F}_{e*}^\sharp \mathbf{g}^b \in \mathbb{S}_+^3 : T\mathcal{B}_p \times T\mathcal{B}_p \rightarrow \mathbb{R}, & \widehat{\mathbf{B}}_e^\sharp &= \mathbf{f}_{e*}^\sharp \mathbf{g}^\sharp \in \mathbb{S}_+^3 : T^*\mathcal{B}_p \times T^*\mathcal{B}_p \rightarrow \mathbb{R}, \\ \mathbf{C}_p^b &= \mathbf{F}_{p*}^\sharp \widehat{\mathbf{G}}^b \in \mathbb{S}_+^3 : T\mathcal{B}_0 \times T\mathcal{B}_0 \rightarrow \mathbb{R}, & \mathbf{B}_p^\sharp &= \mathbf{f}_{p*}^\sharp \widehat{\mathbf{G}}^\sharp \in \mathbb{S}_+^3 : T^*\mathcal{B}_0 \times T^*\mathcal{B}_0 \rightarrow \mathbb{R}, \end{aligned} \quad (3.3)$$

and $\mathbf{b}_e^\sharp = \det^{-1}(\mathbf{c}_e^b) \text{cof}(\mathbf{c}_e^b)$, $\widehat{\mathbf{b}}_p^\sharp = \det^{-1}(\widehat{\mathbf{c}}_p^b) \text{cof}(\widehat{\mathbf{c}}_p^b)$, $\widehat{\mathbf{B}}_e^\sharp = \det^{-1}(\widehat{\mathbf{C}}_e^b) \text{cof}(\widehat{\mathbf{C}}_e^b)$, $\mathbf{B}_p^\sharp = \det^{-1}(\mathbf{C}_p^b) \text{cof}(\mathbf{C}_p^b)$ being obvious, compare Eqs.(2.6) and see Appendix A for notational details. Summarising, Figure 3.1 gives a graphical representation of these kinematic tensor fields and their transformation relations.

3.2 Free Helmholtz energy density

Let the free Helmholtz energy density be given as

$$\psi_0 = \psi_0(\mathbf{g}^b, \mathbf{F}_e^\sharp, \widehat{\mathbf{G}}^\sharp, \widehat{\mathbf{A}}_{1,\dots,n}^\sharp, \kappa; \mathbf{X}) \quad (3.4)$$

whereby $\widehat{\mathbf{A}}_{1,\dots,n}^\sharp \in \mathbb{S}^3 : [T^*\mathcal{B}_p \times T^*\mathcal{B}_p]_{1,\dots,n} \rightarrow \mathbb{R}$ represents a set of additional tensorial arguments and $\kappa \in \mathbb{R}$ is a hardening (softening) variable. Next, in analogy to Section 2.2, we apply the fundamental covariance relation, that is a scalar–valued tensor function remains invariant under the action of any non–singular tangent map (on it’s variables) which relates the tangent space of two affinely connected manifolds. Thus, the free Helmholtz energy density remains un–changed under the following pull–back operation of the incorporated arguments with respect to the intermediate configuration (see Appendix A for notational details)

$$\psi_0 \doteq \psi_0(\mathbf{F}_{e*}^\sharp \mathbf{g}^b, \mathbf{f}_{e*}^\sharp \mathbf{F}_e^\sharp, \widehat{\mathbf{G}}^\sharp, \widehat{\mathbf{A}}_{1,\dots,n}^\sharp, \kappa; \mathbf{X}) = \psi_0^p(\widehat{\mathbf{C}}_e^b, \widehat{\mathbf{G}}^\sharp, \widehat{\mathbf{A}}_{1,\dots,n}^\sharp, \kappa; \mathbf{X}) \quad (3.5)$$

Please note that the incorporation of the mixed–variant identity $\widehat{\mathbf{G}}^\sharp = \mathbf{f}_{e*}^\sharp \mathbf{F}_e^\sharp$ is naturally redundant. Now, with Eq.(3.5) at hand, which obviously incorporates exclusively symmetric kinematic tensors, further transformations in terms of \mathbf{F}_e^\sharp and \mathbf{F}_p^\sharp result in the spatial and material setting

$$\psi_0 \doteq \psi_0^p(\mathbf{f}_e^{\sharp*} \widehat{\mathbf{C}}_e^b, \mathbf{F}_{e*}^\sharp \widehat{\mathbf{G}}^\sharp, \mathbf{F}_{e*}^\sharp \widehat{\mathbf{A}}_{1,\dots,n}^\sharp, \kappa; \mathbf{X}) = \psi_0^t(\mathbf{g}^b, \mathbf{b}_e^\sharp, \mathbf{a}_{1,\dots,n}^\sharp, \kappa; \mathbf{X}) \quad (3.6)$$

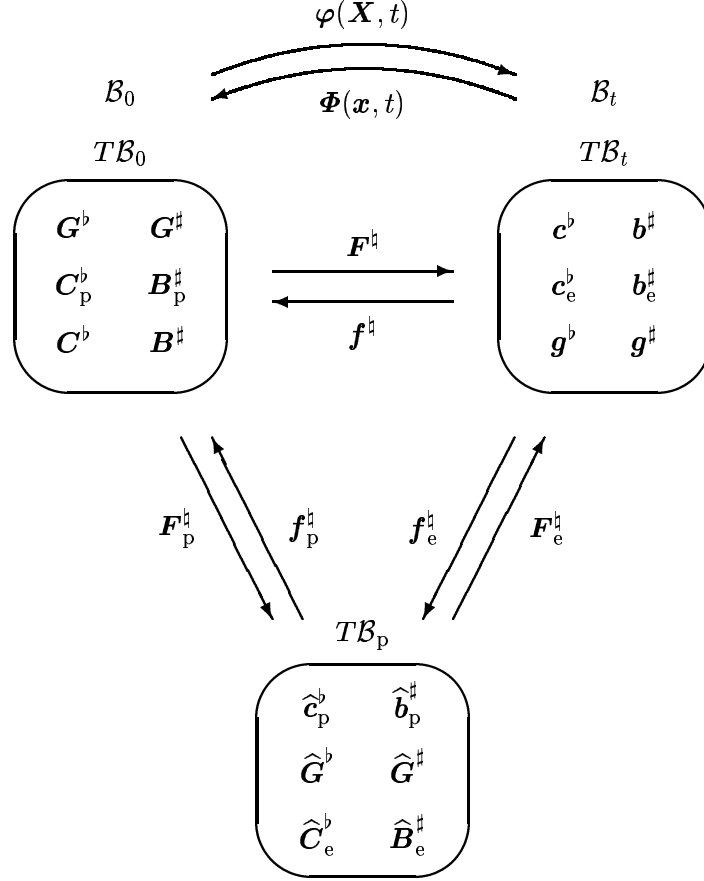


Figure 3.1: Non-linear motion, linear tangent maps and kinematic tensor fields.

$$\boxed{\psi_0 \doteq \psi_0^p(\mathbf{F}_p^\sharp \star \widehat{\mathbf{C}}_e^b, \mathbf{f}_{p^\star}^\sharp \widehat{\mathbf{G}}^\sharp, \mathbf{f}_{p^\star}^\sharp \widehat{\mathbf{A}}_{1,\dots,n}^\sharp; \kappa; \mathbf{X}) = \psi_0^0(\mathbf{C}^b, \mathbf{B}_p^\sharp, \mathbf{A}_{1,\dots,n}^\sharp; \kappa; \mathbf{X})}, \quad (3.7)$$

incorporating standard push-forward and pull-back operations for the set $\widehat{\mathbf{A}}_{1,\dots,n}^\sharp$, i.e.

$$\mathbf{a}_{1,\dots,n}^\sharp = \mathbf{F}_{e^\star}^\sharp \widehat{\mathbf{A}}_{1,\dots,n}^\sharp, \quad \text{and} \quad \mathbf{A}_{1,\dots,n}^\sharp = \mathbf{f}_{p^\star}^\sharp \widehat{\mathbf{A}}_{1,\dots,n}^\sharp. \quad (3.8)$$

As one typical field of application, we interpret these elements in the sequel without loss of generality similar to structural tensors. In this context, the preferred fibre directions define the material symmetry group \mathbb{G} of the body B in \mathcal{B}_0

$$\mathbb{G} = \left\{ \mathbf{Q}^\sharp \in \mathbb{O}^3 \mid \mathbf{Q}^\sharp \star \mathbf{A}_{1,\dots,n}^\sharp = \mathbf{A}_{1,\dots,n}^\sharp \right\}. \quad (3.9)$$

Since the fundamental idea of multiplicative elasto-plasticity relies on the picture of an elastic setting with respect to the intermediate configuration, an isometry with linear tangent map $\widehat{\mathbf{Q}}^\sharp$ is superposed onto the arguments of the free Helmholtz energy density ψ_0^p which must remain invariant under this action

$$\psi_0^p(\widehat{\mathbf{C}}_e^b, \widehat{\mathbf{G}}^\sharp, \widehat{\mathbf{A}}_{1,\dots,n}^\sharp; \mathbf{X}) = \psi_0^p(\widehat{\mathbf{Q}}^\sharp \star \widehat{\mathbf{C}}_e^b, \widehat{\mathbf{Q}}^\sharp \star \widehat{\mathbf{G}}^\sharp, \widehat{\mathbf{Q}}^\sharp \star \widehat{\mathbf{A}}_{1,\dots,n}^\sharp; \mathbf{X}) \quad \forall \widehat{\mathbf{Q}}^\sharp \in \mathbb{O}^3 \quad (3.10)$$

with $\widehat{\mathbf{Q}}^\sharp \star \widehat{\mathbf{G}}^\sharp = \widehat{\mathbf{G}}^\sharp$ being obvious. Recall that this choice of a superposed orthogonal transformation as one specific format of general covariance is one-to-one with the definition of an isotropic tensor function. Based on this, the general representation theorem can be applied, see e.g. the fundamental works by Wang [Wan70], Smith [Smi71a], Boehler [Boe77] or the outline by Antman [Ant95, Chap. XII.13]. In analogy to Table 2.1, the obtained set of invariants is summarised in Table 3.1, see Appendix A for notational details. Please note that the isotropic tensor function has been introduced

with respect to the intermediate configuration. Thus, the appropriate set of invariants is defined by trace operations in terms of the metric tensors $\widehat{\mathbf{G}}^b$ and $\widehat{\mathbf{G}}^\sharp$, respectively. On the contrary, the material symmetry group as given in Eq.(3.9) refers to the reference configuration.

Table 3.1: Complete set of invariants $\psi_0(I_{(i),\dots,(xi)}; \mathbf{X})$ with respect to \mathcal{B}_t , \mathcal{B}_p and \mathcal{B}_0 for all possible choices of $i, j, k, l \in [1, n]$ but $i \neq l$.

(i)	$\mathbf{g}^b : \mathbf{b}_e^\sharp =$	$\widehat{\mathbf{C}}_e^b : \widehat{\mathbf{G}}^\sharp =$	$\mathbf{C}^b : \mathbf{B}_p^\sharp$
(ii)	$[\mathbf{g}^b \cdot \mathbf{b}_e^\sharp \cdot \mathbf{g}^b] : \mathbf{b}_e^\sharp =$	$[\widehat{\mathbf{C}}_e^b \cdot \widehat{\mathbf{G}}^\sharp \cdot \widehat{\mathbf{C}}_e^b] : \widehat{\mathbf{G}}^\sharp =$	$[\mathbf{C}^b \cdot \mathbf{B}_p^\sharp \cdot \mathbf{C}^b] : \mathbf{B}_p^\sharp$
(iii)	$[\mathbf{g}^b \cdot [\mathbf{b}_e^\sharp \cdot \mathbf{g}^b]^2] : \mathbf{b}_e^\sharp =$	$[\widehat{\mathbf{C}}_e^b \cdot [\widehat{\mathbf{G}}^\sharp \cdot \widehat{\mathbf{C}}_e^b]^2] : \widehat{\mathbf{G}}^\sharp =$	$[\mathbf{C}^b \cdot [\mathbf{B}_p^\sharp \cdot \mathbf{C}^b]^2] : \mathbf{B}_p^\sharp$
(iv)	$\mathbf{g}^b : \mathbf{a}_i^\sharp =$	$\widehat{\mathbf{C}}_e^b : \widehat{\mathbf{A}}_i^\sharp =$	$\mathbf{C}^b : \mathbf{A}_i^\sharp$
(v)	$[\mathbf{g}^b \cdot \mathbf{b}_e^\sharp \cdot \mathbf{g}^b] : \mathbf{a}_i^\sharp =$	$[\widehat{\mathbf{C}}_e^b \cdot \widehat{\mathbf{G}}^\sharp \cdot \widehat{\mathbf{C}}_e^b] : \widehat{\mathbf{A}}_i^\sharp =$	$[\mathbf{C}^b \cdot \mathbf{B}_p^\sharp \cdot \mathbf{C}^b] : \mathbf{A}_i^\sharp$
(vi)	$[\mathbf{g}^b \cdot \mathbf{a}_j^\sharp \cdot \mathbf{c}_e^b] : \mathbf{a}_i^\sharp =$	$[\widehat{\mathbf{C}}_e^b \cdot \widehat{\mathbf{A}}_j^\sharp \cdot \widehat{\mathbf{G}}^\sharp] : \widehat{\mathbf{A}}_i^\sharp =$	$[\mathbf{C}^b \cdot \mathbf{A}_j^\sharp \cdot \mathbf{C}_p^b] : \mathbf{A}_i^\sharp$
(vii)	$[\mathbf{g}^b \cdot \mathbf{a}_i^\sharp \cdot \mathbf{g}^b] : \mathbf{a}_i^\sharp =$	$[\widehat{\mathbf{C}}_e^b \cdot \widehat{\mathbf{A}}_i^\sharp \cdot \widehat{\mathbf{C}}_e^b] : \widehat{\mathbf{A}}_i^\sharp =$	$[\mathbf{C}^b \cdot \mathbf{A}_i^\sharp \cdot \mathbf{C}^b] : \mathbf{A}_i^\sharp$
(viii)	$\mathbf{c}_e^b : \mathbf{a}_i^\sharp =$	$\widehat{\mathbf{G}}^\sharp : \widehat{\mathbf{A}}_i^\sharp =$	$\mathbf{C}_p^b : \mathbf{A}_i^\sharp$
(ix)	$[\mathbf{c}_e^b \cdot \mathbf{a}_j^\sharp \cdot \mathbf{c}_e^b] : \mathbf{a}_i^\sharp =$	$[\widehat{\mathbf{G}}^\sharp \cdot \widehat{\mathbf{A}}_j^\sharp \cdot \widehat{\mathbf{G}}^\sharp] : \widehat{\mathbf{A}}_i^\sharp =$	$[\mathbf{C}_p^b \cdot \mathbf{A}_j^\sharp \cdot \mathbf{C}_p^b] : \mathbf{A}_i^\sharp$
(x)	$[\mathbf{c}_e^b \cdot [\mathbf{a}_{j,k}^\sharp \cdot \mathbf{c}_e^b]^2] : \mathbf{a}_i^\sharp =$	$[\widehat{\mathbf{G}}^\sharp \cdot [\widehat{\mathbf{A}}_{j,k}^\sharp \cdot \widehat{\mathbf{G}}^\sharp]^2] : \widehat{\mathbf{A}}_i^\sharp =$	$[\mathbf{C}_p^b \cdot [\mathbf{A}_{j,k}^\sharp \cdot \mathbf{C}_p^b]^2] : \mathbf{A}_i^\sharp$
(xi)	$[\mathbf{c}_e^b \cdot [\mathbf{a}_{i,l,l}^\sharp \cdot \mathbf{c}_e^b]^3] : \mathbf{a}_i^\sharp =$	$[\widehat{\mathbf{G}}^\sharp \cdot [\widehat{\mathbf{A}}_{i,l,l}^\sharp \cdot \widehat{\mathbf{G}}^\sharp]^3] : \widehat{\mathbf{A}}_i^\sharp =$	$[\mathbf{C}_p^b \cdot [\mathbf{A}_{i,l,l}^\sharp \cdot \mathbf{C}_p^b]^3] : \mathbf{A}_i^\sharp$

Remark 3.1 Recall that the particular case where all tensorial arguments $\mathbf{A}_{1,\dots,n}^\sharp$, $\mathbf{a}_{1,\dots,n}^\sharp$ remain spherical during the whole deformation process results in an isotropic setting.

3.3 Coleman–Noll entropy principle

Before adopting the Coleman–Noll entropy principle as based on the Clausius–Duhem inequality – compare the reiteration in the outlook on page 144 and for a detailed outline we refer the reader to e.g. Coleman and Noll [CN63], Truesdell and Noll [TN92, Chap. D II] and Coleman and Gurtin [CG67] – recall that the material time derivative D_t of a, e.g., spatial contra–variant second order tensor field $[\bullet]^t$ decomposes additively into the Lie derivative $L_t[\bullet]^t = \mathbf{F}^\sharp \star D_t(\mathbf{f}^\sharp \star [\bullet]^t)$, or rather the Oldroyd rate, and a symmetrised part in terms of the spatial velocity gradient. In view of the appropriate spatial arguments of the free Helmholtz energy density, one obtains in particular

$$D_t \mathbf{b}_e^\sharp = L_t \mathbf{b}_e^\sharp + 2[\mathbf{l}^\sharp \cdot \mathbf{b}_e^\sharp]^{\text{sym}}, \quad D_t \mathbf{a}_i^\sharp = L_t \mathbf{a}_i^\sharp + 2[\mathbf{l}^\sharp \cdot \mathbf{a}_i^\sharp]^{\text{sym}} \quad (3.11)$$

whereby the spatial velocity gradient reads

$$\mathbf{l}^\sharp = D_t \mathbf{F}^\sharp \cdot \mathbf{f}^\sharp = D_t \mathbf{F}_e^\sharp \cdot \mathbf{f}_e^\sharp + \mathbf{F}_e^\sharp \cdot D_t \mathbf{F}_p^\sharp \cdot \mathbf{f}_p^\sharp = \mathbf{l}_e^\sharp + \mathbf{l}_p^\sharp \in \mathbb{L}^3 : T^* \mathcal{B}_t \times T \mathcal{B}_t \rightarrow \mathbb{R} \quad (3.12)$$

and the symmetry operation is reiterated in Appendix A. Consequently, the pointwise and isothermal format of the dissipation inequality with respect to \mathcal{B}_t results in

$$\begin{aligned} \mathcal{D}_0^t &= [\mathbf{m}^\sharp]^t : \mathbf{l}^\sharp - D_t \psi_0^t(\mathbf{g}^\flat, \mathbf{b}_e^\sharp, \mathbf{a}_{1,\dots,n}^\sharp, \kappa, ; \mathbf{X}) \\ &= \left[[\mathbf{m}^\sharp]^t - 2 \partial_{\mathbf{b}_e^\sharp} \psi_0^t \cdot \mathbf{b}_e^\sharp - 2 \sum_{i=1}^n \partial_{\mathbf{a}_i^\sharp} \psi_0^t \cdot \mathbf{a}_i^\sharp \right] : \mathbf{l}^\sharp \\ &\quad - \partial_{\mathbf{b}_e^\sharp} \psi_0^t : L_t \mathbf{b}_e^\sharp - \sum_{i=1}^n \partial_{\mathbf{a}_i^\sharp} \psi_0^t : L_t \mathbf{a}_i^\sharp - \partial_\kappa \psi_0^t D_t \kappa \geq 0 \end{aligned} \quad (3.13)$$

whereby $[\mathbf{m}^\sharp]^t : \mathbf{l}^\sharp$ computes the stress power and $[\mathbf{m}^\sharp]^t = \mathbf{g}^\flat \cdot \boldsymbol{\tau}^\sharp$ denotes the spatial Mandel tensor with $\boldsymbol{\tau}^\sharp$ characterising a Kirchhoff–type stress measure, compare e.g. Eringen [Eri62, Sects. 38 & 45]. Next, adopting the common Coleman–Noll argumentation of rational thermodynamics, we obtain the following hyper–elastic constitutive function for the mixed–variant stress tensor

$$[\mathbf{m}^\sharp]^t = 2 \partial_{\mathbf{b}_e^\sharp} \psi_0^t \cdot \mathbf{b}_e^\sharp + 2 \sum_{i=1}^n \partial_{\mathbf{a}_i^\sharp} \psi_0^t \cdot \mathbf{a}_i^\sharp. \quad (3.14)$$

This remarkable format allows interpretation as generalisation of the celebrated isotropic Truesdell formula [TN92, Eq.(85.15)] – which has already been given by Murnaghan [Mur37] in terms of \mathbf{c}^\flat – to anisotropic multiplicative elasto–plasticity, compare Section 2.3.1. Nevertheless, the remaining task is to prove that the contra–variant representation of Eq.(3.14) is symmetric and corresponds to the Kirchhoff stress, namely that

$$\boldsymbol{\tau}^\sharp = \mathbf{g}^\flat \cdot [\mathbf{m}^\sharp]^t = 2 \mathbf{g}^\flat \cdot \left[\partial_{\mathbf{b}_e^\sharp} \psi_0^t \cdot \mathbf{b}_e^\sharp + \sum_{i=1}^n \partial_{\mathbf{a}_i^\sharp} \psi_0^t \cdot \mathbf{a}_i^\sharp \right] \doteq 2 \partial_{\mathbf{g}^\flat} \psi_0^t \quad (3.15)$$

holds. The straightforward proof follows in analogy to Chapter 2 but now with respect to the even larger set of invariants as summarised in Table 3.1, see Sections 3.3.1 and 3.3.2. Alternatively, the verification can be performed by applying the fundamental covariance relation of the free Helmholtz energy density, see Appendix B.5.1 for an outline. Naturally, the dissipation inequality is computed with respect to the intermediate configuration in terms of the Mandel stress $[\widehat{\mathbf{M}}^\sharp]^t = \widehat{\mathbf{C}}_e^\flat \cdot \widehat{\mathbf{S}}^\sharp$, with $\widehat{\mathbf{S}}^\sharp = \mathbf{f}_{e^\star}^\sharp \boldsymbol{\tau}^\sharp$, and straightforward transformations yield

$$\begin{aligned} \mathcal{D}_0^p &= \left[[\widehat{\mathbf{M}}^\sharp]^t - 2 \partial_{\widehat{\mathbf{G}}^\sharp} \psi_0^p \cdot \widehat{\mathbf{G}}^\sharp - 2 \sum_{i=1}^n \partial_{\widehat{\mathbf{A}}_i^\sharp} \psi_0^p \cdot \widehat{\mathbf{A}}_i^\sharp \right] : \widehat{\mathbf{L}}^\sharp \\ &\quad - \partial_{\widehat{\mathbf{G}}^\sharp} \psi_0^p : L_t^p \widehat{\mathbf{G}}^\sharp - \sum_{i=1}^n \partial_{\widehat{\mathbf{A}}_i^\sharp} \psi_0^p : L_t^p \widehat{\mathbf{A}}_i^\sharp - \partial_\kappa \psi_0^p D_t \kappa \geq 0, \end{aligned} \quad (3.16)$$

whereby

$$\widehat{\mathbf{L}}^\sharp = \mathbf{f}_{e^\star}^\sharp \cdot \mathbf{l}^\sharp \cdot \mathbf{F}_e^\sharp = \mathbf{f}_{e^\star}^\sharp \cdot D_t \mathbf{F}_e^\sharp + D_t \mathbf{F}_p^\sharp \cdot \mathbf{f}_p^\sharp = \widehat{\mathbf{L}}_e^\sharp + \widehat{\mathbf{L}}_p^\sharp \in \mathbb{L}^3 : T^* \mathcal{B}_p \times T \mathcal{B}_p \rightarrow \mathbb{R} \quad (3.17)$$

denotes the mixed–variant pull–back of the spatial velocity gradient \mathbf{l}^\sharp and the appropriate Lie–derivative reads as $L_t^p [\widehat{\bullet}]^\sharp = \mathbf{F}_{p^\star}^\sharp D_t (\mathbf{f}_{p^\star}^\sharp [\widehat{\bullet}]^\sharp)$. Consequently, the symmetric second Piola–Kirchhoff–type stress tensor is defined via

$$\widehat{\mathbf{S}}^\sharp = \widehat{\mathbf{B}}_e^\sharp \cdot [\widehat{\mathbf{M}}^\sharp]^t = 2 \widehat{\mathbf{B}}_e^\sharp \cdot \left[\partial_{\widehat{\mathbf{G}}^\sharp} \psi_0^p \cdot \widehat{\mathbf{G}}^\sharp + \sum_{i=1}^n \partial_{\widehat{\mathbf{A}}_i^\sharp} \psi_0^p \cdot \widehat{\mathbf{A}}_i^\sharp \right] \doteq 2 \partial_{\widehat{\mathbf{C}}_e^\flat} \psi_0^p. \quad (3.18)$$

Continuing this strategy, the Mandel tensor in the material setting reads $[\mathbf{M}^\sharp]^t = \mathbf{C}^\flat \cdot \mathbf{S}^\sharp$, with $\mathbf{S}^\sharp = \mathbf{f}_{e^\star}^\sharp \boldsymbol{\tau}^\sharp$, and we obtain

$$\begin{aligned} \mathcal{D}_0^0 &= \left[[\mathbf{M}^\sharp]^t - 2 \partial_{\mathbf{B}_p^\sharp} \psi_0^0 \cdot \mathbf{B}_p^\sharp - 2 \sum_{i=1}^n \partial_{\mathbf{A}_i^\sharp} \psi_0^0 \cdot \mathbf{A}_i^\sharp \right] : \mathbf{L}^\sharp \\ &\quad - \partial_{\mathbf{B}_p^\sharp} \psi_0^0 : D_t \mathbf{B}_p^\sharp - \sum_{i=1}^n \partial_{\mathbf{A}_i^\sharp} \psi_0^0 : D_t \mathbf{A}_i^\sharp - \partial_\kappa \psi_0^0 D_t \kappa \geq 0 \end{aligned} \quad (3.19)$$

with

$$\mathbf{L}^\sharp = \mathbf{f}^\sharp \cdot \mathbf{l}^\sharp \cdot \mathbf{F}^\sharp = \mathbf{f}^\sharp \cdot \mathbf{D}_t \mathbf{F}_e^\sharp \cdot \mathbf{F}_p^\sharp + \mathbf{f}_p^\sharp \cdot \mathbf{D}_t \mathbf{F}_p^\sharp = \mathbf{L}_e^\sharp + \mathbf{L}_p^\sharp \in \mathbb{L}^3 : T^* \mathcal{B}_0 \times T \mathcal{B}_0 \rightarrow \mathbb{R} \quad (3.20)$$

being obvious. Thus, the second Piola–Kirchhoff stress is defined as

$$\mathbf{S}^\sharp = \mathbf{B}^\sharp \cdot [\mathbf{M}^\sharp]^\dagger = 2 \mathbf{B}^\sharp \cdot \left[\partial_{\mathbf{B}_p^\sharp} \psi_0^0 \cdot \mathbf{B}_p^\sharp + \sum_{i=1}^n \partial_{\mathbf{A}_i^\sharp} \psi_0^0 \cdot \mathbf{A}_i^\sharp \right] \doteq 2 \partial_{\mathbf{C}^b} \psi_0^0. \quad (3.21)$$

Remark 3.2 *The established format of the reduced dissipation inequality within multiplicative elasto–plasticity refers to the Mandel–type stress and the plastic part of the spatial velocity gradient or appropriate fields obtained after pull–back operations. In order to relate Eqs.(3.13, 3.16, 3.19) to this common representation, we apply the image of spatial Lie–derivatives as the push–forward of Lie–derivatives with respect to the intermediate configuration via the linear elastic tangent map. This strategy results in splitting elastic and plastic contributions of spatial Lie–derivatives. In particular, one obtains the decomposition*

$$\mathbf{L}_t [\bullet]^\sharp = \mathbf{F}_{e^*}^\sharp \mathbf{L}_t^p [\hat{\bullet}]^\sharp = \mathbf{F}_{e^*}^\sharp \mathbf{D}_t [\hat{\bullet}]^\sharp - 2 \left[\mathbf{l}_p^\sharp \cdot [\bullet]^\sharp \right]^{\text{sym}} \quad (3.22)$$

for a contra–variant spatial field $[\bullet]^\sharp = \mathbf{F}_{e^*}^\sharp [\hat{\bullet}]^\sharp$ of second order. Now with this relation at hand, the spatial format of the reduced dissipation inequality, as highlighted in Eq.(3.13), allows representation as

$$\begin{aligned} \mathcal{D}_0^t &= \left[[\mathbf{m}^\sharp]^\dagger - 2 \partial_{\mathbf{b}_e^\sharp} \psi_0^t \cdot \mathbf{b}_e^\sharp - 2 \sum_{i=1}^n \partial_{\mathbf{a}_i^\sharp} \psi_0^t \cdot \mathbf{a}_i^\sharp \right] : \mathbf{l}^\sharp \\ &+ \left[2 \partial_{\mathbf{b}_e^\sharp} \psi_0^t : \mathbf{b}_e^\sharp + 2 \sum_{i=1}^n \partial_{\mathbf{a}_i^\sharp} \psi_0^t : \mathbf{a}_i^\sharp \right] : \mathbf{l}_p^\sharp \\ &- \sum_{i=1}^n \partial_{\mathbf{a}_i^\sharp} \psi_0^t : \left[\mathbf{F}_{e^*}^\sharp \mathbf{D}_t \hat{\mathbf{A}}_i^\sharp \right] - \partial_\kappa \psi_0^t \mathbf{D}_t \kappa \geq 0, \\ \text{red} \mathcal{D}_0^t &= [\mathbf{m}^\sharp]^\dagger : \mathbf{l}_p^\sharp - \sum_{i=1}^n \partial_{\mathbf{a}_i^\sharp} \psi_0^t : \left[\mathbf{F}_{e^*}^\sharp \mathbf{D}_t \hat{\mathbf{A}}_i^\sharp \right] - \partial_\kappa \psi_0^t \mathbf{D}_t \kappa \geq 0. \end{aligned} \quad (3.23)$$

Obviously, pull–back operations can be applied which end up with

$$\text{red} \mathcal{D}_0^p = [\hat{\mathbf{M}}^\sharp]^\dagger : \hat{\mathbf{L}}_p^\sharp - \sum_{i=1}^n \partial_{\hat{\mathbf{A}}_i^\sharp} \psi_0^p : \mathbf{D}_t \hat{\mathbf{A}}_i^\sharp - \partial_\kappa \psi_0^p \mathbf{D}_t \kappa \geq 0, \quad (3.24)$$

compare Mandel [Man74, Eq.(15.13)], and in view of the material setting we obtain

$$\text{red} \mathcal{D}_0^0 = [\mathbf{M}^\sharp]^\dagger : \mathbf{L}_p^\sharp - \sum_{i=1}^n \partial_{\mathbf{A}_i^\sharp} \psi_0^0 : \left[\mathbf{f}_{p^*}^\sharp \mathbf{D}_t \hat{\mathbf{A}}_i^\sharp \right] - \partial_\kappa \psi_0^0 \mathbf{D}_t \kappa \geq 0. \quad (3.25)$$

3.3.1 Derivation of the anisotropic stress relation via invariants

In order to verify the hyper–elastic constitutive equations for the Kirchhoff stress, Eq.(3.15), we compute the derivatives of the set of invariants in Table 3.1 with respect to the arguments in the free Helmholtz energy density and prove the relation

$$\boldsymbol{\tau}^\sharp = 2 \sum_{q=(i)}^{(xi)} \partial_{I_q} \psi_0^t \partial_{\mathbf{g}^b} I_q = 2 \sum_{q=(i)}^{(xi)} \left[\partial_{I_q} \psi_0^t \mathbf{g}^\sharp \cdot \partial_{\mathbf{b}_e^\sharp} I_q \cdot \mathbf{b}_e^\sharp + \sum_{s=1}^n \partial_{I_q} \psi_0^t \mathbf{g}^\sharp \cdot \partial_{\mathbf{a}_s^\sharp} I_q \cdot \mathbf{a}_s^\sharp \right], \quad (3.26)$$

compare Eq.(2.36). The analogous outline for the Piola–type stresses, Eqs.(3.18,3.21), is of course identical and thus omitted here. Moreover, for the non–dissipative setting, the invariants $I_{(vii),\dots,(xi)}$ were redundant and the corresponding proof based on $I_{(i),\dots,(vi)}$ has been highlighted in Chapter 2 (for

multiplicative elasto–plasticity, one simply has to apply the transformation $\mathbf{b}_e^\# \mapsto \mathbf{b}^\#$ and $\mathbf{c}_e^b \mapsto \mathbf{c}^b$. To save space, we do not reiterate these contributions here but focus on the verification of

$$\partial_{\mathbf{g}^b} I_q = \mathbf{g}^\# \cdot \partial_{\mathbf{b}_e^\#} I_q \cdot \mathbf{b}_e^\# + \sum_{s=1}^n \mathbf{g}^\# \cdot \partial_{\mathbf{a}_s^\#} I_q \cdot \mathbf{a}_s^\# \quad \text{for } q \equiv (vii), \dots, (xi). \quad (3.27)$$

In this context, the relevant derivatives of the invariants $I_{(vii), \dots, (xi)}$ with respect to the spatial metric \mathbf{g}^b , the elastic Finger tensor $\mathbf{b}_e^\#$ and the additional variables $\mathbf{a}_{1, \dots, n}^\#$ are given in Appendix B.5. With these equations at hand, the proof of the constitutive equation for the Kirchhoff stress in the format of Eq.(3.27) follows immediately, after some straightforward but tedious algebra

(vii)

$$\begin{aligned} \partial_{\mathbf{g}^b} I_{(vii)} &\doteq \mathbf{0} + \sum_{s=1}^n \mathbf{g}^\# \cdot \partial_{\mathbf{a}_s^\#} I_{(vii)} \cdot \mathbf{a}_s^\# \\ &= 2 \mathbf{g}^\# \cdot \mathbf{g}^b \cdot \mathbf{a}_i^\# \cdot \mathbf{g}^b \cdot \mathbf{a}_i^\# \\ &= 2 \mathbf{a}_i^\# \cdot \mathbf{g}^b \cdot \mathbf{a}_i^\# \end{aligned}$$

(viii)

$$\begin{aligned} \partial_{\mathbf{g}^b} I_{(viii)} &\doteq - \mathbf{g}^\# \cdot \mathbf{c}_e^b \cdot \mathbf{a}_i^\# \cdot \mathbf{c}_e^b \cdot \mathbf{b}_e^\# + \sum_{s=1}^n \mathbf{g}^\# \cdot \partial_{\mathbf{a}_s^\#} I_{(viii)} \cdot \mathbf{a}_s^\# \\ &= - \mathbf{g}^\# \cdot \mathbf{c}_e^b \cdot \mathbf{a}_i^\# + \mathbf{g}^\# \cdot \mathbf{c}_e^b \cdot \mathbf{a}_i^\# \\ &= \mathbf{0} \end{aligned}$$

(ix)

$$\begin{aligned} \partial_{\mathbf{g}^b} I_{(ix)} &\doteq - 2 \mathbf{g}^\# \cdot \mathbf{c}_e^b \cdot [\mathbf{a}_{i,j}^\# \cdot \mathbf{c}_e^b]_2^{\text{sym}} \cdot \mathbf{c}_e^b \cdot \mathbf{b}_e^\# + \sum_{s=1}^n \mathbf{g}^\# \cdot \partial_{\mathbf{a}_s^\#} I_{(ix)} \cdot \mathbf{a}_s^\# \\ &= - \mathbf{g}^\# \cdot \mathbf{c}_e^b \cdot \mathbf{a}_i^\# \cdot \mathbf{c}_e^b \cdot \mathbf{a}_j^\# - \mathbf{g}^\# \cdot \mathbf{c}_e^b \cdot \mathbf{a}_j^\# \cdot \mathbf{c}_e^b \cdot \mathbf{a}_i^\# \\ &\quad + \mathbf{g}^\# \cdot \mathbf{c}_e^b \cdot \mathbf{a}_j^\# \cdot \mathbf{c}_e^b \cdot \mathbf{a}_i^\# + \mathbf{g}^\# \cdot \mathbf{c}_e^b \cdot \mathbf{a}_i^\# \cdot \mathbf{c}_e^b \cdot \mathbf{a}_j^\# \\ &= \mathbf{0} \end{aligned}$$

(x)

$$\begin{aligned} \partial_{\mathbf{g}^b} I_{(x)} &\doteq - \mathbf{g}^\# \cdot \mathbf{c}_e^b \cdot \left[[\mathbf{a}_{i,j,k}^\# \cdot \mathbf{c}_e^b]_3^{\text{sym}} + [\mathbf{a}_{k,i,j}^\# \cdot \mathbf{c}_e^b]_3^{\text{sym}} + [\mathbf{a}_{j,k,i}^\# \cdot \mathbf{c}_e^b]_3^{\text{sym}} \right] \cdot \mathbf{c}_e^b \cdot \mathbf{b}_e^\# \\ &\quad + \sum_{s=1}^n \mathbf{g}^\# \cdot \partial_{\mathbf{a}_s^\#} I_{(x)} \cdot \mathbf{a}_s^\# \\ &= - \mathbf{g}^\# \cdot \mathbf{c}_e^b \cdot \left[[\mathbf{a}_{i,j,k}^\# \cdot \mathbf{c}_e^b]_3^{\text{sym}} + [\mathbf{a}_{k,i,j}^\# \cdot \mathbf{c}_e^b]_3^{\text{sym}} + [\mathbf{a}_{j,k,i}^\# \cdot \mathbf{c}_e^b]_3^{\text{sym}} \right] \\ &\quad + \mathbf{g}^\# \cdot \mathbf{c}_e^b \cdot [\mathbf{a}_{j,k}^\# \cdot \mathbf{c}_e^b]_2^{\text{sym}} \cdot \mathbf{c}_e^b \cdot \mathbf{a}_i^\# + \mathbf{g}^\# \cdot \mathbf{c}_e^b \cdot [\mathbf{a}_{k,i}^\# \cdot \mathbf{c}_e^b]_2^{\text{sym}} \cdot \mathbf{c}_e^b \cdot \mathbf{a}_j^\# \\ &\quad + \mathbf{g}^\# \cdot \mathbf{c}_e^b \cdot [\mathbf{a}_{i,j}^\# \cdot \mathbf{c}_e^b]_2^{\text{sym}} \cdot \mathbf{c}_e^b \cdot \mathbf{a}_k^\# \\ &= \mathbf{0} \end{aligned}$$

(xi)

$$\begin{aligned} \partial_{\mathbf{g}^b} I_{(xi)} &\doteq - \mathbf{g}^\# \cdot \mathbf{c}_e^b \cdot \left[[\mathbf{a}_{l,i,i,l}^\# \cdot \mathbf{c}_e^b]_4 + 2 [\mathbf{a}_{l,l,i,i}^\# \cdot \mathbf{c}_e^b]_4^{\text{sym}} + [\mathbf{a}_{i,i,l,l}^\# \cdot \mathbf{c}_e^b]_4 \right] \cdot \mathbf{c}_e^b \cdot \mathbf{b}_e^\# \\ &\quad + \sum_{s=1}^n \mathbf{g}^\# \cdot \partial_{\mathbf{a}_s^\#} I_{(xi)} \cdot \mathbf{a}_s^\# \\ &= - \mathbf{g}^\# \cdot \mathbf{c}_e^b \cdot \left[[\mathbf{a}_{l,i,i,l}^\# \cdot \mathbf{c}_e^b]_4 + 2 [\mathbf{a}_{l,l,i,i}^\# \cdot \mathbf{c}_e^b]_4^{\text{sym}} + [\mathbf{a}_{i,i,l,l}^\# \cdot \mathbf{c}_e^b]_4 \right] \\ &\quad + 2 \left[\mathbf{g}^\# \cdot \mathbf{c}_e^b \cdot [\mathbf{a}_{i,l,l}^\# \cdot \mathbf{c}_e^b]_3^{\text{sym}} \cdot \mathbf{c}_e^b \cdot \mathbf{a}_i^\# + \mathbf{g}^\# \cdot \mathbf{c}_e^b \cdot [\mathbf{a}_{l,i,i}^\# \cdot \mathbf{c}_e^b]_3^{\text{sym}} \cdot \mathbf{c}_e^b \cdot \mathbf{a}_l^\# \right] \\ &= \mathbf{0} \end{aligned}$$

which obviously proves Eqs.(3.27, 3.26, 3.15), compare Appendix A.1 for notational details.

3.3.2 Derivation of the anisotropic tangent operator via invariants

Next, in view of the elastic tangent operator, we stress the relation

$$\begin{aligned}
\mathbf{e}^\# &= 4 \partial_{\mathbf{g}^b \otimes \mathbf{g}^b}^2 \psi_0^t \\
&= 4 [\mathbf{b}_e^\# \overline{\otimes} \mathbf{g}^\#] : \partial_{\mathbf{b}_e^\# \otimes \mathbf{b}_e^\#}^2 \psi_0^t : [\mathbf{g}^\# \overline{\otimes} \mathbf{b}_e^\#] \\
&+ 4 \sum_{s=1}^n [\mathbf{a}_s^\# \overline{\otimes} \mathbf{g}^\#] : \partial_{\mathbf{a}_s^\# \otimes \mathbf{b}_e^\#}^2 \psi_0^t : [\mathbf{g}^\# \overline{\otimes} \mathbf{b}_e^\#] \\
&+ 4 \sum_{t=1}^n [\mathbf{b}_e^\# \overline{\otimes} \mathbf{g}^\#] : \partial_{\mathbf{b}_e^\# \otimes \mathbf{a}_t^\#}^2 \psi_0^t : [\mathbf{g}^\# \overline{\otimes} \mathbf{a}_t^\#] \\
&+ 4 \sum_{s,t=1}^n [\mathbf{a}_s^\# \overline{\otimes} \mathbf{g}^\#] : \partial_{\mathbf{a}_s^\# \otimes \mathbf{a}_t^\#}^2 \psi_0^t : [\mathbf{g}^\# \overline{\otimes} \mathbf{a}_t^\#]
\end{aligned} \tag{3.28}$$

compare Eq.(2.39) and Appendix A.1 for the definition of the non-standard dyadic products. An outline with respect to \mathcal{B}_p or \mathcal{B}_0 is of course identical and thus omitted here. In terms of the derivatives of the invariants as given in Table 3.1, we obtain in analogy to Eq.(2.45)

$$\mathbf{e}^\# = 4 \sum_{q=(i)}^{(xi)} \partial_{I_q} \psi_0^t \partial_{\mathbf{g}^b \otimes \mathbf{g}^b}^2 I_q + 4 \sum_{q,r=(i)}^{(xi)} \partial_{I_q I_r}^2 \psi_0^t \partial_{\mathbf{g}^b} I_q \otimes \partial_{\mathbf{g}^b} I_r. \tag{3.29}$$

Apparently, the proof for the contributions $\partial_{\mathbf{g}^b} I_q \otimes \partial_{\mathbf{g}^b} I_r$ is included in the verification of Eq.(3.27). Hence the remaining task is to show that the relations

$$\begin{aligned}
\partial_{\mathbf{g}^b \otimes \mathbf{g}^b}^2 I_q &= [\mathbf{b}_e^\# \overline{\otimes} \mathbf{g}^\#] : \partial_{\mathbf{b}_e^\# \otimes \mathbf{b}_e^\#}^2 I_q : [\mathbf{g}^\# \overline{\otimes} \mathbf{b}_e^\#] \\
&+ \sum_{s=1}^n [\mathbf{a}_s^\# \overline{\otimes} \mathbf{g}^\#] : \partial_{\mathbf{a}_s^\# \otimes \mathbf{b}_e^\#}^2 I_q : [\mathbf{g}^\# \overline{\otimes} \mathbf{b}_e^\#] \\
&+ \sum_{t=1}^n [\mathbf{b}_e^\# \overline{\otimes} \mathbf{g}^\#] : \partial_{\mathbf{b}_e^\# \otimes \mathbf{a}_t^\#}^2 I_q : [\mathbf{g}^\# \overline{\otimes} \mathbf{a}_t^\#] \\
&+ \sum_{s,t=1}^n [\mathbf{a}_s^\# \overline{\otimes} \mathbf{g}^\#] : \partial_{\mathbf{a}_s^\# \otimes \mathbf{a}_t^\#}^2 I_q : [\mathbf{g}^\# \overline{\otimes} \mathbf{a}_t^\#]
\end{aligned} \tag{3.30}$$

hold, compare Eq.(2.47). Moreover, the transformations of the second order derivatives $\partial_{\mathbf{g}^b \otimes \mathbf{g}^b}^2 I_{(i), \dots, (vi)}$ are, again, similar to those highlighted in Section 2.3.2.3 and thus not reiterated here. From the list of remaining contributions due to the invariants $I_{(vii), \dots, (xi)}$, the second order derivatives of $I_{(vii)}$ are highlighted in Appendix B.5 which yield

$$\begin{aligned}
\partial_{\mathbf{g}^b \otimes \mathbf{g}^b}^2 I_{(vii)} &\doteq [\mathbf{b}_e^\# \overline{\otimes} \mathbf{g}^\#] : \partial_{\mathbf{b}_e^\# \otimes \mathbf{b}_e^\#}^2 I_{(vii)} : [\mathbf{g}^\# \overline{\otimes} \mathbf{b}_e^\#] \\
&+ \sum_{s=1}^n [\mathbf{a}_s^\# \overline{\otimes} \mathbf{g}^\#] : \partial_{\mathbf{a}_s^\# \otimes \mathbf{b}_e^\#}^2 I_{(vii)} : [\mathbf{g}^\# \overline{\otimes} \mathbf{b}_e^\#] \\
&+ \sum_{t=1}^n [\mathbf{b}_e^\# \overline{\otimes} \mathbf{g}^\#] : \partial_{\mathbf{b}_e^\# \otimes \mathbf{a}_t^\#}^2 I_{(vii)} : [\mathbf{g}^\# \overline{\otimes} \mathbf{a}_t^\#] \\
&+ \sum_{s,t=1}^n [\mathbf{a}_s^\# \overline{\otimes} \mathbf{g}^\#] : \partial_{\mathbf{a}_s^\# \otimes \mathbf{a}_t^\#}^2 I_{(vii)} : [\mathbf{g}^\# \overline{\otimes} \mathbf{a}_t^\#] \\
&= 3 \mathbf{0} + [\mathbf{a}_i^\# \overline{\otimes} \mathbf{g}^\#] : [\mathbf{g}^b \overline{\otimes} \mathbf{g}^b + \mathbf{g}^b \underline{\otimes} \mathbf{g}^b] : [\mathbf{g}^\# \overline{\otimes} \mathbf{a}_i^\#] \\
&= \mathbf{a}_i^\# \overline{\otimes} \mathbf{a}_i^\# + \mathbf{a}_i^\# \underline{\otimes} \mathbf{a}_i^\#
\end{aligned} \tag{3.31}$$

and verify the transformation relation for $\partial_{\mathbf{g}^b \otimes \mathbf{g}^b}^2 I_{(vii)}$ in Eq.(3.28). Although tedious, it is straightforward to show that the contributions due to $\partial_{\mathbf{g}^b \otimes \mathbf{g}^b}^2 I_{(viii), \dots, (xi)}$ cancel out as one can simply estimate from Eqs.(B.25, B.26). Nevertheless, the underlying procedure turns out to be quite lengthy and is thus not reiterated here.

3.3.3 Thermodynamic forces

In order to abbreviate the notation, we denote the introduced thermodynamic forces within the spatial setting as

$$\boxed{\begin{aligned} \mathbf{y}^b &= -\partial_{\mathbf{b}_e^\sharp} \psi_0^t \in \mathbb{S}^3 : T\mathcal{B}_t \times T\mathcal{B}_t \rightarrow \mathbb{R}, \\ \mathbf{z}_i^b &= -\partial_{\mathbf{a}_i^\sharp} \psi_0^t \in \mathbb{S}^3 : T^*\mathcal{B}_t \times T^*\mathcal{B}_t \rightarrow \mathbb{R}, \\ h &= -\partial_\kappa \psi_0^t \in \mathbb{R}, \end{aligned}} \quad (3.32)$$

compare Eq.(3.13). Please note that these definitions are of cardinal importance within the proposed framework of anisotropic multiplicative elasto-plasticity since these stress measures represent the key ingredients of the inelastic potentials, see Section 3.4. Next, focusing on the intermediate configuration, the thermodynamic forces read

$$\boxed{\begin{aligned} \widehat{\mathbf{Y}}^b &= -\partial_{\widehat{\mathbf{G}}^\sharp} \psi_0^p \in \mathbb{S}^3 : T\mathcal{B}_p \times T\mathcal{B}_p \rightarrow \mathbb{R}, \\ \widehat{\mathbf{Z}}_i^b &= -\partial_{\widehat{\mathbf{A}}_i^\sharp} \psi_0^p \in \mathbb{S}^3 : T^*\mathcal{B}_p \times T^*\mathcal{B}_p \rightarrow \mathbb{R}, \\ h &= -\partial_\kappa \psi_0^p \in \mathbb{R}. \end{aligned}} \quad (3.33)$$

which represents nothing else but the pull-back of Eqs.(3.32) in terms of \mathbf{F}^h . Finally, within the material setting, i.e. the pull-back of Eqs.(3.32) in terms of \mathbf{F}^h , we obtain

$$\boxed{\begin{aligned} \mathbf{Y}^b &= -\partial_{\mathbf{B}_p^\sharp} \psi_0^0 \in \mathbb{S}^3 : T\mathcal{B}_0 \times T\mathcal{B}_0 \rightarrow \mathbb{R}, \\ \mathbf{Z}_i^b &= -\partial_{\mathbf{A}_i^\sharp} \psi_0^0 \in \mathbb{S}^3 : T^*\mathcal{B}_0 \times T^*\mathcal{B}_0 \rightarrow \mathbb{R}, \\ h &= -\partial_\kappa \psi_0^0 \in \mathbb{R}. \end{aligned}} \quad (3.34)$$

For convenience of the reader, Figure 3.2 monitors the second order tensorial stress measures, their conjugate variables and in addition, the correlated transformation relations.

3.4 Non-standard dissipative materials

Based on the Coleman–Noll entropy principle, represented in terms of the Clausius–Duhem inequality (compare Section 3.3 and the outlook on page 144), we adopt in the sequel a Lemaitre–type model based on the framework of generalised standard dissipative materials as advocated by Halphen and Nguyen [HN75] *. Following the standard scheme, let an admissible elastic domain be characterised

* Referring to a generalised (simple continuous) standard dissipative material, we take the following relations for granted: (i) the free Helmholtz energy density is convex in it's arguments (appropriate strain measure, internal variables) with the only exception being concave in the temperature field $\theta(\mathbf{X}, t)$, i.e. $\partial_{\theta\theta}^2 \psi_0 < 0$ (compare the outlook on page 144), (ii) the entropy equals the derivative of the free Helmholtz energy density with respect to temperature times minus one, (iii) the thermodynamic forces are defined via derivatives of the free Helmholtz energy density with respect to the introduced internal variables times minus one, (iv) the intrinsic dissipation power (greater/equal zero) is identical to the scalar product of the thermodynamic forces and the rates of the internal variables, (v) the admissible domain \mathbb{A} is a closed convex set in the space spanned by the thermodynamic forces which initially includes the origin, e.g. $\mathbf{y}_1^b + \zeta [\mathbf{y}_2^b - \mathbf{y}_1^b] \in \mathbb{A}^t \forall \mathbf{y}_{1,2}^b \in \mathbb{A}^t$ and $\zeta \in \mathbb{R}_0 : \zeta \leq 1$ (in this direction see e.g. Hill [Hil00] or Mollica and Srinivasa [MS02] with special emphasis on anisotropy and e.g. Mróz and Raniecki [MR76] where restrictions for the non-isothermal case are discussed), (vi) evolution equations are characterised by normality rules which results in ((vii) the postulate of maximal dissipation (positive dissipation within Lemaitre–type models is conveniently guaranteed via dissipation potentials that are homogeneous of degree one in the thermodynamic forces, up to a positive scalar-valued factor).

By simple continuous media we mean that the response functions of the underlying material depend on the set $\{t, \boldsymbol{\varphi}, \mathbf{F}^h, \theta, \text{Grad } \theta, [\bullet]; \mathbf{X}\}$ whereby the notation $[\bullet]$ abbreviates a collection of internal variables as well as additional arguments and, moreover, application of the principle of material objectivity excludes t and $\boldsymbol{\varphi}$ from the above list, see e.g. Noll [Nol58], Truesdell and Noll [TN92, Sect. 28], Truesdell [Tru77, Sect. IV.3] for a detailed outline or the introduction and the outlook on page 1 and 144.

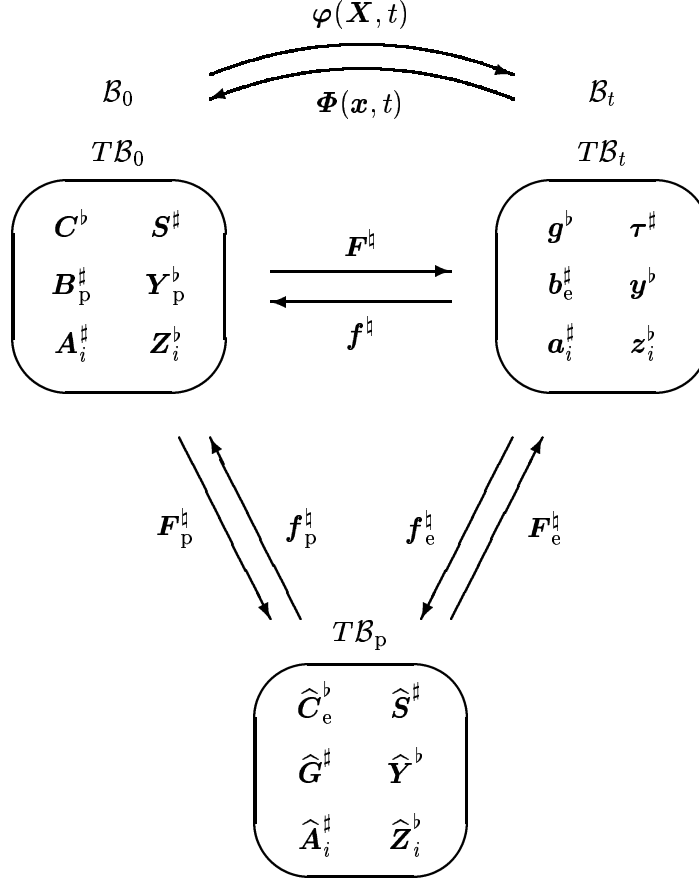


Figure 3.2: Second order tensorial stress measure, conjugate variables and correlated transformation relations.

by a scalar–valued yield function ${}^{\text{vie}}\Phi$. This potential, with respect to \mathcal{B}_t , is assumed to depend on the hardening stress h , the thermodynamic force \mathbf{y}^b , appropriate metric tensors \mathbf{g}^b , $\mathbf{g}^\#$ and additional arguments $\mathbf{a}_{n+1, \dots, m}^\#$ which we specify later on. Accepting an additive decomposition we end up with

$$\mathbb{A}^t = \left\{ (\mathbf{y}^b, h; \mathbf{X}) \mid {}^{\text{vie}}\Phi^t = {}^{\text{pla}}\Phi^t(\mathbf{y}^b, \mathbf{g}^\#, \mathbf{g}^b, \mathbf{a}_{n+1, \dots, m}^\#; \mathbf{X}) + {}^{\text{har}}\Phi(h; \mathbf{X}) \leq 0 \right\}. \quad (3.35)$$

Moreover, by adopting a Lemaitre–type model, a dissipation potential is introduced

$${}^{\text{pot}}\Phi^t = {}^{\text{vie}}\Phi^t(\mathbf{y}^b, h, \mathbf{g}^\#, \mathbf{g}^b, \mathbf{a}_{n+1, \dots, m}^\#; \mathbf{X}) + {}^{\text{fib}}\Phi^t(\mathbf{z}_{1, \dots, n}^b, \mathbf{g}^\#, \mathbf{g}^b, \mathbf{a}_{1, \dots, n}^\#; \mathbf{X}) \quad (3.36)$$

which is additively composed by the yield function ${}^{\text{vie}}\Phi^t$ and an additional potential ${}^{\text{fib}}\Phi^t$ that will account for an evolution of the tensorial arguments $\mathbf{a}_{1, \dots, n}^\#$.

Based on these potentials, the setup of appropriate evolution equations is a natural consequence

$$\begin{aligned} L_t \mathbf{b}_e^\# &= D_t \lambda \partial_{\mathbf{y}^b} {}^{\text{pot}}\Phi^t = D_t \lambda \partial_{\mathbf{y}^b} {}^{\text{pla}}\Phi^t \doteq D_t \lambda \boldsymbol{\xi}_{\mathbf{y}^b}^\# \\ L_t \mathbf{a}_i^\# &= D_t \lambda \partial_{\mathbf{z}_i^b} {}^{\text{pot}}\Phi^t = D_t \lambda \partial_{\mathbf{z}_i^b} {}^{\text{fib}}\Phi^t \doteq D_t \lambda \boldsymbol{\xi}_{\mathbf{z}_i^b}^\# \\ D_t \kappa &= D_t \lambda \partial_h {}^{\text{pot}}\Phi^t = D_t \lambda \partial_h {}^{\text{har}}\Phi \doteq D_t \lambda \xi_h \end{aligned} \quad (3.37)$$

whereby Eqs.(3.37)_{1,3} are obviously of associated format and Eq.(3.37)₂ is non–associated.

Similar to the free Helmholtz energy density, these scalar–valued functions (potentials) satisfy the fundamental covariance relation. In this context, usual pull–back and push–forward operations hold for the additional set of arguments $\mathbf{a}_{n+1, \dots, m}^\#$, namely

$$\widehat{\mathbf{A}}_{n+1, \dots, m}^\# = \mathbf{f}_{e\star}^\# \mathbf{a}_{n+1, \dots, m}^\#, \quad \mathbf{A}_{n+1, \dots, m}^\# = \mathbf{f}_{\star}^\# \mathbf{a}_{n+1, \dots, m}^\#. \quad (3.38)$$

Without loss of generality, we assume these tensorial fields to be of second order and symmetric whereby we will typically choose a rank one property in analogy to the structural tensors $\mathbf{a}_{1,\dots,n}^\sharp$. Moreover, the set $\mathbf{A}_{n+1,\dots,m}^\sharp \in [T^*\mathcal{B}_0 \times T^*\mathcal{B}_0]_{n+1,\dots,m} \rightarrow \mathbb{R}$ defines the material symmetry group in \mathcal{B}_0 of the plastic potential via

$$\mathbb{H} = \left\{ \mathbf{Q}^\sharp \in \mathbb{O}^3 \mid \mathbf{Q}^\sharp \star \mathbf{A}_{n+1,\dots,m}^\sharp = \mathbf{A}_{n+1,\dots,m}^\sharp \right\}. \quad (3.39)$$

Similar to Eq.(3.10), a spatial isometry is now superposed onto the arguments of the covariant inelastic potentials ${}^{\text{pla}}\Phi^t$ and ${}^{\text{fib}}\Phi^t$, i.e.

$$\left. \begin{aligned} {}^{\text{pla}}\Phi^t(\mathbf{y}^b, \mathbf{g}^\sharp, \mathbf{g}^b, \mathbf{a}_{n+1,\dots,m}^\sharp; \mathbf{X}) &= {}^{\text{pla}}\Phi^t(\mathbf{q}^\sharp \star \mathbf{y}^b, \mathbf{q}^\sharp \star \mathbf{g}^\sharp, \mathbf{q}^\sharp \star \mathbf{g}^b, \mathbf{q}^\sharp \star \mathbf{a}_{n+1,\dots,m}^\sharp; \mathbf{X}) \\ {}^{\text{fib}}\Phi^t(\mathbf{z}_{1,\dots,n}^b, \mathbf{g}^\sharp, \mathbf{g}^b, \mathbf{a}_{1,\dots,n}^\sharp; \mathbf{X}) &= {}^{\text{fib}}\Phi^t(\mathbf{q}^\sharp \star \mathbf{z}_{1,\dots,n}^b, \mathbf{q}^\sharp \star \mathbf{g}^\sharp, \mathbf{q}^\sharp \star \mathbf{g}^b, \mathbf{q}^\sharp \star \mathbf{a}_{1,\dots,n}^\sharp; \mathbf{X}) \end{aligned} \right\} \forall \mathbf{q}^\sharp \in \mathbb{O}^3 \quad (3.40)$$

and $\mathbf{q}^\sharp \star \mathbf{g}^\sharp = \mathbf{g}^\sharp$, $\mathbf{q}^\sharp \star \mathbf{g}^b = \mathbf{g}^b$ being obvious. With these definitions of scalar-valued isotropic tensor functions at hand, the representation theorem can be applied in order to construct an appropriate set of invariants. Table 3.2 summarises the complete list for the plastic potential ${}^{\text{pla}}\Phi$, see Appendix A for notational details. Please note that we have defined the isotropic tensor functions in Eq.(3.40) with respect to the Eulerian configuration \mathcal{B}_t . The trace operations within the computation of the invariants are thus computed in terms of the spatial metric tensors \mathbf{g}^b and \mathbf{g}^\sharp , respectively. This is in contrast to the previous introduction of the free Helmholtz energy density which we set up with respect to the intermediate configuration. Moreover, the definition of the material symmetry group of the plastic potential refers to the reference configuration \mathcal{B}_0 , Eq.(3.39). The set of invariants due to ${}^{\text{fib}}\Phi$ is even larger but otherwise similar to that in Table 3.2, since we deal with the complete set $\mathbf{z}_{1,\dots,n}^b$ instead of only one thermodynamic force \mathbf{y}^b , and is thus not reiterated here.

Table 3.2: Complete set of invariants ${}^{\text{pla}}\Phi(I_{(i),\dots,(xi)}; \mathbf{X})$ with respect to \mathcal{B}_t , \mathcal{B}_p and \mathcal{B}_0 for all possible choices of $i, j, k, l \in [1, n]$ but $i \neq l$.

(i)	$\mathbf{g}^\sharp : \mathbf{y}^b =$	$\widehat{\mathbf{B}}_e^\sharp : \widehat{\mathbf{Y}}^b =$	$\mathbf{B}^\sharp : \mathbf{Y}^b$
(ii)	$[\mathbf{g}^\sharp \cdot \mathbf{y}^b \cdot \mathbf{g}^\sharp] : \mathbf{y}^b =$	$[\widehat{\mathbf{B}}_e^\sharp \cdot \widehat{\mathbf{Y}}^b \cdot \widehat{\mathbf{B}}_e^\sharp] : \widehat{\mathbf{Y}}^b =$	$[\mathbf{B}^\sharp \cdot \mathbf{Y}^b \cdot \mathbf{B}^\sharp] : \mathbf{Y}^b$
(iii)	$[\mathbf{g}^\sharp \cdot [\mathbf{y}^b \cdot \mathbf{g}^\sharp]^2] : \mathbf{y}^b =$	$[\widehat{\mathbf{B}}_e^\sharp \cdot [\widehat{\mathbf{Y}}^b \cdot \widehat{\mathbf{B}}_e^\sharp]^2] : \widehat{\mathbf{Y}}^b =$	$[\mathbf{B}^\sharp \cdot [\mathbf{Y}^b \cdot \mathbf{B}^\sharp]^2] : \mathbf{Y}^b$
(iv)	$\mathbf{y}^b : \mathbf{a}_i^\sharp =$	$\widehat{\mathbf{Y}}^b : \widehat{\mathbf{A}}_i^\sharp =$	$\mathbf{Y}^b : \mathbf{A}_i^\sharp$
(v)	$[\mathbf{y}^b \cdot \mathbf{g}^\sharp \cdot \mathbf{y}^b] : \mathbf{a}_i^\sharp =$	$[\widehat{\mathbf{Y}}^b \cdot \widehat{\mathbf{B}}_e^\sharp \cdot \widehat{\mathbf{Y}}^b] : \widehat{\mathbf{A}}_i^\sharp =$	$[\mathbf{Y}^b \cdot \mathbf{B}^\sharp \cdot \mathbf{Y}^b] : \mathbf{A}_i^\sharp$
(vi)	$[\mathbf{y}^b \cdot \mathbf{a}_j^\sharp \cdot \mathbf{g}^b] : \mathbf{a}_i^\sharp =$	$[\widehat{\mathbf{Y}}^b \cdot \widehat{\mathbf{A}}_j^\sharp \cdot \widehat{\mathbf{C}}_e^b] : \widehat{\mathbf{A}}_i^\sharp =$	$[\mathbf{Y}^b \cdot \mathbf{A}_j^\sharp \cdot \mathbf{C}^b] : \mathbf{A}_i^\sharp$
(vii)	$[\mathbf{y}^b \cdot \mathbf{a}_i^\sharp \cdot \mathbf{y}^b] : \mathbf{a}_i^\sharp =$	$[\widehat{\mathbf{Y}}^b \cdot \widehat{\mathbf{A}}_i^\sharp \cdot \widehat{\mathbf{Y}}^b] : \widehat{\mathbf{A}}_i^\sharp =$	$[\mathbf{Y}^b \cdot \mathbf{A}_i^\sharp \cdot \mathbf{Y}^b] : \mathbf{A}_i^\sharp$
(viii)	$\mathbf{g}^b : \mathbf{a}_i^\sharp =$	$\widehat{\mathbf{C}}_e^b : \widehat{\mathbf{A}}_i^\sharp =$	$\mathbf{C}^b : \mathbf{A}_i^\sharp$
(ix)	$[\mathbf{g}^b \cdot \mathbf{a}_j^\sharp \cdot \mathbf{g}^b] : \mathbf{a}_i^\sharp =$	$[\widehat{\mathbf{C}}_e^b \cdot \widehat{\mathbf{A}}_j^\sharp \cdot \widehat{\mathbf{C}}_e^b] : \widehat{\mathbf{A}}_i^\sharp =$	$[\mathbf{C}^b \cdot \mathbf{A}_j^\sharp \cdot \mathbf{C}^b] : \mathbf{A}_i^\sharp$
(x)	$[\mathbf{g}^b \cdot [\mathbf{a}_{j,k}^\sharp \cdot \mathbf{g}^b]^2] : \mathbf{a}_i^\sharp =$	$[\widehat{\mathbf{C}}_e^b \cdot [\widehat{\mathbf{A}}_{j,k}^\sharp \cdot \widehat{\mathbf{C}}_e^b]^2] : \widehat{\mathbf{A}}_i^\sharp =$	$[\mathbf{C}^b \cdot [\mathbf{A}_{j,k}^\sharp \cdot \mathbf{C}^b]^2] : \mathbf{A}_i^\sharp$
(xi)	$[\mathbf{g}^b \cdot [\mathbf{a}_{i,l,l}^\sharp \cdot \mathbf{g}^b]^3] : \mathbf{a}_i^\sharp =$	$[\widehat{\mathbf{C}}_e^b \cdot [\widehat{\mathbf{A}}_{i,l,l}^\sharp \cdot \widehat{\mathbf{C}}_e^b]^3] : \widehat{\mathbf{A}}_i^\sharp =$	$[\mathbf{C}^b \cdot [\mathbf{A}_{i,l,l}^\sharp \cdot \mathbf{C}^b]^3] : \mathbf{A}_i^\sharp$

Apparently one has different possibilities to correlate the sets $\mathbf{a}_{1,\dots,n}^\sharp$ and $\mathbf{a}_{n+1,\dots,m}^\sharp$ which enter e.g. the free Helmholtz energy density ψ_0^t and the plastic potential $^{\text{pla}}\Phi^t$. We account for three different options in this work, specifically

$$\boxed{\begin{array}{ll} \text{(i)} & \mathbf{a}_{1,\dots,n}^\sharp \cap \mathbf{a}_{n+1,\dots,m}^\sharp = \emptyset \\ \text{(ii)} & \mathbf{a}_{1,\dots,n}^\sharp \cap \mathbf{a}_{n+1,\dots,m}^\sharp = \mathbf{a}_{s,\dots,t}^\sharp \\ \text{(iii)} & \mathbf{a}_{1,\dots,n}^\sharp \cap \mathbf{a}_{n+1,\dots,m}^\sharp = \mathbf{a}_{1,\dots,n}^\sharp \end{array}} \quad (3.41)$$

that is, (i) all arguments $\mathbf{a}_{n+1,\dots,m}^\sharp$ in the plastic potential are different from those incorporated into ψ_0^t ; (ii) at least some of these arguments are identical; (iii) all arguments $\mathbf{a}_{n+1,\dots,m}^\sharp$ equal the tensorial fields $\mathbf{a}_{1,\dots,n}^\sharp$ and $m = 2n$.

3.5 Reduction to isotropy

Now, with the complete framework at hand, we can boil the anisotropic setting down to isotropy in order to see how the proposed formulation is related to well–established isotropic approaches.

Recall once more that we obtain the well–known Truesdell or rather Murnaghan formula

$$[\mathbf{m}^\sharp]^t = 2 \partial_{\mathbf{b}_e^\sharp} \psi_0^t \cdot \mathbf{b}_e^\sharp = -2 \mathbf{c}_e^b \cdot \partial_{\mathbf{c}_e^b} \psi_0^t \quad (3.42)$$

for $\mathbf{a}_{1,\dots,n}^\sharp = \mathbf{0}$ whereby $[\mathbf{m}^\sharp]^t = \mathbf{g}^b \cdot \boldsymbol{\tau}^\sharp$ denotes the mixed–variant spatial Mandel stress. Within the current framework, the symmetric thermodynamic force which enters the plastic potential but not the equilibrium equations, reads in terms of the Kirchhoff stress as

$$\mathbf{y}^b = -\partial_{\mathbf{b}_e^\sharp} \psi_0^t = -\frac{1}{2} \mathbf{g}^b \cdot \boldsymbol{\tau}^\sharp \cdot \mathbf{c}_e^b = -\frac{1}{2} [\mathbf{m}^\sharp]^t \cdot \mathbf{c}_e^b = \mathbf{c}_e^b \cdot \partial_{\mathbf{c}_e^b} \psi_0^t \cdot \mathbf{c}_e^b, \quad (3.43)$$

compare Miehe [Mie98b, Eq.(38)₂]. Pausing for a moment, we observe that in the case of metal plasticity where the elastic strains are usually small, i.e. $\mathbf{c}_e^b \rightarrow \mathbf{g}^b$, the norms of \mathbf{y}^b and $\boldsymbol{\tau}^\sharp$ differ only by a factor of two. Moreover, the reduced isothermal pointwise dissipation inequality allows the following representation

$$\begin{aligned} \text{red} \mathcal{D}_0^t &= [\mathbf{y}^b \cdot \mathbf{b}_e^\sharp] : [\mathbb{L}_t \mathbf{b}_e^\sharp \cdot \mathbf{c}_e^b] = -\frac{1}{2} [\mathbf{m}^\sharp]^t : [\mathbb{L}_t \mathbf{b}_e^\sharp \cdot \mathbf{c}_e^b] \\ &= [[\mathbf{m}^\sharp]^t \cdot \mathbf{c}_e^b] : [\mathbb{I}_p^\sharp \cdot \mathbf{b}_e^\sharp]^{\text{sym}} = [[\mathbf{m}^\sharp]^t \cdot \mathbf{c}_e^b] : [\mathbb{I}_p^\sharp \cdot \mathbf{b}_e^\sharp] \\ &= [\mathbf{m}^\sharp]^t : \mathbb{I}_p^\sharp \geq 0 \end{aligned} \quad (3.44)$$

whereby hardening contributions have been neglected for the sake of clarity and $\mathbb{L}_t \mathbf{b}_e^\sharp = -2 [\mathbb{I}_p^\sharp \cdot \mathbf{b}_e^\sharp]^{\text{sym}}$ is obvious. On this basis, an associated evolution equation is a natural outcome

$$\boxed{-\frac{1}{2} \mathbb{L}_t \mathbf{b}_e^\sharp \cdot \mathbf{c}_e^b = \text{D}_t \lambda \mathbf{g}^\sharp \cdot \partial_{\boldsymbol{\tau}^\sharp} \text{pla} \Phi^t \quad \text{or} \quad \mathbb{I}_p^\sharp = \text{D}_t \lambda \partial_{[\mathbf{m}^\sharp]^t} \text{pla} \Phi^t}, \quad (3.45)$$

compare Simo and Miehe [SM92, Eq.(2.19)]. Please note that the crucial relation $\partial_{[\mathbf{m}^\sharp]^t} \text{pla} \Phi^t = \mathbf{g}^\sharp \cdot \partial_{\boldsymbol{\tau}^\sharp} \text{pla} \Phi^t$ is a direct consequence of the Mandel–type stress tensor $[\mathbf{m}^\sharp]^t$ being a product of two symmetric tensors with one always remaining positive definite. Moreover, the spectral representation theorem $[\mathbf{m}^\sharp]^t = \mathbf{g}^b \cdot \boldsymbol{\tau}^\sharp = \sum_{i=1}^3 [\mathbf{m}^\sharp]^t \lambda_i \text{rig} \mathbf{n}_i^b \otimes \text{lef} \mathbf{n}_i^\sharp$ with $[\mathbf{m}^\sharp]^t \lambda_i \in \mathbb{R}$ can be applied for this specific case, compare Ericksen [Eri60, Sect. 37], Eringen [Eri71, Sect. 1.10] or Lodge [Lod74, Sect. 2.8].

Next, applying a pull–back operation to the intermediate configuration, we obtain

$$\hat{\mathbf{Y}}^b = -\partial_{\hat{\mathbf{G}}^\sharp} \psi_0^p = -\frac{1}{2} \hat{\mathbf{C}}_e^b \cdot \hat{\mathbf{S}}^\sharp \cdot \hat{\mathbf{G}}^b = -\frac{1}{2} [\hat{\mathbf{M}}^\sharp]^t \cdot \hat{\mathbf{G}}^b = \hat{\mathbf{G}}^b \cdot \partial_{\hat{\mathbf{G}}^b} \psi_0^p \cdot \hat{\mathbf{G}}^b \quad (3.46)$$

for the considered isotropic setting with $[\widehat{\mathbf{M}}^{\natural}]^t = \widehat{\mathbf{C}}_e^b \cdot \widehat{\mathbf{S}}^{\natural}$ representing the Mandel stress in \mathcal{B}_p . Continuing this strategy, the dissipation inequality (3.44) results in

$$\begin{aligned} \text{red}\mathcal{D}_0^p &= [\widehat{\mathbf{Y}}^b \cdot \widehat{\mathbf{G}}^{\natural}] : [\mathbf{L}_t^p \widehat{\mathbf{G}}^{\natural} \cdot \widehat{\mathbf{G}}^b] = -\frac{1}{2} [\widehat{\mathbf{M}}^{\natural}]^t : [\mathbf{L}_t^p \widehat{\mathbf{G}}^{\natural} \cdot \widehat{\mathbf{G}}^b] \\ &= [[\widehat{\mathbf{M}}^{\natural}]^t \cdot \widehat{\mathbf{G}}^b] : [\widehat{\mathbf{L}}_p^{\natural} \cdot \widehat{\mathbf{G}}^{\natural}]^{\text{sym}} = [[\widehat{\mathbf{M}}^{\natural}]^t \cdot \widehat{\mathbf{G}}^b] : [\widehat{\mathbf{L}}_p^{\natural} \cdot \widehat{\mathbf{G}}^{\natural}] \\ &= [\widehat{\mathbf{M}}^{\natural}]^t : \widehat{\mathbf{L}}_p^{\natural} \geq 0 \end{aligned} \quad (3.47)$$

with $\mathbf{L}_t^p \widehat{\mathbf{G}}^{\natural} = -2 [\widehat{\mathbf{L}}_p^{\natural} \cdot \widehat{\mathbf{G}}^{\natural}]^{\text{sym}}$. The associated evolution equation is consequently given by

$$\boxed{-\frac{1}{2} \mathbf{L}_t^p \widehat{\mathbf{G}}^{\natural} \cdot \widehat{\mathbf{G}}^b = D_t \lambda \widehat{\mathbf{B}}_e^{\natural} \cdot \partial_{\widehat{\mathbf{S}}^{\natural}}^{\text{pla}} \Phi^p \quad \text{or} \quad \widehat{\mathbf{L}}_p^{\natural} = D_t \lambda \partial_{[\widehat{\mathbf{M}}^{\natural}]^t}^{\text{pla}} \Phi^p}, \quad (3.48)$$

see e.g. Lubliner [Lub90, Sect. 8.2.4] and Miehe and Stein [MS92] or Maugin [Mau94] with special emphasis on the framework of Eshelbian mechanics. In this direction, another pull-back to the reference configuration yields in analogy to Eqs.(3.42, 3.46)

$$\mathbf{Y}^b = -\partial_{\mathbf{B}_p^{\natural}} \psi_0^0 = -\frac{1}{2} \mathbf{C}^b \cdot \mathbf{S}^{\natural} \cdot \mathbf{C}_p^b = -\frac{1}{2} [\mathbf{M}^{\natural}]^t \cdot \mathbf{C}_p^b = \mathbf{C}_p^b \cdot \partial_{\mathbf{C}_p^b} \psi_0^0 \cdot \mathbf{C}_p^b \quad (3.49)$$

incorporating the Mandel stress $[\mathbf{M}^{\natural}]^t = \mathbf{C}^b \cdot \mathbf{S}^{\natural}$, compare Miehe [Mie98b, Eq.(38)₁]. Now, the reduced dissipation inequality follows as

$$\begin{aligned} \text{red}\mathcal{D}_0^0 &= [\mathbf{Y}^b \cdot \mathbf{B}_p^{\natural}] : [D_t \mathbf{B}_p^{\natural} \cdot \mathbf{C}_p^b] = -\frac{1}{2} [\mathbf{M}^{\natural}]^t : [D_t \mathbf{B}_p^{\natural} \cdot \mathbf{C}_p^b] \\ &= [[\mathbf{M}^{\natural}]^t \cdot \mathbf{C}_p^b] : [\mathbf{L}_p^{\natural} \cdot \mathbf{B}_p^{\natural}]^{\text{sym}} = [[\mathbf{M}^{\natural}]^t \cdot \mathbf{C}_p^b] : [\mathbf{L}_p^{\natural} \cdot \mathbf{B}_p^{\natural}] \\ &= [\mathbf{M}^{\natural}]^t : \mathbf{L}_p^{\natural} \geq 0 \end{aligned} \quad (3.50)$$

with $D_t \mathbf{B}_p^{\natural} = -2 [\mathbf{L}_p^{\natural} \cdot \mathbf{B}_p^{\natural}]^{\text{sym}}$ and the appropriate associated evolution equation results in

$$\boxed{-\frac{1}{2} D_t \mathbf{B}_p^{\natural} \cdot \mathbf{C}_p^b = D_t \lambda \mathbf{B}^{\natural} \cdot \partial_{\mathbf{S}^{\natural}}^{\text{pla}} \Phi^0 \quad \text{or} \quad \mathbf{L}_p^{\natural} = \partial_{[\mathbf{M}^{\natural}]^t}^{\text{pla}} \Phi^0}, \quad (3.51)$$

see e.g. Ibrahimbegović [Ibr94, Eq.(47)].

3.6 Relation to Eshelbian mechanics

The driving force within a deformation process of an inhomogeneous or generally inelastic body B is accurately described by the framework of Eshelbian mechanics, see the recent monographs by Maugin [Mau93], Šilhavý [Šil97] and Gurtin [Gur00]. In this context, e.g., Epstein and Maugin [EM90, EM96] and Cleja-Țigoiu and Maugin [CTM00] placed special emphasis on finite elasto-plasticity, see also references cited in these works.

We focus on the relation between Eshelbian stress tensors and the thermodynamic forces within the proposed framework for anisotropic plasticity in the following. The significant stress field, e.g. \mathbf{y}^b in \mathcal{B}_t , is defined by the derivative of the free Helmholtz energy density ψ_0^t with respect to the elastic Finger tensor. For this reason (in order to incorporate ψ_0), we consider the inverse motion problem characterised by $\Phi(\mathbf{x}, t)$ whereby the connection

$$\boxed{\psi_t = \det(\mathbf{f}^{\natural}) \psi_0 \iff \psi_0 = \det(\mathbf{F}^{\natural}) \psi_t} \quad (3.52)$$

is of cardinal importance, compare e.g. Steinmann [Ste00, Ste01]. With this relation at hand, we compute the following useful representation of the elastic inverse motion first Piola–Kirchhoff stress $[\boldsymbol{\pi}_e^{\natural}]^t \in \mathbb{L}^3 : T^* \mathcal{B}_t \rightarrow T^* \mathcal{B}_p$, namely

$$\boxed{[\boldsymbol{\pi}_e^{\natural}]^t = \partial_{\mathbf{f}_e^{\natural}} \psi_t^t = \det(\mathbf{f}_p^{\natural}) \psi_0^t \text{ cof}(\mathbf{f}_e^{\natural}) + \det(\mathbf{f}^{\natural}) \partial_{\mathbf{f}_e^{\natural}} \psi_0^t} \quad (3.53)$$

with $\text{cof}(\mathbf{f}_e^{\sharp}) = \det(\mathbf{f}_e^{\sharp}) [\mathbf{F}_e^{\sharp}]^t$ being obvious, compare Appendix B.1. Moreover, a Piola transformation with respect to \mathcal{B}_p yields the intermediate elastic inverse motion Cauchy stress $[\widehat{\boldsymbol{\pi}}_e^{\sharp}]^t \cdot \text{cof}(\mathbf{F}_e^{\sharp}) \doteq [\widehat{\boldsymbol{\Sigma}}_e^{\sharp}]^t \in \mathbb{L}^3 : T\mathcal{B}_p \times T^*\mathcal{B}_p \rightarrow \mathbb{R}$, see e.g. Murnaghan [Mur51, Sect. 1.3]. After some straightforward computations, we obtain

$$\begin{aligned}
[\widehat{\boldsymbol{\Sigma}}_e^{\sharp}]^t &= \det(\mathbf{F}_e^{\sharp}) [\boldsymbol{\pi}_e^{\sharp}]^t \cdot [\mathbf{f}_e^{\sharp}]^t \\
&= \det(\mathbf{f}_p^{\sharp}) \psi_0^p [\widehat{\mathbf{G}}^{\sharp}]^t + \det(\mathbf{f}_p^{\sharp}) \partial_{\mathbf{f}_e^{\sharp}} \psi_0^p \cdot [\mathbf{f}_e^{\sharp}]^t \\
&= \det(\mathbf{f}_p^{\sharp}) \psi_0^p [\widehat{\mathbf{G}}^{\sharp}]^t + 2 \det(\mathbf{f}_p^{\sharp}) \left[[\mathbf{g}^b \cdot \mathbf{F}_e^{\sharp} \cdot \partial_{\widehat{\mathbf{C}}_e^b} \psi_0^p] : \partial_{\mathbf{f}_e^{\sharp}} \mathbf{F}_e^{\sharp} + \sum_{i=1}^n \partial_{\widehat{\mathbf{A}}_i^{\sharp}} \psi_0^p \cdot \mathbf{f}_e^{\sharp} \cdot \mathbf{a}_i^{\sharp} \right] \cdot [\mathbf{f}_e^{\sharp}]^t \\
&= \det(\mathbf{f}_p^{\sharp}) \psi_0^p [\widehat{\mathbf{G}}^{\sharp}]^t - 2 \det(\mathbf{f}_p^{\sharp}) \left[\widehat{\mathbf{C}}_e^b \cdot \partial_{\widehat{\mathbf{C}}_e^b} \psi_0^p - \sum_{i=1}^n \partial_{\widehat{\mathbf{A}}_i^{\sharp}} \psi_0^p \cdot \widehat{\mathbf{A}}_i^{\sharp} \right],
\end{aligned} \tag{3.54}$$

based on Eq.(3.5), which allows interpretation as one possible Eshelby stress tensor. Please note that alternative derivatives of appropriate representations of the free Helmholtz energy densities (ψ_p^p and ψ_t^t) with respect to \mathbf{f}_p^{\sharp} and \mathbf{f}^{\sharp} render further formats of Eshelbian stress tensors. One could additionally consider the direct motion problem monitored by $\boldsymbol{\varphi}(\mathbf{X}, t)$, see e.g. Steinmann [Ste01] for a comprehensive survey within a non–dissipative setting.

Next, by summarising terms and from Eqs.(3.18, 3.33), we observe

$$\boxed{\det(\mathbf{F}_p^{\sharp}) [\widehat{\boldsymbol{\Sigma}}_e^{\sharp}]^t - \psi_0^p [\widehat{\mathbf{G}}^{\sharp}]^t = -[\widehat{\mathbf{M}}^{\sharp}]^t - 2 \sum_{i=1}^n \widehat{\mathbf{Z}}_i^b \cdot \widehat{\mathbf{A}}_i^{\sharp} = 2 \widehat{\mathbf{Y}}^b \cdot \widehat{\mathbf{G}}^{\sharp}} \tag{3.55}$$

together with the remarkable result

$$\boxed{\widehat{\mathbf{G}}^{\sharp} \cdot [\widehat{\boldsymbol{\Sigma}}_e^{\sharp}]^t = \widehat{\boldsymbol{\Sigma}}_e^{\sharp} \cdot \widehat{\mathbf{G}}^{\sharp} \quad \text{and} \quad [\widehat{\boldsymbol{\Sigma}}_e^{\sharp}]^t \cdot \widehat{\mathbf{G}}^b = \widehat{\mathbf{G}}^b \cdot \widehat{\boldsymbol{\Sigma}}_e^{\sharp}} \tag{3.56}$$

since $\widehat{\mathbf{Y}}^b$ is symmetric throughout, compare Svendsen [Sve01b] for a similar approach in terms of \mathbf{F}_p^{\sharp} . Naturally, push–forward and pull–back operations with respect to \mathbf{F}_e^{\sharp} and \mathbf{f}_p^{\sharp} can be applied to this introduced Eshelbian stress measure which result in

$$\begin{aligned}
[\boldsymbol{\sigma}_e^{\sharp}]^t \doteq [\mathbf{f}_e^{\sharp}]^t \cdot [\widehat{\boldsymbol{\Sigma}}_e^{\sharp}]^t \cdot [\mathbf{F}_e^{\sharp}]^t &\implies \mathbf{b}_e^{\sharp} \cdot [\boldsymbol{\sigma}_e^{\sharp}]^t = \boldsymbol{\sigma}_e^{\sharp} \cdot \mathbf{b}_e^{\sharp} \quad \text{and} \quad [\boldsymbol{\sigma}_e^{\sharp}]^t \cdot \mathbf{c}_e^b = \mathbf{c}_e^b \cdot \boldsymbol{\sigma}_e^{\sharp}, \\
[\boldsymbol{\Sigma}_e^{\sharp}]^t \doteq [\mathbf{F}_p^{\sharp}]^t \cdot [\widehat{\boldsymbol{\Sigma}}_e^{\sharp}]^t \cdot [\mathbf{f}_p^{\sharp}]^t &\implies \mathbf{B}_p^{\sharp} \cdot [\boldsymbol{\Sigma}_e^{\sharp}]^t = \boldsymbol{\Sigma}_e^{\sharp} \cdot \mathbf{B}_p^{\sharp} \quad \text{and} \quad [\boldsymbol{\Sigma}_e^{\sharp}]^t \cdot \mathbf{C}_p^b = \mathbf{C}_p^b \cdot \boldsymbol{\Sigma}_e^{\sharp}.
\end{aligned} \tag{3.57}$$

Moreover, the isothermal pointwise dissipation inequality in \mathcal{B}_p allows representation as

$$\begin{aligned}
\mathcal{D}_0^p &= [\widehat{\mathbf{M}}^{\sharp}]^t : \widehat{\mathbf{L}}^{\sharp} - \partial_{\mathbf{f}_e^{\sharp}} \psi_0^p : D_t \mathbf{f}_e^{\sharp} - \sum_{i=1}^n \partial_{\widehat{\mathbf{A}}_i^{\sharp}} \psi_0^p : [\mathbf{f}_{e^{\star}}^{\sharp} D_t \mathbf{a}_i^{\sharp}] - \partial_{\kappa} \psi_0^p D_t \kappa \\
&= [\widehat{\mathbf{M}}^{\sharp}]^t : \widehat{\mathbf{L}}^{\sharp} - \left[\partial_{\mathbf{f}_e^{\sharp}} \psi_0^p \cdot [\mathbf{f}_e^{\sharp}]^t \right] : [D_t \mathbf{f}_e^{\sharp} \cdot \mathbf{F}_e^{\sharp}] \\
&+ \sum_{i=1}^n \widehat{\mathbf{Z}}_i^b : \left[\mathbf{f}_{e^{\star}}^{\sharp} L_t \mathbf{a}_i^{\sharp} + 2 \mathbf{f}_{e^{\star}}^{\sharp} [L^{\sharp} \cdot \mathbf{a}_i^{\sharp}]^{\text{sym}} \right] + h D_t \kappa \\
&= \left[[\widehat{\mathbf{M}}^{\sharp}]^t + 2 \sum_{i=1}^n \widehat{\mathbf{Z}}_i^b \cdot \widehat{\mathbf{A}}_i^{\sharp} \right] : \widehat{\mathbf{L}}^{\sharp} \\
&+ \left[\det(\mathbf{F}_p^{\sharp}) [\widehat{\boldsymbol{\Sigma}}_e^{\sharp}]^t - \psi_0^p [\widehat{\mathbf{G}}^{\sharp}]^t \right] : \widehat{\mathbf{L}}^{\sharp} + \sum_{i=1}^n \widehat{\mathbf{Z}}_i^b : L_t^p \widehat{\mathbf{A}}_i^{\sharp} + h D_t \kappa \\
&= \left[[\widehat{\mathbf{M}}^{\sharp}]^t + 2 \sum_{i=1}^n \widehat{\mathbf{Z}}_i^b \cdot \widehat{\mathbf{A}}_i^{\sharp} + \det(\mathbf{F}_p^{\sharp}) [\widehat{\boldsymbol{\Sigma}}_e^{\sharp}]^t - \psi_0^p [\widehat{\mathbf{G}}^{\sharp}]^t \right] : \widehat{\mathbf{L}}^{\sharp} \\
&+ \left[[\widehat{\mathbf{M}}^{\sharp}]^t + 2 \sum_{i=1}^n \widehat{\mathbf{Z}}_i^b \cdot \widehat{\mathbf{A}}_i^{\sharp} \right] : \widehat{\mathbf{L}}_p^{\sharp} + \sum_{i=1}^n \widehat{\mathbf{Z}}_i^b : L_t^p \widehat{\mathbf{A}}_i^{\sharp} + h D_t \kappa \geq 0
\end{aligned} \tag{3.58}$$

whereby the relation $D_t(\mathbf{f}_e^\sharp \cdot \mathbf{F}_e^\sharp) = \mathbf{0} \implies -D_t \mathbf{f}_e^\sharp \cdot \mathbf{F}_e^\sharp = \mathbf{f}_e^\sharp \cdot D_t \mathbf{F}_e^\sharp = \widehat{\mathbf{L}}_e^\sharp = \widehat{\mathbf{L}}^\sharp - \widehat{\mathbf{L}}_p^\sharp$ and Eq.(3.54) have been applied. Thus, based on the common argumentation of rational thermodynamics, the reduced format of the dissipation inequality reads

$$\begin{aligned} \text{red} \mathcal{D}_0^p &= \left[\psi_0^p [\widehat{\mathbf{G}}^\sharp]^t - \det(\mathbf{F}_p^\sharp) [\widehat{\boldsymbol{\Sigma}}_e^\sharp]^t \right] : \widehat{\mathbf{L}}_p^\sharp + \sum_{i=1}^n \widehat{\mathbf{Z}}_i^b : L_t^p \widehat{\mathbf{A}}_i^\sharp + h D_t \kappa \\ &= -2 \left[\widehat{\mathbf{Y}}^b \cdot \widehat{\mathbf{G}}^\sharp \right] : \widehat{\mathbf{L}}_p^\sharp + \sum_{i=1}^n \widehat{\mathbf{Z}}_i^b : L_t^p \widehat{\mathbf{A}}_i^\sharp + h D_t \kappa \geq 0, \end{aligned} \quad (3.59)$$

compare Eqs.(3.55). Apparently the incorporated stress measure $\widehat{\mathbf{Y}}^b \cdot \widehat{\mathbf{G}}^\sharp$ turns out to be symmetric with respect to $[\widehat{\mathbf{G}}^\sharp]^t$ with the Eshelbian stress $[\widehat{\boldsymbol{\Sigma}}_e^\sharp]^t$ being likewise symmetric but the Mandel tensor $[\widehat{\mathbf{M}}^\sharp]^t$ being obviously non-symmetric in general, compare Eq.(3.56). In this context, the non-symmetric part of $\widehat{\mathbf{L}}_p^\sharp$ (with respect to $[\widehat{\mathbf{G}}^\sharp]^t$) remains undetermined and thus the incorporation of a plastic spin is superfluous within the proposed framework with respect to \mathcal{B}_p (when choosing a Cartesian setting), compare Svendsen [Sve01b]. For a general discussion on plastic spin, we refer to Dafalias [Daf98] and references cited therein. Push-forward and pull-back operations of the isothermal pointwise dissipation inequality in \mathcal{B}_p to the spatial and material setting nevertheless yield

$$\begin{aligned} \text{red} \mathcal{D}_0^t &= -2 \left[\mathbf{y}^b \cdot \mathbf{b}_e^\sharp \right] : \mathbf{l}_p^\sharp + \sum_{i=1}^n \mathbf{z}_i^b : L_t \mathbf{a}_i^\sharp + h D_t \kappa \geq 0, \\ \text{red} \mathcal{D}_0^0 &= -2 \left[\mathbf{Y}^b \cdot \mathbf{B}_p^\sharp \right] : \mathbf{L}_p^\sharp + \sum_{i=1}^n \mathbf{Z}_i^b : D_t \mathbf{A}_i^\sharp + h D_t \kappa \geq 0, \end{aligned} \quad (3.60)$$

with $\mathbf{y}^b \cdot \mathbf{b}_e^\sharp$ and $\mathbf{Y}^b \cdot \mathbf{B}_p^\sharp$ being non-symmetric in the general anisotropic case (with respect to $[\mathbf{g}^\sharp]^t$ and $[\mathbf{G}^\sharp]^t$). The corresponding associated evolution equations for the hardening variable κ and the incorporated strain measure, e.g. \mathbf{b}_e^\sharp , which leaves the evolution of the plastic spin undetermined are exactly those which are proposed in the current framework, compare Eqs.(3.37, 3.23–3.25, 3.44, 3.47, 3.50).

3.7 Numerical time integration

Concerning the integration of the evolution equations within the proposed anisotropic framework, we consider the usual decomposition into a finite number of time intervals

$$\mathbb{T} = \bigcup_{n=0}^N [{}^n t, {}^{n+1} t]. \quad (3.61)$$

In order to guarantee incrementally objective integration algorithms within the spatial setting, we apply pull-back operations of the spatial fields to the reference configuration, then the integration is performed in \mathcal{B}_0 and finally, a push-forward of the obtained quantities to the Eulerian setting yields the demanded variables. The approach allows similar interpretation as the concept of a Lie-derivative. Without loss of generality, the incorporated contra-variant spatial flow directions are defined by

$$\mathbf{F}_\star^\sharp \partial_{[\bullet^0]^b} \text{pot} \Phi^0 = \partial_{[\bullet^t]^b} \text{pot} \Phi^t = \boldsymbol{\xi}_{[\bullet^t]^b}^\sharp \quad (3.62)$$

whereby the notations $[\bullet^0]^b$ and $[\bullet^t]^b$ indicate the thermodynamic forces \mathbf{Y}^b , \mathbf{Z}_i^b and \mathbf{y}^b , \mathbf{z}_i^b , respectively. Moreover, spatial contravariant trial fields are obtained via

$${}^{n+1} \mathbf{F}_\star^\sharp n[\bullet^0]^\sharp = {}^{n+1} \mathbf{F}_\star^\sharp n \mathbf{f}_\star^\sharp n[\bullet^t]^\sharp = \Delta t \mathbf{F}_\star^\sharp n[\bullet^t]^\sharp = \text{trial}[\bullet^t]^\sharp, \quad (3.63)$$

incorporating the abbreviations $[\bullet^0]^\sharp$ for \mathbf{B}_p^\sharp , \mathbf{A}_i^\sharp and $[\bullet^t]^\sharp$ characterising \mathbf{b}_e^\sharp , \mathbf{a}_i^\sharp . Based on these spatial fields, we seek a robust and simple integration technique. Since no exponential algorithm is conveniently available, due to the non-coaxiality of the trial values and the flow directions, we apply a

simple Euler backward approach which results in

$$\begin{aligned} n+1 \mathbf{b}_e^\# &= \text{trial} \mathbf{b}_e^\# + \Delta \lambda \ n+1 \boldsymbol{\xi}_{y^b}^\#, \\ n+1 \mathbf{a}_i^\# &= \text{trial} \mathbf{a}_i^\# + \Delta \lambda \ n+1 \boldsymbol{\xi}_{z_i^b}^\#, \\ n+1 \kappa &= \text{trial} \kappa + \Delta \lambda \ n+1 \xi_h. \end{aligned} \quad (3.64)$$

see Section 5.3 and Appendix E.1 for applications of higher order (implicit and explicit) Runge–Kutta methods.

Within the subsequent numerical examples, a staggered solution technique is applied, that is a Newton–type algorithm to solve the system (3.64) is embedded into a scalar–valued iteration for the Lagrange multiplier $\Delta \lambda$, see Algorithm 3.1 and e.g. Engeln–Müllges and Uhlig [EMU96, Chap. 2 & 6] for a survey on standard procedures to solve non–linear equations. In view of the Newton iteration, we obtain the following residua

$$\begin{aligned} \text{pla}_{\mathcal{R}}^\# &= n+1 \mathbf{b}_e^\# - \text{trial} \mathbf{b}_e^\# - \Delta \lambda \ n+1 \boldsymbol{\xi}_{y^b}^\#, \\ \text{fib}_{\mathcal{R}_i}^\# &= n+1 \mathbf{a}_i^\# - \text{trial} \mathbf{a}_i^\# - \Delta \lambda \ n+1 \boldsymbol{\xi}_{z_i^b}^\#, \\ \text{har}_{\mathcal{R}} &= n+1 \kappa - \text{trial} \kappa - \Delta \lambda \ n+1 \xi_h, \end{aligned} \quad (3.65)$$

and Jacobians

$$\begin{aligned} \text{pla}_{\mathbf{J}_{b_e^\#}}^\# &= \partial_{b_e^\#} \text{pla}_{\mathcal{R}}^\#, & \text{pla}_{\mathbf{J}_{a_i^\#}}^\# &= \partial_{a_i^\#} \text{pla}_{\mathcal{R}}^\#, \\ \text{fib}_{\mathbf{J}_{i b_e^\#}}^\# &= \partial_{b_e^\#} \text{fib}_{\mathcal{R}_i}^\#, & \text{fib}_{\mathbf{J}_{i a_j^\#}}^\# &= \partial_{a_j^\#} \text{pla}_{\mathcal{R}_i}^\#, \\ \text{har}_j &= \partial_h \text{har}_{\mathcal{R}}, \end{aligned} \quad (3.66)$$

which define a system of linear equations within each iteration step

$$\begin{bmatrix} \text{pla}_{\mathbf{J}_{b_e^\#}}^\# & \text{pla}_{\mathbf{J}_{a_1^\#}}^\# & \cdots & \text{pla}_{\mathbf{J}_{a_n^\#}}^\# \\ \text{fib}_{\mathbf{J}_{1 b_e^\#}}^\# & \text{fib}_{\mathbf{J}_{1 a_1^\#}}^\# & \cdots & \text{fib}_{\mathbf{J}_{1 a_n^\#}}^\# \\ \vdots & \vdots & \ddots & \vdots \\ \text{fib}_{\mathbf{J}_{n b_e^\#}}^\# & \text{fib}_{\mathbf{J}_{n a_1^\#}}^\# & \cdots & \text{fib}_{\mathbf{J}_{n a_n^\#}}^\# \\ \text{har}_j \end{bmatrix} \circ \begin{bmatrix} \Delta b_e^\# \\ \Delta a_1^\# \\ \vdots \\ \Delta a_n^\# \\ \Delta \kappa \end{bmatrix} = \begin{bmatrix} - \text{pla}_{\mathcal{R}}^\# \\ - \text{fib}_{\mathcal{R}_1}^\# \\ \vdots \\ - \text{fib}_{\mathcal{R}_n}^\# \\ - \text{har}_{\mathcal{R}} \end{bmatrix}, \quad (3.67)$$

with the notation \circ denoting the appropriate contraction. It thereby turns out to be convenient to approximate the Jacobians by a first order difference scheme, see Appendix E.2 and Dennis and Schnabel [DS96, Chaps. 4 & 5]. A similar approach is applied within a finite element setting for the spatial algorithmic tangent operator, $L_t \boldsymbol{\tau}^\# = \frac{1}{2} \text{algo} \mathbf{e}^\# : L_t \mathbf{g}^b$, as advocated by Miehe [Mie96b].

Remark 3.3 *Apparently, the Euler backward integration scheme does not satisfy the commonly assumed constraint of plastic incompressibility, i.e. $\det(\mathbf{F}_p^\#) \doteq 1 \implies \det(\mathbf{b}_e^\#) = \det(\mathbf{b}^\#)$. This topic needs further investigations and interpretations within a general anisotropic setting and is beyond the scope of this Chapter (see also Remark 6.6). However, a numerical correction (within every iteration step) is advocated in Sarma and Zacharia [SZ99] which – transmitted to the present framework – yields $n+1 \mathbf{b}_{e \text{ cor}}^\# \doteq \det^{\frac{1}{3}}(n+1 \mathbf{b}^\#) \det^{-\frac{1}{3}}(n+1 \mathbf{b}_e^\#) n+1 \mathbf{b}_e^\#$.[†]*

[†] For the specific case of a plastic incompressible and isotropic setting we usually deal with inelastic potentials that are un–affected by the spherical part $y^b g^\# I_1 \doteq \mathbf{g}^\# : \mathbf{y}^b = \text{tr}(\mathbf{y}^b)$ or $g^b \tau^\# I_1 \doteq \mathbf{g}^b : \boldsymbol{\tau}^\# = \text{tr}(\boldsymbol{\tau}^\#)$ respectively, see e.g. Remark 3.4. Therefore, the contribution $g^b b_e^\# I_1 \doteq \mathbf{g}^b : \mathbf{b}_e^\# = \text{tr}(\mathbf{b}_e^\#)$ is un–determined and can be chosen such that the constraint

Algorithm 3.1 *Staggered solution technique: Newton–type algorithm to solve the set of non–linear equations in \mathbf{b}_e^\sharp , $\mathbf{a}_{1,\dots,n}^\sharp$ and κ embedded into a scalar–valued iteration (e.g. modified regula–falsi schemes) to compute the Lagrange multiplier $\Delta\lambda$.*

```

(Finite Element Method)   for given  $n+1 \mathbf{F}^\sharp$  do
                           if  $y^{ie}\Phi^t|_{n+1} > 0$  then
(scalar–valued iteration) dowhile  $|y^{ie}\Phi^t(\Delta\lambda)|_{n+1} > \text{tol}$ 
                            $\Delta\lambda = \dots$ 
(Newton–type method)     dowhile  $\|\text{pla}\mathbf{r}^\sharp\| + \|\text{fib}\mathbf{r}^\sharp\| + |\text{har}r| > \text{tol}$ 
                            $\dots$ 
                            $n+1 \mathbf{b}_e^\sharp + \Delta\mathbf{b}_e^\sharp \mapsto n+1 \mathbf{b}_e^\sharp$ 
                            $n+1 \mathbf{a}_{1,\dots,n}^\sharp + \Delta\mathbf{a}_{1,\dots,n}^\sharp \mapsto n+1 \mathbf{a}_{1,\dots,n}^\sharp$ 
                            $n+1 \kappa + \Delta\kappa \mapsto n+1 \kappa$ 
                           enddo
                           enddo
                           endif

```

3.8 Prototype model

In view of the subsequent numerical examples, a specific prototype model is chosen that accounts for elastic, plastic and deformation induced anisotropy. In order to obtain a manageable setting, we incorporate a subset of the complete list of invariants as monitored in Tables 3.1 and 3.2, respectively.

3.8.1 Free Helmholtz energy density

In the sequel, the assumption of an additive decomposition of the free Helmholtz energy density is adopted which is well–established in the computational mechanics literature and reads with respect of plastic incompressibility is generally satisfied. In particular we seek $f \in \mathbb{R}$ as the solution of ($n_{\text{dim}} \doteq 3$)

$$\det(\text{dev}\mathbf{b}_e^\sharp + f\mathbf{g}^\sharp) - \det(\mathbf{b}^\sharp) \doteq 0 \quad \text{with} \quad \text{dev}\mathbf{b}_e^\sharp = \mathbf{b}_e^\sharp - \frac{1}{3}g^b b_e^\sharp I_1 \mathbf{g}^\sharp \quad \text{and} \quad [\text{dev}\mathbf{b}_e^\sharp + f\mathbf{g}^\sharp] \mapsto \mathbf{b}_e^\sharp \quad (\dagger.1)$$

being obvious, compare e.g. Miehe [Mie95] or Bonet [Bon01]. The fundamental relation

$$\det(\mathbf{d} + \mathbf{e}) = \det(\mathbf{d}) + \text{cof}^t(\mathbf{d}) : \mathbf{e} + \mathbf{d} : \text{cof}^t(\mathbf{e}) + \det(\mathbf{e}) \quad \forall \mathbf{d}, \mathbf{e} \in \mathbb{L}^3, \quad (\dagger.2)$$

whereby, e.g., $\text{cof}(\mathbf{d}) = \mathbf{d}^2 - \text{tr}(\mathbf{d})\mathbf{d} + \frac{1}{2}[\text{tr}^2(\mathbf{d}) - \text{tr}(\mathbf{d}^2)]\mathbf{I}$ is always defined and $\mathbf{I} \in \mathbb{S}_+^3$ denotes the second order identity, results for the present context in (recall the relations $\det(f\mathbf{f}) = f^3 \det(\mathbf{f})$ and $\text{cof}(f\mathbf{f}) = f^2 \text{cof}(\mathbf{f})$ with $f \in \mathbb{R}$, $\mathbf{f} \in \mathbb{L}^3$)

$$\det(\mathbf{d} + f\mathbf{f}) - d \doteq 0 \quad \iff \quad f^3 \det(\mathbf{f}) + f^2 \mathbf{d} : \text{cof}^t(\mathbf{f}) + f \text{cof}^t(\mathbf{d}) : \mathbf{f} + [\det(\mathbf{d}) - d] \doteq 0 \quad (\dagger.3)$$

which apparently is a cubic equation in f . Next, by placing emphasis on Eq.(†.1) we obtain

$$\frac{1}{\sqrt{g}} f^3 + f^2 g^b \text{dev} b_e^\sharp I_1 + \frac{1}{2} f \left[g^b \text{dev} b_e^\sharp I_1^2 - g^b \text{dev} b_e^\sharp I_2 \right] = \frac{1}{\sqrt{g}} f^3 - \frac{1}{2} f g^b \text{dev} b_e^\sharp I_2 \doteq \det(\mathbf{b}^\sharp) - \det(\text{dev}\mathbf{b}_e^\sharp) \quad (\dagger.4)$$

with $g^b \text{dev} b_e^\sharp I_2 \doteq g^b : \left[\text{dev}\mathbf{b}_e^\sharp \cdot g^b \cdot \text{dev}\mathbf{b}_e^\sharp \right] = \text{tr}([\text{dev}\mathbf{b}_e^\sharp]^2)$, $g^b \text{dev} b_e^\sharp I_1 = 0$ and $\det(\mathbf{g}^\sharp) \doteq \frac{1}{\sqrt{g}} \in \mathbb{R}_+$. Alternatively, the substitution $f \doteq \frac{1}{3} g^b b_e^\sharp I_1$, from Eq.(†.1), yields a cubic equation in $\text{tr}(\mathbf{b}_e^\sharp)$, namely

$$\frac{1}{\sqrt{g}} g^b b_e^\sharp I_1^3 - \frac{9}{2} g^b b_e^\sharp I_1 g^b \text{dev} b_e^\sharp I_2 \doteq 27 [\det(\mathbf{b}^\sharp) - \det(\text{dev}\mathbf{b}_e^\sharp)] \quad (\dagger.5)$$

Eqs.(†.4, †.5) can be solved either numerically by any appropriate iteration scheme or analytically via Cardan's formula. The latter approach is based on the normalised format of cubic equations, say $\vartheta^3 + r\vartheta^2 + s\vartheta + t = 0$ with $\vartheta \equiv f$ or $\vartheta \equiv g^b b_e^\sharp I_1$, respectively, and $r = 0$ since $\text{tr}(\text{dev}\mathbf{b}_e^\sharp) = 0$. Hence, the first (real) solution (the others possibly being conjugate complex) to the problem at hand is represented by $\vartheta_{(1)} = v - \frac{s}{3v}$ with $v = \sqrt[3]{-\frac{t}{2} + \sqrt{\frac{s^3}{27} + \frac{t^2}{4}}}$.

to the spatial setting as

$$\psi_0^t \doteq \text{iso}\psi_0^t(\mathbf{g}^b, \mathbf{b}_e^\sharp; \mathbf{X}) + \text{ani}\psi_0^t(\mathbf{g}^b, \mathbf{b}_e^\sharp, \mathbf{a}_{1,\dots,n}^\sharp; \mathbf{X}) + \text{har}\psi_0(\kappa; \mathbf{X}). \quad (3.68)$$

Moreover, we only consider two additional arguments in the anisotropic part of the free Helmholtz energy density, i.e. $\mathbf{a}_{1,2}^\sharp \neq \mathbf{0}$ and $\mathbf{a}_{3,\dots,n}^\sharp = \mathbf{0}$. Thus, if $\mathbf{a}_{1,2}^\sharp|_{t_0}$ are of rank one, we model an initially orthotropic material within the elastic domain.

The isotropic contribution $\text{iso}\psi_0^t$ is consequently defined by three basic invariants or, alternatively, three principal invariants as appearing in the underlying characteristic polynomial, e.g. the determinant,

$$\begin{aligned} g^b b_e^\sharp I_1 &= \mathbf{g}^b : \mathbf{b}_e^\sharp, & g^b b_e^\sharp I_2 &= [\mathbf{g}^b \cdot \mathbf{b}_e^\sharp \cdot \mathbf{g}^b] : \mathbf{b}_e^\sharp, & g^b b_e^\sharp I_3 &= [\mathbf{g}^b \cdot [\mathbf{b}_e^\sharp \cdot \mathbf{g}^b]^2] : \mathbf{b}_e^\sharp, \\ \det(\mathbf{b}_e^\sharp) &= \frac{1}{6} \left[2 g^b b_e^\sharp I_3 - 3 g^b b_e^\sharp I_1 g^b b_e^\sharp I_2 + g^b b_e^\sharp I_1^3 \right], \end{aligned} \quad (3.69)$$

compare Appendix B.2. Next, in analogy to the work by Spencer [Spe84] within linear elastic orthotropy, we incorporate the following four invariants

$$\begin{aligned} g^b a_{1,2}^\sharp I_4 &= \mathbf{g}^b : \mathbf{a}_1^\sharp, & g^b a_{1,2}^\sharp I_5 &= [\mathbf{g}^b \cdot \mathbf{b}_e^\sharp \cdot \mathbf{g}^b] : \mathbf{a}_1^\sharp, \\ g^b a_{1,2}^\sharp I_6 &= \mathbf{g}^b : \mathbf{a}_2^\sharp, & g^b a_{1,2}^\sharp I_7 &= [\mathbf{g}^b \cdot \mathbf{b}_e^\sharp \cdot \mathbf{g}^b] : \mathbf{a}_2^\sharp \end{aligned} \quad (3.70)$$

into the anisotropic part $\text{ani}\psi_0^t$ of the free Helmholtz energy density and additionally consider two further invariants

$$c_e^b a_{1,2}^\sharp I_1 = \mathbf{c}_e^b : \mathbf{a}_1^\sharp, \quad c_e^b a_{1,2}^\sharp I_2 = \mathbf{c}_e^b : \mathbf{a}_2^\sharp \quad (3.71)$$

which account for the fact that the structural or rather anisotropy tensors are not constant in \mathcal{B}_p .

In view of the isotropic contribution, we apply a standard Neo–Hooke–type function, namely

$$\text{iso}\psi_0^t \doteq \frac{G}{2} \left[\det^{-1/3}(\mathbf{b}_e^\sharp) g^b b_e^\sharp I_1 - 3 \right] + \frac{K}{2} \left[\frac{1}{2} [\det(\mathbf{b}_e^\sharp) - 1] - \ln \left(\det^{1/2}(\mathbf{b}_e^\sharp) \right) \right] \quad (3.72)$$

as reiterated in Eq.(C.7). The anisotropic part $\text{ani}\psi_0^t$ of the proposed prototype model reads as

$$\begin{aligned} \text{ani}\psi_0^t &\doteq \left[\gamma_1 [g^b a_{1,2}^\sharp I_4 - 1] + \gamma_2 [g^b a_{1,2}^\sharp I_6 - 1] \right] [g^b b_e^\sharp I_1 - 3] \\ &+ \frac{1}{2} \gamma_3 [g^b a_{1,2}^\sharp I_5 - 1]^2 + \frac{1}{2} \gamma_4 [g^b a_{1,2}^\sharp I_7 - 1]^2 \\ &+ \frac{1}{2} \gamma_5 [g^b a_{1,2}^\sharp I_4 - 1]^2 + \frac{1}{2} \gamma_6 [g^b a_{1,2}^\sharp I_6 - 1]^2 \\ &+ \gamma_7 [g^b a_{1,2}^\sharp I_4 - 1] [g^b a_{1,2}^\sharp I_6 - 1] \\ &+ \gamma_8 \left[\exp(g^b a_{1,2}^\sharp I_4 - 1) - g^b a_{1,2}^\sharp I_4 \right] \\ &+ \gamma_9 \left[\exp(g^b a_{1,2}^\sharp I_6 - 1) - g^b a_{1,2}^\sharp I_6 \right] \\ &+ \frac{1}{2} \gamma_{10} c_e^b a_{1,2}^\sharp I_1 [g^b b_e^\sharp I_1 - 3]^2 + \frac{1}{2} \gamma_{11} c_e^b a_{1,2}^\sharp I_2 [g^b b_e^\sharp I_1 - 3]^2 \end{aligned} \quad (3.73)$$

within orthotropic symmetry if $\mathbf{a}_{1,2}^\sharp$ have rank one, compare Eq.(3.9). The chosen prototype free Helmholtz energy density is similar to the approach by Spencer [Spe84] – for two orthogonal fibres which are not mechanically identical – but additionally enlarged by two exponential contributions and two further terms that account for $\widehat{\mathbf{A}}_{1,2}^\sharp$ not being constant. Concerning the hardening part $\text{har}\psi_0$ in terms of the scalar–valued internal variable κ , an additive combination of an exponential saturation–type and a parabolic function is adopted

$$\text{har}\psi_0 \doteq [Y_\infty - Y_0] [\kappa + \delta_1^{-1} \exp(-\delta_1 \kappa) - \delta_1^{-1}] + \frac{1}{2} \delta_2 \kappa^2 \quad (3.74)$$

see e.g. Steinmann et al. [SMS96].

With this model at hand, the corresponding stress fields can be computed. Based on Eq.(3.15), the isotropic part of the Kirchhoff stress, $\boldsymbol{\tau}^\# = \text{iso}\boldsymbol{\tau}^\# + \text{ani}\boldsymbol{\tau}^\#$ from Eq.(3.68), is given by

$$\text{iso}\boldsymbol{\tau}^\# = \left[\frac{K}{2} [\det(\mathbf{b}_e^\#) - 1] - \frac{G}{3} \det^{-1/3}(\mathbf{b}_e^\#) g^b b_e^\# I_1 \right] \mathbf{g}^\# + G \det^{-1/3}(\mathbf{b}_e^\#) \mathbf{b}_e^\# \quad (3.75)$$

and the anisotropic complement reads

$$\begin{aligned} \text{ani}\boldsymbol{\tau}^\# = 2 \left[\right. & \left[\begin{aligned} & \gamma_1 [g^b a_{1,2}^\# I_4 - 1] + \gamma_2 [g^b a_{1,2}^\# I_6 - 1] \\ & + [\gamma_{10} c_e^b a_{1,2}^\# I_1 + \gamma_{11} c_e^b a_{1,2}^\# I_2] [g^b b_e^\# I_1 - 3] \end{aligned} \right] \mathbf{b}_e^\# \\ & + \left[\begin{aligned} & \gamma_5 [g^b a_{1,2}^\# I_4 - 1] + \gamma_7 [g^b a_{1,2}^\# I_6 - 1] \\ & + \gamma_8 [\exp(g^b a_{1,2}^\# I_4 - 1) - 1] + \gamma_1 [g^b b_e^\# I_1 - 3] \end{aligned} \right] \mathbf{a}_1^\# \\ & + \left[\begin{aligned} & \gamma_6 [g^b a_{1,2}^\# I_6 - 1] + \gamma_7 [g^b a_{1,2}^\# I_4 - 1] \\ & + \gamma_9 [\exp(g^b a_{1,2}^\# I_6 - 1) - 1] + \gamma_2 [g^b b_e^\# I_1 - 3] \end{aligned} \right] \mathbf{a}_2^\# \\ & + 2 \gamma_3 [g^b a_{1,2}^\# I_5 - 1] [\mathbf{b}_e^\# \cdot \mathbf{g}^b \cdot \mathbf{a}_1^\#]^{\text{sym}} \\ & + 2 \gamma_4 [g^b a_{1,2}^\# I_7 - 1] [\mathbf{b}_e^\# \cdot \mathbf{g}^b \cdot \mathbf{a}_2^\#]^{\text{sym}} \left. \right]. \end{aligned} \quad (3.76)$$

Furthermore, the thermodynamic forces can be computed and within this prototype model, Eqs.(3.68, 3.72–3.74), we obtain for the stress conjugate to the elastic Finger tensor

$$\text{iso}\mathbf{y}^b = \left[\frac{K}{4} [1 - \det(\mathbf{b}_e^\#)] + \frac{G}{6} \det^{-1/3}(\mathbf{b}_e^\#) g^b b_e^\# I_1 \right] \mathbf{c}_e^b - \frac{G}{2} \det^{-1/3}(\mathbf{b}_e^\#) \mathbf{g}^b, \quad (3.77)$$

$$\begin{aligned} \text{ani}\mathbf{y}^b = & \left[\gamma_1 [1 - g^b a_{1,2}^\# I_4] + \gamma_2 [1 - g^b a_{1,2}^\# I_6] + [\gamma_{10} c_e^b a_{1,2}^\# I_1 + \gamma_{11} c_e^b a_{1,2}^\# I_2] [3 - g^b b_e^\# I_1] \right] \mathbf{g}^b \\ & + \gamma_3 [3 - g^b b_e^\# I_1] \mathbf{g}^b \cdot \mathbf{a}_1^\# \cdot \mathbf{g}^b + \gamma_4 [3 - g^b b_e^\# I_1] \mathbf{g}^b \cdot \mathbf{a}_2^\# \cdot \mathbf{g}^b \\ & + \frac{1}{2} [g^b b_e^\# I_1 - 3]^2 [\gamma_{10} \mathbf{c}_e^b \cdot \mathbf{a}_1^\# \cdot \mathbf{c}_e^b + \gamma_{11} \mathbf{c}_e^b \cdot \mathbf{a}_2^\# \cdot \mathbf{c}_e^b] \end{aligned} \quad (3.78)$$

with $\mathbf{y}^b = \text{iso}\mathbf{y}^b + \text{ani}\mathbf{y}^b$. Further straightforward computations render the thermodynamic forces due to the fields $\mathbf{a}_{1,2}^\#$ that account for anisotropy

$$\begin{aligned} \mathbf{z}_{1,2}^b = & \left[\begin{aligned} & \gamma_{5,6} [1 - g^b a_{1,2}^\# I_{4,6}] + \gamma_7 [1 - g^b a_{1,2}^\# I_{6,4}] \\ & + \gamma_{8,9} [1 - \exp(g^b a_{1,2}^\# I_{4,6} - 1)] + \gamma_{1,2} [3 - g^b b_e^\# I_1] \end{aligned} \right] \mathbf{g}^b \\ & + \gamma_{3,4} [3 - g^b a_{1,2}^\# I_{5,7}] \mathbf{g}^b \cdot \mathbf{b}_e^\# \cdot \mathbf{g}^b - \frac{1}{2} \gamma_{10,11} [g^b b_e^\# I_1 - 3]^2 \mathbf{c}_e^b \end{aligned} \quad (3.79)$$

and the (proportional) hardening stress results in

$$h = [Y_0 - Y_\infty] [1 - \exp(-\delta_1 \kappa)] - \delta_2 \kappa. \quad (3.80)$$

Finally, placing emphasis on the implementation of the model within a finite element setting, the computation of the elastic tangent operator is a straightforward exercise. Once more separating into an isotropic and anisotropic contribution, we end up with

$$\begin{aligned} \text{iso}\mathbf{e}^\# = & \left[\frac{2G}{9} \det^{-1/3}(\mathbf{b}_e^\#) g^b b_e^\# I_1 + K \det(\mathbf{b}_e^\#) \right] \mathbf{g}^\# \otimes \mathbf{g}^\# \\ & + \left[\frac{G}{3} \det^{-1/3}(\mathbf{b}_e^\#) g^b b_e^\# I_1 + \frac{K}{2} [1 - \det(\mathbf{b}_e^\#)] \right] [\mathbf{g}^\# \overline{\otimes} \mathbf{g}^\# + \mathbf{g}^\# \underline{\otimes} \mathbf{g}^\#] \\ & - \frac{2G}{3} \det^{-1/3}(\mathbf{b}_e^\#) [\mathbf{b}_e^\# \overline{\otimes} \mathbf{g}^\# + \mathbf{g}^\# \underline{\otimes} \mathbf{b}_e^\#], \end{aligned} \quad (3.81)$$

$$\begin{aligned}
\text{ani } \mathbf{e}^\# &= 4 \left[\gamma_{10} c_e^b a_{1,2}^\# I_1 + \gamma_{11} c_e^b a_{1,2}^\# I_2 \right] \mathbf{b}_e^\# \otimes \mathbf{b}_e^\# \\
&+ 4 \gamma_1 [\mathbf{b}_e^\# \otimes \mathbf{a}_1^\# + \mathbf{a}_1^\# \otimes \mathbf{b}_e^\#] \\
&+ 4 \gamma_2 [\mathbf{b}_e^\# \otimes \mathbf{a}_2^\# + \mathbf{a}_2^\# \otimes \mathbf{b}_e^\#] \\
&+ 4 \left[\gamma_5 + \gamma_8 \exp(g^b a_{1,2}^\# I_4 - 1) \right] \mathbf{a}_1^\# \otimes \mathbf{a}_1^\# \\
&+ 4 \left[\gamma_6 + \gamma_9 \exp(g^b a_{1,2}^\# I_6 - 1) \right] \mathbf{a}_2^\# \otimes \mathbf{a}_2^\# \\
&+ 4 \gamma_7 [\mathbf{a}_1^\# \otimes \mathbf{a}_2^\# + \mathbf{a}_2^\# \otimes \mathbf{a}_1^\#] \\
&+ 16 \gamma_3 [\mathbf{b}_e^\# \cdot \mathbf{g}^b \cdot \mathbf{a}_1^\#]^{\text{sym}} \otimes [\mathbf{b}_e^\# \cdot \mathbf{g}^b \cdot \mathbf{a}_1^\#]^{\text{sym}} \\
&+ 16 \gamma_4 [\mathbf{b}_e^\# \cdot \mathbf{g}^b \cdot \mathbf{a}_2^\#]^{\text{sym}} \otimes [\mathbf{b}_e^\# \cdot \mathbf{g}^b \cdot \mathbf{a}_2^\#]^{\text{sym}} \\
&+ 2 \gamma_3 \left[g^b a_{1,2}^\# I_5 - 1 \right] [\mathbf{b}_e^\# \overline{\otimes} \mathbf{a}_1^\# + \mathbf{b}_e^\# \underline{\otimes} \mathbf{a}_1^\# + \mathbf{a}_1^\# \overline{\otimes} \mathbf{b}_e^\# + \mathbf{a}_1^\# \underline{\otimes} \mathbf{b}_e^\#] \\
&+ 2 \gamma_4 \left[g^b a_{1,2}^\# I_7 - 1 \right] [\mathbf{b}_e^\# \overline{\otimes} \mathbf{a}_2^\# + \mathbf{b}_e^\# \underline{\otimes} \mathbf{a}_2^\# + \mathbf{a}_2^\# \overline{\otimes} \mathbf{b}_e^\# + \mathbf{a}_2^\# \underline{\otimes} \mathbf{b}_e^\#].
\end{aligned} \tag{3.82}$$

3.8.2 Inelastic potentials

In view of the computation of the plastic potential, recall Eq.(3.35), we define the deviator of the stress conjugate to the elastic Finger tensor via

$$\boxed{\text{dev } \mathbf{y}^b = \mathbf{y}^b - n_{\text{dim}}^{-1} [\mathbf{y}^b : \mathbf{g}^\#] \mathbf{g}^b} \tag{3.83}$$

with n_{dim} characterising the appropriate dimension in space, compare Appendix A.1. The invariants of the deviator ${}^{\text{dev } \mathbf{y}^b} g^\# I_{1,2,3}$ are obviously functions of the three basic invariants of \mathbf{y}^b , say $I_{(i),(ii),(iii)}$ as given in Table 3.2. Thus, we introduce the invariant

$${}^{\text{dev } \mathbf{y}^b} g^\# I_2 = [\text{dev } \mathbf{y}^b \cdot \mathbf{g}^\# \cdot \text{dev } \mathbf{y}^b] : \mathbf{g}^\#, \tag{3.84}$$

in order to account for J_2 -type contributions in the plastic potential, see e.g. Simo [Sim98, Sect. 50] for an outline on the numerical treatment of (isotropic) J_2 -plasticity. Moreover, we incorporate two additional tensorial arguments of second order, namely $\mathbf{a}_{3,4}^\#$, for the construction of the plastic potential ${}^{\text{pla}} \Phi^t$. Thereby, without loss of generality, rank one properties

$$\mathbf{a}_3^\# = \mathbf{F}^\natural_\star A_3^\# \mathbf{N}^\# \otimes \mathbf{F}^\natural_\star A_3^\# \mathbf{N}^\#, \quad \mathbf{a}_4^\# = \mathbf{F}^\natural_\star A_4^\# \mathbf{N}^\# \otimes \mathbf{F}^\natural_\star A_4^\# \mathbf{N}^\#, \quad A_{3,4}^\# \mathbf{N}^\# \in \mathbb{U}^2 : T^* \mathcal{B}_0 \rightarrow \mathbb{R} \tag{3.85}$$

in the spirit of structural tensors are assumed. A rank three second order tensor $\mathbf{a}_5^\#$ could alternatively be introduced to set up a Hill-type criterion in terms of a fourth order tensor $\mathbf{a}_5^\#(\mathbf{a}_5^\#; \mathbf{X})$ via ${}^{\text{pla}} \Phi^t \doteq \mathbf{y}^b : \mathbf{a}_5^\# : \mathbf{y}^b$, compare Steinmann et al. [SMS96]. Next, similar to the construction of the prototype free Helmholtz energy density ψ_0^t , the following contributions are selected from the complete list of invariants as monitored in Table 3.2

$$\begin{aligned}
{}^{\text{dev } \mathbf{y}^b} a_{3,4}^\# I_4 &= \text{dev } \mathbf{y}^b : \mathbf{a}_3^\#, & {}^{\text{dev } \mathbf{y}^b} a_{3,4}^\# I_5 &= [\text{dev } \mathbf{y}^b \cdot \mathbf{g}^\# \cdot \text{dev } \mathbf{y}^b] : \mathbf{a}_3^\#, \\
{}^{\text{dev } \mathbf{y}^b} a_{3,4}^\# I_6 &= \text{dev } \mathbf{y}^b : \mathbf{a}_4^\#, & {}^{\text{dev } \mathbf{y}^b} a_{3,4}^\# I_7 &= [\text{dev } \mathbf{y}^b \cdot \mathbf{g}^\# \cdot \text{dev } \mathbf{y}^b] : \mathbf{a}_4^\#, \\
{}^g a_{3,4}^\# I_8 &= [\mathbf{a}_3^\# \cdot \mathbf{g}^b \cdot \mathbf{a}_4^\#] : \mathbf{g}^b.
\end{aligned} \tag{3.86}$$

Based on these ingredients and in analogy to Eq.(3.73), we consider the following prototype plastic potential

$$\begin{aligned}
{}^{\text{pla}} \Phi^t &\doteq \left[\eta_1 + \eta_8 g^b a_{3,4}^\# I_8 \right] {}^{\text{dev } \mathbf{y}^b} g^\# I_2 + \eta_6 {}^{\text{dev } \mathbf{y}^b} a_{3,4}^\# I_4 {}^{\text{dev } \mathbf{y}^b} a_{3,4}^\# I_6 \\
&+ 2 \eta_2 {}^{\text{dev } \mathbf{y}^b} a_{3,4}^\# I_5 + 2 \eta_3 {}^{\text{dev } \mathbf{y}^b} a_{3,4}^\# I_7 + \frac{1}{2} \eta_4 {}^{\text{dev } \mathbf{y}^b} a_{3,4}^\# I_4^2 + \frac{1}{2} \eta_5 {}^{\text{dev } \mathbf{y}^b} a_{3,4}^\# I_6^2
\end{aligned} \tag{3.87}$$

within orthotropic symmetry, compare Eq.(3.39). Please note that the term $\eta_1 \text{dev } \mathbf{y}^b g^\# I_2$ represents a classical J_2 -type plasticity which has been enlarged by the additional contribution $\eta_8 g^b a_{3,4}^\# I_8 \text{dev } \mathbf{y}^b g^\# I_2$ whereby $g^b a_{3,4}^\# I_8$ essentially characterises the angle between the fibres $\mathbf{F}^\# \star A_{3,4}^\# \mathbf{N}^\#$ which define $\mathbf{a}_{3,4}^\#$. The computation of the corresponding associated flow direction is straightforward and results (for the three-dimensional setting) in

$$\begin{aligned}
\boldsymbol{\xi}_{\mathbf{y}^b}^\# &= \partial_{\mathbf{y}^b} \text{pla} \Phi^t = \partial_{\text{dev } \mathbf{y}^b} \text{pla} \Phi^t : \partial_{\mathbf{y}^b} \text{dev } \mathbf{y}^b \\
&= \partial_{\text{dev } \mathbf{y}^b} \text{pla} \Phi^t : \left[\frac{1}{2} [\mathbf{g}^\# \otimes \mathbf{g}^\# + \mathbf{g}^\# \underline{\otimes} \mathbf{g}^\#] - \frac{1}{3} \mathbf{g}^b \otimes \mathbf{g}^\# \right] \\
&= 2 [\eta_1 + \eta_8 g^b a_{3,4}^\# I_8] \mathbf{g}^\# \cdot \text{dev } \mathbf{y}^b \cdot \mathbf{g}^\# \\
&+ [\eta_4 \text{dev } \mathbf{y}^b a_{3,4}^\# I_4 + \eta_6 \text{dev } \mathbf{y}^b a_{3,4}^\# I_6] \text{dev } \mathbf{a}_3^\# \\
&+ [\eta_5 \text{dev } \mathbf{y}^b a_{3,4}^\# I_6 + \eta_6 \text{dev } \mathbf{y}^b a_{3,4}^\# I_4] \text{dev } \mathbf{a}_4^\# \\
&+ 4 \eta_2 [\mathbf{g}^\# \cdot \text{dev } \mathbf{y}^b \cdot \mathbf{a}_3^\#]_{\text{sym}} - \frac{4}{3} \eta_2 [\text{dev } \mathbf{y}^b : \mathbf{a}_3^\#] \mathbf{g}^\# \\
&+ 4 \eta_3 [\mathbf{g}^\# \cdot \text{dev } \mathbf{y}^b \cdot \mathbf{a}_4^\#]_{\text{sym}} - \frac{4}{3} \eta_3 [\text{dev } \mathbf{y}^b : \mathbf{a}_4^\#] \mathbf{g}^\#
\end{aligned} \tag{3.88}$$

with $\text{dev } \mathbf{a}_{3,4}^\# = \mathbf{a}_{3,4}^\# - n_{\text{dim}}^{-1} [\mathbf{g}^b : \mathbf{a}_{3,4}^\#] \mathbf{g}^\#$ being obvious.

The prototype hardening potential, in terms of the hardening stress $h(\kappa)$, as well as the associated flow direction are rather standard and follow as

$$\text{har} \Phi \doteq -\frac{1}{3} [Y_0 - h]^2, \quad \xi_h = \partial_h \text{har} \Phi = \frac{2}{3} [Y_0 - h], \tag{3.89}$$

whereby Y_0 represents a constant threshold.

Finally, we assume possible prototype, say fibre potentials $\text{fib} \Phi^t$ to depend on the following two sets of invariants

$$\begin{aligned}
z_{1,2}^{b, a_{1,2}^\#} I_1 &= \mathbf{z}_1^b : \mathbf{a}_1^\#, & z_{1,2}^{b, a_{1,2}^\#} I_3 &= [\mathbf{z}_1^b \cdot \mathbf{a}_1^\# \cdot \mathbf{z}_1^b] : \mathbf{a}_1^\#, \\
z_{1,2}^{b, a_{1,2}^\#} I_2 &= \mathbf{z}_2^b : \mathbf{a}_2^\#, & z_{1,2}^{b, a_{1,2}^\#} I_4 &= [\mathbf{z}_2^b \cdot \mathbf{a}_2^\# \cdot \mathbf{z}_2^b] : \mathbf{a}_2^\#, \\
z_{1,2}^{b, g^\#} I_1 &= \mathbf{z}_1^b : \mathbf{g}^\#, & z_{1,2}^{b, g^\#} I_3 &= [\mathbf{z}_1^b \cdot \mathbf{g}^\# \cdot \mathbf{z}_1^b] : \mathbf{g}^\#, \\
z_{1,2}^{b, g^\#} I_2 &= \mathbf{z}_2^b : \mathbf{g}^\#, & z_{1,2}^{b, g^\#} I_4 &= [\mathbf{z}_2^b \cdot \mathbf{g}^\# \cdot \mathbf{z}_2^b] : \mathbf{g}^\#.
\end{aligned} \tag{3.90}$$

These ingredients enable us to construct different types of evolution equations. To be specific, we chose on the one hand

$$\text{fib} \Phi_{\text{fix}}^t \doteq \frac{1}{2} \eta_9 z_{1,2}^{b, a_{1,2}^\#} I_1^2 + \frac{1}{2} \eta_{10} z_{1,2}^{b, a_{1,2}^\#} I_2^2 + \frac{1}{2} \eta_{11} z_{1,2}^{b, a_{1,2}^\#} I_3^2 + \frac{1}{2} \eta_{12} z_{1,2}^{b, a_{1,2}^\#} I_4^2 \tag{3.91}$$

which retains the symmetry class of the body B since the corresponding flow directions

$$\boldsymbol{\xi}_{z_{1,2}^b}^\# = \partial_{z_{1,2}^b} \text{fib} \Phi_{\text{fix}}^t = \eta_9 z_{1,2}^{b, a_{1,2}^\#} I_{1,2} \mathbf{a}_{1,2}^\# + \eta_{10} z_{1,2}^{b, a_{1,2}^\#} I_{3,4} \mathbf{a}_{1,2}^\# \cdot \mathbf{z}_{1,2}^b \cdot \mathbf{a}_{1,2}^\# \tag{3.92}$$

show identical rank and principal directions as the structural tensors $\mathbf{a}_{1,2}^\#$, respectively. On the other hand, the introduction of

$$\text{fib} \Phi_{\text{cha}}^t \doteq \frac{1}{2} \eta_9 z_{1,2}^{b, g^\#} I_1^2 + \frac{1}{2} \eta_{10} z_{1,2}^{b, g^\#} I_2^2 + \frac{1}{2} \eta_{11} z_{1,2}^{b, g^\#} I_3^2 + \frac{1}{2} \eta_{12} z_{1,2}^{b, g^\#} I_4^2 \tag{3.93}$$

results in a change of the underlying symmetry class of the material, defined by ψ_0 , since the corresponding flow directions

$$\boldsymbol{\xi}_{z_{1,2}^b}^\# = \partial_{z_{1,2}^b} \text{fib} \Phi_{\text{cha}}^t = \eta_9 z_{1,2}^{b, g^\#} I_{1,2} \mathbf{g}^\# + \eta_{10} z_{1,2}^{b, g^\#} I_{3,4} \mathbf{g}^\# \cdot \mathbf{z}_{1,2}^b \cdot \mathbf{g}^\# \tag{3.94}$$

are of rank three and thus do not preserve the rank one property of the initial anisotropy tensors $\mathbf{a}_{1,2}^\# |_{t_0}$ (compare Section 5.2 for a detailed discussion in this regard with application to continuum damage mechanics where we additionally comment on the positive dissipation contribution of the chosen prototype model).

Remark 3.4 For comparative reasons, assume a J_2 , or rather a v . Mises–type, plasticity in terms of \mathbf{y}^b or $\boldsymbol{\tau}^\sharp$, respectively, within an isotropic setting, $\mathbf{a}_{1,\dots,n}^\sharp \doteq \mathbf{0}$. The appropriate yield functions and the associated evolution equations follow immediately as

$$\begin{aligned}
\text{yie } \Phi_{\mathbf{y}^b}^t &\doteq \text{dev } \mathbf{y}^b g^\sharp I_2^{1/2} - \sqrt{\frac{2}{3}} [Y_0 - h], \\
\boldsymbol{\xi}_{\mathbf{y}^b}^\sharp &\doteq \text{dev } \mathbf{y}^b g^\sharp I_2^{-1/2} \mathbf{g}^\sharp \cdot \text{dev } \mathbf{y}^b \cdot \mathbf{g}^\sharp \implies L_t \mathbf{b}_e^\sharp = D_t \lambda \boldsymbol{\xi}_{\mathbf{y}^b}^\sharp, \\
\text{yie } \Phi_{\boldsymbol{\tau}^\sharp}^t &\doteq g^b \text{dev } \boldsymbol{\tau}^\sharp I_2^{1/2} - \sqrt{\frac{2}{3}} [Y_0 - h], \\
\boldsymbol{\xi}_{\boldsymbol{\tau}^\sharp}^b &\doteq g^b \text{dev } \boldsymbol{\tau}^\sharp I_2^{-1/2} \mathbf{g}^b \cdot \text{dev } \boldsymbol{\tau}^\sharp \cdot \mathbf{g}^b \implies L_t \mathbf{b}_e^\sharp = -2 D_t \lambda \mathbf{g}^\sharp \cdot \boldsymbol{\xi}_{\boldsymbol{\tau}^\sharp}^b \cdot \mathbf{b}_e^\sharp,
\end{aligned} \tag{3.95}$$

with $\text{dev } \boldsymbol{\tau}^\sharp = \boldsymbol{\tau}^\sharp - n_{\text{dim}}^{-1} [\mathbf{g}^b : \boldsymbol{\tau}^\sharp] \mathbf{g}^\sharp$ being obvious, compare Eqs.(3.37, 3.45)₁. Since the mixed–variant tensor fields $\mathbf{g}^b \cdot \mathbf{b}_e^\sharp$, $\mathbf{c}_e^b \cdot \mathbf{g}^\sharp$, $\mathbf{y}^b \cdot \mathbf{g}^\sharp$, $\mathbf{g}^b \cdot \boldsymbol{\tau}^\sharp$, $\mathbf{g}^b \cdot \boldsymbol{\xi}_{\mathbf{y}^b}^\sharp$ and $\boldsymbol{\xi}_{\boldsymbol{\tau}^\sharp}^b \cdot \mathbf{g}^\sharp$ commute for this specific case, we observe from Eqs.(3.95) that the evolution equation for $L_t \mathbf{b}_e^\sharp$ due to \mathbf{y}^b or $\boldsymbol{\tau}^\sharp$ have identical principal directions and sign (recall that \mathbf{y}^b and $\boldsymbol{\tau}^\sharp$ have different signs and \mathbf{b}_e^\sharp always being positive definite). Moreover, in the case of metal plasticity with $\mathbf{b}_e^\sharp \rightarrow \mathbf{g}^\sharp$ and $\mathbf{c}_e^b \rightarrow \mathbf{g}^b$, both representations of associated v . Mises–type evolution equations in Eqs.(3.37, 3.45)₁ differ only by a scalar factor.

As previously mentioned, we have several options to relate the fields $\mathbf{a}_{3,4}^\sharp$, which enter the plastic potential $\text{pla } \Phi^t$, to the anisotropy tensors $\mathbf{a}_{1,2}^\sharp$ defining the functions ψ_0^t and $\text{fib } \Phi^t$, compare Eqs.(3.41). In this context, single invariants in terms of $\mathbf{a}_{3,4}^\sharp$ determining $\text{pla } \Phi^t$ could be replaced by the correlated invariants due to $\mathbf{a}_{1,2}^\sharp$ or the complete set could even be substituted. Within the subsequent numerical examples, we account for four representative options

(o) case a :	$\text{pla } \Phi^t = \text{pla } \Phi^t \left(\text{dev } \mathbf{y}^b g^\sharp I_2; \mathbf{X} \right)$	(3.96)
(i) case b :	$\text{pla } \Phi^t = \text{pla } \Phi^t \left(\text{dev } \mathbf{y}^b g^\sharp I_2, \text{dev } \mathbf{y}^b a_{3,4}^\sharp I_{4,\dots,7}, g^b a_{3,4}^\sharp I_8; \mathbf{X} \right)$	
(ii) case c :	$\text{pla } \Phi^t = \text{pla } \Phi^t \left(\text{dev } \mathbf{y}^b g^\sharp I_2, \text{dev } \mathbf{y}^b a_{3,4}^\sharp I_{4,\dots,7}, g^b a_{1,2}^\sharp I_8; \mathbf{X} \right)$	
	$\text{fib } \Phi_{\text{fix}}^t = \text{fib } \Phi_{\text{fix}}^t \left(z_{1,2}^b a_{1,2}^\sharp I_{1,\dots,4}; \mathbf{X} \right)$	
(iii) case d :	$\text{pla } \Phi^t = \text{pla } \Phi^t \left(\text{dev } \mathbf{y}^b g^\sharp I_2, \text{dev } \mathbf{y}^b a_{1,2}^\sharp I_{4,\dots,7}, g^b a_{1,2}^\sharp I_8; \mathbf{X} \right)$	
	$\text{fib } \Phi_{\text{cha}}^t = \text{fib } \Phi_{\text{cha}}^t \left(z_{1,2}^b g^\sharp I_{1,\dots,4}; \mathbf{X} \right)$	

with respect to Eq.(3.95) for case a and Eqs.(3.87, 3.91, 3.93) concerning cases b–d. In particular, case a accounts for isotropic v . Mises–type plasticity. Within cases b–d, orthotropic elasticity defined via $\mathbf{a}_{1,2}^\sharp$ and orthotropic plasticity characterised by $\mathbf{a}_{3,4}^\sharp$ are incorporated. For case b, all structural tensors are assumed to remain constant in \mathcal{B}_0 but $\mathbf{a}_{1,2}^\sharp \neq \mathbf{a}_{3,4}^\sharp$. On top of that, case c accounts for an evolution of $\mathbf{a}_{1,2}^\sharp$ which retains the material symmetry group of the body B . Finally, within case d, we set $\mathbf{a}_{3,4}^\sharp = \mathbf{a}_{1,2}^\sharp$ and incorporate evolution equations for $\mathbf{a}_{1,2}^\sharp$ which result in a change of the underlying symmetry group of the material.

3.9 Numerical examples

The following numerical examples account for the four different combinations of the coupling due to the elastic and inelastic properties of the considered material as summarised in Eqs.(3.96). Thereby,

the set of material parameter has been chosen as

$$\begin{aligned}
K &= 164.28, & G &= 80.23, & Y_0 &= 0.45, & Y_\infty &= 0.715, \\
\delta_1 &= 16.93, & \delta_2 &= 0.01, & \alpha &= \frac{2}{3} Y_0^2, \\
\gamma_1 &= 10, & \gamma_2 &= 15, & \eta_1 &= \alpha/6, & \eta_2 &= \alpha/10, \\
\gamma_3 &= 20, & \gamma_4 &= 25, & \eta_3 &= \alpha/8, & \eta_4 &= \alpha/20, \\
\gamma_5 &= 30, & \gamma_6 &= 35, & \eta_5 &= \alpha/16, & \eta_6 &= \alpha/10, \\
\gamma_7 &= 10, & \gamma_8 &= 10, & \eta_7 &= \alpha/10, & \eta_8 &= \alpha/20, \\
\gamma_9 &= 15, & \gamma_{10} &= 10, & \eta_9 &= \alpha/10^2, & \eta_{10} &= \alpha/10^2, \\
\gamma_{11} &= 15, & & & \eta_{11} &= \alpha/10^3, & \eta_{12} &= \alpha/10^3,
\end{aligned} \tag{3.97}$$

similar to the work by Steinmann et al. [SMS96]. Moreover, the incorporated initial fibre-orientations read with respect to a Cartesian frame as

$$\begin{aligned}
A_1|_{t_0} \mathbf{N} &= [+2 \mathbf{e}_1 + 1 \mathbf{e}_2 + 0 \mathbf{e}_3]/\sqrt{5}, & A_3|_{t_0} \mathbf{N} &= [+1 \mathbf{e}_1 + 2 \mathbf{e}_2 + 1 \mathbf{e}_3]/\sqrt{6}, \\
A_2|_{t_0} \mathbf{N} &= [-1 \mathbf{e}_1 + 2 \mathbf{e}_2 + 1 \mathbf{e}_3]/\sqrt{6}, & A_4|_{t_0} \mathbf{N} &= [+2 \mathbf{e}_1 - 1 \mathbf{e}_2 + 0 \mathbf{e}_3]/\sqrt{5},
\end{aligned} \tag{3.98}$$

with $[A_1|_{t_0} \mathbf{N}]^t \cdot A_2|_{t_0} \mathbf{N} = [A_3|_{t_0} \mathbf{N}]^t \cdot A_4|_{t_0} \mathbf{N} = 0$ and $\|A_{1,\dots,4}|_{t_0}\| = 1$ being obvious.

3.9.1 Simple shear

To set the stage, we discuss in the sequel the homogeneous deformation in simple shear, i.e. $\mathbf{F} = \mathbf{I} + \gamma \mathbf{e}_1 \otimes \mathbf{e}^2$ with respect to a Cartesian frame whereby $\mathbf{I} = \delta_j^i \mathbf{e}_i \otimes \mathbf{e}^j$ denotes the second order identity tensor and γ the shear number, respectively. The loading behaviour for $\gamma \in [0 \rightarrow 1]$ is discussed in particular and on top of that we consider unloading/reloading with respect to the deformation history $\gamma \in [0 \rightarrow 1, 1 \rightarrow 0]$.

Case a: For comparison reasons, let the body B transform isotropic elasto-plastic, i.e. v. Mises-type plasticity and no structural tensors are incorporated. For this setting, Figure 3.3 monitors the deviatoric norm of the Kirchhoff stress $\|\text{dev } \boldsymbol{\tau}^\sharp\|$ and the appropriate thermodynamic force $\|\text{dev } \mathbf{y}^\flat\|$ over the shear number γ . Furthermore, stress components of interest are highlighted with respect to a Cartesian frame, $\tau^{ij} = \mathbf{e}^i \cdot \boldsymbol{\tau}^\sharp \cdot \mathbf{e}^j$ and $y_{ij} = \mathbf{e}_i \cdot \mathbf{y}^\flat \cdot \mathbf{e}_j$, respectively. In addition, the unloading/reloading behaviour is visualised in Figure 3.4.

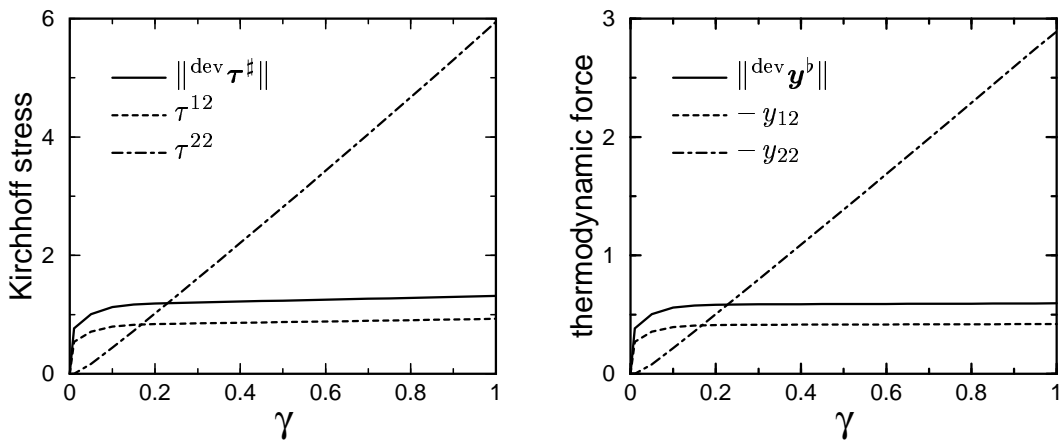


Figure 3.3: Simple shear, case a: Deviatoric norm and components of the Kirchhoff stress $\|\text{dev } \boldsymbol{\tau}^\sharp\|$, τ^{12} , τ^{22} (left) and deviatoric norm and components of the thermodynamic force $\|\text{dev } \mathbf{y}^\flat\|$, $-y_{12}$, $-y_{22}$ (right).

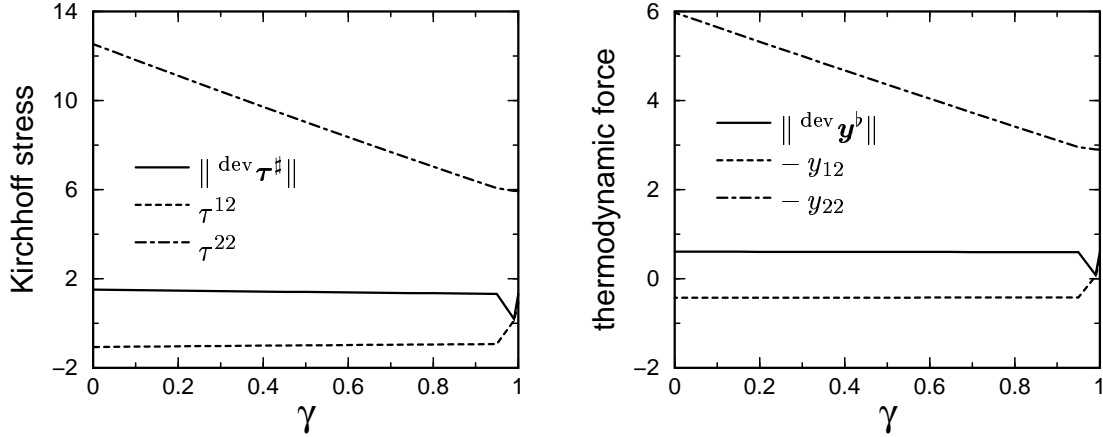


Figure 3.4: Simple shear, case a, unloading/reloading: Deviatoric norm and components of the Kirchhoff stress $\|\text{dev } \boldsymbol{\tau}^\sharp\|$, τ^{12} , τ^{22} (left) and deviatoric norm and components of the thermodynamic force $\|\text{dev } \mathbf{y}^b\|$, $-y_{12}$, $-y_{22}$ (right).

Case b: Next, with four different structural tensors at hand which enter the free Helmholtz energy density and the inelastic potentials, compare Eqs.(3.98), we apparently obtain a rather different response of the Kirchhoff stress $\boldsymbol{\tau}^\sharp$ and the introduced thermodynamic force \mathbf{y}^b as visualised in Figure 3.5. Moreover, the anisotropy measure $\delta(\mathbf{b}_e^\sharp, \boldsymbol{\tau}^\sharp)$ is not equal to zero due to the incorporated structural tensors which are assumed to be constant with respect to \mathcal{B}_0 , see Figure 3.6 and Appendix D.1 for the definition of the anisotropy measure. The unloading/reloading behaviour is monitored in Figures 3.7 and 3.8.

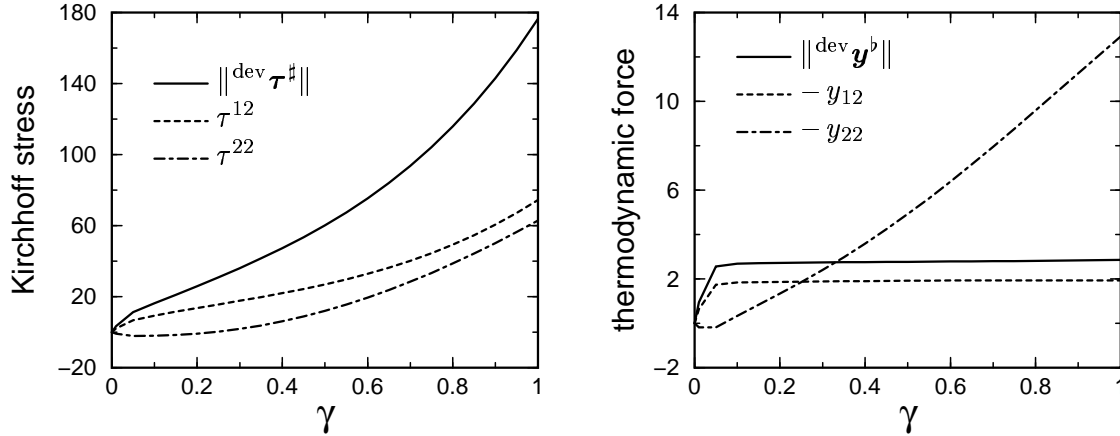


Figure 3.5: Simple shear, case b: Deviatoric norm and components of the Kirchhoff stress $\|\text{dev } \boldsymbol{\tau}^\sharp\|$, τ^{12} , τ^{22} (left) and deviatoric norm and components of the thermodynamic force $\|\text{dev } \mathbf{y}^b\|$, $-y_{12}$, $-y_{22}$ (right).

Case c: Now, we additionally account for an evolution of the structural tensors $\mathbf{a}_{1,2}^\sharp$ which nevertheless, does not change the material symmetry of the body B of interest. Figure 3.9 reflects the character of the Kirchhoff stress and the thermodynamic force whereby, once more, the saturation effect of the non-linear hardening model is clearly seen in the plot of \mathbf{y}^b . The anisotropy measure due to strain and stress as well as the evolution of the norm of the structural tensors $\mathbf{A}_{1,2}^\sharp$ are additionally shown in Figure 3.10. In analogy to case b, the response under unloading/reloading is monitored in Figures 3.11 and 3.12.

Case d: Finally, the anisotropy tensors in the free Helmholtz energy density and in the plastic potential are assumed to coincide. The corresponding operation of the relevant stress fields are monitored in Figure 3.13. Beside this, the incorporated evolution equation of the anisotropy tensors results in a change of the underlying material symmetry group. In other words, the actual anisotropy

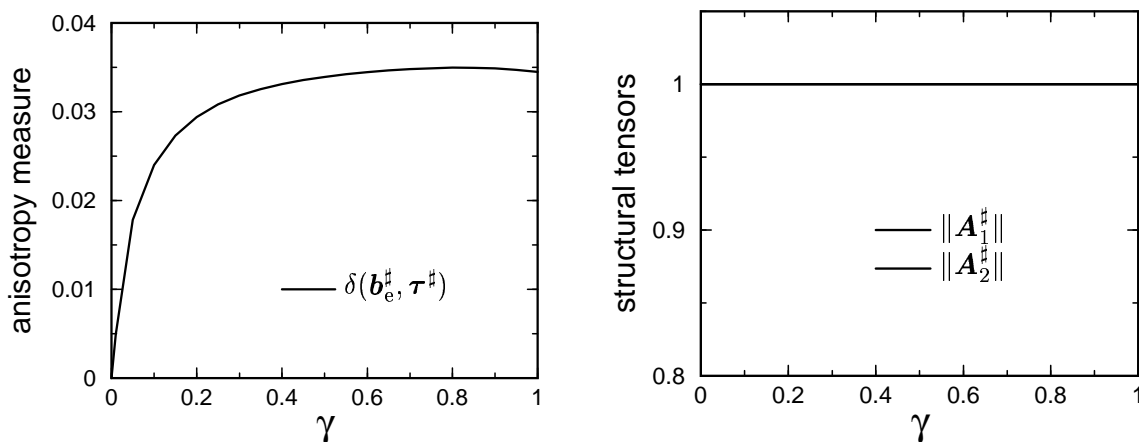


Figure 3.6: Simple shear, case b: Anisotropy measure $\delta(\mathbf{b}_e^\#, \boldsymbol{\tau}^\#)$ (left) and norm of the structural tensors $\|\mathbf{A}_1^\#\|$, $\|\mathbf{A}_2^\#\|$ (right).

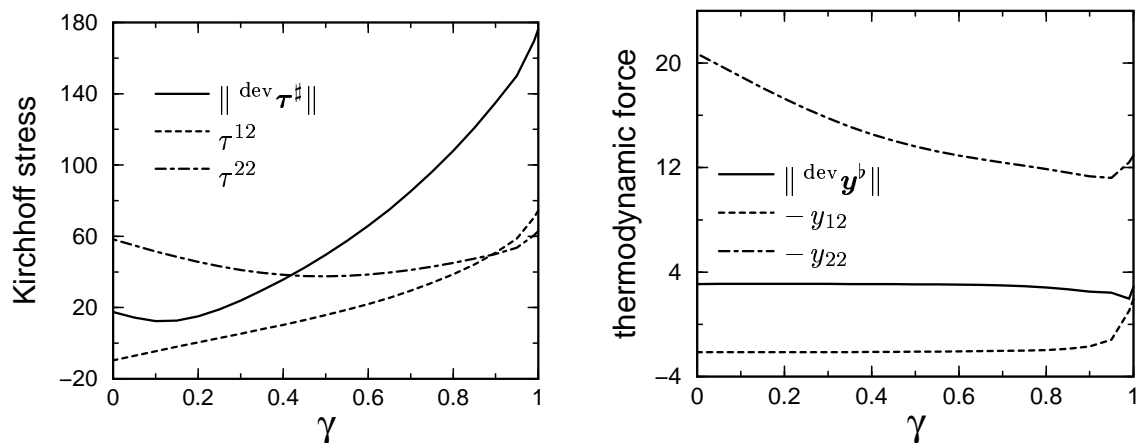


Figure 3.7: Simple shear, case b, unloading/reloading: Deviatoric norm and components of the Kirchhoff stress $\|\text{dev } \boldsymbol{\tau}^\#\|$, τ^{12} , τ^{22} (left) and deviatoric norm and components of the thermodynamic force $\|\text{dev } \mathbf{y}^b\|$, $-y_{12}$, $-y_{22}$ (right).

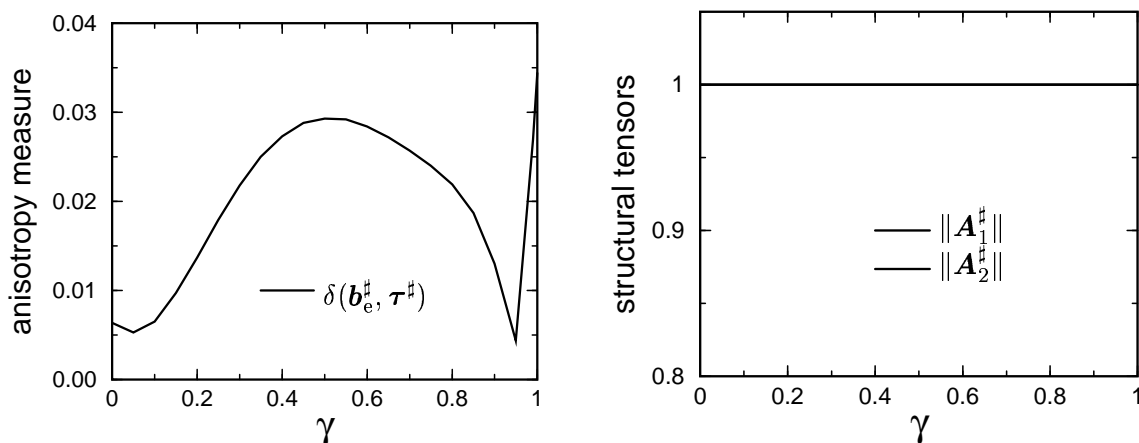


Figure 3.8: Simple shear, case b, unloading/reloading: Anisotropy measure $\delta(\mathbf{b}_e^\#, \boldsymbol{\tau}^\#)$ (left) and norm of the structural tensors $\|\mathbf{A}_1^\#\|$, $\|\mathbf{A}_2^\#\|$ (right).

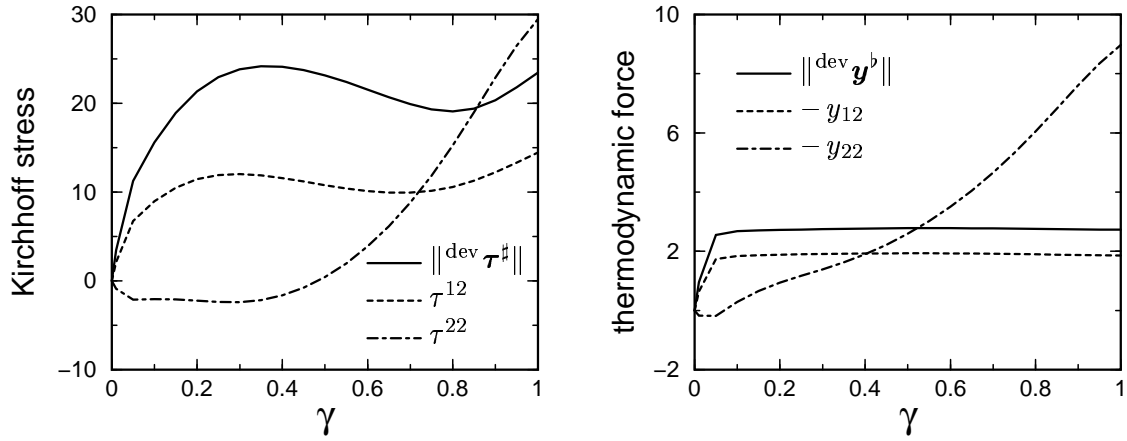


Figure 3.9: Simple shear, case c: Deviatoric norm and components of the Kirchhoff stress $\|\text{dev } \boldsymbol{\tau}^\sharp\|$, τ^{12} , τ^{22} (left) and deviatoric norm and components of the thermodynamic force $\|\text{dev } \boldsymbol{y}^b\|$, $-y_{12}$, $-y_{22}$ (right).

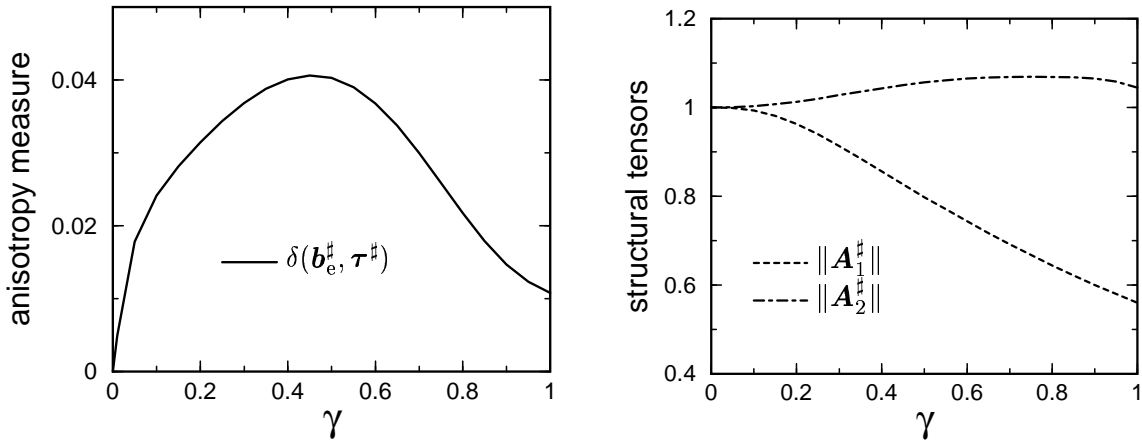


Figure 3.10: Simple shear, case c: Anisotropy measure $\delta(\boldsymbol{b}_e^\sharp, \boldsymbol{\tau}^\sharp)$ (left) and norm of the structural tensors $\|\boldsymbol{A}_1^\sharp\|$, $\|\boldsymbol{A}_2^\sharp\|$ (right).

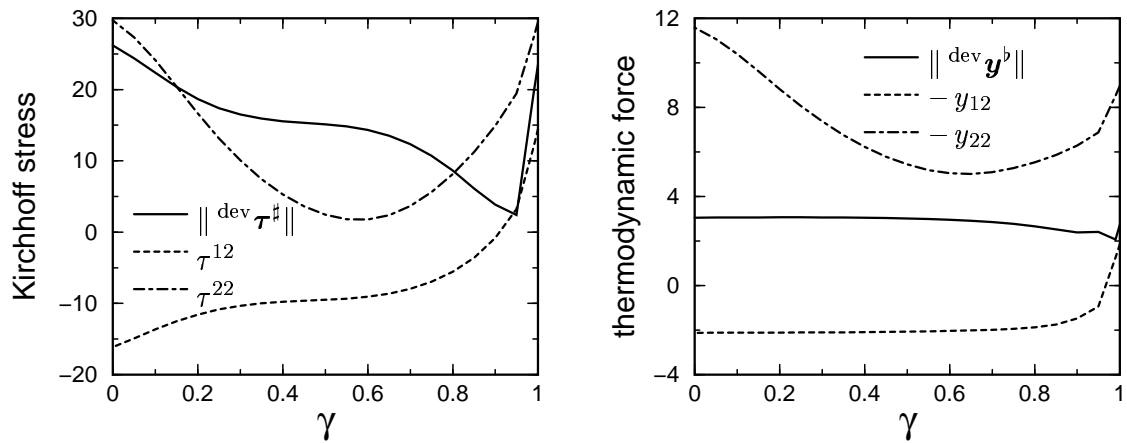


Figure 3.11: Simple shear, case c, unloading/reloading: Deviatoric norm and components of the Kirchhoff stress $\|\text{dev } \boldsymbol{\tau}^\sharp\|$, τ^{12} , τ^{22} (left) and deviatoric norm and components of the thermodynamic force $\|\text{dev } \boldsymbol{y}^b\|$, $-y_{12}$, $-y_{22}$ (right).

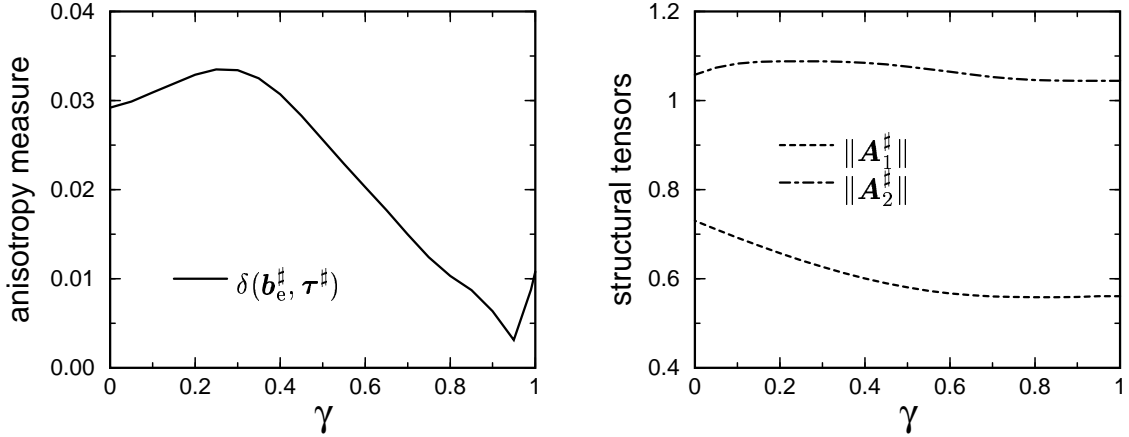


Figure 3.12: Simple shear, case c, unloading/reloading: Anisotropy measure $\delta(\mathbf{b}_e^\#, \boldsymbol{\tau}^\#)$ (left) and norm of the structural tensors $\|\mathbf{A}_1^\#\|$, $\|\mathbf{A}_2^\#\|$ (right).

tensors $\mathbf{A}_{1,2}^\#$ are not coaxial to the initial structural tensors $\mathbf{A}_{1,2}^\#|_{t_0}$. Thus, in addition to $\delta(\mathbf{b}_e^\#, \boldsymbol{\tau}^\#)$, we can compute a non-vanishing anisotropy measure $\delta(\mathbf{A}_{1,2}^\#, \mathbf{A}_{1,2}^\#|_{t_0})$, see Figure 3.14. Lastly, Figures 3.15 and 3.16 summarise the unloading/reloading behaviour.

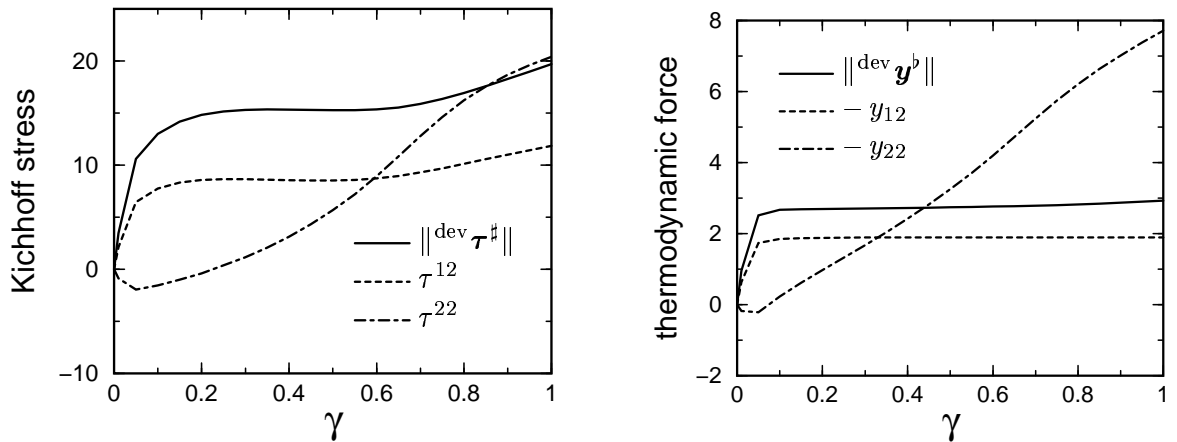


Figure 3.13: Simple shear, case d: Deviatoric norm and components of the Kirchhoff stress $\|\text{dev } \boldsymbol{\tau}^\#\|$, τ^{12} , τ^{22} (left) and deviatoric norm and components of the thermodynamic force $\|\text{dev } \mathbf{y}^b\|$, $-y_{12}$, $-y_{22}$ (right).

Please note that the amount of single stress components or appropriate norms of the stress tensors strongly depend on the considered model, here case a–d. This effect is apparently due to the increase in stiffness of the anisotropic material when additional fibre orientations and evolutions are incorporated.

3.9.2 Strip with a hole

As a typical boundary value problem, we consider an initially symmetric strip with a hole of dimensions $120 \times 40 \times 5$ (length \times width \times height) whereby the radius of the drilled hole is 10. To solve this problem numerically, the finite element method is adopted, see e.g. Oden [Ode72]. Thereby, the chosen discretisation of the geometry of the specimen is performed by $32 \times 8 \times 4$ enhanced eight node bricks (Q1E9) as advocated by Simo and Armero [SA92]. Usual Dirichlet boundary conditions are applied, namely one end of the strip is completely clamped, say $\mathbf{u}^p = \mathbf{0}$ at $\mathbf{X} \cdot \mathbf{e}_1 = 0$ with respect to a Cartesian frame, while the other end is stretched in longitudinal direction, $\mathbf{u}^p = u^p \mathbf{e}_1$ at $\mathbf{X} \cdot \mathbf{e}_1 = 120$.

Case a: We once more consider the isotropic v. Mises–type, or rather J_2 –type, setting for comparison reasons. Figure 3.17 highlights the undeformed initial geometry and the deformed configuration

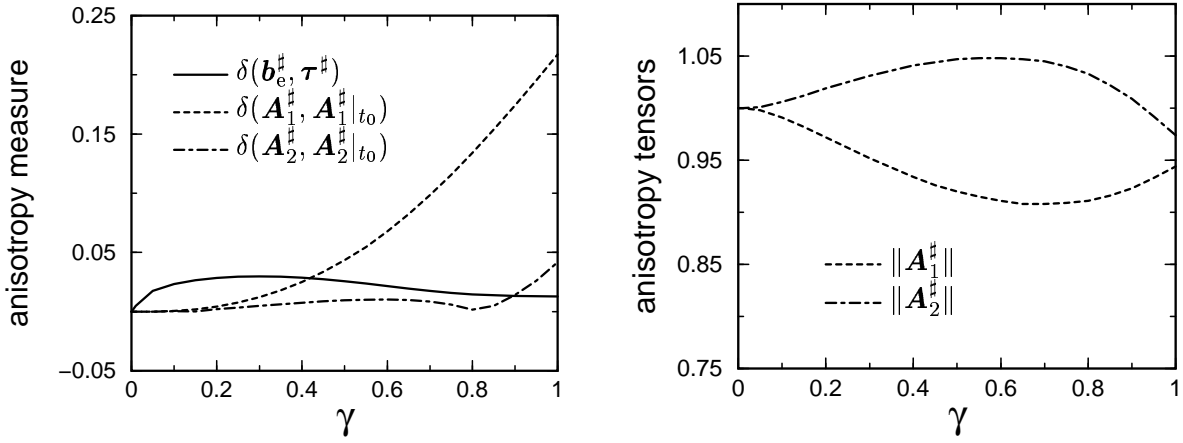


Figure 3.14: Simple shear, case d: Anisotropy measure $\delta(\mathbf{b}_e^\#, \boldsymbol{\tau}^\#)$, $\delta(\mathbf{A}_1^\#, \mathbf{A}_1^\#|_{t_0})$, $\delta(\mathbf{A}_2^\#, \mathbf{A}_2^\#|_{t_0})$ (left) and norm of the anisotropy tensors $\|\mathbf{A}_1^\#\|$, $\|\mathbf{A}_2^\#\|$ (right).

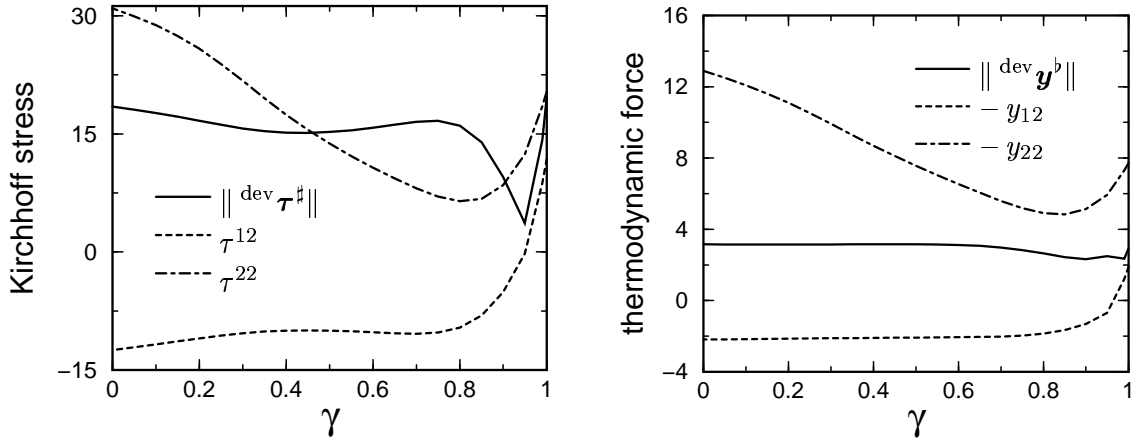


Figure 3.15: Simple shear, case d, unloading/reloading: Deviatoric norm and components of the Kirchhoff stress $\|\text{dev } \boldsymbol{\tau}^\#\|$, τ^{12} , τ^{22} (left) and deviatoric norm and components of the thermodynamic force $\|\text{dev } \mathbf{y}^b\|$, $-y_{12}$, $-y_{22}$ (right).

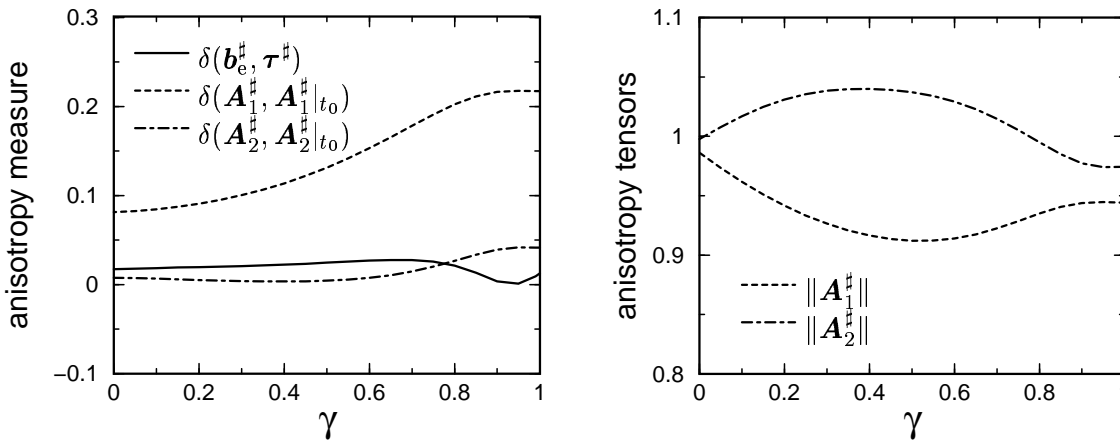


Figure 3.16: Simple shear, case d, unloading/reloading: Anisotropy measure $\delta(\mathbf{b}_e^\#, \boldsymbol{\tau}^\#)$, $\delta(\mathbf{A}_1^\#, \mathbf{A}_1^\#|_{t_0})$, $\delta(\mathbf{A}_2^\#, \mathbf{A}_2^\#|_{t_0})$ (left) and norm of the anisotropy tensors $\|\mathbf{A}_1^\#\|$, $\|\mathbf{A}_2^\#\|$ (right).

at a longitudinal stretch $\lambda = 1.2 = 1 + u^p/120$. Due to the applied boundary conditions and the lack of anisotropy, we observe a completely symmetric response of the specimen, see the plots of a longitudinal section in Figure 3.18. Moreover, the typical necking effect is clearly monitored by the corresponding load–displacement curve as given in Figure 3.20. In addition, Figures 3.20 and 3.21 visualise the dispositions of $\|\text{dev } \boldsymbol{\tau}^\sharp\|$, $\|\text{dev } \boldsymbol{y}^b\|$ and κ , respectively. As an interesting side aspect, we examine that $\|\text{dev } \boldsymbol{\tau}^\sharp\|$ and $\|\text{dev } \boldsymbol{y}^b\|$ are related by a factor of about two since the elastic strains are almost small; compare Section 3.5.

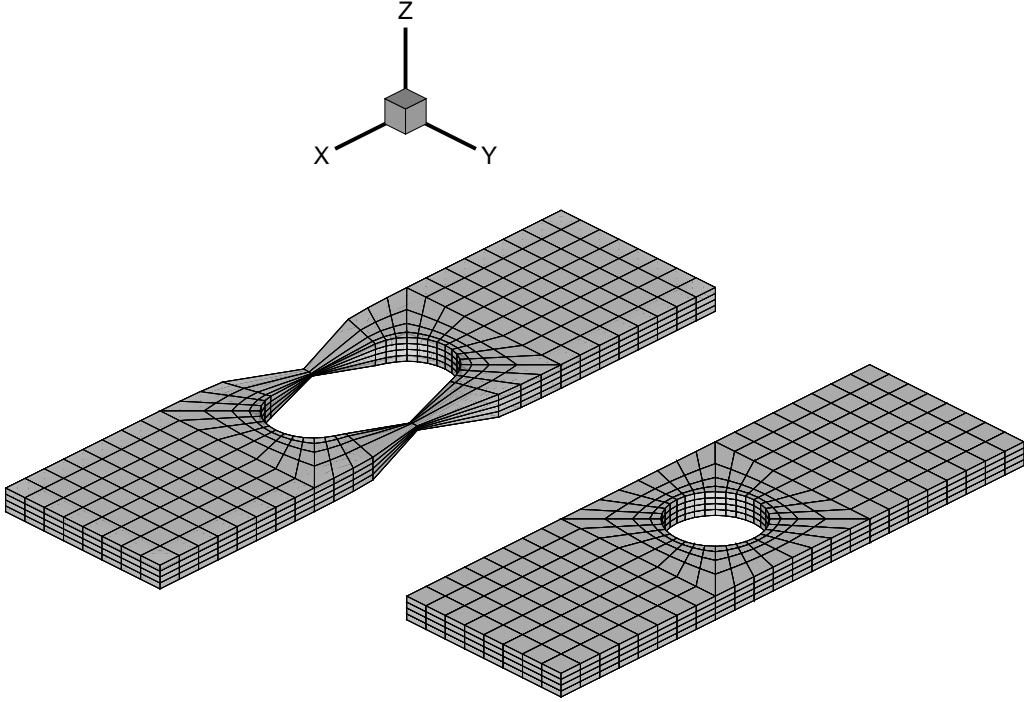


Figure 3.17: Strip with a hole, case a: Deformed configuration at a longitudinal stretch $\lambda = 1.2$ and initial undeformed geometry.

Case b: Now, within an anisotropic setting and constant structural tensors in \mathcal{B}_0 , the deformed configuration generally features a non–symmetric response under symmetric loading and boundary conditions. This effect is clearly shown in Figure 3.22 with respect to a longitudinal stretch $\lambda = 1.2$. Thereby, a sharp “out–off–plane” deformation is recognised, see Figure 3.23. The corresponding load–displacement curve monitors a weaker necking compared to the overall isotropic case and is given in Figure 3.24. Furthermore, Figure 3.25 visualises the contributions of $\|\text{dev } \boldsymbol{\tau}^\sharp\|$ and $\|\text{dev } \boldsymbol{y}^b\|$ which are obviously not related by the factor two. In addition to the proportional hardening variable κ , the now non–vanishing anisotropy measure $\delta(\mathbf{b}_e^\sharp, \boldsymbol{\tau}^\sharp)$ is monitored in Figure 3.26.

Case c: This anisotropic case incorporates an evolution of the structural tensors $\mathbf{a}_{1,2}^\sharp$ which retains the material symmetry group. Figures 3.27–3.31 highlight the deformed configuration at $\lambda = 1.2$, a cut through the specimen, the underlying load–displacement curve, $\|\text{dev } \boldsymbol{\tau}^\sharp\|$, $\|\text{dev } \boldsymbol{y}^b\|$, κ and $\delta(\mathbf{b}_e^\sharp, \boldsymbol{\tau}^\sharp)$. In addition, Figure 3.32 monitors the evolution of the norm of the structural tensors $\mathbf{A}_{1,2}^\sharp$. Remarkably, we observe a strong decrease and increase which allow interpretation as damage and hardening effects, respectively.

Case d: Finally, we account for an evolution of the anisotropy tensors which results in a change of the initial material symmetry group. Figures 3.33–3.38 are in analogy to the presentation of the previous cases a–c. Supplementary, Figure 3.39 highlights the anisotropy measure $\delta(\mathbf{A}_{1,2}^\sharp, \mathbf{A}_{1,2}^\sharp|_{t_0})$ which apparently differs from zero as soon as an inelastic deformation takes place.

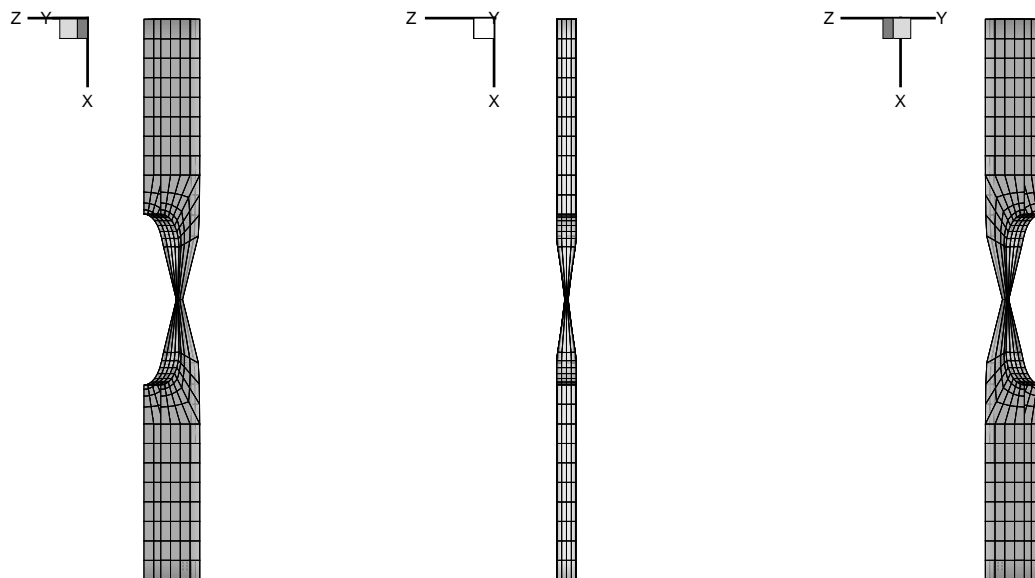


Figure 3.18: Strip with a hole, case a: Different views on a longitudinal section of the specimen.

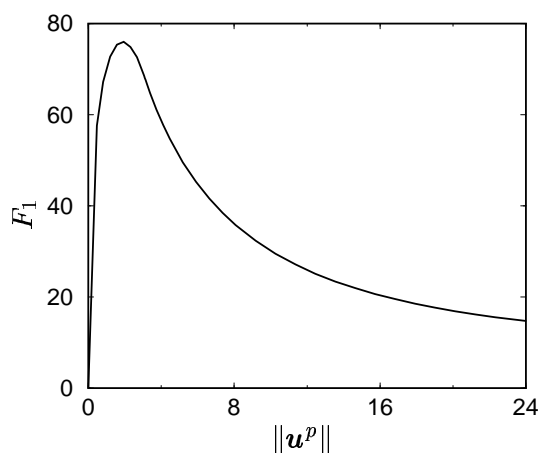


Figure 3.19: Strip with a hole, case a: Load–displacement curve (longitudinal).

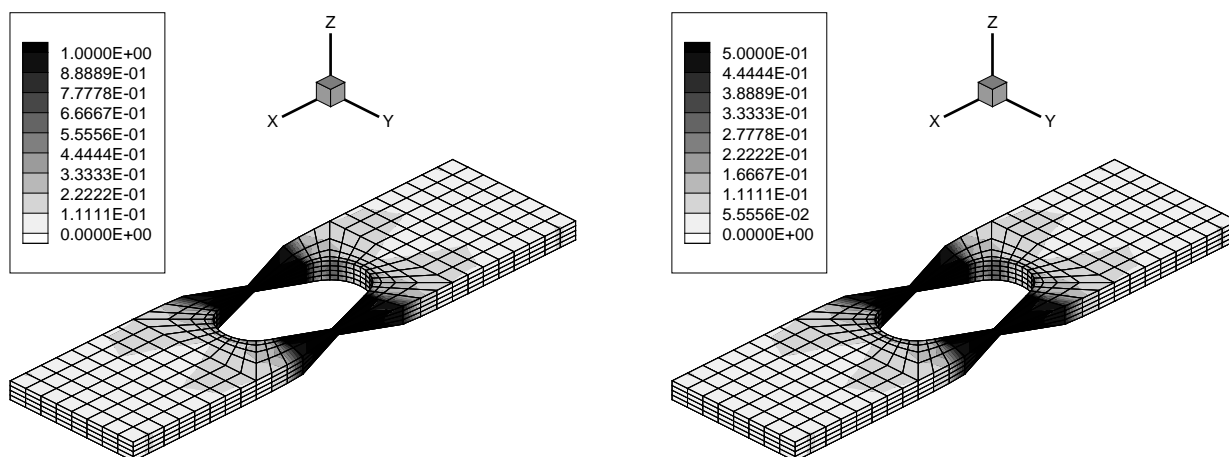


Figure 3.20: Strip with a hole, case a: Norm of the deviatoric Kirchhoff stress $\|\text{dev} \boldsymbol{\tau}^\sharp\|$ (left) and of the proposed thermodynamic force $\|\text{dev} \boldsymbol{y}^b\|$ (right).

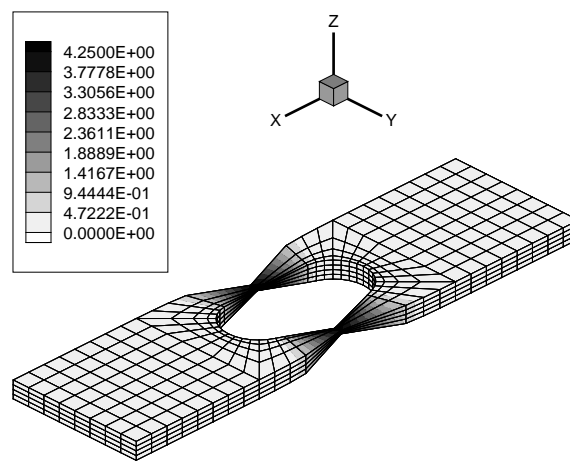


Figure 3.21: Strip with a hole, case a: Hardening variable κ .

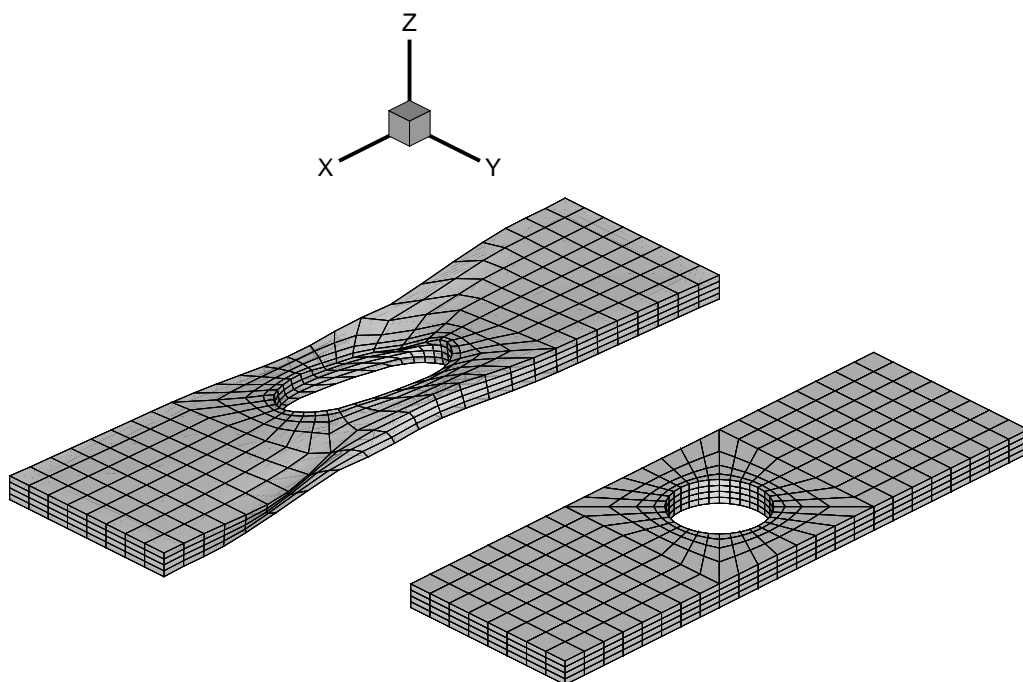


Figure 3.22: Strip with a hole, case b: Deformed configuration at a longitudinal stretch $\lambda = 1.2$ and initial undeformed geometry.

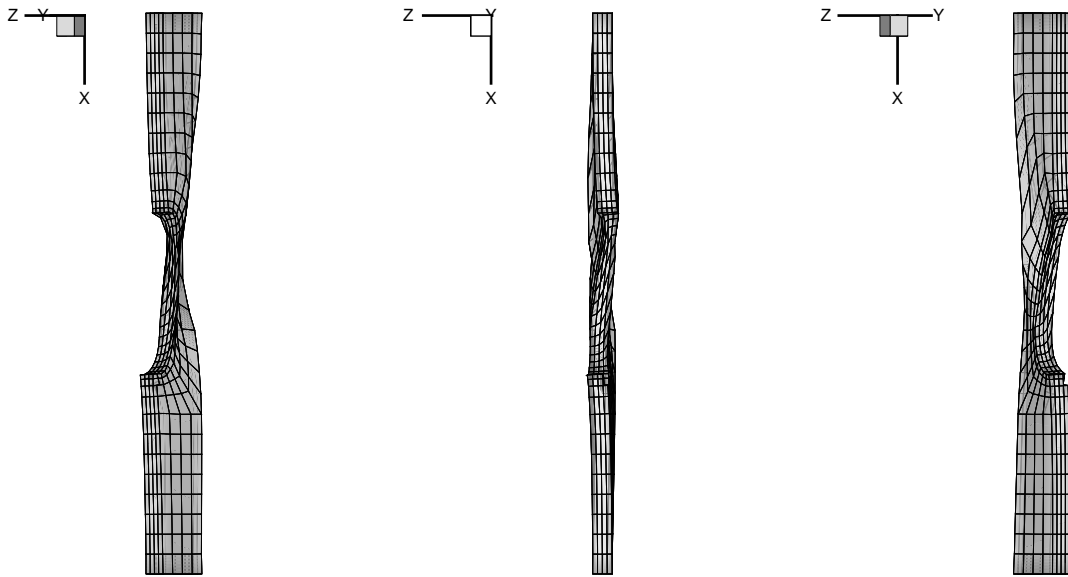


Figure 3.23: Strip with a hole, case b: Different views on a longitudinal section of the specimen.

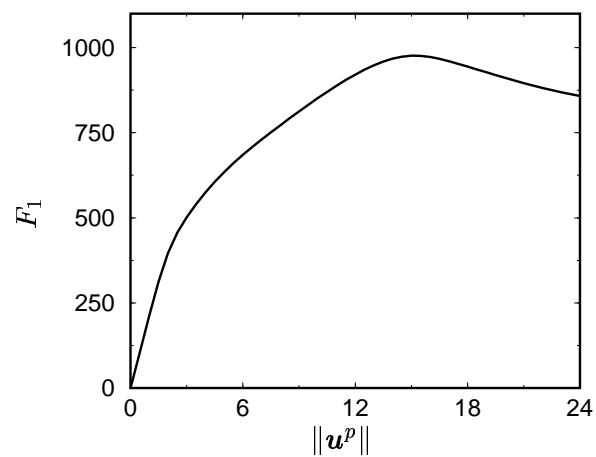


Figure 3.24: Strip with a hole, case b: Load–displacement curve (longitudinal).

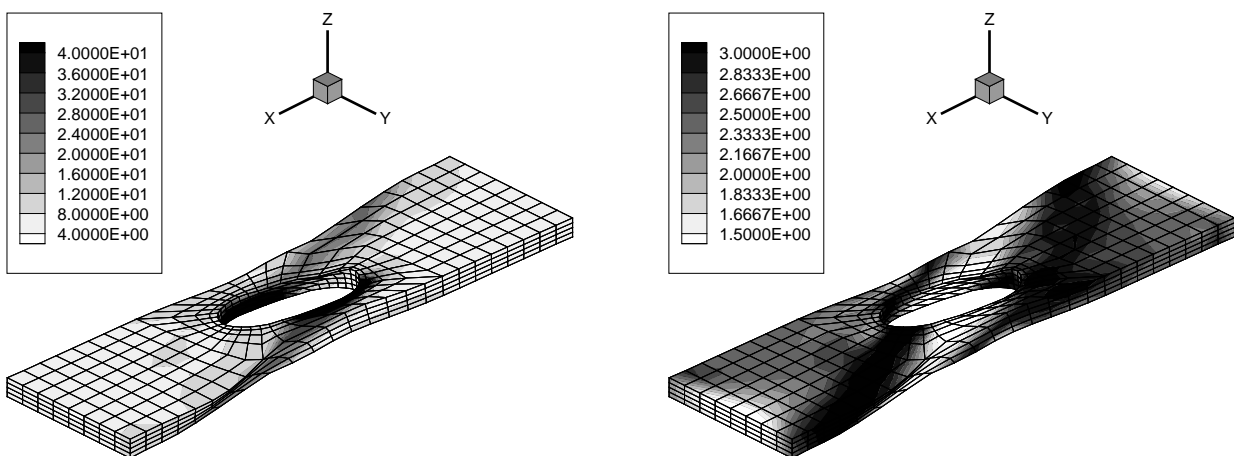


Figure 3.25: Strip with a hole, case b: Norm of the deviatoric Kirchhoff stress $\|{}^{\text{dev}}\boldsymbol{\tau}^{\#}\|$ (left) and of the proposed thermodynamic force $\|{}^{\text{dev}}\boldsymbol{y}^b\|$ (right).

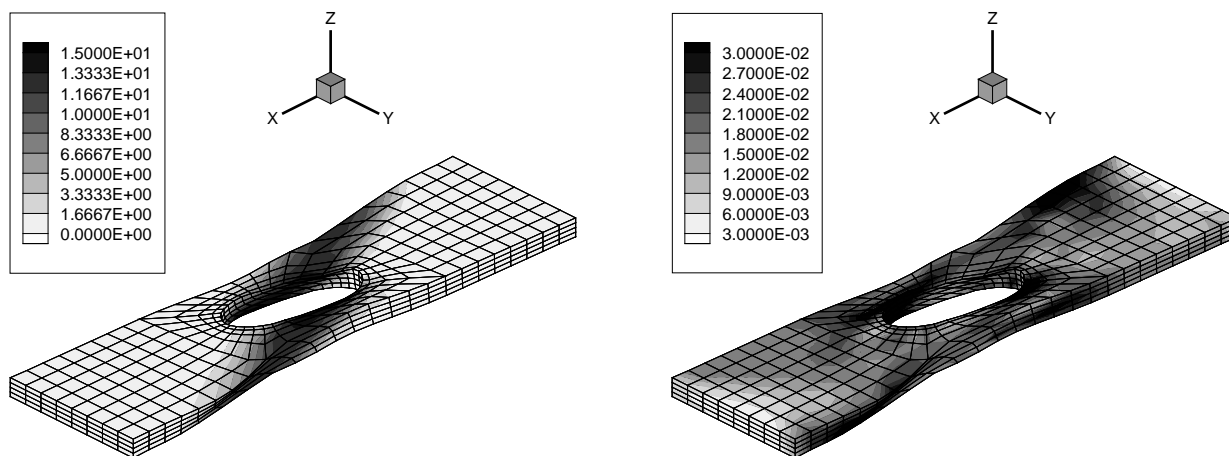


Figure 3.26: Strip with a hole, case b: Hardening variable κ (left) and anisotropy measure $\delta(\mathbf{b}_e^\#, \boldsymbol{\tau}^\#)$ (right).

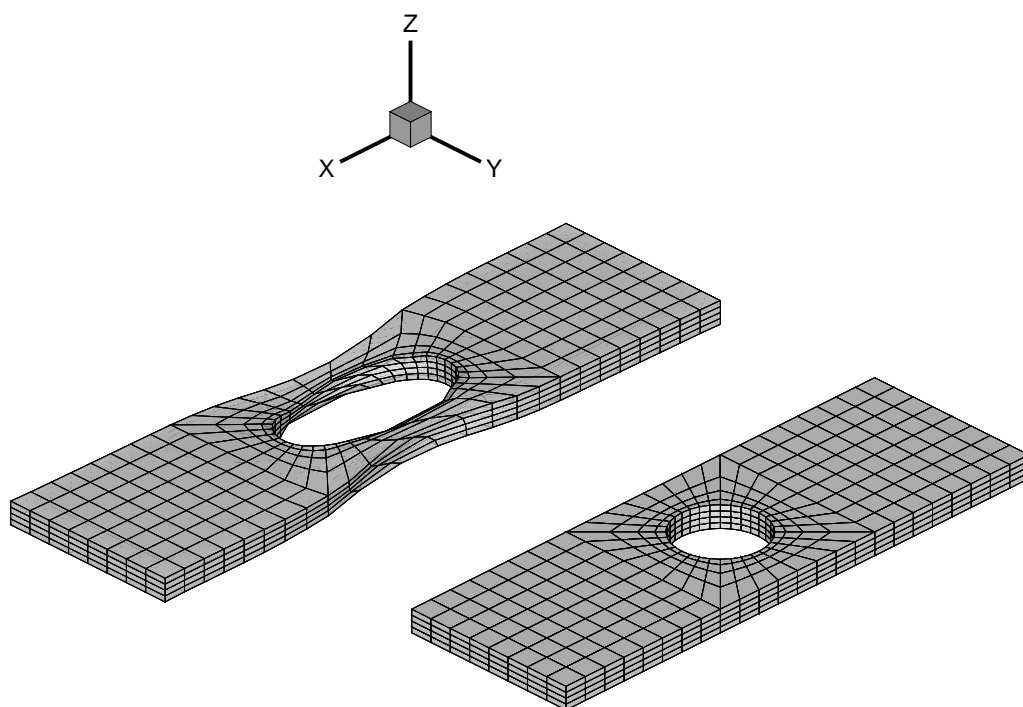


Figure 3.27: Strip with a hole, case c: Deformed configuration at a longitudinal stretch $\lambda = 1.2$ and initial undeformed geometry.

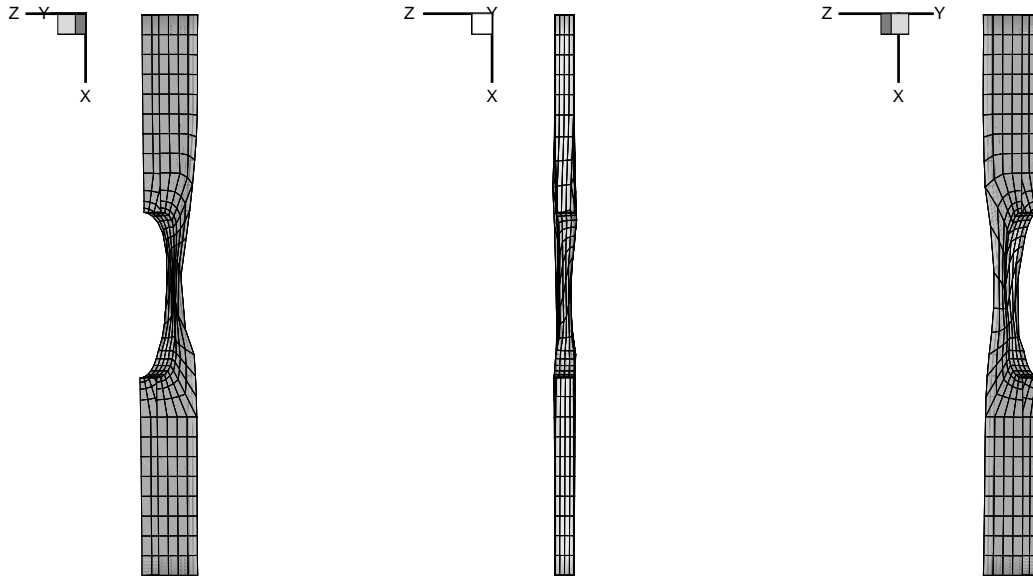


Figure 3.28: Strip with a hole, case c: Different views on a longitudinal section of the specimen.

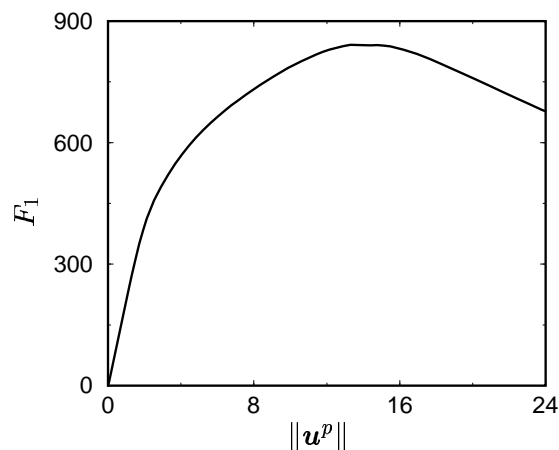


Figure 3.29: Strip with a hole, case c: Load–displacement curve (longitudinal).

It is clearly seen from the load–displacement curves in Figures 3.19, 3.24, 3.29 and 3.35 that the force level in the longitudinal direction F_1 for given prescribed displacements \mathbf{u}^p strongly depends on the considered model, here case a–d. This effect is obviously due to the type of incorporated fibres and the correlated increase of stiffness of the material.

Lastly, note that the Jacobians within the solution of the local ordinary differential evolution equations and the global finite element setting have been approximated numerically, recall Section 3.7. Thus, we should spend some words on the convergence of the performed examples. In this context, the machine precision was set to 16 digits and a perturbation parameter $\varepsilon = 10^{-8}$ has been adopted, see Appendix E.2 for a reminder on the numerical approximation technique of Jacobians. In this context, Table 3.3 highlights the quadratic convergence for an elastic and an inelastic setting. Thereby, we observe almost identical performances within the elastic range when applying the exact or numerically approximated tangent operator. Moreover, the convergence behaviour for the isotropic v. Mises–type case a is monitored. In the same direction, Table 3.4 highlights typical convergence properties within the inelastic anisotropic cases b–d. Obviously, the overall property for all these examples is monitored by quadratic rates of convergence.

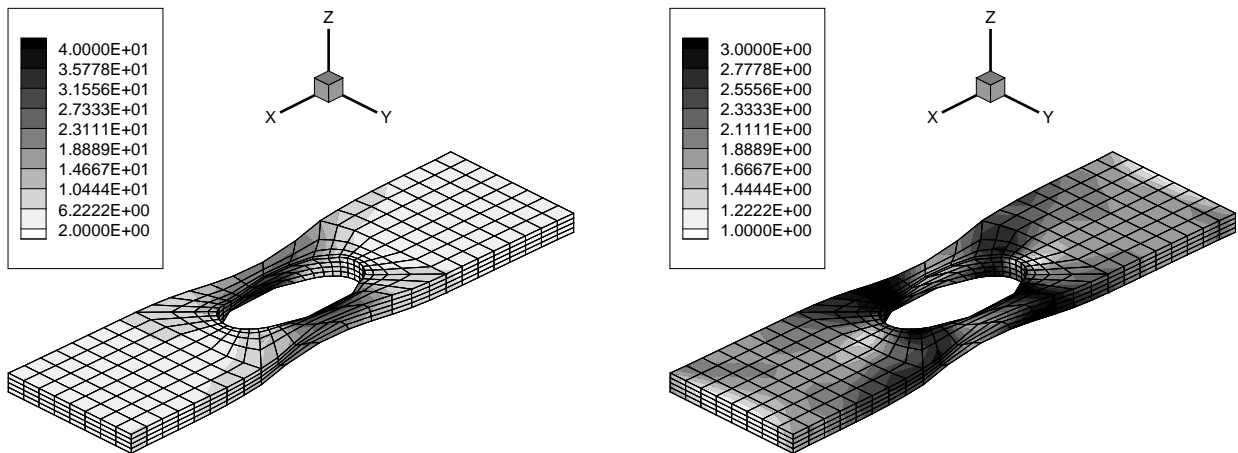


Figure 3.30: Strip with a hole, case c: Norm of the deviatoric Kirchhoff stress $\|\text{dev } \boldsymbol{\tau}^\sharp\|$ (left) and of the proposed thermodynamic force $\|\text{dev } \boldsymbol{y}^\flat\|$ (right).

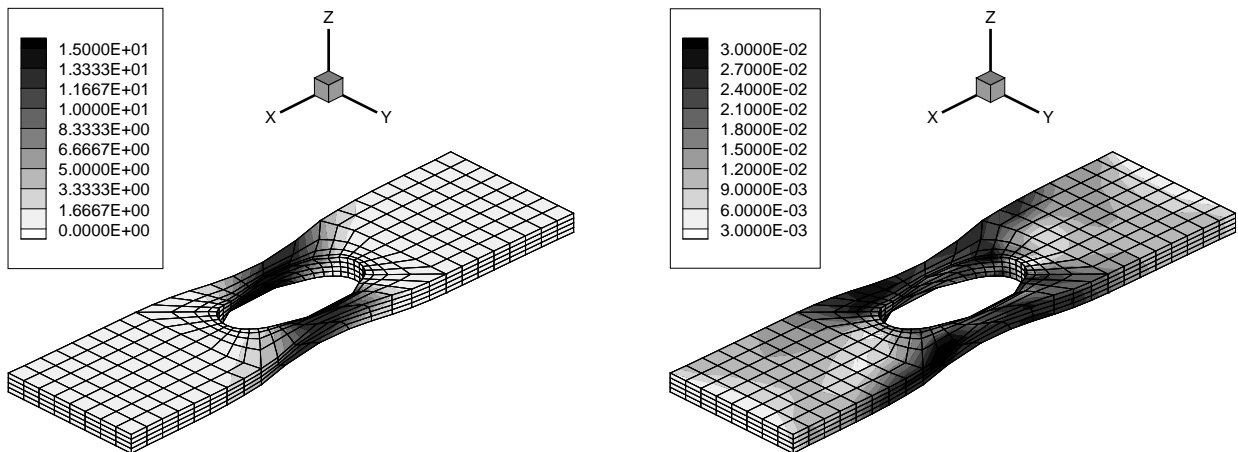


Figure 3.31: Strip with a hole, case c: Hardening variable κ (left) and anisotropy measure $\delta(\boldsymbol{b}_e^\sharp, \boldsymbol{\tau}^\sharp)$ (right).

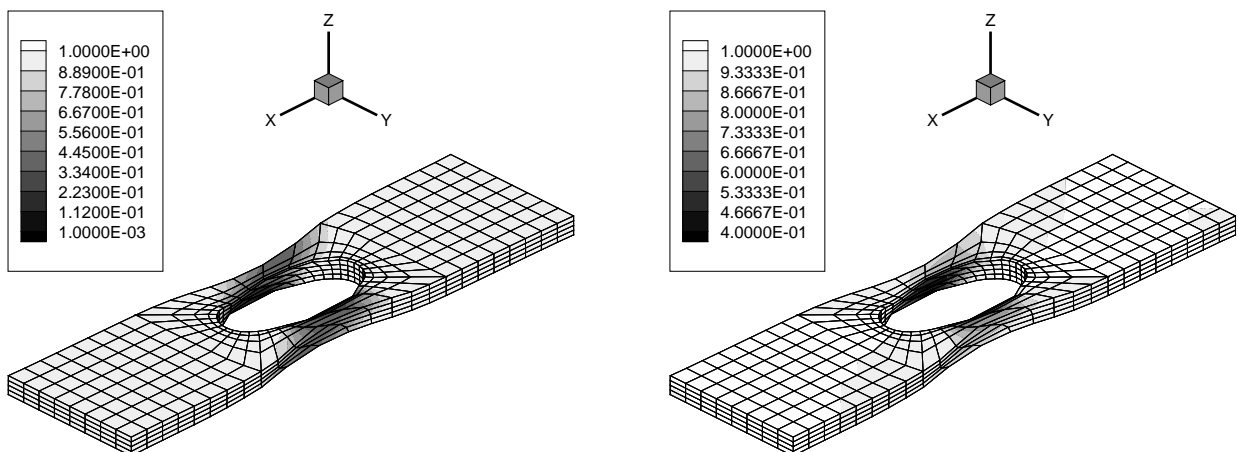


Figure 3.32: Strip with a hole, case c: Norm of the first structural tensor $\|\boldsymbol{A}_1^\sharp\|$ (left) and Norm of the second structural tensor $\|\boldsymbol{A}_2^\sharp\|$ (right).

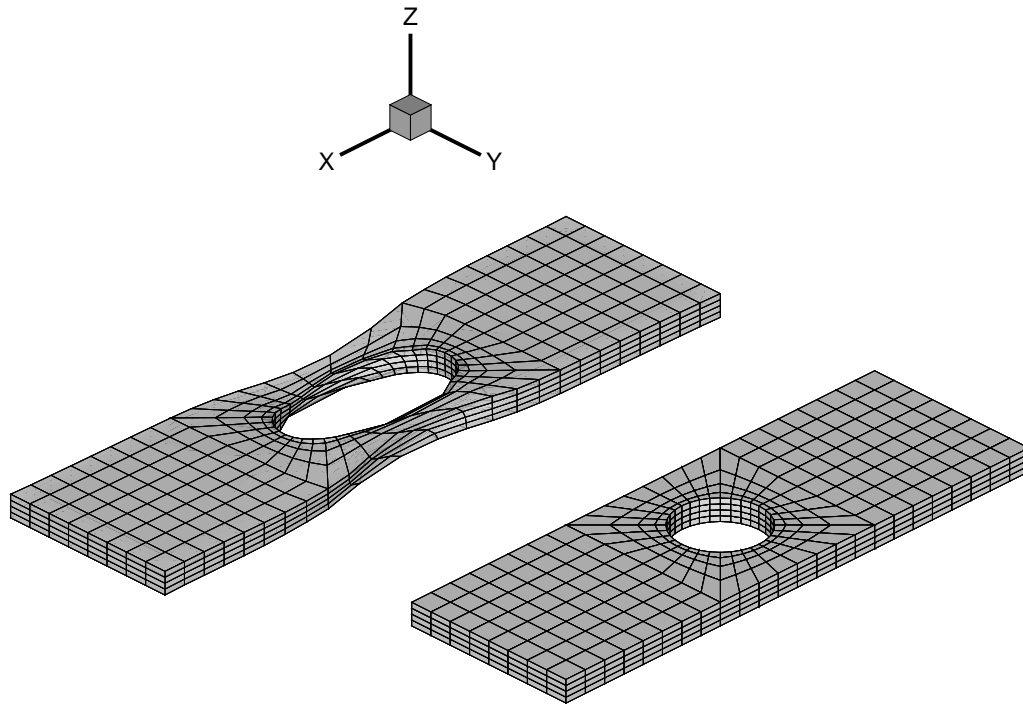


Figure 3.33: Strip with a hole, case d: Deformed configuration at a longitudinal stretch $\lambda = 1.2$ and initial undeformed geometry.

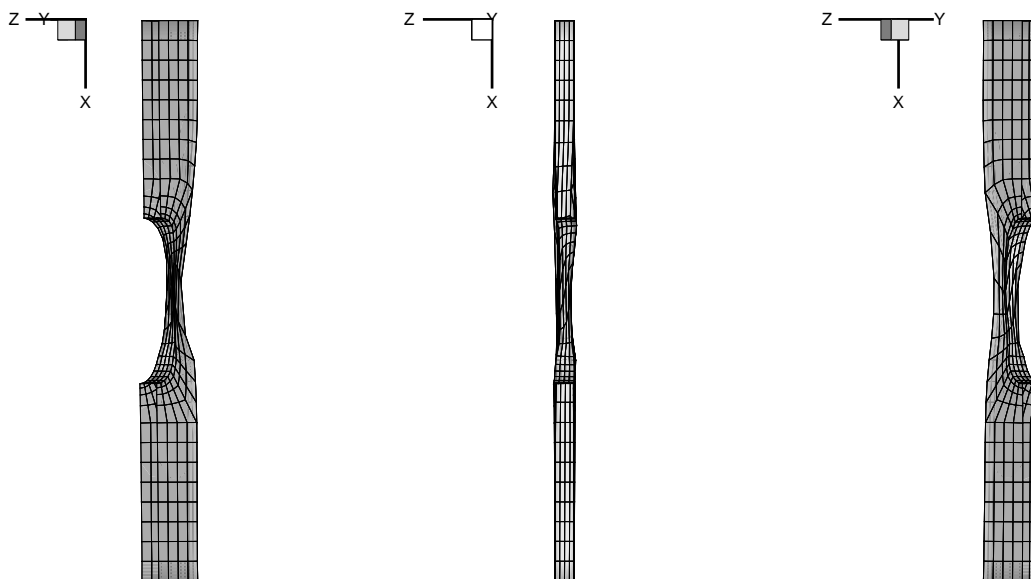


Figure 3.34: Strip with a hole, case d: Different views on a longitudinal section of the specimen.

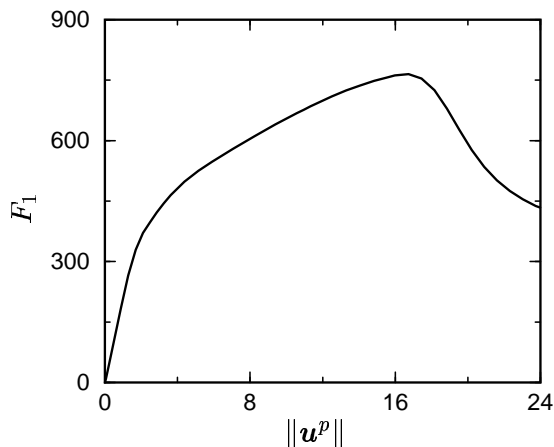


Figure 3.35: Strip with a hole, case d: Load–displacement curve (longitudinal).

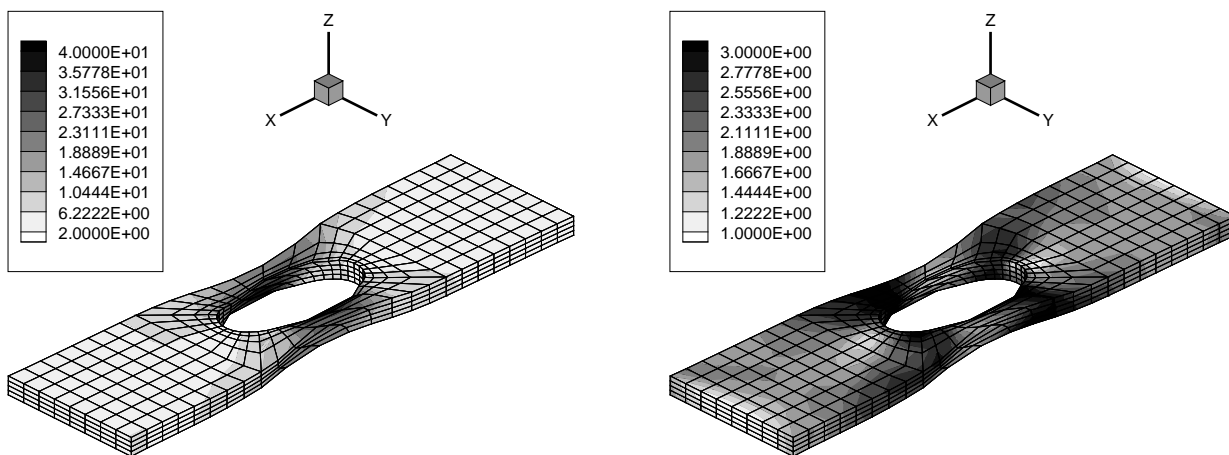


Figure 3.36: Strip with a hole, case d: Norm of the deviatoric Kirchhoff stress $\|{}^{\text{dev}}\boldsymbol{\tau}^{\#}\|$ (left) and of the proposed thermodynamic force $\|{}^{\text{dev}}\boldsymbol{y}^b\|$ (right).

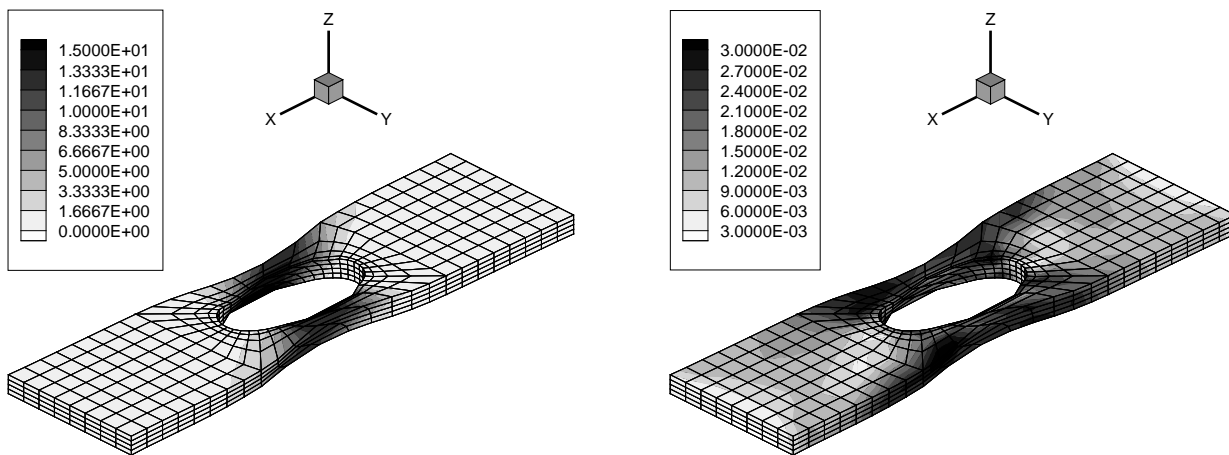


Figure 3.37: Strip with a hole, case d: Hardening variable κ (left) and anisotropy measure $\delta(\boldsymbol{b}_e^{\#}, \boldsymbol{\tau}^{\#})$ (right).

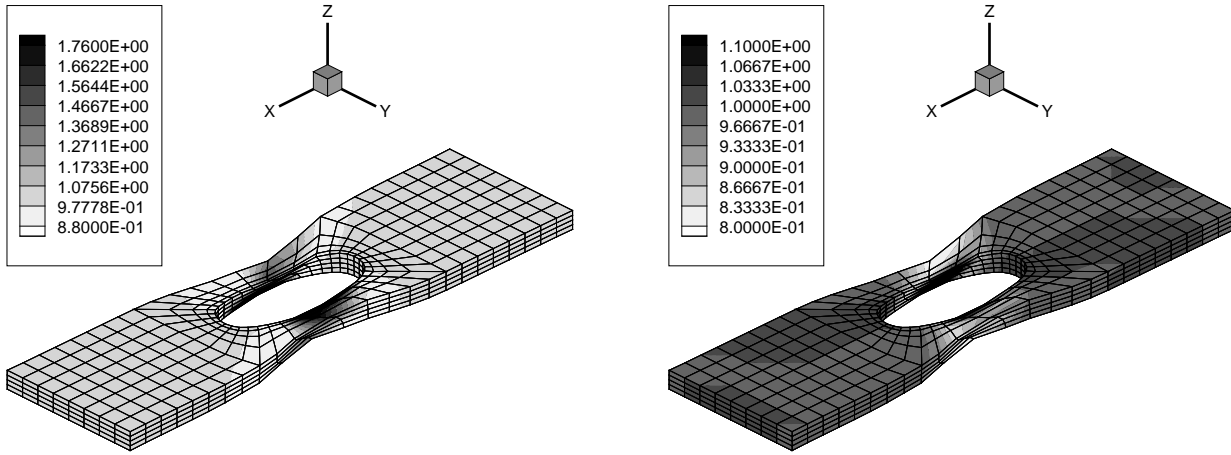


Figure 3.38: Strip with a hole, case d: Norm of the first structural tensor $\|\mathbf{A}_1^\sharp\|$ (left) and Norm of the second structural tensor $\|\mathbf{A}_2^\sharp\|$ (right).

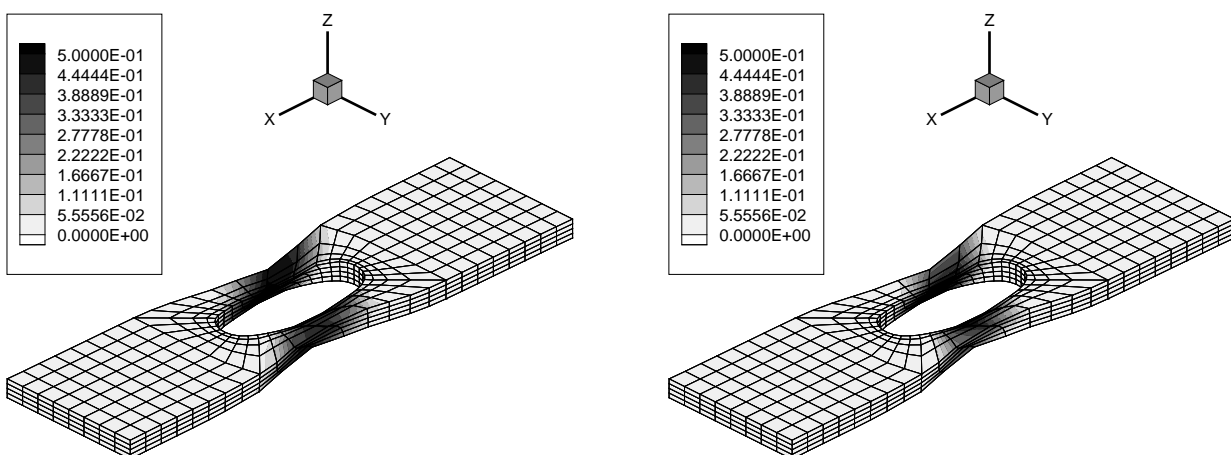


Figure 3.39: Strip with a hole, case d: Anisotropy measure $\delta(\mathbf{A}_1^\sharp, \mathbf{A}_1^\sharp|_{t_0})$ (left) and anisotropy measure $\delta(\mathbf{A}_2^\sharp, \mathbf{A}_2^\sharp|_{t_0})$ (right).

Table 3.3: Strip with a hole: Residual norm. Elastic range: Cases b–d, load step $u^p \in [0, 48]$ with exact tangent operator (left) and numerically approximated tangent operator (middle). Inelastic range: Case a, load step $u^p \in [0, 2]$ with numerically approximated tangent operator (right).

cases b–d: $Y_0 \rightarrow \infty$ exact: $u^p \in [0, 48]$			cases b–d: $Y_0 \rightarrow \infty$ numer.: $u^p \in [0, 48]$			case a: $Y_0 = 0.45$ numer.: $u^p \in [0, 2]$		
no.	$\ \mathbf{R}\ $		no.	$\ \mathbf{R}\ $		no.	$\ \mathbf{R}\ $	
1	3.21994	$E + 02$	1	3.21994	$E + 02$	1	1.34164	$E + 01$
2	2.21262	$E + 05$	2	2.21262	$E + 05$	2	4.55349	$E + 02$
3	7.56261	$E + 04$	3	7.56261	$E + 04$	3	1.23884	$E + 02$
4	2.45944	$E + 04$	4	2.45944	$E + 04$	4	7.07282	$E + 01$
5	7.17088	$E + 03$	5	7.17089	$E + 03$	5	1.83575	$E + 01$
6	1.46425	$E + 03$	6	1.46425	$E + 03$	6	1.13941	$E + 01$
7	2.64768	$E + 02$	7	2.64768	$E + 02$	7	8.83643	$E + 00$
8	4.37246	$E + 01$	8	4.37247	$E + 01$	8	6.03734	$E + 00$
9	1.75701	$E + 00$	9	1.75702	$E + 00$	9	3.76384	$E + 00$
10	2.50026	$E - 03$	10	2.50030	$E - 03$	10	5.64753	$E - 02$
11	5.94743	$E - 09$	11	5.93833	$E - 09$	11	5.06373	$E - 05$
						12	3.00627	$E - 10$

Table 3.4: Strip with a hole: Residual norm. Inelastic range: Case b, load step $u^p \in [0, 4]$ (left); case c, load step $u^p \in [0, 4]$ (middle); case d, load step $u^p \in [0, 2]$ (right) – all of them based on numerically approximated tangent operators.

case b: $Y_0 = 0.45$ numer.: $u^p \in [0, 4]$			case c: $Y_0 = 0.45$ numer.: $u^p \in [0, 4]$			case d: $Y_0 = 0.45$ numer.: $u^p \in [0, 2]$		
no.	$\ \mathbf{R}\ $		no.	$\ \mathbf{R}\ $		no.	$\ \mathbf{R}\ $	
1	2.68328	$E + 01$	1	2.68328	$E + 01$	1	2.01246	$E + 01$
2	5.98994	$E + 02$	2	5.66343	$E + 02$	2	2.95349	$E + 02$
3	3.47484	$E + 02$	3	3.59314	$E + 02$	3	1.71933	$E + 02$
4	5.27901	$E + 01$	4	4.71192	$E + 01$	4	1.62065	$E + 02$
5	1.11731	$E + 01$	5	1.37008	$E + 01$	5	1.13449	$E + 01$
6	2.29268	$E - 01$	6	1.28591	$E - 01$	6	8.86933	$E - 01$
7	1.03728	$E - 03$	7	7.46116	$E - 04$	7	1.20462	$E - 02$
8	7.35647	$E - 09$	8	9.85912	$E - 10$	8	2.63357	$E - 06$
						9	1.80916	$E - 10$

Chapter 4

Anisotropic hyper–elasticity based on a fictitious configuration

Ungeachtet der Vollständigkeit meiner analytischen Ergebnisse blieb mir nichts übrig, als dem Beispiel jener Forscher zu folgen, welche so glücklich sind, die unschätzbaren, wenn auch verflümmelten Reste des Altertums aus langer Begrabenheit an den Tag zu bringen.

Sigmund Freud [1856 – 1939]

Within the setting of geometrically non–linear continuum mechanics, the incorporation of structural tensors into the free Helmholtz energy density is one common strategy to model anisotropic materials, see the previous Chapters 2 and 3. Here we highlight an alternative approach based on an additional, fictitious configuration which is related to the standard reference configuration via a linear tangent map. Anisotropy comes into the picture if this mapping is non–spherical. Consequently, we deal with a reduced, but physically motivated set of invariants in terms of pre–specified combinations of the invariants of the structural tensor approach. Without loss of generality, this formulation holds for elastic and inelastic processes. Nevertheless, in order to clarify concepts, we place emphasis on the case of hyper–elasticity in this Chapter and focus on continuum damage mechanics and the coupling to multiplicative elasto–plasticity in the subsequent Chapters 5 and 6.

The Chapter is organised as follows: As the key issue of this Chapter, Section 4.1 presents the kinematical framework of anisotropic hyper–elasticity based on a fictitious, isotropic configuration. The relations between this formulation and the classical structural tensor approach are highlighted in Section 4.2. Specifically, we compare the invariants implied by the fictitious configuration concept for various cases of anisotropy with the invariants that are obtained by the introduction of structural tensors. Finally, numerical examples within the homogeneous deformation in simple shear and a general finite element setting are highlighted in Section 4.3 which underline the practicability of the proposed framework.

4.1 The concept of a fictitious configuration

The proposed concept of a fictitious isotropic configuration allows the interpretation as a multiplicative composition of the standard deformation gradient and an attached additional anisotropy map. The principle of strain energy equivalence (or rather the fundamental covariance relation) – well known in continuum damage mechanics, see e.g. Sidoroff [Sid81], Betten [Bet82b] and Murakami [Mur88] – renders two sets of invariants with respect to either the fictitious isotropic configuration or the undeformed anisotropic reference configuration. Based on these sets, stress–strain relations within the

hyper-elastic context are obtained. Obviously, anisotropy is incorporated as soon as the fictitious map is non-spherical. In particular, the specific form of the anisotropy map affects the type of material symmetry and it turns out that a reduced formulation of orthotropy is obtained.

4.1.1 Kinematics of the fictitious configuration

In addition to the Lagrangian (\mathcal{B}_0) and the Eulerian setting (\mathcal{B}_t), we introduce a fictitious isotropic configuration ($\bar{\mathcal{B}}$) with natural tangent space $T\bar{\mathcal{B}}$ and corresponding co-tangent or rather dual space $T^*\bar{\mathcal{B}}$ (and naturally identify $T^*\bar{\mathcal{B}} \doteq T\bar{\mathcal{B}}$). In analogy to the intermediate configuration within the multiplicative decomposition of elasto-plasticity, the fictitious configuration is generally incompatible. Mathematically speaking, we deal with a non-Euclidian space, i.e. the underlying metric tensors determine a non-vanishing Riemann-Christoffel tensor and the conditions of compatibility are generally not fulfilled. The corresponding non-singular direct fictitious linear tangent map, which transforms fictitious tangent vectors into material tangent vectors in reference to curves in \mathcal{B}_0 , is denoted by $\bar{\mathbf{F}}^\natural \in \mathbb{L}_+^3 : T\bar{\mathcal{B}} \rightarrow T\mathcal{B}_0$ and takes the interpretation of a non-holonomic Pfaffian, see e.g. Haupt [Hau00, Sect. 1.10] or Eringen [Eri71, Chap. 4]. For the proposed multiplicative composition, $\bar{\mathbf{F}}^\natural$ allows interpretation as pre-deformation. Figure 4.1 gives a symbolic graphical representation of the multiplicative composition of the linear tangent maps $\bar{\mathbf{F}}^\natural$ and \mathbf{F}^\natural .

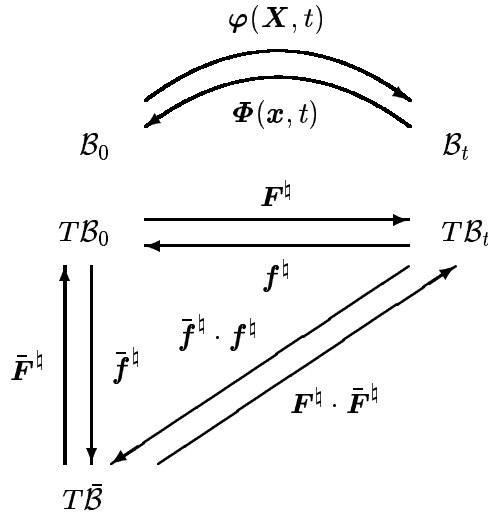


Figure 4.1: Non-linear point map φ and linear tangent maps $\bar{\mathbf{F}}^\natural$ and \mathbf{F}^\natural .

Accordingly, we introduce the convected base vectors in the fictitious configuration, which are not derivable from position vectors but are rather defined by the linear map $\bar{\mathbf{F}}^\natural$,

$$\bar{\mathbf{G}}_i \in \mathbb{R}^3 : T^*\bar{\mathcal{B}} \rightarrow \mathbb{R} \quad \text{and} \quad \bar{\mathbf{G}}^i \in \mathbb{R}^3 : T\bar{\mathcal{B}} \rightarrow \mathbb{R}. \quad (4.1)$$

Then, similar to Eqs.(2.2), the corresponding metric tensors of the fictitious configuration follow as usual

$$\begin{aligned} \bar{\mathbf{G}}^b &= \bar{G}_{ij} \bar{\mathbf{G}}^i \otimes \bar{\mathbf{G}}^j \in \mathbb{S}_+^3 : T\bar{\mathcal{B}} \times T\bar{\mathcal{B}} \rightarrow \mathbb{R}, & \bar{G}_{ij} &= \bar{\mathbf{G}}_i \cdot \bar{\mathbf{G}}_j, \\ \bar{\mathbf{G}}^\sharp &= \bar{G}^{ij} \bar{\mathbf{G}}_i \otimes \bar{\mathbf{G}}_j \in \mathbb{S}_+^3 : T^*\bar{\mathcal{B}} \times T^*\bar{\mathcal{B}} \rightarrow \mathbb{R}, & \bar{G}^{ij} &= \bar{\mathbf{G}}^i \cdot \bar{\mathbf{G}}^j \end{aligned} \quad (4.2)$$

and, in analogy to Eq.(2.3), the appropriate mixed-variant identity is obtained as

$$\bar{\mathbf{G}}^\natural = \bar{\mathbf{G}}_i \otimes \bar{\mathbf{G}}^i \in \mathbb{L}_+^3 : T^*\bar{\mathcal{B}} \times T\bar{\mathcal{B}} \rightarrow \mathbb{R}. \quad (4.3)$$

Therefore, the linear tangent or rather anisotropy map of the direct and the inverse fictitious mapping respectively read

$$\boxed{\bar{\mathbf{F}}^\natural = \mathbf{G}_i \otimes \bar{\mathbf{G}}^i \in \mathbb{L}_+^3 : T\bar{\mathcal{B}} \rightarrow T\mathcal{B}_0 \quad \text{and} \quad \bar{\mathbf{f}}^\natural = \bar{\mathbf{G}}_i \otimes \mathbf{G}^i \in \mathbb{L}_+^3 : T\mathcal{B}_0 \rightarrow T\bar{\mathcal{B}}}. \quad (4.4)$$

Consequently, four different symmetric kinematic tensor in the fictitious configuration are a natural outcome (compare Eqs.(2.6) and footnote ** on page 27)

$$\begin{aligned}
\bar{\mathbf{C}}^b &= \bar{\mathbf{F}}^{\sharp*} \mathbf{C}^b = [\bar{\mathbf{F}}^{\sharp}]^t \cdot \mathbf{C}^b \cdot \bar{\mathbf{F}}^{\sharp} = g_{ij} \bar{\mathbf{G}}^i \otimes \bar{\mathbf{G}}^j \in \mathbb{S}_+^3 : T\bar{\mathcal{B}} \times T\bar{\mathcal{B}} \rightarrow \mathbb{R}, \\
\bar{\mathbf{B}}^{\sharp} &= \bar{\mathbf{f}}^{\sharp*} \mathbf{B}^{\sharp} = \bar{\mathbf{f}}^{\sharp} \cdot \mathbf{B}^{\sharp} \cdot [\bar{\mathbf{f}}^{\sharp}]^t = g^{ij} \bar{\mathbf{G}}_i \otimes \bar{\mathbf{G}}_j \in \mathbb{S}_+^3 : T^*\bar{\mathcal{B}} \times T^*\bar{\mathcal{B}} \rightarrow \mathbb{R}, \\
\bar{\mathbf{C}}_0^b &= \bar{\mathbf{F}}^{\sharp*} \mathbf{G}^b = [\bar{\mathbf{F}}^{\sharp}]^t \cdot \mathbf{G}^b \cdot \bar{\mathbf{F}}^{\sharp} = G_{ij} \bar{\mathbf{G}}^i \otimes \bar{\mathbf{G}}^j \in \mathbb{S}_+^3 : T\bar{\mathcal{B}} \times T\bar{\mathcal{B}} \rightarrow \mathbb{R}, \\
\bar{\mathbf{B}}_0^{\sharp} &= \bar{\mathbf{f}}^{\sharp*} \mathbf{G}^{\sharp} = \bar{\mathbf{f}}^{\sharp} \cdot \mathbf{G}^{\sharp} \cdot [\bar{\mathbf{f}}^{\sharp}]^t = G^{ij} \bar{\mathbf{G}}_i \otimes \bar{\mathbf{G}}_j \in \mathbb{S}_+^3 : T^*\bar{\mathcal{B}} \times T^*\bar{\mathcal{B}} \rightarrow \mathbb{R},
\end{aligned} \tag{4.5}$$

with $\bar{\mathbf{B}}^{\sharp} = \det^{-1}(\bar{\mathbf{C}}^b) \text{cof}(\bar{\mathbf{C}}^b)$ and $\bar{\mathbf{B}}_0^{\sharp} = \det^{-1}(\bar{\mathbf{C}}_0^b) \text{cof}(\bar{\mathbf{C}}_0^b)$ being obvious, see Appendix A for notational details. Now, among several possible strain measures as highlighted in Eqs.(2.7, 2.8), we apply similar to the standard Green–Lagrange strain tensor \mathbf{E}^b a fictitious strain metric tensor in the sequel, which is introduced as

$$\boxed{\bar{\mathbf{E}}^b = \bar{\mathbf{F}}^{\sharp*} \mathbf{E}^b = [\bar{\mathbf{F}}^{\sharp}]^t \cdot \mathbf{E}^b \cdot \bar{\mathbf{F}}^{\sharp} = \frac{1}{2} [g_{ij} - G_{ij}] \bar{\mathbf{G}}^i \otimes \bar{\mathbf{G}}^j \in \mathbb{S}_+^3 : T\bar{\mathcal{B}} \times T\bar{\mathcal{B}} \rightarrow \mathbb{R}}. \tag{4.6}$$

Remark 4.1 *For conceptual simplicity, we restrict ourselves in this Chapter to the composition $\mathbf{F}^{\sharp} \cdot \bar{\mathbf{F}}^{\sharp}$ and the introduction of a Lagrangian fictitious configuration which is related to the material setting. Alternatively, one could account for an additional Eulerian fictitious configuration that allows interpretation as an intermediate configuration with respect to the Lagrangian fictitious configuration and the spatial setting, compare Chapter 6 in the context of Continuum damage mechanics coupled to multiplicative elasto–plasticity.*

4.1.2 Energy metric tensors

Next, for the computation of the scalar–valued free Helmholtz energy density ψ_0 , we introduce the contra–variant energy metric tensors $\bar{\mathbf{A}}^{\sharp}$ and \mathbf{A}^{\sharp} in addition to the co–variant strain metric tensors $\bar{\mathbf{E}}^b$ and \mathbf{E}^b

$$\bar{\mathbf{A}}^{\sharp} = \bar{A}^{ij} \bar{\mathbf{G}}_i \otimes \bar{\mathbf{G}}_j \in \mathbb{S}_+^3 : T^*\bar{\mathcal{B}} \times T^*\bar{\mathcal{B}} \rightarrow \mathbb{R}, \quad \mathbf{A}^{\sharp} = A^{ij} \mathbf{G}_i \otimes \mathbf{G}_j \in \mathbb{S}_+^3 : T^*\mathcal{B}_0 \times T^*\mathcal{B}_0 \rightarrow \mathbb{R}. \tag{4.7}$$

Thereby, we set

$$\boxed{\bar{\mathbf{F}}^{\sharp*} \bar{\mathbf{A}}^{\sharp} = \bar{\mathbf{F}}^{\sharp} \cdot \bar{\mathbf{A}}^{\sharp} \cdot [\bar{\mathbf{F}}^{\sharp}]^t \doteq \mathbf{A}^{\sharp} \implies \bar{A}^{ij} = A^{ij} \doteq \text{const}}. \tag{4.8}$$

Note that constant coefficients of the energy metric tensor are assumed since we deal with a non–dissipative material in this Chapter and furthermore that \mathbf{A}^{\sharp} is supposed to substitute the contra–variant metric tensor \mathbf{G}^{\sharp} in the definition of the free Helmholtz energy density. As the underlying idea of the proposed formulation, the fictitious configuration is isotropic and thus the fictitious energy metric tensor has to be spherical. We therefore set

$$\boxed{\bar{\mathbf{A}}^{\sharp} \doteq \bar{\mathbf{G}}^{\sharp}} \tag{4.9}$$

throughout this contribution. Consequently, $\bar{\mathbf{F}}^{\sharp}$ may be interpreted as a pre–deformation of a fictitious isotropic hyper–elastic material. Finally, the scalar–valued free Helmholtz energy density is restricted to remain invariant under a superposed diffeomorphism (covariance), which is represented here by the linear tangent map $\bar{\mathbf{F}}^{\sharp}$, and we consequently obtain

$$\boxed{\bar{\psi}_0(\bar{\mathbf{E}}^b, \bar{\mathbf{A}}^{\sharp}; \mathbf{X}) = \psi_0^0(\mathbf{E}^b, \mathbf{A}^{\sharp}; \mathbf{X})} \tag{4.10}$$

which is established as the principle of strain energy equivalence in the context of continuum damage mechanics, see e.g. Sidoroff [Sid81] †.

† Following the outline in Section 2.2, the free Helmholtz energy density allows representation as

$$\psi_0 = \psi_0(\mathbf{g}^b, \mathbf{F}^{\sharp} \cdot \bar{\mathbf{F}}^{\sharp}, \bar{\mathbf{A}}^{\sharp} \doteq \bar{\mathbf{G}}^{\sharp}; \mathbf{X}) \in \mathbb{R}. \tag{†.1}$$

To underline the nature of the proposed framework, we now stress that Eq.(4.10) includes all assumptions of the material modelling. Nevertheless we clearly deal with a reduced representation of anisotropy which is highlighted in Section 4.2. As an advantage, note that besides the introduction of the fictitious configuration, no further assumptions or additional material parameters have to be included since standard isotropic free energy functions can be applied to model anisotropic behaviour. Of course isotropy is included for $\mathbf{A}^\sharp \doteq \beta_0 \mathbf{G}^\sharp$, $\beta_0 \in \mathbb{R}_0$ and anisotropy enters the formulation if \mathbf{A}^\sharp is a non-spherical tensor.

4.1.3 Hyper-elasticity

Since $T\bar{\mathcal{B}}$, $T^*\bar{\mathcal{B}}$ refer to a fictitious isotropic configuration, a set of merely three basic invariants $\bar{E}^b \bar{A}^\sharp I_{1,2,3}$ defined in terms of the fictitious strain and energy metric tensors $\bar{\mathbf{E}}^b$ and $\bar{\mathbf{A}}^\sharp$ is given as

$$\bar{E}^b \bar{A}^\sharp I_i = \bar{\mathbf{G}}^\sharp : [\bar{\mathbf{E}}^b \cdot \bar{\mathbf{A}}^\sharp]^i \quad (4.11)$$

with $i = 1, 2, 3$, compare Table 3.1 and Appendix B.2. Next, the set of invariants $E^b A^\sharp I_{1,2,3}$ with respect to the anisotropic reference configuration \mathcal{B}_0 is obtained by expressing $\bar{\mathbf{E}}^b$ and $\bar{\mathbf{A}}^\sharp$ in terms of \mathbf{E}^b and \mathbf{A}^\sharp via a pull-back operation determined by $\bar{\mathbf{F}}^\sharp$ as defined via Eqs.(4.6, 4.8). Then, straightforward calculations result in the following set of basic invariants in \mathcal{B}_0 ($i = 1, 2, 3$)

$$E^b A^\sharp I_i = \mathbf{G}^\sharp : [\mathbf{E}^b \cdot \mathbf{A}^\sharp]^i. \quad (4.12)$$

The relations $\bar{E}^b \bar{A}^\sharp I_i = E^b A^\sharp I_i$ obviously hold and moreover, the hyper-elastic constitutive law for the second Piola-Kirchhoff stress tensor $\mathbf{S}^\sharp = \partial_{\mathbf{E}^b} \psi_0^0$ is now expressed as

$$\mathbf{S}^\sharp = \partial_{E^b A^\sharp I_1} \psi_0^0 \mathbf{A}^\sharp + 2 \partial_{E^b A^\sharp I_2} \psi_0^0 [\mathbf{A}^\sharp \cdot \mathbf{E}^b \cdot \mathbf{A}^\sharp] + 3 \partial_{E^b A^\sharp I_3} \psi_0^0 [\mathbf{A}^\sharp \cdot \mathbf{E}^b \cdot \mathbf{A}^\sharp \cdot \mathbf{E}^b \cdot \mathbf{A}^\sharp], \quad (4.13)$$

obeying the identical structure of an isotropic setting. Next, the correlated tangent operator $\mathbf{E}^\sharp = \partial_{\mathbf{E}^b \otimes \mathbf{E}^b}^2 \psi_0^0 \in \mathbb{S}^{3 \times 3} : T^* \mathcal{B}_0 \times T^* \mathcal{B}_0 \times T^* \mathcal{B}_0 \times T^* \mathcal{B}_0 \rightarrow \mathbb{R}$ results in (see Appendix A.1 for notational details)

$$\begin{aligned} \mathbf{E}^\sharp &= \partial_{E^b A^\sharp I_1}^2 \psi_0^0 \mathbf{A}^\sharp \otimes \mathbf{A}^\sharp \\ &+ 4 \partial_{E^b A^\sharp I_2}^2 \psi_0^0 [\mathbf{A}^\sharp \cdot \mathbf{E}^b \cdot \mathbf{A}^\sharp] \otimes [\mathbf{A}^\sharp \cdot \mathbf{E}^b \cdot \mathbf{A}^\sharp] \\ &+ 9 \partial_{E^b A^\sharp I_3}^2 \psi_0^0 [\mathbf{A}^\sharp \cdot \mathbf{E}^b \cdot \mathbf{A}^\sharp \cdot \mathbf{E}^b \cdot \mathbf{A}^\sharp] \otimes [\mathbf{A}^\sharp \cdot \mathbf{E}^b \cdot \mathbf{A}^\sharp \cdot \mathbf{E}^b \cdot \mathbf{A}^\sharp] \\ &+ 4 \partial_{E^b A^\sharp I_1}^2 \psi_0^0 \left[\mathbf{A}^\sharp \otimes [\mathbf{A}^\sharp \cdot \mathbf{E}^b \cdot \mathbf{A}^\sharp] \right]^{\text{SYM}} \\ &+ 12 \partial_{E^b A^\sharp I_2}^2 \psi_0^0 \left[[\mathbf{A}^\sharp \cdot \mathbf{E}^b \cdot \mathbf{A}^\sharp] \otimes [\mathbf{A}^\sharp \cdot \mathbf{E}^b \cdot \mathbf{A}^\sharp \cdot \mathbf{E}^b \cdot \mathbf{A}^\sharp] \right]^{\text{SYM}} \\ &+ 6 \partial_{E^b A^\sharp I_3}^2 \psi_0^0 \left[\mathbf{A}^\sharp \otimes [\mathbf{A}^\sharp \cdot \mathbf{E}^b \cdot \mathbf{A}^\sharp \cdot \mathbf{E}^b \cdot \mathbf{A}^\sharp] \right]^{\text{SYM}} \\ &+ \partial_{E^b A^\sharp I_2} \psi_0^0 [\mathbf{A}^\sharp \bar{\otimes} \mathbf{A}^\sharp + \mathbf{A}^\sharp \underline{\otimes} \mathbf{A}^\sharp] \\ &+ 3 \partial_{E^b A^\sharp I_3} \psi_0^0 \left[\mathbf{A}^\sharp \bar{\otimes} [\mathbf{A}^\sharp \cdot \mathbf{E}^b \cdot \mathbf{A}^\sharp] + \mathbf{A}^\sharp \underline{\otimes} [\mathbf{A}^\sharp \cdot \mathbf{E}^b \cdot \mathbf{A}^\sharp] \right]^{\text{SYM}} \end{aligned} \quad (4.14)$$

A transformation of the arguments to $\bar{\mathcal{B}}$ together with the fundamental covariance relation yields

$$\psi_0 \doteq \psi_0(\mathbf{F}^{\sharp*} \bar{\mathbf{F}}^{\sharp*} \mathbf{g}^b, \mathbf{f}^{\sharp*} \bar{\mathbf{f}}^{\sharp*} [\mathbf{F}^{\sharp*} \cdot \bar{\mathbf{F}}^{\sharp*}], \bar{\mathbf{A}}^\sharp; \mathbf{X}) = \bar{\psi}_0(\bar{\mathbf{C}}^b, \bar{\mathbf{A}}^\sharp; \mathbf{X}) \implies \bar{\psi}_0(\bar{\mathbf{E}}^b, \bar{\mathbf{A}}^\sharp; \mathbf{X}) \quad (\ddagger.2)$$

whereby $\mathbf{f}^{\sharp*} \bar{\mathbf{f}}^{\sharp*} [\mathbf{F}^{\sharp*} \cdot \bar{\mathbf{F}}^{\sharp*}] = \bar{\mathbf{G}}^\sharp$ is redundant and the replacement $\bar{\mathbf{E}}^b \mapsto \bar{\mathbf{C}}^b$ being obvious. Naturally, we can apply push-forward operations to obtain representations of the free Helmholtz energy density in \mathcal{B}_0 and \mathcal{B}_t , respectively, namely

$$\begin{aligned} \psi_0 = \bar{\psi}_0(\bar{\mathbf{E}}^b, \bar{\mathbf{A}}^\sharp; \mathbf{X}) &\doteq \bar{\psi}_0(\bar{\mathbf{f}}^{\sharp*} \bar{\mathbf{E}}^b, \bar{\mathbf{F}}^{\sharp*} \bar{\mathbf{A}}^\sharp; \mathbf{X}) = \psi_0^0(\mathbf{E}^b, \mathbf{A}^\sharp; \mathbf{X}), \\ &\doteq \psi_0^0(\mathbf{f}^{\sharp*} \mathbf{E}^b, \mathbf{F}^{\sharp*} \mathbf{A}^\sharp; \mathbf{X}) = \psi_0^t(\mathbf{e}^b, \mathbf{a}^\sharp; \mathbf{X}). \end{aligned} \quad (\ddagger.3)$$

which is apparently similar to an isotropic setting and relatively concise compared to the Hessian based on structural tensors in Eqs.(2.52–2.54). It is obvious that the general formulation in terms of structural tensors ends up in enormous analytical and numerical costs. In contrast, the approach based on a fictitious configuration is much cheaper. Actually, the computational effort is in the same range as that for standard isotropy.

Remark 4.2 *Usually, isotropic hyper-elasticity is formulated in terms of the three principal invariants ${}^{C^b G^\sharp} J_{1,2,3}$ of the right Cauchy–Green tensor \mathbf{C}^b (or alternatively in terms of the Finger tensor \mathbf{b}^\sharp) instead of the basic invariants ${}^{E^b G^\sharp} I_{1,2,3}$ determined by the Green–Lagrange tensor, compare Appendix B. Selecting the principal invariants ${}^{E^b G^\sharp} J_{1,2,3}$ with respect to the strain metric tensor \mathbf{E}^b renders contributions that include the inverse $[\mathbf{E}^b]^{-1}$ when the stress tensor \mathbf{S}^\sharp and the corresponding Hessian \mathbf{E}^\sharp are computed. Since $[\mathbf{E}^b]^{-1}$ might not be defined, especially for the undeformed state (or any other deformation that results in a strain measure of improper rank), one has to re-express the inverse strain metric tensor via the Cayley–Hamilton theorem to end up with a singularity-free formulation, compare Appendices B.1, B.2 and footnote † on page 60. We alternatively invoke the basic invariants here – as given in Eq.(4.12) – defined by the strain metric tensor because the fictitious configuration is directly based on the concept of strain energy equivalence and these invariants turn out to be conveniently applicable.*

4.2 Relations between structural tensors and the fictitious configuration

The main goal of this section is to highlight the relations between the two frameworks based on either structural tensors or on the advocated fictitious configuration, respectively. Therefore, one has to compare the arguments of the free Helmholtz energy functions, i.e. the corresponding sets of invariants. Conceptually speaking, the task is to compute ${}^{E^b A^\sharp} I_{1,2,3} = {}^{E^b A^\sharp} I_{1,2,3}({}^{E^b A^\sharp} I_{1,\dots,9})$.

4.2.1 Review of orthotropic hyper-elasticity based on structural tensors

For convenience of the reader, we briefly reiterate the Lagrangian setting of orthotropic hyper-elasticity based on two structural tensors $\mathbf{A}_{1,2}^\sharp = A_{1,2}^\sharp \mathbf{N}^\sharp \otimes A_{1,2}^\sharp \mathbf{N}^\sharp \doteq \text{const}$ in \mathcal{B}_0 with $A_{1,2}^\sharp \mathbf{N}^\sharp \in \mathbb{U}^2 : T^* \mathcal{B}_0 \rightarrow \mathbb{R}$, fully outlined in Chapter 2. Thus, the appropriate set of invariants reads as ($i = 1, 2, 3$)

$$\begin{aligned}
{}^{E^b A_{12}^\sharp} I_i &= \mathbf{G}^\sharp : [\mathbf{E}^b \cdot \mathbf{G}^\sharp]^i, \\
{}^{E^b A_{12}^\sharp} I_4 &= \mathbf{A}_1^\sharp : \mathbf{E}^b, & {}^{E^b A_{12}^\sharp} I_5 &= \mathbf{A}_1^\sharp : [\mathbf{E}^b \cdot \mathbf{G}^\sharp \cdot \mathbf{E}^b], \\
{}^{E^b A_{12}^\sharp} I_6 &= \mathbf{A}_2^\sharp : \mathbf{E}^b, & {}^{E^b A_{12}^\sharp} I_7 &= \mathbf{A}_2^\sharp : [\mathbf{E}^b \cdot \mathbf{G}^\sharp \cdot \mathbf{E}^b], \\
{}^{E^b A_{12}^\sharp} I_8 &= \mathbf{A}_1^\sharp : [\mathbf{G}^b \cdot \mathbf{A}_2^\sharp], & {}^{E^b A_{12}^\sharp} I_9 &= \mathbf{A}_1^\sharp : [\mathbf{G}^b \cdot \mathbf{A}_2^\sharp \cdot \mathbf{E}^b],
\end{aligned} \tag{4.15}$$

compare Table 2.1. Note that the denomination ${}^{E^b A_{12}^\sharp} I_8$ has been chosen for notational simplicity and that this contribution, which is practically related to the angle between the two incorporated fibre orientations, stays constant during the deformation. Further restrictions like the orthogonality of $A_{1,2}^\sharp \mathbf{N}^\sharp$ or a vanishing fibre vector $A_2^\sharp \mathbf{N}^\sharp$ yield classical orthotropic and transversely isotropic behaviour, respectively. The hyper-elastic constitutive law for the second Piola–Kirchhoff stress tensor $\mathbf{S}^\sharp = \partial_{\mathbf{E}^b} \psi_0^0(\mathbf{E}^b, \mathbf{A}_{1,2}^\sharp; \mathbf{X})$ renders (see Appendix A.1 for notational details)

$$\begin{aligned}
\mathbf{S}^\sharp &= \partial_{E^b A_{12}^\sharp I_1} \psi_0^0 \mathbf{G}^\sharp + 2 \partial_{E^b A_{12}^\sharp I_2} \psi_0^0 [\mathbf{G}^\sharp \cdot \mathbf{E}^b \cdot \mathbf{G}^\sharp] + 3 \partial_{E^b A_{12}^\sharp I_3} \psi_0^0 [\mathbf{G}^\sharp \cdot \mathbf{E}^b \cdot \mathbf{G}^\sharp \cdot \mathbf{E}^b \cdot \mathbf{G}^\sharp] \\
&+ \partial_{E^b A_{12}^\sharp I_4} \psi_0^0 \mathbf{A}_1^\sharp + 2 \partial_{E^b A_{12}^\sharp I_5} \psi_0^0 [\mathbf{G}^\sharp \cdot \mathbf{E}^b \cdot \mathbf{A}_1^\sharp]^{\text{sym}} \\
&+ \partial_{E^b A_{12}^\sharp I_6} \psi_0^0 \mathbf{A}_2^\sharp + 2 \partial_{E^b A_{12}^\sharp I_7} \psi_0^0 [\mathbf{G}^\sharp \cdot \mathbf{E}^b \cdot \mathbf{A}_2^\sharp]^{\text{sym}} + 2 \partial_{E^b A_{12}^\sharp I_9} \psi_0^0 [\mathbf{A}_1^\sharp \cdot \mathbf{G}^b \cdot \mathbf{A}_2^\sharp]^{\text{sym}}
\end{aligned} \tag{4.16}$$

which obviously incorporates more than twice as many terms than Eq.(4.13). The corresponding Hessian within the Eulerian setting is highlighted in Eqs.(2.52–2.54) and therefore skipped here.

4.2.2 Incorporation of structural tensors into the fictitious linear tangent map

In order to demonstrate the nature of the energy metric tensor, we make a specific ansatz for the fictitious dual base vectors. In particular, we give a representation of $\bar{\mathbf{G}}^i$ which reads

$$\bar{\mathbf{G}}^i = [\bar{\mathbf{F}}^{\sharp}]^t \cdot \mathbf{G}^i \doteq \alpha_0 \mathbf{G}^i + \sum_{j=1}^2 \alpha_i A_j^{\sharp} N^i A_j^b \mathbf{N}^b \quad (4.17)$$

and emphasises the heart of the proposed formulation whereby $A_j^{\sharp} N^i$ represent the components of the contra-variant fibre orientations and $A_j^b \mathbf{N}^b$ denote the co-variant complement of these unit-vectors[§]. Conceptually speaking, Eq.(4.17) defines $\bar{\mathbf{G}}^i$ in terms of \mathbf{G}^i and the fibre directions $A_{1,2}^{\sharp} \mathbf{N}^{\sharp}$. The two-point tensor $\bar{\mathbf{F}}^{\sharp} = \mathbf{G}_i \otimes \bar{\mathbf{G}}^i$ now takes the following format with respect to \mathcal{B}_0

$$\bar{\mathbf{F}}^{\sharp} \doteq \alpha_0 \mathbf{G}^{\sharp} + \sum_{i=1}^2 \alpha_i \mathbf{A}_i^{\sharp} \quad \text{with} \quad \mathbf{A}_i^{\sharp} = A_i^{\sharp} \mathbf{N}^{\sharp} \otimes A_i^b \mathbf{N}^b \quad (4.18)$$

Remarkably, beside this ansatz, no further assumptions to model anisotropy are required. The introduction of $\bar{\mathbf{F}}^{\sharp}$ as a symmetric quantity with respect to \mathbf{G}^{\sharp} is no severe restriction since the energy metric tensor \mathbf{A}^{\sharp} remains generally symmetric. Next, straightforward calculations with $\mathbf{A}^{\sharp} = \bar{\mathbf{F}}_{\star} \bar{\mathbf{A}}^{\sharp}$ and $\bar{\mathbf{A}}^{\sharp} \doteq \bar{\mathbf{G}}^{\sharp}$ render the energy metric tensor in \mathcal{B}_0

$$\mathbf{A}^{\sharp} = \beta_0 \mathbf{G}^{\sharp} + \beta_1 \mathbf{A}_1^{\sharp} + \beta_2 \mathbf{A}_2^{\sharp} + 2 \beta_3 [\mathbf{A}_1^{\sharp} \cdot \mathbf{G}^b \cdot \mathbf{A}_2^{\sharp}]^{\text{sym}} \quad (4.19)$$

whereby we introduce the abbreviated notations

$$\beta_0 = \alpha_0^2, \quad \beta_1 = 2 \alpha_0 \alpha_1 + \alpha_1^2, \quad \beta_2 = 2 \alpha_0 \alpha_2 + \alpha_2^2, \quad \beta_3 = \alpha_1 \alpha_2, \quad (4.20)$$

and $\mathbf{A}_{1,2}^{\sharp} = A_{1,2}^{\sharp} \mathbf{N}^{\sharp} \otimes A_{1,2}^b \mathbf{N}^b$ allow similar interpretation as structural tensors. Consequently, the relations between structural tensors and the fictitious configuration with respect to the proposed ansatz can easily be verified by the incorporation of Eq.(4.19) into Eq.(4.12) and comparing the obtained result to Eq.(4.15).

Remark 4.3 *The parameters $\alpha_{0,1,2}$ have to be chosen such that $\det(\mathbf{F}^{\sharp}) \in \mathbb{R}_+$. In this context, we consider the following cases:*

- (i) $\alpha_0 \neq 0, \alpha_1 = \alpha_2 = 0$: *This isotropic situation ends up in the restriction $\alpha_0 > 0$ which is assumed to hold throughout.*
- (ii) $\alpha_0 > 0, \alpha_1 \neq 0, \alpha_2 = 0$: *Application of the Sherman–Morrison–Woodbury theorem, see e.g. Householder [Hou75, Sect. 5.1], results in the constraint $\alpha_1 > -\alpha_0$ for this transversely isotropic case.*
- (iii) $\alpha_0 > 0, \alpha_{1,2} \neq 0$: *Within this general case, the determinant is again computed via the Sherman–Morrison–Woodbury theorem and takes the following format*

$$\det(\bar{\mathbf{F}}^{\sharp}) = \alpha_0^2 [\alpha_0 + \alpha_1] \left[1 + \frac{\alpha_2}{\alpha_0} - \frac{\alpha_1 \alpha_2}{\alpha_0 + \alpha_1 / \alpha_0} E^b A_{12}^{\sharp} I_8 \right] > 0 \quad (4.21)$$

with $E^b A_{12}^{\sharp} I_8 = \mathbf{A}_1^{\sharp} : [\mathbf{A}_2^{\sharp}]^t$. Thus, possible solutions can be obtained by the restrictions

$$\alpha_1 > \max \left\{ -\alpha_0, \frac{\alpha_0^2 [\alpha_0 + \alpha_2]}{\alpha_0^2 \alpha_2 E^b A_{12}^{\sharp} I_8 - \alpha_0 - \alpha_2} \right\}, \quad \alpha_2 > \frac{\alpha_0 [\alpha_0^2 + \alpha_1]}{\alpha_0^2 \alpha_1 E^b A_{12}^{\sharp} I_8 - \alpha_0^2 - \alpha_1} \quad (4.22)$$

[§]For notational simplicity the underlying shifter, say $[\text{shi}_{\sharp}^{\sharp}]^t : T^* \mathcal{B}_0 \rightarrow T^* \bar{\mathcal{B}}$, is omitted in Eq.(4.17).

4.2.3 Two arbitrary fibres

In the following, the most general case of two arbitrary, mechanically non-equivalent ($\alpha_1 \neq \alpha_2$) fibres $A_{1,2}^\sharp \mathbf{N}^\sharp$ is discussed in detail. Within this setting, the first invariant ${}^{E^b A^\sharp} I_1$ in terms of ${}^{E^b A_{12}^\sharp} I_{1,\dots,9}$ reads

$${}^{E^b A^\sharp} I_1 = \gamma_{10} {}^{E^b A_{12}^\sharp} I_1 + \gamma_{11} {}^{E^b A_{12}^\sharp} I_4 + \gamma_{12} {}^{E^b A_{12}^\sharp} I_6 + \gamma_{13} {}^{E^b A_{12}^\sharp} I_9 \quad (4.23)$$

together with the scalar-valued coefficients $\gamma_{1n}(\beta_i)$

$$\gamma_{10} = \beta_0, \quad \gamma_{11} = \beta_1, \quad \gamma_{12} = \beta_2, \quad \gamma_{13} = 2\beta_3. \quad (4.24)$$

Similar computations for the second basic invariant, which is quadratic in the strain metric tensor, end up with

$$\begin{aligned} {}^{E^b A^\sharp} I_2 = & \gamma_{20} {}^{E^b A_{12}^\sharp} I_2 + \gamma_{21} {}^{E^b A_{12}^\sharp} I_5 + \gamma_{22} {}^{E^b A_{12}^\sharp} I_4^2 \\ & + \gamma_{23} {}^{E^b A_{12}^\sharp} I_6^2 + \gamma_{24} {}^{E^b A_{12}^\sharp} I_7 + \gamma_{25} {}^{E^b A_{12}^\sharp} I_9^2 {}^{E^b A_{12}^\sharp} I_8^{-1} \\ & + \gamma_{26} \left[{}^{E^b A_{12}^\sharp} I_4 {}^{E^b A_{12}^\sharp} I_6 {}^{E^b A_{12}^\sharp} I_8 + {}^{E^b A_{12}^\sharp} I_9^2 \right] \\ & + \gamma_{27} {}^{E^b A_{12}^\sharp} I_4 {}^{E^b A_{12}^\sharp} I_9 + \gamma_{28} {}^{E^b A_{12}^\sharp} I_6 {}^{E^b A_{12}^\sharp} I_9 \\ & + \gamma_{29} {}^{E^b A_{12}^\sharp} I_8^{1/2} {}^{E^b A_{12}^\sharp} I_{\text{red}} \end{aligned} \quad (4.25)$$

and the corresponding coefficients $\gamma_{2n}(\beta_i)$ result in

$$\begin{aligned} \gamma_{20} &= \beta_0^2, & \gamma_{21} &= 2\beta_0\beta_1, & \gamma_{22} &= \beta_1^2, \\ \gamma_{23} &= \beta_2^2, & \gamma_{24} &= 2\beta_0\beta_2, & \gamma_{25} &= 2\beta_1\beta_2, \\ \gamma_{26} &= 2\beta_3^2, & \gamma_{27} &= 4\beta_1\beta_3, & \gamma_{28} &= 4\beta_2\beta_3, \\ \gamma_{29} &= 4\beta_0\beta_3, \end{aligned} \quad (4.26)$$

with ${}^{E^b A_{12}^\sharp} I_{\text{red}} = A_1^\sharp \mathbf{N}^\sharp \cdot \mathbf{E}^b \cdot \mathbf{G}^\sharp \cdot \mathbf{E}^b \cdot A_2^\sharp \mathbf{N}^\sharp$ – see Remark 4.4. The invariants ${}^{E^b A_{12}^\sharp} I_{4,\dots,9}$ of the structural tensors as given in Eq.(4.15) include only terms up to order two with respect to the strain metric tensor. Thus, we have to apply the Cayley–Hamilton theorem for the comparison of the third invariant. Thereby, the relations $\mathbf{G}^b : \mathbf{A}_{1,2}^\sharp \doteq 1$ have been taken into account and moreover, the determinant of the strain metric tensor $\gamma_{\det} \mathbf{E}^b$ comes into play which reads in terms of the basic invariants as

$$\gamma_{\det} \mathbf{E}^b = \frac{1}{6} \left[2 {}^{E^b A_{12}^\sharp} I_3 - 3 {}^{E^b A_{12}^\sharp} I_1 {}^{E^b A_{12}^\sharp} I_2 + {}^{E^b A_{12}^\sharp} I_1^3 \right]. \quad (4.27)$$

After some tedious algebra we obtain the result

$$\begin{aligned} {}^{E^b A^\sharp} I_3 = & \gamma_{30} {}^{E^b A_{12}^\sharp} I_3 + \gamma_{31} {}^{E^b A_{12}^\sharp} I_4 {}^{E^b A_{12}^\sharp} I_5 + \gamma_{32} {}^{E^b A_{12}^\sharp} I_4^3 \\ & + \gamma_{33} \left[{}^{E^b A_{12}^\sharp} I_1 {}^{E^b A_{12}^\sharp} I_5 - \frac{1}{2} \left[{}^{E^b A_{12}^\sharp} I_1^2 - {}^{E^b A_{12}^\sharp} I_2 \right] {}^{E^b A_{12}^\sharp} I_4 + \gamma_{\det} \mathbf{E}^b \right] \\ & + \gamma_{34} {}^{E^b A_{12}^\sharp} I_6 {}^{E^b A_{12}^\sharp} I_7 + \gamma_{35} {}^{E^b A_{12}^\sharp} I_6^3 + \gamma_{36} {}^{E^b A_{12}^\sharp} I_4 {}^{E^b A_{12}^\sharp} I_9^2 {}^{E^b A_{12}^\sharp} I_8^{-1} \\ & + \gamma_{37} {}^{E^b A_{12}^\sharp} I_6 {}^{E^b A_{12}^\sharp} I_9^2 {}^{E^b A_{12}^\sharp} I_8^{-1} + \gamma_{38} {}^{E^b A_{12}^\sharp} I_9 {}^{E^b A_{12}^\sharp} I_8^{-1/2} {}^{E^b A_{12}^\sharp} I_{\text{red}} \\ & + \gamma_{39} \left[{}^{E^b A_{12}^\sharp} I_1 {}^{E^b A_{12}^\sharp} I_7 - \frac{1}{2} \left[{}^{E^b A_{12}^\sharp} I_1^2 - {}^{E^b A_{12}^\sharp} I_2 \right] {}^{E^b A_{12}^\sharp} I_6 + \gamma_{\det} \mathbf{E}^b \right] \\ & + \gamma_{310} {}^{E^b A_{12}^\sharp} I_4^2 {}^{E^b A_{12}^\sharp} I_9 + \gamma_{311} {}^{E^b A_{12}^\sharp} I_6^2 {}^{E^b A_{12}^\sharp} I_9 \\ & + \gamma_{312} {}^{E^b A_{12}^\sharp} I_8 \left[{}^{E^b A_{12}^\sharp} I_5 {}^{E^b A_{12}^\sharp} I_6 + {}^{E^b A_{12}^\sharp} I_4 {}^{E^b A_{12}^\sharp} I_7 + 2 {}^{E^b A_{12}^\sharp} I_9 {}^{E^b A_{12}^\sharp} I_8^{-1/2} {}^{E^b A_{12}^\sharp} I_{\text{red}} \right] \\ & + \gamma_{313} \left[{}^{E^b A_{12}^\sharp} I_4 {}^{E^b A_{12}^\sharp} I_9^2 {}^{E^b A_{12}^\sharp} I_8^{-1} + {}^{E^b A_{12}^\sharp} I_4^2 {}^{E^b A_{12}^\sharp} I_6 \right] \\ & + \gamma_{314} \left[{}^{E^b A_{12}^\sharp} I_6 {}^{E^b A_{12}^\sharp} I_9^2 {}^{E^b A_{12}^\sharp} I_8^{-1} + {}^{E^b A_{12}^\sharp} I_4 {}^{E^b A_{12}^\sharp} I_6^2 \right] \\ & + \gamma_{315} \left[{}^{E^b A_{12}^\sharp} I_4 {}^{E^b A_{12}^\sharp} I_8^{-1/2} {}^{E^b A_{12}^\sharp} I_{\text{red}} + {}^{E^b A_{12}^\sharp} I_5 {}^{E^b A_{12}^\sharp} I_9 \right] \end{aligned} \quad (4.28)$$

$$\begin{aligned}
& + \gamma_{316} \left[E^b A_{12}^\# I_6 E^b A_{12}^\# I_8^{-1/2} E^b A_{12}^\# I_{\text{red}} + E^b A_{12}^\# I_7 E^b A_{12}^\# I_9 \right] \\
& + \gamma_{317} \left[E^b A_{12}^\# I_4 E^b A_{12}^\# I_6 E^b A_{12}^\# I_9 + E^b A_{12}^\# I_9^3 E^b A_{12}^\# I_8^{-1} \right] \\
& + \gamma_{318} \left[E^b A_{12}^\# I_1 E^b A_{12}^\# I_8^{1/2} E^b A_{12}^\# I_{\text{red}} - \frac{1}{2} \left[E^b A_{12}^\# I_1^2 - E^b A_{12}^\# I_2 \right] E^b A_{12}^\# I_9 + 2 \gamma_{\det} E^b A_{12}^\# I_8 \right] \\
& + \gamma_{319} \left[E^b A_{12}^\# I_4 E^b A_{12}^\# I_6 E^b A_{12}^\# I_8 E^b A_{12}^\# I_9 + \frac{1}{3} E^b A_{12}^\# I_9^3 \right].
\end{aligned}$$

The scalar-valued coefficients $\gamma_{3n}(\beta_i)$ are defined by the following formulae

$$\begin{aligned}
\gamma_{30} &= \beta_0^3, & \gamma_{31} &= 3 \beta_0 \beta_1^2, & \gamma_{32} &= \beta_1^3, \\
\gamma_{33} &= 3 \beta_0^2 \beta_1, & \gamma_{34} &= 3 \beta_0 \beta_2^2, & \gamma_{35} &= \beta_2^3, \\
\gamma_{36} &= 3 \beta_1^2 \beta_2, & \gamma_{37} &= 3 \beta_1 \beta_2^2, & \gamma_{38} &= 6 \beta_0 \beta_1 \beta_2, \\
\gamma_{39} &= 3 \beta_0^2 \beta_2, & \gamma_{310} &= 6 \beta_1^2 \beta_3, & \gamma_{311} &= 6 \beta_2^2 \beta_3, \\
\gamma_{312} &= 3 \beta_0 \beta_3^2, & \gamma_{313} &= 3 \beta_1 \beta_3^2, & \gamma_{314} &= 3 \beta_2 \beta_3^2, \\
\gamma_{315} &= 6 \beta_0 \beta_1 \beta_3, & \gamma_{316} &= 6 \beta_0 \beta_2 \beta_3, & \gamma_{317} &= 6 \beta_1 \beta_2 \beta_3, \\
\gamma_{318} &= 6 \beta_0^2 \beta_3, & \gamma_{319} &= 6 \beta_3^3.
\end{aligned} \tag{4.29}$$

So far we have chosen two arbitrary vectors $A_{1,2}^\# \mathbf{N}^\#$ with $\alpha_1 \neq \alpha_2$ in order to keep the relation to the fibre orientations as transparent as possible. In the sequel, emphasis is placed on certain dependencies of these vectors which result e.g. in classical orthotropy or transverse isotropy. Trivially – for vanishing $A_{1,2}^\# \mathbf{N}^\#$ – isotropy is included. Moreover, the energy metric tensor $\mathbf{A}^\#$ is generally symmetric such that it's spectral decomposition can be applied which is pointed out in Section 4.2.8.

Remark 4.4 Please note that $\mathbf{G}^\# : [\mathbf{E}^b \cdot \mathbf{A}_1^\# \cdot \mathbf{E}^b \cdot \mathbf{A}_2^\# \cdot \mathbf{E}^b] \doteq E^b A_{12}^\# I_8^{-1/2} E^b A_{12}^\# I_9 E^b A_{12}^\# I_{\text{red}}$ is not an invariant but reducible. For an outline on the derivation we refer to Spencer [Spe84, Eq.(33)].

4.2.4 Two equivalent fibres

As a special application of constitutive equations that incorporate two structural tensors, we consider the case of two different fibre orientations $A_{1,2}^\# \mathbf{N}^\#$, with identical characteristics, namely $\alpha_2 \doteq \alpha_1$. With respect to Eq.(4.19), the corresponding scalars to compute the energy metric tensor $\mathbf{A}^\#$ read

$$\beta_0 = \alpha_0^2, \quad \beta_1 = 2 \alpha_0 \alpha_1 + \alpha_1^2, \quad \beta_2 = \beta_1, \quad \beta_3 = \alpha_1^2. \tag{4.30}$$

Next, in view of Eq.(4.23) the first invariant $E^b A^\# I_1$ is related to structural tensors via

$$\gamma_{10} = \beta_0, \quad \gamma_{11} = \beta_1, \quad \gamma_{12} = \gamma_{11}, \quad \gamma_{13} = 2 \beta_3. \tag{4.31}$$

Taking Eq.(4.25) into account, we find that the correlated scalars γ_{2n} for two mechanically equivalent fibres are

$$\begin{aligned}
\gamma_{20} &= \beta_0^2, & \gamma_{21} &= 2 \beta_0 \beta_1, & \gamma_{22} &= \beta_1^2, \\
\gamma_{23} &= \gamma_{22}, & \gamma_{24} &= \gamma_{21}, & \gamma_{25} &= \gamma_{21}, \\
\gamma_{26} &= \beta_3^2, & \gamma_{27} &= 4 \beta_1 \beta_3, & \gamma_{28} &= \gamma_{27}, \\
\gamma_{29} &= 4 \beta_0 \beta_3,
\end{aligned} \tag{4.32}$$

and furthermore with respect to Eq.(4.28), the computation of the third invariant ends up with

$$\begin{aligned}
\gamma_{30} &= \beta_0^3, & \gamma_{31} &= 3\beta_0\beta_1^2, & \gamma_{32} &= \beta_1^3, \\
\gamma_{33} &= 3\beta_0^2\beta_1, & \gamma_{34} &= \gamma_{31}, & \gamma_{35} &= \gamma_{32}, \\
\gamma_{36} &= 3\gamma_{32}, & \gamma_{37} &= \gamma_{36}, & \gamma_{38} &= 2\gamma_{31}, \\
\gamma_{39} &= \gamma_{33}, & \gamma_{310} &= 6\beta_1^2\beta_3, & \gamma_{311} &= \gamma_{310}, \\
\gamma_{312} &= 3\beta_0\beta_3^2, & \gamma_{313} &= 3\beta_1\beta_3^2, & \gamma_{314} &= \gamma_{313}, \\
\gamma_{315} &= 6\beta_0\beta_1\beta_3, & \gamma_{316} &= \gamma_{315}, & \gamma_{317} &= \gamma_{310}, \\
\gamma_{318} &= 6\beta_0^2\beta_3, & \gamma_{319} &= 6\beta_3^3.
\end{aligned} \tag{4.33}$$

4.2.5 Two orthogonal fibres

Next, we consider the case of two orthogonal fibres $A_{1,2}^\# \mathbf{N}^\#$ with generally different mechanical characteristics, often denoted as classical orthotropy. This orthogonality assumption results in ${}^{E^b A_{1,2}^\#} I_{8,9} = 0$ and moreover, the energy metric tensor $\mathbf{A}^\#$ can be computed via

$$\beta_0 = \alpha_0^2, \quad \beta_1 = 2\alpha_0\alpha_1 + \alpha_1^2, \quad \beta_2 = 2\alpha_0\alpha_2 + \alpha_2^2, \quad \beta_3 = 0. \tag{4.34}$$

The first basic invariant is characterised by

$$\gamma_{10} = \beta_0, \quad \gamma_{11} = \beta_1, \quad \gamma_{12} = \beta_2 \tag{4.35}$$

and $\gamma_{13} = 0$. The second basic invariant correlates to

$$\begin{aligned}
\gamma_{20} &= \beta_0^2, & \gamma_{21} &= 2\beta_0\beta_1, & \gamma_{22} &= \beta_1^2, \\
\gamma_{23} &= \beta_2^2, & \gamma_{24} &= 2\beta_0\beta_2, & \gamma_{25} &= 2\beta_1\beta_2
\end{aligned} \tag{4.36}$$

and $\gamma_{2[6,\dots,9]} = 0$. Finally, ${}^{E^b A^\#} I_3$ is related to structural tensors via the following equations

$$\begin{aligned}
\gamma_{30} &= \beta_0^3, & \gamma_{31} &= 3\beta_0\beta_1^2, & \gamma_{32} &= \beta_1^3, \\
\gamma_{33} &= 3\beta_0^2\beta_1, & \gamma_{34} &= 3\beta_0\beta_2^2, & \gamma_{35} &= \beta_2^3, \\
\gamma_{36} &= 3\beta_1^2\beta_2, & \gamma_{37} &= 3\beta_1\beta_2^2, & \gamma_{38} &= 6\beta_0\beta_1\beta_2, \\
\gamma_{39} &= 3\beta_0^2\beta_2
\end{aligned} \tag{4.37}$$

and $\gamma_{3[10,\dots,19]} = 0$.

4.2.6 Transverse isotropy

For a transversely isotropic material with only one fibre we obtain ${}^{E^b A_{1,2}^\#} I_{6,\dots,9} = 0$ in terms of structural tensors and the coefficients to compute $\mathbf{A}^\#$ read

$$\beta_0 = \alpha_0^2, \quad \beta_1 = 2\alpha_0\alpha_1 + \alpha_1^2, \quad \beta_2 = 0 \quad \beta_3 = 0. \tag{4.38}$$

These relations render ${}^{E^b A^\#} I_1$ in terms of

$$\gamma_{10} = \beta_0, \quad \gamma_{11} = \beta_1 \tag{4.39}$$

and $\gamma_{1[2,3]} = 0$. The second basic invariant is obtained via

$$\gamma_{20} = \beta_0^2, \quad \gamma_{21} = 2\beta_0\beta_1, \quad \gamma_{22} = \beta_1^2 \tag{4.40}$$

and $\gamma_{2[3,\dots,9]} = 0$. Moreover, exploiting Eq.(4.38) results in

$$\gamma_{30} = \beta_0^3, \quad \gamma_{31} = 3\beta_0\beta_1^2, \quad \gamma_{32} = \beta_1^3, \quad \gamma_{33} = 3\beta_0^2\beta_1 \tag{4.41}$$

and $\gamma_{3[4,\dots,19]} = 0$.

4.2.7 Isotropy

For completeness, we finally consider the case of an isotropic material whereby it is obvious that no structural tensors are taken into account via ${}^{E^b A_{12}^\#} I_{4,\dots,9} = 0$. The computation of the energy metric tensor $\mathbf{A}^\#$ and the isotropic invariants ${}^{E^b A_{12}^\#} I_{1,2,3}$ are defined by the following formulae

$$\gamma_{10} = \beta_0, \quad \gamma_{20} = \beta_0^2, \quad \gamma_{30} = \beta_0^3 \quad (4.42)$$

and $\gamma_{1[1,2,3]} = \gamma_{2[1,\dots,8]} = \gamma_{3[1,\dots,19]} = 0$.

4.2.8 Spectral representation

Since the energy metric tensor $\mathbf{A}^\#$ is of second order, positive definite and symmetric, the appropriate spectral decomposition reads

$$\mathbf{A}^\# = \sum_{i=1}^3 {}^A \lambda_i {}^A \mathbf{N}_i^\# \otimes {}^A \mathbf{N}_i^\# = \eta_0 \mathbf{G}^\# + \eta_1 {}^A \mathbf{N}_1^\# \otimes {}^A \mathbf{N}_1^\# + \eta_2 {}^A \mathbf{N}_2^\# \otimes {}^A \mathbf{N}_2^\# \quad (4.43)$$

with ${}^A \lambda_i \in \mathbb{R}_+$, $\eta_0 = {}^A \lambda_3$, $\eta_1 = {}^A \lambda_1 - {}^A \lambda_3$, $\eta_2 = {}^A \lambda_2 - {}^A \lambda_3$ and ${}^A \mathbf{N}_j^\# \in \mathbb{U}^2 : T^* \mathcal{B}_0 \rightarrow \mathbb{R}$, compare Svendsen [Sve01b]. The relations to classical orthotropy, transverse isotropy and isotropy are self-evident (see Eq.(4.19) or e.g. Negahban and Wineman [NW93] among others), namely

$$\eta_i \doteq \beta_i, \quad \beta_3 = 0 \quad \text{and} \quad {}^A \mathbf{N}_j^\# \otimes {}^A \mathbf{N}_j^\# \doteq \mathbf{A}_j^\# \quad \text{with} \quad i = 0, 1, 2; \quad j = 1, 2. \quad (4.44)$$

For two mechanically equivalent fibres ($\alpha_2 \doteq \alpha_1$) with arbitrary orientations, these representations are not that obvious. Without loss of generality, the following relations between the vectors ${}^{A_{1,2}^\#} \mathbf{N}^\#$ which define the incorporated anisotropy (fibre directions) and the eigenvectors ${}^A \mathbf{N}_j^\#$ hold by taking basic geometrical considerations into account

$$\begin{aligned} {}^A \mathbf{N}_1^\# &= \left[{}^{A_1^\#} \mathbf{N}^\# + {}^{A_2^\#} \mathbf{N}^\# \right] / [2 \cos(\phi)], & {}^{A_1^\#} \mathbf{N}^\# &= \cos(\phi) {}^A \mathbf{N}_1^\# + \sin(\phi) {}^A \mathbf{N}_2^\#, \\ {}^A \mathbf{N}_2^\# &= \left[{}^{A_1^\#} \mathbf{N}^\# - {}^{A_2^\#} \mathbf{N}^\# \right] / [2 \sin(\phi)], & {}^{A_2^\#} \mathbf{N}^\# &= \cos(\phi) {}^A \mathbf{N}_1^\# - \sin(\phi) {}^A \mathbf{N}_2^\#, \end{aligned} \quad (4.45)$$

whereby $2\phi = \arccos({}^{E^b A_{12}^\#} I_8^{1/2})$ denotes the angle between the two fibres – compare Spencer [Spe84]. The underlying idea is based on the fact that ${}^{A_1^\#} \mathbf{N}^\#$ and ${}^{A_2^\#} \mathbf{N}^\#$ have to be interchangeable for two mechanically equivalent fibres and hence ${}^A \mathbf{N}_{1,2}^\#$ denote admissible reflections that allow representation as $\text{ref } \mathbf{R}_{1,2}^\# = \mathbf{G}^\# - 2 {}^A \mathbf{N}_{1,2}^\# \otimes {}^A \mathbf{N}_{1,2}^\#$, compare Eq.(2.19)₁. With these relations at hand, the symmetric part $[\mathbf{A}_1^\# \cdot \mathbf{G}^\# \cdot \mathbf{A}_2^\#]^{\text{sym}}$ of Eq.(4.19) reads

$$[\mathbf{A}_1^\# \cdot \mathbf{G}^\# \cdot \mathbf{A}_2^\#]^{\text{sym}} = \frac{1}{2} \left[2 \cos^2(\phi) {}^A \mathbf{N}_1^\# \otimes {}^A \mathbf{N}_1^\# - 2 \sin^2(\phi) {}^A \mathbf{N}_2^\# \otimes {}^A \mathbf{N}_2^\# \right] \quad (4.46)$$

and the computation of the coefficients $\eta_{0,1,2}$ yields

$$\eta_0 = \alpha_0^2, \quad \eta_1 = 4\alpha_1 [\alpha_0 \cos^2(\phi) + \alpha_1 \cos^4(\phi)], \quad \eta_2 = 4\alpha_1 [\alpha_0 \sin^2(\phi) + \alpha_1 \sin^4(\phi)]. \quad (4.47)$$

Furthermore, based on these modified scalars – which as a matter of fact bring the invariant ${}^{E^b A_{12}^\#} I_8$ into the picture – the standard formulae of classical orthotropy as pointed out in Eqs.(4.35–4.37) can be applied.

Remark 4.5 *A computation based on the proposed (reduced) framework with respect to the fictitious configuration is numerically significantly cheaper than the standard approach in terms of structural tensors as presented in Chapter 2. Eqs.(4.16, 4.13) of the corresponding stress tensors and especially the Hessians in Eqs.(2.52–2.54) and (4.14) underline this fact most impressively. It is our belief that the general structural tensor approach with no further constitutive assumptions results in an almost unmanageable numerical setting, especially within the computation of inelastic materials. On the contrary, the proposed framework based on a fictitious configuration ends up with nearly identical numerical costs compared to standard isotropy.*

Remark 4.6 For geometrically linear anisotropic elasticity based on structural tensors, transverse isotropy and orthotropy contain five and nine independent material parameters, respectively. On the contrary, the formulation based on the fictitious configuration incorporates three independent material parameters in the case of a transversely isotropic material and four independent parameters for orthotropy (thereby the two Lamé constants are taken into account, and thus the additional isotropic parameter α_0 is not independent). This underlines that we deal with a reduced formulation. For the sake of clarity, we consider, e.g., a linear elastic material of St.-Venant Kirchhoff type, $\psi_0^0(\mathbf{E}^b, \mathbf{A}^\sharp; \mathbf{X}) = \lambda/2 {}^{EbA^\sharp}I_1^2 + \mu {}^{EbA^\sharp}I_2$, which results in the following tangent operator

$$\mathbf{E}^\sharp = \partial_{\mathbf{E}^b \otimes \mathbf{E}^b}^2 \psi_0^0 = \lambda \mathbf{A}^\sharp \otimes \mathbf{A}^\sharp + \mu [\mathbf{A}^\sharp \overline{\otimes} \mathbf{A}^\sharp + \mathbf{A}^\sharp \underline{\otimes} \mathbf{A}^\sharp]. \quad (4.48)$$

Now, referring to a Cartesian frame we choose in view of Eq.(4.43) or Eq.(4.19), respectively, the specific case of $\mathbf{A} \doteq \eta_0 \mathbf{I} + \eta_1 \mathbf{e}_1 \otimes \mathbf{e}_1 + \eta_2 \mathbf{e}_2 \otimes \mathbf{e}_2$ (with \mathbf{I} representing the second order identity and \mathbf{e}_i obviously denoting the principal axis of \mathbf{A}). Based on Voigt's notation, the coefficients of the Hessian read

$$\text{voi} \mathbf{E}_{ij} = \begin{bmatrix} \mathbf{E}_1 & \mathbf{E}_2 & \mathbf{E}_3 & 0 & 0 & 0 \\ \mathbf{E}_2 & \mathbf{E}_4 & \mathbf{E}_5 & 0 & 0 & 0 \\ \mathbf{E}_3 & \mathbf{E}_5 & \mathbf{E}_6 & 0 & 0 & 0 \\ 0 & 0 & 0 & \mathbf{E}_7 & 0 & 0 \\ 0 & 0 & 0 & 0 & \mathbf{E}_8 & 0 \\ 0 & 0 & 0 & 0 & 0 & \mathbf{E}_9 \end{bmatrix} \quad (4.49)$$

whereby $\mathbf{E}_{1,\dots,9}$ are not entirely independent but are defined via four (independent) material parameters

$$\begin{aligned} \mathbf{E}_1 &= [\lambda + 2\mu][\eta_0 + \eta_1]^2, & \mathbf{E}_2 &= \lambda[\eta_0 + \eta_1] + 2\mu[\eta_0 + \eta_2], & \mathbf{E}_3 &= \lambda\eta_0[\eta_0 + \eta_1], \\ \mathbf{E}_4 &= [\lambda + 2\mu][\eta_0 + \eta_2]^2, & \mathbf{E}_5 &= \lambda\eta_0[\eta_0 + \eta_2], & \mathbf{E}_6 &= [\lambda + 2\mu]\eta_0^2, \\ \mathbf{E}_7 &= \mu[\eta_0 + \eta_1][\eta_0 + \eta_2], & \mathbf{E}_8 &= \mu\eta_0[\eta_0 + \eta_2], & \mathbf{E}_9 &= \mu\eta_0[\eta_0 + \eta_1]. \end{aligned} \quad (4.50)$$

We obviously deal with a sub-class of rhombic symmetry – compare e.g. Haupt [Hau00, Sect. 9.3.2], Şuhubi [Şuh75, Sect. 2.15.1] or Love [Lov44, Sect. 109] – and the corresponding symmetry group reads $\mathbb{G} = \{\pm \mathbf{I}, {}^{\text{ref}}\mathbf{R}(\mathbf{e}_1), {}^{\text{ref}}\mathbf{R}(\mathbf{e}_2)\}$, compare Eq.(2.19). Nevertheless, the general linear constitutive equation $\psi_0^0(\mathbf{E}, \mathbf{A}_{1,2}; \mathbf{X})$ incorporating two orthogonal fibres in terms of structural tensors

$$\begin{aligned} \psi_0^0 &= \frac{\lambda}{2} {}^{EA_{12}}I_1^2 + \mu {}^{EA_{12}}I_2 + [\delta_1 {}^{EA_{12}}I_4 + \delta_2 {}^{EA_{12}}I_6] {}^{EA_{12}}I_1 \\ &+ 2\mu_1 {}^{EA_{12}}I_5 + 2\mu_2 {}^{EA_{12}}I_7 + \frac{\delta_3}{2} {}^{EA_{12}}I_4^2 + \frac{\delta_4}{2} {}^{EA_{12}}I_6^2 + \delta_5 {}^{EA_{12}}I_4 {}^{EA}I_6, \end{aligned} \quad (4.51)$$

as given e.g. by Spencer [Spe84], results with respect to a Cartesian frame and $\mathbf{A}_i \doteq \mathbf{e}_j \otimes \mathbf{e}_j$, for $j = 1, 2$ in

$$\begin{aligned} \mathbf{E}_1 &= \lambda + 2\delta_1 + \delta_3 + 2\mu + 4\mu_1, & \mathbf{E}_2 &= \lambda + \delta_1 + \delta_2 + \delta_5, & \mathbf{E}_3 &= \lambda + \delta_1, \\ \mathbf{E}_4 &= \lambda + 2\delta_2 + \delta_4 + 2\mu + 4\mu_2, & \mathbf{E}_5 &= \lambda + \delta_2, & \mathbf{E}_6 &= \lambda + 2\mu, \\ \mathbf{E}_7 &= 2[\mu + \mu_2], & \mathbf{E}_8 &= 2[\mu + \mu_1], & \mathbf{E}_9 &= 2[\mu + \mu_1 + \mu_2], \end{aligned} \quad (4.52)$$

whereby nine independent material parameters are incorporated. Thus, the coefficients $\mathbf{E}_{1,\dots,9}$ within the framework of a fictitious configuration represent a specific reduced form but with identical symmetry properties. The derivation of the corresponding relations for transversal isotropy is straightforward. Recall that the determination of the formulation based on the fictitious configuration in terms of structural tensors is always possible while the opposite does not hold. Moreover, the proposed framework allows representation as a specific application of the introduction of a (rank three) fabric tensor as e.g. outlined by Cowin [Cow85] and Zysset and Curnier [ZC95].

4.3 Numerical examples

To discuss the implications of anisotropic material behaviour, we first point out an example of a homogeneous deformation in simple shear. Three-dimensional finite element computations subsequently

underline the applicability and the numerical efficiency of the proposed anisotropic framework. A non-linear constitutive equation of Kauderer-type is thereby incorporated

$$\mathbf{S}^\sharp \doteq \left[3K \text{ sph } \kappa - \frac{2}{3} G \text{ dev } \kappa \right] \mathbf{E}^b \mathbf{A}^\sharp + 2G \text{ dev } \kappa \mathbf{A}^\sharp \cdot \mathbf{E}^b \cdot \mathbf{A}^\sharp, \quad (4.53)$$

as highlighted in Eq.(C.8) and the material parameters are chosen as: $K = 8.3333 \times 10^4$, $G = 3.8461 \times 10^4$, $\text{ sph } \kappa_1 = \text{ dev } \kappa_2 = 0.5$ and $\text{ sph } \kappa_2 = \text{ dev } \kappa_4 = 0.25$. The energy metric tensor is constructed by two unit vectors which we define via the following spherical coordinates $\vartheta_1^1 = 5/6 \pi$, $\vartheta_1^2 = 1/6 \pi$, $\vartheta_2^1 = 1/3 \pi$, $\vartheta_2^2 = 1/2 \pi$, compare Figure D.12. Moreover, the corresponding scalars are set to $\alpha_0 = 1.0$, $\alpha_1 = 0.25$ and $\alpha_2 = 0.5$. In order to visualise the effects of the underlying anisotropy, we apply the anisotropy measure δ , the method of stereo-graphic projection and the determinant of the acoustic tensor, compare Appendix D.

4.3.1 Simple shear

In the sequel, we consider a homogeneous deformation in simple shear. Hence, referring to a Cartesian frame, the deformation gradient reads $\mathbf{F} = \mathbf{I} + \gamma \mathbf{e}_1 \otimes \mathbf{e}_2$ with $\mathbf{I} = \delta_j^i \mathbf{e}_i \otimes \mathbf{e}^j$ characterising the second order identity. The non-coaxiality of the strain metric tensor and the stress tensor is monitored for three different shear numbers γ by the stereo-graphic projection and highlighted in Figure 4.2.

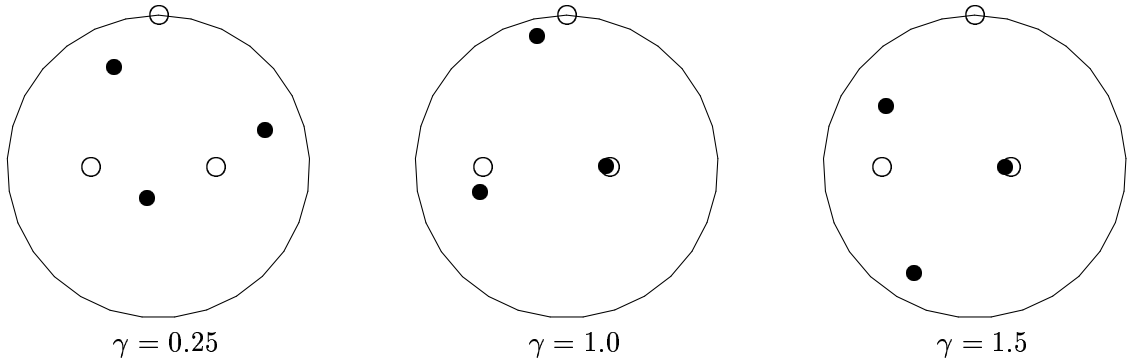


Figure 4.2: Simple shear: Stereo-graphic projection due to the principal directions of strain \mathbf{E}^b : \circ and stress \mathbf{S}^\sharp : \bullet for different shear numbers γ .

Next, as a measure of the degree of anisotropy we compute the scalar-valued quantity $\delta(\mathbf{E}^b, \mathbf{S}^\sharp)$, see Appendix D.1. Figure 4.3 monitors that this anisotropy measure shows a strong dependence on the shear number γ .

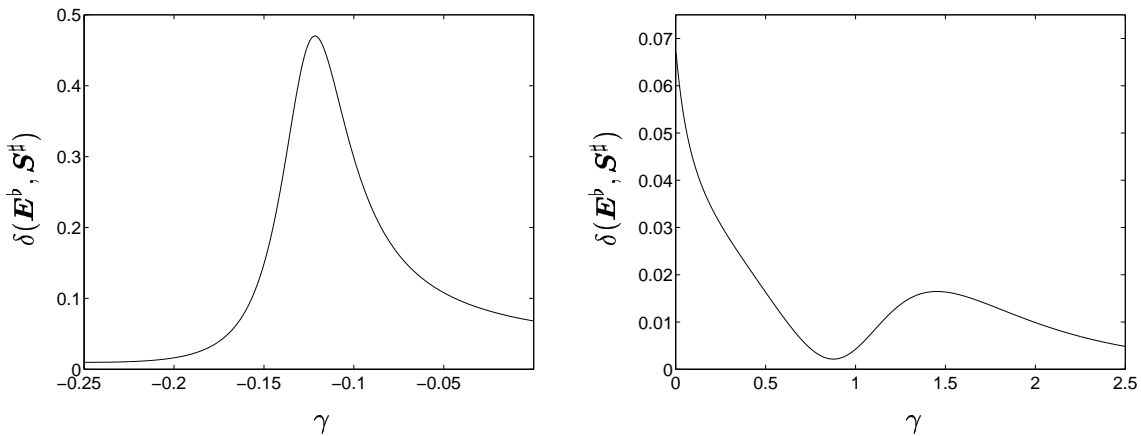


Figure 4.3: Simple shear: Anisotropy measure $\delta(\mathbf{E}^b, \mathbf{S}^\sharp)$ for $\gamma \in [-0.25, 0.0]$ (left) and $\gamma \in [0.0, 2.5]$ (right).

Finally, the acoustic tensor \mathbf{q}^\sharp within the proposed anisotropic framework based on the fictitious configuration is discussed, see Appendix D.3 for a short reminder on the underlying theory. Within

an isotropic linear elastic St. Venant–Kirchhoff material, the determinant of the acoustic tensor turns out to be independent of the wave propagation direction and hence persists constant. In particular one obtains

$$\det(\mathbf{q}^\sharp)^{\text{lin,iso}} = G^2 \left[\frac{3}{4} G + K \right], \quad (4.54)$$

see e.g. Marsden and Hughes [MH94, Sect. 4.3]. Nevertheless, in the context of non-linear hyper-elasticity at large strain kinematics, $\det(\mathbf{q}^\sharp)$ remains no longer constant. Figure 4.4 highlights this dependence on the wave propagation direction $\mathbf{n}^b \in \mathbb{U}^2 : T\mathcal{B}_t \rightarrow \mathbb{R}$ at $\gamma = 0.25$ for the anisotropic case with $\alpha_1 = 0.25$, $\alpha_2 = 0.5$ ($\det(\mathbf{q}^\sharp)^{\text{ani}}$) and the isotropic setting based on $\alpha_1 = \alpha_2 = 0.0$ ($\det(\mathbf{q}^\sharp)^{\text{iso}}$). Thereby, the spherical coordinates $\vartheta^{1,2}$ define the wave propagation direction, compare Figure D.12.

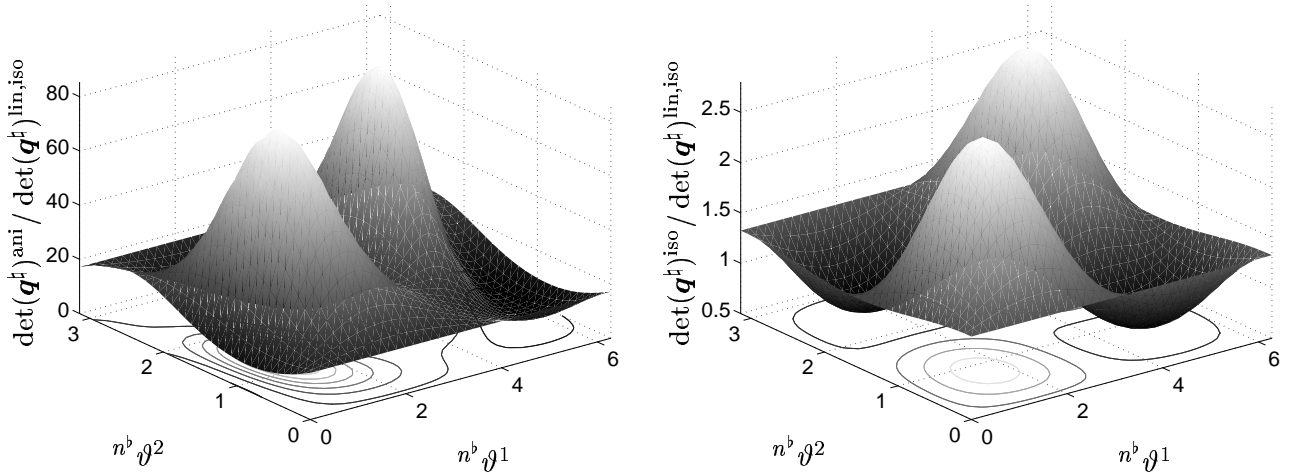


Figure 4.4: Simple shear: Determinant of the acoustic tensor \mathbf{q}^\sharp at $\gamma = 0.25$; anisotropic setting (left) and isotropic setting (right).

4.3.2 Cook's problem

For this finite element example, we investigate a three dimensional version of the classical two dimensional Cook's membrane problem (in analogy to Section 2.4.2.2). Thus, the standard discretisation in the $\mathbf{e}_{1,2}$ plane, is extended into the \mathbf{e}_3 direction. The geometry as well as the boundary and loading conditions are visualised in Figure 4.5 whereby the following parameters are chosen: $L = 48$, $H_1 = 44$, $H_2 = 16$, $T = 4$. The discretisation consists of $16 \times 16 \times 4$ eight node bricks and invokes enhanced elements (Q1E9) as advocated by Simo and Armero [SA92]. Recall, that the conservative force \mathbf{F} is considered as the resultant of a continuous shear stress with respect to the undeformed reference geometry.

Since the axes $A^\sharp \mathbf{N}_{1,2}$, which characterise the incorporated anisotropy, do not lie in the $\mathbf{e}_{1,2}$ plane we consequently observe a severe out-of-plane deformation. Figures 4.5 and 4.6 show the deformed mesh for $\|\mathbf{F}\| = 1.28 \times 10^5$. Furthermore, we study the displacement of the mid point node at the top corner, ${}^{\text{top}}\mathbf{u}$, which is highlighted in Figure 4.7. In order to compare these results to an isotropic setting incorporating a spherical energy metric tensor ${}^{\text{sph}}\mathbf{A}^\sharp$ we demand

$${}^{\text{sph}}\mathbf{A}^\sharp = {}^{\text{sph}}\alpha_0 \mathbf{G}^\sharp \quad \text{with} \quad \|{}^{\text{sph}}\mathbf{A}^\sharp\| \doteq \|\mathbf{A}^\sharp\|. \quad (4.55)$$

Based on Eq.(4.34), this evident assumption renders

$${}^{\text{sph}}\alpha_0 = \left[\beta_0^2 + [\beta_0 + \beta_1]^2 + [\beta_0 + \beta_2]^2 \right]^{1/2}, \quad (4.56)$$

with $\beta_0 = \alpha_0$, $\beta_1 = 2\alpha_0\alpha_1 + \alpha_1^2$, $\beta_2 = 2\alpha_0\alpha_2 + \alpha_2^2$. Figure 4.8 monitors the corresponding displacement curves of the mid point node at the top corner, which are obviously within the same range as those of the anisotropic setting. We additionally highlight the results of a computation based on standard tri-linear eight node bricks (Q1), which show a stiffer behaviour compared to the previous computation with enhanced elements (Q1E9). Table 4.1 summarises the convergence of the computations within these three different settings. Thereby the residual norm of the corresponding Newton iteration steps are tabulated for the rather large load step $\|\mathbf{F}\| : [0, 5.12 \times 10^4]$.

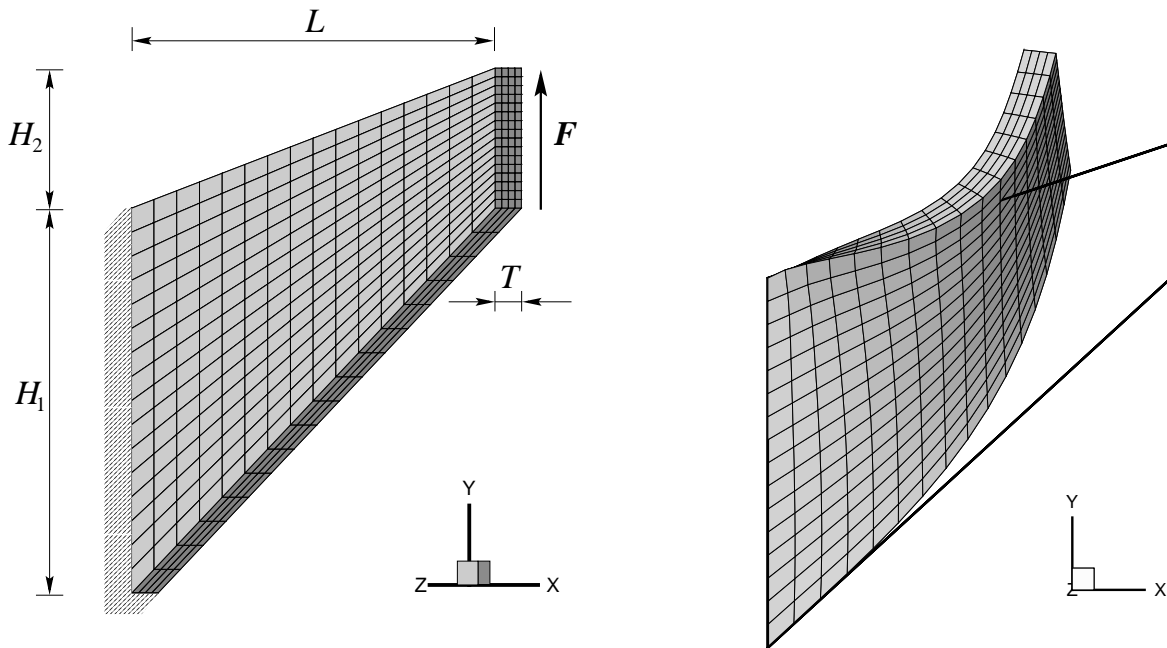


Figure 4.5: Cook's problem: Anisotropic (Q1E9); geometry, boundary and loading conditions, discretisation with $16 \times 16 \times 4$ eight node bricks (left) and deformed mesh at $\|\mathbf{F}\| = 1.28 \times 10^5$.

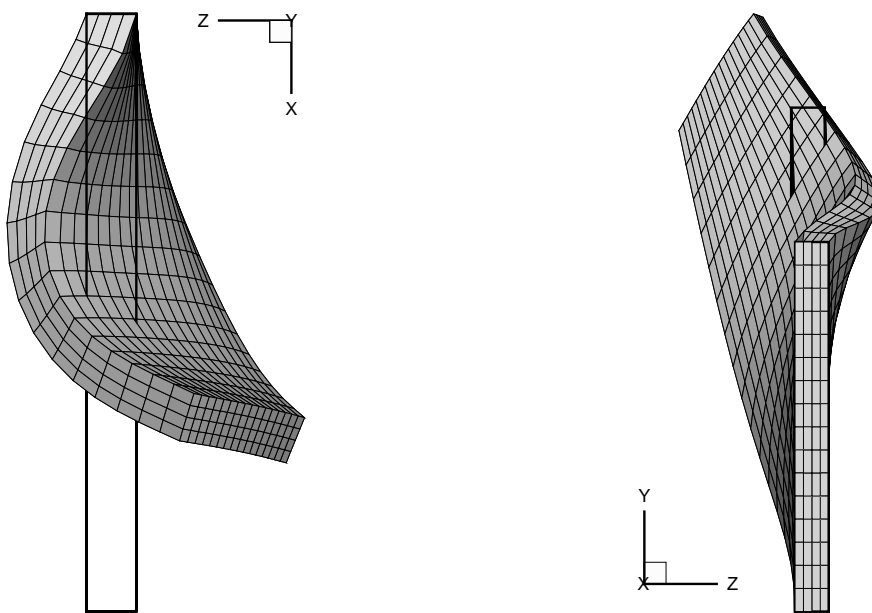


Figure 4.6: Cook's problem: Anisotropic (Q1E9); different views on the deformed mesh at $\|\mathbf{F}\| = 1.28 \times 10^5$.

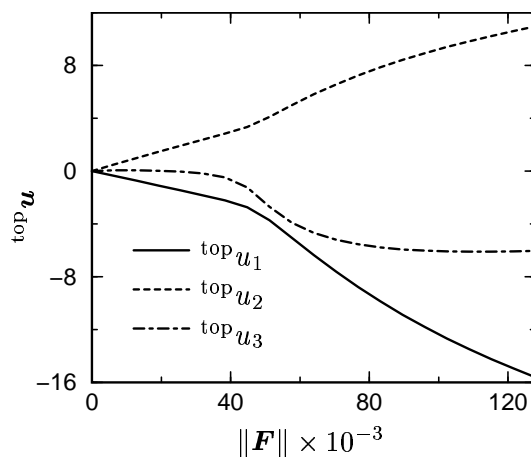


Figure 4.7: Cook's problem: Anisotropic (Q1E9); displacement curves of the mid point node at the top corner.

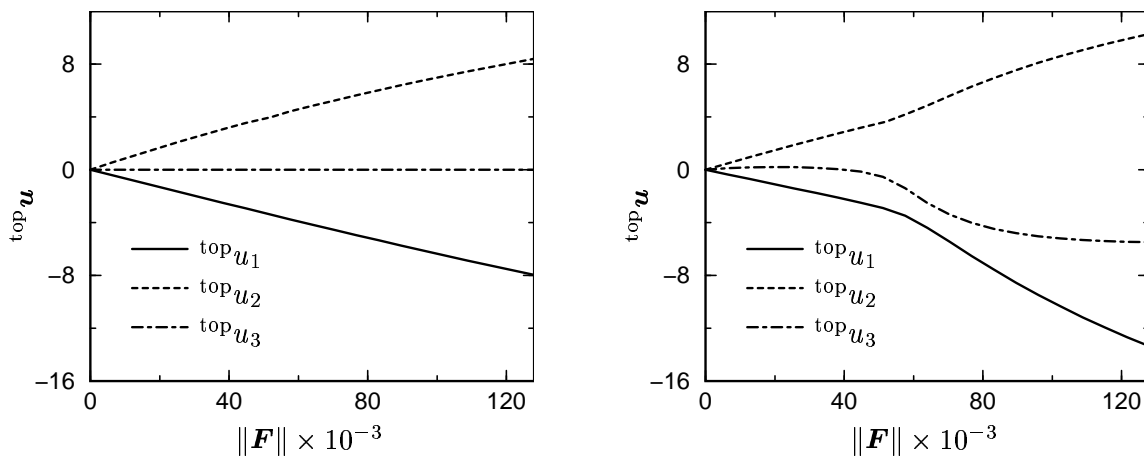



Figure 4.8: Cook's problem: Load-displacement curves of the mid point node at the top corner; isotropic setting (Q1E9, left) and anisotropic setting (Q1, right).

Table 4.1: Cook's problem: Residual norm for the load step $\|\mathbf{F}\| : [0, 5.12 \times 10^4]$.

Q1E9, anisotropic		Q1E9, isotropic		Q1, anisotropic	
no.	$\ \mathbf{R}\ $	no.	$\ \mathbf{R}\ $	no.	$\ \mathbf{R}\ $
1	$2.35695 E + 04$	1	$2.35695 E + 04$	1	$2.35695 E + 04$
2	$1.70059 E + 05$	2	$2.35936 E + 05$	2	$1.57264 E + 05$
3	$3.71217 E + 03$	3	$5.65492 E + 03$	3	$3.81568 E + 03$
4	$2.59480 E + 06$	4	$1.24521 E + 02$	4	$6.76394 E + 04$
5	$1.16144 E + 04$	5	$5.51955 E - 02$	5	$7.16359 E + 03$
6	$1.32396 E + 04$	6	$1.89174 E - 08$	6	$5.46791 E + 00$
7	$3.76553 E + 03$			7	$1.47482 E + 00$
8	$3.93106 E + 03$			8	$3.25775 E - 07$
9	$4.76101 E + 02$			9	$1.95022 E - 08$
10	$1.17589 E + 02$				
11	$5.68824 E - 01$				
12	$1.48105 E - 04$				
13	$1.02527 E - 08$				

Chapter 5

Anisotropic damage based on a fictitious configuration

er große deutsche Mathematiker Kronecker sagte über die Mathematik: Die natürlichen Zahlen sind von Gott geschaffen; alles andere ist Menschenwerk. Im Gegensatz dazu sage ich: Die natürlichen Zahlen sind Menschenwerk, sie sind ein Nebenprodukt der menschlichen Sprache, der Erfindung des Zählens und des Weiterzählens. Das Addieren ist auch eine menschliche Erfindung, und ebenso das Multiplizieren.

Sir Karl Raimund Popper [1902 – 1994]
Vorlesung in Mannheim, 08.05.1972

To capture the anisotropic nature of damage within a phenomenological model, one has at least to introduce a second order internal variable, see e.g. Leckie and Onat [LO81]. Hence, the main goal of this Chapter is the development of a framework for geometrically non-linear, anisotropic, tensorial second order continuum damage whereby, depending on the corresponding rate equations, the categories of quasi isotropic and anisotropic damage evolution are classified.

We enlarge the framework highlighted in Chapter 4 in particular to tensorial second order continuum damage whereby the incorporated fictitious, isotropic configuration is assumed to represent the undamaged material. Conceptually speaking, the fictitious, undamaged, microscopic configuration corresponds to the effective space of the classical, isotropic $[1 - D]$ damage theory which is supplemented to the damaged, macroscopic, undeformed and deformed configurations. In contrast to the classical approaches of Betten [Bet82a] and Murakami [Mur88], the present damage theory, is based on the notion of a second order damage metric tensor. The framework of generalised standard dissipative materials is strictly applied. This approach consequently leads to the introduction of an admissible domain, the postulate of maximum dissipation and associated evolution equations. For the general anisotropic case, these rate equations represent a reduced set compared to a general tensor-valued tensor function in terms of e.g. the strain metric and internal variables, see e.g. Betten [Bet85] and the reiteration in Appendix B.3.

Concerning the numerical integration of the evolution equations with respect to multi-stage Runge-Kutta methods, two different categories of algorithms are classified. Namely, within the first category, only the actual configuration is forced to remain in the admissible domain whereby the second category additionally demands the algorithmic intermediate stages to satisfy this constraint. The algorithmic treatment is straightforward and several implicit and explicit Runge-Kutta algorithms of different order are outlined.

The Chapter is organised as follows: Based on Chapters 3 and 4, Section 5.1 reiterates the application of the Coleman–Noll entropy principle in the present context. The framework of generalised standard dissipative materials is subsequently highlighted in Section 5.2. Finally, after the introduction of appropriate integration algorithms in Section 5.3, we give several numerical examples, Section 5.4.

5.1 Coleman–Noll entropy principle

Similar to the outline in Section 3.3 on the Coleman–Noll entropy principle as represented by the Clausius–Duhem inequality, we now focus on the Lagrangian setting in the following. Furthermore, an additional internal, scalar-valued hardening variable κ is introduced for completeness and an additive split of the free Helmholtz energy density ψ_0^0 of the form

$$\boxed{\psi_0^0(\mathbf{E}^b, \mathbf{A}^\sharp, \kappa; \mathbf{X}) \doteq \text{dam}\psi_0^0(\mathbf{E}^b, \mathbf{A}^\sharp; \mathbf{X}) + \text{har}\psi_0(\kappa; \mathbf{X})} \quad (5.1)$$

is assumed, compare footnote † on page 87. Thereby, based on the concept of a fictitious configuration, the symmetric, positive definite second order tensor \mathbf{A}^\sharp replaces the contra-variant metric tensor \mathbf{G}^\sharp and represents an internal variable which will be denoted as damage metric tensor in the sequel. The local format of the dissipation inequality in \mathcal{B}_0 for an isothermal processes consequently reads as

$$\mathcal{D}_0^0 = \mathbf{S}^\sharp : \text{D}_t \mathbf{E}^b - \text{D}_t \psi_0^0 = \left[\mathbf{S}^\sharp - \partial_{\mathbf{E}^b} \psi_0^0 \right] : \text{D}_t \mathbf{E}^b - \partial_{\mathbf{A}^\sharp} \psi_0^0 : \text{D}_t \mathbf{A}^\sharp - \partial_\kappa \psi_0^0 \text{D}_t \kappa \geq 0. \quad (5.2)$$

Following the common argumentation of rational thermodynamics, being that for a purely elastic, non-dissipative motion the constitutive equation is defined via $[\mathbf{S}^\sharp - \partial_{\mathbf{E}^b} \psi_0^0] : \text{D}_t \mathbf{E}^b \doteq 0 \forall \text{D}_t \mathbf{E}^b$, we obtain reasonable definitions for the hyper-elastic second Piola–Kirchhoff stress tensor \mathbf{S}^\sharp , a co-variant damage stress tensor $\mathbf{Z}^b \in \mathbb{S}^3 : T\mathcal{B}_0 \times T\mathcal{B}_0 \rightarrow \mathbb{R}$ and a scalar-valued hardening stress $h \in \mathbb{R}$

$$\boxed{\mathbf{S}^\sharp = \partial_{\mathbf{E}^b} \psi_0^0, \quad \mathbf{Z}^b = -\partial_{\mathbf{A}^\sharp} \psi_0^0, \quad h = -\partial_\kappa \psi_0^0.} \quad (5.3)$$

Based on this, application of the introduced stress fields to the pointwise isothermal Clausius–Duhem inequality (5.2) results in the reduced format

$$\text{red}\mathcal{D}_0^0 = \mathbf{Z}^b : \text{D}_t \mathbf{A}^\sharp + h \text{D}_t \kappa \geq 0. \quad (5.4)$$

Moreover, following the standard scheme, a convex dissipation surface ${}^{\text{vie}}\Phi$ is introduced which defines an admissible domain \mathbb{A} where no damage evolution or hardening takes place

$$\boxed{\mathbb{A}^0 = \left\{ (\mathbf{Z}^b, h; \mathbf{X}) \mid {}^{\text{vie}}\Phi^0 = {}^{\text{vie}}\Phi^0(\mathbf{Z}^b, h; \mathbf{A}^\sharp, \mathbf{X}) \doteq \text{dam}\Phi^0(\mathbf{Z}^b; \mathbf{A}^\sharp, \mathbf{X}) + \text{har}\Phi(h; \mathbf{X}) \leq 0 \right\}} \quad (5.5)$$

with $\text{dam}\Phi^0(\mathbf{Z}^b; \mathbf{A}^\sharp, \mathbf{X})$ representing the damage potential and $\text{har}\Phi(h; \mathbf{X}) \doteq h(\kappa; \mathbf{X}) - Y_0$ whereby Y_0 denotes a constant threshold and $\text{har}\Phi$ is known as equivalent stress. Next, the postulate of maximum dissipation renders associated evolution equations

$$\boxed{\text{D}_t \mathbf{A}^\sharp \doteq \text{D}_t \lambda \partial_{\mathbf{Z}^b} {}^{\text{vie}}\Phi^0 = \text{D}_t \lambda \partial_{\mathbf{Z}^b} \text{dam}\Phi^0, \quad \text{D}_t \kappa = \text{D}_t \lambda \partial_h {}^{\text{vie}}\Phi^0 = \text{D}_t \lambda \partial_h \text{har}\Phi = \text{D}_t \lambda.} \quad (5.6)$$

Here $\text{D}_t \lambda$ denotes the Lagrange multiplier and the Kuhn–Tucker conditions completed by the consistency condition read

$$\text{D}_t \lambda \geq 0, \quad {}^{\text{vie}}\Phi^0 \leq 0, \quad \text{D}_t \lambda {}^{\text{vie}}\Phi^0 = 0, \quad \text{D}_t \lambda \text{D}_t {}^{\text{vie}}\Phi^0 = 0. \quad (5.7)$$

For notational convenience, the (relevant) second order derivatives of the free Helmholtz energy density ψ_0^0 are abbreviated by

$$\begin{aligned} \mathbf{E}^\sharp &= \partial_{\mathbf{E}^b \otimes \mathbf{E}^b}^2 \psi_0^0 \in \mathbb{S}^{3 \times 3} : T^* \mathcal{B}_0 \times T^* \mathcal{B}_0 \times T^* \mathcal{B}_0 \times T^* \mathcal{B}_0 \rightarrow \mathbb{R}, \\ \mathbf{A}^b &= \partial_{\mathbf{A}^\sharp \otimes \mathbf{A}^\sharp}^2 \psi_0^0 \in \mathbb{S}^{3 \times 3} : T\mathcal{B}_0 \times T\mathcal{B}_0 \times T\mathcal{B}_0 \times T\mathcal{B}_0 \rightarrow \mathbb{R}, \\ \mathbf{B}^\sharp &= \partial_{\mathbf{A}^\sharp \otimes \mathbf{E}^b}^2 \psi_0^0 \in \mathbb{S}^{3 \times 3} : T\mathcal{B}_0 \times T\mathcal{B}_0 \times T^* \mathcal{B}_0 \times T^* \mathcal{B}_0 \rightarrow \mathbb{R}, \\ \mathbf{C}^\sharp &= \partial_{\mathbf{E}^b \otimes \mathbf{A}^\sharp}^2 \psi_0^0 \in \mathbb{S}^{3 \times 3} : T^* \mathcal{B}_0 \times T^* \mathcal{B}_0 \times T\mathcal{B}_0 \times T\mathcal{B}_0 \rightarrow \mathbb{R}, \\ k &= \partial_{\kappa \kappa}^2 \psi_0^0 \in \mathbb{R}, \end{aligned} \quad (5.8)$$

with $\mathbf{C}^\sharp = [\mathbf{B}^\sharp]^\top$ being obvious, compare Appendix A.1. Next, based on the consistency condition, the Lagrange multiplier $D_t \lambda$ allows the following representation for an inelastic process

$$D_t \lambda = \frac{\partial_{\mathbf{Z}^b} \text{yie} \Phi^0 : \mathbf{B}^\sharp : D_t \mathbf{E}^b}{\left[\partial_{\mathbf{A}^\sharp} \text{yie} \Phi^0 - \partial_{\mathbf{Z}^b} \text{yie} \Phi^0 : \mathbf{A}^b \right] : \partial_{\mathbf{Z}^b} \text{yie} \Phi^0 - k}. \quad (5.9)$$

Ultimately, the material time derivatives of the hyper-elastic second Piola–Kirchhoff stress tensor $D_t \mathbf{S}^\sharp$ and the Green–Lagrange strain tensor $D_t \mathbf{E}^b$ are combined by a symmetric fourth order tensor which is denoted as $\text{ine} \mathbf{E}^\sharp \in \mathbb{S}^{3 \times 3} : T^* \mathcal{B}_0 \times T^* \mathcal{B}_0 \times T^* \mathcal{B}_0 \times T^* \mathcal{B}_0 \rightarrow \mathbb{R}$ (continuum tangent stiffness), in detail

$$D_t \mathbf{S}^\sharp = \text{ine} \mathbf{E}^\sharp : D_t \mathbf{E}^b \quad \text{with} \quad \text{ine} \mathbf{E}^\sharp = \mathbf{E}^\sharp - \frac{[\mathbf{C}^\sharp : \partial_{\mathbf{Z}^b} \text{yie} \Phi^0] \otimes [\partial_{\mathbf{Z}^b} \text{yie} \Phi^0 : \mathbf{B}^\sharp]}{\left[\partial_{\mathbf{Z}^b} \text{yie} \Phi^0 : \mathbf{A}^b - \partial_{\mathbf{A}^\sharp} \text{yie} \Phi^0 \right] : \partial_{\mathbf{Z}^b} \text{yie} \Phi^0 + k}. \quad (5.10)$$

Standard pull-back and push-forward operations applied to the second order stress tensors again render

$$\begin{aligned} \bar{\mathbf{f}}_\star \mathbf{S}^\sharp &= \bar{\mathbf{f}}^\sharp \cdot \mathbf{S}^\sharp \cdot [\bar{\mathbf{f}}^\sharp]^\top = \bar{\mathbf{S}}^\sharp \in \mathbb{S}^3 : T^* \bar{\mathcal{B}}_0 \times T^* \bar{\mathcal{B}}_0 \rightarrow \mathbb{R}, \\ \bar{\mathbf{F}}^\star \mathbf{Z}^b &= [\bar{\mathbf{F}}^\sharp]^\top \cdot \mathbf{Z}^b \cdot \bar{\mathbf{F}}^\sharp = \bar{\mathbf{Z}}^b \in \mathbb{S}^3 : T \bar{\mathcal{B}}_0 \times T \bar{\mathcal{B}}_0 \rightarrow \mathbb{R}, \end{aligned} \quad (5.11)$$

whereby $\bar{\mathbf{S}}^\sharp$ and $\bar{\mathbf{Z}}^b$ allow interpretation as effective stress fields, see footnote ** on page 27 Appendix C.3 for a reminder on homogenisation concepts in the context of isotropic continuum damage mechanics. Moreover, the set of invariants due to Eq.(4.12) defines the tensorial stresses in Eq.(5.3) and straightforward computations in analogy to Eq.(4.13) yield

$$\boxed{\begin{aligned} \mathbf{S}^\sharp &= \partial_{E^b A^\sharp I_1} \psi_0^0 \mathbf{A}^\sharp + 2 \partial_{E^b A^\sharp I_2} \psi_0^0 \mathbf{A}^\sharp \cdot \mathbf{E}^b \cdot \mathbf{A}^\sharp + 3 \partial_{E^b A^\sharp I_3} \psi_0^0 \mathbf{A}^\sharp \cdot \mathbf{E}^b \cdot \mathbf{A}^\sharp \cdot \mathbf{E}^b \cdot \mathbf{A}^\sharp, \\ -\mathbf{Z}^b &= \partial_{E^b A^\sharp I_1} \psi_0^0 \mathbf{E}^b + 2 \partial_{E^b A^\sharp I_2} \psi_0^0 \mathbf{E}^b \cdot \mathbf{A}^\sharp \cdot \mathbf{E}^b + 3 \partial_{E^b A^\sharp I_3} \psi_0^0 \mathbf{E}^b \cdot \mathbf{A}^\sharp \cdot \mathbf{E}^b \cdot \mathbf{A}^\sharp \cdot \mathbf{E}^b. \end{aligned}} \quad (5.12)$$

Remark 5.1 Note that for the general case, when \mathbf{A}^\sharp is a non-spherical tensor, the introduced stresses \mathbf{S}^\sharp and \mathbf{Z}^b in Eq.(5.3) do not commute with respect to their conjugate variables \mathbf{E}^b and \mathbf{A}^\sharp .

Remark 5.2 Since the damage metric tensor \mathbf{A}^\sharp is determined by the fictitious stretch field, one could assume the rotational part of $\bar{\mathbf{F}}^\sharp$ to be constant. Then, with this reduced mapping at hand, it is obvious that standard, not necessarily isotropic, damage formulations can conveniently be applied in $\bar{\mathcal{B}}$, compare Section 6.4.3.1 in regard to the coupling with plasticity or the contributions by Carol et al. [CRW01] where emphasis is placed on small strain continuum damage.

5.2 Generalised standard dissipative materials

Referring to the theory of generalised standard dissipative materials, as introduced by Halphen and Nguyen [HN75] – compare footnote * on page 53, the construction of rate equations for the internal variables is highlighted in the following, whereby the hardening stress $h(\kappa; \mathbf{X})$ and thus $\text{har} \Phi$ are assumed to remain constant throughout this Chapter without loss of generality (the case $\text{har} \Phi \neq \text{const}$ is discussed in Chapter 6).

Based on this, the existence of a damage potential $\text{dam} \Phi$ within an associated setting is adopted which represents a reduced ansatz compared to a general tensor-valued tensor function to compute the rate $D_t \mathbf{A}^\sharp$ in terms of the damage stress \mathbf{Z}^b and the damage metric itself \mathbf{A}^\sharp , see Appendix B.3 where the general canonical form of the evolution equation is reiterated.

In this direction, the overall representation of the damage potential $\text{dam} \Phi^0 = \text{dam} \Phi^0(\mathbf{Z}^b; \mathbf{A}^\sharp, \mathbf{X})$ is of course based on the set of ten invariants, say $Z^b A^\sharp I_{1, \dots, 10}^{\text{gen}}$ similar to Table 3.2, which renders the (re-

stricted format of an) associated evolution equation

$$\begin{aligned}
D_t \mathbf{A}^\sharp &\doteq D_t \lambda \partial_{\mathbf{Z}^b} \text{dam} \Phi^0 \left(Z^b A^\sharp I_{1,\dots,10}^{\text{gen}}; \mathbf{X} \right) = D_t \lambda \sum_{i=1}^{10} \partial_{Z^b A^\sharp I_i^{\text{gen}}} \text{dam} \Phi^0 \partial_{\mathbf{Z}^b} Z^b A^\sharp I_i^{\text{gen}} \\
&= D_t \lambda \left[\begin{aligned} &\partial_{Z^b A^\sharp I_1^{\text{gen}}} \text{dam} \Phi^0 \mathbf{G}^\sharp + 2 \partial_{Z^b A^\sharp I_2^{\text{gen}}} \text{dam} \Phi^0 \mathbf{G}^\sharp \cdot \mathbf{Z}^b \cdot \mathbf{G}^\sharp \\ &+ 3 \partial_{Z^b A^\sharp I_3^{\text{gen}}} \text{dam} \Phi^0 \mathbf{G}^\sharp \cdot \mathbf{Z}^b \cdot \mathbf{G}^\sharp \cdot \mathbf{Z}^b \cdot \mathbf{G}^\sharp \\ &+ \partial_{Z^b A^\sharp I_7^{\text{gen}}} \text{dam} \Phi^0 \mathbf{A}^\sharp + \partial_{Z^b A^\sharp I_8^{\text{gen}}} \text{dam} \Phi^0 \mathbf{A}^\sharp \cdot \mathbf{G}^b \cdot \mathbf{A}^\sharp \\ &+ 2 \partial_{Z^b A^\sharp I_9^{\text{gen}}} \text{dam} \Phi^0 [\mathbf{G}^\sharp \cdot \mathbf{Z}^b \cdot \mathbf{A}^\sharp]_{\text{sym}} \\ &+ 2 \partial_{Z^b A^\sharp I_{10}^{\text{gen}}} \text{dam} \Phi^0 \mathbf{A}^\sharp \cdot \mathbf{Z}^b \cdot \mathbf{A}^\sharp \end{aligned} \right]. \tag{5.13}
\end{aligned}$$

In this work, we nevertheless adopt the concept of a fictitious isotropic configuration for the damage potential in analogy to the free Helmholtz energy density. Hence, the appropriate set of three invariants reads as ($i = 1, 2, 3$)

$$\bar{Z}^b \bar{A}^\sharp I_i = \bar{\mathbf{G}}^\sharp : [\bar{\mathbf{Z}}^b \cdot \bar{\mathbf{A}}^\sharp]^i = \mathbf{G}^\sharp : [\mathbf{Z}^b \cdot \mathbf{A}^\sharp]^i = Z^b A^\sharp I_i \tag{5.14}$$

and the associated format of the evolution equation results in

$$\begin{aligned}
D_t \mathbf{A}^\sharp &\doteq D_t \lambda \partial_{\mathbf{Z}^b} \text{dam} \Phi^0 (Z^b A^\sharp I_{1,2,3}; \mathbf{X}) = D_t \lambda \sum_{i=1}^3 \partial_{Z^b A^\sharp I_i} \text{dam} \Phi^0 \partial_{\mathbf{Z}^b} Z^b A^\sharp I_i \\
&= D_t \lambda \left[\begin{aligned} &\partial_{Z^b A^\sharp I_1} \text{dam} \Phi^0 \mathbf{A}^\sharp + 2 \partial_{Z^b A^\sharp I_2} \text{dam} \Phi^0 \mathbf{A}^\sharp \cdot \mathbf{Z}^b \cdot \mathbf{A}^\sharp \\ &+ 3 \partial_{Z^b A^\sharp I_3} \text{dam} \Phi^0 \mathbf{A}^\sharp \cdot \mathbf{Z}^b \cdot \mathbf{A}^\sharp \cdot \mathbf{Z}^b \cdot \mathbf{A}^\sharp \end{aligned} \right]. \tag{5.15}
\end{aligned}$$

On this basis, two selected representations of Eq.(5.13) seem to be natural, compare Schreyer [Sch95]:

The *direct formulation* is actually based on a second order, positive definite tensor $\boldsymbol{\Xi}^\sharp(\mathbf{A}^\sharp; \mathbf{X}) \in \mathbb{S}_+^3 : T^* \mathcal{B}_0 \times T^* \mathcal{B}_0 \rightarrow \mathbb{R}$ which is assumed to be negatively proportional to the damage rate itself, namely $D_t \mathbf{A}^\sharp = -D_t \lambda \boldsymbol{\Xi}^\sharp$. Within an associated setting, this relation is one-to-one with $\text{dam} \Phi_{\text{fix}}^0 = -\mathbf{Z}^b : \boldsymbol{\Xi}^\sharp$ and straightforward calculations using the inelastic loading conditions $\text{vie} \Phi^0 \leq 0$ and $D_t \lambda \geq 0$ yield the reduced, pointwise and isothermal dissipation inequality $\text{red} \mathcal{D}_0^0 = -D_t \lambda \text{har} \Phi \geq 0$. As a first example, the simplest case of this direct formulation is introduced via $\boldsymbol{\Xi}^\sharp \doteq \mathbf{A}^\sharp$ which ends up with

$$\begin{aligned}
\text{dam} \Phi_{\text{fix}}^0 &\doteq -\mathbf{Z}^b : \mathbf{A}^\sharp = -Z^b A^\sharp I_1, \\
D_t \mathbf{A}^\sharp &= -D_t \lambda \mathbf{A}^\sharp. \tag{5.16}
\end{aligned}$$

Although the damage metric is just scaled down (in the case of damage evolution), this approach differs significantly from the standard isotropic $[1 - D]$ continuum damage formulation since \mathbf{A}^\sharp is not necessarily a spherical tensor and thus possibly renders overall anisotropic material behaviour. However, in the context that the damage rate $D_t \mathbf{A}^\sharp$ commutes with the damage metric \mathbf{A}^\sharp itself, Eq.(5.16) is denoted as *quasi isotropic* damage evolution in the sequel.

The *formulation based on conjugate variables* constitutes the damage rate via a linear map of the damage stress, in detail $D_t \mathbf{A}^\sharp = D_t \lambda \boldsymbol{\Xi}^\sharp : \mathbf{Z}^b$ whereby $\boldsymbol{\Xi}^\sharp(\mathbf{A}^\sharp; \mathbf{X}) \in \mathbb{S}^{3 \times 3} : T^* \mathcal{B}_0 \times T^* \mathcal{B}_0 \times T^* \mathcal{B}_0 \times T^* \mathcal{B}_0 \rightarrow \mathbb{R}$ represents an appropriate fourth order tensor. For the considered associated setting we obtain the damage potential $\text{dam} \Phi_{\text{cha}}^0 = \frac{1}{2} \mathbf{Z}^b : \boldsymbol{\Xi}^\sharp : \mathbf{Z}^b$ which renders the reduced, pointwise and isothermal Clausius–Duhem inequality of the format $\text{red} \mathcal{D}_0^0 = -2 D_t \lambda \text{har} \Phi \geq 0$.

The damage evolution is identified as truly *anisotropic* if $D_t \mathbf{A}^\sharp$ and \mathbf{A}^\sharp are not coaxial. The rotation of the principle damage directions is generally included, e.g. for $\Xi^\sharp = \mathbf{A}^\sharp \bar{\otimes} \mathbf{A}^\sharp$ which represents the simplest choice within the formulation based on the conjugate variable and results in (see Appendix B.1 for notational details)

$$\begin{aligned} \text{dam}\Phi_{\text{cha}}^0 &\doteq \frac{1}{2} \mathbf{Z}^b : [\mathbf{A}^\sharp \bar{\otimes} \mathbf{A}^\sharp] : \mathbf{Z}^b = \frac{1}{2} Z^b A^\sharp I_2, \\ D_t \mathbf{A}^\sharp &= D_t \lambda [\mathbf{A}^\sharp \bar{\otimes} \mathbf{A}^\sharp] : \mathbf{Z}^b = D_t \lambda \mathbf{A}^\sharp \cdot \mathbf{Z}^b \cdot [\mathbf{A}^\sharp]^t. \end{aligned} \quad (5.17)$$

Based on these two introduced types of damage potentials, together with the character of the initial damage metric tensor $\mathbf{A}^\sharp|_{t_0}$, a general classification of the coupling of hyper-elasticity and damage becomes possible and the following four categories are obtained:

$$\begin{aligned} \text{(i)} & \quad \text{isotropic hyper-elasticity } (\mathbf{A}^\sharp|_{t_0} = \beta_0 \mathbf{G}^\sharp) \ \& \ \text{quasi isotropic damage } (\text{dam}\Phi_{\text{fix}}^0) \\ \text{(ii)} & \quad \text{isotropic hyper-elasticity } (\mathbf{A}^\sharp|_{t_0} = \beta_0 \mathbf{G}^\sharp) \ \& \ \text{anisotropic damage } (\text{dam}\Phi_{\text{cha}}^0) \\ \text{(iii)} & \quad \text{anisotropic hyper-elasticity } (\mathbf{A}^\sharp|_{t_0} \neq \beta_0 \mathbf{G}^\sharp) \ \& \ \text{quasi isotropic damage } (\text{dam}\Phi_{\text{fix}}^0) \\ \text{(iv)} & \quad \text{anisotropic hyper-elasticity } (\mathbf{A}^\sharp|_{t_0} \neq \beta_0 \mathbf{G}^\sharp) \ \& \ \text{anisotropic damage } (\text{dam}\Phi_{\text{cha}}^0) \end{aligned} \quad (5.18)$$

Moreover, by assuming a material of St. Venant–Kirchhoff type, category (i) correlates to the classical $[1 - D]$ damage formulation via $\mathbf{A}^\sharp = \beta_0 \mathbf{G}^\sharp = [1 - D]^2 \mathbf{G}^\sharp$. In this case, β_0 represents three equal eigenvalues, which degrade for increasing damage, e.g. characterised by D . Note that formulations within category (ii) become especially anisotropic within the purely elastic domain for unloading after damage evolution has taken place.

Remark 5.3 *An alternative motivation for Eqs.(5.16, 5.17), which practically characterises the type of inelastic anisotropy, is based on the quadratic form*

$$\text{dam}\Phi_{\mathbf{G}^\sharp}^0 \doteq \frac{1}{2} \mathbf{Z}^b : [\delta_1 \mathbf{G}^\sharp \otimes \mathbf{G}^\sharp + \delta_2 [\mathbf{G}^\sharp \bar{\otimes} \mathbf{G}^\sharp + \mathbf{G}^\sharp \underline{\otimes} \mathbf{G}^\sharp]] : \mathbf{Z}^b = \frac{1}{2} \delta_1 Z^b G^\sharp I_1^2 + \delta_2 Z^b G^\sharp I_2, \quad (5.19)$$

whereby the structure of the fourth order tensor $\Xi^\sharp(\mathbf{G}^\sharp; \mathbf{X})$ coincides with the representation of linear isotropic elasticity. Now, due to the central idea of the proposed framework, the contra-variant metric tensor \mathbf{G}^\sharp is replaced by the damage metric \mathbf{A}^\sharp

$$\text{dam}\Phi_{\mathbf{A}^\sharp}^0 \doteq \frac{1}{2} \mathbf{Z}^b : [\delta_1 \mathbf{A}^\sharp \otimes \mathbf{A}^\sharp + \delta_2 [\mathbf{A}^\sharp \bar{\otimes} \mathbf{A}^\sharp + \mathbf{A}^\sharp \underline{\otimes} \mathbf{A}^\sharp]] : \mathbf{Z}^b = \frac{1}{2} \delta_1 Z^b A^\sharp I_1^2 + \delta_2 Z^b A^\sharp I_2. \quad (5.20)$$

Note that the first term, incorporating the scalar δ_1 , correlates to quasi isotropic damage evolution and that the second term, incorporating the scalar δ_2 , represents an anisotropic damage potential.

5.3 Numerical time integration

Based on the rate-independent framework given in Section 5.1, a staggered algorithmic treatment is applied (similar to Algorithm 3.1). Thus, from the computational point of view, the time interval of interest $\mathbb{T} = \bigcup_{n=0}^N [{}^n t, {}^{n+1} t]$ is actually split up into n time steps which define the strain driven algorithm. Please note that for the subsequent Algorithms 5.1, 5.2 and 5.3 loading and unloading conditions are exclusively checked by the trial step at ${}^{n+1} \mathbf{E}^b$.

To set the stage, we firstly consider quasi isotropic damage evolution. Since the principle directions of the damage metric \mathbf{A}^\sharp stay constant during the inelastic process, an exponential scheme can be conveniently applied, compare Weber and Anand [WA90, Eq.(26)]. For the specific example as given in Eq.(5.16), the obtained algorithm reduces to a scalar-valued iteration with respect to the Lagrange multiplier, see Algorithm 5.1.

Algorithm 5.1 *Exponential integration algorithm for quasi isotropic damage, Eq.(5.16).*

```

(Finite Element Method) for given  ${}^{n+1}\mathbf{F}^{\natural}$  do
    if  ${}^{\text{yie}}\Phi^0(\mathbf{Z}^{\flat}({}^{n+1}\mathbf{E}^{\flat}, {}^n\mathbf{A}^{\natural}); {}^n\mathbf{A}^{\natural}) > 0$ 
    (scalar-valued iteration)    dowhile  $|{}^{\text{yie}}\Phi^0(\Delta\lambda, \mathbf{Z}^{\flat}({}^{n+1}\mathbf{E}^{\flat}, {}^{n+1}\mathbf{A}^{\natural}); {}^{n+1}\mathbf{A}^{\natural})| > \text{tol}$ 
         $\Delta\lambda = \dots$ 
         ${}^{n+1}\mathbf{A}^{\natural} = \exp(-\Delta\lambda) {}^n\mathbf{A}^{\natural}$ 
    enddo
    endif

```

Several families of algorithms to solve for the roots of non-linear scalar-valued equations exist, see e.g. Engeln-Müllges and Uhlig [EMU96, Chap. 2] for a detailed outline. Within the subsequent numerical examples, we prefer modified regula-falsi schemes, e.g. the algorithm by Anderson and Björck which results in more stable computations than interpolation or Newton-type methods (in this case).

For the general anisotropic case as highlighted in Eq.(5.17), exponential schemes can no longer conveniently be applied since the damage rate does not commute with the damage metric itself. Nevertheless, e.g. multi-stage methods of the Runge-Kutta family can be adopted for the integration of the obtained system of ordinary differential equations (initial value problem), see e.g. Hairer et al. [HNW93, Chap. II] among many others. In the following outline, we focus on implicit methods. Apparently, explicit schemes are included and result in scalar-valued iterations with respect to the Lagrange multipliers. The underlying (s-stage) Butcher array defines general Runge-Kutta methods and is reiterated in Appendix E.1 where the coefficients of some typical algorithms are briefly summarised. On this basis, general higher order methods with several intermediate stages \mathbf{A}_i^{\natural} are (implicitly) defined by ¶

$$\mathbf{A}_i^{\natural} = {}^n\mathbf{A}^{\natural} + \Delta\lambda_i \sum_{j=1}^s a_{ij} \partial_{\mathbf{Z}_j^{\flat}} {}^{\text{yie}}\Phi^0({}^{n+c_j}\mathbf{E}^{\flat}, \mathbf{A}_j^{\natural}) \quad (5.21)$$

and the actual damage metric ${}^{n+1}\mathbf{A}^{\natural}$ is computed via

$${}^{n+1}\mathbf{A}^{\natural} = {}^n\mathbf{A}^{\natural} + \Delta\lambda \sum_{i=1}^s b_i \partial_{\mathbf{Z}_i^{\flat}} {}^{\text{yie}}\Phi^0({}^{n+c_i}\mathbf{E}^{\flat}, \mathbf{A}_i^{\natural}) \quad (5.22)$$

These non-linear equations are solved for given $\Delta\lambda_i$ by a local Newton algorithm which yields the following linear system of equations within each iteration k (the notation \circ denotes the appropriate type of contraction and the incorporated fourth order identity is defined in Appendix A.1)

$$\begin{bmatrix} \text{sym}\mathbf{G}^{\natural} - \Delta\lambda_1 a_{11} \mathbf{J}_1^{\natural} & -\Delta\lambda_1 a_{12} \mathbf{J}_2^{\natural} & \dots & -\Delta\lambda_1 a_{1s} \mathbf{J}_s^{\natural} \\ -\Delta\lambda_2 a_{21} \mathbf{J}_1^{\natural} & \text{sym}\mathbf{G}^{\natural} - \Delta\lambda_2 a_{22} \mathbf{J}_2^{\natural} & \dots & -\Delta\lambda_2 a_{2s} \mathbf{J}_s^{\natural} \\ \vdots & \vdots & \ddots & \vdots \\ -\Delta\lambda_s a_{s1} \mathbf{J}_1^{\natural} & -\Delta\lambda_s a_{s2} \mathbf{J}_2^{\natural} & \dots & \text{sym}\mathbf{G}^{\natural} - \Delta\lambda_s a_{ss} \mathbf{J}_s^{\natural} \end{bmatrix} \circ \begin{bmatrix} \Delta\mathbf{A}_1^{\natural} \\ \Delta\mathbf{A}_1^{\natural} \\ \vdots \\ \Delta\mathbf{A}_s^{\natural} \end{bmatrix} = - \begin{bmatrix} \mathbf{R}_1^{\natural} \\ \mathbf{R}_1^{\natural} \\ \vdots \\ \mathbf{R}_s^{\natural} \end{bmatrix} \quad (5.23)$$

together with

$$\begin{aligned} \text{the residua:} \quad \mathbf{R}_i^{\natural} &= {}_k\mathbf{A}_i^{\natural} - {}^n\mathbf{A}^{\natural} - \Delta\lambda_i \sum_{j=1}^s a_{ij} \partial_{\mathbf{Z}_j^{\flat}} {}^{\text{yie}}\Phi^0({}^{n+c_j}\mathbf{E}^{\flat}, {}_k\mathbf{A}_j^{\natural}) \\ \text{the Jacobians:} \quad \mathbf{J}_i^{\natural} &= \partial_{\mathbf{Z}_i^{\flat} \otimes {}_k\mathbf{A}_i^{\natural}} {}^{\text{yie}}\Phi^0({}^{n+c_i}\mathbf{E}^{\flat}, {}_k\mathbf{A}_i^{\natural}) \\ \text{and the update:} \quad {}_{k+1}\mathbf{A}_i^{\natural} &= {}_k\mathbf{A}_i^{\natural} + \Delta\mathbf{A}_i^{\natural} \end{aligned} \quad (5.24)$$

¶For notational simplicity we abbreviate ${}^{\text{yie}}\Phi^0({}^{n+c_j} \mathbf{Z}^{\flat}({}^{n+c_j}\mathbf{E}^{\flat}, \mathbf{A}_j^{\natural}); \mathbf{A}_j^{\natural})$ by ${}^{\text{yie}}\Phi^0({}^{n+c_j}\mathbf{E}^{\flat}, \mathbf{A}_j^{\natural})$ and furthermore \mathbf{Z}_j^{\flat} represents $\mathbf{Z}^{\flat}({}^{n+c_j}\mathbf{E}^{\flat}, \mathbf{A}_j^{\natural})$.

Remark 5.4 It turns out to be useful to apply Voigt's notation within the solution of the system of equations (5.23); $\Delta \mathbf{A}_i^\sharp \mapsto \Delta^{\text{voi}} \mathbf{A}_i$, $\Delta \mathbf{R}_i^\sharp \mapsto \Delta^{\text{voi}} \mathbf{R}_i$, ${}^{\text{sym}} \mathbf{G}^\sharp \mapsto {}^{\text{voi, sym}} \mathbf{I}$ and $\mathbf{J}_i^\sharp \mapsto {}^{\text{voi}} \mathbf{J}_i$. Then, symmetry relations yield $\Delta^{\text{voi}} \mathbf{A}_i, \Delta^{\text{voi}} \mathbf{R}_i \in \mathbb{R}^6$ and consequently ${}^{\text{voi, sym}} \mathbf{I}, {}^{\text{voi}} \mathbf{J}_i \in \mathbb{R}^6 \times \mathbb{R}^6$.

Remark 5.5 The Jacobians with respect to Eq.(5.17), are defined by

$$\begin{aligned} \mathbf{J}_i^\sharp &= \partial_{k \mathbf{A}_i^\sharp} ([k \mathbf{A}_i^\sharp \overline{\otimes} k \mathbf{A}_i^\sharp] : k \mathbf{Z}_i^b) \\ &= [\partial_{k \mathbf{A}_i^\sharp} (k \mathbf{A}_i^\sharp \overline{\otimes} k \mathbf{A}_i^\sharp)] : k \mathbf{Z}_i^b - [k \mathbf{A}_i^\sharp \overline{\otimes} k \mathbf{A}_i^\sharp] : k \mathbf{A}_i^b \\ &= \left[\mathbf{G}^\sharp \overline{\otimes} [k \mathbf{A}_i^\sharp \cdot k \mathbf{Z}_i^b] + \mathbf{G}^\sharp \underline{\otimes} [k \mathbf{A}_i^\sharp \cdot k \mathbf{Z}_i^b] \right]^{\text{SYM}} - [k \mathbf{A}_i^\sharp \overline{\otimes} k \mathbf{A}_i^\sharp] : k \mathbf{A}_i^b. \end{aligned} \quad (5.25)$$

The fourth order Hessian $\mathbf{A}^b = -\partial_{\mathbf{A}^\sharp} \mathbf{Z}^b$ has already been defined in Eq.(5.8) and reads in detail (after some straightforward computations) as

$$\begin{aligned} \mathbf{A}^b &= \partial_{E^b A^\sharp I_1 E^b A^\sharp I_1} \psi_0^0 \mathbf{E}^b \otimes \mathbf{E}^b \\ &+ 4 \partial_{E^b A^\sharp I_2 E^b A^\sharp I_2} \psi_0^0 [\mathbf{E}^b \cdot \mathbf{A}^\sharp \cdot \mathbf{E}^b] \otimes [\mathbf{E}^b \cdot \mathbf{A}^\sharp \cdot \mathbf{E}^b] \\ &+ 9 \partial_{E^b A^\sharp I_3 E^b A^\sharp I_3} \psi_0^0 [\mathbf{E}^b \cdot \mathbf{A}^\sharp \cdot \mathbf{E}^b \cdot \mathbf{A}^\sharp \cdot \mathbf{E}^b] \otimes [\mathbf{E}^b \cdot \mathbf{A}^\sharp \cdot \mathbf{E}^b \cdot \mathbf{A}^\sharp \cdot \mathbf{E}^b] \\ &+ 4 \partial_{E^b A^\sharp I_1 E^b A^\sharp I_2} \psi_0^0 \left[\mathbf{E}^b \otimes [\mathbf{E}^b \cdot \mathbf{A}^\sharp \cdot \mathbf{E}^b] \right]^{\text{SYM}} \\ &+ 12 \partial_{E^b A^\sharp I_2 E^b A^\sharp I_3} \psi_0^0 \left[[\mathbf{E}^b \cdot \mathbf{A}^\sharp \cdot \mathbf{E}^b] \otimes [\mathbf{E}^b \cdot \mathbf{A}^\sharp \cdot \mathbf{E}^b \cdot \mathbf{A}^\sharp \cdot \mathbf{E}^b] \right]^{\text{SYM}} \\ &+ 6 \partial_{E^b A^\sharp I_1 E^b A^\sharp I_3} \psi_0^0 \left[\mathbf{E}^b \otimes [\mathbf{E}^b \cdot \mathbf{A}^\sharp \cdot \mathbf{E}^b \cdot \mathbf{A}^\sharp \cdot \mathbf{E}^b] \right]^{\text{SYM}} \\ &+ \partial_{E^b A^\sharp I_2} \psi_0^0 [\mathbf{E}^b \overline{\otimes} \mathbf{E}^b + \mathbf{E}^b \underline{\otimes} \mathbf{E}^b] \\ &+ 3 \partial_{E^b A^\sharp I_3} \psi_0^0 \left[\mathbf{E}^b \overline{\otimes} [\mathbf{E}^b \cdot \mathbf{A}^\sharp \cdot \mathbf{E}^b] + \mathbf{E}^b \underline{\otimes} [\mathbf{E}^b \cdot \mathbf{A}^\sharp \cdot \mathbf{E}^b] \right]^{\text{SYM}}. \end{aligned} \quad (5.26)$$

Referring to the applied staggered solution strategy, namely the Newton iteration for the damage metric embedded into a scalar-valued iteration to compute the Lagrange multiplier, two different approaches are possible. Within the first type of algorithm, the intermediate stages, \mathbf{A}_i^\sharp , are not forced to satisfy the constraint of the damage condition and ${}^{\text{yie}} \Phi^0(\mathbf{Z}_i^b; \mathbf{A}_i^\sharp, \mathbf{X}) > 0$ is possible. Since solely the actual setting must lie in the admissible elastic domain \mathbb{A} , which requires ${}^{\text{yie}} \Phi^0({}^{n+1} \mathbf{Z}^b; {}^{n+1} \mathbf{A}^\sharp, \mathbf{X}) = 0$, this scheme results in only one damage multiplier, see Algorithm 5.2.

Algorithm 5.2 Integration Scheme 1: Intermediate stages may violate the damage condition.

```

(Finite Element Method) for given  ${}^{n+1} \mathbf{F}^\sharp$  do
    if  ${}^{\text{yie}} \Phi^0(\mathbf{Z}^b({}^{n+1} \mathbf{E}^b, {}^n \mathbf{A}^\sharp); {}^n \mathbf{A}^\sharp) > 0$ 
(scalar-valued iteration)    while  $|{}^{\text{yie}} \Phi^0(\Delta \lambda, \mathbf{Z}^b({}^{n+1} \mathbf{E}^b, {}^{n+1} \mathbf{A}^\sharp); {}^{n+1} \mathbf{A}^\sharp)| > \text{tol}$ 
         $\Delta \lambda = \dots$ 
(Newton-type methods)    while  $\|\mathbf{R}_i^\sharp\| > \text{tol}$ 
        ...
         $\mathbf{A}_i^\sharp = {}^n \mathbf{A}^\sharp + \Delta \lambda \sum_{j=1}^s a_{ij} \partial_{\mathbf{Z}_j^b} {}^{\text{yie}} \Phi^0({}^{n+c_j} \mathbf{E}^b, \mathbf{A}_j^\sharp)$ 
        enddo
         ${}^{n+1} \mathbf{A}^\sharp = {}^n \mathbf{A}^\sharp + \Delta \lambda \sum_{i=1}^s b_i \partial_{\mathbf{Z}_i^b} {}^{\text{yie}} \Phi^0({}^{n+c_i} \mathbf{E}^b, \mathbf{A}_i^\sharp)$ 
        enddo
    endif

```

Alternatively, the second integration category forces the intermediate stages to satisfy the damage condition. All stages of interest now lie in the admissible elastic domain \mathbb{A} but from the numerical point of view several scalar-valued iterations for different Lagrange multipliers due to each intermediate stage come into the picture, see Algorithm 5.3. Furthermore, if the considered interval includes damaged and purely elastic regions as well, the rate equation is no longer smooth which may cause numerical instabilities for large integration intervals.

Algorithm 5.3 *Integration Scheme 2: Intermediate stages are forced to fulfil the damage condition.*

```

(Finite Element Method) for given  ${}^{n+1}\mathbf{F}^\sharp$  do
    if  ${}^{\text{yie}}\Phi^0(\mathbf{Z}^b({}^{n+1}\mathbf{E}^b, {}^n\mathbf{A}^\sharp); {}^n\mathbf{A}^\sharp) > 0$ 
    if  ${}^{\text{yie}}\Phi^0(\mathbf{Z}^b({}^{n+c_i}\mathbf{E}^b, {}^n\mathbf{A}^\sharp); {}^n\mathbf{A}^\sharp) > 0$ 
    (scalar-valued iterations)    dowhile  $|{}^{\text{yie}}\Phi^0(\Delta\lambda_i, \mathbf{Z}_i^b; \mathbf{A}_i^\sharp)| > \text{tol}$ 
         $\Delta\lambda_i = \dots$ 
    (Newton-type methods)    dowhile  $\|\mathbf{R}_i^\sharp\| > \text{tol}$ 
         $\dots$ 
         $\mathbf{A}_i^\sharp = {}^n\mathbf{A}^\sharp + \Delta\lambda_i \sum_{j=1}^s a_{ij} \partial_{\mathbf{Z}_j^b} {}^{\text{yie}}\Phi^0({}^{n+c_j}\mathbf{E}^b, \mathbf{A}_j^\sharp)$ 
    enddo
    enddo
endif
    (scalar-valued iteration)    dowhile  $|{}^{\text{yie}}\Phi^0(\Delta\lambda, \mathbf{Z}^b({}^{n+1}\mathbf{E}^b, {}^{n+1}\mathbf{A}^\sharp); {}^{n+1}\mathbf{A}^\sharp)| > \text{tol}$ 
         $\Delta\lambda = \dots$ 
         ${}^{n+1}\mathbf{A}^\sharp = {}^n\mathbf{A}^\sharp + \Delta\lambda \sum_{i=1}^s b_i \partial_{\mathbf{Z}_i^b} {}^{\text{yie}}\Phi^0({}^{n+c_i}\mathbf{E}^b, \mathbf{A}_i^\sharp)$ 
    enddo
endif

```

Remark 5.6 *Note that both algorithms (5.2, 5.3) are identical in the case of an Euler backward integration.*

Remark 5.7 *The intermediate strain metrics are usually defined by linear interpolation ${}^{n+c_i}\mathbf{E}^b = c_i {}^{n+1}\mathbf{E}^b + [1 - c_i] {}^n\mathbf{E}^b$. Moreover, it is useful to choose ${}^{\text{ini}}\mathbf{A}_j^\sharp \doteq \mathbf{A}_i^\sharp$ for $c_j > c_i$ as an initial guess (ini) within diagonally implicit Runge–Kutta schemes instead of the standard initialisation ${}^{\text{ini}}\mathbf{A}_j^\sharp \doteq {}^n\mathbf{A}^\sharp$.*

5.4 Numerical examples

To discuss overall anisotropic behaviour within the proposed framework of coupling hyper-elasticity to continuum damage, the homogeneous deformation in simple shear is considered. Both types of damage evolution as highlighted in Eqs.(5.16, 5.17) are discussed. Furthermore, even the initial hyper-elastic setting is anisotropic and the subsequent examples consequently represent categories (iii) and (iv). Thereby, the constitutive function of a compressible Mooney–Rivlin material has been applied with respect to the fictitious undamaged and isotropic configuration

$$\psi_0^0 = c_1 \left[{}^{C^b A^\sharp} J_1 - 3 \right] + c_2 \left[{}^{C^b A^\sharp} J_2 - 3 \right] + \frac{\lambda^p}{2} \ln^2 \left({}^{C^b A^\sharp} J_3^{1/2} \right) - 2 [c_1 + 2c_2] \ln \left({}^{C^b A^\sharp} J_3^{1/2} \right), \quad (5.27)$$

compare Eq.(C.3). The chosen material parameters read $c_1 = 10$, $c_2 = 20$ and $\lambda^p = 5$ and a constant threshold ${}^{\text{har}}\Phi = -10$ is adopted. Moreover, the initial damage metric $\mathbf{A}^\sharp|_{t_0}$ is determined by $\eta_0 = 1$, $\eta_1 = \frac{1}{2}$, $\eta_2 = \frac{1}{4}$, $\vartheta_1^1 = \frac{2}{3}\pi$, $\vartheta_1^2 = \frac{1}{3}\pi$, $\vartheta_2^1 = \frac{4}{3}\pi$ and $\vartheta_2^2 = \frac{1}{6}\pi$ – see Eq.(4.43) and Figure D.1.2. In order to visualise the anisotropic material behaviour, the method of stereographic projection is applied, as emphasised in Appendix D.2.

5.4.1 Simple shear

Within the subsequently considered homogeneous deformation in simple shear, i.e. $\mathbf{F} = \mathbf{I} + \gamma \mathbf{e}_1 \otimes \mathbf{e}_2$ with $\mathbf{I} = \delta_j^i \mathbf{e}_i \otimes \mathbf{e}_j$ when referring to a Cartesian frame, anisotropic hyper-elasticity coupled to quasi isotropic and anisotropic damage are discussed in detail.

5.4.1.1 Quasi isotropic damage

For quasi isotropic damage evolution in terms of the potential ${}^{\text{dam}}\Phi_{\text{fix}}^0$ as defined in Eq.(5.16) together with the non-spherical metric $\mathbf{A}^\#|_{t_0}$, we end up with a damage formulation in category (iii). Thus, the strain field \mathbf{E}^b and the stress field $\mathbf{S}^\#$ do not commute but, nevertheless, the eigenvectors of the damage metric $\mathbf{A}^\#$ remain constant for arbitrary deformations. Figure 5.1 visualises these effects by the method of stereo-graphic projection for different shear numbers γ .

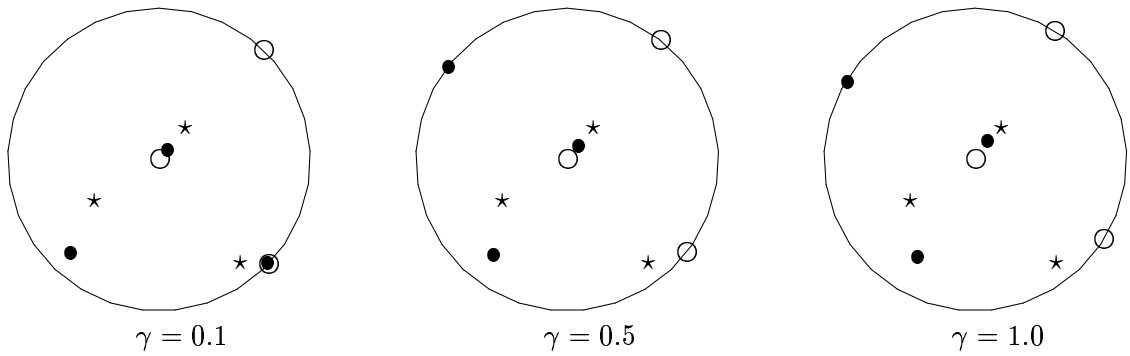


Figure 5.1: Simple shear, quasi isotropic damage: Stereo-graphic projection due to the principal directions of strain \mathbf{E}^b : \circ , stress $\mathbf{S}^\#$: \bullet and the damage metric $\mathbf{A}^\#$: \star for different shear numbers γ .

Concerning the numerical integration of the obtained rate equation for $D_t \mathbf{A}^\#$, see Eq.(5.16), an exponential scheme is applied, as summarised in Algorithm 5.1. Finally, the corresponding degradation of the eigenvalues ${}^{\mathbf{A}^\#} \lambda_i$ of the damage metric is depicted in Figure 5.2.

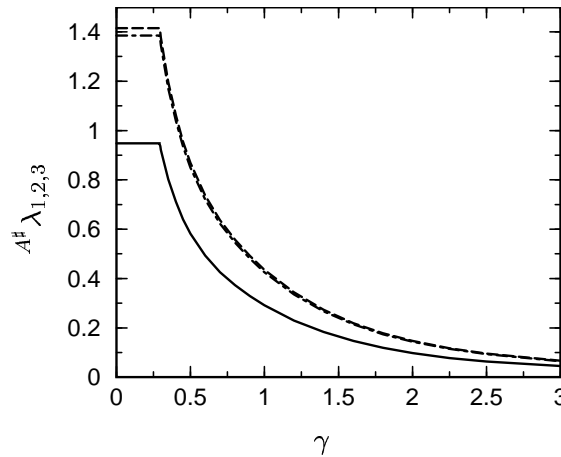


Figure 5.2: Simple shear, quasi isotropic damage: Degradation of the eigenvalues ${}^{\mathbf{A}^\#} \lambda_i$.

5.4.1.2 Anisotropic damage

Next, within the same setting as above, we account for anisotropic damage evolution in terms of the potential ${}^{\text{dam}}\Phi_{\text{cha}}^0$, compare Eq.(5.17). Since the initial damage metric $\mathbf{A}^\#|_{t_0}$ is non-spherical, we deal with a damage formulation in category (iv). The strain field \mathbf{E}^b and the stress field $\mathbf{S}^\#$ are consequently non-coaxial and the initial damage metric $\mathbf{A}^\#|_{t_0}$ and actual damage metric $\mathbf{A}^\#|_t$ additionally

do not commute as soon as damage evolution takes place. Once more adopting the method of stereographic projection, we give graphical representations of these anisotropic characteristics in Figure 5.3 for different shear numbers γ .

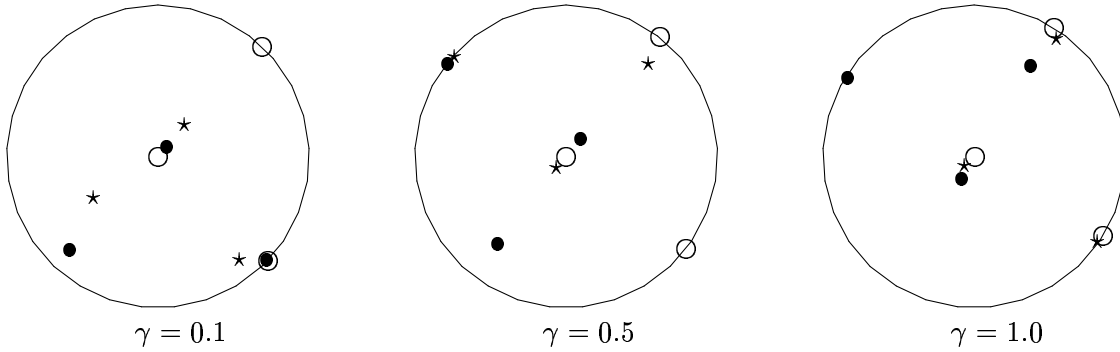


Figure 5.3: Simple shear, anisotropic damage: Stereo-graphic projection due to the principal directions of strain \mathbf{E}^b : \circ , stress \mathbf{S}^\sharp : \bullet and the damage metric \mathbf{A}^\sharp : \star for different shear numbers γ .

Since the eigenvectors of the initial damage metric $A^\sharp|_{t_0} \mathbf{N}_i^\sharp$ feature non-vanishing components with respect to all three Cartesian directions \mathbf{e}_i , and, moreover, since the anisotropic damage potential $\text{dam} \Phi_{\text{cha}}^0$ is additionally applied, the eigenvalues of the damage metric $A^\sharp \lambda_i$ degrade differently, see Figure 5.4 (this reference solution has been computed within a fourth order Runge–Kutta scheme for rather small load steps, $h : \Delta\gamma = 0.02$).

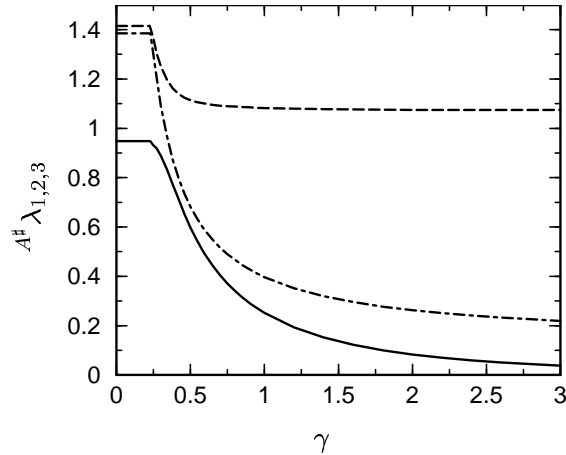


Figure 5.4: Simple shear, anisotropic damage: Degradation of the eigenvalues $A^\sharp \lambda_i$.

Now, for the integration of the rate equation of $D_t \mathbf{A}^\sharp$ – Eq.(5.17) – explicit Runge–Kutta schemes of order one up to four are applied. Because of stability reasons, the load steps h , actually in terms of strains, must be so small (here e.g. $h : \Delta\gamma = 0.1$) that the accuracy of the integration scheme is no longer substantially significant, as depicted in Figure 5.5 for the smallest and second damage eigenvalue $A^\sharp \lambda_{1,2}$. Although the considered integration algorithms render somewhat different results at $\gamma = 0.4$, they end up with identical eigenvalues $A^\sharp \lambda_i$ for increasing damage – as far as can be seen. Furthermore, integration Scheme 2 was applied (see Algorithm 5.3) which is not of fundamental importance for such small load steps.

Next, a rather large integration interval is considered which starts in the elastic area and ends up in the damaged domain, ($h : [\gamma = 0.1, \gamma = 1.0]$). Thereby, implicit Runge–Kutta methods within Scheme 1 and 2 are applied (see Algorithms 5.2 and 5.3). Recall that the intermediate stages are required to satisfy the damage condition within Scheme 2 and otherwise are not constrained (Scheme 1). Figures 5.6_{1,...,4} again visualise the numerical results for the smallest and second damage eigenvalue with respect to integration Scheme 1 whereby algorithms of order one up to four are analysed, see Appendix E.1 for some details. For this rather large loading interval, the numerical results for dif-

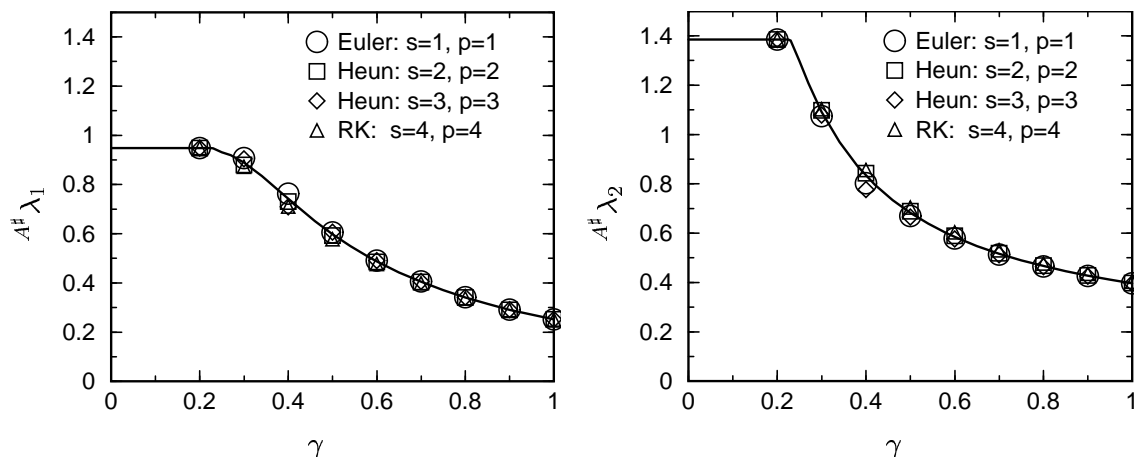


Figure 5.5: Simple shear, anisotropic damage: Degradation of the smallest and second damage eigenvalue $A^\# \lambda_{1,2}$ within explicit integration algorithms due to Scheme 2, Algorithm 5.3.

ferent integration algorithms deviate significantly – especially for the smallest eigenvalue of the damage metric. Diagonally implicit Runge–Kutta schemes (DIRK) within Scheme 1 (Algorithm 5.2), as monitored in Figures 5.6_{3,4}, show similar upshots as standard Runge–Kutta schemes which are highlighted in Figures 5.6_{1,2}. On the contrary, integration Scheme 2 (Algorithm 5.3) forces the intermediate stages to satisfy the damage condition. As depicted in Figures 5.6_{5,6}, the numerical results obtained by DIRK methods are most accurate.

Finally, an integration interval is considered which lies completely in the damage domain ($h : [\gamma = 0.25, \gamma = 1.0]$). In analogy to Figure 5.6, the corresponding numerical results are depicted in Figure 5.7. Now, the integration interval is comparatively smaller than in the above example and, moreover, the integrated function is smooth. Hence, the numerical results for all settings become more accurate. Nevertheless, the standard implicit Runge–Kutta algorithms within Scheme 1, see Figures 5.7_{1,2}, render aberrant eigenvalues and, again, DIRK methods within Scheme 2 end up with the most accurate computations, compare Figures 5.7_{5,6}.

Remark 5.8 Obviously, integration algorithms within Scheme 2 require several scalar-valued iterations to compute all Lagrange multipliers. Nevertheless, the overall numerical costs are in general not necessarily higher than applying Scheme 1 since each iteration reaches faster convergence compared to the single one within integration Scheme 1. Apparently, Scheme 2 behaves numerically more stable than Scheme 1 as far as large integration intervals for a sufficiently smooth function are considered.

5.4.2 Cracked plate under mode 3 loading

The subsequent finite element setting is based on anisotropic damage evolution in terms of the potential $^{\text{dam}}\mathcal{F}_{\text{cha}}^0$, compare Eq.(5.17). In analogy to Section 5.4.1.2, the initial damage metric $A^\#|_{t_0}$ is non-spherical which results in a damage formulation within category (iv). We consider a plate-like structure of dimensions $40 \times 80 \times 4$ whereby the discretisation is performed by $12 \times 24 \times 4$ enhanced eight node bricks (Q1E9) as advocated by Simo and Armero [SA92], see Figures 5.8 and 5.9. One side of the specimen is completely clamped while we apply typical mode 3-type displacement constraints (u_3) to the opposite ripped side. Similar to Section 3.9.2, simple Euler backward integration and a numerical perturbation scheme to approximate the “global” numerical tangent operator are adopted whereby the perturbation parameter $\varepsilon = 10^{-8}$ has been chosen and the precision corresponds to 16 decimal points, compare Section E.2.

The overall behaviour of the considered setting is monitored by representative load–displacement curves. In this context, let the notation F_3 characterises force–components with respect to the direction which is perpendicular to the initial plane of the specimen. Moreover, the abbreviation F_3^\pm denotes the sum over $\text{sign}(u_3) F_3$ with respect to the free boundary at the ripped side, see Figure 5.10. Likewise, we additionally highlight the norm of the resultant force $\|\mathbf{F}\|$ at the same constrained surface which would obviously vanish for an isotropic setting.

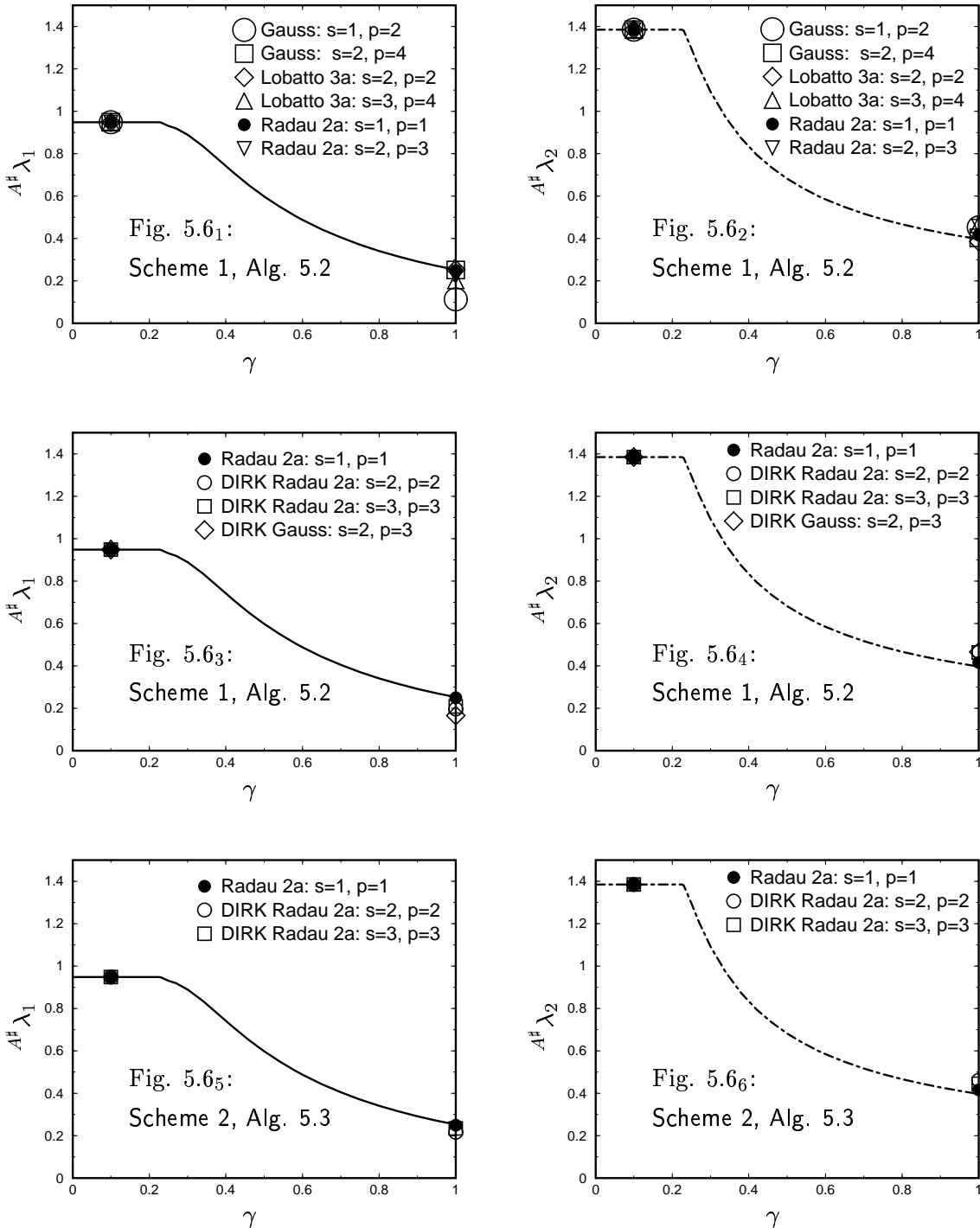


Figure 5.6: Simple shear, anisotropic damage: Degradation of the smallest and second damage eigenvalue $A^\# \lambda_{1,2}$ within implicit integration algorithms due to an elastic–damage interval.

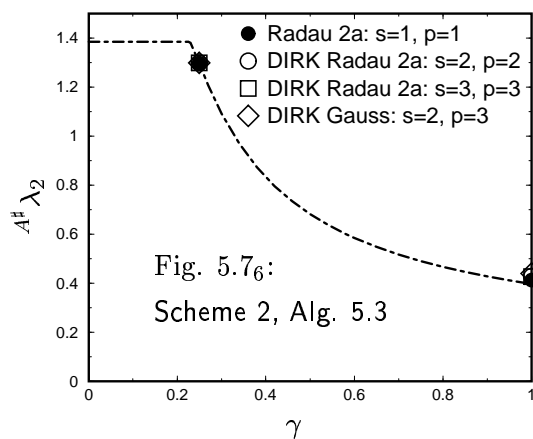
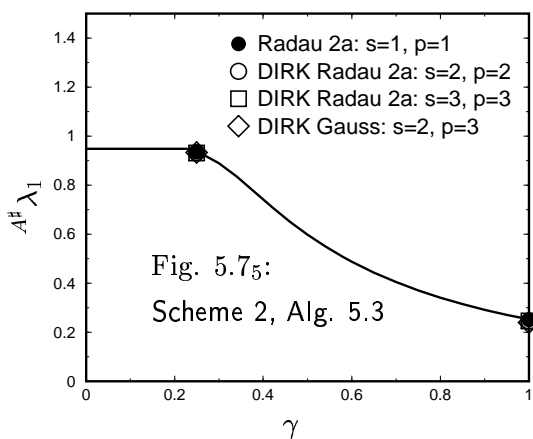
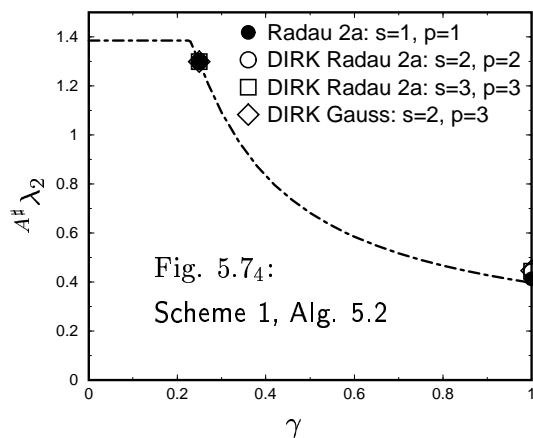
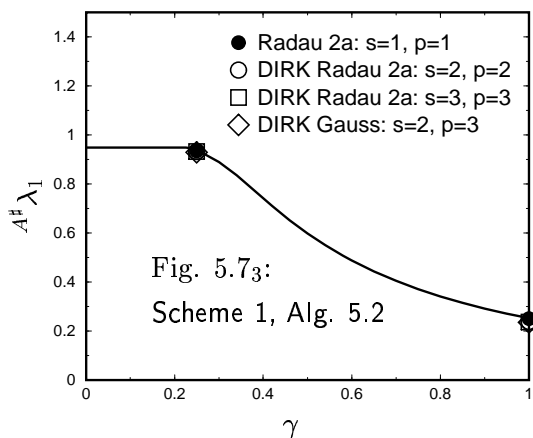
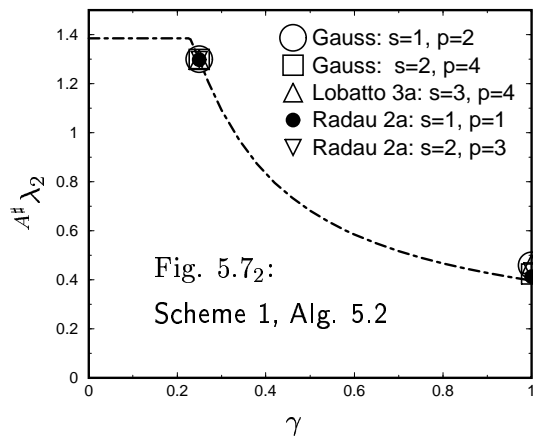
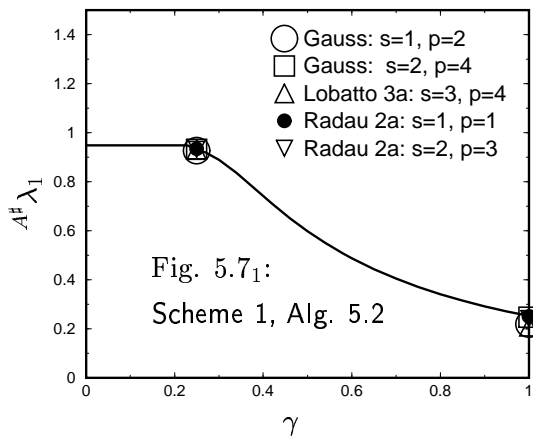


Figure 5.7: Simple shear, anisotropic damage: Degradation of the smallest and second damage eigenvalue $A^\# \lambda_{1,2}$ within implicit integration algorithms due to an damage–damage interval.

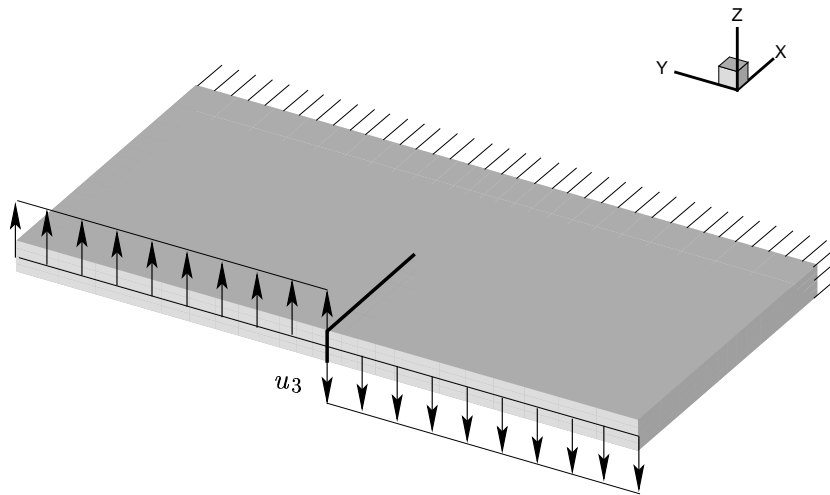


Figure 5.8: Cracked plate under mode 3 loading, anisotropic damage: Geometry and boundary conditions of the specimen.

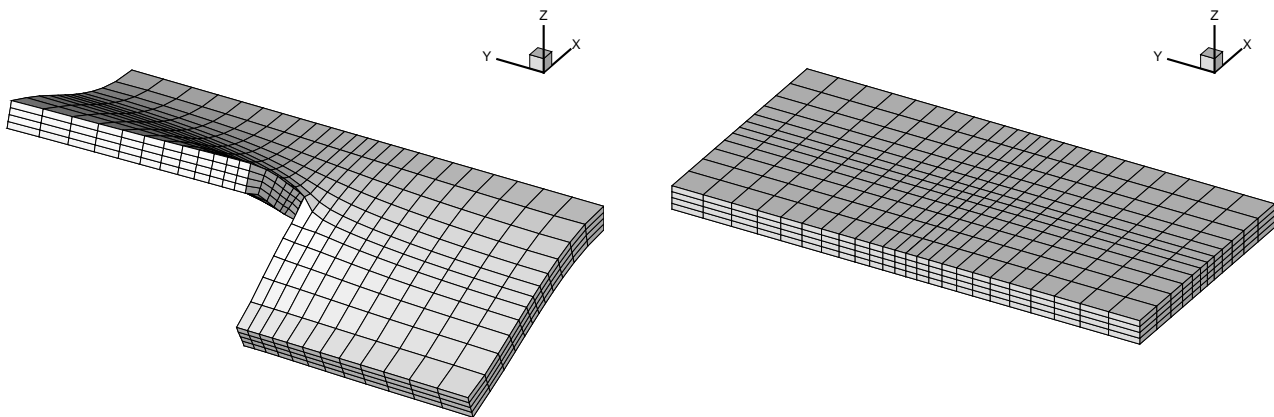


Figure 5.9: Cracked plate under mode 3 loading, anisotropic damage: Deformed mesh at $|u_3| = 13.34$ and discretisation of the specimen.

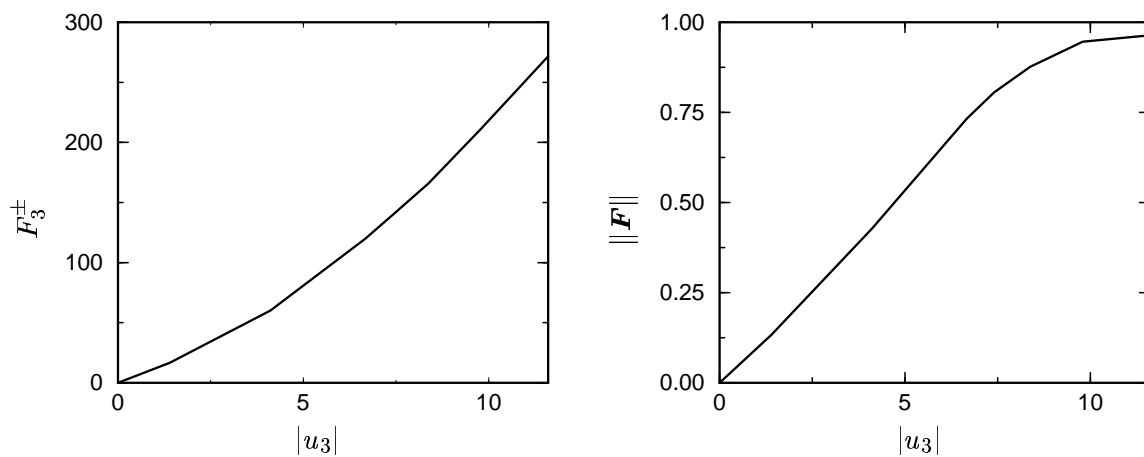


Figure 5.10: Cracked plate under mode 3 loading, anisotropic damage: Load–displacement curves.

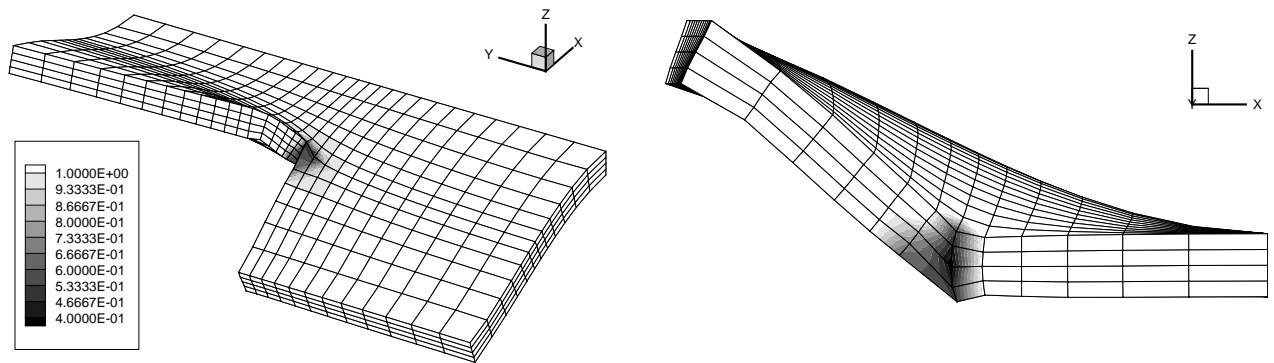


Figure 5.11: Cracked plate under mode 3 loading, anisotropic damage: Smallest damage eigenvalue $A^\# \lambda_1$ at $|u_3| = 13.34$.

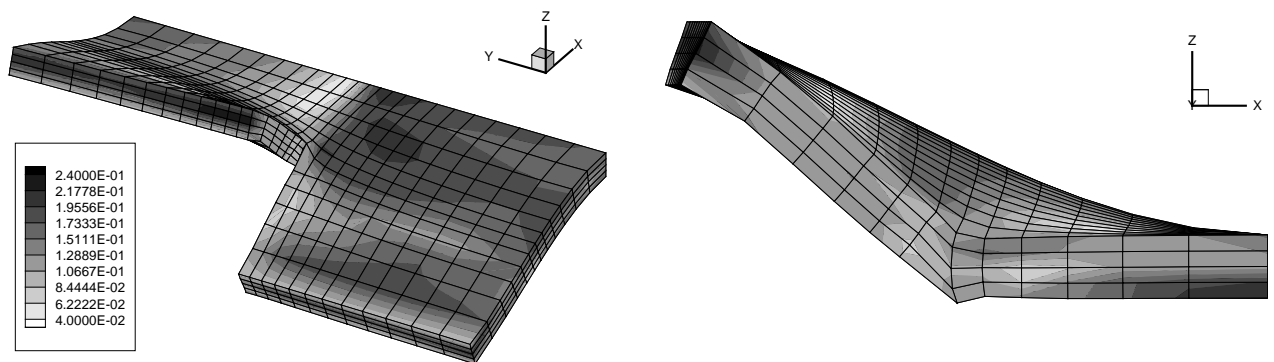


Figure 5.12: Cracked plate under mode 3 loading, anisotropic damage: Anisotropy measure $\delta(\mathbf{E}^b, \mathbf{S}^\#)$ at $|u_3| = 13.34$.

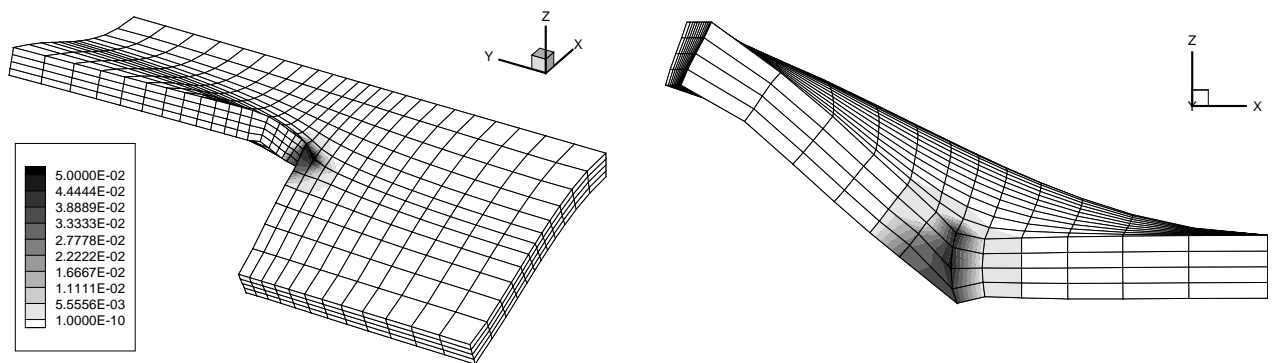



Figure 5.13: Cracked plate under mode 3 loading, anisotropic damage: Anisotropy measure $\delta(\mathbf{A}^\#, \mathbf{A}^\#|_{t_0})$ at $|u_3| = 13.34$.

The contribution of the smallest damage eigenvalue is visualised in Figure 5.11. Remarkably, the amount of this damage indicator boils down from 1.00 to 0.32 which corresponds to a high degree of damage evolution. In order to focus on the “fracture zone”, a cut through the specimen is additionally highlighted in the sequel. For the considered anisotropic setting neither the strain field (\mathbf{E}^b) and the stress field (\mathbf{S}^\sharp) commute nor the initial ($\mathbf{A}^\sharp|_{t_0}$) and the actual damage metric (\mathbf{A}^\sharp) possess identical principal directions as soon as damage evolution takes place. Hence we obtain non-vanishing anisotropy measures which are monitored in Figures 5.12 and 5.13.

Chapter 6

Anisotropic damage coupled to multiplicative elasto–plasticity based on fictitious configurations

 It is the nature of a real thing to be inexhaustible in content; we can get an ever deeper insight into this content by the continual addition of new experiences, partly in apparent contradiction, by bringing them into harmony with one another. In this interpretation, things of the real world are approximate ideas. From this arises the empirical character of all our knowledge of reality.

Hermann Weyl [1885 – 1955]
Space–Time–Matter, 1922

Based on the concept of fictitious configurations as worked out in Chapters 4 and 5, we develop a model formulation for anisotropic damage which is kinematically coupled to inelastic deformations, see e.g. the work by Hansen and Schreyer [HS94] or Menzel et al. [MS01g, MESR02]. Here we adopt the well-established framework of multiplicative elasto–plasticity; compare Chapter 3 and for a survey the reader is referred to Lubliner [Lub90, Chap. 8], Haupt [Hau00, Chap. 11], see also references cited therein, and the discussion by Naghdi [Nag90]. For conceptual clarity, we restrict ourselves to the rate-independent case without loss of generality. In particular, the previously highlighted framework of Lagrangian fictitious, microscopic configurations is adopted which has until now been mainly used in continuum damage mechanics; see e.g. Brüning [Brü01] for a similar approach. In this contribution, we relate elements of the tangent spaces of an undamaged, microscopic configuration and the standard intermediate configuration of multiplicative elasto–plasticity via a damage deformation gradient. Thereby, the previously mentioned covariance postulate is applied to the free Helmholtz energy density and the assumed damage dissipation potential. On top of this, a second fictitious configuration of Eulerian type is introduced and claimed to represent an isotropic setting with respect to the assumed plastic dissipation potential. Then, based on an essential kinematic assumption, the well-accepted concept of effective stress with respect to the construction of a yield function is a natural outcome of standard transformations in non-linear continuum mechanics, compare e.g. Lemaitre and Chaboche [LC98, Chap. 7].

The Chapter is organised as follows: To set the stage, the underlying kinematics related to the introduction of fictitious configurations are given in Section 6.1. Based on this, we set up the specific format of the free Helmholtz energy density, see Section 6.2. Later on, the Coleman–Noll entropy principle as based on the Clausius–Duhem inequality is applied within multiplicative elasto–plasticity as highlighted in Section 6.3. Thereby, the incorporated Finger-type metric tensor in terms of a fictitious linear tangent map is treated as an internal variable and denoted as damage metric tensor. Sec-

tion 6.4 deals with the framework of non–standard dissipative materials. Finally, we focus on the integration of the obtained evolution equations – Section 6.5 – and give some numerical examples in simple shear and a general finite element setting, see Section 6.6.

6.1 Kinematical framework of fictitious configurations

For convenience of the reader, this Section reiterates the concept of fictitious configurations in the context of multiplicative elasto–plasticity. In particular, we deal with two additional incompatible fictitious configurations, one of Lagrangian type ($\bar{\mathcal{B}}$) which is attached to the intermediate setting and a second of Eulerian type ($\tilde{\mathcal{B}}$) being connected to the spatial configuration.

In this direction, we first consider the fictitious configuration $\bar{\mathcal{B}}$ which is assumed to be isotropic with respect to the free Helmholtz energy density and attached to the intermediate configuration of multiplicative elasto–plasticity. The corresponding tangent space and the dual space are denoted by $T\bar{\mathcal{B}}$ and $T^*\bar{\mathcal{B}}$ (with $T^{**}\bar{\mathcal{B}} \doteq \bar{\mathcal{B}}$, respectively). Consequently, the direct fictitious linear tangent map $\bar{\mathbf{F}}^\sharp$ allows interpretation as pre–deformation. The corresponding fictitious natural and dual base vectors, the metric tensors and the identity are defined in Eqs.(4.1–4.3). In contrast to Chapters 4 and 5, this Lagrangian fictitious configuration $\bar{\mathcal{B}}$ is here attached to the intermediate setting \mathcal{B}_p (and not to \mathcal{B}_0) since the framework of multiplicative elasto–plasticity allows the picture of an elastic setting with respect to the intermediate configuration \mathcal{B}_p . Now the linear tangent maps of the direct and inverse Lagrangian fictitious motion consequently read

$$\boxed{\bar{\mathbf{F}}^\sharp = \bar{\mathbf{G}}_i \otimes \bar{\mathbf{G}}^i \in \mathbb{L}_+^3 : T\bar{\mathcal{B}} \rightarrow T\mathcal{B}_p, \quad \bar{\mathbf{f}}^\sharp = \bar{\mathbf{G}}_i \otimes \bar{\mathbf{G}}^i \in \mathbb{L}_+^3 : T\mathcal{B}_p \rightarrow T\bar{\mathcal{B}},} \quad (6.1)$$

see Figure 6.1 for a graphical representation.

Second, think of an Eulerian fictitious configuration ($\tilde{\mathcal{B}}$) which is isotropic with respect to an assumed plastic dissipation potential. Moreover, let this configuration $\tilde{\mathcal{B}}$ be attached to the previously introduced fictitious configuration $\bar{\mathcal{B}}$ and as well to the spatial setting \mathcal{B}_t . The corresponding tangent space and the dual space are respectively denoted by $T\tilde{\mathcal{B}}$ and $T^*\tilde{\mathcal{B}}$ (naturally we identify $T^{**}\tilde{\mathcal{B}} \doteq T\tilde{\mathcal{B}}$) and in analogy to Eq.(4.1) one obtains fictitious natural and dual base vectors

$$\tilde{\mathbf{g}}_i \in \mathbb{R}^3 : T^*\tilde{\mathcal{B}} \rightarrow \mathbb{R}, \quad \tilde{\mathbf{g}}^i \in \mathbb{R}^3 : T\tilde{\mathcal{B}} \rightarrow \mathbb{R} \quad (6.2)$$

whereby it is again the outcome that no interpretations as derivatives with respect to position vectors hold. The corresponding fictitious metric tensors and the second order identity consequently follow straightforward as

$$\begin{aligned} \tilde{\mathbf{g}}^b &= \tilde{g}_{ij} \tilde{\mathbf{g}}^i \otimes \tilde{\mathbf{g}}^j \in \mathbb{S}_+^3 : T\tilde{\mathcal{B}} \times T\tilde{\mathcal{B}} \rightarrow \mathbb{R}, \\ \tilde{\mathbf{g}}^\sharp &= \tilde{g}^{ij} \tilde{\mathbf{g}}_i \otimes \tilde{\mathbf{g}}_j \in \mathbb{S}_+^3 : T^*\tilde{\mathcal{B}} \times T^*\tilde{\mathcal{B}} \rightarrow \mathbb{R}, \\ \tilde{\mathbf{g}}^\sharp &= \tilde{\mathbf{g}}_i \otimes \tilde{\mathbf{g}}^i \in \mathbb{S}_+^3 : T^*\tilde{\mathcal{B}} \times T\tilde{\mathcal{B}} \rightarrow \mathbb{R}, \end{aligned} \quad (6.3)$$

and $\tilde{\mathbf{g}}^\sharp = \det^{-1}(\tilde{\mathbf{g}}^b) \text{cof}(\tilde{\mathbf{g}}^b)$. Likewise, the linear tangent maps of the direct and inverse fictitious motions read as

$$\boxed{\begin{aligned} \bar{\mathbf{F}}_e^\sharp &= \tilde{\mathbf{g}}_i \otimes \bar{\mathbf{G}}^i \in \mathbb{L}_+^3 : T\bar{\mathcal{B}} \rightarrow T\tilde{\mathcal{B}}, & \bar{\mathbf{f}}_e^\sharp &= \bar{\mathbf{G}}_i \otimes \tilde{\mathbf{g}}^i \in \mathbb{L}_+^3 : T\tilde{\mathcal{B}} \rightarrow T\bar{\mathcal{B}}, \\ \tilde{\mathbf{F}}^\sharp &= \mathbf{g}_i \otimes \tilde{\mathbf{g}}^i \in \mathbb{L}_+^3 : T\tilde{\mathcal{B}} \rightarrow T\mathcal{B}_t, & \tilde{\mathbf{f}}^\sharp &= \tilde{\mathbf{g}}_i \otimes \mathbf{g}^i \in \mathbb{L}_+^3 : T\mathcal{B}_t \rightarrow T\tilde{\mathcal{B}}, \end{aligned}} \quad (6.4)$$

see Figure 6.1 for a graphical representation. In particular we end up with the useful relations

$$\tilde{\mathbf{F}}^\sharp = \mathbf{F}_e^\sharp \cdot \bar{\mathbf{F}}^\sharp \cdot \bar{\mathbf{f}}_e^\sharp, \quad \tilde{\mathbf{f}}^\sharp = \bar{\mathbf{F}}_e^\sharp \cdot \tilde{\mathbf{f}}^\sharp \cdot \mathbf{f}_e^\sharp. \quad (6.5)$$

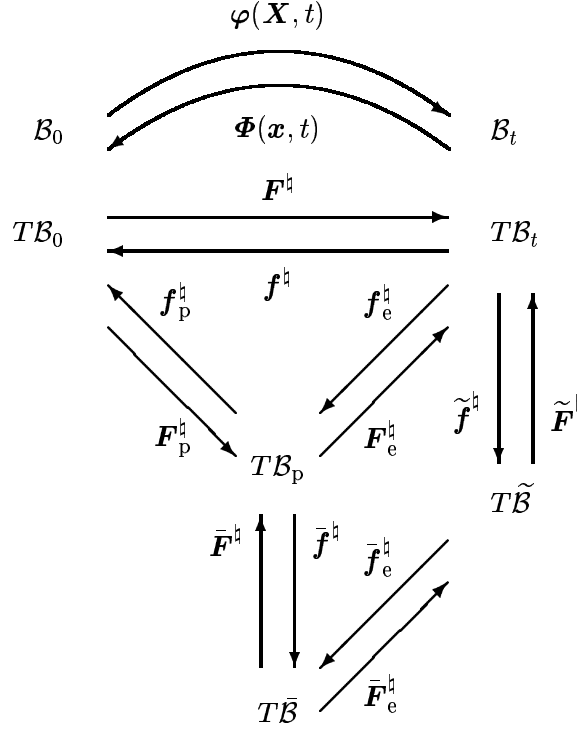


Figure 6.1: Non-linear point map φ and linear tangent maps \mathbf{F}^\sharp , \mathbf{F}_p^\sharp , \mathbf{F}_e^\sharp , $\bar{\mathbf{F}}^\sharp$, $\bar{\mathbf{F}}_e^\sharp$, $\tilde{\mathbf{F}}^\sharp$.

6.2 Construction of the free Helmholtz energy density

For the construction of the free Helmholtz energy density ψ_0^p with respect to the intermediate configuration, a contra-variant energy metric or rather damage tensor (Finger-type) is introduced and, in analogy to Chapters 4 and 5, denoted by $\bar{\mathbf{A}}^\sharp$ in $\bar{\mathcal{B}}$ and $\hat{\mathbf{A}}^\sharp \in \mathbb{S}_+^3 : T^*\mathcal{B}_p \times T^*\mathcal{B}_p \rightarrow \mathbb{R}$, respectively, with $\hat{\mathbf{A}}^\sharp = \bar{\mathbf{F}}^\sharp_* \bar{\mathbf{A}}^\sharp$ being obvious.

In this context, we adopt the common ansatz of an additive decomposition of the free Helmholtz energy density into an elastic or rather damage contribution and an additional hardening term defined by a scalar-valued hardening variable κ , i.e. $\psi_0^0(\mathbf{E}^b, \mathbf{A}^\sharp; \mathbf{X}) \doteq \text{dam}\psi_0^0(\mathbf{E}^b, \mathbf{A}^\sharp; \mathbf{X}) + \text{har}\psi_0(\kappa; \mathbf{X})$ in \mathcal{B}_0 , compare Eq.(5.1) and footnote † on page 87. For the crucial relation between the intermediate and the attached Lagrangian fictitious configuration, we obtain

$$\boxed{\text{dam}\psi_0^0(\bar{\mathbf{E}}_e^b, \bar{\mathbf{A}}^\sharp; \mathbf{X}) + \text{har}\psi_0(\kappa; \mathbf{X}) = \text{dam}\psi_0^p(\hat{\mathbf{E}}_e^b, \hat{\mathbf{A}}^\sharp; \mathbf{X}) + \text{har}\psi_0(\kappa; \mathbf{X})} \quad (6.6)$$

with $\hat{\mathbf{E}}_e^b = \frac{1}{2}[\hat{\mathbf{C}}_e^b - \hat{\mathbf{G}}^b]$, compare Eqs.(2.7, 3.3). Conceptually speaking, the free Helmholtz energy density remains invariant under any covariant action of a non-singular linear tangent map, here $\bar{\mathbf{F}}^\sharp$ whereby it is obvious that the elastic strain tensor transforms as

$$\bar{\mathbf{f}}^\sharp_* \bar{\mathbf{E}}_e^b = [\bar{\mathbf{f}}^\sharp]^\sharp \cdot \bar{\mathbf{E}}_e^b \cdot \bar{\mathbf{f}}^\sharp = \hat{\mathbf{E}}_e^b. \quad (6.7)$$

Since the fictitious configuration is assumed to be isotropic, three (basic) invariants in terms of $\bar{\mathbf{E}}_e^b \in \mathbb{S}^3 : T\bar{\mathcal{B}} \times T\bar{\mathcal{B}} \rightarrow \mathbb{R}$ and $\bar{\mathbf{A}}^\sharp$ determine the elastic or rather damage contribution to the free Helmholtz energy density. Application of standard transformations renders two corresponding sets of invariants ($i = 1, 2, 3$)

$$\bar{\mathbf{E}}_e^b \bar{\mathbf{A}}^\sharp I_i = \bar{\mathbf{G}}^\sharp : [\bar{\mathbf{E}}_e^b \cdot \bar{\mathbf{A}}^\sharp]^i = \hat{\mathbf{G}}^\sharp : [\hat{\mathbf{E}}_e^b \cdot \hat{\mathbf{A}}^\sharp]^i = \hat{\mathbf{E}}_e^b \hat{\mathbf{A}}^\sharp I_i, \quad (6.8)$$

now in terms of the elastic Green-Lagrange strain tensor.

Remark 6.1 *As an alternative formulation to the classical scalar–valued hardening contribution $\text{har}\psi_0(\kappa; \mathbf{X})$ in Eq.(6.6), one could introduce $\text{har}\psi_0^{\text{P}}(\widehat{\mathbf{K}}^b, \widehat{\mathbf{A}}^\sharp; \mathbf{X})$ incorporating a symmetric second order tensor $\widehat{\mathbf{K}}^b \in \mathbb{S}^3 : \mathcal{TB}_{\text{p}} \times \mathcal{TB}_{\text{p}} \rightarrow \mathbb{R}$ or $\widehat{\mathbf{K}}^b \doteq \widehat{\mathbf{F}}^{\text{P}*} \widehat{\mathbf{K}}^b$, respectively, as an internal hardening variable. Then, based on the assumption of an isotropic fictitious configuration, similar to Eq.(6.8), we obtain two sets of three invariants which determine the hardening contribution to the free Helmholtz energy density*

$$\widehat{\mathbf{K}}^b \widehat{\mathbf{A}}^\sharp I_i = \widehat{\mathbf{G}}^\sharp : [\widehat{\mathbf{K}}^b \cdot \widehat{\mathbf{A}}^\sharp]^i = \widehat{\mathbf{G}}^\sharp : [\widehat{\mathbf{K}}^b \cdot \widehat{\mathbf{A}}^\sharp]^i = \widehat{\mathbf{K}}^b \widehat{\mathbf{A}}^\sharp I_i \quad (6.9)$$

with $i = 1, 2, 3$. Nevertheless, for the sake of conceptual clarity, we focus on the classical scalar–valued hardening approach in this Chapter as highlighted in Eq.(6.6). For a detailed outline on the application of Eq.(6.9) within small strain kinematics see Menzel et al. [MESR02] or Ekh et al. [EMRS02].

6.3 Coleman–Noll entropy principle

We now reiterate the Coleman–Noll entropy principle in analogy to Sections 3.3 and 5.1 and obtain the local form of the iso–thermal Clausius–Duhem inequality with respect to the intermediate configuration as

$$\mathcal{D}_0^{\text{P}} = [\widehat{\mathbf{M}}^\sharp]^t : \widehat{\mathbf{L}}^\sharp - \partial_{\widehat{\mathbf{E}}_e^b} \psi_0^{\text{P}} : \text{D}_t \widehat{\mathbf{E}}_e^b - \partial_{\widehat{\mathbf{A}}^\sharp} \psi_0^{\text{P}} : \text{D}_t \widehat{\mathbf{A}}^\sharp - \partial_\kappa \psi_0^{\text{P}} \text{D}_t \kappa \geq 0. \quad (6.10)$$

whereby the notation D_t denotes the material time derivative, $[\widehat{\mathbf{M}}^\sharp]^t$ characterises the Mandel tensor, see Eq.(3.16), and

$$\widehat{\mathbf{L}}^\sharp = \mathbf{f}_e^\sharp \cdot \mathbf{l}^\sharp \cdot \mathbf{F}_e^\sharp = \mathbf{f}_e^\sharp \cdot \text{D}_t \mathbf{F}_e^\sharp + \text{D}_t \mathbf{F}_e^\sharp \cdot \mathbf{f}_p^\sharp = \widehat{\mathbf{L}}_e^\sharp + \widehat{\mathbf{L}}_p^\sharp \quad (6.11)$$

determines the mixed–variant pull–back of the spatial velocity gradient with respect to the intermediate configuration, compare Eqs.(3.12, 3.17). Now, by taking into account the relationship

$$2 \text{D}_t \widehat{\mathbf{E}}_e^b = \text{D}_t [\mathbf{F}_e^\sharp]^t \cdot \mathbf{g}^b \cdot \mathbf{F}_e^\sharp + [\mathbf{F}_e^\sharp]^t \cdot \mathbf{g}^b \cdot \text{D}_t \mathbf{F}_e^\sharp = [\widehat{\mathbf{L}}_e^\sharp]^t \cdot \widehat{\mathbf{C}}_e^b + \widehat{\mathbf{C}}_e^b \cdot \widehat{\mathbf{L}}_e^\sharp = 2 \left[\widehat{\mathbf{C}}_e^b \cdot \widehat{\mathbf{L}}_e^\sharp \right]^{\text{sym}}, \quad (6.12)$$

the dissipation inequality allows the representation

$$\begin{aligned} \mathcal{D}_0^{\text{P}} &= [\widehat{\mathbf{M}}^\sharp]^t : \widehat{\mathbf{L}}^\sharp - \left[\widehat{\mathbf{C}}_e^b \cdot \partial_{\widehat{\mathbf{E}}_e^b} \psi_0^{\text{P}} \right] : \widehat{\mathbf{L}}_e^\sharp - \partial_{\widehat{\mathbf{A}}^\sharp} \psi_0^{\text{P}} : \text{D}_t \widehat{\mathbf{A}}^\sharp - \partial_\kappa \psi_0^{\text{P}} \text{D}_t \kappa \\ &= \left[[\widehat{\mathbf{M}}^\sharp]^t - \widehat{\mathbf{C}}_e^b \cdot \partial_{\widehat{\mathbf{E}}_e^b} \psi_0^{\text{P}} \right] : \widehat{\mathbf{L}}_e^\sharp + \left[\widehat{\mathbf{C}}_e^b \cdot \partial_{\widehat{\mathbf{E}}_e^b} \psi_0^{\text{P}} \right] : \widehat{\mathbf{L}}_p^\sharp - \partial_{\widehat{\mathbf{A}}^\sharp} \psi_0^{\text{P}} : \text{D}_t \widehat{\mathbf{A}}^\sharp - \partial_\kappa \psi_0^{\text{P}} \text{D}_t \kappa \geq 0. \end{aligned} \quad (6.13)$$

Following the standard argumentation of rational thermodynamics, appropriate stress fields are defined by

$$\boxed{\begin{aligned} [\widehat{\mathbf{M}}^\sharp]^t &\doteq \widehat{\mathbf{C}}_e^b \cdot \partial_{\widehat{\mathbf{E}}_e^b} \psi_0^{\text{P}} \doteq \widehat{\mathbf{C}}_e^b \cdot \partial_{\widehat{\mathbf{E}}_e^b}^{\text{dam}} \psi_0^{\text{P}} \doteq \widehat{\mathbf{C}}_e^b \cdot \widehat{\mathbf{S}}^\sharp, \\ -\widehat{\mathbf{Z}}^b &\doteq \partial_{\widehat{\mathbf{A}}^\sharp} \psi_0^{\text{P}} \doteq \partial_{\widehat{\mathbf{A}}^\sharp}^{\text{dam}} \psi_0^{\text{P}}, \\ -h &\doteq \partial_\kappa \psi_0^{\text{P}} \doteq \partial_\kappa^{\text{har}} \psi_0. \end{aligned}} \quad (6.14)$$

Thereby, with respect to the representation of the basic invariants in Eq.(6.8), the derivatives of the damage contribution of the free Helmholtz energy function $\text{dam}\psi_0^{\text{P}}$ take the following format

$$\begin{aligned} \widehat{\mathbf{S}}^\sharp &= \sum_{i=1}^3 i \partial_{\widehat{\mathbf{E}}_e^b \widehat{\mathbf{A}}^\sharp I_i} \text{dam}\psi_0^{\text{P}} \widehat{\mathbf{A}}^\sharp \cdot [\widehat{\mathbf{E}}_e^b \cdot \widehat{\mathbf{A}}^\sharp]^{[i-1]}, \\ -\widehat{\mathbf{Z}}^b &= \sum_{i=1}^3 i \partial_{\widehat{\mathbf{E}}_e^b \widehat{\mathbf{A}}^\sharp I_i} \text{dam}\psi_0^{\text{P}} \widehat{\mathbf{E}}_e^b \cdot [\widehat{\mathbf{A}}^\sharp \cdot \widehat{\mathbf{E}}_e^b]^{[i-1]}, \end{aligned} \quad (6.15)$$

compare Eq.(5.12). Now, with these definitions at hand, the reduced format of the isothermal dissipation inequality results in

$$\text{red}\mathcal{D}_0^{\text{P}} = [\widehat{\mathbf{M}}^\sharp]^t : \widehat{\mathbf{L}}_p^\sharp + \widehat{\mathbf{Z}}^b : \text{D}_t \widehat{\mathbf{A}}^\sharp + h \text{D}_t \kappa = \widehat{\mathbf{S}}^\sharp : \widehat{\mathbf{D}}_p^b + \widehat{\mathbf{Z}}^b : \text{D}_t \widehat{\mathbf{A}}^\sharp + h \text{D}_t \kappa \geq 0 \quad (6.16)$$

whereby the symmetric tensor $\widehat{\mathbf{D}}_p^b = [\widehat{\mathbf{C}}_e^b \cdot \widehat{\mathbf{L}}_p^{\sharp}]^{\text{sym}} \in \mathbb{S}^3 : \mathcal{TB}_p \times \mathcal{TB}_p \rightarrow \mathbb{R}$ has been introduced, compare Maugin [Mau94] with application to the more general framework based on the Eshelby stress tensor and $\det(\mathbf{F}_p^{\sharp}) \neq 1$. Note that $\widehat{\mathbf{W}}_p^b = [\widehat{\mathbf{C}}_e^b \cdot \widehat{\mathbf{L}}_p^{\sharp}]^{\text{skw}} \in \mathbb{W}^3 : \mathcal{TB}_p \times \mathcal{TB}_p \rightarrow \mathbb{R}$, which characterises the plastic spin with respect to $\widehat{\mathbf{C}}_e^b$, is obviously undetermined within the representation in Eq.(6.16)₂.

Next, following the standard framework, we introduce an admissible elastic cone with respect to the intermediate configuration

$$\mathbb{A}^p = \left\{ \left([\widehat{\mathbf{M}}^{\sharp}]^t, \bar{\mathbf{F}}^{\sharp}, h; \widehat{\mathbf{G}}^{\sharp}, \mathbf{X} \right) \mid \text{yie} \Phi^p \left([\widehat{\mathbf{M}}^{\sharp}]^t, \bar{\mathbf{F}}^{\sharp}, h; \widehat{\mathbf{G}}^{\sharp}, \mathbf{X} \right) \right. \\ \left. \doteq \text{pla} \Phi^p \left([\widehat{\mathbf{M}}^{\sharp}]^t, \bar{\mathbf{F}}^{\sharp}; \widehat{\mathbf{G}}^{\sharp}, \mathbf{X} \right) + \text{har} \Phi(h; \mathbf{X}) \leq 0 \right\} \quad (6.17)$$

which is determined by the convex functions $\text{pla} \Phi^p$ and $\text{har} \Phi$. Moreover, the existence of a dissipation potential of Lemaitre–type is assumed, see e.g. Lemaitre and Chaboche [LC98, Sect. 7.5.2] and Section 3.4, namely

$$\text{pot} \Phi^p \left([\widehat{\mathbf{M}}^{\sharp}]^t, \bar{\mathbf{F}}^{\sharp}, h, \widehat{\mathbf{Z}}^b; \widehat{\mathbf{G}}^{\sharp}, \widehat{\mathbf{A}}^{\sharp}, \mathbf{X} \right) \doteq \text{yie} \Phi^p \left([\widehat{\mathbf{M}}^{\sharp}]^t, \bar{\mathbf{F}}^{\sharp}, h; \widehat{\mathbf{G}}^{\sharp}, \mathbf{X} \right) + \text{dam} \Phi^p(\widehat{\mathbf{Z}}^b; \widehat{\mathbf{A}}^{\sharp}, \mathbf{X}) \quad (6.18)$$

which are specified in Section 6.4. In this context, appropriate evolution equations allow e.g. the following representation

$$\begin{aligned} \widehat{\mathbf{L}}_p^{\sharp} &= D_t \lambda \partial_{[\widehat{\mathbf{M}}^{\sharp}]^t} \text{pot} \Phi^p = D_t \lambda \partial_{[\widehat{\mathbf{M}}^{\sharp}]^t} \text{pla} \Phi^p, \\ D_t \widehat{\mathbf{A}}^{\sharp} &= D_t \lambda \partial_{\widehat{\mathbf{Z}}^b} \text{pot} \Phi^p = D_t \lambda \partial_{\widehat{\mathbf{Z}}^b} \text{dam} \Phi^p, \\ D_t \kappa &= D_t \lambda \partial_h \text{pot} \Phi^p = D_t \lambda \partial_h \text{har} \Phi. \end{aligned} \quad (6.19)$$

We obviously deal with associated evolution equations for the plasticity and hardening contributions but the damage part nevertheless remains non–associated.

Remark 6.2 Recall that, in view of Eq.(6.16)₂, an alternative format of an associated evolution equation for $\widehat{\mathbf{L}}_p^{\sharp}$ can be introduced via

$$\begin{aligned} \widehat{\mathbf{D}}_p^b &= D_t \lambda \partial_{\widehat{\mathbf{S}}^{\sharp}} \text{pla} \Phi^p \\ &= D_t \lambda \partial_{[\widehat{\mathbf{M}}^{\sharp}]^t} \text{pla} \Phi^p : \partial_{\widehat{\mathbf{S}}^{\sharp}} \left[\widehat{\mathbf{C}}_e^b \cdot \widehat{\mathbf{S}}^{\sharp} \right] \\ &= D_t \lambda \partial_{[\widehat{\mathbf{M}}^{\sharp}]^t} \text{pla} \Phi^p : \frac{1}{2} \left[\widehat{\mathbf{C}}_e^b \overline{\otimes} \widehat{\mathbf{G}}^{\sharp} + \widehat{\mathbf{C}}_e^b \underline{\otimes} \widehat{\mathbf{G}}^{\sharp} \right] \\ &= D_t \lambda \left[\widehat{\mathbf{C}}_e^b \cdot \partial_{[\widehat{\mathbf{M}}^{\sharp}]^t} \text{pla} \Phi^p \right]^{\text{sym}}, \end{aligned} \quad (6.20)$$

compare Miehe and Stein [MS92] and Section 3.5.

Remark 6.3 Please note that the incorporation of the second order tensor $\widehat{\mathbf{K}}^b \in \mathbb{S}^3 : \mathcal{TB}_p \times \mathcal{TB}_p \rightarrow \mathbb{R}$, which accounts for hardening, results in a reduced dissipation inequality of the format

$$\text{red} \mathcal{D}_0^p = [\widehat{\mathbf{M}}^{\sharp}]^t : \widehat{\mathbf{L}}_p^{\sharp} + \widehat{\mathbf{Z}}^b : D_t \widehat{\mathbf{A}}^{\sharp} + \widehat{\mathbf{H}}^{\sharp} : D_t \widehat{\mathbf{K}}^b \geq 0 \quad (6.21)$$

with $\widehat{\mathbf{H}}^{\sharp} = -\partial_{\widehat{\mathbf{K}}^b} \text{har} \psi_0^p \in \mathbb{S}^3 : T^* \mathcal{B}_p \times T^* \mathcal{B}_p \rightarrow \mathbb{R}$. In addition, the evolution equation $D_t \widehat{\mathbf{K}}^b = D_t \lambda \partial_{\widehat{\mathbf{H}}^{\sharp}} \text{pot} \Phi^p = D_t \lambda \partial_{\widehat{\mathbf{H}}^{\sharp}} \text{har} \Phi^p(\widehat{\mathbf{H}}^{\sharp}; \widehat{\mathbf{A}}^b, \mathbf{X})$ is a natural consequence, compare Menzel et al. [MESR02] or Ekh et al. [EMRS02].

6.4 Non–standard dissipative materials

In this Section we discuss the construction of the inelastic potentials within a Lemaitre–type model. We thereby choose different approaches concerning each single contribution. For the damage part, we apply the fundamental covariance postulate with respect to the intermediate and the Lagrangian fictitious configuration – similar to Section 5.2. Concerning the scalar–valued hardening contribution, well–established constitutive equations are adopted as introduced in Eq.(3.89). Finally, a specific kinematic assumption is incorporated for the plasticity framework, which essentially enables us to deal with the concept of effective stress.

6.4.1 Construction of the damage potential

We choose a quasi isotropic potential in the sequel which is quadratic in the damage stress field, namely

$$\text{dam}\Phi_{\text{fix}}^{\text{p}} \doteq \frac{1}{2} \delta_1 \widehat{\mathbf{Z}}^{\text{b}} \widehat{\mathbf{A}}^{\sharp} I_1^2 \implies \text{D}_t \widehat{\mathbf{A}}^{\sharp} = \text{D}_t \lambda \delta_1 \left[\widehat{\mathbf{Z}}^{\text{b}} : \widehat{\mathbf{A}}^{\sharp} \right] \widehat{\mathbf{A}}^{\sharp}. \quad (6.22)$$

compare Eqs.(3.91, 5.16). For anisotropic damage evolution, the previously applied representation

$$\text{dam}\Phi_{\text{cha}}^{\text{p}} \doteq \frac{1}{2} \delta_2 \widehat{\mathbf{Z}}^{\text{b}} \widehat{\mathbf{A}}^{\sharp} I_2 \implies \text{D}_t \widehat{\mathbf{A}}^{\sharp} = \text{D}_t \lambda \delta_2 \widehat{\mathbf{A}}^{\sharp} \cdot \widehat{\mathbf{Z}}^{\text{b}} \cdot [\widehat{\mathbf{A}}^{\sharp}]^{\text{t}} \quad (6.23)$$

is adopted, see Eqs.(3.93, 5.17). Recall that a detailed discussion of this prototype damage model (without coupling to plasticity) was given in Section 5.2 where we additionally commented on its positive dissipation contribution).

6.4.2 Construction of the hardening potential

For completeness, we reiterate the applied proportional hardening potential

$$\text{har}\Phi \doteq -\frac{1}{3} [Y_0 - h(\kappa)]^2 \implies \text{D}_t \kappa = \text{D}_t \lambda \frac{2}{3} [Y_0 - h(\kappa)] \quad (6.24)$$

as introduced in Eq.(3.89).

Remark 6.4 *Similar to Remark 6.1, we alternatively obtain two sets of invariants under the isotropy assumption $\bar{\mathbf{A}}^{\text{b}} \doteq \bar{\mathbf{G}}^{\text{b}}$ for the fictitious configuration ($i = 1, 2, 3$)*

$$\bar{\mathbf{A}}^{\text{b}} \bar{\mathbf{H}}^{\sharp} I_i = \bar{\mathbf{G}}^{\text{b}} : \left[\bar{\mathbf{A}}^{\text{b}} \cdot \bar{\mathbf{H}}^{\sharp} \right]^i = \widehat{\mathbf{G}}^{\text{b}} : \left[\widehat{\mathbf{A}}^{\text{b}} \cdot \widehat{\mathbf{H}}^{\sharp} \right]^i = \widehat{\mathbf{A}}^{\text{b}} \widehat{\mathbf{H}}^{\sharp} I_i \quad (6.25)$$

with $\widehat{\mathbf{H}}^{\sharp} = -\partial_{\widehat{\mathbf{K}}^{\text{b}}} \text{har}\psi_0^{\text{p}}(\widehat{\mathbf{K}}^{\text{b}}, \widehat{\mathbf{A}}^{\sharp}; \mathbf{X})$ and $\bar{\mathbf{H}}^{\sharp} = \bar{\mathbf{f}}_{\star} \widehat{\mathbf{H}}^{\sharp}$, which define the alternative hardening potential $\text{har}\Phi^{\text{p}}(\widehat{\mathbf{A}}^{\text{b}} \widehat{\mathbf{H}}^{\sharp} I_{1,2,3})$.

6.4.3 Construction of the plastic potential

Next, for the definition of the invariants which enter the plastic contribution of the dissipation potential, we assume the Eulerian fictitious configuration $\widetilde{\mathcal{B}}$ to represent an isotropic setting. Now, similar to $\bar{\mathbf{A}}^{\text{b}}$ within the damage formulation, $\widetilde{\mathbf{p}}^{\text{b}} \in \mathbb{S}_+^3 : T\widetilde{\mathcal{B}} \times T\widetilde{\mathcal{B}} \rightarrow \mathbb{R}$ denotes a co–variant inelastic metric. In the following, $\widetilde{\mathbf{p}}^{\text{b}} \doteq \widetilde{\mathbf{g}}^{\text{b}}$ is assumed and we thus define an isotropic configuration for

$$\boxed{\text{pla}\widetilde{\Phi} = \text{pla}\widetilde{\Phi}(\widetilde{\boldsymbol{\tau}}^{\sharp}; \widetilde{\mathbf{p}}^{\text{b}}; \mathbf{X}) \doteq \text{pla}\widetilde{\Phi}(\widetilde{\boldsymbol{\tau}}^{\sharp}; \widetilde{\mathbf{g}}^{\text{b}}; \mathbf{X})} \quad (6.26)$$

whereby $\widetilde{\boldsymbol{\tau}}^{\sharp} = \widetilde{\mathbf{f}}_{\star}^{\sharp} \boldsymbol{\tau}^{\sharp} \in \mathbb{S}^3 : T^*\widetilde{\mathcal{B}} \times T^*\widetilde{\mathcal{B}} \rightarrow \mathbb{R}$ represents the pull–back to $\widetilde{\mathcal{B}}$ of the Kirchhoff stress tensor in \mathcal{B}_t . Standard transformations now yield the plastic potential with respect to the intermediate configuration

$$\text{pla}\widetilde{\Phi} = \text{pla}\widetilde{\Phi}(\bar{\mathbf{F}}^{\text{b}} \star \bar{\mathbf{f}}_{\text{e}\star}^{\sharp} \widetilde{\boldsymbol{\tau}}^{\sharp}; \bar{\mathbf{f}}_{\text{e}\star}^{\sharp} \bar{\mathbf{F}}_{\text{e}\star}^{\text{b}} \widetilde{\mathbf{p}}^{\text{b}}, \mathbf{X}) = \text{pla}\bar{\Phi}(\bar{\mathbf{F}}^{\text{b}} \star \bar{\mathbf{S}}^{\sharp}; \bar{\mathbf{f}}_{\text{e}\star}^{\sharp} \bar{\mathbf{P}}^{\text{b}}, \mathbf{X}) = \text{pla}\Phi^{\text{p}}(\widehat{\mathbf{S}}^{\sharp}; \widehat{\mathbf{P}}^{\text{b}}, \mathbf{X}). \quad (6.27)$$

Please note that $\widehat{\mathbf{S}}^\sharp = \bar{\mathbf{F}}^\sharp \star \bar{\mathbf{f}}_{e^\star}^\sharp \widehat{\mathbf{f}}_{e^\star}^\sharp \boldsymbol{\tau}^\sharp = \mathbf{f}_{e^\star}^\sharp \boldsymbol{\tau}^\sharp$ denotes the pull-back of the Kirchhoff stress to the intermediate configuration. Based on this, we make the key assumption of the proposed plasticity framework, namely that the fictitious elastic linear tangent map $\bar{\mathbf{F}}_e^\sharp$ equals the elastic linear tangent map \mathbf{F}_e^\sharp of the multiplicative decomposition. Consequently, in view of the involved Cauchy–Green–type tensors, we obtain the crucial relationship (for notational simplicity the underlying shifters are ignored)

$$\boxed{\begin{aligned} \bar{\mathbf{F}}_e^\sharp &\equiv \mathbf{F}_e^\sharp &\implies \bar{\mathbf{P}}^b &= \bar{\mathbf{F}}_e^\sharp \star \widehat{\mathbf{p}}^b = [\bar{\mathbf{F}}_e^\sharp]^\dagger \cdot \widehat{\mathbf{p}}^b \cdot \bar{\mathbf{F}}_e^\sharp \\ & & &\equiv \mathbf{F}_e^\sharp \star \mathbf{g}^b = [\mathbf{F}_e^\sharp]^\dagger \cdot \mathbf{g}^b \cdot \mathbf{F}_e^\sharp = \widehat{\mathbf{C}}_e^b \end{aligned}} \quad (6.28)$$

based on $\widehat{\mathbf{p}}^b \doteq \widehat{\mathbf{g}}^b$. In this direction, the plastic part of the yield function with respect to the intermediate configuration results in

$$\boxed{\begin{aligned} \text{pla}_{\widehat{\Phi}}(\widehat{\boldsymbol{\tau}}^\sharp; \widehat{\mathbf{p}}^b, \mathbf{X}) &= \text{pla}_{\widehat{\Phi}}(\bar{\mathbf{F}}^\sharp \star \bar{\mathbf{f}}_{e^\star}^\sharp \widehat{\boldsymbol{\tau}}^\sharp; \bar{\mathbf{f}}^\sharp \star \bar{\mathbf{F}}_e^\sharp \star \widehat{\mathbf{p}}^b, \mathbf{X}) = \text{pla}_{\Phi^p}(\widehat{\mathbf{S}}^\sharp; \bar{\mathbf{f}}^\sharp \star \bar{\mathbf{P}}^b, \mathbf{X}) \\ &\equiv \text{pla}_{\Phi^p}(\widehat{\mathbf{S}}^\sharp; \bar{\mathbf{f}}^\sharp \star \widehat{\mathbf{C}}_e^b, \mathbf{X}) = \text{pla}_{\Phi^p}(\bar{\mathbf{f}}^\sharp \star \widehat{\mathbf{C}}_e^b \cdot \widehat{\mathbf{S}}^\sharp; \widehat{\mathbf{G}}^\sharp, \mathbf{X}) \\ &= \text{pla}_{\Phi^p}([\widehat{\mathbf{M}}_d^\sharp]^\dagger; \widehat{\mathbf{G}}^\sharp, \mathbf{X}) = \text{pla}_{\Phi^p}([\widehat{\mathbf{M}}_d^\sharp]^\dagger, \bar{\mathbf{F}}^\sharp; \widehat{\mathbf{G}}^\sharp, \mathbf{X}) \end{aligned}} \quad (6.29)$$

with the modified Mandel stress $[\widehat{\mathbf{M}}_d^\sharp]^\dagger \equiv \bar{\mathbf{f}}^\sharp \star \widehat{\mathbf{C}}_e^b \cdot \widehat{\mathbf{S}}^\sharp \in \mathbb{L}^3 : T\mathcal{B}_p \times T^*\mathcal{B}_p \rightarrow \mathbb{R}$. The fundamental covariance postulate has thereby been applied and an appropriate set of invariants is given by

$$\begin{aligned} \widehat{\mathbf{p}}^b \star \widehat{\boldsymbol{\tau}}^\sharp I_i &= \widehat{\mathbf{g}}^\sharp : [\widehat{\mathbf{p}}^b \cdot \widehat{\boldsymbol{\tau}}^\sharp]^i \\ &= \widehat{\mathbf{G}}^\sharp : [\bar{\mathbf{P}}^b \cdot \widehat{\mathbf{S}}^\sharp]^i = \bar{P}^b \bar{S}^\sharp I_i \\ &\equiv \widehat{\mathbf{G}}^\sharp : [\bar{\mathbf{f}}^\sharp \star \widehat{\mathbf{C}}_e^b \cdot \widehat{\mathbf{S}}^\sharp]^i = \bar{f}^\sharp \star \widehat{\mathbf{C}}_e^b \widehat{S}^\sharp I_i \\ &= \widehat{\mathbf{G}}^\sharp : [\widehat{\mathbf{C}}_e^b \cdot \bar{\mathbf{f}}^\sharp \star \widehat{\mathbf{S}}^\sharp]^i = \widehat{\mathbf{C}}_e^b \bar{f}^\sharp \star \widehat{S}^\sharp I_i \\ &\equiv \widehat{\mathbf{G}}^\sharp : [[\widehat{\mathbf{M}}_d^\sharp]^\dagger]^i = \widehat{G}^\sharp [\widehat{\mathbf{M}}_d^\sharp]^\dagger I_i \end{aligned} \quad (6.30)$$

for $i = 1, 2, 3$ which is based essentially on the assumed isotropy of $\widehat{\mathbf{B}}$ for the plastic potential. Note that in contrast to the free Helmholtz energy density, the linear tangent map $\bar{\mathbf{F}}^\sharp$ explicitly enters the yield function. Pausing for a moment, we see that this is obviously a nice feature since the introduction of a damage spin within the coupling to plasticity is possible. Note that the set of invariants allows the representations

$$\begin{aligned} \widehat{G}^\sharp [\widehat{\mathbf{M}}_d^\sharp]^\dagger I_i &= \widehat{G}^\sharp [\widehat{\mathbf{M}}_d^\sharp]^\dagger I_i \\ &= \widehat{\mathbf{G}}^\sharp : [\widehat{\mathbf{C}}_e^b \cdot [\bar{\mathbf{f}}^\sharp]^\dagger \cdot \widehat{\mathbf{S}}^\sharp]^i = \widehat{\mathbf{C}}_e^b \cdot [\bar{\mathbf{f}}^\sharp]^\dagger \widehat{S}^\sharp I_i \\ &= \widehat{\mathbf{G}}^\sharp : [\widehat{\mathbf{C}}_e^b \cdot \widehat{\mathbf{S}}_{\bar{\mathbf{f}}^\sharp}^\sharp]^i = \widehat{\mathbf{C}}_e^b \widehat{S}_{\bar{\mathbf{f}}^\sharp}^\sharp I_i \end{aligned} \quad (6.31)$$

$$\begin{aligned} \text{with } \widehat{\mathbf{C}}_e^b \cdot [\bar{\mathbf{f}}^\sharp]^\dagger &= [[\bar{\mathbf{f}}^\sharp]^\dagger \otimes [\bar{\mathbf{f}}^\sharp]^\dagger] : \widehat{\mathbf{C}}_e^b \\ \text{and } \widehat{\mathbf{S}}_{\bar{\mathbf{f}}^\sharp}^\sharp &= [\bar{\mathbf{f}}^\sharp \otimes \bar{\mathbf{f}}^\sharp] : \widehat{\mathbf{S}}^\sharp \end{aligned}$$

for $i = 1, 2, 3$, which underlines that the modified Mandel stress tensor $[\widehat{\mathbf{M}}_d^\sharp]^\dagger \equiv \widehat{\mathbf{C}}_e^b \cdot [\bar{\mathbf{f}}^\sharp]^\dagger \cdot \widehat{\mathbf{S}}^\sharp$, entering the plastic part of the yield function, is essentially obtained by a linear map of $\widehat{\mathbf{C}}_e^b$ via the fourth order tensor $[\bar{\mathbf{f}}^\sharp]^\dagger \otimes [\bar{\mathbf{f}}^\sharp]^\dagger$ which accounts for anisotropy and degradation. Conceptually speaking, the appropriate metric tensor, with respect to the intermediate configuration, is modified such that anisotropy

and degradation are incorporated into the yield function. Alternatively, a modified or rather effective stress tensor can be introduced to construct the appropriate set of invariants which is then determined by the linear mapping of $\widehat{\mathbf{S}}^\sharp$ under the action of $\widehat{\mathbf{f}}^\sharp \otimes \widehat{\mathbf{f}}^\sharp$. Further, when referring to the Lagrangian fictitious configuration, we deal with the well–accepted postulate of effective stress for the construction of the plastic potential.

Next, in view of Eq.(6.19)₁, the corresponding associated evolution equation is given as

$$\begin{aligned}\widehat{\mathbf{L}}_p^\sharp &= D_t \lambda \partial_{[\widehat{\mathbf{M}}_d^\sharp]^\dagger}^{\text{pot}} \Phi^p \\ &= D_t \lambda \partial_{[\widehat{\mathbf{M}}_d^\sharp]^\dagger}^{\text{pla}} \Phi^p : \partial_{\widehat{\mathbf{S}}^\sharp} [\widehat{\mathbf{M}}_d^\sharp]^\dagger : \partial_{[\widehat{\mathbf{M}}_d^\sharp]^\dagger} \widehat{\mathbf{S}}^\sharp \\ &= D_t \lambda \partial_{[\widehat{\mathbf{M}}_d^\sharp]^\dagger}^{\text{pla}} \Phi^p : \frac{1}{2} \left[\widehat{\mathbf{C}}_e^b [\widehat{\mathbf{f}}^\sharp]^\dagger \cdot \widehat{\mathbf{B}}_e^\sharp \right] \overline{\otimes} \widehat{\mathbf{G}}^\sharp + \widehat{\mathbf{C}}_e^b [\widehat{\mathbf{f}}^\sharp]^\dagger \underline{\otimes} \widehat{\mathbf{B}}_e^\sharp \end{aligned} \quad (6.32)$$

$$\text{with } \partial_{\widehat{\mathbf{S}}^\sharp} [\widehat{\mathbf{M}}_d^\sharp]^\dagger = \frac{1}{2} \left[\widehat{\mathbf{C}}_e^b [\widehat{\mathbf{f}}^\sharp]^\dagger \overline{\otimes} \widehat{\mathbf{G}}^\sharp + \widehat{\mathbf{C}}_e^b [\widehat{\mathbf{f}}^\sharp]^\dagger \underline{\otimes} \widehat{\mathbf{G}}^\sharp \right]$$

$$\text{and } \partial_{[\widehat{\mathbf{M}}_d^\sharp]^\dagger} \widehat{\mathbf{S}}^\sharp = \widehat{\mathbf{B}}_e^\sharp \overline{\otimes} \widehat{\mathbf{G}}^\sharp$$

whereby the applied relation $\widehat{\mathbf{B}}_e^\sharp = \det^{-1}(\widehat{\mathbf{C}}_e^b) \text{cof}(\widehat{\mathbf{C}}_e^b)$ has been introduced in Eq.(3.3). Summarising, we obtain the more compact format

$$\boxed{\begin{aligned}\widehat{\mathbf{L}}_p^\sharp &= D_t \lambda \frac{1}{2} \left[\widehat{\mathbf{B}}_e^\sharp \cdot \widehat{\mathbf{C}}_e^b [\widehat{\mathbf{f}}^\sharp]^\dagger \cdot \partial_{[\widehat{\mathbf{M}}_d^\sharp]^\dagger}^{\text{pla}} \Phi^p + \widehat{\mathbf{B}}_e^\sharp \cdot \left[\partial_{[\widehat{\mathbf{M}}_d^\sharp]^\dagger}^{\text{pla}} \Phi^p \right]^\dagger \cdot \widehat{\mathbf{C}}_e^b [\widehat{\mathbf{f}}^\sharp]^\dagger \right] \\ &= D_t \lambda \left[\widehat{\mathbf{B}}_e^\sharp \cdot \left[\widehat{\mathbf{C}}_e^b [\widehat{\mathbf{f}}^\sharp]^\dagger \cdot \partial_{[\widehat{\mathbf{M}}_d^\sharp]^\dagger}^{\text{pla}} \Phi^p \right]^{\text{sym}} \right] \\ &\doteq D_t \lambda \widehat{\mathbf{N}}_{\widehat{\mathbf{f}}^\sharp}^\sharp \left(\widehat{\mathbf{N}}_d^\sharp, \widehat{\mathbf{C}}_e^b [\widehat{\mathbf{f}}^\sharp]^\dagger, \widehat{\mathbf{B}}_e^\sharp \right) \quad \text{with } \widehat{\mathbf{N}}_d^\sharp = \partial_{[\widehat{\mathbf{M}}_d^\sharp]^\dagger}^{\text{pla}} \Phi^p\end{aligned}} \quad (6.33)$$

which has a surprisingly similar structure compared to Eq.(6.20).

Remark 6.5 *For the sake of transparency, consider the isotropic case of a spherical damage mapping with $\|\widehat{\mathbf{F}}^\sharp\| \doteq \sqrt{3[1-D]}$. The proposed framework then boils down to the classical isotropic $[1-D]$ damage formulation with coupling to plasticity, see e.g. Steinmann et al. [SMS94] or Lämmer and Tsakmakis [LT00].*

6.4.3.1 Prototype model

Concerning the plastic part of the dissipation function, the evolution of the damage spin is neglected for clarity's sake and the rotational term of $\widehat{\mathbf{f}}^\sharp$ is thus not incorporated; for a discussion on plastic spin, we refer to Dafalias [Daf98] and references cited therein. In this context, the polar decomposition theorem yields

$$\begin{aligned}\widehat{\mathbf{F}}^\sharp &= \widehat{\mathbf{R}}^\sharp \cdot \widehat{\mathbf{U}}^\sharp = \widehat{\mathbf{V}}^\sharp \cdot \widehat{\mathbf{R}}^\sharp, & \widehat{\mathbf{f}}^\sharp &= \widehat{\mathbf{r}}^\sharp \cdot \widehat{\mathbf{u}}^\sharp = \widehat{\mathbf{v}}^\sharp \cdot \widehat{\mathbf{r}}^\sharp, \\ \widehat{\mathbf{R}}^\sharp &\in \mathbb{O}_+^3 : \quad T\widehat{\mathbf{B}} \rightarrow T\mathcal{B}_p, & \widehat{\mathbf{r}}^\sharp &\in \mathbb{O}_+^3 : \quad T\mathcal{B}_p \rightarrow T\widehat{\mathbf{B}}, \\ \widehat{\mathbf{U}}^\sharp &\in \mathbb{L}_+^3 : \quad T^*\widehat{\mathbf{B}} \times T\widehat{\mathbf{B}} \rightarrow \mathbb{R}, & \widehat{\mathbf{u}}^\sharp &\in \mathbb{L}_+^3 : \quad T^*\mathcal{B}_p \times T\mathcal{B}_p \rightarrow \mathbb{R}, \\ \widehat{\mathbf{V}}^\sharp &\in \mathbb{L}_+^3 : \quad T^*\mathcal{B}_p \times T\mathcal{B}_p \rightarrow \mathbb{R}, & \widehat{\mathbf{v}}^\sharp &\in \mathbb{L}_+^3 : \quad T^*\widehat{\mathbf{B}} \times T\widehat{\mathbf{B}} \rightarrow \mathbb{R},\end{aligned} \quad (6.34)$$

with $[\widehat{\mathbf{R}}^\sharp]^\dagger = [\widehat{\mathbf{R}}^\sharp]^{-1} = \widehat{\mathbf{r}}^\sharp$ and $\widehat{\mathbf{u}}^\sharp, \widehat{\mathbf{V}}^\sharp, \widehat{\mathbf{v}}^\sharp, \widehat{\mathbf{U}}^\sharp$ turn out to be symmetric with respect to $\widehat{\mathbf{G}}^\sharp$ and $\widehat{\mathbf{G}}^\sharp$, respectively. Furthermore, note that the fictitious right and left stretch tensors are now determined by the damage metric tensor $\widehat{\mathbf{A}}^\sharp$ since the rotational part is assumed to equal the identity mapping; $\widehat{\mathbf{R}}^\sharp \equiv \widehat{\mathbf{r}}^\sharp$. In particular, we obtain

$$\widehat{\mathbf{A}}^\sharp \equiv \widehat{\mathbf{U}}^\sharp \cdot \widehat{\mathbf{G}}^\sharp \cdot [\widehat{\mathbf{U}}^\sharp]^\dagger \equiv \widehat{\mathbf{V}}^\sharp \cdot \widehat{\mathbf{G}}^\sharp \cdot [\widehat{\mathbf{V}}^\sharp]^\dagger, \quad [\widehat{\mathbf{A}}^\sharp]^{-1} \equiv [\widehat{\mathbf{u}}^\sharp]^\dagger \cdot \widehat{\mathbf{G}}^\sharp \cdot \widehat{\mathbf{u}}^\sharp \equiv [\widehat{\mathbf{v}}^\sharp]^\dagger \cdot \widehat{\mathbf{G}}^\sharp \cdot \widehat{\mathbf{v}}^\sharp. \quad (6.35)$$

With these assumptions at hand, the following restricted format of the plastic dissipation function is a natural outcome,

$$\begin{aligned} \text{pla}\Phi^{\#} &\doteq \text{pla}\Phi^{\#} \left(\left[[\widehat{\mathbf{v}}^{\natural}]^t \otimes \overline{[\widehat{\mathbf{v}}^{\natural}]^t} : \widehat{\mathbf{C}}_e^b \right] \cdot \widehat{\mathbf{S}}^{\#}; \widehat{\mathbf{G}}^{\natural}, \mathbf{X} \right) \\ &= \text{pla}\Phi^{\#} \left([\widehat{\mathbf{M}}_{\text{d}[\widehat{\mathbf{v}}^{\natural}]^t}^{\natural}]^t; \widehat{\mathbf{G}}^{\natural}, \mathbf{X} \right) = \text{pla}\Phi^{\#} \left(\widehat{\mathbf{G}}^{\natural} [\widehat{\mathbf{M}}_{\text{d}[\widehat{\mathbf{v}}^{\natural}]^t}^{\natural}]^t I_{1,2,3}; \mathbf{X} \right) \end{aligned} \quad (6.36)$$

whereby a similar abbreviation as defined in Eq.(6.31) has been applied. Recall that the alternative representation of the invariants, which was directly related to the postulate of effective stress referring to the fictitious configuration, results in $\text{pla}\Phi^{\#} \left(\widehat{\mathbf{C}}_e^b \cdot [\widehat{\mathbf{u}}^{\natural} \otimes \widehat{\mathbf{u}}^{\natural}] : \widehat{\mathbf{S}}^{\#}; \widehat{\mathbf{G}}^{\natural}, \mathbf{X} \right)$. Next, we define a stress deviator with respect to the Eulerian fictitious configuration (recall $\widetilde{\mathbf{p}}^{\#} \doteq \widetilde{\mathbf{g}}^{\#}$)

$$\begin{aligned} \text{dev} \widetilde{\boldsymbol{\tau}}^{\#} &\doteq \widetilde{\boldsymbol{\tau}}^{\#} - \frac{1}{3} [\widetilde{\mathbf{p}}^b : \widetilde{\boldsymbol{\tau}}^{\#}] \widetilde{\mathbf{p}}^{\#} \\ \text{dev} \widehat{\mathbf{S}}^{\#} &\doteq \widehat{\mathbf{S}}^{\#} - \frac{1}{3} [\widehat{\mathbf{C}}_e^b \cdot \widehat{\mathbf{S}}^{\#}] \widehat{\mathbf{B}}_e^{\#} \overline{\mathbf{U}}^{\natural} \\ \text{dev} [\widehat{\mathbf{M}}_{\text{d}[\widehat{\mathbf{v}}^{\natural}]^t}^{\natural}]^t &\doteq [\widehat{\mathbf{M}}_{\text{d}[\widehat{\mathbf{v}}^{\natural}]^t}^{\natural}]^t - \frac{1}{3} [\widehat{\mathbf{G}}^{\natural} : [\widehat{\mathbf{M}}_{\text{d}[\widehat{\mathbf{v}}^{\natural}]^t}^{\natural}]^t] [\widehat{\mathbf{G}}^{\natural}]^t = \widehat{\mathbf{C}}_e^b \cdot \text{dev} \widehat{\mathbf{S}}^{\#} \end{aligned} \quad (6.37)$$

which allows us to set up a v. Mises–type function

$$\text{pla}\Phi^{\#} \left([\widehat{\mathbf{M}}_{\text{d}[\widehat{\mathbf{v}}^{\natural}]^t}^{\natural}]^t; \widehat{\mathbf{G}}^{\natural} \right) \doteq \widehat{\mathbf{G}}^{\natural} \text{dev} [\widehat{\mathbf{M}}_{\text{d}[\widehat{\mathbf{v}}^{\natural}]^t}^{\natural}]^t I_2 = \widehat{\mathbf{G}}^{\natural} : \left[\widehat{\mathbf{C}}_e^b \cdot \text{dev} \widehat{\mathbf{S}}^{\#} \right]^2. \quad (6.38)$$

Finally, for completeness, we take into account the relation

$$\text{dev} \widehat{\mathbf{G}}^{\natural} \doteq \partial_{[\widehat{\mathbf{M}}_{\text{d}[\widehat{\mathbf{v}}^{\natural}]^t}^{\natural}]^t} \text{dev} [\widehat{\mathbf{M}}_{\text{d}[\widehat{\mathbf{v}}^{\natural}]^t}^{\natural}]^t = [\widehat{\mathbf{G}}^{\natural}]^t \otimes \widehat{\mathbf{G}}^{\natural} - \frac{1}{3} [\widehat{\mathbf{G}}^{\natural}]^t \otimes \widehat{\mathbf{G}}^{\natural} \quad (6.39)$$

with $\text{dev} \widehat{\mathbf{G}}^{\natural} : [\widehat{\mathbf{M}}_{\text{d}[\widehat{\mathbf{v}}^{\natural}]^t}^{\natural}]^t = \text{dev} [\widehat{\mathbf{M}}_{\text{d}[\widehat{\mathbf{v}}^{\natural}]^t}^{\natural}]^t$ being obvious (compare Appendix A.1) and with these definitions at hand, the v. Mises–type model results in the associated evolution equation

$$\begin{aligned} \widehat{\mathbf{L}}_p^{\natural} &= D_t \lambda \widehat{\mathbf{N}}_{[\widehat{\mathbf{v}}^{\natural}]^t}^{\natural} \left(\widehat{\mathbf{N}}_{\text{d}}^{\natural}, \widehat{\mathbf{C}}_e^b \cdot \widehat{\mathbf{N}}_{[\widehat{\mathbf{v}}^{\natural}]^t}^{\natural}, \widehat{\mathbf{B}}_e^{\#} \right), \\ \text{with } \widehat{\mathbf{N}}_{\text{d}}^{\natural} &= \partial_{\text{dev} [\widehat{\mathbf{M}}_{\text{d}[\widehat{\mathbf{v}}^{\natural}]^t}^{\natural}]^t} \text{pla}\Phi^{\#} : \text{dev} \widehat{\mathbf{G}}^{\natural} = 2 \text{dev} [\widehat{\mathbf{M}}_{\text{d}[\widehat{\mathbf{v}}^{\natural}]^t}^{\natural}]^t : \left[[\widehat{\mathbf{G}}^{\natural}]^t \otimes \widehat{\mathbf{G}}^{\natural} \right], \\ \text{and } \widehat{\mathbf{C}}_e^b \cdot \widehat{\mathbf{N}}_{[\widehat{\mathbf{v}}^{\natural}]^t}^{\natural} &= \left[[\widehat{\mathbf{v}}^{\natural}]^t \otimes \overline{[\widehat{\mathbf{v}}^{\natural}]^t} \right] : \left[[\mathbf{F}_e^{\natural}]^t \cdot \mathbf{g}^b \cdot \mathbf{F}_e^{\natural} \right], \\ \text{for } [\widehat{\mathbf{A}}^{\#}]^{-1} &\equiv [\widehat{\mathbf{v}}^{\natural}]^t \cdot \widehat{\mathbf{G}}^b \cdot \overline{\mathbf{v}}^{\natural}, \\ \text{and } \widehat{\mathbf{B}}_e^{\#} &= \mathbf{f}_e^{\natural} \cdot \mathbf{g}^{\#} \cdot [\mathbf{f}_e^{\natural}]^t, \end{aligned} \quad (6.40)$$

compare Eq.(6.33).

6.5 Numerical time integration

Let the time interval of interest be given by N time steps $\mathbb{T} = \bigcup_{n=0}^N [{}^n t, {}^{n+1} t]$. In the following, we highlight a strain driven staggered algorithm with respect to the Lagrange multiplier $D_t \lambda$ and the variables \mathbf{F}_e^{\natural} , $\widehat{\mathbf{A}}^{\#}$, κ . Recall that loading and un–loading have to be checked by each trial step at ${}^{n+1} \mathbf{F}_e^{\natural}$. An outline of the numerical setting for multiplicative elasto–plasticity is given, e.g., by Simo [Sim98, Chaps. III,IV] and Miehe and Stein [MS92].

For conceptual clarity, we apply an Euler backward integration with respect to the quasi isotropic damage setting

$${}^{n+1} \widehat{\mathbf{A}}^{\#} = {}^n \widehat{\mathbf{A}}^{\#} + \Delta \lambda \delta_1 [{}^{n+1} \widehat{\mathbf{Z}}^b : {}^{n+1} \widehat{\mathbf{A}}^{\#}] {}^{n+1} \widehat{\mathbf{A}}^{\#}, \quad (6.41)$$

as well as for anisotropic damage evolution (compare Section 5.3)

$${}^{n+1}\widehat{\mathbf{A}}^\sharp = {}^n\widehat{\mathbf{A}}^\sharp + \Delta\lambda \delta_2 {}^{n+1}\widehat{\mathbf{A}}^\sharp \cdot {}^{n+1}\widehat{\mathbf{Z}}^b \cdot {}^{n+1}\widehat{\mathbf{A}}^\sharp \quad (6.42)$$

and, once more for the proportional hardening variable

$${}^{n+1}\kappa = {}^n\kappa + \Delta\lambda \frac{2}{3} [Y_0 - h({}^{n+1}\kappa)]. \quad (6.43)$$

Although plastic incompressibility is not a key issue here, since plasticity is coupled to continuum damage, we adopt an exponential integration scheme for \mathbf{F}_p^\sharp . The corresponding evolution equation is constructed via Eqs.(6.11, 6.40) and reads as

$$D_t \mathbf{F}_p^\sharp \cdot \mathbf{f}_p^\sharp = \widehat{\mathbf{L}}_p^\sharp = D_t \lambda \widehat{\mathbf{N}}_{[\widehat{\mathbf{f}}^\sharp]^\dagger}^\sharp \implies D_t \mathbf{F}_p^\sharp = D_t \lambda \widehat{\mathbf{N}}_{[\widehat{\mathbf{f}}^\sharp]^\dagger}^\sharp \cdot \mathbf{F}_p^\sharp. \quad (6.44)$$

Based on this, straightforward application of the exponential integration scheme results in

$$\boxed{{}^{n+1}\mathbf{F}_p^\sharp = \exp(\Delta\lambda {}^{n+1}\widehat{\mathbf{N}}_{[\widehat{\mathbf{f}}^\sharp]^\dagger}^\sharp) \cdot {}^n\mathbf{F}_p^\sharp \implies {}^{n+1}\mathbf{f}_p^\sharp = {}^n\mathbf{f}_p^\sharp \cdot \exp(-\Delta\lambda {}^{n+1}\widehat{\mathbf{N}}_{[\widehat{\mathbf{f}}^\sharp]^\dagger}^\sharp)}, \quad (6.45)$$

see Weber and Anand [WA90]. In this direction, the elastic part of the deformation gradient allows the representation

$$\boxed{{}^{n+1}\mathbf{F}_e^\sharp = {}^{n+1}\mathbf{F}^\sharp \cdot {}^{n+1}\mathbf{f}_p^\sharp = {}^{n+1}\mathbf{F}_{e\text{tri}}^\sharp \cdot \exp(-\Delta\lambda {}^{n+1}\widehat{\mathbf{N}}_{[\widehat{\mathbf{f}}^\sharp]^\dagger}^\sharp)} \quad (6.46)$$

and ${}^{n+1}\widehat{\mathbf{N}}_{[\widehat{\mathbf{f}}^\sharp]^\dagger}^\sharp$ being obviously neither symmetric nor coaxial to ${}^{n+1}\widehat{\mathbf{C}}_e^b = [{}^{n+1}\mathbf{F}_e^\sharp]^\dagger \cdot \mathbf{g}^b \cdot {}^{n+1}\mathbf{F}_e^\sharp$, compare Eqs.(6.34,6.40) and Remark 6.6. With these integration schemes at hand, we are able to set up an outline of the applied algorithm – similar to Sections 3.7 and 5.3, see Algorithm 6.1. We choose a modified regula–falsi scheme in particular for the iteration of the Lagrange multiplier and a Newton algorithm to compute the set of internal variables. This strategy results in the following system of linear equations within each Newton iteration k

$$\begin{bmatrix} \text{dam } \widehat{\mathbf{J}}_{\widehat{\mathbf{A}}^\sharp}^\sharp & \text{dam } \widehat{\mathbf{J}}_{\mathbf{F}_e^\sharp}^\sharp \\ \text{pla } \mathbf{J}_{\widehat{\mathbf{A}}^\sharp}^\sharp & \text{pla } \mathbf{J}_{\mathbf{F}_e^\sharp}^\sharp \\ & \text{har } j_\kappa \end{bmatrix} \circ \begin{bmatrix} \Delta \widehat{\mathbf{A}}^\sharp \\ \Delta \mathbf{F}_e^\sharp \\ \Delta \kappa \end{bmatrix} = \begin{bmatrix} - \text{dam } \widehat{\mathbf{R}}^\sharp \\ - \text{pla } \mathbf{R}^\sharp \\ - \text{har } r \end{bmatrix} \quad (6.47)$$

whereby the notation \circ denotes the appropriate type of contraction and additional abbreviations have been introduced, in particular the residua

$$\begin{aligned} \text{dam } \widehat{\mathbf{R}}_{\text{fix}}^\sharp &= {}^{n+1}\widehat{\mathbf{A}}_k^\sharp - {}^n\widehat{\mathbf{A}}^\sharp - \Delta\lambda \delta_1 [{}^{n+1}\widehat{\mathbf{Z}}_k^b : {}^{n+1}\widehat{\mathbf{A}}_k^\sharp] {}^{n+1}\widehat{\mathbf{A}}_k^\sharp \\ \text{dam } \widehat{\mathbf{R}}_{\text{cha}}^\sharp &= {}^{n+1}\widehat{\mathbf{A}}_k^\sharp - {}^n\widehat{\mathbf{A}}^\sharp - \Delta\lambda \delta_2 {}^{n+1}\widehat{\mathbf{A}}_k^\sharp \cdot {}^{n+1}\widehat{\mathbf{Z}}_k^b \cdot {}^{n+1}\widehat{\mathbf{A}}_k^\sharp \\ \text{pla } \mathbf{R}^\sharp &= {}^{n+1}\mathbf{F}_{e\text{tri}}^\sharp - {}^{n+1}\mathbf{F}_{e\text{tri}}^\sharp \cdot \exp(-\Delta\lambda {}^{n+1}\widehat{\mathbf{N}}_{[\widehat{\mathbf{f}}^\sharp]^\dagger}^\sharp) \\ \text{har } r &= {}^{n+1}\kappa_k - {}^n\kappa - \Delta\lambda \frac{2}{3} [Y_0 - {}^{n+1}h_k] \end{aligned} \quad (6.48)$$

and the Jacobians

$$\begin{aligned} \text{dam } \widehat{\mathbf{J}}_{\widehat{\mathbf{A}}^\sharp}^\sharp &= \partial_{n+1}\widehat{\mathbf{A}}_k^\sharp \text{dam } \widehat{\mathbf{R}}^\sharp, & \text{dam } \widehat{\mathbf{J}}_{\mathbf{F}_e^\sharp}^\sharp &= \partial_{n+1}\mathbf{F}_{e\text{tri}}^\sharp \text{dam } \widehat{\mathbf{R}}^\sharp, \\ \text{pla } \mathbf{J}_{\widehat{\mathbf{A}}^\sharp}^\sharp &= \partial_{n+1}\widehat{\mathbf{A}}_k^\sharp \text{pla } \mathbf{R}^\sharp, & \text{pla } \mathbf{J}_{\mathbf{F}_e^\sharp}^\sharp &= \partial_{n+1}\mathbf{F}_{e\text{tri}}^\sharp \text{pla } \mathbf{R}^\sharp, \\ \text{har } j_\kappa &= \partial_{n+1}\kappa_k \text{har } r. \end{aligned} \quad (6.49)$$

An outline on the “exact” derivation of a Jacobian similar to $\text{pla } \mathbf{J}_{\mathbf{F}_e^\sharp}^\sharp$ is discussed by de Souza Neto [dSN01]. Here, we nevertheless adopt a numerical perturbation scheme to compute the Jacobians within the subsequent numerical examples. Moreover, within a finite element setting, it turns out to be advantageous to apply this finite difference approximation in addition to the global tangent operator. For convenience of the reader, Appendix E.2 reiterates the adopted algorithm.

Algorithm 6.1 *Staggered solution technique: Newton–type algorithm to solve the set of non–linear equations in $\widehat{\mathbf{A}}^\sharp$, \mathbf{F}_e^\sharp and κ embedded into a scalar–valued iteration (e.g. modified regula–falsi schemes) to compute the Lagrange multiplier $\Delta\lambda$.*

```

(Finite Element Method)   for given  ${}^{n+1}\mathbf{F}^\sharp$  do
                           if  ${}^{\text{vie}}\Phi^{\text{P}}|_{n+1} > 0$  then
(scalar–valued iteration)   dowhile  $|{}^{\text{vie}}\Phi^{\text{P}}(\Delta\lambda)|_{n+1} > \text{tol}$ 
                                $\Delta\lambda = \dots$ 
(Newton–type method)       dowhile  $\|{}^{\text{dam}}\widehat{\mathbf{R}}^\sharp\| + \|{}^{\text{pla}}\mathbf{R}^\sharp\| + |{}^{\text{har}}r| > \text{tol}$ 
                                $\dots$ 
                                ${}^{n+1}\widehat{\mathbf{A}}_{k+1}^\sharp = {}^{n+1}\widehat{\mathbf{A}}_k^\sharp + \Delta\widehat{\mathbf{A}}^\sharp$ 
                                ${}^{n+1}\mathbf{F}_{ek+1}^\sharp = {}^{n+1}\mathbf{F}_{ek}^\sharp + \Delta\mathbf{F}_e^\sharp$ 
                                ${}^{n+1}\kappa_{k+1} = {}^{n+1}\kappa_k + \Delta\kappa$ 
                               enddo
                           enddo
                           endif

```

Remark 6.6 *Recall that closed representations of exponential functions of second order tensors conveniently exist if the argument is symmetric or skew–symmetric (spectral representation, Euler–Rodrigues formula). In the case of a non–symmetric second order tensor, one has to apply a series expansion. From the computational point of view this procedure might be comparatively expensive since the series expansion should not be terminated until an appropriate norm of an element falls below a chosen tolerance. However, higher order powers allow representation via the Cayley–Hamilton theorem, which yields in the present context*

$$\exp(\widehat{\mathbf{N}}^\sharp) = \sum_{m=0}^{\infty} \frac{1}{m!} [\widehat{\mathbf{N}}^\sharp]^m, \quad [\widehat{\mathbf{N}}^\sharp]^m = J_1 [\widehat{\mathbf{N}}^\sharp]^{m-1} - J_2 [\widehat{\mathbf{N}}^\sharp]^{m-2} + J_3 [\widehat{\mathbf{N}}^\sharp]^{m-3}, \quad (6.50)$$

compare e.g. Miehe [Mie96a] and Appendix B.1 ^{||}. For a discussion on the computation of general tensor function we refer the reader to Betten [Bet84].

Remark 6.7 *In order to underline that the numerical approximation of the Jacobians is appropriate for the presented framework, we give an example of the exact, analytical evaluation of one single fourth order contribution. Thus, the derivation of the “simplest” Jacobian ${}^{\text{dam}}\widehat{\mathbf{J}}_{\widehat{\mathbf{A}}^\sharp}^\sharp$ is highlighted. In the case of quasi isotropic damage evolution, we obtain*

$${}^{\text{dam}}\widehat{\mathbf{J}}_{\widehat{\mathbf{A}}^\sharp}^\sharp = \left[1 - \Delta\lambda \delta_1 {}^{n+1}\widehat{\mathbf{Z}}^b : {}^{n+1}\widehat{\mathbf{A}}^\sharp \right] \text{sym}\widehat{\mathbf{G}}^\sharp - \Delta\lambda \delta_1 {}^{n+1}\widehat{\mathbf{A}}^\sharp \otimes \left[{}^{n+1}\widehat{\mathbf{Z}}^b - {}^{n+1}\widehat{\mathbf{A}}^\sharp : \widehat{\mathbf{A}}^b \right] \quad (6.51)$$

and anisotropic damage results in

$$\begin{aligned} {}^{\text{dam}}\widehat{\mathbf{J}}_{\widehat{\mathbf{A}}^\sharp}^\sharp &= \text{sym}\widehat{\mathbf{G}}^\sharp + \Delta\lambda \delta_2 \left[{}^{n+1}\widehat{\mathbf{A}}^\sharp \overline{\otimes} {}^{n+1}\widehat{\mathbf{A}}^\sharp \right] : \widehat{\mathbf{A}}^b \\ &- \Delta\lambda \delta_1 \left[\widehat{\mathbf{G}}^\sharp \overline{\otimes} \left[{}^{n+1}\widehat{\mathbf{A}}^\sharp \cdot {}^{n+1}\widehat{\mathbf{Z}}^b \right] + \widehat{\mathbf{G}}^\sharp \underline{\otimes} \left[{}^{n+1}\widehat{\mathbf{A}}^\sharp \cdot {}^{n+1}\widehat{\mathbf{Z}}^b \right] \right]^{\text{SYM}} \end{aligned} \quad (6.52)$$

^{||} Application of the identity $\det(\exp(\mathbf{d})) = \exp(\text{tr}(\mathbf{d})) \forall \mathbf{d} \in \mathbb{L}^n$ to the problem at hand yields $\det(\exp(\Delta\lambda \widehat{\mathbf{N}}^\sharp)) = \exp(\text{tr}(\Delta\lambda \widehat{\mathbf{N}}^\sharp))$ whereby the tr–operation refers to the appropriate metric, compare e.g. Weber and Anand [WA90] and Gurtin [Gur81, Sect. 36]. From Eq.(6.45) it is then obvious, that $\mathbf{F}_p^\sharp \in \mathbb{M}_+^3 : \mathcal{TB}_0 \rightarrow \mathcal{TB}_p$ if $\text{tr}(\widehat{\mathbf{N}}^\sharp) = 0$, which represents plastic incompressibility, see Remark 3.3 and footnote [†] on page 60 with respect to non–exponential integration schemes. Similar we obtain with Eq.(6.44) the equivalent relation $D_t \det(\mathbf{F}_p^\sharp) = \text{cof}(\mathbf{F}_p^\sharp) : [\widehat{\mathbf{L}}_p^\sharp \cdot \mathbf{F}_p^\sharp] \doteq 0 \implies \text{tr}(\widehat{\mathbf{L}}_p^\sharp) = 0$.

whereby the fourth order tensor ${}^{\text{sym}}\widehat{\mathbf{G}}^{\sharp}$ and $\widehat{\mathbf{A}}^{\flat}$ are defined in Appendix A.1 and in Eq.(5.26), respectively. The complexity of this “comparatively simple” contribution justifies the numerical approximation of the Jacobians in Eqs.(6.51,6.52), and apparently the approximation of the other fourth order Jacobians in Eq.(6.49). Moreover, it turns out that this approach is not immoderately expensive.

6.6 Numerical examples

For the following numerical examples where we discuss the overall anisotropic behaviour of the proposed framework, a typical compressible Neo–Hooke material is adopted. In particular, we choose

$$\text{dam}\psi_0^{\text{p}} = \frac{\mu}{2} \left[\widehat{C}_e^{\flat} \widehat{A}^{\sharp} J_1 - 3 \right] - \mu \ln \left(\widehat{C}_e^{\flat} \widehat{A}^{\sharp} J_3 \right) + \frac{\lambda}{2} \ln^2 \left(\widehat{C}_e^{\flat} \widehat{A}^{\sharp} J_3 \right) \quad (6.53)$$

as given in Eq.(C.4). The setting of anisotropic elasto–plasticity and the coupling to quasi isotropic and anisotropic damage are considered in detail. For both cases the anisotropy, or rather damage metric $\mathbf{A}^{\sharp}|_{t_0}$ is assumed to be non–spherical. In particular, we choose the initial anisotropy metric to be determined by the spherical coordinates $\vartheta_1^1 = \frac{5}{6}\pi$, $\vartheta_1^2 = \frac{1}{6}\pi$, $\vartheta_2^1 = \frac{1}{3}\pi$, $\vartheta_2^2 = \frac{1}{2}\pi$ and the scalars $\alpha_0 = 1$, $\alpha_1 = \frac{1}{4}$, $\alpha_2 = \frac{1}{2}$. Thus, from the beginning, the elastic behaviour is anisotropic. The material parameters for the Neo–Hooke material are assumed as $\mu = 10^4$ and $\lambda = 10^3$.

Moreover, concerning the hardening part of the free Helmholtz energy density, we account for the established additive decomposition into a saturation–type contribution and a quadratic term with respect to the scalar–valued hardening variable

$$\begin{aligned} \text{har}\psi_0(\kappa) &\doteq [Y_{\infty} - Y_0] [\kappa + \delta_3^{-1} \exp(-\delta_3 \kappa) - \delta_3^{-1}] + \frac{1}{2} \delta_4 \kappa^2 \\ \Rightarrow h(\kappa) &= [Y_0 - Y_{\infty}] [1 - \exp(-\delta_3 \kappa)] - \delta_4 \kappa \end{aligned} \quad (6.54)$$

as introduced in Section 3.8 with $Y_0 = 10^3$, $Y_{\infty} = 2 \times 10^3$ and $\delta_{3,4} = 10$.

In order to highlight the principal directions of specific symmetric second order tensors, like e.g. stress and strain, the method of stereo–graphic projection is applied and in view of the overall anisotropic material behaviour, the anisotropy measure δ is monitored, compare Appendix D.

6.6.1 Simple shear

Within the subsequent numerical examples of a homogeneous deformation in simple shear ($\mathbf{F} = \mathbf{I} + \gamma \mathbf{e}_1 \otimes \mathbf{e}^2$ with respect to a Cartesian frame and $\mathbf{I} = \delta^i_j \mathbf{e}_i \otimes \mathbf{e}^j$), it is clearly seen that the evolution of the norm of the deviatoric modified Mandel tensor $\|\text{dev}[\widehat{\mathbf{M}}_{\text{d}[\widehat{\mathbf{v}}^{\flat}]\sharp}^{\sharp}]\|$, which essentially enters the yield function, displays a typical saturation effect. On the contrary, due to the incorporated continuum damage, the corresponding norm of the spatial nominal Kirchhoff stress $\|\text{dev}\boldsymbol{\tau}^{\sharp}\|$, decreases. In the sequel, components of tensorial fields refer to a Cartesian frame, e.g. $[\bullet]^{ij} = \mathbf{e}^i \cdot [\bullet]^{\sharp} \cdot \mathbf{e}^j$.

6.6.1.1 Anisotropic elasto–plasticity

To set the stage, we firstly discuss a purely elasto–plastic body whereby no damage evolution takes place, $\delta_{1,2} = 0$. In this context, Figures 6.2–6.4 highlight the overall anisotropic behaviour. Representative properties of the Kirchhoff stress and the non–symmetric, modified Mandel tensor are given in Figure 6.2. The anisotropy measure in terms of strain and stress, $\delta(\widehat{\mathbf{E}}_e^{\flat}, \widehat{\mathbf{S}}^{\sharp})$, shows a strong dependence on the shear number γ and, due to the fact that no damage evolution is incorporated, all eigenvalues of the anisotropy metric remain constant during the deformation process, see Figure 6.3. In addition, the non–coaxiality of stress and strain is highlighted in Figure 6.4 for different shear numbers γ by applying the method of stereo–graphic projection. Next, we reverse the shear direction and consider unloading/reloading with respect to the deformation history $\gamma \in [0 \rightarrow 1, 1 \rightarrow 0]$. Figures 6.5 and 6.6 monitor the contributions of the Kirchhoff stress, the modified Mandel stress, the

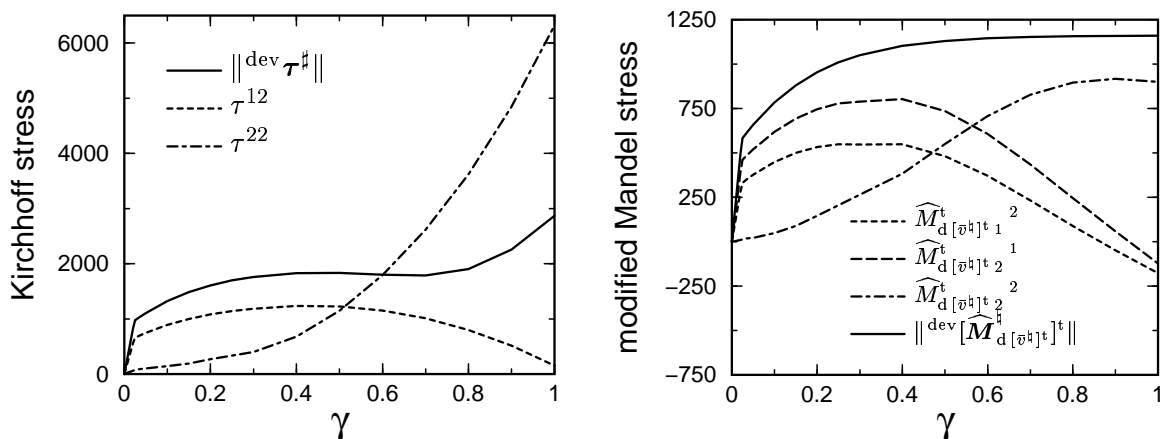


Figure 6.2: Simple shear, anisotropic elasto–plasticity: Kirchhoff stress $\tau^\#$ and modified Mandel stress $[\widehat{\mathbf{M}}_d^\#]_{[\widehat{\nu}^\#]^t}$.

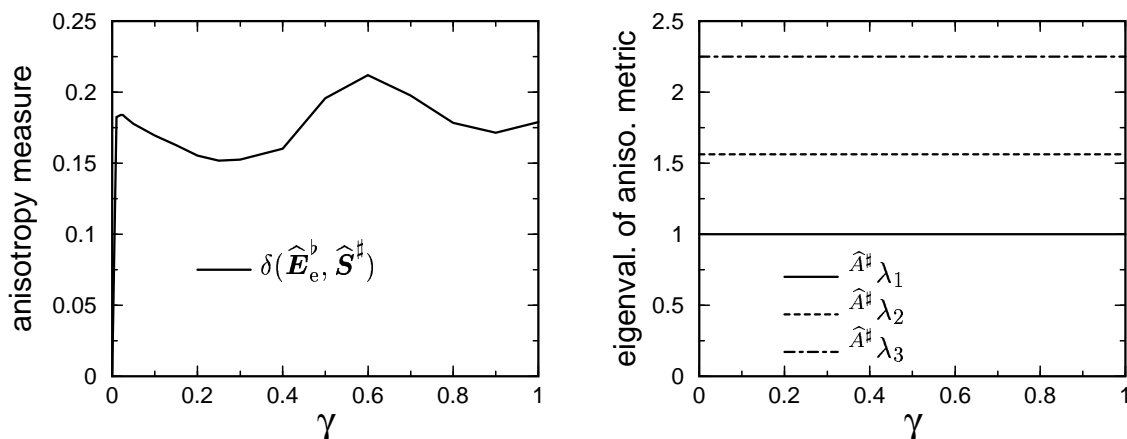


Figure 6.3: Simple shear, anisotropic elasto–plasticity: Anisotropy measure $\delta(\widehat{\mathbf{E}}_e^b, \widehat{\mathbf{S}}^\#)$ and eigenvalues of the anisotropy metric $\widehat{\mathbf{A}}^\# \lambda_{1,2,3}$.

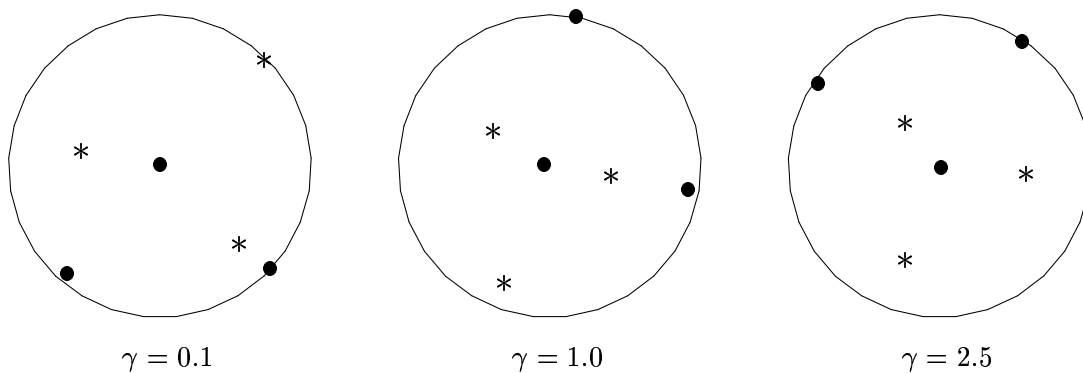


Figure 6.4: Simple shear, anisotropic elasto–plasticity: Stereo–graphic projection of strain $(\widehat{\mathbf{E}}_e^b : \bullet)$ and stress $(\widehat{\mathbf{S}}^\# : *)$ for different shear numbers γ .

anisotropy measure and the damage eigenvalues which are trivially constant for the considered setting. Against intuition, we do not observe an exclusive reloading behaviour as experienced in an isotropic setting, i.e. $\mathbf{A}^\sharp \propto \mathbf{G}^\sharp$. Apparently, this immediate loading effect results from the incorporated anisotropy and the comparatively small threshold. Finally, in analogy to Figure 6.4 we discuss

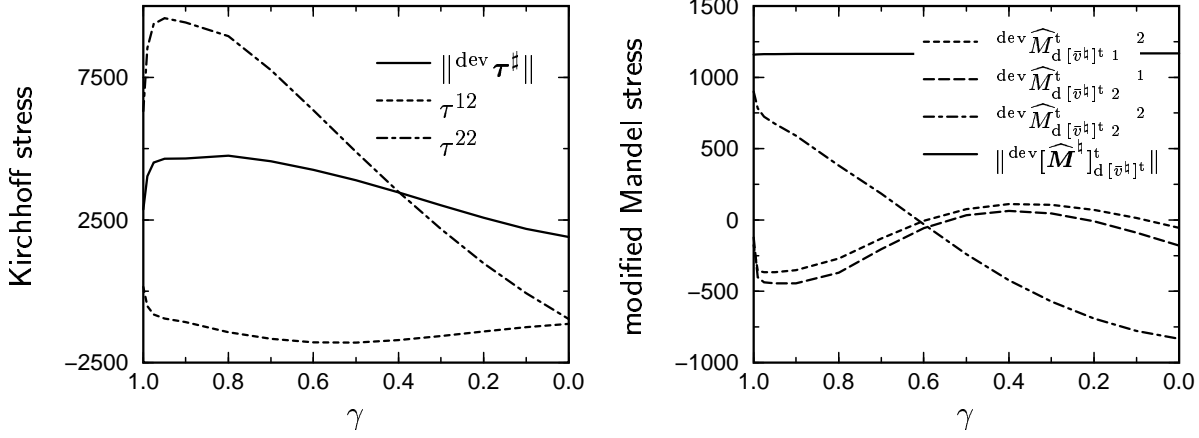


Figure 6.5: Simple shear, anisotropic elasto–plasticity, unloading/reloading: Kirchhoff stress τ^\sharp and modified Mandel stress $[\widehat{\mathbf{M}}_d^\sharp]^\dagger$.

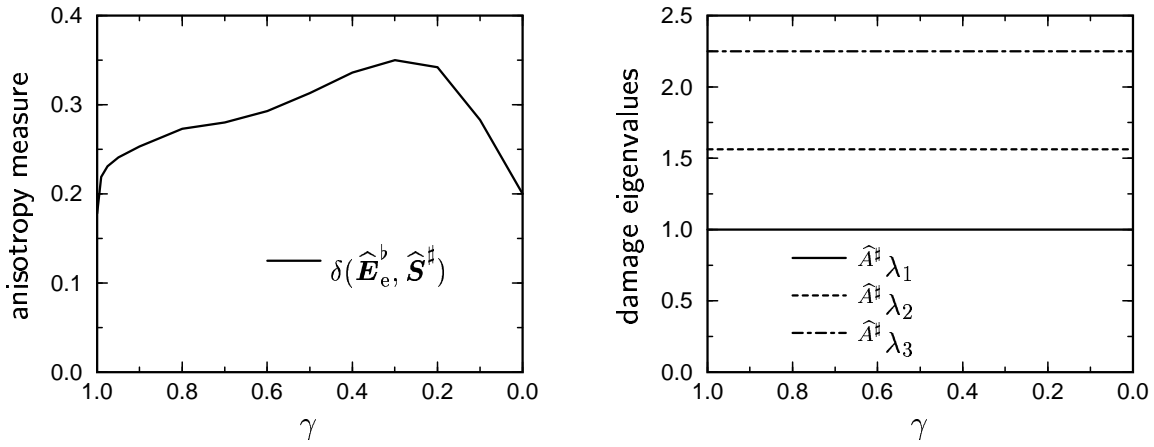


Figure 6.6: Simple shear, anisotropic elasto–plasticity, unloading/reloading: Anisotropy measure $\delta(\widehat{\mathbf{E}}_e^b, \widehat{\mathbf{S}}^\sharp)$ and eigenvalues of the anisotropy metric $\widehat{\mathbf{A}}^\sharp \lambda_{1,2,3}$.

the evolution of the principal directions of strain and stress for reverse loading within the shear interval $\gamma \in [0 \rightarrow 2.5, 2.5 \rightarrow 0.1]$, see Figure 6.7.

6.6.1.2 Anisotropic elasto–plasticity coupled to quasi isotropic damage

Next, we consider the coupling to quasi isotropic damage, with $\delta_1 = 10^2$ and $\delta_2 = 0$. Similar to the previous setting, Figure 6.8 monitors the Kirchhoff stress and the non–symmetric, modified Mandel tensor. Now the eigenvalues of the damage metric decrease, see Figure 6.9. Apparently, these eigenvalues, $\widehat{\mathbf{A}}^\sharp \lambda_{1,2,3}$, are uniformly scaled down during the deformation process which is due to the nature of quasi isotropic damage evolution. Moreover, Figure 6.10 highlights the non–commutativity of strain and stress for different shear numbers γ and the case of reverse loading is visualised in Figures 6.11–6.13 in analogy to Section 6.6.1.1.

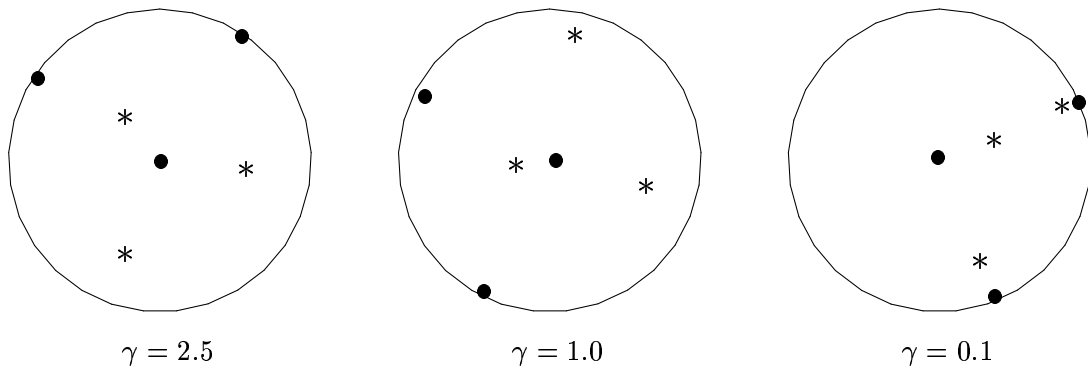


Figure 6.7: Simple shear, anisotropic elasto–plasticity, unloading/reloading: Stereographic projection of strain ($\hat{\mathbf{E}}_e^b : \bullet$) and stress ($\hat{\mathbf{S}}^\sharp : *$).

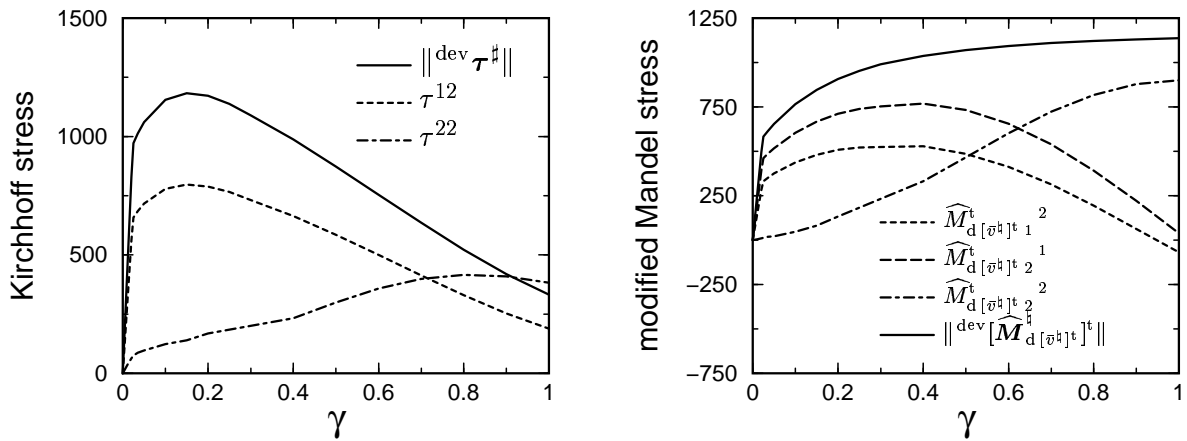


Figure 6.8: Simple shear, anisotropic elasto–plasticity coupled to quasi isotropic damage: Kirchhoff stress τ^\sharp and modified Mandel stress $[\hat{\mathbf{M}}_{d[\bar{\nu}^h]^\sharp}^\sharp]^\sharp$.

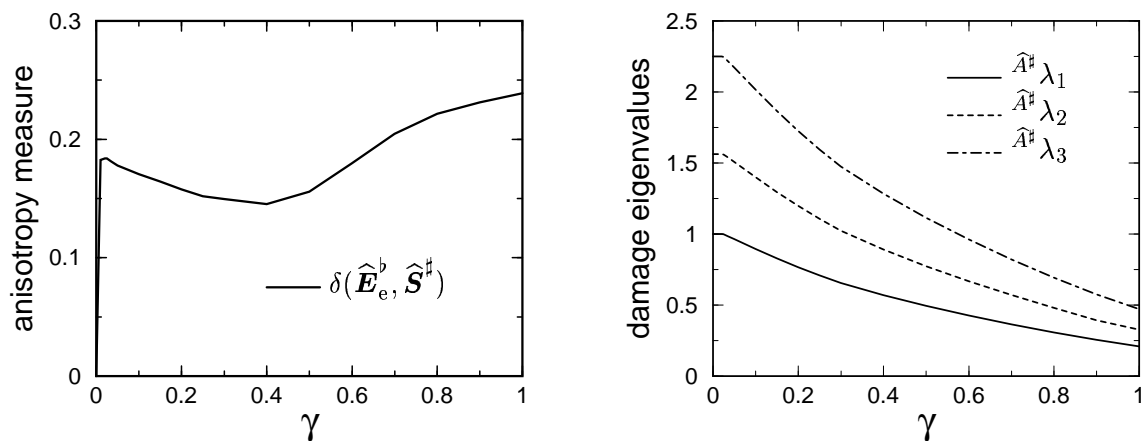


Figure 6.9: Simple shear, anisotropic elasto–plasticity coupled to quasi isotropic damage: Anisotropy measure $\delta(\hat{\mathbf{E}}_e^b, \hat{\mathbf{S}}^\sharp)$ and eigenvalues of the damage metric $\hat{\mathbf{A}}^\sharp \lambda_{1,2,3}$.

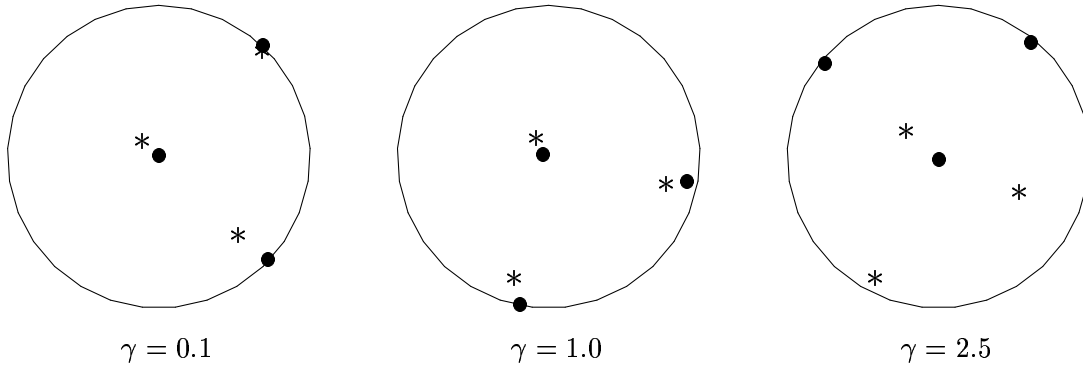


Figure 6.10: Simple shear, anisotropic elasto–plasticity coupled to quasi isotropic damage: Stereographic projection of strain ($\widehat{\mathbf{E}}_e^b : \bullet$) and stress ($\widehat{\mathbf{S}}^\sharp : *$) for different shear numbers γ .

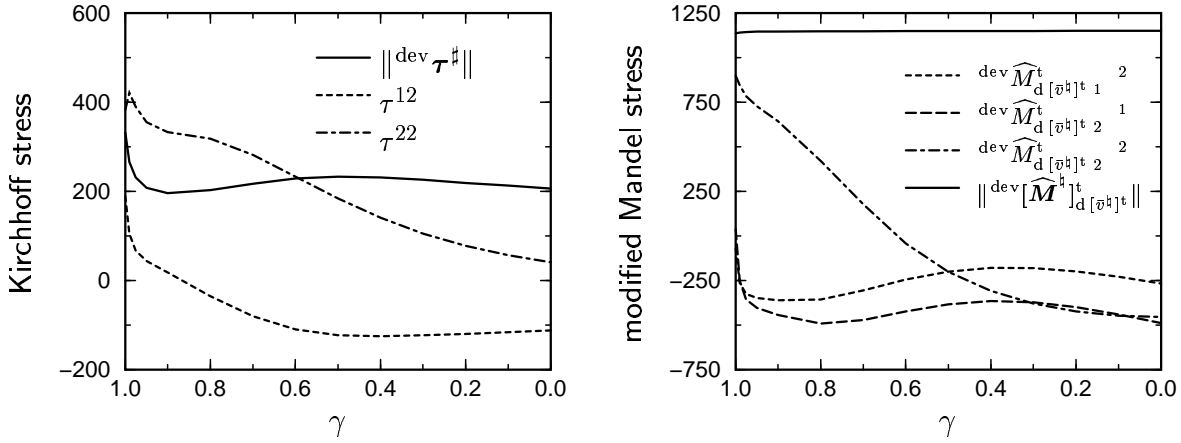


Figure 6.11: Anisotropic elasto–plasticity coupled to quasi isotropic damage, unloading/reloading: Kirchhoff stress $\boldsymbol{\tau}^\sharp$ and modified Mandel stress $[\widehat{\mathbf{M}}_d^\sharp]_{[v^\sharp]^t}^t$.

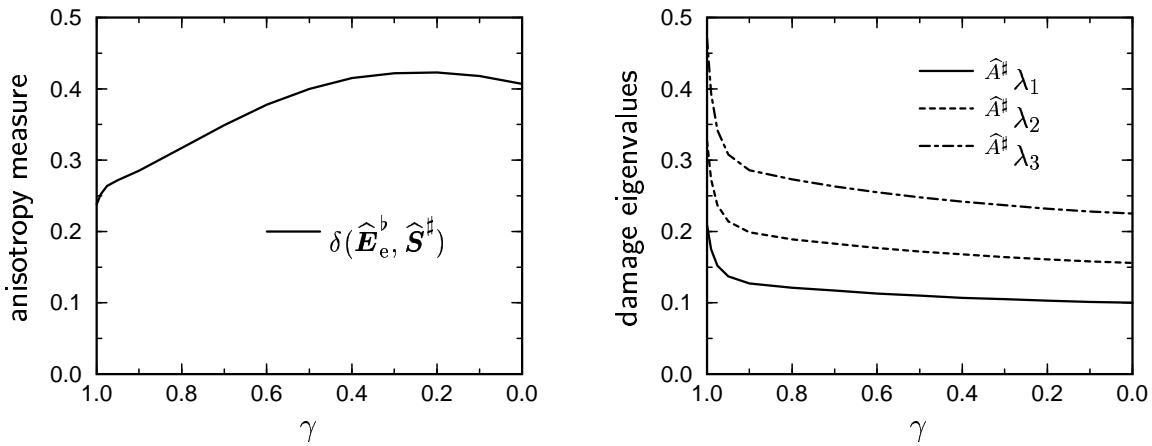


Figure 6.12: Anisotropic elasto–plasticity coupled to quasi isotropic damage, unloading/reloading: Anisotropy measure $\delta(\widehat{\mathbf{E}}_e^b, \widehat{\mathbf{S}}^\sharp)$ and eigenvalues of the damage metric $\widehat{\mathbf{A}}^\sharp \lambda_{1,2,3}$.

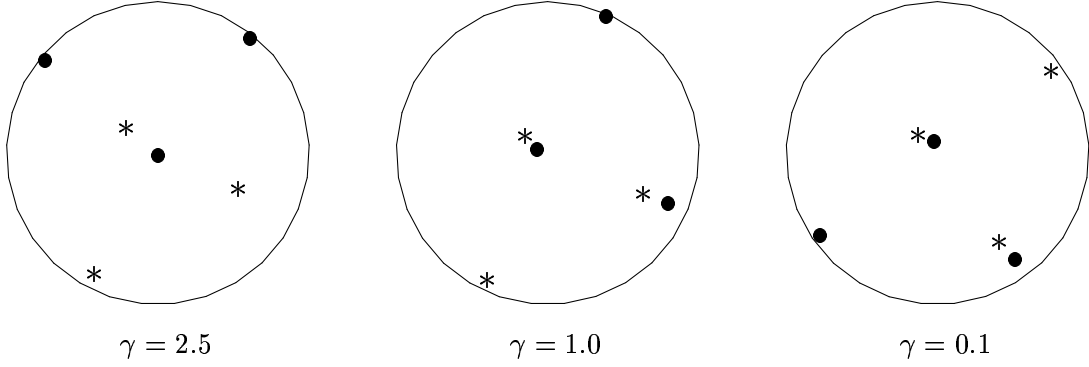


Figure 6.13: Anisotropic elasto–plasticity coupled to quasi isotropic damage, unloading/reloading: Stereo–graphic projection of strain ($\widehat{\mathbf{E}}_e^b : \bullet$) and stress ($\widehat{\mathbf{S}}^\sharp : *$).

6.6.1.3 Anisotropic elasto–plasticity coupled to anisotropic damage

Lastly, we take anisotropic damage evolution into account with $\delta_1 = 0$ and $\delta_2 = 10^2$. Figures 6.14–6.21 highlight the corresponding results in analogy to the previous settings. Please note that besides $\delta(\widehat{\mathbf{E}}_e^b, \widehat{\mathbf{S}}^\sharp)$ Figures 6.15 and 6.19 monitor the anisotropy measure $\delta(\widehat{\mathbf{A}}^\sharp, \widehat{\mathbf{A}}^\sharp|_{t_0})$ which underlines the evolution of the principal axes of the damage metric. Furthermore, due to the nature of anisotropic damage, the eigenvalues of the damage metric now degrade differently during the deformation process. The same effect is clearly reflected by the method of stereo–graphic projection in Figures 6.17 and 6.21 where the contributions of the actual damage metric $\widehat{\mathbf{A}}^\sharp$ are compared to the initial damage metric $\widehat{\mathbf{A}}^\sharp|_{t_0}$. Similar to the previous examples, Figures 6.16 and 6.20 visualises the non–coaxiality of strain and stress for different shear numbers γ .

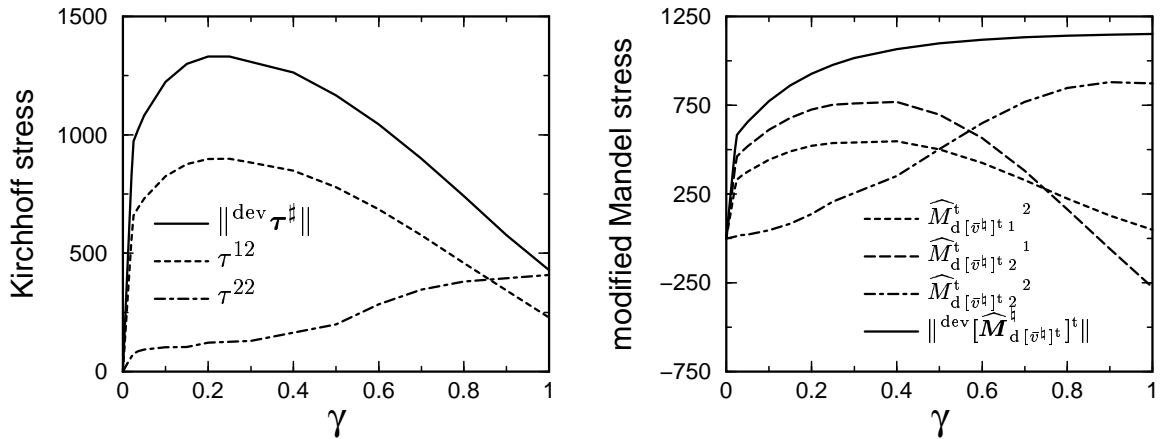


Figure 6.14: Simple shear, anisotropic elasto–plasticity coupled to anisotropic damage: Kirchhoff stress τ^\sharp and modified Mandel stress $[\widehat{\mathbf{M}}_{d[\bar{\sigma}^\sharp]^\sharp}^\sharp]^\sharp$.

6.6.1.4 Numerical aspects

As mentioned in Section 6.5, we applied a regula–falsi–type algorithm for the iteration for the Lagrange multiplier and Newton’s method based on approximated Jacobians for the damage and plastic contributions and the exact Jacobian for the hardening part. Concerning the scalar–valued iteration scheme for the Lagrange multiplier, one must choose two initial values in order to start the computation. The trial guess zero is obvious but the second value affects the convergence of the iteration. Table 6.1 highlights this influence within the setting of anisotropic elasto–plasticity coupled to anisotropic

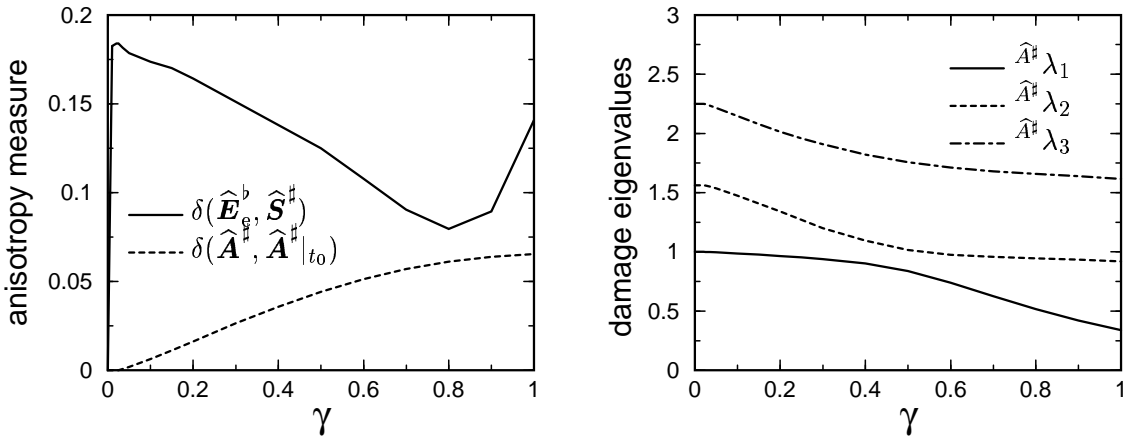


Figure 6.15: Simple shear, anisotropic elasto–plasticity coupled to anisotropic damage: Anisotropy measure $\delta(\widehat{\mathbf{E}}_e^b, \widehat{\mathbf{S}}^\#)$, $\delta(\widehat{\mathbf{A}}^\#, \widehat{\mathbf{A}}^\#|_{t_0})$ and eigenvalues of the damage metric $A^\# \lambda_{1,2,3}$.

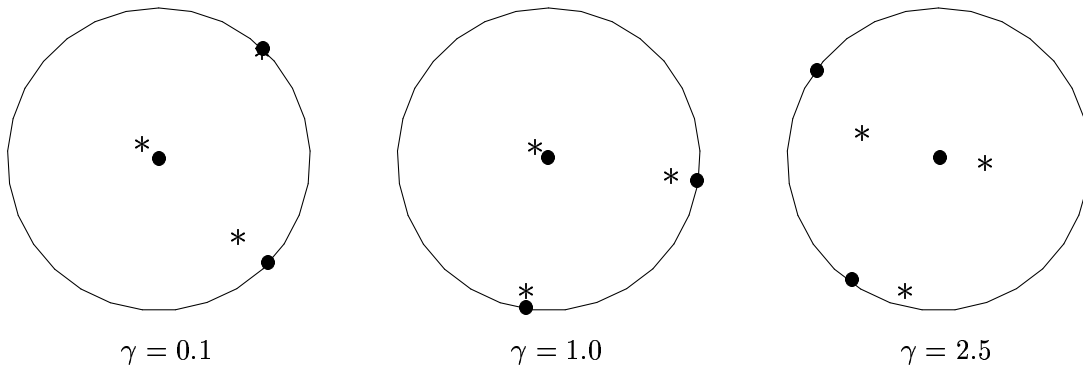


Figure 6.16: Simple shear, anisotropic elasto–plasticity coupled to anisotropic damage: Stereo–graphic projection of strain ($\widehat{\mathbf{E}}_e^b : \bullet$) and stress ($\widehat{\mathbf{S}}^\# : *$) for different shear numbers γ .

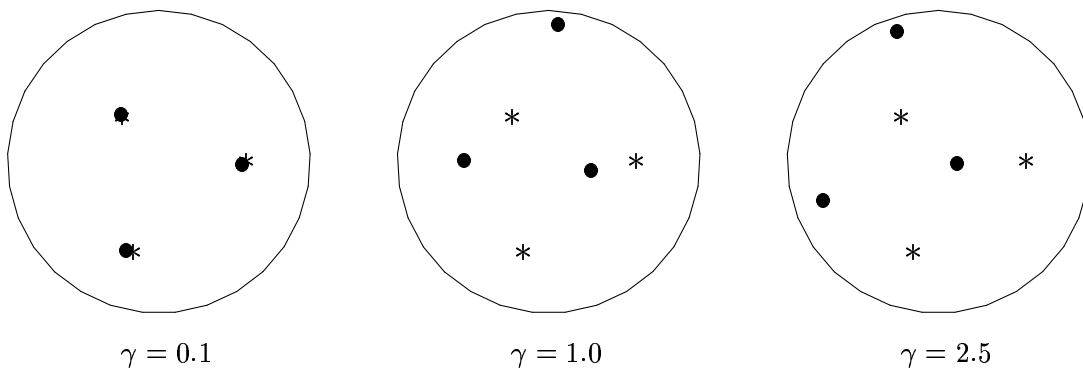


Figure 6.17: Simple shear, anisotropic elasto–plasticity coupled to anisotropic damage: Stereo–graphic projection of the actual damage metric ($\widehat{\mathbf{A}}^\# : \bullet$) and the initial damage metric ($\widehat{\mathbf{A}}^\#|_{t_0} : *$) for different shear numbers γ .

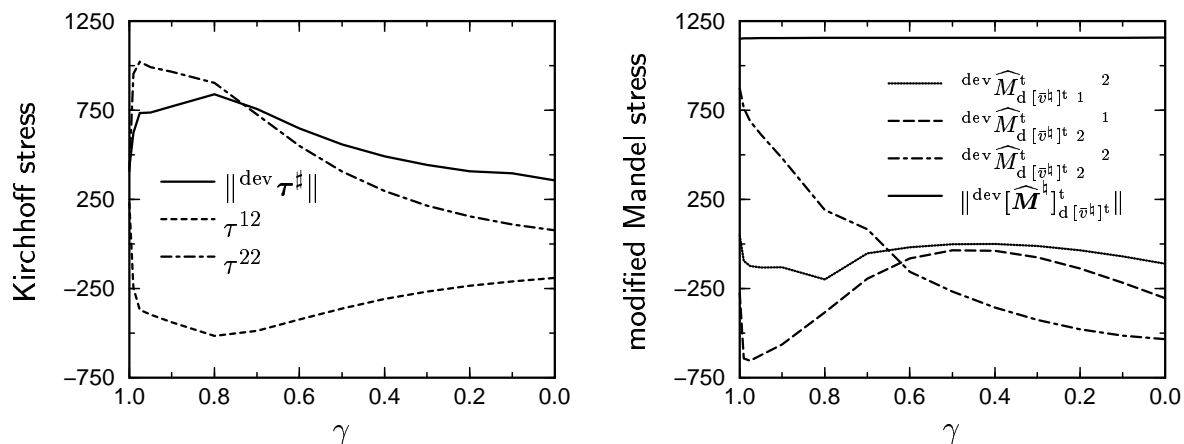


Figure 6.18: Anisotropic elasto–plasticity coupled to anisotropic damage, unloading/reloading: Kirchhoff stress $\tau^\#$ and modified Mandel stress $[\widehat{M}_d^\#]_{d[\widehat{v}^h]^t}^t$.

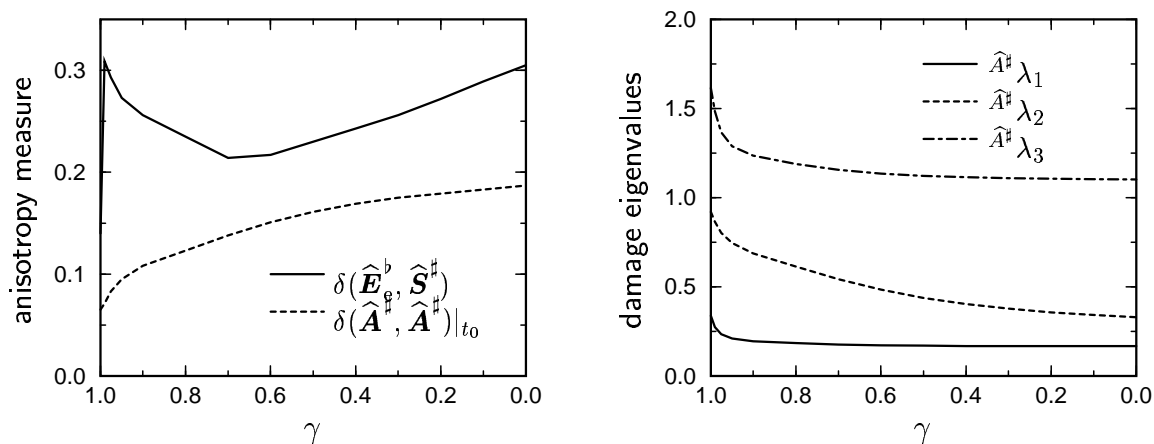


Figure 6.19: Anisotropic elasto–plasticity coupled to anisotropic damage, unloading/reloading: Anisotropy measure $\delta(\widehat{E}_e^b, \widehat{S}^\#)$, $\delta(\widehat{A}^\#, \widehat{A}^\#|_{t_0})$ and eigenvalues of the damage metric $\widehat{A}^\# \lambda_{1,2,3}$.

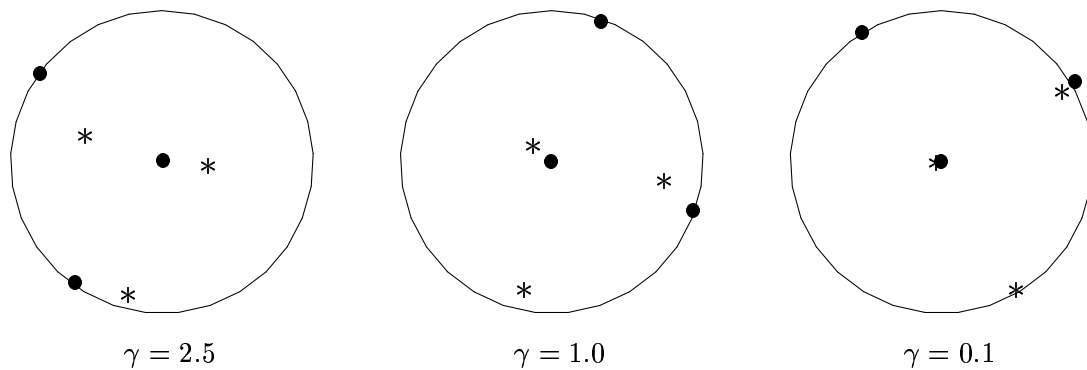


Figure 6.20: Anisotropic elasto–plasticity coupled to anisotropic damage, unloading/reloading: Stereo–graphic projection of strain ($\widehat{E}_e^b : \bullet$) and stress ($\widehat{S}^\# : *$).

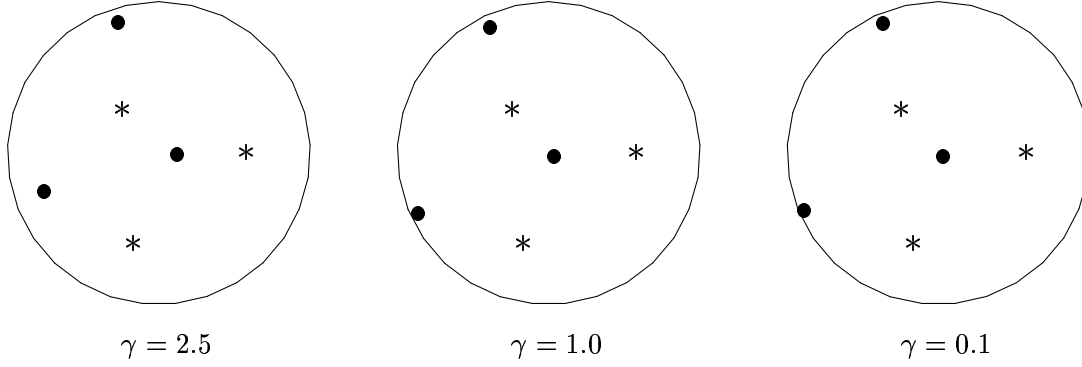


Figure 6.21: Anisotropic elasto–plasticity coupled to anisotropic damage, unloading/reloading: Stereo–graphic projection of the actual damage metric ($\hat{\mathbf{A}}^\sharp : \bullet$) and the initial damage metric ($\hat{\mathbf{A}}^\sharp|_{t_0} : *$).

damage evolution for the rather large load step $\gamma \in [0, 0.5]$. Moreover, the convergence of the New-

Table 6.1: Influence of different initial values for $\Delta\lambda_1$ on the convergence of the regula–falsi–type iteration for the Lagrange multiplier within the load step $\gamma \in [0, 0.5]$.

No.	$\Delta\lambda_1$	$y_{ie}\Phi^p$	$\Delta\lambda_1$	$y_{ie}\Phi^p$	$\Delta\lambda_1$	$y_{ie}\Phi^p$
	0.000 E–16	2.068 E+08	0.000 E–16	2.068 E+08	0.000 E–16	2.068 E+08
1	1.000 E–06	1.018 E+08	1.000 E–05	2.803 E+07	1.000 E–04	1.325 E+06
2	1.969 E–06	7.710 E+07	1.156 E–05	2.482 E+07	1.010 E–04	1.301 E+06
3	4.995 E–06	4.640 E+07	2.369 E–05	1.246 E+07	1.370 E–04	3.621 E+05
4	9.569 E–06	2.905 E+07	3.591 E–05	7.704 E+06	1.500 E–04	1.282 E+05
5	1.722 E–05	1.726 E+07	5.570 E–05	4.217 E+06	1.580 E–04	1.955 E+04
6	4.454 E–05	1.017 E+07	7.963 E–05	2.259 E+06	1.590 E–04	1.260 E+03
7	6.607 E–05	5.821 E+06	1.070 E–04	1.079 E+06	1.600 E–04	1.335 E+01
8	9.232 E–05	3.198 E+06	1.330 E–04	4.418 E+05	1.600 E–04	9.230 E–03
9	1.200 E–04	1.628 E+06	1.500 E–04	1.351 E+05	1.600 E–04	1.752 E–03
10	1.420 E–04	7.330 E+05	1.580 E–04	2.416 E+04	1.600 E–04	4.346 E–07
11	1.550 E–04	2.679 E+05	1.590 E–04	1.631 E+03		
12	1.590 E–04	6.663 E+04	1.600 E–04	2.128 E+01		
13	1.600 E–04	8.115 E+03	1.600 E–04	1.902 E–02		
14	1.600 E–04	2.836 E+02	1.600 E–04	3.610 E–03		
15	1.600 E–04	1.255 E+00	1.600 E–04	1.141 E–06		
16	1.600 E–04	8.920 E–04	1.600 E–04	1.711 E–09		
17	1.600 E–04	1.690 E–04				
18	1.600 E–04	1.202 E–08				

ton algorithm inside each regula–falsi step is crucially affected by the incorporated perturbation parameter ε for the numerically approximated Jacobians, compare Appendix E.2. For the above examples we chosen a precision of 16 decimal points. The influence of the perturbation parameter is given in Table 6.2 within the load step $\gamma \in [0, 0.5]$ whereby $\|\mathbf{R}\|$ abbreviates the sum $\|\mathbf{R}^{\text{dam}}\| + \|\mathbf{R}^{\text{pla}}\|$.

6.6.2 Stamping of a sheet

Within the subsequent finite element setting, we account for anisotropic elasto–plasticity coupled to anisotropic damage evolution with $\delta_1 = 0$ and $\delta_2 = 10$. The considered specimen consists of a plate–like structure of dimensions $10 \times 10 \times 0.5$ and a rigid square block with a cross–sectional area measuring 2.5×2.5 , see Figure 6.22. The discretisation of the plate is performed by $16 \times 16 \times 8$ enhanced

Table 6.2: Influence of different perturbation factors ε on the convergence of the local Newton iteration within the load step $\gamma \in [0, 0.5]$ for $\Delta\lambda_1 = 10^{-4}$.

No.	$\ \mathbf{R}\ $ for $\varepsilon = 10^{-12}$		$\ \mathbf{R}\ $ for $\varepsilon = 10^{-8}$		$\ \mathbf{R}\ $ for $\varepsilon = 10^{-4}$	
	step 1	step 2	step 1	step 2	step 1	step 2
1	2.970 E+01	3.264 E-06	2.995 E+01	3.451 E-06	3.001 E+01	9.142 E-06
2	7.390 E+01	2.570 E-09	7.397 E+01	1.584 E-11	7.448 E+01	1.522 E-08
3	9.324 E+00		9.383 E+00		9.366 E+00	
4	7.997 E-01		6.915 E-01		6.663 E-01	
5	1.296 E-01		1.217 E-01		1.191 E-01	
6	3.985 E-03		3.525 E-03		3.360 E-03	
7	4.920 E-06		4.418 E-06		5.030 E-06	
8	1.405 E-09		1.889 E-12		1.771 E-09	

eight node bricks (Q1E9), as advocated by Simo and Armero [SA92]. Boundary conditions and the applied loading are given in Figure 6.23.

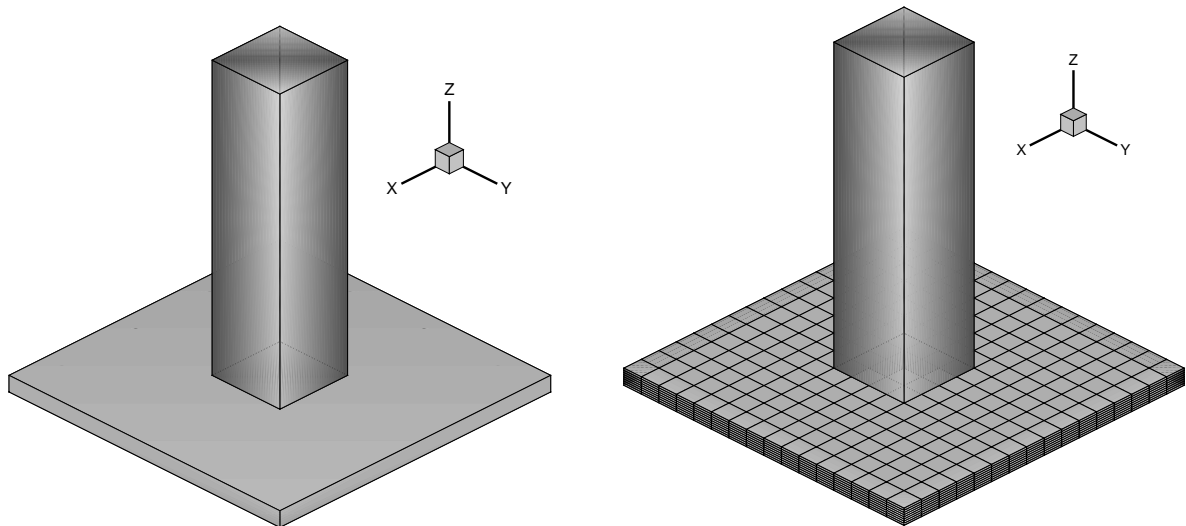


Figure 6.22: Stamping of a sheet, anisotropic elasto-plasticity coupled to anisotropic damage evolution: Geometry and discretisation of the specimen.

A typical necking behaviour is indicated by the load-displacement curve in Figure 6.24. Furthermore, the subsequent plots refer to a deformation $\|\mathbf{u}\| = 1.46$ which is almost triple the thickness of the plate itself. Figure 6.25 monitors the distribution of the deviatoric norm of the Kirchhoff stress $\|\text{dev} \boldsymbol{\tau}^\sharp\|$. In addition, one quarter of the body is zoomed. Even though geometry, boundary conditions and loading imply certain symmetries, the response of the specimen is completely non-symmetric which is due to the incorporated anisotropies. Apparently, the property of the contribution of the deviatoric norm of the modified Mandel stress $\|\text{dev} [\widehat{\mathbf{M}}^\sharp]_{\text{d}[\widehat{\nu}^\sharp]_t}^\sharp\|$ is different from those of the Kirchhoff stress, see Figure 6.26. The smallest eigenvalue of the damage metric tensor is visualised in Figure 6.27. Please note that $\widehat{\mathbf{A}}^\sharp \lambda_1$ boils down from 1.00 to 0.55 which underlines a high degree of damage evolution. A typical indicator for anisotropy is the anisotropy measure $\delta(\widehat{\mathbf{E}}_e^b, \widehat{\mathbf{S}}^\sharp)$ as highlighted in Figure 6.28. Moreover, the evolution of the principal axes of the damage metric is represented via the non-vanishing scalar $\delta(\widehat{\mathbf{A}}^\sharp, \widehat{\mathbf{A}}^\sharp|_{t_0})$ which allows interpretation as deformation induced anisotropy, see Figure 6.29. Finally the contributions of the hardening variable κ are monitored in Figure 6.30.

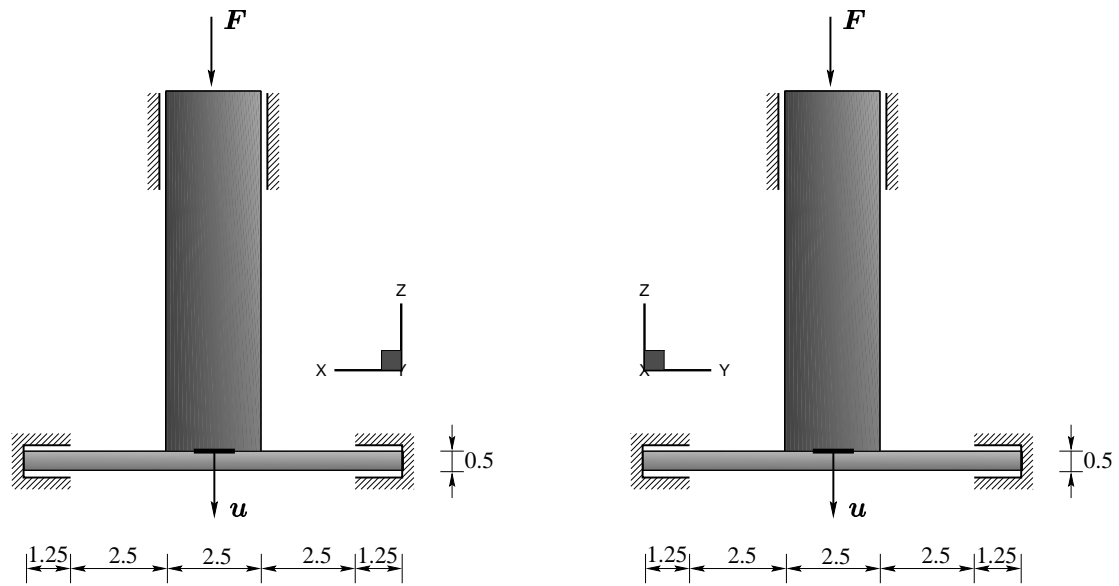


Figure 6.23: Stamping of a sheet, anisotropic elasto–plasticity coupled to anisotropic damage evolution: Boundary conditions and loading of the specimen.

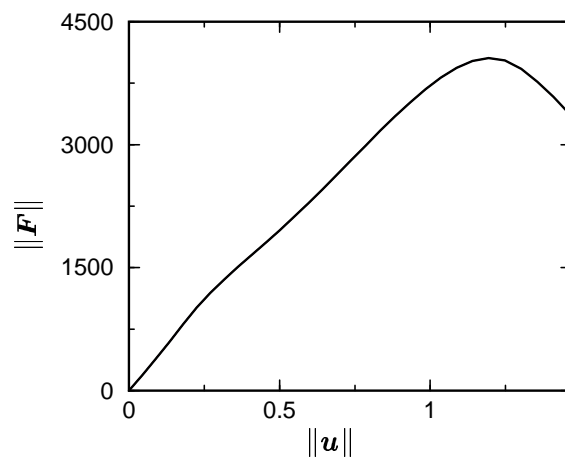


Figure 6.24: Stamping of a sheet, anisotropic elasto–plasticity coupled to anisotropic damage evolution: Load–displacement curve.

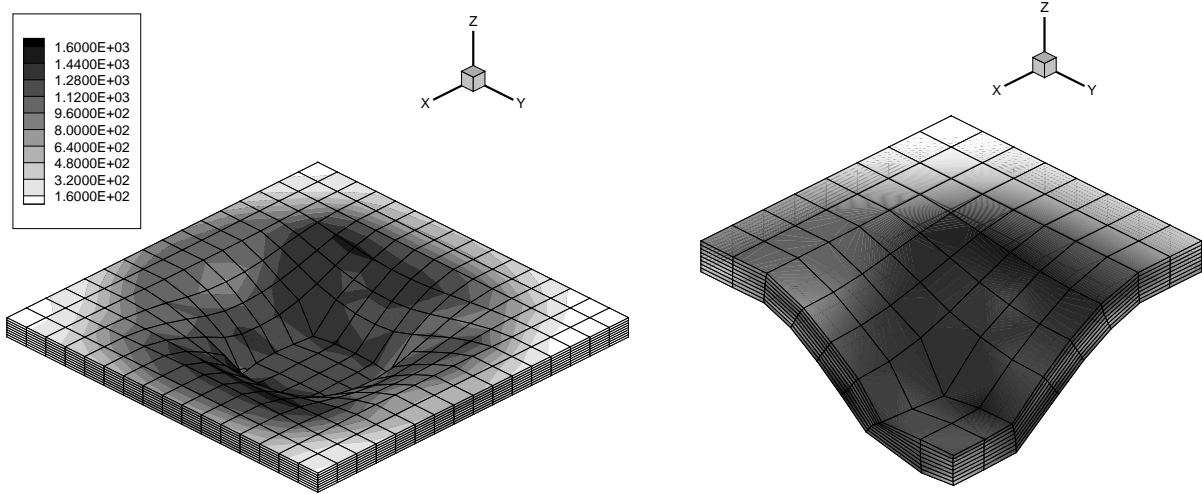


Figure 6.25: Stamping of a sheet, anisotropic elasto-plasticity coupled to anisotropic damage evolution: Deviatoric norm of the Kirchhoff stress $\|\text{dev } \boldsymbol{\tau}^{\sharp}\|$ at $\|\mathbf{u}\| = 1.46$.

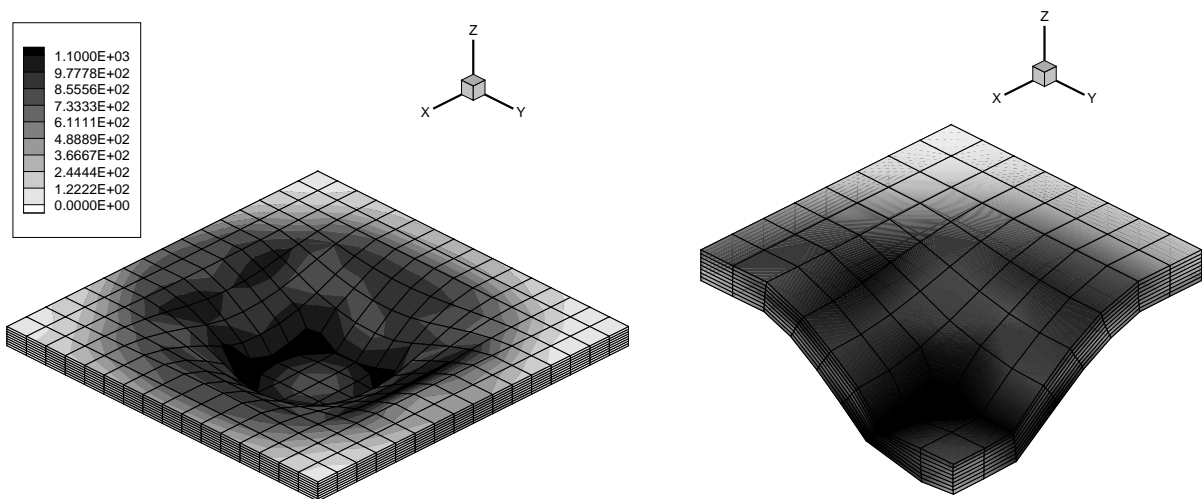


Figure 6.26: Stamping of a sheet, anisotropic elasto-plasticity coupled to anisotropic damage evolution: Deviatoric norm of the modified Mandel stress $\|\text{dev } [\widehat{\mathbf{M}}_{\text{d}}^{\sharp}]^t\|$ at $\|\mathbf{u}\| = 1.46$.

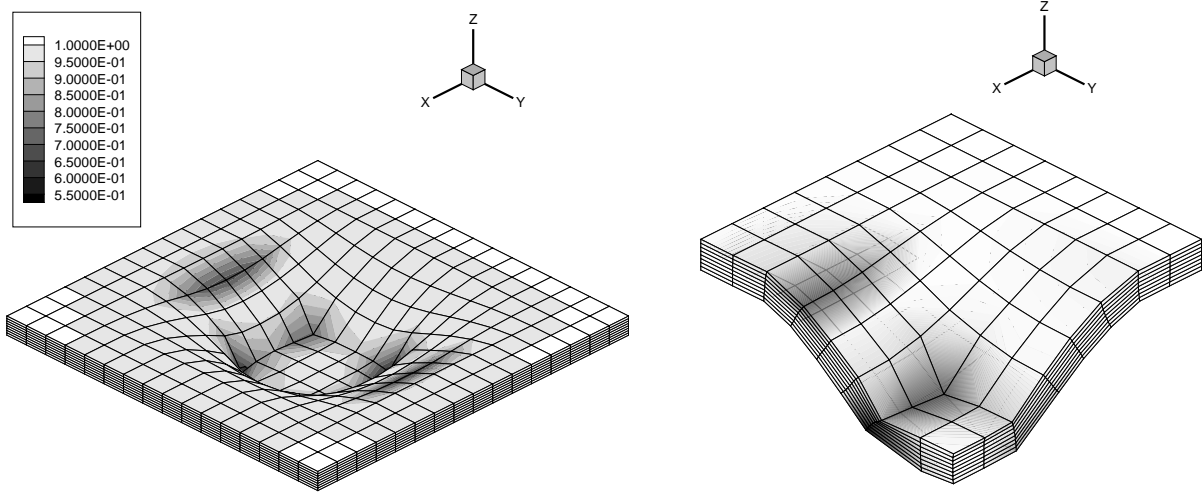


Figure 6.27: Stamping of a sheet, anisotropic elasto–plasticity coupled to anisotropic damage evolution: Smallest damage eigenvalue $\hat{A}^\sharp \lambda_1$ at $\|\mathbf{u}\| = 1.46$.

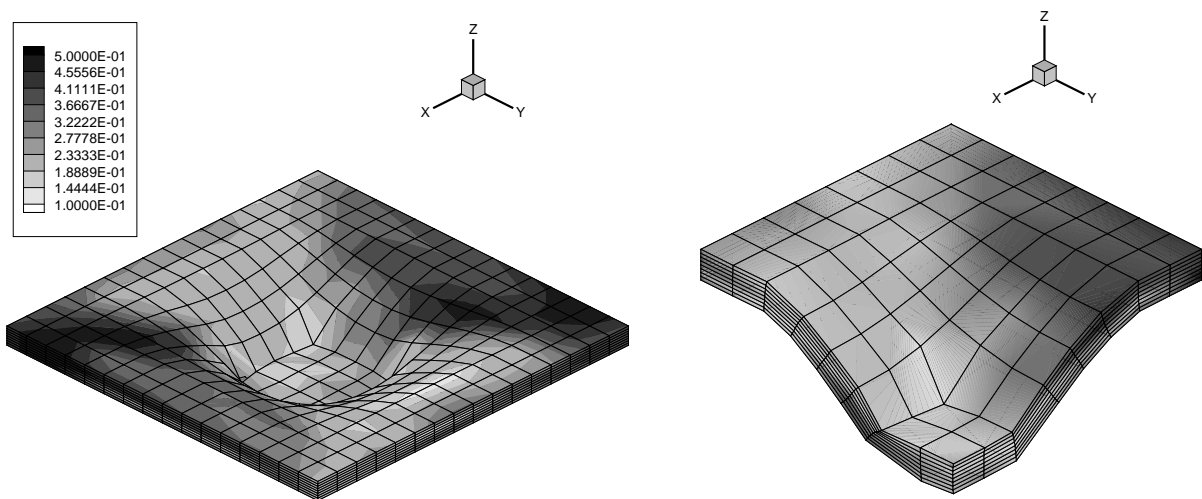


Figure 6.28: Stamping of a sheet, anisotropic elasto–plasticity coupled to anisotropic damage evolution: Anisotropy measure $\delta(\hat{\mathbf{E}}_e^b, \hat{\mathbf{S}}^\sharp)$ at $\|\mathbf{u}\| = 1.46$.

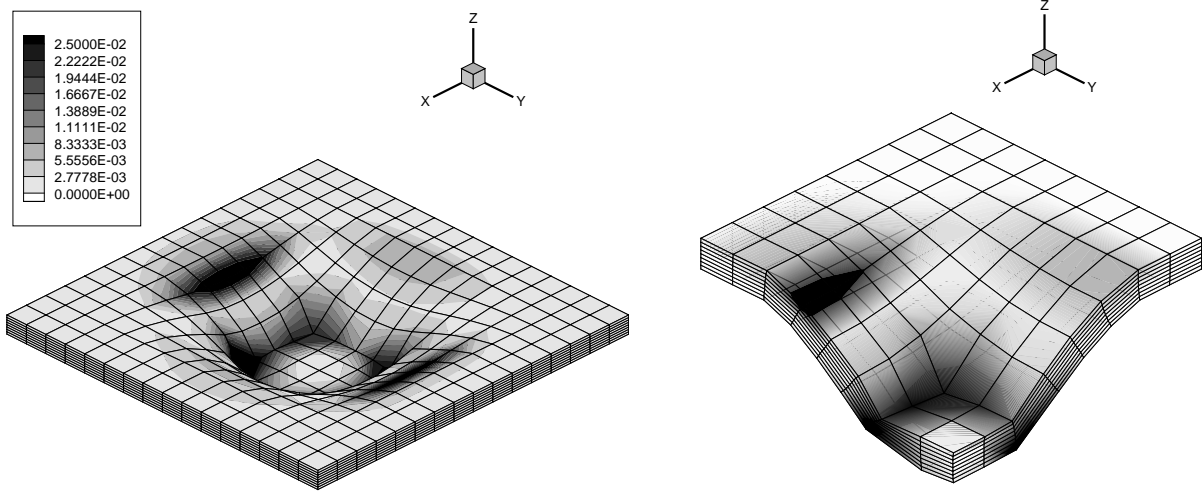


Figure 6.29: Stamping of a sheet, anisotropic elasto-plasticity coupled to anisotropic damage evolution: Anisotropy measure $\delta(\widehat{\mathbf{A}}^\sharp, \widehat{\mathbf{A}}^\sharp|_{t_0})$ at $\|\mathbf{u}\| = 1.46$.

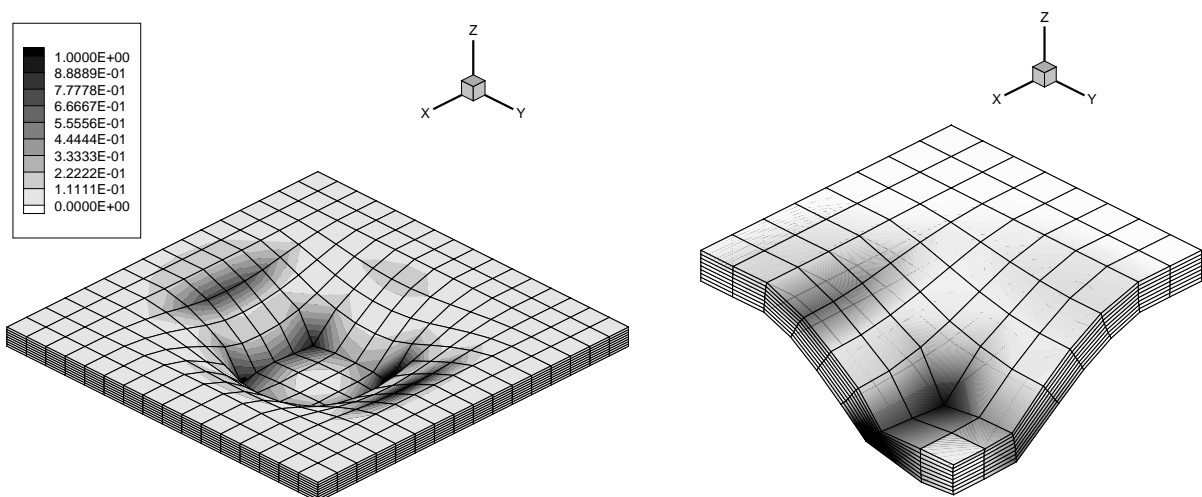


Figure 6.30: Stamping of a sheet, anisotropic elasto-plasticity coupled to anisotropic damage evolution: Hardening variable κ at $\|\mathbf{u}\| = 1.46$.


6.6.2.1 Numerical aspects

As previously mentioned, we numerically approximated the algorithmic tangent operator within the finite element setting, compare Appendix E.2. In this context, Table 6.3 monitors the dependence of the global convergence of the finite element scheme on the perturbation factor ε with respect to the residual norm $\|\mathbf{R}\|$, similar to Section 3.9. We thereby chose one load step which results from $\|\mathbf{u}\| = 0$ in $\|\mathbf{u}\| = 0.34$ and $\hat{\lambda}_1 \in [1, 0.98]$ whereby the computations have been performed with the arc-length method. Recall that the chosen precision corresponds to 16 decimal points.

Table 6.3: Influence of different perturbation factors ε on the convergence of the global Newton iteration within the load step $\|\mathbf{u}\| \in [0, 0.34]$.

	$\varepsilon = 10^{-12}$	$\varepsilon = 10^{-8}$	$\varepsilon = 10^{-4}$
No.	$\ \mathbf{R}\ $	$\ \mathbf{R}\ $	$\ \mathbf{R}\ $
1	2.6998 E+03	2.6983 E+03	2.6985 E+03
2	6.8412 E+02	6.7962 E+02	6.8185 E+02
3	5.9166 E+01	5.1878 E+01	5.1816 E+01
4	2.4510 E+00	1.0577 E+00	1.0275 E+00
5	1.4148 E-01	2.0344 E-02	2.0650 E-02
6	1.2744 E-02	8.3972 E-07	2.4782 E-04
7	7.6180 E-04	2.7513 E-09	3.2112 E-05
8	4.7580 E-05		4.5746 E-06
9	5.2422 E-06		6.5566 E-07
10	1.1622 E-06		9.4023 E-08
11	1.3666 E-07		1.3699 E-08
12	1.8831 E-08		

Discussion

as habe ich getan – sagt mein Gedächtnis. Das kann ich nicht getan haben – sagt mein Stolz und bleibt unerbitterlich. Endlich – gibt das Gedächtnis nach.

Friederich Nietzsche [1844 – 1900]
Jenseits von Gut und Böse, 1886


The main objective of this work is to develop and compare two rational, modular and thermodynamically consistent frameworks of anisotropic inelasticity which are especially well suited for general numerical settings, e.g. the finite element method.

On the one hand, a spatial formulation of anisotropic multiplicative elasto–plasticity is deduced in terms of the elastic Finger tensor and an arbitrary number of additional symmetric second order tensors (typically structural tensors). In particular, the derivation is based on the general representation theorem of isotropic tensor functions – or alternatively on the fundamental covariance relation of the free Helmholtz energy density. As a result, we proved the generalisation of the celebrated Truesdell or rather Murnaghan formula to anisotropic multiplicative elasto–plasticity. On this basis, it seemed natural to incorporate the thermodynamic force conjugate to the elastic Finger tensor into the plastic potential, although this stress measure differs from the stress in the equilibrium equations. Furthermore, we discussed the interpretation of this thermodynamic force within the framework of Eshelbian mechanics and additionally showed that the proposed approach embeds the well–established formulations of isotropic large strain plasticity. It turns out that the stress tensors and the elastic tangent operators result in a specific additive structure with respect to the appropriate ingredients of the free Helmholtz energy density. Thus, in view of numerical applications, standard formulations for non–linear hyper–elasticity or multiplicative elasto–plasticity can be conveniently enlarged to anisotropic constitutive equations. In analogy to a texture development, we accounted for an evolution of the additional second order internal variables, whereby a Lemaitre–type model has been adopted. The character of the obtained evolution equations for these tensorial fields is of cardinal importance since they influence the material symmetry group of the modelled body of interest. Concerning the numerical examples, the chosen prototype models accounted for an initially (elastic) transversally isotropic and orthotropic material, respectively. Furthermore, the initial symmetry group of the plastic potential is assumed to be orthotropic. As it is clearly monitored by the numerical examples within a homogeneous deformation in simple shear and finite element settings, the proposed formulation allows the representation of strongly anisotropic solids. For the inelastic case, an evolution and change of the incorporated anisotropy is optionally included. Recall that due to the conceptual beauty of this framework, we are not restricted to a specific configuration and thus choose the most convenient environment – the physical space. As an interesting side aspect, all internal variables and flow directions remain symmetric and simple integration techniques were suitably applied. Summarising, it is believed that the developed formulation serves as a very convenient framework for anisotropic hyper–elasticity and multiplicative elasto–plasticity.

On the other hand, we compared the previous approach to the concept of fictitious configurations within a hyper–elastic setting. Thereby, the underlying motivation for the latter strategy relies in the consideration of an energy metric tensor which allows the interpretation as a fictitious Finger tensor

characterising a pre-stretched material. The concept of strain energy equivalence between an isotropic fictitious and the anisotropic reference configuration was strictly applied and a specific ansatz for the fictitious linear map has been chosen in order to introduce an analogue to structural tensors. On this basis, the comparison of the incorporated sets of invariants underlines that the framework within the fictitious configuration deals with a reduced set of invariants and generators compared to the structural tensor approach and is restricted at least to orthotropic symmetry. As a main advantage of this framework, standard isotropic constitutive equations can be applied to model orthotropic material behaviour. Recall that correlated numerical computations end up in similar costs compared to the computation of an isotropic material which is a significant benefit of the formulation. With this framework at hand, a large strain second order continuum damage formulation has been discussed whereby the well established concept of generalised standard dissipative materials was adopted. Based on the introduction of a dissipation potential and appropriate flow rules, two types of damage evolution were classified, namely quasi isotropic damage with constant principal damage directions and generally anisotropic damage incorporating an evolution of the principal damage directions. Both categories allow the coupling to either isotropic or anisotropic hyper-elasticity, respectively. Then, the coupling of continuum damage to multiplicative elasto-plasticity was developed in a kinematically consistent manner. Consequently, the previously introduced fictitious configuration has been attached to the intermediate configuration and another additional fictitious configuration for the yield function has been introduced. A specific kinematical assumption enabled us to define a modified stress tensor of Mandel-type which enters the plastic potential with respect to the intermediate configuration. This particular stress tensor accounted for anisotropy and degradation in view of the plasticity framework. Referring to time integration for the proposed rate-independent staggered formulation, different higher order methods have been applied. Since no exponential scheme for the general anisotropic damage case is conveniently available, Runge-Kutta algorithms have been used for the computations. Thereby, two different schemes were outlined, either tolerating intermediate stages outside of the elastic domain or forcing the intermediate stages to remain in the elastic domain. For the highlighted numerical examples diagonally implicit Runge-Kutta algorithms especially rendered results of satisfying accuracy for large integration intervals. In the case of full coupling of hyper-elasticity, continuum damage and plasticity in the context of overall anisotropy at large strains a simple Euler backward integration for the damage part and an exponential scheme for the plasticity contributions were successfully applied. In conclusion, it turns out that the developed kinematically and thermodynamically consistent framework for anisotropic second order continuum damage coupled to plasticity results in a manageable numerical setting which is a main advantage of the proposed formulation.

Outlook

 es ist sinnlos, alle Aspekte des Verhaltens eines Materials als zugleich erfassen zu wollen. . . . 'Die' Stoffgleichung für ein reales Material, die wirklich das gesamte Verhalten korrekt wiedergibt, wird man nie angeben können.

Arnold Krawietz
Materialtheorie, 1986

It is obvious that the development of specific physically and micro-mechanically motivated evolution equations, the comparison of the numerical results with appropriate experimental data and the identification of the incorporated material parameters are of cardinal importance and constitute future research – however, neither of these tasks being trivial.

The extension of the proposed anisotropic frameworks to more general thermomechanical formula-

tions seems to be worthwhile. In this context, the set of (possibly hemitropic) response functions reads

$$\begin{aligned}
 [\mathbf{II}^\sharp]^\dagger &= [\mathbf{II}^\sharp]^\dagger([\bullet]) \in \mathbb{L}^3 : T^*\mathcal{B}_0 \rightarrow T^*\mathcal{B}_t, \\
 \mathbf{q}^\sharp &= \mathbf{q}^\sharp([\bullet]) \in \mathbb{R}^3 : T^*\mathcal{B}_0 \rightarrow \mathbb{R}, \\
 \epsilon_0 &= \epsilon_0([\bullet]) \in \mathbb{R}, \\
 \eta_0 &= \eta_0([\bullet]) \in \mathbb{R}_0, \\
 \psi_0 &= \psi_0([\bullet]) \in \mathbb{R}, \\
 [\bullet] &\doteq \{ \mathbf{F}^\sharp, \mathbf{D}_{t^m}^m \mathbf{F}^\sharp, \mathbf{G}^\sharp, \theta, \text{Grad } \theta, \mathbf{A}_{1,\dots,n}^\sharp; \mathbf{X} \},
 \end{aligned} \tag{O.1}$$

whereby t and $\varphi(\mathbf{X}, t)$ are excluded from the set $[\bullet]$ due to the principle of material objectivity, $[\mathbf{II}^\sharp]^\dagger$ denotes a mixed-variant stress tensor, \mathbf{q}^\sharp characterises the heat flux vector, $\mathbf{A}_{1,\dots,n}^\sharp$ collects a set of additional (possibly internal) variables and $\theta, \epsilon_0, \eta_0 \in \mathbb{R}_+$ as well as $\psi_0 \in \mathbb{R}$ represent the absolute temperature field, internal energy, entropy and the free Helmholtz energy densities, respectively, with $\psi_0 = \epsilon_0 - \theta \eta_0$, $\text{Grad } \theta \in \mathbb{R}^3 : T\mathcal{B}_0 \rightarrow \mathbb{R}$ and usually $m = 0$ or $m = 1$, compare e.g. Truesdell and Toupin [TT60, Chap. E], Truesdell and Noll [TN92, Chap. D II], Green and Adkins [GA70, Chap. VIII], Şuhubi [Şuh75], Lavenda [Lav93, Chap. 3], Capriz [Cap89, Part III], Antman [Ant95, Sect. XII.14], Šilhavý [Šil97, Chap. 9], Maugin [Mau99, Sect. 3.3.B], Gurtin [Gur00, Chap. A.9] or Rivlin [Riv73] for an overview **. Then, the Coleman–Noll entropy principle as based on the Clausius–Duhem inequality is assumed to take the following local format

$$-D_t \psi_0 - \eta_0 D_t \theta + [\mathbf{II}^\sharp]^\dagger : D_t \mathbf{F}^\sharp + \theta^{-1} \mathbf{q}^\sharp \cdot \text{Grad } \theta \geq 0 \tag{O.2}$$

which results in (the notation \circ denotes the appropriate contraction)

$$\begin{aligned}
 & [[\mathbf{II}^\sharp]^\dagger - \partial_{\mathbf{F}^\sharp} \psi_0] : D_t \mathbf{F}^\sharp - \partial_{\mathbf{D}_{t^m}^m \mathbf{F}^\sharp} \psi_0 : \mathbf{D}_{t^{m+1}}^{m+1} \mathbf{F}^\sharp - \sum_{i=1}^n \partial_{\mathbf{A}_i^\sharp} \psi_0 \circ D_t \mathbf{A}_i^\sharp \\
 & - [\eta_0 + \partial_\theta \psi_0] : D_t \theta - \partial_{\text{Grad } \theta} \psi_0 : D_t \text{Grad } \theta + \theta^{-1} \mathbf{q}^\sharp \cdot \text{Grad } \theta \geq 0
 \end{aligned} \tag{O.3}$$

with $D_t \mathbf{A}_{1,\dots,n}^\sharp = D_t \mathbf{A}_{1,\dots,n}^\sharp([\bullet])^{\dagger\dagger}$. Following the lines of rational thermodynamics by applying the classical Coleman–Noll argumentation, we demand this inequality to restrict the constitutive equations (O.1). In particular, inequality (O.3) is claimed to hold at a material point at fixed time t for arbitrary variables of the set $[\bullet]$ and $D_t \mathbf{F}^\sharp, \mathbf{D}_{t^{m+1}}^{m+1} \mathbf{F}^\sharp, D_t \theta, D_t \text{Grad } \theta$ since it is always possible to find a motion and temperature field which satisfy this constraint (every deformation–temperature path allows realisation in a process). Please note that the response functions (O.1) are unaffected by $D_t \mathbf{F}^\sharp$,

** For conceptual clarity, the dependence of the constitutive functions on the temperature rate is neglected. Indeed, for rigid bodies ($\mathbf{C}^b \doteq \mathbf{G}^b$) it turns out that we deal with a parabolic heat conduction equation (infinite propagation velocity of the thermal field) while the incorporation of $D_t \theta$ results in second order time derivatives of θ in the energy balance and consequently in a hyperbolic setting (finite propagation velocity of the thermal field). A detailed outline is given in Şuhubi [Şuh75, Sects. 2.3 & 2.7].

$\dagger\dagger$ Naturally, balance of mass ($dM = dm$) and angular momentum ($\mathbf{S}^\sharp, \boldsymbol{\tau}^\sharp \in \mathbb{S}^3$) is assumed to hold throughout and from linear momentum, we obtain the pointwise balance equation

$$D_t \mathbf{p}_0^b = \text{Div} [\mathbf{II}^\sharp]^\dagger + {}^{\text{bod}} \mathbf{b}_0^b \tag{\dagger\dagger.1}$$

with $\mathbf{p}_0^b \doteq \rho_0 \mathbf{g}^b \cdot D_t \mathbf{x} \in \mathbb{R}^3 : T\mathcal{B}_t \rightarrow \mathbb{R}$ whereby ρ_0 denotes the referential density in \mathcal{B}_0 and ${}^{\text{bod}} \mathbf{b}_0^b \in \mathbb{R}^3 : T\mathcal{B}_t \rightarrow \mathbb{R}$. Apparently, balance of entropy is defined in terms of the difference in increase of total and reversible entropy, namely the entropy production $\Gamma_0 \doteq D_t S_0 - D_t {}^{\text{rev}} S_0 \geq 0$ with $\Gamma_0 = \int_{\mathcal{B}_0} \gamma_0 dM$, $S_0 = \int_{\mathcal{B}_0} \eta_0 dM$ and ${}^{\text{rev}} S_0 = \int_{\mathcal{B}_0} {}^{\text{ent}} r_0 dM + \int_{\partial \mathcal{B}_0} \mathbf{h}^\sharp \cdot \mathbf{n}^b dA$ whereby ${}^{\text{ent}} r_0$ characterises a source of entropy and $\mathbf{h}^\sharp \in \mathbb{R}^3 : T^*\mathcal{B}_0 \rightarrow \mathbb{R}$ denotes the entropy flux vector in connection with the outward unit-vector $\mathbf{n}^b \in \mathbb{U}^2 : T\mathcal{B}_0 \rightarrow \mathbb{R}$. The corresponding local format results in

$$\gamma_0 = D_t \eta_0 - \left[{}^{\text{ent}} r_0 + \text{Div } \mathbf{h}^\sharp \right], \tag{\dagger\dagger.2}$$

$$\gamma_0 = D_t \eta_0 - \theta^{-1} \left[{}^{\text{ene}} r_0 + \text{Div } \mathbf{q}^\sharp + \theta^{-1} \mathbf{q}^\sharp \cdot \text{Grad } \theta \right], \tag{\dagger\dagger.3}$$

whereby the representation ($\dagger\dagger.3$) is based on the constitutive relations $\mathbf{h}^\sharp \doteq \theta^{-1} \mathbf{q}^\sharp$ and ${}^{\text{ent}} r_0 \doteq \theta^{-1} {}^{\text{ene}} r_0$ (${}^{\text{ene}} r_0$ denotes an energy source term), compare e.g. Truesdell and Toupin [TT60, Sect. E IIb] or Šilhavý [Šil97, Sect. 9.2].

$D_{t^{m+1}}^{m+1} \mathbf{F}^\sharp$, $D_t \theta$, $D_t \text{Grad } \theta$ and that the contributions $D_t \mathbf{A}_{1,\dots,n}^\sharp$ allow interpretation as being constitutive functions themselves and thus do not permit to be independently varied. Based on these relations and the fact that the inequality (O.3) depends linearly on $D_t \mathbf{F}^\sharp$, $D_{t^{m+1}}^{m+1} \mathbf{F}^\sharp$, $D_t \theta$, $D_t \text{Grad } \theta$, constitutive equations for a mixed-variant hyper-elastic stress field (first Piola–Kirchhoff stress) and the entropy density as well as the independency of ψ_0 (just as ϵ_0 and η_0) on the m th time derivative of the motion and temperature gradient in addition to the reduced format of the Clausius–Duhem inequality are a natural consequence $\ddagger\ddagger$.

$$\boxed{\begin{aligned} [\mathbf{\Pi}^\sharp]^\dagger &\doteq \partial_{\mathbf{F}^\sharp} \psi_0, \quad \eta_0 \doteq -\partial_\theta \psi_0, \quad \partial_{D_{t^m} \mathbf{F}^\sharp} \psi_0 \doteq \mathbf{0}, \quad \partial_{\text{Grad } \theta} \psi_0 \doteq \mathbf{0}, \\ &-\sum_{i=1}^n \partial_{\mathbf{A}_i^\sharp} \psi_0 \circ D_t \mathbf{A}_i^\sharp + \theta^{-1} \mathbf{q}^\sharp \cdot \text{Grad } \theta \geq 0. \end{aligned}} \quad (\text{O.4})$$

Next, we consider a moderate and simple prototype model with respect to the Lagrangian setting. The following ingredients $[\bullet] \doteq \{\mathbf{C}^b, \mathbf{G}^\sharp, \theta, \mathbf{A}^\sharp; \mathbf{X}\}$ with $\mathbf{A}^\sharp \in \mathbb{S}^3 : T^* \mathcal{B}_0 \times T^* \mathcal{B}_0 \rightarrow \mathbb{R}$ and $\mathbf{q}^\sharp = \mathbf{q}^\sharp(\text{Grad } \theta, [\bullet])$ together with the assumption $D_t \mathbf{A}_{1,\dots,n}^\sharp \doteq \mathbf{0}$ result in the hyper-elastic format ($i = 1, 2, 3$)

$$\begin{aligned} \mathbf{S}^\sharp &= 2 \partial_{\mathbf{C}^b} \psi_0^0 = 2 \mathbf{B}^\sharp \cdot \left[\partial_{\mathbf{G}^\sharp} \psi_0^0 \cdot \mathbf{G}^\sharp + \partial_{\mathbf{A}^\sharp} \psi_0^0 \cdot \mathbf{A}^\sharp \right] \\ &= S^\sharp \phi_i \mathbf{G}^\sharp \cdot [\mathbf{C}^b \cdot \mathbf{G}^\sharp]^{i-1} + S^\sharp \phi_4 \mathbf{A}^\sharp + S^\sharp \phi_5 [\mathbf{A}^\sharp \cdot \mathbf{C}^b \cdot \mathbf{G}^\sharp]_{\text{sym}} \quad (\text{O.5}) \\ \text{with } S^\sharp \phi_{1,\dots,5} &= S^\sharp \phi_{1,\dots,5} \left(\mathbf{G}^\sharp : [\mathbf{C}^b \cdot \mathbf{G}^\sharp]^i, \mathbf{C}^b : \mathbf{A}^\sharp, [\mathbf{C}^b \cdot \mathbf{G}^\sharp \cdot \mathbf{C}^b] : \mathbf{A}^\sharp, \theta \right), \end{aligned}$$

whereby the free Helmholtz energy density is assumed to represent a hemitropic scalar-valued tensor function. Since the constitutive equation for the heat flux vector is generally not based on any potential, we obtain ($i = 1, 2, 3$)

$$\begin{aligned} \mathbf{q}^\sharp &= q^\sharp \phi_i \text{Grad } \theta \cdot \mathbf{G}^\sharp \cdot [\mathbf{C}^b \cdot \mathbf{G}^\sharp]^{i-1} \\ &+ q^\sharp \phi_4 \text{Grad } \theta \cdot \mathbf{A}^\sharp + q^\sharp \phi_5 \text{Grad } \theta \cdot \mathbf{A}^\sharp \cdot \mathbf{C}^b \cdot \mathbf{G}^\sharp + q^\sharp \phi_6 \text{Grad } \theta \cdot \mathbf{G}^\sharp \cdot \mathbf{C}^b \cdot \mathbf{A}^\sharp \\ \text{with } q^\sharp \phi_{1,\dots,6} &= q^\sharp \phi_{1,\dots,6} \left(\mathbf{G}^\sharp : [\mathbf{C}^b \cdot \mathbf{G}^\sharp]^i, \mathbf{C}^b : \mathbf{A}^\sharp, [\mathbf{C}^b \cdot \mathbf{G}^\sharp \cdot \mathbf{C}^b] : \mathbf{A}^\sharp, \theta, \right. \\ &\quad \text{Grad } \theta \cdot \mathbf{G}^\sharp \cdot [\mathbf{C}^b \cdot \mathbf{G}^\sharp]^{i-1} \cdot \text{Grad } \theta, \\ &\quad \left. \text{Grad } \theta \cdot \mathbf{A}^\sharp \cdot \text{Grad } \theta, \text{Grad } \theta \cdot \mathbf{A}^\sharp \cdot \mathbf{C}^b \cdot \mathbf{G}^\sharp \cdot \text{Grad } \theta \right), \end{aligned} \quad (\text{O.6})$$

compare Zheng [Zhe93a] or Antman [Ant95, Sect. XII.13.9] for the applied representation theorem of hemitropic vector-valued tensor functions and see Wang [Wan84] for a discussion on the underlying symmetry. Alternatively, Eqs.(O.5,O.6) allow a direct formulation in the Eulerian setting whereby the stress relation is essentially defined by the general covariance of the free Helmholtz energy density and the heat flux vector results in the Piola transformation $\mathbf{q}^\sharp|_{\mathcal{B}_0} \cdot \text{cof}(\mathbf{f}^\sharp) \doteq \mathbf{q}^\sharp|_{\mathcal{B}_t}(\mathbf{g}^b, \mathbf{b}^\sharp, \theta, \text{grad } \theta, \mathbf{a}^\sharp; \mathbf{X})$. Nevertheless, the incorporation of additional arguments $\mathbf{A}_{1,\dots,n}^\sharp$ (possibly higher order structural tensors), the introduction of different sets $\mathbf{A}_{q,\dots,r}^\sharp$ and $\mathbf{A}_{s,\dots,t}^\sharp$ into ψ_0 and the constitutive function for \mathbf{q}^\sharp , respectively, or the definition and application of appropriate evolution equations such that $D_t \mathbf{A}_{1,\dots,n}^\sharp \neq \mathbf{0}$ is straightforward but tedious. Finally, it is clear that the incorporation of the temperature field generally allows the modelling via multiplicative decompositions with respect to an additional thermal linear tangent map $\mathbf{F}_\theta^\sharp \in \mathbb{L}_+^3$, see Figure 7.31₁ for a graphical representation of the decomposition $\mathbf{F}^\sharp \doteq \mathbf{F}_\theta^\sharp \cdot \mathbf{F}_e^\sharp \cdot \mathbf{F}_p^\sharp$.

$\ddagger\ddagger$ It is clear that the highlighted thermomechanical framework deals throughout with dissipative processes (even if $D_t \mathbf{A}_{1,\dots,n}^\sharp \doteq \mathbf{0}$ we end up with $\theta^{-1} \mathbf{q}^\sharp \cdot \text{Grad } \theta > 0$ for a non-isothermal setting, $0 < \theta \neq \text{const}$ and $\mathbf{q}^\sharp \neq \mathbf{0}$). An alternative non-dissipative framework, which nevertheless accounts for thermal effects, is highlighted in Green and Naghdi [GN91, GN93]. Thereby, the key idea relies on the introduction of a thermal displacement field $\alpha = \alpha(\mathbf{X}, t) \in \mathbb{R}$ which essentially characterises the integral of the thermal field with respect to time, $\alpha(\mathbf{X}, t) = \int_{t_0}^t \theta(\mathbf{X}, t) dt + \alpha_0(\mathbf{X})$. Then, from the list of arguments of the set $[\bullet]$, the contribution $\text{Grad } \theta$ is replaced by $\text{Grad } \alpha \in \mathbb{R}^3 : T\mathcal{B}_0 \rightarrow \mathbb{R}$ which finally results in a hyper-elastic format for the heat flux (determined via the derivative of the free Helmholtz energy density with respect to $\text{Grad } \alpha$).

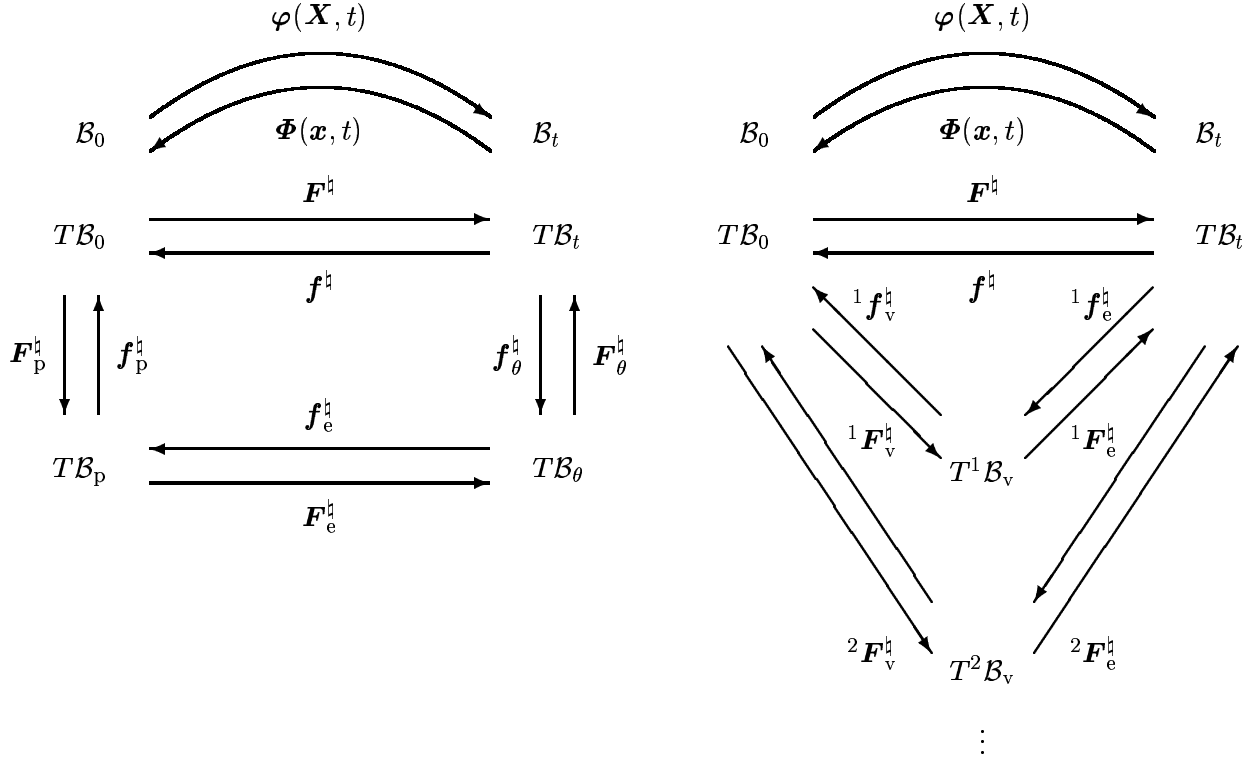


Figure 7.31: Non-linear point map φ and linear tangent maps $\mathbf{F}^\sharp, \mathbf{F}_p^\sharp, \mathbf{F}_e^\sharp, \mathbf{F}_\theta^\sharp$ within a thermomechanical setting (left) and linear tangent maps $\mathbf{F}^\sharp, {}^i\mathbf{F}_v^\sharp, {}^i\mathbf{F}_e^\sharp$ for the generalised Maxwell model (right).

The extension of the developed hyper-elastic framework to visco-elasticity is straightforward and allows a similar outline as multiplicative elasto-plasticity, see Chapter 3. In this context, let (no summation over the positive integer i)

$$\boxed{\mathbf{F}^\sharp \doteq ({}^i)\mathbf{F}_e^\sharp \cdot ({}^i)\mathbf{F}_v^\sharp \quad \text{with} \quad {}^i\mathbf{F}_v^\sharp \in \mathbb{L}_+^3 : T\mathcal{B}_0 \rightarrow T^i\mathcal{B}_v \quad \text{and} \quad {}^i\mathbf{F}_e^\sharp \in \mathbb{L}_+^3 : T^i\mathcal{B}_v \rightarrow T\mathcal{B}_t} \quad (\text{O.7})$$

represent a generalised Maxwell model with respect to a finite number of intermediate configurations ${}^i\mathcal{B}_v$, compare Govindjee and Reese [GR97], Haupt [Hau00, Sect. 10.2], Bonet [Bon01] and Nedjar [Ned02] and see Figure 7.31₂ for a descriptive visualisation. Next, we accept the following additive decomposition of the free Helmholtz energy density into

$$\psi_0^0 \doteq \infty\psi_0^0(\mathbf{C}^b, \mathbf{G}^\sharp, \mathbf{A}_{1,\dots,n}^\sharp; \mathbf{X}) + \sum_i {}^i\psi_0^0(\mathbf{C}^b, {}^i\mathbf{B}_v^\sharp, {}^i\mathbf{A}_{n+1,\dots,m}^\sharp; \mathbf{X}) \quad (\text{O.8})$$

whereby $\mathbf{A}_{1,\dots,n}^\sharp, {}^i\mathbf{A}_{n+1,\dots,m}^\sharp \in \mathbb{S}^3 : [T^*\mathcal{B}_0 \times T^*\mathcal{B}_0]_{1,\dots,m} \rightarrow \mathbb{R}$ collect symmetric second order tensor fields and the relations ${}^i\mathbf{A}_{n+1,\dots,m}^\sharp = {}^i\mathbf{f}_{v^*}^\sharp \cdot \widehat{\mathbf{A}}_{n+1,\dots,m}^\sharp, {}^i\mathbf{B}_v^\sharp = {}^i\mathbf{f}_{v^*}^\sharp \cdot \widehat{\mathbf{G}}^\sharp \in \mathbb{S}_+^3 : T^*\mathcal{B}_0 \times T^*\mathcal{B}_0 \rightarrow \mathbb{R}$ are obvious. With these relations at hand, the isothermal dissipation inequality in local format reads

$$\begin{aligned} \mathcal{D}_0^0 = & \left[[\mathbf{M}^\sharp]^\dagger - 2 \partial_{\mathbf{G}^\sharp} \infty\psi_0^0 \cdot \mathbf{G}^\sharp - 2 \sum_j \partial_{\mathbf{A}_j^\sharp} \infty\psi_0^0 \cdot \mathbf{A}_j^\sharp \right. \\ & \left. - 2 \sum_i \partial_{{}^i\mathbf{B}_v^\sharp} {}^i\psi_0^0 \cdot {}^i\mathbf{B}_v^\sharp - 2 \sum_{i,j} \partial_{{}^i\mathbf{A}_j^\sharp} {}^i\psi_0^0 \cdot {}^i\mathbf{A}_j^\sharp \right] : \mathbf{L}^\sharp \\ & - \sum_i \partial_{{}^i\mathbf{B}_v^\sharp} {}^i\psi_0^0 : \text{D}_t {}^i\mathbf{B}_v^\sharp - \sum_j \partial_{\mathbf{A}_j^\sharp} \infty\psi_0^0 : \text{D}_t \mathbf{A}_j^\sharp - \sum_{i,j} \partial_{{}^i\mathbf{A}_j^\sharp} {}^i\psi_0^0 : \text{D}_t {}^i\mathbf{A}_j^\sharp \geq 0. \end{aligned} \quad (\text{O.9})$$

The tensor series $\mathbf{A}_{1,\dots,n}^\sharp$ and ${}^i\mathbf{A}_{n+1,\dots,m}^\sharp$ are usually assumed to remain constant in \mathcal{B}_0 (material, deformation induced anisotropy) and the strict constraints $-\partial_{{}^i\mathbf{B}_v^\sharp} {}^i\psi_0^0 : \text{D}_t {}^i\mathbf{B}_v^\sharp \geq 0$ are commonly accepted. Based on this, the visco-hyper-elastic constitutive function for the Mandel stress $[\mathbf{M}^\sharp]^\dagger = \mathbf{C}^b \cdot \mathbf{S}^\sharp$

suggests an additive decomposition of the second Piola–Kirchhoff stress into a symmetric equilibrium (∞) and a symmetric non–equilibrium (neq) part, namely

$$\begin{aligned} \infty \mathbf{S}^\sharp &= 2 \mathbf{B}^\sharp \cdot \left[\partial_{\mathbf{G}^\sharp} \infty \psi_0^0 \cdot \mathbf{G}^\sharp + \sum_j \partial_{\mathbf{A}_j^\sharp} \infty \psi_0^0 \cdot \mathbf{A}_j^\sharp \right], \\ \text{neq} \mathbf{S}^\sharp &= 2 \mathbf{B}^\sharp \cdot \left[\sum_i \partial_{\mathbf{B}_v^\sharp} \text{neq} \psi_0^0 \cdot \mathbf{B}_v^\sharp + \sum_{i,j} \partial_{\mathbf{A}_j^\sharp} \text{neq} \psi_0^0 \cdot \mathbf{A}_j^\sharp \right]. \end{aligned} \quad (\text{O.10})$$

Concerning the evolution equations for the viscous contributions \mathbf{B}_v^\sharp , it is established to introduce the mapping

$$\text{D}_t \mathbf{B}_v^\sharp \doteq \mathbf{B}_v^\sharp : \mathbf{B}_v^\sharp \quad (\text{O.11})$$

whereby $\mathbf{B}_v^\sharp \in \mathbb{S}^{3 \times 3} : T^* \mathcal{B}_0 \times T^* \mathcal{B}_0 \times T \mathcal{B}_0 \times T \mathcal{B}_0 \rightarrow \mathbb{R}$ is negative definite in order to satisfy the reduced dissipation inequality and generally accounts for the deformation history and anisotropy, compare Section 5.2. For applications of anisotropic visco–elasticity within finite element settings, we refer to the recent contributions by Kaliske [Kal00] and Holzapfel and Gasser [HG01].

It is straightforward to expand the developed frameworks to visco–plastic models of classical Perzyna–type. Thereby, the Lagrange multiplier $\text{D}_t \lambda$ is replaced by the constitutive functional $\text{D}_t \lambda_v \doteq [2 \eta]^{-1} [{}^{\text{yie}} \Phi + |{}^{\text{yie}} \Phi|]$, see e.g. Mähler et al. [MER01] or the contributions by Spencer [Spe01] and Sansour and Kollmann [SK01] with special application to anisotropy. Finally, recall that the framework of a fictitious configurations is optionally included in the previous reiterations on thermo–mechanical materials, visco–elasticity and –plasticity when neglecting the additional tensor series, like e.g. $\mathbf{A}_{1,\dots,n}^\sharp$, and replacing the Lagrangian metric tensor by an anisotropy or rather damage tensor.

In order to manage the occurring localisation (e.g. for softening behaviour), a number of modifications of the standard Boltzmann continuum description, so called regularisations, have been proposed during the recent years, e.g. non–simple, non–local and micropolar continua, higher order gradient methods, rate dependency, fracture energy approaches or the introduction of discontinuous displacement fields (and combinations thereof). Practically speaking, an internal length scale is introduced. One of the most promising approaches in computational mechanics relies on the incorporation of higher gradients, typically second order material gradients in terms of the Laplace operator of a scalar measure. For the developed anisotropic continuum damage model, these gradients should be somehow related to the second order damage metric tensor \mathbf{A}^\sharp . In the subsequent brief outline, we adopt the approach highlighted in Borino et al. [BFP99] and introduce an inelastic domain $\mathcal{B}_0^{\text{ine}} \subseteq \mathcal{B}_0$ in connection with a split (internal, external) of the boundary surface $\partial \mathcal{B}_0^{\text{ine}} = \partial^{\text{int}} \mathcal{B}_0^{\text{ine}} \cup \partial^{\text{ext}} \mathcal{B}_0^{\text{ine}}$. In particular, $\mathcal{B}_0^{\text{ine}}$ represents a finite region, namely larger than a specific limit which is e.g. determined by an internal length scale ℓ_0 . Referring to the anisotropic continuum damage model of Chapter 5, the local format of the isothermal reduced dissipation inequality results in

$$\text{red} \mathcal{D}_0^0 = \mathbf{Z}^b : \text{D}_t \mathbf{A}^\sharp + \zeta_0^0 \geq 0 \quad \text{with} \quad \int_{\mathcal{B}_0^{\text{ine}}} \zeta_0^0 \, dV = 0 \quad (\text{O.12})$$

whereby hardening contributions have been neglected and $\zeta_0 \in \mathbb{R}$ is established as a non–locality residual ($\zeta_0^0 = 0$ in $\mathcal{B}_0 \setminus \mathcal{B}_0^{\text{ine}}$). Next, the gradient of the damage metric and the conjugate stress field are additionally introduced as

$$\begin{aligned} \mathfrak{A}^\sharp &\doteq \text{Grad} \mathbf{A}^\sharp && : T \mathcal{B}_0 \times T \mathcal{B}_0 \times T^* \mathcal{B}_0 \rightarrow \mathbb{R}, \\ \mathfrak{Z}^\sharp &\doteq - \partial_{\mathfrak{A}^\sharp} \psi_0^0(\mathbf{E}^b, \mathfrak{A}^\sharp; \mathbf{A}^\sharp, \mathbf{X}) && : T^* \mathcal{B}_0 \times T^* \mathcal{B}_0 \times T \mathcal{B}_0 \rightarrow \mathbb{R} \end{aligned} \quad (\text{O.13})$$

and incorporated into the reduced isothermal dissipation inequality

$$\begin{aligned} \text{red} \mathcal{D}_0^0 &= \mathbf{Z}^b : \text{D}_t \mathbf{A}^\sharp + \mathfrak{Z}^\sharp : \text{D}_t \mathfrak{A}^\sharp + \zeta_0^0 \doteq \dagger \mathbf{Z}^b : \text{D}_t \mathbf{A}^\sharp \geq 0 \\ \Rightarrow \zeta_0^0 &= - \mathbf{Z}^b : \text{D}_t \mathbf{A}^\sharp - \mathfrak{Z}^\sharp : \text{D}_t \mathfrak{A}^\sharp + \dagger \mathbf{Z}^b : \text{D}_t \mathbf{A}^\sharp. \end{aligned} \quad (\text{O.14})$$

With this setting at hand, the constraint in Eq.(O.12)₂ yields

$$\int_{\mathcal{B}_0^{\text{ine}}} \zeta_0^0 \, dV = \int_{\mathcal{B}_0^{\text{ine}}} \left[\dagger \mathbf{Z}^b - \mathbf{Z}^b - \text{Div} [\mathbf{z}^{\natural}]^t \right] : \text{D}_t \mathbf{A}^\sharp \, dV + \int_{\partial \mathcal{B}_0^{\text{ine}}} \mathbf{N}^b \cdot [\mathbf{z}^{\natural}]^t : \text{D}_t \mathbf{A}^\sharp \, dA = 0, \quad (\text{O.15})$$

whereby $\mathbf{N}^b \in \mathbb{U}^2 : T^* \mathcal{B}_0 \rightarrow \mathbb{R}$ denotes the surface normal and $\mathbf{N}^b \cdot [\mathbf{z}^{\natural}]^t = \mathbf{z}^\natural \cdot \mathbf{N}^b$. Apparently, Eq.(O.15) is satisfied for

$$\boxed{\dagger \mathbf{Z}^b - \mathbf{Z}^b - \text{Div} [\mathbf{z}^{\natural}]^t \doteq \mathbf{0} \text{ in } \mathcal{B}_0^{\text{ine}} \text{ and } \mathbf{z}^\natural \cdot \mathbf{N}^b \doteq \mathbf{0} \text{ on } \partial^{\text{ext}} \mathcal{B}_0^{\text{ine}}, \text{D}_t \mathbf{A}^\sharp \doteq \mathbf{0} \text{ on } \partial^{\text{int}} \mathcal{B}_0^{\text{ine}}.} \quad (\text{O.16})$$

Based on this, the correlated inelastic potential is determined in terms of $\dagger \mathbf{Z}^b \in \mathbb{S}^3 : T\mathcal{B}_0 \times T\mathcal{B}_0 \rightarrow \mathbb{R}$. Apparently, in the case of scalar-valued internal variables, anisotropy optionally enters the non-local formulation if specific weighting characteristics for the gradients of the internal variables are introduced. Likewise, different length scales with respect to the gradients of diverse scalar-valued internal variables (which could be attached to typical deformation modes like tension and compression) allow the modelling of anisotropic material behaviour, see e.g. Comi [Com01]. For a detailed discussion of the underlying gradient enhanced theory and numerical applications to damage and plasticity, we refer to Steinmann [Ste96, Ste99], Svedberg [Sve99] and references cited in these works. A physical motivation of higher gradient methods for single and polycrystal plasticity within small strain kinematics is highlighted in Menzel and Steinmann [MS98, MS00].

Until now, we solely incorporated linear fictitious tangent maps $\bar{\mathbf{F}}^\natural \in \mathbb{L}_+^3 : T\bar{\mathcal{B}} \rightarrow T\mathcal{B}_0$ to represent the relations between fictitious and nominal configurations, e.g. $\mathbf{A}^\sharp \doteq [\bar{\mathbf{F}}^\natural \bar{\otimes} \bar{\mathbf{F}}^\natural] : \bar{\mathbf{A}}^\sharp \in \mathbb{S}_+^3$. Apparently, “more” general mappings are possible whereby the map $\mathbf{A}^\sharp \doteq \bar{\mathbf{F}}^\natural : \bar{\mathbf{A}}^\sharp \in \mathbb{L}_+^3$, with $\bar{\mathbf{F}}^\natural([\bar{\circ}]; \mathbf{X}) \in \mathbb{L}^{3 \times 3} : [T\bar{\mathcal{B}} \times T\bar{\mathcal{B}}] \rightarrow [T\mathcal{B}_0 \times T\mathcal{B}_0]$, represents a typical reduced format (compare Section 1.3.4) which needs to be further investigated – especially in the context of large deformations. Other enhancements in terms of additional contributions of a Taylor series of the fictitious mapping like $\mathbf{A}^\sharp \doteq \bar{\mathbf{F}}^\natural : \bar{\mathbf{A}}^\sharp + \mathbf{f}^\natural : [\bar{\mathbf{A}}^\sharp \otimes \bar{\mathbf{A}}^\sharp] + \dots \in \mathbb{L}_+^3$, with $\mathbf{f}^\natural([\bar{\circ}]; \mathbf{X}) : [T\bar{\mathcal{B}} \times T\bar{\mathcal{B}} \times T\bar{\mathcal{B}} \times T\bar{\mathcal{B}}] \rightarrow [T\mathcal{B}_0 \times T\mathcal{B}_0]$, seem to be unmanageable in an appropriate numerical setting. However, the incorporation of gradients of the linear tangent map $\bar{\mathbf{F}}^\natural$ likely constitute future research. It is obvious that these gradient fields enter the definition of the Christoffel symbols (of the first kind or rather the connection coefficients) via

$$\boxed{\bar{\Gamma}_{ijk} = \bar{\mathbf{G}}_i \cdot \partial_{\theta^k} \bar{\mathbf{G}}_j = \bar{\mathbf{G}}_i \cdot [\bar{\mathbf{f}}^\natural]^t \cdot \partial_{\theta^k} \bar{\mathbf{f}}^\natural \cdot \bar{\mathbf{G}}_j = \frac{1}{2} [\partial_{\theta^k} G_{ji} + \partial_{\theta^j} G_{ik} - \partial_{\theta^i} G_{kj}]} \quad (\text{O.17})$$

compare e.g. Murnaghan [Mur51, Sect. 2.4] or Lodge [Lod51] among others. The corresponding integrability, or rather compatibility conditions, are satisfied if $\text{Curl} \bar{\mathbf{f}}^\natural = \mathbf{0}$, i.e. $\partial_{\theta^k} \bar{f}_j^i = \partial_{\theta^j} \bar{f}_k^i$, which constitutes another likely argument to enlarge the framework developed so far, compare the contributions by Steinmann [Ste96] and Acharya and Bassani [AB00] – with application to plasticity – and references cited therein.

Finally, the introduction of a fictitious configuration allows convenient extension to the modelling of materials with growth (recall that we deal with a reduced representation of a fabric tensor approach), see Epstein and Maugin [EM00], Rodriguez et al. [RHM94], Chen and Hoger [CH00] for a general outline. A (very) simple prototype model could be defined via the following evolution equations

$$\boxed{\begin{aligned} \text{D}_t \gamma &\doteq \beta^e \left[\gamma^{\frac{l-m-1}{m}} \psi_0^0 - \text{ref} \psi_0^e \right] & \text{with} & \quad \gamma \doteq \varrho_0^{-m} \varrho_t^m \text{ and } m \succ l, \\ \text{D}_t \mathbf{A}^\sharp &\doteq \beta^{A^\sharp} \partial_{\mathbf{Z}^b} \text{pot} \Phi^0 & \text{with} & \quad \text{pot} \Phi^0 \doteq \text{fib} \Phi^0(\mathbf{Z}^b; \mathbf{A}^\sharp, \mathbf{X}) - \text{ref} \psi_0^{A^\sharp} \doteq 0, \end{aligned}} \quad (\text{O.18})$$

whereby $\varrho_0, \varrho_t \in \mathbb{R}_+$ characterise initial and actual density-type fields, respectively, $\beta^e, \beta^{A^\sharp}, \text{ref} \psi_0^e, \text{ref} \psi_0^{A^\sharp} \in \mathbb{R}_0$ and m, l denote positive integers *. In addition, the introduction of dead zones is a natural consequence and specific assumptions on the coaxiality of the anisotropy metric \mathbf{A}^\sharp

* Due to the nature of materials with growth, the mass of such bodies no longer remains constant. We therefore obtain in general $\text{D}_t \int_{\mathcal{B}_0} \rho_0 \, dV = \int_{\mathcal{B}_0} {}^V G \, dV + \int_{\partial \mathcal{B}_0} {}^A G \, dA \neq 0$ whereby $\rho_0 \in \mathbb{R}_+$ represents the density in \mathcal{B}_0 , ${}^V G \in \mathbb{R}$ denotes a volumetric mass source and ${}^A G = {}^A \mathbf{G}^\sharp \cdot \mathbf{N}^b$ characterises a boundary flux term (${}^A \mathbf{G}^\sharp \in \mathbb{R}^3 : T^* \mathcal{B}_0 \rightarrow \mathbb{R}$,

and the stress field \mathbf{S}^\sharp as well as decompositions for the evolution equation of \mathbf{A}^\sharp e.g. in a spherical and a deviatoric part are established approaches for small strain kinematics. Based on the framework of linear elasticity, numerical applications within finite element settings are developed in Jacobs et al. [JSBC97] and moreover, Weng [Wen98] advocated a formulation which is based essentially on the spectral decomposition of the continuum tangent operator.


$\mathcal{N}^\flat \in \mathbb{U}^2 : T\mathcal{B}_0 \rightarrow \mathbb{R}$), compare footnote †† on page 145. The corresponding local form with respect to the Eulerian setting consequently results in the mass balance

$$D_t \rho = {}^v g + \operatorname{div} {}^a \mathbf{g}^\sharp - \rho \operatorname{div} D_t \mathbf{x} \quad (*.1)$$

via Cauchy's theorem $\partial_t \rho_0|_{\mathbf{x}} = {}^V G + \operatorname{Div} {}^A \mathbf{G}^\sharp$ with the density $\rho = \det(\mathbf{f}^\sharp) \rho_0 \in \mathbb{R}_+$ in \mathcal{B}_t , ${}^v g = \det(\mathbf{f}^\sharp) {}^V G \in \mathbb{R}$ and ${}^a \mathbf{g}^\sharp = {}^A \mathbf{G}^\sharp \cdot \operatorname{cof}(\mathbf{f}^\sharp) \in \mathbb{R}^3 : T^* \mathcal{B}_t \rightarrow \mathbb{R}$. Please note that the balance of linear momentum (similar to Eq.(††.1)) together with Eq.(*.1) yields a coupled problem in analogy to the previously highlighted thermomechanical setting – Eqs.(††.1, ††.2). A detailed outline on the balance of linear and angular momentum ($\mathbf{S}^\sharp, \boldsymbol{\tau}^\sharp \in \mathbb{L}^3$) as well as energy and entropy are given in Epstein and Maugin [EM00]. Moreover, volumetric growth allows similar representation with thermal expansion. Therefore, a multiplicative decomposition of the total deformation gradient – like e.g. $\mathbf{F}^\sharp \doteq \mathbf{F}_1^\sharp \cdot \mathbf{F}_e^\sharp \cdot \mathbf{F}_g^\sharp$ with $\mathbf{F}_1^\sharp, \mathbf{F}_g^\sharp \in \mathbb{L}_+^3$ – is a natural consequence, compare Figure 7.31₁. The physical interpretation of these three contributions is essentially based on a stress-free, unloaded reference configuration \mathcal{B}_0 of the body B . The linear tangent map \mathbf{F}_g^\sharp relates the tangent space of \mathcal{B}_0 to the tangent space of an intermediate configuration which takes the image of stress-free infinitesimal elements which are obtained from cutting B into infinitesimal sections. Thereby the growth of each element (increase or decrease in volume) may be anisotropic and we obtain a geometrical misfit, i.e. the considered intermediate configuration is incompatible. Consequently, the linear tangent map \mathbf{F}_e^\sharp deforms every section such that we can “glue” the (grown) elements together and thus deal with a compatible but stressed intermediated configuration whereby the underlying tangent space is related to the tangent space of \mathcal{B}_0 by the inverse of the linear tangent map $\mathbf{F}_e^\sharp \cdot \mathbf{F}_g^\sharp$. Finally, external loading is represented via the linear tangent map \mathbf{F}_1^\sharp which relates the tangent space of the compatible intermediate configuration to the tangent space of the spatial configuration \mathcal{B}_t .

Appendix A

Notation

he proper manner of calligraphy is nothing other than not being careless, but in this way one's writing will simply be sluggish and stiff. One should go beyond this and depart from the norm. This principle applies to all things.

Yamamoto Tsunetomo [1658 – 1719]
Hagakure, The Book of the Samurai, 1979

Referring to convective coordinates, we adopt the notation highlighted in the monograph by Marsden and Hughes [MH94, Chap. 1] and indicate e.g. the spatial co-variant metric tensor with $\mathbf{g}^{\flat} \in \mathbb{S}_+^n$, the spatial contra-variant metric tensor with $\mathbf{g}^{\sharp} \in \mathbb{S}_+^n$ and spatial contra-, co-variant second order identity tensor with $\mathbf{g}^{\natural} \in \mathbb{L}_+^n$ (mixed-variant fields are generally characterised by the symbol \natural). Now, let $\mathbf{a}_{1,2}^{\sharp}, \mathbf{b}_{1,2}^{\flat} \in \mathbb{R}^n$ be spatial vectors, $\mathbf{u}_{1,2}^{\natural} \in \mathbb{L}^n$ represent spatial contra-, co-variant second order fields and $\mathbf{u}_{3,4}^{\natural} \in \mathbb{L}^n$ spatial co-, contra-variant second order fields, $\mathbf{v}_{1,2}^{\sharp}, \mathbf{w}_{1,2}^{\flat} \in \mathbb{L}^n$ are assumed to denote spatial second order tensors, $\mathbf{y}_{1,\dots,n}^{\sharp}, \mathbf{z}_{1,2}^{\flat} \in \mathbb{S}^n$ characterise spatial symmetric tensors of second order and $\mathbf{v}_1^{\sharp}, \mathbf{w}_1^{\flat} \in \mathbb{L}^{n \times n}$ are fourth order tensors, respectively; see Section A.2 for a definition of the underlying spaces.

A.1 Useful abbreviations

In this work, we apply two types of non-standard dyadic products which are defined via [†]

$$\begin{aligned}
 [\mathbf{u}_1^{\natural} \overline{\otimes} \mathbf{u}_3^{\natural}] : \mathbf{u}_2^{\flat} &= \mathbf{u}_1^{\natural} \cdot \mathbf{u}_2^{\flat} \cdot [\mathbf{u}_3^{\natural}]^{\flat}, & [\mathbf{u}_1^{\natural} \underline{\otimes} \mathbf{u}_3^{\natural}] : \mathbf{u}_4^{\flat} &= \mathbf{u}_1^{\natural} \cdot [\mathbf{u}_4^{\natural}]^{\flat} \cdot [\mathbf{u}_3^{\natural}]^{\flat}, \\
 [\mathbf{u}_3^{\natural} \overline{\otimes} \mathbf{u}_1^{\natural}] : \mathbf{u}_4^{\flat} &= \mathbf{u}_3^{\natural} \cdot \mathbf{u}_4^{\flat} \cdot [\mathbf{u}_1^{\natural}]^{\flat}, & [\mathbf{u}_3^{\natural} \underline{\otimes} \mathbf{u}_1^{\natural}] : \mathbf{u}_2^{\flat} &= \mathbf{u}_3^{\natural} \cdot [\mathbf{u}_2^{\natural}]^{\flat} \cdot [\mathbf{u}_1^{\natural}]^{\flat}, \\
 [\mathbf{u}_1^{\natural} \overline{\otimes} \mathbf{u}_2^{\natural}] : \mathbf{v}_1^{\sharp} &= \mathbf{u}_1^{\natural} \cdot \mathbf{v}_1^{\sharp} \cdot [\mathbf{u}_2^{\natural}]^{\flat}, & [\mathbf{u}_1^{\natural} \underline{\otimes} \mathbf{u}_2^{\natural}] : \mathbf{v}_1^{\sharp} &= \mathbf{u}_1^{\natural} \cdot [\mathbf{v}_1^{\sharp}]^{\flat} \cdot [\mathbf{u}_2^{\natural}]^{\flat}, \\
 [\mathbf{u}_3^{\natural} \overline{\otimes} \mathbf{u}_4^{\natural}] : \mathbf{w}_1^{\flat} &= \mathbf{u}_3^{\natural} \cdot \mathbf{w}_1^{\flat} \cdot [\mathbf{u}_4^{\natural}]^{\flat}, & [\mathbf{u}_3^{\natural} \underline{\otimes} \mathbf{u}_4^{\natural}] : \mathbf{w}_1^{\flat} &= \mathbf{u}_3^{\natural} \cdot [\mathbf{w}_1^{\flat}]^{\flat} \cdot [\mathbf{u}_4^{\natural}]^{\flat}, \\
 [\mathbf{w}_1^{\flat} \overline{\otimes} \mathbf{w}_2^{\flat}] : \mathbf{v}_1^{\sharp} &= \mathbf{w}_1^{\flat} \cdot \mathbf{v}_1^{\sharp} \cdot [\mathbf{w}_2^{\flat}]^{\flat}, & [\mathbf{w}_1^{\flat} \underline{\otimes} \mathbf{w}_2^{\flat}] : \mathbf{v}_1^{\sharp} &= \mathbf{w}_1^{\flat} \cdot [\mathbf{v}_1^{\sharp}]^{\flat} \cdot [\mathbf{w}_2^{\flat}]^{\flat}, \\
 [\mathbf{v}_1^{\sharp} \overline{\otimes} \mathbf{v}_2^{\sharp}] : \mathbf{w}_1^{\flat} &= \mathbf{v}_1^{\sharp} \cdot \mathbf{w}_1^{\flat} \cdot [\mathbf{v}_2^{\sharp}]^{\flat}, & [\mathbf{v}_1^{\sharp} \underline{\otimes} \mathbf{v}_2^{\sharp}] : \mathbf{w}_1^{\flat} &= \mathbf{v}_1^{\sharp} \cdot [\mathbf{w}_1^{\flat}]^{\flat} \cdot [\mathbf{v}_2^{\sharp}]^{\flat},
 \end{aligned} \tag{A.1}$$

whereby the applied transposition operation for second order fields reads as (see footnote ** on page 27)

$$\mathbf{b}_1^{\flat} \cdot \mathbf{u}_1^{\natural} \cdot \mathbf{a}_1^{\sharp} = \mathbf{a}_1^{\sharp} \cdot [\mathbf{u}_1^{\natural}]^{\flat} \cdot \mathbf{b}_1^{\flat}, \quad \mathbf{b}_1^{\flat} \cdot \mathbf{v}_1^{\sharp} \cdot \mathbf{b}_2^{\flat} = \mathbf{b}_2^{\flat} \cdot [\mathbf{v}_1^{\sharp}]^{\flat} \cdot \mathbf{b}_1^{\flat}, \quad \mathbf{a}_1^{\sharp} \cdot \mathbf{w}_1^{\flat} \cdot \mathbf{a}_2^{\sharp} = \mathbf{a}_2^{\sharp} \cdot [\mathbf{w}_1^{\flat}]^{\flat} \cdot \mathbf{a}_1^{\sharp}. \tag{A.2}$$

[†]Eqs.(A.1) highlight the definitions of the applied non-standard dyadic products by double contraction to the right. The corresponding double contraction to the left (e.g. $\mathbf{w}_1^{\flat} : [\mathbf{v}_1^{\sharp} \overline{\otimes} \mathbf{v}_2^{\sharp}] = [\mathbf{v}_1^{\sharp}]^{\flat} \cdot \mathbf{w}_1^{\flat} \cdot \mathbf{v}_2^{\sharp}$ and $\mathbf{w}_1^{\flat} : [\mathbf{v}_1^{\sharp} \underline{\otimes} \mathbf{v}_2^{\sharp}] = [\mathbf{v}_1^{\sharp}]^{\flat} \cdot [\mathbf{w}_1^{\flat}]^{\flat} \cdot \mathbf{v}_2^{\sharp}$) is obvious and thus omitted.

When referring to fourth order tensors, two different types of transposition are similarly introduced, i.e.

$$\begin{aligned} \mathbf{w}_1^b : \mathbf{v}_1^\sharp : \mathbf{w}_2^b &= \mathbf{w}_1^b : [\mathbf{v}_1^\sharp]^t : [\mathbf{w}_2^b]^t, & \mathbf{w}_1^b : \mathbf{v}_1^\sharp : \mathbf{w}_2^b &= \mathbf{w}_2^b : [\mathbf{v}_1^\sharp]^T : \mathbf{w}_1^b, \\ \mathbf{v}_1^\sharp : \mathbf{w}_1^b : \mathbf{v}_2^\sharp &= \mathbf{v}_1^\sharp : [\mathbf{w}_1^b]^t : [\mathbf{v}_2^\sharp]^t, & \mathbf{v}_1^\sharp : \mathbf{w}_1^b : \mathbf{v}_2^\sharp &= \mathbf{v}_2^\sharp : [\mathbf{w}_1^b]^T : \mathbf{v}_1^\sharp \end{aligned} \quad (\text{A.3})$$

which are established as minor (t) and major (T) transposition. The definition of transposition operations for different mixed-variant fourth order tensors is straightforward and thus not highlighted here for clarity's sake.

It arises naturally to introduce specific notations for higher order tensors. We apply the following abbreviations specifically for mixed-variant spatial fourth order fields

$$\begin{aligned} \mathbf{g}^\sharp &\doteq \mathbf{g}^\sharp \overline{\otimes} \mathbf{g}^\sharp, & \mathbf{v}_1^\sharp &= \mathbf{g}^\sharp : \mathbf{v}_1^\sharp, \\ \text{sym} \mathbf{g}^\sharp &\doteq \frac{1}{2} [\mathbf{g}^\sharp \overline{\otimes} \mathbf{g}^\sharp + \mathbf{g}^\sharp \underline{\otimes} \mathbf{g}^\sharp], & [\mathbf{v}_1^\sharp]^{\text{sym}} &= \text{sym} \mathbf{g}^\sharp : \mathbf{v}_1^\sharp, \\ \text{skw} \mathbf{g}^\sharp &\doteq \frac{1}{2} [\mathbf{g}^\sharp \overline{\otimes} \mathbf{g}^\sharp - \mathbf{g}^\sharp \underline{\otimes} \mathbf{g}^\sharp], & [\mathbf{v}_1^\sharp]^{\text{skw}} &= \text{skw} \mathbf{g}^\sharp : \mathbf{v}_1^\sharp, \\ \text{sph} \mathbf{g}^\sharp &\doteq \frac{1}{n} \mathbf{g}^\sharp \otimes \mathbf{g}^\sharp, & [\mathbf{v}_1^\sharp]^{\text{sph}} &= \text{sph} \mathbf{g}^\sharp : \mathbf{v}_1^\sharp, \\ \text{dev} \mathbf{g}^\sharp &\doteq \mathbf{g}^\sharp - \text{sph} \mathbf{g}^\sharp, & [\mathbf{v}_1^\sharp]^{\text{dev}} &= \text{dev} \mathbf{g}^\sharp : \mathbf{v}_1^\sharp, \\ \text{dev} \mathbf{g}_{\text{sym}}^\sharp &\doteq \text{sym} \mathbf{g}^\sharp - \text{sph} \mathbf{g}^\sharp, & [\mathbf{v}_1^\sharp]^{\text{dev}}_{\text{sym}} &= \text{dev} \mathbf{g}_{\text{sym}}^\sharp : \mathbf{v}_1^\sharp, \\ \text{dev} \mathbf{g}_{\text{skw}}^\sharp &\doteq \text{skw} \mathbf{g}^\sharp - \text{sph} \mathbf{g}^\sharp, & [\mathbf{v}_1^\sharp]^{\text{dev}}_{\text{skw}} &= \text{dev} \mathbf{g}_{\text{skw}}^\sharp : \mathbf{v}_1^\sharp, \end{aligned} \quad (\text{A.4})$$

which map contra-variant second order tensors to contra-variant second order tensors[‡]. The derivation of mixed-variant fourth order fields which map co-variant second order tensors is straightforward and thus skipped here. Generally, similar abbreviations for symmetric, skew-symmetric, etc. co-variant second order tensors are adopted. Even for mixed-variant second order fields, the spherical and deviatoric operations are a natural outcome. On the contrary, the symmetry and skew-symmetry transformations need further attention since a mixed-variant field and its transposed belong to different spaces and thus cannot be added, compare footnote ** on page 27. We can nevertheless introduce these operations for mixed-variant fields with respect to the identity. To give an example, let the symmetry and skew-symmetry operation for \mathbf{u}_1^\sharp refer to the mixed-variant identity \mathbf{g}^\sharp , to be specific

$$[\mathbf{u}_1^\sharp \cdot \mathbf{g}^\sharp]^{\text{sym}} = \text{sym} \mathbf{g}^\sharp : [\mathbf{u}_1^\sharp \cdot \mathbf{g}^\sharp] \quad \text{and} \quad [\mathbf{u}_1^\sharp \cdot \mathbf{g}^\sharp]^{\text{skw}} = \text{skw} \mathbf{g}^\sharp : [\mathbf{u}_1^\sharp \cdot \mathbf{g}^\sharp]. \quad (\text{A.5})$$

Furthermore, within the Lagrangian setting, the fourth order tensors in Eq.(A.4) are denoted by \mathbf{G}^\sharp, \dots and when applying a Cartesian frame, we prefer to use the abbreviations \mathbf{I}, \dots . Next, as examples of frequently considered derivatives, we highlight the following relations

$$\begin{aligned} \partial_{\mathbf{v}_1^\sharp} \mathbf{v}_1^\sharp &= \mathbf{g}^\sharp \overline{\otimes} \mathbf{g}^\sharp, & -\partial_{\mathbf{v}_1^\sharp} [\mathbf{v}_1^\sharp]^{-1} &= [\mathbf{v}_1^\sharp]^{-1} \overline{\otimes} [\mathbf{v}_1^\sharp]^{-t}, \\ \partial_{\mathbf{v}_1^\sharp} [\mathbf{v}_1^\sharp]^t &= \mathbf{g}^\sharp \underline{\otimes} \mathbf{g}^\sharp, & -\partial_{\mathbf{v}_1^\sharp} [\mathbf{v}_1^\sharp]^{-t} &= [\mathbf{v}_1^\sharp]^{-t} \underline{\otimes} [\mathbf{v}_1^\sharp]^{-1}, \\ \partial_{\mathbf{u}_1^\sharp} \mathbf{u}_1^\sharp &= \mathbf{g}^\sharp \overline{\otimes} [\mathbf{g}^\sharp]^t, & -\partial_{\mathbf{u}_1^\sharp} [\mathbf{u}_1^\sharp]^{-1} &= \left[[\mathbf{u}_1^\sharp]^{-1} \cdot \mathbf{g}^\sharp \right] \overline{\otimes} \left[[\mathbf{u}_1^\sharp]^{-t} \cdot \mathbf{g}^\sharp \right], \\ \partial_{\mathbf{u}_1^\sharp} [\mathbf{u}_1^\sharp]^t &= [\mathbf{g}^\sharp]^t \underline{\otimes} \mathbf{g}^\sharp, & -\partial_{\mathbf{u}_1^\sharp} [\mathbf{u}_1^\sharp]^{-t} &= \left[[\mathbf{u}_1^\sharp]^{-t} \cdot \mathbf{g}^\sharp \right] \underline{\otimes} \left[[\mathbf{u}_1^\sharp]^{-1} \cdot \mathbf{g}^\sharp \right], \\ \partial_{\mathbf{y}_1^\sharp} \mathbf{y}_1^\sharp &= \text{sym} \mathbf{g}^\sharp, & -\partial_{\mathbf{y}_1^\sharp} [\mathbf{y}_1^\sharp]^{-1} &= \frac{1}{2} \left[[\mathbf{y}_1^\sharp]^{-1} \overline{\otimes} [\mathbf{y}_1^\sharp]^{-1} + [\mathbf{y}_1^\sharp]^{-1} \underline{\otimes} [\mathbf{y}_1^\sharp]^{-1} \right], \end{aligned} \quad (\text{A.6})$$

with the corresponding derivatives in terms of a co-variant fields, e.g. \mathbf{w}_1^b and \mathbf{z}_1^b or co-, contra-variant fields, e.g. \mathbf{u}_3^\sharp , being obvious.

Concerning the symmetry and skew-symmetry operation for fourth order contra- or co-variant fields, we prefer not to introduce mappings via eighth order tensors and thus define the correlated

[‡]The components of all fields are assumed to be real. Thus the (general) Hermitian is throughout denoted as a symmetric field.

transformations by

$$\begin{aligned} [\mathbf{v}^\#]^{\text{sym}} &= \frac{1}{2} \left[[\mathbf{v}^\#] + [\mathbf{v}^\#]^t \right], & [\mathbf{v}^\#]^{\text{SYM}} &= \frac{1}{2} \left[[\mathbf{v}^\#] + [\mathbf{v}^\#]^T \right], \\ [\mathbf{w}^b]^{\text{skw}} &= \frac{1}{2} \left[[\mathbf{w}^b] - [\mathbf{w}^b]^t \right], & [\mathbf{w}^b]^{\text{SKW}} &= \frac{1}{2} \left[[\mathbf{w}^b] - [\mathbf{w}^b]^T \right] \end{aligned} \quad (\text{A.7})$$

whereby these representations are respectively established as minor (sym, skw) and major (SYM, SKW) symmetry and skew-symmetry.

Finally, in order to keep the notation of some formulae manageable, we apply the following simplifications

$$\underbrace{[\mathbf{y}_{i,j,\dots,k}^\# \cdot \mathbf{z}_1^b]_{q \times}}^q = \underbrace{[\mathbf{y}_i^\# \cdot \mathbf{z}_1^b] \cdot [\mathbf{y}_j^\# \cdot \mathbf{z}_1^b] \cdot \dots \cdot [\mathbf{y}_k^\# \cdot \mathbf{z}_1^b]}_{q \times [\dots]} = \underbrace{[\mathbf{z}_1^b \cdot \mathbf{y}_{k,j,\dots,i}^\#]_{q \times}}^q \quad (\text{A.8})$$

and

$$\underbrace{[\mathbf{y}_{i,j,\dots,k}^\# \cdot \mathbf{z}_1^b]_q}_{q \times} = [\mathbf{y}_i^\# \cdot \mathbf{z}_1^b \cdot \mathbf{y}_j^\# \cdot \mathbf{z}_1^b \cdot \dots \cdot \mathbf{z}_1^b \cdot \mathbf{y}_k^\#] = \underbrace{[\mathbf{z}_1^b \cdot \mathbf{y}_{k,j,\dots,i}^\#]_q}_{q \times} \quad (\text{A.9})$$

A.2 Denomination of spaces

In the following, the applied notation of spaces is reiterated, which is standard as far as possible. Thus the set of real numbers is denoted by \mathbb{R} with useful subsets $\mathbb{R}_{\text{inv}} = \{x \in \mathbb{R} : x \neq 0\}$, $\mathbb{R}_0 = \{x \in \mathbb{R} : x \geq 0\}$ and $\mathbb{R}_+ = \{x \in \mathbb{R} : x > 0\}$. The Euclidian point-space of dimension n (with n being a positive integer) is indicated by \mathbb{E}^n and moreover, let \mathbb{V}^n specify an associated affine vector-space. The representation $\mathbb{U}^m = \{\mathbf{x} \in \mathbb{R}^n : \|\mathbf{x}\| = 1\}$ characterises a unit-sphere in \mathbb{R}^n with $m = n - 1$ whereby the norm refers to an appropriate metric. As usual, the space of mappings of \mathbb{R}^n into \mathbb{R}^n is denoted by \mathbb{L}^n with useful subspaces $\mathbb{L}_{\text{inv}}^n = \{\mathbf{y} \in \mathbb{L}^n : \det(\mathbf{y}) \in \mathbb{R}_{\text{inv}}\}$, $\mathbb{L}_0^n = \{\mathbf{y} \in \mathbb{L}^n : \det(\mathbf{y}) \in \mathbb{R}_0\}$, $\mathbb{L}_+^n = \{\mathbf{y} \in \mathbb{L}^n : \det(\mathbf{y}) \in \mathbb{R}_+\}$, $\mathbb{S}^n = \{\mathbf{y} \in \mathbb{L}^n : \mathbf{y} = \mathbf{y}^t\}$, $\mathbb{S}_{\text{inv}}^n = \{\mathbf{y} \in \mathbb{S}^n : \mathbf{x} \cdot \mathbf{y} \cdot \mathbf{x} \in \mathbb{R}_{\text{inv}}, \forall \mathbf{x} \in \mathbb{R}^n, \mathbf{x} \neq \mathbf{0}\}$, $\mathbb{S}_0^n = \{\mathbf{y} \in \mathbb{S}^n : \mathbf{x} \cdot \mathbf{y} \cdot \mathbf{x} \in \mathbb{R}_0, \forall \mathbf{x} \in \mathbb{R}^n, \mathbf{x} \neq \mathbf{0}\}$, $\mathbb{S}_+^n = \{\mathbf{y} \in \mathbb{S}^n : \mathbf{x} \cdot \mathbf{y} \cdot \mathbf{x} \in \mathbb{R}_+, \forall \mathbf{x} \in \mathbb{R}^n, \mathbf{x} \neq \mathbf{0}\}$, $\mathbb{W}^n = \{\mathbf{y} \in \mathbb{L}^n : \mathbf{y}^t = -\mathbf{y}\}$, $\mathbb{O}^n = \{\mathbf{y} \in \mathbb{L}^n : \mathbf{y}^t \cdot \mathbf{y} = \mathbf{y} \cdot \mathbf{y}^t = \mathbf{I}\}$, $\mathbb{O}_+^n = \{\mathbf{y} \in \mathbb{O}^n : \det(\mathbf{y}) = 1\}$, $\mathbb{M}^n = \{\mathbf{y} \in \mathbb{L}^n : \det^2(\mathbf{y}) = 1\}$, $\mathbb{M}_+^n = \{\mathbf{y} \in \mathbb{L}^n : \det(\mathbf{y}) = 1\}$, whereby \mathbf{I} denotes the second order identity and $[\bullet]^t$ indicates transposition. Finally, let the space of linear mappings of \mathbb{L}^n into \mathbb{L}^o (with o being a positive integer) be represented by $\mathbb{L}^{o \times n}$ and the mapping of \mathbb{L}^n into \mathbb{S}^o by $\mathbb{S}^{o \times n}$.

A.3 Denomination of functions

What we call mapping is a sufficient smooth function α from one space \mathbb{X} to another space \mathbb{Y} ; $\alpha : \mathbb{X} \rightarrow \mathbb{Y}$. A composite mapping $\beta \circ \alpha : \mathbb{X} \rightarrow \mathbb{Z}$ with $\beta : \mathbb{Y} \rightarrow \mathbb{Z}$ is defined by $(\alpha \circ \beta)(\mathbf{x}) = \beta(\alpha(\mathbf{x}))$, $\mathbf{x} \in \mathbb{X}$. Moreover, the mapping induced by α between spaces on differential forms (\mathbf{D} , elements of the dual- or rather co-tangent space) are denoted by α^* and the mapping induced by α between spaces on chains (\mathbf{C} , elements of the tangent space) read α_* , compare e.g. Flanders [Fla89, Sects. 3.3 & 5.11] or Abraham and Marsden [AM78, Def. 1.7.16]. Figure A.1 gives a graphical representation of these mappings.

Push-forward and pull-back operations are applied throughout this work especially to contra-, co-variant, contra-variant and co-variant second order tensors with respect to linear tangent maps, e.g. $\mathbf{F} \in \mathbb{L}_+^3 : T\mathcal{B}_0 \rightarrow T\mathcal{B}_t$ and $\mathbf{f} \in \mathbb{L}_+^3 : T\mathcal{B}_t \rightarrow T\mathcal{B}_0$ defined by the diffeomorphisms $\varphi(\mathbf{X}, t) : \mathcal{B}_0 \times \mathbb{R} \rightarrow \mathcal{B}_t$ and $\Phi(\mathbf{x}, t) : \mathcal{B}_t \times \mathbb{R} \rightarrow \mathcal{B}_0$, respectively. We denote these operations by φ_* , φ^* and Φ_* , Φ^* and adopt the abbreviations \mathbf{F}^\natural_* , \mathbf{F}^\natural^* and \mathbf{f}^\natural_* , \mathbf{f}^\natural^* for the analogous operations in terms of the linear tangent maps. Moreover, since φ represents the direct non-linear deformation mapping and Φ the inverse complement, we often do not thoroughly distinguish between φ^* and Φ_* or φ_* and Φ^* , respectively. For convenience of the reader Eqs.(A.10) summarise these transformations with respect to sec-

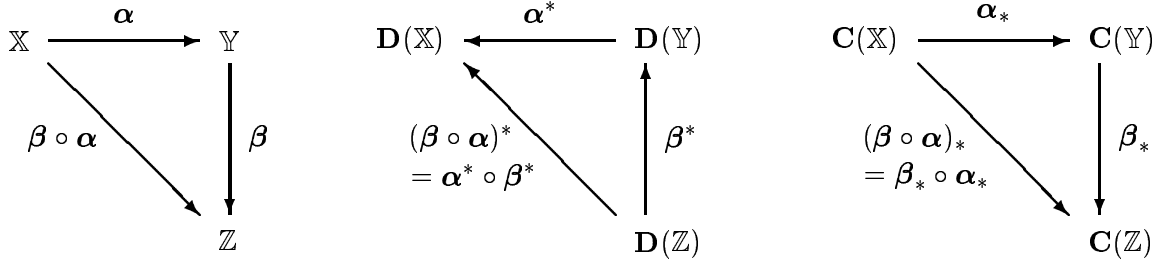


Figure A.1: Composite mappings between spaces.

and order tensors, denoted $\mathbf{u}^\natural, \mathbf{v}^\sharp, \mathbf{w}^\flat$ in the spatial setting and $\mathbf{U}^\natural, \mathbf{V}^\sharp, \mathbf{W}^\flat$ as their material counterpart (with a slight misusage of notation for the mixed-variant transformations)

$$\begin{array}{l}
 \varphi^* \mathbf{u}^\natural = \mathbf{f}^\natural_* \mathbf{u}^\natural = \mathbf{f}^\natural \cdot \mathbf{u}^\natural \cdot \mathbf{F}^\natural = u^i_j \mathbf{G}_i \otimes \mathbf{G}^j = \mathbf{U}^\natural, \\
 \Phi_* \mathbf{v}^\sharp = \mathbf{f}^\sharp_* \mathbf{v}^\sharp = \mathbf{f}^\sharp \cdot \mathbf{v}^\sharp \cdot [\mathbf{f}^\natural]^\flat = v^{ij} \mathbf{G}_i \otimes \mathbf{G}_j = \mathbf{V}^\sharp, \\
 \varphi^* \mathbf{w}^\flat = \mathbf{F}^\flat_* \mathbf{w}^\flat = [\mathbf{F}^\natural]^\flat \cdot \mathbf{w}^\flat \cdot \mathbf{F}^\natural = w_{ij} \mathbf{G}^i \otimes \mathbf{G}^j = \mathbf{W}^\flat, \\
 \varphi_* \mathbf{U}^\natural = \mathbf{F}^\natural_* \mathbf{U}^\natural = \mathbf{F}^\natural \cdot \mathbf{U}^\natural \cdot \mathbf{f}^\natural = U^i_j \mathbf{g}_i \otimes \mathbf{g}^j = \mathbf{u}^\natural, \\
 \varphi_* \mathbf{V}^\sharp = \mathbf{F}^\sharp_* \mathbf{V}^\sharp = \mathbf{F}^\sharp \cdot \mathbf{V}^\sharp \cdot [\mathbf{F}^\natural]^\flat = V^{ij} \mathbf{g}_i \otimes \mathbf{g}_j = \mathbf{v}^\sharp, \\
 \Phi^* \mathbf{W}^\flat = \mathbf{f}^\flat_* \mathbf{W}^\flat = [\mathbf{f}^\natural]^\flat \cdot \mathbf{W}^\flat \cdot \mathbf{f}^\natural = W_{ij} \mathbf{g}^i \otimes \mathbf{g}^j = \mathbf{w}^\flat,
 \end{array} \tag{A.10}$$

compare footnote ** on page 27.

Appendix B

Some comments on isotropic tensor functions

Seder, der mich kennt, weiß, wie verhaßt mir Fehler sind. ... Wenn ich in einem Buch auf einen Fehler stoße, werde ich sogleich äußerst ungehalten und frage mich, was ich wohl von einem Autor lernen kann, der sich bereits in mindestens einem Punkt erwiefenermaßen geirrt hat. Gehen die Fehler auf mein Konto oder betreffen sie meine Arbeit, erfährt mich maßloser Zorn. Der Leser dieses Buches kann sich daher unschwer die Zerknirschung ausmalen, die mich beim bloßen Gedanken daran überkommt, daß meine Freunde und Kollegen nach der Veröffentlichung Duzende schwerwiegender Fehler finden, die sie schadenfroh oder mitfühlend dem perfektionistischen Autor hinterbringen.

Murray Gell-Mann
Das Quark und der Jaguar, 1994

An (hemitropic) isotropic tensor-function remains invariant under the action of (proper) orthogonal tensors. The underlying painstaking analysis to compute general irreducible representations has been developed over several decades, see Spencer [Spe71] for the polynomial case and Wang [Wan70], Rivlin [Riv70], Smith [Smi71a], Boehler [Boe77] and Zheng [Zhe93a] with emphasis on non-polynomial settings. In this Chapter, we place special emphasis on the scalar-valued case, i.e. the free Helmholtz energy density which is assumed to define hyper-elastic constitutive functions.

B.1 Characteristic polynomial

Let $\mathbf{u}^\natural \in \mathbb{L}^n$ be an Eulerian contra-, co-variant second order field. The underlying eigenvalue problem

$${}^{\text{lef}}\mathbf{n}_i^\flat \cdot [\lambda_i \mathbf{g}^\natural - \mathbf{u}^\natural] \doteq \mathbf{0} \quad \text{and} \quad [\lambda_i \mathbf{g}^\natural - \mathbf{u}^\natural] \cdot {}^{\text{rig}}\mathbf{n}_i^\sharp \doteq \mathbf{0} \quad (\text{B.1})$$

corresponds to the characteristic polynomial

$$\det(\lambda \mathbf{g}^\natural - \mathbf{u}^\natural) = \sum_{m=0}^n [-1]^m J_m(\mathbf{u}^\natural; [\mathbf{g}^\natural]^\dagger) \lambda^{n-m} \doteq 0 \quad (\text{B.2})$$

whereby ${}^{\text{lef}}\mathbf{n}_i^\flat, {}^{\text{rig}}\mathbf{n}_i^\sharp \in \mathbb{R}^n$ denote the left and right eigenvectors and let $\lambda_i, J_m \in \mathbb{R}$ represent the sets of eigenvalues and principal invariants (with $J_0 = 1$ and $J_n = \det(\mathbf{u}^\natural)$), respectively, compare Ericksen [Eri60, Sect. 37 & 38], Eringen [Eri71, Sect. 1.10] or Lodge [Lod74, Sect. 2.8] [§]. Furthermore, the

[§]A sufficient condition for non-complex eigenvalues $\lambda_i \in \mathbb{R}$ – which implies $J_m \in \mathbb{R}$, ${}^{\text{lef}}\mathbf{n}_i^\flat : TB_t \rightarrow \mathbb{R}$ and ${}^{\text{rig}}\mathbf{n}_i^\sharp : TB_t \rightarrow \mathbb{R}$ – is given by $\mathbf{u}^\natural \doteq \mathbf{y}^\sharp \cdot \mathbf{z}^\flat$ with $\mathbf{y}^\sharp \in \mathbb{S}_+^n$ and $\mathbf{z}^\flat \in \mathbb{S}^n$, compare Section 3.5.

constraint that \mathbf{u}^\sharp satisfies its characteristic polynomial results in

$$\boxed{\sum_{m=0}^n [-1]^m J_m(\mathbf{u}^\sharp; [\mathbf{g}^\sharp]^\dagger) [\mathbf{u}^\sharp]^{n-m} \doteq \mathbf{0}} \quad (\text{B.3})$$

and with these equations (Cayley–Hamilton theorem) at hand, we obtain the derivatives of the principal invariants with respect to the argument \mathbf{u}^\sharp via the relation ($m > 0$)

$$\boxed{\partial_{\mathbf{u}^\sharp} J_m(\mathbf{u}^\sharp; [\mathbf{g}^\sharp]^\dagger) = \sum_{l=0}^{m-1} J_{m-l-1}(\mathbf{u}^\sharp; [\mathbf{g}^\sharp]^\dagger) [-[\mathbf{u}^\sharp]^\dagger]^l}. \quad (\text{B.4})$$

In case that $\mathbf{u}^\sharp \in \mathbb{L}_{\text{inv}}^n$, i.e. \mathbf{u}^\sharp is non-singular, Eqs.(B.3, B.4) result in $\partial_{\mathbf{u}^\sharp} \det(\mathbf{u}^\sharp) = \det(\mathbf{u}^\sharp) [\mathbf{u}^\sharp]^{-\dagger} \doteq \text{cof}(\mathbf{u}^\sharp) \spadesuit$.

B.2 Useful relations between different types of invariants

The specific case of a three-dimensional setting in terms of the positive definite co-variant and symmetric right Cauchy–Green tensor $\mathbf{C}^b \in \mathbb{S}_+^3$ ends up with

$$\begin{aligned} C^b \lambda^3 - C^b G^\sharp J_1 C^b \lambda^2 + C^b G^\sharp J_2 C^b \lambda - C^b G^\sharp J_3 \mathbf{1} &= \mathbf{0}, \\ C^b \cdot \mathbf{G}^\sharp \cdot C^b \cdot \mathbf{G}^\sharp \cdot C^b - C^b G^\sharp J_1 C^b \cdot \mathbf{G}^\sharp \cdot C^b + C^b G^\sharp J_2 C^b - C^b G^\sharp J_3 \mathbf{G}^b &= \mathbf{0}, \end{aligned} \quad (\text{B.5})$$

and the principal invariants and their derivatives read

$$\begin{aligned} C^b G^\sharp J_1 &= \mathbf{C}^b : \mathbf{G}^\sharp, & \partial_{\mathbf{C}^b} C^b G^\sharp J_1 &= \mathbf{G}^\sharp, \\ C^b G^\sharp J_2 &= \frac{1}{2} \left[C^b G^\sharp J_1^2 - [\mathbf{C}^b \cdot \mathbf{G}^\sharp \cdot C^b] : \mathbf{G}^\sharp \right], & \partial_{\mathbf{C}^b} C^b G^\sharp J_2 &= C^b G^\sharp J_1 \mathbf{G}^\sharp - \mathbf{G}^\sharp \cdot C^b \cdot \mathbf{G}^\sharp, \\ C^b G^\sharp J_3 &= \det(\mathbf{C}^b), & \partial_{\mathbf{C}^b} C^b G^\sharp J_3 &= \text{cof}(\mathbf{C}^b) = C^b G^\sharp J_3 \mathbf{B}^\sharp, \end{aligned} \quad (\text{B.6})$$

with $\mathbf{B}^\sharp = \det^{-1}(\mathbf{C}^b) \text{cof}(\mathbf{C}^b) = [\mathbf{B}^\sharp]^\dagger$ and, moreover, the relation $C^b G^\sharp J_2 = \mathbf{G}^b : \text{cof}(\mathbf{C}^b)$ holds, compare e.g. Murnaghan [Mur51, Sect. 3]. From Eq.(B.5), it is obvious that the principal invariants allow representation in terms of eigenvalues which are summarised in Eq.(B.7). For completeness, these connections are additionally highlighted for the set of basic invariants

$$\begin{aligned} C^b G^\sharp J_1 &= C^b \lambda_1 + C^b \lambda_2 + C^b \lambda_3, & C^b G^\sharp I_1 &= C^b \lambda_1 + C^b \lambda_2 + C^b \lambda_3, \\ C^b G^\sharp J_2 &= C^b \lambda_1 C^b \lambda_2 + C^b \lambda_2 C^b \lambda_3 + C^b \lambda_1 C^b \lambda_3, & C^b G^\sharp I_2 &= C^b \lambda_1^2 + C^b \lambda_2^2 + C^b \lambda_3^2, \\ C^b G^\sharp J_3 &= C^b \lambda_1 C^b \lambda_2 C^b \lambda_3, & C^b G^\sharp I_3 &= C^b \lambda_1^3 + C^b \lambda_2^3 + C^b \lambda_3^3. \end{aligned} \quad (\text{B.7})$$

For an isotropic Lagrangian setting, the free Helmholtz energy density is usually defined in terms of the invariants with respect to \mathbf{C}^b or, alternatively, with respect to an appropriate strain measure, e.g. the Green–Lagrangian tensor $\mathbf{E}^b = \frac{1}{2} [\mathbf{C}^b - \mathbf{G}^b]$. In this context, the following equations

$$\begin{aligned} C^b G^\sharp J_1 &= 3 + 2 E^b G^\sharp I_1 \\ C^b G^\sharp J_2 &= 3 + 4 E^b G^\sharp I_1 - 2 E^b G^\sharp I_2 + 2 E^b G^\sharp I_1^2 \\ C^b G^\sharp J_3 &= 1 + 2 E^b G^\sharp I_1 - 2 E^b G^\sharp I_2 + \frac{8}{3} E^b G^\sharp I_3 + 2 E^b G^\sharp I_1^2 - 4 E^b G^\sharp I_1 E^b I G^\sharp_2 + \frac{4}{3} E^b I_1^3 \end{aligned} \quad (\text{B.8})$$

and

$$\begin{aligned} E^b G^\sharp I_1 &= \frac{1}{2} \left[-3 + C^b G^\sharp J_1 \right] \\ E^b G^\sharp I_2 &= \frac{1}{4} \left[3 - 2 C^b G^\sharp J_1 - 2 C^b G^\sharp J_2 + C^b G^\sharp J_1^2 \right] \\ E^b G^\sharp I_3 &= \frac{1}{8} \left[-3 + 3 C^b G^\sharp J_1 + 6 C^b G^\sharp J_2 + 3 C^b G^\sharp J_3 - 3 C^b G^\sharp J_1^2 - 3 C^b G^\sharp J_1 C^b G^\sharp J_2 + C^b G^\sharp J_1^3 \right]. \end{aligned} \quad (\text{B.9})$$

[‡]The definition of the cofactor for singular fields (i.e. tensors of improper rank) is highlighted in Šilhavý [Šil97, Prop. 1.1.5].

summarises the relations between the principal and basic invariants of \mathbf{C}^b and \mathbf{E}^b .

The introduction of several typical dissipation potentials is often conveniently based on the application of Haigh–Westergard invariants, see e.g. Maugin [Mau92, Sect. 1.4] or de Boer [dB00, App. C]. These coordinates (here denoted by $H_{1,2,3}$) have a specific geometric interpretation in the space spanned by the principal axes of a symmetric second order tensor (length along the space diagonal, radius in the deviatoric plane, Lode angle) and allow interpretation as invariants. In terms of, e.g., the Kirchhoff stress $\boldsymbol{\tau}^\sharp = \sum_{i=1}^3 \tau_i^\sharp \mathbf{n}_i^\sharp \otimes \tau_i^\sharp \mathbf{n}_i^\sharp \in \mathbb{S}^3$, one obtains

$$g^b \tau^\sharp H_1 = \frac{1}{\sqrt{3}} g^b \tau^\sharp I_1, \quad g^b \tau^\sharp H_2 = \left[\frac{1}{2} g^{b \text{ dev } \tau^\sharp} I_2 \right]^{1/2}, \quad g^b \tau^\sharp H_3 = \frac{1}{3} \left[\arccos \left(\sqrt{6} g^b \tau^\sharp H_2^{-3} g^{b \text{ dev } \tau^\sharp} I_3 \right) \right] \quad (\text{B.10})$$

and the corresponding derivatives with respect to $\boldsymbol{\tau}^\sharp$ result in

$$\begin{aligned} \partial_{\boldsymbol{\tau}^\sharp} g^b \tau^\sharp H_1 &= \frac{1}{\sqrt{3}} \mathbf{g}^b, \\ \partial_{\boldsymbol{\tau}^\sharp} g^b \tau^\sharp H_2 &= g^{b \text{ dev } \tau^\sharp} I_2^{-1/2} \mathbf{g}^b \cdot \text{dev } \boldsymbol{\tau}^\sharp \cdot \mathbf{g}^b, \\ \partial_{\boldsymbol{\tau}^\sharp} g^b \tau^\sharp H_3 &= -\sqrt{\frac{2}{3}} \left[1 - \left[\sqrt{6} g^{b \text{ dev } \tau^\sharp} I_3 g^b \tau^\sharp H_2^{-3} \right]^2 \right]^{-1/2} \\ &\quad \mathbf{g}^b \cdot \left[\frac{3 [\boldsymbol{\tau}^\sharp \cdot \mathbf{g}^b \cdot \boldsymbol{\tau}^\sharp] - 2 g^b \tau^\sharp I_1 \boldsymbol{\tau}^\sharp + [2 \tau^\sharp I_1^2 / 3 - g^b \tau^\sharp I_2] \mathbf{g}^\sharp}{g^b \tau^\sharp H_2^3} - \frac{3 g^{b \text{ dev } \tau^\sharp} I_3 \text{ dev } \boldsymbol{\tau}^\sharp}{g^b \text{ dev } \tau^\sharp H_2^4 g^{b \text{ dev } \tau^\sharp} I_2^{1/2}} \right] \cdot \mathbf{g}^b. \end{aligned} \quad (\text{B.11})$$

B.3 Tensor-valued isotropic tensor functions of second order

Let $L_t \mathbf{z}_1^b, \mathbf{z}_1^b, \mathbf{z}_2^b, \mathbf{y}^\sharp \in \mathbb{S}^3$ denote symmetric, second order Eulerian tensors which define the tensor-valued tensor function $L_t \mathbf{z}_1^b = L_t \mathbf{z}_1^b(\mathbf{z}_2^b, \mathbf{y}^\sharp)$. Furthermore, \mathbf{z}_1^b and \mathbf{y}^\sharp represent conjugate variables which are assumed to be connected within an associated setting via $L_t \mathbf{z}_1^b = D_t \lambda \partial_{\mathbf{y}^\sharp} \Phi^t(\mathbf{z}_2^b, \mathbf{y}^\sharp)$ whereby Φ represents an appropriate dissipation potential and $D_t \lambda$ denotes the correlated Lagrange multiplier of the underlying constrained optimisation problem. Now, following the outline given in Betten [Bet85], the general canonical form of this rate equation reads

$$\begin{aligned} L_t \mathbf{z}_1^b &= L_t \mathbf{z}_1^b(\mathbf{z}_2^b, \mathbf{y}^\sharp) = \sum_{i=0}^2 {}^i \mathbf{z}_2^b : [\mathbf{g}^\sharp \cdot [\mathbf{g}^b \cdot \mathbf{y}^\sharp]^i] \quad \text{with} \\ {}^i \mathbf{z}_2^b &= \sum_{j=0}^2 \frac{1}{2} z_{2i,j} \left[[\mathbf{g}^b \cdot [\mathbf{g}^\sharp \cdot \mathbf{z}_2^b]^j] \overline{\otimes} \mathbf{g}^b + [\mathbf{g}^b \cdot [\mathbf{g}^\sharp \cdot \mathbf{z}_2^b]^j] \underline{\otimes} \mathbf{g}^b \right]^{\text{SYM}}, \end{aligned} \quad (\text{B.12})$$

whereby the nine scalar-valued functions $z_{2i,j}$ with $i, j = 0, 1, 2$ are generally defined by the appropriate set of ten invariants; $z_{2i,j} = z_{2i,j}(z_2^b y^\sharp I_{1,\dots,10})$, compare e.g. Table 3.1. The assumption of a dissipation potential $\Phi^t = \Phi^t(\mathbf{z}_2^b, \mathbf{y}^\sharp)$ within an associated setting yields

$$\begin{aligned} z_{20,0} &= D_t \lambda \partial_{z_2^b y^\sharp I_4} \Phi^t, & z_{20,1} &= D_t \lambda \partial_{z_2^b y^\sharp I_7} \Phi^t, & z_{20,2} &= D_t \lambda \partial_{z_2^b y^\sharp I_8} \Phi^t, \\ z_{21,0} &= \frac{1}{2} D_t \lambda \partial_{z_2^b y^\sharp I_5} \Phi^t, & z_{21,1} &= \frac{1}{2} D_t \lambda \partial_{z_2^b y^\sharp I_9} \Phi^t, & z_{21,2} &= \frac{1}{2} D_t \lambda \partial_{z_2^b y^\sharp I_{10}} \Phi^t, \\ z_{22,0} &= \frac{1}{3} D_t \lambda \partial_{z_2^b y^\sharp I_6} \Phi^t, & z_{22,1} &= 0, & z_{22,2} &= 0. \end{aligned} \quad (\text{B.13})$$

These relations apparently represent a restricted form of Eq.(B.12) which is naturally based on the fact that $z_2^b y^\sharp I_{1,2,3} = \mathbf{g}^\sharp : [\mathbf{z}_2^b \cdot \mathbf{g}^\sharp]^{1,2,3}$ are independent of \mathbf{y}^\sharp which consequently yields $\partial_{\mathbf{y}^\sharp} z_2^b y^\sharp I_{1,2,3} = \mathbf{0}$.

B.4 First and second derivatives of the basic invariants

For the presented non-dissipative anisotropic hyper-elastic setting in Chapter 2 we obtain invariants $I_{(i),\dots,(vi)}$ as given in Table 2.1 with the help of the general representation theorem of isotropic scalar-valued tensor functions whereby $\mathbf{A}_{1,\dots,n}^\sharp \doteq \text{const}$ has been assumed. This set enters the definition of

the free Helmholtz energy density as highlighted in Eq.(2.9). In the sequel, we focus on the Eulerian setting. Hence the second order generators, determined by the first derivatives of these invariants with respect to the spatial metric tensor \mathbf{g}^b , read (see Appendix A for notational details)

$$\begin{aligned}
\partial_{\mathbf{g}^b} I_{(i)} &= \mathbf{b}^\#, \\
\partial_{\mathbf{g}^b} I_{(ii)} &= 2 \mathbf{b}^\# \cdot \mathbf{g}^b \cdot \mathbf{b}^\#, \\
\partial_{\mathbf{g}^b} I_{(iii)} &= 3 \mathbf{b}^\# \cdot [\mathbf{g}^b \cdot \mathbf{b}^\#]^2, \\
\partial_{\mathbf{g}^b} I_{(iv)} &= \mathbf{a}_i^\#, \\
\partial_{\mathbf{g}^b} I_{(v)} &= 2 [\mathbf{b}^\# \cdot \mathbf{g}^b \cdot \mathbf{a}_i^\#]^{\text{sym}}, \\
\partial_{\mathbf{g}^b} I_{(vi)} &= [\mathbf{a}_{i,j}^\# \cdot \mathbf{c}^b]_2^{\text{sym}}.
\end{aligned} \tag{B.14}$$

Moreover, the computation of the derivatives with respect to the Finger tensor $\mathbf{b}^\#$ results in

$$\begin{aligned}
\partial_{\mathbf{b}^\#} I_{(i)} &= \mathbf{g}^b, \\
\partial_{\mathbf{b}^\#} I_{(ii)} &= 2 \mathbf{g}^b \cdot \mathbf{b}^\# \cdot \mathbf{g}^b, \\
\partial_{\mathbf{b}^\#} I_{(iii)} &= 3 \mathbf{g}^b \cdot [\mathbf{b}^\# \cdot \mathbf{g}^b]^2, \\
\partial_{\mathbf{b}^\#} I_{(v)} &= \mathbf{g}^b \cdot \mathbf{a}_i^\# \cdot \mathbf{g}^b, \\
\partial_{\mathbf{b}^\#} I_{(vi)} &= - \mathbf{c}^b \cdot [\mathbf{a}_{i,j}^\# \cdot \mathbf{g}^b]_2^{\text{sym}} \cdot \mathbf{c}^b.
\end{aligned} \tag{B.15}$$

Finally, taking derivatives with respect to the elements of the tensor series $\mathbf{a}_{1,\dots,n}^\#$, we end up with

$$\begin{aligned}
\partial_{\mathbf{a}_i^\#} I_{(iv)} &= \mathbf{g}^b, \\
\partial_{\mathbf{a}_i^\#} I_{(v)} &= \mathbf{g}^b \cdot \mathbf{b}^\# \cdot \mathbf{g}^b, \\
\partial_{\mathbf{a}_i^\#} I_{(vi)} &= [\mathbf{g}^b \cdot \mathbf{a}_j^\# \cdot \mathbf{c}^b]^{\text{sym}}, \\
\partial_{\mathbf{a}_j^\#} I_{(vi)} &= [\mathbf{g}^b \cdot \mathbf{a}_i^\# \cdot \mathbf{c}^b]^{\text{sym}}.
\end{aligned} \tag{B.16}$$

Next, again referring to the spatial setting, the derivatives of these generators due to \mathbf{g}^b , $\mathbf{b}^\#$ and $\mathbf{a}_{1,\dots,n}^\#$ are computed which are, practically speaking, second derivatives of the invariants. In particular, one obtains (see Appendix A for notational details)

$$\begin{aligned}
\partial_{\mathbf{g}^b \otimes \mathbf{g}^b}^2 I_{(ii)} &= [\mathbf{b}^\# \overline{\otimes} \mathbf{b}^\# + \mathbf{b}^\# \underline{\otimes} \mathbf{b}^\#], \\
\partial_{\mathbf{g}^b \otimes \mathbf{g}^b}^2 I_{(iii)} &= 3 \left[\mathbf{b}^\# \overline{\otimes} [\mathbf{b}^\# \cdot \mathbf{g}^b \cdot \mathbf{b}^\#] + \mathbf{b}^\# \underline{\otimes} [\mathbf{b}^\# \cdot \mathbf{g}^b \cdot \mathbf{b}^\#] \right]^{\text{SYM}}, \\
\partial_{\mathbf{g}^b \otimes \mathbf{g}^b}^2 I_{(v)} &= [\mathbf{b}^\# \overline{\otimes} \mathbf{a}_i^\# + \mathbf{b}^\# \underline{\otimes} \mathbf{a}_i^\#]^{\text{SYM}}
\end{aligned} \tag{B.17}$$

for the second derivative with respect to the spatial co-variant metric tensor, compare Eq.(B.14). Next, based on the generators in terms of the Finger tensor, see Eq.(B.15), we end up with

$$\begin{aligned}
\partial_{\mathbf{b}^\# \otimes \mathbf{b}^\#}^2 I_{(ii)} &= [\mathbf{g}^b \overline{\otimes} \mathbf{g}^b + \mathbf{g}^b \underline{\otimes} \mathbf{g}^b], \\
\partial_{\mathbf{b}^\# \otimes \mathbf{b}^\#}^2 I_{(iii)} &= 3 \left[\mathbf{g}^b \overline{\otimes} [\mathbf{g}^b \cdot \mathbf{b}^\# \cdot \mathbf{g}^b] + \mathbf{g}^b \underline{\otimes} [\mathbf{g}^b \cdot \mathbf{b}^\# \cdot \mathbf{g}^b] \right]^{\text{SYM}}, \\
\partial_{\mathbf{b}^\# \otimes \mathbf{b}^\#}^2 I_{(vi)} &= \left[\mathbf{c}^b \overline{\otimes} [\mathbf{c}^b \cdot \mathbf{a}_j^\# \cdot \mathbf{g}^b \cdot \mathbf{a}_i^\# \cdot \mathbf{c}^b]^{\text{sym}} \right. \\
&\quad \left. + \mathbf{c}^b \underline{\otimes} [\mathbf{c}^b \cdot \mathbf{a}_j^\# \cdot \mathbf{g}^b \cdot \mathbf{a}_i^\# \cdot \mathbf{c}^b]^{\text{sym}} \right]^{\text{SYM}}, \\
\partial_{\mathbf{b}^\# \otimes \mathbf{a}_i^\#}^2 I_{(v)} &= \frac{1}{2} [\mathbf{g}^b \overline{\otimes} \mathbf{g}^b + \mathbf{g}^b \underline{\otimes} \mathbf{g}^b], \\
\partial_{\mathbf{b}^\# \otimes \mathbf{a}_i^\#}^2 I_{(vi)} &= -\frac{1}{2} \left[\mathbf{c}^b \overline{\otimes} [\mathbf{c}^b \cdot \mathbf{a}_j^\# \cdot \mathbf{g}^b] + \mathbf{c}^b \underline{\otimes} [\mathbf{c}^b \cdot \mathbf{a}_j^\# \cdot \mathbf{g}^b] \right]^{\text{SYM}}, \\
\partial_{\mathbf{b}^\# \otimes \mathbf{a}_j^\#}^2 I_{(vi)} &= -\frac{1}{2} \left[\mathbf{c}^b \overline{\otimes} [\mathbf{c}^b \cdot \mathbf{a}_i^\# \cdot \mathbf{g}^b] + \mathbf{c}^b \underline{\otimes} [\mathbf{c}^b \cdot \mathbf{a}_i^\# \cdot \mathbf{g}^b] \right]^{\text{SYM}}.
\end{aligned} \tag{B.18}$$

Finally, the derivatives with respect to the elements of the additional tensor series result in

$$\begin{aligned}
\partial_{\mathbf{a}_i^\sharp \otimes \mathbf{b}^\sharp}^2 I(v) &= \frac{1}{2} [\mathbf{g}^b \overline{\otimes} \mathbf{g}^b + \mathbf{g}^b \underline{\otimes} \mathbf{g}^b], \\
\partial_{\mathbf{a}_i^\sharp \otimes \mathbf{b}^\sharp}^2 I(v_i) &= -\frac{1}{2} \left[\mathbf{c}^b \overline{\otimes} [\mathbf{g}^b \cdot \mathbf{a}_j^\sharp \cdot \mathbf{c}^b] + \mathbf{c}^b \underline{\otimes} [\mathbf{g}^b \cdot \mathbf{a}_j^\sharp \cdot \mathbf{c}^b] \right]^{\text{SYM}}, \\
\partial_{\mathbf{a}_j^\sharp \otimes \mathbf{b}^\sharp}^2 I(v_i) &= -\frac{1}{2} \left[\mathbf{c}^b \overline{\otimes} [\mathbf{g}^b \cdot \mathbf{a}_i^\sharp \cdot \mathbf{c}^b] + \mathbf{c}^b \underline{\otimes} [\mathbf{g}^b \cdot \mathbf{a}_i^\sharp \cdot \mathbf{c}^b] \right]^{\text{SYM}}, \\
\partial_{\mathbf{a}_i^\sharp \otimes \mathbf{a}_j^\sharp}^2 I(v_i) &= \frac{1}{2} [\mathbf{g}^b \overline{\otimes} \mathbf{c}^b + \mathbf{g}^b \underline{\otimes} \mathbf{c}^b]^{\text{SYM}} = \partial_{\mathbf{a}_j^\sharp \otimes \mathbf{a}_i^\sharp}^2 I(v_i).
\end{aligned} \tag{B.19}$$

The correlated outline within the Lagrangian setting is obvious and thus omitted here.

B.4.1 Alternative proof of the spatial anisotropic stress relation: Application to hyper-elasticity

In the following, we highlight an alternative proof of Proposition 2.1. Conceptually speaking, the point of departure is based on the material covariance of the free Helmholtz energy density $\psi_0^0(\mathbf{C}^b, \mathbf{G}^\sharp, \mathbf{A}_{1,\dots,n}^\sharp; \mathbf{X})$, compare Marsden and Hughes [MH94, Chap. 2 & 3], Menzel and Steinmann [MS01h] and Lu and Papadopoulos [LP00].

We consider a material diffeomorphism $\boldsymbol{\omega}(\mathbf{X}, t) : \mathcal{B}_0 \times \mathbb{R} \rightarrow \mathcal{B}_\tau$, as introduced in Eq.(2.15), which defines the linear tangent map $\mathbf{F}_\tau^\sharp(\mathbf{X}, t) \in \mathbb{L}_{\text{inv}}^3 : T\mathcal{B}_0 \rightarrow T\mathcal{B}_\tau$. Then the correlated material time derivative reads $D_t \mathbf{F}_\tau^\sharp = \mathbf{l}_\tau^\sharp \cdot \mathbf{F}_\tau^\sharp$ with $\mathbf{l}_\tau^\sharp \in \mathbb{L}^3 : T^* \mathcal{B}_\tau \times T\mathcal{B}_\tau \rightarrow \mathbb{R}$ (compare Section 2.2.1.1) and the common ansatz $D_t \mathbf{F}_\tau^\sharp \cdot \mathbf{f}_\tau^\sharp + \mathbf{F}_\tau^\sharp \cdot D_t \mathbf{f}_\tau^\sharp = \mathbf{0}$ (recall the notation $\mathbf{f}_\tau^\sharp \doteq [\mathbf{F}_\tau^\sharp]^{-1}$) ends up with $D_t \mathbf{f}_\tau^\sharp = -\mathbf{f}_\tau^\sharp \cdot \mathbf{l}_\tau^\sharp$. Now, the definition of material covariance $\psi_0^0(\mathbf{C}^b, \mathbf{G}^\sharp, \mathbf{A}_{1,\dots,n}^\sharp; \mathbf{X}) = \psi_0^0(\boldsymbol{\Omega}^* \mathbf{C}^b, \boldsymbol{\omega}_* \mathbf{G}^\sharp, \boldsymbol{\omega}_* \mathbf{A}_{1,\dots,n}^\sharp; \mathbf{X})$ – compare Section 2.2 (and recall the abbreviation $\boldsymbol{\Omega} \doteq \boldsymbol{\omega}^{-1}$) – results in the necessary condition

$$D_t \psi_0^0 \left(\boldsymbol{\Omega}^* \mathbf{C}^b, \boldsymbol{\omega}_* \mathbf{G}^\sharp, \boldsymbol{\omega}_* \mathbf{A}_{1,\dots,n}^\sharp; \mathbf{X} \right) \Big|_{\mathbf{F}^\sharp} = 0 \quad \forall \quad \boldsymbol{\omega} : \mathcal{B}_0 \times \mathbb{R} \rightarrow \mathcal{B}_\tau. \tag{B.20}$$

One obtains in particular

$$\begin{aligned}
& D_t \psi_0^0 \left(\boldsymbol{\Omega}^* \mathbf{C}^b, \boldsymbol{\omega}_* \mathbf{G}^\sharp, \boldsymbol{\omega}_* \mathbf{A}_{1,\dots,n}^\sharp; \mathbf{X} \right) \Big|_{\mathbf{F}^\sharp} \\
&= \partial_{\boldsymbol{\Omega}^* \mathbf{C}^b} \psi_0^0 : D_t (\boldsymbol{\Omega}^* \mathbf{C}^b) \Big|_{\mathbf{F}^\sharp} \\
&+ \partial_{\boldsymbol{\omega}_* \mathbf{G}^\sharp} \psi_0^0 : D_t (\boldsymbol{\omega}_* \mathbf{G}^\sharp) \Big|_{\mathbf{F}^\sharp} \\
&+ \sum_{s=1}^n \partial_{\boldsymbol{\omega}_* \mathbf{A}_s^\sharp} \psi_0^0 : D_t (\boldsymbol{\omega}_* \mathbf{A}_s^\sharp) \Big|_{\mathbf{F}^\sharp} \\
&= \partial_{\boldsymbol{\Omega}^* \mathbf{C}^b} \psi_0^0 : D_t ([\mathbf{f}_\tau^\sharp]^\text{t} \cdot \mathbf{C}^b \cdot \mathbf{f}_\tau^\sharp) \Big|_{\mathbf{F}^\sharp} \\
&+ \partial_{\boldsymbol{\omega}_* \mathbf{G}^\sharp} \psi_0^0 : D_t (\mathbf{F}_\tau^\sharp \cdot \mathbf{G}^\sharp \cdot [\mathbf{F}_\tau^\sharp]^\text{t}) \Big|_{\mathbf{F}^\sharp} \\
&+ \sum_{s=1}^n \partial_{\boldsymbol{\omega}_* \mathbf{A}_s^\sharp} \psi_0^0 : D_t (\mathbf{F}_\tau^\sharp \cdot \mathbf{A}_s^\sharp \cdot [\mathbf{F}_\tau^\sharp]^\text{t}) \Big|_{\mathbf{F}^\sharp} \\
&= - \partial_{\boldsymbol{\Omega}^* \mathbf{C}^b} \psi_0^0 : \left[[\mathbf{l}_\tau^\sharp]^\text{t} \cdot \boldsymbol{\Omega}^* \mathbf{C}^b + \boldsymbol{\Omega}^* \mathbf{C}^b \cdot \mathbf{l}_\tau^\sharp \right] \\
&+ \partial_{\boldsymbol{\omega}_* \mathbf{G}^\sharp} \psi_0^0 : \left[\mathbf{l}_\tau^\sharp \cdot \boldsymbol{\omega}_* \mathbf{G}^\sharp + \boldsymbol{\omega}_* \mathbf{G}^\sharp \cdot [\mathbf{l}_\tau^\sharp]^\text{t} \right] \\
&+ \sum_{s=1}^n \partial_{\boldsymbol{\omega}_* \mathbf{A}_s^\sharp} \psi_0^0 : \left[\mathbf{l}_\tau^\sharp \cdot \boldsymbol{\omega}_* \mathbf{A}_s^\sharp + \boldsymbol{\omega}_* \mathbf{A}_s^\sharp \cdot [\mathbf{l}_\tau^\sharp]^\text{t} \right] \\
&= 0.
\end{aligned} \tag{B.21}$$

Next, by taking advantage of the symmetry of the terms $\partial_{\boldsymbol{\Omega}^* [\bullet]^\flat} \psi_0^0$, $\partial_{\boldsymbol{\omega}_* [\bullet]^\sharp} \psi_0^0$, and $\boldsymbol{\Omega}^* [\bullet]^\flat$, $\boldsymbol{\omega}_* [\bullet]^\sharp$, respectively, we end up with

$$2 \left[- \partial_{\boldsymbol{\Omega}^* \mathbf{C}^b} \psi_0^0 : [\boldsymbol{\Omega}^* \mathbf{C}^b \cdot \mathbf{l}_\tau^\sharp]^{\text{sym}} + \partial_{\boldsymbol{\omega}_* \mathbf{G}^\sharp} \psi_0^0 : [\mathbf{l}_\tau^\sharp \cdot \boldsymbol{\omega}_* \mathbf{G}^\sharp]^{\text{sym}} + \sum_{s=1}^n \partial_{\boldsymbol{\omega}_* \mathbf{A}_s^\sharp} \psi_0^0 : [\mathbf{l}_\tau^\sharp \cdot \boldsymbol{\omega}_* \mathbf{A}_s^\sharp]^{\text{sym}} \right]$$

$$\begin{aligned}
&= 2 \left[-\partial_{\Omega^*} \mathbf{C}^b \psi_0^0 \cdot \Omega^* \mathbf{C}^b + \omega_* \mathbf{G}^\sharp \cdot \partial_{\omega_*} \mathbf{G}^\sharp \psi_0^0 + \sum_{s=1}^n \omega_* \mathbf{A}_s^\sharp \cdot \partial_{\omega_* \mathbf{A}_s^\sharp} \psi_0^0 \right] : \mathbf{l}_\tau^\sharp \\
&\doteq 2 \Xi_\tau^\sharp : \mathbf{l}_\tau^\sharp = 0 \quad \forall \quad \mathbf{l}_\tau^\sharp : T^* \mathcal{B}_\tau \times T \mathcal{B}_\tau \rightarrow \mathbb{R}.
\end{aligned} \tag{B.22}$$

Hence the contribution Ξ_τ^\sharp must vanish. In this context, we choose the cases $\mathbf{F}_\tau^\sharp \doteq \mathbf{F}^\sharp \in \mathbb{L}_+^3 : T \mathcal{B}_0 \rightarrow T \mathcal{B}_t$ and $\mathbf{F}_\tau^\sharp \doteq \mathbf{G}^\sharp \in \mathbb{L}_+^3 : T^* \mathcal{B}_0 \times T \mathcal{B}_0 \rightarrow \mathbb{R}$ as special applications without loss of generality and obtain the anisotropic spatial and material stress relations (recall the notation $\mathbf{B}^\sharp = \det^{-1}(\mathbf{C}^b) \text{cof}(\mathbf{C}^b)$)

$$\boxed{
\begin{aligned}
\mathbf{F}_\tau^\sharp \doteq \mathbf{F}^\sharp &\implies \partial_{\mathbf{g}^b} \psi_0^t = \mathbf{b}^\sharp \cdot \partial_{\mathbf{b}^\sharp} \psi_0^t \cdot \mathbf{g}^\sharp + \sum_{s=1}^n \mathbf{a}_s^\sharp \cdot \partial_{\mathbf{a}_s^\sharp} \psi_0^t \cdot \mathbf{g}^\sharp = [\partial_{\mathbf{g}^b} \psi_0^t]^t, \\
\mathbf{F}_\tau^\sharp \doteq \mathbf{G}^\sharp &\implies \partial_{\mathbf{C}^b} \psi_0^0 = \mathbf{G}^\sharp \cdot \partial_{\mathbf{G}^\sharp} \psi_0^0 \cdot \mathbf{B}^\sharp + \sum_{s=1}^n \mathbf{A}_s^\sharp \cdot \partial_{\mathbf{A}_s^\sharp} \psi_0^0 \cdot \mathbf{B}^\sharp = [\partial_{\mathbf{C}^b} \psi_0^0]^t,
\end{aligned}
} \tag{B.23}$$

which obviously proves Proposition 2.1. Note that the specific choice of a material isometry with $\mathbf{F}_\tau^\sharp \in \mathbb{O}^3$, $\mathbf{l}_\tau^\sharp \in \mathbb{W}^3$ results in the definition of a scalar-valued isotropic tensor function, which has been applied for one tensorial argument in, e.g., Truesdell and Noll [TN92, Sect.84] or Šilhavý [Šil97, Prop. 8.2.2]. Then, due to the skew-symmetry of \mathbf{l}_τ^\sharp , the contribution Ξ_τ^\sharp is forced to be symmetric, i.e. $\partial_{\Omega^*} \mathbf{C}^b \psi_0^0$ and $\Omega^* \mathbf{C}^b$ commute (for this isotropic case).

B.5 First and second derivatives of the basic invariants

For the presented dissipative anisotropic hyper-elastic setting in Chapter 3 we obtain invariants $I_{(i), \dots, (xi)}$ as given in Table 3.1 with the help of the general representation theorem of isotropic scalar-valued tensor functions. Recall that the developed elasto-plastic framework allows interpretation as an elastic setting with respect to the intermediate configuration (\mathcal{B}_p) , that the additional tensor series $\widehat{\mathbf{A}}_{1, \dots, n}^\sharp$ was generally not constrained to remain constant (in \mathcal{B}_0 , \mathcal{B}_p or \mathcal{B}_t) and furthermore, that the set of invariants enters the definition of the free Helmholtz energy density.

The first and second derivatives of the invariants $I_{(i), \dots, (vi)}$ are of course similar to those highlighted for the non-dissipative setting in Section B.4. In the context of multiplicative elasto-plasticity and with respect to the spatial configuration, one simply has to replace the fields $\mathbf{b}_e^\sharp \mapsto \mathbf{b}^\sharp$ and $\mathbf{c}_e^b \mapsto \mathbf{c}^b$, respectively. The remaining task is to compute the derivatives of $I_{(vii), \dots, (xi)}$. In this context, we obtain with respect to the spatial metric \mathbf{g}^b the contributions

$$\partial_{\mathbf{g}^b} I_{(vii)} = 2 \mathbf{a}_i^\sharp \cdot \mathbf{g}^b \cdot \mathbf{a}_i^\sharp, \quad \partial_{\mathbf{g}^b} I_{(viii), \dots, (xi)} = \mathbf{0} \tag{B.24}$$

and in view of the elastic Finger tensor \mathbf{b}_e^\sharp , one ends up with

$$\begin{aligned}
\partial_{\mathbf{b}_e^\sharp} I_{(vii)} &= \mathbf{0}, \\
\partial_{\mathbf{b}_e^\sharp} I_{(viii)} &= - \mathbf{c}_e^b \cdot \mathbf{a}_i^\sharp \cdot \mathbf{c}_e^b, \\
\partial_{\mathbf{b}_e^\sharp} I_{(ix)} &= -2 \mathbf{c}_e^b \cdot [\mathbf{a}_{i,j}^\sharp \cdot \mathbf{c}_e^b]_2^{\text{sym}} \cdot \mathbf{c}_e^b, \\
\partial_{\mathbf{b}_e^\sharp} I_{(x)} &= - \mathbf{c}_e^b \cdot \left[[\mathbf{a}_{i,j,k}^\sharp \cdot \mathbf{c}_e^b]_3^{\text{sym}} + [\mathbf{a}_{k,i,j}^\sharp \cdot \mathbf{c}_e^b]_3^{\text{sym}} + [\mathbf{a}_{j,k,i}^\sharp \cdot \mathbf{c}_e^b]_3^{\text{sym}} \right] \cdot \mathbf{c}_e^b, \\
\partial_{\mathbf{b}_e^\sharp} I_{(xi)} &= - \mathbf{c}_e^b \cdot \left[[\mathbf{a}_{l,i,i,l}^\sharp \cdot \mathbf{c}_e^b]_4 + 2 [\mathbf{a}_{l,l,i,i}^\sharp \cdot \mathbf{c}_e^b]_4^{\text{sym}} + [\mathbf{a}_{i,l,l,i}^\sharp \cdot \mathbf{c}_e^b]_4 \right] \cdot \mathbf{c}_e^b,
\end{aligned} \tag{B.25}$$

see Appendix A.1 for notational details. Finally, the correlated derivatives in terms of the anisotropy

tensors $\mathbf{a}_{1,\dots,n}^\sharp$ read

$$\begin{aligned}
\partial_{\mathbf{a}_i^\sharp} I_{(vii)} &= 2 \mathbf{g}^b \cdot \mathbf{a}_i^\sharp \cdot \mathbf{g}^b, \\
\partial_{\mathbf{a}_i^\sharp} I_{(viii)} &= \mathbf{c}_e^b, \\
\partial_{\mathbf{a}_i^\sharp} I_{(ix)} &= \mathbf{c}_e^b \cdot \mathbf{a}_j^\sharp \cdot \mathbf{c}_e^b, \\
\partial_{\mathbf{a}_j^\sharp} I_{(ix)} &= \mathbf{c}_e^b \cdot \mathbf{a}_i^\sharp \cdot \mathbf{c}_e^b, \\
\partial_{\mathbf{a}_i^\sharp} I_{(x)} &= \mathbf{c}_e^b \cdot [\mathbf{a}_{j,k}^\sharp \cdot \mathbf{c}_e^b]_2^{\text{sym}} \cdot \mathbf{c}_e^b, \\
\partial_{\mathbf{a}_j^\sharp} I_{(x)} &= \mathbf{c}_e^b \cdot [\mathbf{a}_{k,i}^\sharp \cdot \mathbf{c}_e^b]_2^{\text{sym}} \cdot \mathbf{c}_e^b, \\
\partial_{\mathbf{a}_k^\sharp} I_{(x)} &= \mathbf{c}_e^b \cdot [\mathbf{a}_{i,j}^\sharp \cdot \mathbf{c}_e^b]_2^{\text{sym}} \cdot \mathbf{c}_e^b, \\
\partial_{\mathbf{a}_i^\sharp} I_{(xi)} &= 2 \mathbf{c}_e^b \cdot [\mathbf{a}_{i,l,l}^\sharp \cdot \mathbf{c}_e^b]_3^{\text{sym}} \cdot \mathbf{c}_e^b, \\
\partial_{\mathbf{a}_l^\sharp} I_{(xi)} &= 2 \mathbf{c}_e^b \cdot [\mathbf{a}_{l,i,i}^\sharp \cdot \mathbf{c}_e^b]_3^{\text{sym}} \cdot \mathbf{c}_e^b.
\end{aligned} \tag{B.26}$$

The computations of $\partial_{\mathbf{g}^b \otimes \mathbf{g}^b}^2 I_{(vii),\dots,(xi)}$ consequently result in

$$\partial_{\mathbf{g}^b \otimes \mathbf{g}^b}^2 I_{(vii)} = \mathbf{a}_i^\sharp \overline{\otimes} \mathbf{a}_i^\sharp + \mathbf{a}_i^\sharp \underline{\otimes} \mathbf{a}_i^\sharp, \quad \partial_{\mathbf{g}^b \otimes \mathbf{g}^b}^2 I_{(viii),\dots,(xi)} = \mathbf{0}. \tag{B.27}$$

The remaining second order derivatives of the invariants $I_{(vii)}$ yield

$$\partial_{\mathbf{b}_e^\sharp \otimes \mathbf{b}_e^\sharp}^2 I_{(vii)} = \partial_{\mathbf{a}_i^\sharp \otimes \mathbf{b}_e^\sharp}^2 I_{(vii)} = \partial_{\mathbf{b}_e^\sharp \otimes \mathbf{a}_i^\sharp}^2 I_{(vii)} = \mathbf{0}, \quad \partial_{\mathbf{a}_i^\sharp \otimes \mathbf{a}_i^\sharp}^2 I_{(vii)} = \mathbf{g}^b \overline{\otimes} \mathbf{g}^b + \mathbf{g}^b \underline{\otimes} \mathbf{g}^b. \tag{B.28}$$

Although tedious, it is straightforward to specify the extant derivatives due to $I_{(viii),\dots,(xi)}$. Nevertheless, the procedure is quite lengthy and thus not reiterated here. A final note is that the outline with respect to \mathcal{B}_p or \mathcal{B}_0 is of course similar and thus omitted.

B.5.1 Alternative proof of the spatial anisotropic stress relation: Application to multiplicative elasto–plasticity

In analogy to Section B.4.1, the fundamental covariance property of the function ψ_0 can be applied to prove the constitutive equations (3.15, 3.18, 3.21). The free Helmholtz energy density thus remains invariant under the action of any arbitrary but non–singular linear tangent map, namely

$$D_t \psi_0^p \left(\mathbf{f}_\tau^\sharp \star \widehat{\mathbf{C}}_e^b, \mathbf{F}_{\tau^\star}^\sharp \widehat{\mathbf{G}}^\sharp, \mathbf{F}_{\tau^\star}^\sharp \widehat{\mathbf{A}}_{1,\dots,n}^\sharp; \mathbf{X} \right) \Big|_{\mathbf{F}_{e,p}^\sharp} = 0 \quad \forall \mathbf{F}_\tau^\sharp \in \mathbb{L}_{\text{inv}}^3 : T\mathcal{B}_p \rightarrow T\mathcal{B}_\tau. \tag{B.29}$$

with $\mathbf{f}_\tau^\sharp \doteq [\mathbf{F}_\tau^\sharp]^{-1}$. Note that ψ_0^p in Eq.(B.29) could be replaced by ψ_0^t or ψ_0^0 and a correlated linear tangent map without loss of generality. Next, let the velocity gradient in terms of \mathbf{F}_τ^\sharp be denoted by $\mathbf{l}_\tau^\sharp = D_t \mathbf{F}_\tau^\sharp \cdot \mathbf{f}_\tau^\sharp$ – and we additionally obtain $\mathbf{l}_\tau^\sharp = -D_t \mathbf{f}_\tau^\sharp \cdot \mathbf{F}_\tau^\sharp$ from $D_t (\mathbf{F}_\tau^\sharp \cdot \mathbf{f}_\tau^\sharp) = \mathbf{0}$ – which allows to represent Eq.(B.29) as

$$\begin{aligned}
& D_t \psi_0^p \left(\mathbf{f}_\tau^\sharp \star \widehat{\mathbf{C}}_e^b, \mathbf{F}_{\tau^\star}^\sharp \widehat{\mathbf{G}}^\sharp, \mathbf{F}_{\tau^\star}^\sharp \widehat{\mathbf{A}}_{1,\dots,n}^\sharp; \mathbf{X} \right) \Big|_{\mathbf{F}_{e,p}^\sharp} \\
&= \partial_{\mathbf{f}_\tau^\sharp \star \widehat{\mathbf{C}}_e^b} \psi_0^p : D_t (\mathbf{f}_\tau^\sharp \star \widehat{\mathbf{C}}_e^b) \Big|_{\mathbf{F}_{e,p}^\sharp} \\
&+ \partial_{\mathbf{F}_{\tau^\star}^\sharp \widehat{\mathbf{G}}^\sharp} \psi_0^p : D_t (\mathbf{F}_{\tau^\star}^\sharp \widehat{\mathbf{G}}^\sharp) \Big|_{\mathbf{F}_{e,p}^\sharp} \\
&+ \sum_{s=1}^n \partial_{\mathbf{F}_{\tau^\star}^\sharp \widehat{\mathbf{A}}_s^\sharp} \psi_0^p : D_t (\mathbf{F}_{\tau^\star}^\sharp \widehat{\mathbf{A}}_s^\sharp) \Big|_{\mathbf{F}_{e,p}^\sharp}
\end{aligned} \tag{B.30}$$

$$\begin{aligned}
&= - \quad \partial_{\mathbf{f}_\tau^{\sharp*} \widehat{\mathbf{C}}_e^b} \psi_0^{\mathbb{P}} : \left[[\mathbf{l}_\tau^{\sharp}]^t \cdot \mathbf{f}_\tau^{\sharp*} \widehat{\mathbf{C}}_e^b + \mathbf{f}_\tau^{\sharp*} \widehat{\mathbf{C}}_e^b \cdot \mathbf{l}_\tau^{\sharp} \right] \\
&\quad + \quad \partial_{\mathbf{F}_{\tau^*}^{\sharp} \widehat{\mathbf{G}}^{\sharp}} \psi_0^{\mathbb{P}} : \left[\mathbf{l}_\tau^{\sharp} \cdot \mathbf{F}_{\tau^*}^{\sharp} \widehat{\mathbf{G}}^{\sharp} + \mathbf{F}_{\tau^*}^{\sharp} \widehat{\mathbf{G}}^{\sharp} \cdot [\mathbf{l}_\tau^{\sharp}]^t \right] \\
&\quad + \quad \sum_{s=1}^n \partial_{\mathbf{F}_{\tau^*}^{\sharp} \widehat{\mathbf{A}}_s^{\sharp}} \psi_0^{\mathbb{P}} : \left[\mathbf{l}_\tau^{\sharp} \cdot \mathbf{F}_{\tau^*}^{\sharp} \widehat{\mathbf{A}}_s^{\sharp} + \mathbf{F}_{\tau^*}^{\sharp} \widehat{\mathbf{A}}_s^{\sharp} \cdot [\mathbf{l}_\tau^{\sharp}]^t \right] \\
&= 0 \quad .
\end{aligned}$$

Please note that \mathbf{F}_e^{\sharp} and \mathbf{F}_p^{\sharp} are kept fixed and as a result, no additional time derivatives as, e.g., $D_t \widehat{\mathbf{A}}_{1,\dots,n}^{\sharp}$ occur. Moreover, all incorporated derivatives of the free Helmholtz energy density are obviously symmetric which enables us to rewrite Eq.(B.30) as

$$2 \left[- \partial_{\mathbf{f}_\tau^{\sharp*} \widehat{\mathbf{C}}_e^b} \psi_0^{\mathbb{P}} \cdot \mathbf{f}_\tau^{\sharp*} \widehat{\mathbf{C}}_e^b + \mathbf{F}_{\tau^*}^{\sharp} \widehat{\mathbf{G}}^{\sharp} \cdot \partial_{\mathbf{F}_{\tau^*}^{\sharp} \widehat{\mathbf{G}}^{\sharp}} \psi_0^{\mathbb{P}} + \sum_{s=1}^n \mathbf{F}_{\tau^*}^{\sharp} \widehat{\mathbf{A}}_s^{\sharp} \cdot \partial_{\mathbf{F}_{\tau^*}^{\sharp} \widehat{\mathbf{A}}_s^{\sharp}} \psi_0^{\mathbb{P}} \right] : \mathbf{l}_\tau^{\sharp} = 0 \quad (\text{B.31})$$

$$\forall \quad \mathbf{l}_\tau^{\sharp} : T^* \mathcal{B}_\tau \times T \mathcal{B}_\tau \rightarrow \mathbb{R}.$$

Thus, the terms in brackets have to vanish identically and with this relation at hand, specific choices for \mathbf{F}_τ^{\sharp} , i.e. $\mathbf{F}_\tau^{\sharp} \doteq \mathbf{F}_e^{\sharp} \in \mathbb{L}_+^3 : T \mathcal{B}_p \rightarrow T \mathcal{B}_t$, $\mathbf{F}_\tau^{\sharp} \doteq \widehat{\mathbf{G}}^{\sharp} \in \mathbb{L}_+^3 : T^* \mathcal{B}_p \times T \mathcal{B}_p \rightarrow \mathbb{R}$ and $\mathbf{F}_\tau^{\sharp} \doteq \mathbf{f}_p^{\sharp} \in \mathbb{L}_+^3 : T \mathcal{B}_p \rightarrow T \mathcal{B}_o$, yield

$$\boxed{
\begin{aligned}
\mathbf{F}_\tau^{\sharp} \doteq \mathbf{F}_e^{\sharp} &\implies \partial_{\mathbf{g}^b} \psi_0^t = \mathbf{b}_e^{\sharp} \cdot \partial_{\mathbf{b}_e^{\sharp}} \psi_0^t \cdot \mathbf{g}^{\sharp} + \sum_{s=1}^n \mathbf{a}_s^{\sharp} \cdot \partial_{\mathbf{a}_s^{\sharp}} \psi_0^t \cdot \mathbf{g}^{\sharp} = [\partial_{\mathbf{g}^b} \psi_0^t]^t, \\
\mathbf{F}_\tau^{\sharp} \doteq \widehat{\mathbf{G}}^{\sharp} &\implies \partial_{\widehat{\mathbf{C}}_e^b} \psi_0^{\mathbb{P}} = \widehat{\mathbf{G}}^{\sharp} \cdot \partial_{\widehat{\mathbf{G}}^{\sharp}} \psi_0^{\mathbb{P}} \cdot \widehat{\mathbf{B}}_e^{\sharp} + \sum_{s=1}^n \widehat{\mathbf{A}}_s^{\sharp} \cdot \partial_{\widehat{\mathbf{A}}_s^{\sharp}} \psi_0^{\mathbb{P}} \cdot \widehat{\mathbf{B}}_e^{\sharp} = [\partial_{\widehat{\mathbf{C}}_e^b} \psi_0^{\mathbb{P}}]^t, \\
\mathbf{F}_\tau^{\sharp} \doteq \mathbf{f}_p^{\sharp} &\implies \partial_{\mathbf{C}^b} \psi_0^0 = \mathbf{B}_p^{\sharp} \cdot \partial_{\mathbf{B}_p^{\sharp}} \psi_0^0 \cdot \mathbf{B}^{\sharp} + \sum_{s=1}^n \mathbf{A}_s^{\sharp} \cdot \partial_{\mathbf{A}_s^{\sharp}} \psi_0^0 \cdot \mathbf{B}^{\sharp} = [\partial_{\mathbf{C}^b} \psi_0^0]^t,
\end{aligned}
} \quad (\text{B.32})$$

which proves Eqs.(3.15, 3.18, 3.21).

Appendix C

Hyper–elastic constitutive functions

Wir müssen die ... Anschauung aufgeben, daß man sich auf die jedem individuellen oder einzelnen Ding inhärenten wesentlichen Eigenschaften berufen kann, um das Verhalten dieses Dinges zu erklären. Denn dieser Anschauung gelingt es durchaus nicht, Licht auf das Problem zu werfen, warum verschiedene individuelle Dinge sich auf ähnliche Weise verhalten sollen. Wenn gesagt wird: „Weil ihre wesentlichen Eigenschaften ähnlich sind“, so erhebt sich die neue Frage, warum es nicht ebenso viele verschiedene wesentliche Eigenschaften geben soll, wie es verschiedene Dinge gibt.

Sir Karl Raimund Popper [1902–1994]
Ratio, Vol. 1, 1957

In the sequel we briefly reiterate some typical examples of free Helmholtz energy densities whereby special emphasis is placed on the isotropic and transversely isotropic case.

C.1 Isotropy

The free Helmholtz energy density of an isotropic material allows modelling in terms of, e.g., the principal $C^b G^\sharp J_{1,2,3}$, $E^b G^\sharp J_{1,2,3}$ or basic $C^b G^\sharp I_{1,2,3}$, $E^b G^\sharp I_{1,2,3}$ invariants (here referring to the right Cauchy–Green tensor $C^b \in \mathbb{S}_+^3$ with respect to the Lagrangian setting without loss of generality for the isotropic case). The unconstrained general format is typically represented by

$$\begin{aligned} \psi_0^0 &= \psi_0^0 \left(C^b G^\sharp J_{1,2,3} \right) = \sum_{p,q,r=0}^{\infty} C^b c_{pqr} \left[C^b G^\sharp J_1 - 3 \right]^p \left[C^b G^\sharp J_2 - 3 \right]^q \left[C^b G^\sharp J_3 - 1 \right]^r, \\ \psi_0^0 &= \psi_0^0 \left(E^b G^\sharp I_{1,2,3} \right) = \sum_{p,q,r=0}^{\infty} E^b c_{pqr} E^b G^\sharp I_1^p E^b G^\sharp I_2^q E^b G^\sharp I_3^r, \end{aligned} \quad (C.1)$$

compare Ogden [Ogd97, Sect. 4.3.5]. Two fundamental restrictions thereby have to be obeyed, namely

$$\begin{aligned} \psi_0^0|_{\mathbf{F}^\sharp = \mathbf{G}^\sharp} = 0 &\implies C^b c_{000} = E^b c_{000} = 0, \\ 2 \partial_{C^b} \psi_0^0|_{\mathbf{F}^\sharp = \mathbf{G}^\sharp} = \partial_{E^b} \psi_0^0|_{\mathbf{F}^\sharp = \mathbf{G}^\sharp} = \mathbf{0} &\implies C^b c_{100} + 2 C^b c_{010} C^b c_{001} = E^b c_{100} = 0. \end{aligned} \quad (C.2)$$

Several additional constraints can now be incorporated into the free Helmholtz energy density ^{||}, such as the restriction $C^b G^\sharp J_3 = 1$ which represents an incompressible material defined in terms of

^{||} It is obvious that physics restrict the response functions. In view of the constitutive equation for appropriate stress fields we commonly agree to the picture that “stress follows strain”, namely the strict monotony condition

$$\begin{aligned} \omega &= \left[[\mathbf{\Pi}^\sharp]^\sharp(\mathbf{g}^b, \mathbf{F}^\sharp + \delta \mathbf{\Xi}^\sharp, \mathbf{G}^\sharp; \mathbf{X}) - [\mathbf{\Pi}^\sharp]^\sharp(\mathbf{g}^b, \mathbf{F}^\sharp, \mathbf{G}^\sharp; \mathbf{X}) \right] : \mathbf{\Xi}^\sharp \in \mathbb{R}_+ \\ \forall \mathbf{F}^\sharp &\in \mathbb{L}_+^3, \quad \forall \mathbf{\Xi}^\sharp \neq \mathbf{0} \in \mathbb{L}^3, \quad \forall \delta \in \mathbb{R} : 0 < \delta \leq 1, \quad [\mathbf{F}^\sharp + \delta \mathbf{\Xi}^\sharp] \in \mathbb{L}_+^3 \end{aligned} \quad (||.1)$$

$\text{con}\psi_0^0 \doteq \text{con}\psi_0^0(C^b G^\sharp J_{1,2})$. The specific case where all c_{pq} are zero with the exception of $c_{10} \doteq c_1$ and $c_{01} \doteq c_2$, is established as Mooney–Rivlin material. Here, we apply a compressible version that is additively enlarged by the function $U_0^0(C^b G^\sharp J_3)$ which takes the format

$$\begin{aligned} \psi_0^0 &= \psi_0^0(C^b G^\sharp J_{1,2,3}) \\ &\doteq \text{con}\psi_0^0(C^b G^\sharp J_{1,2}) + U_0^0(C^b G^\sharp J_3) \\ &\doteq c_1 [C^b G^\sharp J_1 - 3] + c_2 [C^b G^\sharp J_2 - 3] + \frac{\lambda^p}{2} \ln^2(C^b G^\sharp J_3^{1/2}) - 2[c_1 + 2c_2] \ln(C^b G^\sharp J_3^{1/2}), \end{aligned} \quad (\text{C.3})$$

see Simo and Taylor [ST82]. Further restrictions like, e.g., $\text{con}\psi_0^0 \doteq \text{con}\psi_0^0(C^b G^\sharp J_1)$ result in Neo–Hookian functions. In this work, two different compressible types are adopted, namely

$$\psi_0^0(C^b G^\sharp J_{1,2,3}) \doteq \frac{\mu}{2} [C^b G^\sharp J_1 - 3] - \mu \ln(C^b G^\sharp J_3^{1/2}) + \frac{\lambda^p}{2} \ln^2(C^b G^\sharp J_3^{1/2}) \quad (\text{C.4})$$

and

$$\psi_0^0(C^b G^\sharp J_{1,2,3}) \doteq \frac{G}{2} [C^b G^\sharp J_1 - 3] + \frac{K}{2} \left[\frac{1}{2} [C^b G^\sharp J_3 - 1] - \ln(C^b G^\sharp J_3^{1/2}) \right]. \quad (\text{C.5})$$

Furthermore, a decomposition of Flory–type can be applied by separating the volume preserving and changing part of the linear tangent map

$$\mathbf{F}^\natural = [C^b G^\sharp J_3^{1/2 n_{\text{dim}}} \mathbf{g}^\natural] \cdot [C^b G^\sharp J_3^{-1/2 n_{\text{dim}}} \mathbf{F}^\natural] = [C^b G^\sharp J_3^{-1/2 n_{\text{dim}}} \mathbf{F}^\natural] \cdot [C^b G^\sharp J_3^{1/2 n_{\text{dim}}} \mathbf{G}^\natural] \quad (\text{C.6})$$

with n_{dim} characterising the dimension in space. On this basis, the contribution $\text{con}\psi_0^0$ is constructed via $C^b G^\sharp J_3^{-1/n_{\text{dim}}} \mathbf{F}^\natural \mapsto \mathbf{F}^\natural$. To give an example, the Neo–Hookian material in Eq.(C.5) then reads as

$$\psi_0^0(C^b G^\sharp J_{1,2,3}) \doteq \frac{G}{2} [C^b G^\sharp J_3^{-1/n_{\text{dim}}} C^b G^\sharp J_1 - 3] + \frac{K}{2} \left[\frac{1}{2} [C^b G^\sharp J_3 - 1] - \ln(C^b G^\sharp J_3^{1/2}) \right]. \quad (\text{C.7})$$

We additionally adopt a non–linear constitutive equation in the spirit of Kauderer [Kau49] in this work which is determined by the first and second invariant, $\psi_0^0 = \psi_0^0({}^{E^b} G^\sharp I_{1,2}) = \sum_{p,q=0}^{\infty} {}^{E^b} G^\sharp c_{pq} {}^{E^b} G^\sharp I_1^p {}^{E^b} G^\sharp I_2^q$. Consequently, the second Piola–Kirchhoff stress tensor reads

$$\mathbf{S}^\sharp \doteq [3K \text{sph}\kappa - \frac{2}{3} G \text{dev}\kappa] {}^{E^b} G^\sharp I_1 \mathbf{G}^\sharp + 2G \text{dev}\kappa \mathbf{G}^\sharp \cdot \mathbf{E}^b \cdot \mathbf{G}^\sharp, \quad (\text{C.8})$$

whereby $[\mathbf{II}^\natural]^\natural$ is the stress field dual to \mathbf{F}^\natural , and that extreme strains give extreme stresses, i.e. for a hyper–elastic material we claim

$$\psi_0(\mathbf{g}^b, \mathbf{F}^\natural, \mathbf{G}^\sharp; \mathbf{X}) \rightarrow \infty \quad \text{as} \quad \det(\mathbf{F}^\natural) \rightarrow 0_+ \quad \text{or as} \quad [\|\mathbf{F}^\natural\| + \|\text{cof}(\mathbf{F}^\natural)\| + \det(\mathbf{F}^\natural)] \rightarrow \infty \quad (\|\cdot\|_2) \quad (\text{||.2})$$

which allows alternative representation in terms of principal stretches. The second constraint can be replaced by the sharper version $\exists\{\alpha, a, b, c \in \mathbb{R}_+; \beta \in \mathbb{R}\}$ such that $\psi_0(\mathbf{g}^b, \mathbf{F}^\natural, \mathbf{G}^\sharp; \mathbf{X}) \geq \alpha [\|\mathbf{F}^\natural\|^a + \|\text{cof}(\mathbf{F}^\natural)\|^b + \det^c(\mathbf{F}^\natural)] + \beta$. Moreover, assuming that $[\mathbf{II}^\natural]^\natural$ is differentiable and taking the derivative of ω with respect to δ at $\delta = 0$ yields $\varpi = \mathfrak{E}^\natural : \partial_{\mathbf{F}^\natural} [\mathbf{II}^\natural]^\natural : \mathfrak{E}^\natural \in \mathbb{R}_+ \forall \mathfrak{E}^\natural \neq \mathbf{0} \in \mathbb{L}^3$. For \mathfrak{E}^\natural rank one, $\omega \in \mathbb{R}_+$ defines the strong ellipticity condition together with it's stronger restriction $\varpi \in \mathbb{R}_+$ (the latter one being directly related to the (determinant of the) acoustic tensor, compare Appendix D.3). For the considered hyper–elastic setting as based on the free Helmholtz energy density ψ_0 , the strong form of ellipticity allows generalisation to rank–one convexity

$$\begin{aligned} \psi_0(\mathbf{g}^b, \mathbf{F}^\natural + \delta \mathfrak{E}^\natural, \mathbf{G}^\sharp; \mathbf{X}) &\leq [1 - \delta] \psi_0(\mathbf{g}^b, \mathbf{F}^\natural, \mathbf{G}^\sharp; \mathbf{X}) + \delta \psi_0(\mathbf{g}^b, \mathbf{F}^\natural + \mathfrak{E}^\natural, \mathbf{G}^\sharp; \mathbf{X}) \\ \forall \mathbf{F}^\natural \in \mathbb{L}_+^3, \forall \mathfrak{E}^\natural \in \mathbb{L}^3 : \text{rank one}, \forall \delta \in \mathbb{R} : 0 < \delta \leq 1, \omega \in \mathbb{R}_+, [\mathbf{F}^\natural + \delta \mathfrak{E}^\natural] \in \mathbb{L}_+^3 \end{aligned} \quad (\|\cdot\|_2) \quad (\text{||.3})$$

compare e.g. Ball [Bal77, Def. 3.2] or the monographs by Ciarlet [Cia88, Exer. 5.15], Antman [Ant95, Eq. XII/12(2.9)] and Šilhavý [Šil97, Prop. 17.3.3] (for $\psi_0 \in C^2$ (at least) the relation $\varpi \in \mathbb{R}_+ \forall \mathfrak{E}^\natural \in \mathbb{L}^3 : \text{rank one}$, corresponds to the strong Legendre–Hadamard condition). However, the properties: *convexity* \rightarrow *poly-convexity* ($\psi_0(\mathbf{g}^b, \mathbf{F}^\natural, \mathbf{G}^\sharp; \mathbf{X}) = \psi_0^\dagger(\mathbf{g}^b, \mathbf{F}^\natural, \text{cof}(\mathbf{F}^\natural), \det(\mathbf{F}^\natural), \mathbf{G}^\sharp; \mathbf{X})$ with ψ_0^\dagger being convex in $\{\mathbf{F}^\natural, \text{cof}(\mathbf{F}^\natural), \det(\mathbf{F}^\natural)\}$) \rightarrow *quasi-convexity* ($\text{volume}^{-1}(\mathcal{B}_\xi) \int_{\mathcal{B}_\xi} \psi_0(\mathbf{g}^b, \mathbf{F}_\xi^\natural + \mathfrak{E}^\natural, \mathbf{G}^\sharp; \mathbf{X}) d\mathbf{X} \geq \psi_0(\mathbf{g}^b, \mathbf{F}_\xi^\natural, \mathbf{G}^\sharp; \mathbf{X})$ at a particular $\mathbf{F}_\xi^\natural \in \mathbb{L}_+^3$ and with $\mathcal{B}_\xi \subseteq \mathcal{B}_0$, $\mathfrak{E}^\natural(\mathbf{X}) = \partial_{\mathbf{X}} \chi(\mathbf{X}) \in \mathbb{L}^3 \forall \chi(\mathbf{X}) : \mathcal{B}_\xi \rightarrow \mathcal{B}_t$ such that $\mathbf{F}_\xi^\natural + \mathfrak{E}^\natural(\mathbf{X}) \in \mathbb{L}_+^3$) \rightarrow *rank-one convexity* hold throughout and especially the existence theory (of hyper–elastic materials, static settings and dead loading) as based on the minimisation of the potential energy, is substantially based on the poly–convexity condition. Detailed background informations are given in the previously cited references; Ball [Bal77], Ciarlet [Cia88, Chaps. 4,5 & 7], Antman [Ant95, Sect. XII/12] or Šilhavý [Šil97, Chaps. 16–18].

whereby K and G respectively denote the constant compression- and shear-moduli. Note that this structure coincides with a St. Venant–Kirchhoff-type material, whereby non-linearities are introduced via the scalar-valued dimensionless functions $^{\text{sph}}\kappa$ and $^{\text{dev}}\kappa$. We choose a polynomial ansatz in the following

$$\begin{aligned} ^{\text{sph}}\kappa(^{\text{sph}}l^1) &= 1 + ^{\text{sph}}\kappa_1 ^{\text{sph}}l^1 + ^{\text{sph}}\kappa_2 ^{\text{sph}}l^2 + \dots, \\ ^{\text{dev}}\kappa(^{\text{dev}}l^2) &= 1 + ^{\text{dev}}\kappa_2 ^{\text{dev}}l^2 + ^{\text{dev}}\kappa_4 ^{\text{dev}}l^4 + \dots, \end{aligned} \quad (\text{C.9})$$

$$\text{with } ^{\text{sph}}l^1 = \frac{1}{3} E^b G^\# I_1 \text{ and } ^{\text{dev}}l^2 = \frac{4}{3} \left[E^b G^\# I_2 - \frac{1}{3} E^b G^\# I_1^2 \right].$$

The incorporation of constant, linear and quadratic terms – $^{\text{sph}}\kappa_i = 0$, $i = 3, \dots, \infty$ and $^{\text{dev}}\kappa_j = 0$, $j = 6, \dots, \infty$ – renders the following identification of constants

$$\begin{aligned} c_{20} &= \frac{1}{2} K - \frac{1}{3} G, & c_{01} &= G, \\ c_{30} &= \frac{1}{9} K ^{\text{sph}}\kappa_1, & c_{02} &= \frac{2}{3} G ^{\text{dev}}\kappa_2, \\ c_{40} &= \frac{2}{27} G ^{\text{dev}}\kappa_2 + \frac{1}{12} K ^{\text{sph}}\kappa_2, & c_{21} &= -\frac{4}{9} G ^{\text{dev}}\kappa_2, \\ c_{60} &= -\frac{16}{729} G ^{\text{dev}}\kappa_4, & c_{41} &= \frac{16}{81} G ^{\text{dev}}\kappa_4, \\ c_{03} &= \frac{16}{27} G ^{\text{dev}}\kappa_4, & c_{22} &= -\frac{16}{27} G ^{\text{dev}}\kappa_4 \end{aligned} \quad (\text{C.10})$$

and $c_{pq} = 0$ otherwise. Moreover, additionally neglecting the second order terms ($^{\text{sph}}\kappa_{i \setminus 1} = 0$ and $^{\text{dev}}\kappa_{i \setminus 2} = 0$) results in the following coefficients

$$\begin{aligned} c_{20} &= \frac{1}{2} K - \frac{1}{3} G, & c_{01} &= G, \\ c_{30} &= \frac{1}{9} K ^{\text{sph}}\kappa_1, & c_{02} &= \frac{2}{3} G ^{\text{dev}}\kappa_2, \\ c_{40} &= \frac{2}{27} G ^{\text{dev}}\kappa_2, & c_{21} &= -\frac{4}{9} G ^{\text{dev}}\kappa_2 \end{aligned} \quad (\text{C.11})$$

with $c_{pq} = 0$ otherwise.

Finally, please note that an outline with respect to an intermediate or Eulerian setting is straightforward. Moreover, within the framework of fictitious configurations, anisotropy enters the constitutive equations simply by replacing the set of three invariants. It is clear that these anisotropic formulations can alternatively be expressed in terms of structural tensors. The opposite – to represent a constitutive equations based on structural tensors within the framework of a fictitious configurations – is obviously not generally possible.

C.2 Transversal isotropy

For the formulation of a transversely isotropic material based on one structural tensor within the Lagrangian setting, we adopt an additive decomposition of the free Helmholtz energy density into a purely isotropic part and an anisotropic contribution

$$\psi_0^0 \doteq \psi_0^0(\mathbf{C}^b, \mathbf{A}_1^\#; \mathbf{X}) \doteq {}^{\text{iso}}\psi_0^0(\mathbf{C}^b; \mathbf{X}) + {}^{\text{ani}}\psi_0^0(\mathbf{C}^b, \mathbf{A}_1^\#; \mathbf{X}). \quad (\text{C.12})$$

Thereby, the isotropic term ${}^{\text{iso}}\psi_0^0$ is generally defined by Eq.(C.1) and for the anisotropic contribution we choose (see e.g. Eq.(2.49) for the definition of the invariants ${}^{\text{C}^b \mathbf{A}_1^\#} I_{4,5}$)

$$\begin{aligned} {}^{\text{ani}}\psi_0^0 &= \alpha \left[{}^{\text{C}^b G^\#} J_3^{-n} \exp \left(\beta \left[{}^{\text{C}^b \mathbf{A}_1^\#} I_4 - 1 \right] + \delta \left[{}^{\text{C}^b \mathbf{A}_1^\#} I_4 - 1 \right]^2 + \epsilon \left[{}^{\text{C}^b \mathbf{A}_1^\#} I_5 - 1 \right] \right. \right. \\ &\quad \left. \left. + \eta \left[{}^{\text{C}^b G^\#} J_1 - 3 \right] \left[{}^{\text{C}^b \mathbf{A}_1^\#} I_4 - 1 \right] \right) \right. \\ &\quad \left. + n \left[{}^{\text{C}^b G^\#} J_3 - 1 \right] - \beta \left[{}^{\text{C}^b \mathbf{A}_1^\#} I_4 - 1 \right] - \epsilon \left[{}^{\text{C}^b \mathbf{A}_1^\#} I_5 - 1 \right] \right] \end{aligned} \quad (\text{C.13})$$

for the anisotropic contribution which is frequently employed in the literature on soft tissues whereby $\alpha, \beta, \delta, \epsilon, \eta$ and n are additional material parameters, see e.g. Almeida and Spilker [AS98].

C.3 Some remarks on homogenisation concepts

Three different homogenisation approaches are well established and are usually directly related to continuum damage mechanics, namely the concepts of equivalent strain, equivalent stress and equivalent strain energy, see e.g. Lemaitre and Chaboche [LC98, Chap. 7]. For the sake of clarity, we restrict our brief outline here to the common $[1 - D]$ model whereby the scalar-valued variable D is assumed to represent inhomogeneities.

Within the *equivalent strain* concept, the homogenised, effective and nominal metric fields are dictated to be identical; $\bar{\mathbf{C}}^b \doteq \mathbf{C}^b$. We consequently end up with different stress fields and obtain the relation $\bar{\mathbf{S}}^\sharp = 2 \partial_{\bar{\mathbf{C}}^b} \bar{\psi}_0^0 = [1 - D]^{-1} \mathbf{S}^\sharp$ with $\psi_0^0(\mathbf{C}^b, D; \mathbf{X}) \doteq [1 - D] \bar{\psi}_0^0(\bar{\mathbf{C}}^b; \mathbf{X})$.

Next, based on the assumption of *equivalent* homogenised, effective and nominal *stress*, $\bar{\mathbf{S}}^\sharp \doteq \mathbf{S}^\sharp$, we obviously end up with different strain fields. Via $\psi_0^0(\mathbf{C}^b, D; \mathbf{X}) \doteq [1 - D]^{-1} \bar{\psi}_0^0(\bar{\mathbf{C}}^b; \mathbf{X})$, straightforward computations yield $\bar{\mathbf{C}}^b = [1 - D] \mathbf{C}^b$.

Finally, the hypothesis of *equivalent strain energy*, $\psi_0^0(\mathbf{C}^b, D; \mathbf{X}) \doteq \bar{\psi}_0^0(\bar{\mathbf{C}}^b; \mathbf{X})$, results in different homogenised, effective and nominal strain and stress fields. Apparently, this assumption is satisfied for $\bar{\mathbf{S}}^\sharp : \bar{\mathbf{C}}^b \doteq [[1 - D]^{-1} \mathbf{S}^\sharp] : [[1 - D] \mathbf{C}^b] = \mathbf{S}^\sharp : \mathbf{C}^b$.

Recall that the fundamental covariance relation of the free Helmholtz energy density is directly correlated to the postulate of equivalent strain energy and possibly the concept of a fictitious configuration.

Appendix D

Visualisation of anisotropy

Sch gestehe zwar, daß das Fermatsche Theorem als isolierter Satz für mich wenig Interesse hat, denn es lassen sich eine Menge solcher Sätze leicht aufstellen, die man weder beweisen, noch wiederlegen kann. ...
Allein ich bin überzeugt, wenn das Glück mehr tun sollte, als ich erwarten darf und mir einige Hauptschritte in jener Theorie glücken, auch der Fermatsche Satz nur als eines der am wenigsten interessanten Corollarien dabei erscheinen wird (Disquisitiones Arithmeticae).

Carl Friedrich Gauß [1777 – 1855]
Brief an W. Olbers, Göttingen, 21.03.1816

Unfortunately, it is a non-trivial task to give a clear graphical representation of anisotropic material behaviour – especially within a three-dimensional setting. In the following we reiterate three different approaches and with that, try to handle this problem.

D.1 A scalar-valued anisotropy measure

For an anisotropic constitutive equation, e.g., the stress ($\mathbf{S}^\sharp \in \mathbb{S}^3$) and the strain ($\mathbf{E}^b \in \mathbb{S}^3$) metric tensors are generally not coaxial. Here we highlight the material setting and the non-symmetric part of their product thus reads

$$\mathbf{E}^b \cdot \mathbf{S}^\sharp - \mathbf{G}^b \cdot \mathbf{S}^\sharp \cdot \mathbf{E}^b \doteq {}^{E^b S^\sharp} \mathbf{W}^b(\mathbf{E}^b, \mathbf{S}^\sharp) \in \mathbb{W}^3 : TB_0 \times TB_0 \rightarrow \mathbb{R}. \quad (\text{D.1})$$

In the general anisotropic case, when the strain and stress field do not commute, we have ${}^{E^b S^\sharp} \mathbf{W}^b(\mathbf{E}^b, \mathbf{S}^\sharp) \neq \mathbf{0}$ and thus, as an appropriate scalar-valued measure of anisotropy, we propose to compute the quantity $\delta(\mathbf{E}^b, \mathbf{S}^\sharp) \in \mathbb{R}_0$ to indicate anisotropy which is essentially determined by the skew-symmetric tensor ${}^{E^b S^\sharp} \mathbf{W}^b(\mathbf{E}^b, \mathbf{S}^\sharp)$ in a normalised format

$$\delta(\mathbf{E}^b, \mathbf{S}^\sharp) = \frac{\| {}^{E^b S^\sharp} \mathbf{W}^b(\mathbf{E}^b, \mathbf{S}^\sharp) \|}{\| \mathbf{E}^b \| \| \mathbf{S}^\sharp \|} \quad \text{for } \mathbf{E}^b, \mathbf{S}^\sharp \neq \mathbf{0} \quad (\text{D.2})$$

and $\delta(\mathbf{E}^b, \mathbf{S}^\sharp) = 0$ otherwise, whereby the notation $\|[\bullet]\|$ abbreviates the appropriate norm with $\|[\bullet]^\sharp\|^2 = [[\bullet]^\sharp \cdot \mathbf{G}^b] : [\mathbf{G}^b \cdot [\bullet]^\sharp]$ and $\|[\bullet]^b\|^2 = [[\bullet]^b \cdot \mathbf{G}^\sharp] : [\mathbf{G}^\sharp \cdot [\bullet]^b]$. Apparently, this anisotropy measure can be applied to any arbitrary pair of second order tensors (in one configuration).

D.2 Stereo-graphic projection

To visualise the non-coaxiality of, e.g., the strain and stress fields (or any other appropriate pair of symmetric second order tensors) the method of stereo-graphic projection is adopted, which is well-known from crystallography and represents the homomorphism $\mathbb{O}_+^3 \rightarrow \mathbb{M}^2$, see e.g. Altmann [Alt86,

Chap. 7]. Conceptually speaking, the eigenvectors of symmetric second order tensors – interpreted as elements of the unit sphere \mathbb{U}^2 – are projected onto the equatorial plane by viewing from the south pole, see Figure D.1₁.

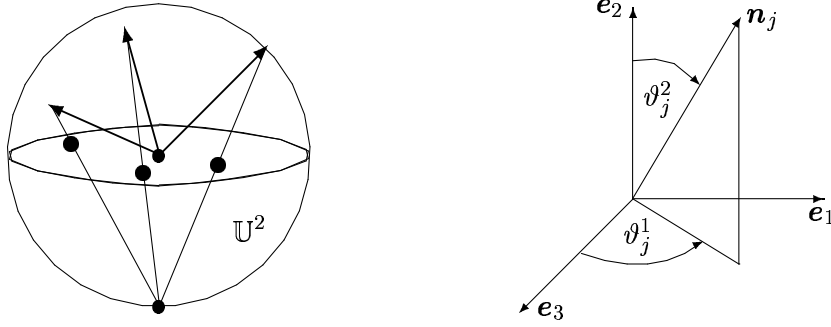


Figure D.1: Stereo-graphic projection and spherical coordinates.

Moreover, to define the axis of anisotropy we apply spherical coordinates. For the sake of simplicity we refer to a Cartesian frame \mathbf{e}_i , thus one possible parametrisation of the direction-vectors of interest $\mathbf{n}_j = n_j^i \mathbf{e}_i \in \mathbb{U}^2$ results in $n_j^1 = \sin \vartheta_j^1 \sin \vartheta_j^2$, $n_j^2 = \cos \vartheta_j^2$ and $n_j^3 = \cos \vartheta_j^1 \sin \vartheta_j^2$, see Figure D.1₂.

D.3 The acoustic tensor

As point of departure, we consider the incremental equation of motion in the absence of body forces

$$\begin{aligned}
 \text{Div } \delta(\mathbf{F}^\natural \cdot \mathbf{S}^\natural) &= \text{Div} (\delta \mathbf{F}^\natural \cdot \mathbf{S}^\natural + \mathbf{F}^\natural \cdot \delta \mathbf{S}^\natural) \\
 &= \text{Grad } \delta \mathbf{F}^\natural : \mathbf{S}^\natural + \delta \mathbf{F}^\natural \cdot \text{Div } \mathbf{S}^\natural + \text{Grad } \mathbf{F}^\natural : \delta \mathbf{S}^\natural + \mathbf{F}^\natural \cdot \text{Div } \delta \mathbf{S}^\natural \\
 &= \partial_{\mathbf{X}} \delta \mathbf{F}^\natural : \mathbf{S}^\natural + \delta \mathbf{F}^\natural \cdot [\partial_{\mathbf{X}} \mathbf{S}^\natural : [\mathbf{G}^\natural]^\dagger] + \partial_{\mathbf{X}} \mathbf{F}^\natural : \delta \mathbf{S}^\natural + \mathbf{F}^\natural \cdot [\partial_{\mathbf{X}} \delta \mathbf{S}^\natural : [\mathbf{G}^\natural]^\dagger] \\
 &\doteq \rho_0 \partial_{tt}^2 \delta \mathbf{x}
 \end{aligned} \tag{D.3}$$

whereby ρ_0 denotes the initial mass density and t represents time, compare e.g. Antman [Ant95, Sect. XIII/2] or Ogden [Ogd97, Sect. 6.4]. Typically a homogeneous state is examined ($\mathbf{F}^\natural \doteq \text{const}$) and, moreover, the following incremental relation holds

$$\mathbf{F}^\natural \cdot \delta \mathbf{S}^\natural = \dagger \mathbf{E}^\natural : \delta \mathbf{F}^\natural \quad \text{with} \quad \dagger \mathbf{E}^\natural = \mathbf{F}^\natural \cdot \mathbf{E}^\natural : \left[[[\mathbf{F}^\natural]^\dagger \cdot \mathbf{g}^b] \overline{\otimes} [\mathbf{G}^\natural]^\dagger \right] \tag{D.4}$$

and $\dagger \mathbf{E}^\natural = \dagger \mathbf{E}^{ijl} \mathbf{g}_i \otimes \mathbf{G}_j \otimes \mathbf{g}^k \otimes \mathbf{G}_l \in \mathbb{L}^{3 \times 3} : [T^* \mathcal{B}_0 \rightarrow T^* \mathcal{B}_t] \rightarrow [T^* \mathcal{B}_0 \rightarrow T \mathcal{B}_t]$ whereby the minor symmetry of the Hessian \mathbf{E}^\natural has been taken into account. For an overview on Eulerian tangent operators, see e.g. Steinmann et al. [SLR97]. Next, we adopt the usual wave propagation ansatz

$$\begin{aligned}
 \delta \mathbf{x} &\doteq \mathbf{m}^\natural f(\mathbf{n}^b \cdot \mathbf{x} - ct), \\
 c \in \mathbb{R}_+, \quad t \in \mathbb{R}, \quad \mathbf{m}^\natural \in \mathbb{R}^3 : T^* \mathcal{B}_t \rightarrow \mathbb{R}, \quad \mathbf{n}^b \in \mathbb{U}^2 : T \mathcal{B}_t \rightarrow \mathbb{R}, \quad f \in C^2.
 \end{aligned} \tag{D.5}$$

Straightforward calculations with $\delta \mathbf{F}^\natural = \partial_{\mathbf{X}} \delta \mathbf{x} \in \mathbb{L}^3$ render the acoustic tensor $\mathbf{q}^\natural = q_j^i \mathbf{g}_i \otimes \mathbf{g}^j \in \mathbb{L}^3 : T^* \mathcal{B}_t \times T \mathcal{B}_t \rightarrow \mathbb{R}$ which occurs in the following eigenvalue problem for the wave speed c in the propagation direction \mathbf{n}^b with corresponding polarisation vector \mathbf{m}^\natural

$$\begin{aligned}
 \mathbf{q}^\natural \cdot \mathbf{m}^\natural &= \left[\dagger \mathbf{q}^\natural + [\mathbf{N}^b \cdot \mathbf{S}^\natural \cdot \mathbf{N}^b] \mathbf{g}^\natural \right] \cdot \mathbf{m}^\natural = \rho_0 c^2 \mathbf{m}^\natural \\
 \text{with } \mathbf{N}^b &= [\mathbf{F}^\natural]^\dagger \cdot \mathbf{n}^b \in \mathbb{R}^3 : T \mathcal{B}_0 \rightarrow \mathbb{R} \quad \text{and} \quad \dagger \mathbf{q}^\natural = [\mathbf{g}^\natural \otimes \mathbf{N}^b] : \dagger \mathbf{E}^\natural \cdot \mathbf{N}^b.
 \end{aligned} \tag{D.6}$$

Appendix E

Numerical aspects



ur wills and fates do so contrary run
That our devices still are overthrown,
Our thoughts are ours, their end none of our own.

William Shakespeare [1564 – 1616]
The Player King in Hamlet, 1604

We focus on two subjects that are frequently applied in this work for the computation of the numerical examples. Some essentials on specific Runge–Kutta integration schemes and the numerical approximation of Jacobians are particularly reiterated.

E.1 Some Runge–Kutta schemes

For completeness and convenience of the reader, some Runge–Kutta schemes are given in the following with respect to the Butcher array (whereby the relations $\sum_{i=1}^s b_i = 1$ and $c_i = \sum_{j=1}^s a_{ij}$ hold)

$$\begin{array}{c|cccc} c_1 & a_{11} & a_{12} & \cdots & a_{1s} \\ c_2 & a_{21} & a_{22} & \cdots & a_{2s} \\ \vdots & \vdots & \vdots & \ddots & \vdots \\ c_s & a_{s1} & a_{s2} & \cdots & a_{ss} \\ \hline & b_1 & b_2 & \cdots & b_s \end{array}$$

which is documented in various standard textbooks, e.g. Ascher and Petzold [AP98, Chap. 4] or Lambert [Lam91, Chap. 5]. Without loss of generality, the intermediate stages are defined by $c_i = \sum_{j=1}^s a_{ij}$ and furthermore, all other subsequently not mentioned coefficients equal zero. Following standard notation, s denotes the stage and p the order of accuracy.

The simplest explicit method (Euler forward, $s = p = 1$) is defined by $b_1 = 1$. Combining several Euler steps ends up in Heun methods, e.g. $s = p = 2$ for $a_{21} = 1$ and $b_1 = b_2 = \frac{1}{2}$, which practically represent explicit predictor/corrector schemes.

Next, three families of implicit Runge–Kutta methods are outlined, Gauß (including the midpoint rule), Radau IIa (including Euler backward) and Lobatto IIIa (including the trapezoidal rule). One considered algorithm of the family of highest possible order – Gauß – for $s = 2$ and $p = 4$ is given by $a_{11} = a_{22} = \frac{1}{4}$, $a_{12} = \frac{1}{12} [3 - 2\sqrt{3}]$, $a_{21} = \frac{1}{12} [3 + 2\sqrt{3}]$ and $b_1 = b_2 = \frac{1}{2}$. A two stage scheme of the Radau IIa type of order $p = 3$, generally including stiff decay, reads $a_{11} = \frac{5}{12}$, $a_{12} = -\frac{1}{12}$, $a_{21} = b_1 = \frac{3}{4}$ and $a_{22} = b_2 = \frac{1}{4}$. From the computational point of view, algorithms due to Lobatto IIIa are less expensive than expressed by their stage s since the first intermediate state 1t coincides with the known

one at $^n t$. For $s = 3$ and $p = 4$ one has $a_{21} = \frac{5}{24}$, $a_{22} = \frac{1}{3}$, $a_{23} = -\frac{1}{24}$, $a_{31} = b_1 = a_{33} = b_3 = \frac{1}{6}$ and $a_{32} = b_2 = \frac{2}{3}$.

Finally, diagonally implicit Runge–Kutta methods (DIRK) are numerically interesting since they do not blow up the system of equations within the Newton iteration. A two stage Gauß DIRK scheme with $p = 3$ is determined by $a_{11} = a_{22} = \alpha_G$, $a_{21} = 1 - 2\alpha_G$ and $b_1 = b_2 = \frac{1}{2}$ with $\alpha_G = \frac{1}{6} [3 + \sqrt{3}]$. The Radau IIa DIRK algorithm for $s = 2$ and order $p = 2$ similarly takes the form $a_{11} = a_{22} = b_2 = \alpha_R$ and $a_{21} = b_1 = 1 - \alpha_R$ with $\alpha_R = \frac{1}{2} [2 - \sqrt{2}]$.

E.2 Numerical approximation of Jacobians

A variety of algorithms can be applied to solve non–linear (systems of) equations. Among the most effective strategies, the standard Newton–Raphson scheme is usually a good choice since quadratic convergence can be obtained (at least close to the solution). As a drawback, the correlated Jacobians have to be computed which may result in tremendous analytical costs. The underlying idea to avoid this analysis is based on a numerical approximation of these fields. Conceptually speaking, the analytical tangent is replaced by an appropriate difference scheme. To be specific, following the outline given in Dennis and Schnabel [DS96, Chap. 5], we consider a function $f(\mathbf{x})$ with $\mathbf{x} \in \mathbb{R}^n$ and appropriate step sizes $\varepsilon_i \in \mathbb{R}_+$ referring to a Cartesian frame \mathbf{e}_i . Then, the analytical tangent operator can be approximated by, e.g., a (first order) forward difference formula or a (second order) central difference formula

$$\frac{\partial f(\mathbf{x})}{\partial x_i} = \frac{f(\mathbf{x} + \varepsilon_i \mathbf{e}_i) - f(\mathbf{x})}{\varepsilon_i} + \mathcal{O}(\varepsilon_i), \quad \frac{\partial f(\mathbf{x})}{\partial x_i} = \frac{f(\mathbf{x} + \varepsilon_i \mathbf{e}_i) - f(\mathbf{x} - \varepsilon_i \mathbf{e}_i)}{2\varepsilon_i} + \mathcal{O}(\varepsilon_i^2) \quad (\text{E.1})$$

with $x_i = \mathbf{x} \cdot \mathbf{e}_i$. The optimal step sizes ε_i again guarantee quadratic convergence; for a discussion and examples with respect to applications in computational plasticity at small strains, see Pérez–Foguet et al. [PFRFH00].

In this work, we are concerned with the (global) consistent tangent operator for a geometrically non–linear finite element setting, see Algorithm E.1, and the computation of (local) Jacobians within the integration of evolution equations, see Algorithm E.2. We adopt and briefly re–iterate here – for convenience of the reader – an approximation algorithm as highlighted by Miehe [Mie96b]. In practice, the chosen step sizes ε_i crucially affect the quality of the convergence. It turns out and can be proved that a perturbation factor of 10^{-8} is an optimal choice for a store up of 16 digits.

Algorithm E.1 *Numerical computation of the consistent algorithmic tangent operator by a (first order) forward difference scheme whereby $\boldsymbol{\gamma}^\sharp(k,l)$, $\boldsymbol{\gamma}^b(k,l)$ and $\mathbf{I}^\sharp(k,l)$, $\mathbf{I}^b(k,l)$ denote appropriate spatial and material base vectors and $i, j, (k), (l) = 1, 2, 3$.*

Eulerian algo. tangent operator, $\text{alg}\mathbf{e}^\sharp \in \mathbb{L}^{3 \times 3} : T^* \mathcal{B}_t \times T^* \mathcal{B}_t \times T^* \mathcal{B}_t \times T \mathcal{B}_t \rightarrow \mathbb{R}$

$${}^{n+1} \mathbf{F}_{\varepsilon}^\sharp(kl) = {}^{n+1} \mathbf{F}^\sharp + \frac{\varepsilon}{2} \left[[\mathbf{g}^\sharp \cdot \boldsymbol{\gamma}_{(k)}^b] \otimes [\boldsymbol{\gamma}_{(l)}^b \cdot \mathbf{F}^\sharp] + [\mathbf{g}^\sharp \cdot \boldsymbol{\gamma}_{(l)}^b] \otimes [\boldsymbol{\gamma}_{(k)}^b \cdot \mathbf{F}^\sharp] \right]$$

$${}^{n+1} \boldsymbol{\tau}_{\varepsilon}^\sharp(kl) = {}^{n+1} \boldsymbol{\tau}_{\varepsilon}^\sharp(kl) \left({}^{n+1} \mathbf{F}_{\varepsilon}^\sharp(kl), \dots \right)$$

$$\text{alg}\mathbf{e}_{\varepsilon}^{ij(kl)} = \frac{1}{\varepsilon} \left[\tau_{\varepsilon}^{ij(kl)} - \tau^{ij} \right] - \frac{1}{2} \left[g^{ik} \tau^{jl} + g^{il} \tau^{jk} + \tau^{ik} g^{jl} + \tau^{il} g^{jk} \right]$$

Lagrangian algo. tangent operator, $\text{alg}\mathbf{E}^\sharp \in \mathbb{L}^{3 \times 3} : T^* \mathcal{B}_0 \times T^* \mathcal{B}_0 \times T^* \mathcal{B}_0 \times T^* \mathcal{B}_0 \rightarrow \mathbb{R}$

$${}^{n+1} \mathbf{F}_{\varepsilon}^\sharp(kl) = {}^{n+1} \mathbf{F}^\sharp + \frac{\varepsilon}{2} \left[[\mathbf{g}^\sharp \cdot [\mathbf{f}^\sharp]^\dagger \cdot \mathbf{I}_{(k)}^b] \otimes \mathbf{I}_{(l)}^b + [\mathbf{g}^\sharp \cdot [\mathbf{f}^\sharp]^\dagger \cdot \mathbf{I}_{(l)}^b] \otimes \mathbf{I}_{(k)}^b \right]$$

$${}^{n+1} \mathbf{S}_{\varepsilon}^\sharp(kl) = {}^{n+1} \mathbf{S}_{\varepsilon}^\sharp(kl) \left({}^{n+1} \mathbf{F}_{\varepsilon}^\sharp(kl), \dots \right)$$

$$\text{alg}\mathbf{E}_{\varepsilon}^{ij(kl)} = \frac{1}{\varepsilon} \left[S_{\varepsilon}^{ij(kl)} - S^{ij} \right]$$

Algorithm E.2 *Representative examples of (first order) forward difference schemes to approximate Jacobians whereby $\boldsymbol{\gamma}^{\sharp(k,l)}$, $\boldsymbol{\gamma}_{(k,l)}^b$ and $\boldsymbol{\Gamma}_{(l)}^b$ denote appropriate spatial and material base vectors and $i, j, (k), (l) = 1, 2, 3$ (The outline in the material or intermediate setting is similar and thus omitted).*

Numerical derivatives wrt $[\bullet]^\sharp, \mathbf{j}^\sharp \in \mathbb{L}^{3 \times 3} : T^* \mathcal{B}_t \times T^* \mathcal{B}_t \times T \mathcal{B}_t \times T \mathcal{B}_t \rightarrow \mathbb{R}$

$${}^{n+1}[\bullet]_\varepsilon^{\sharp(kl)} = {}^{n+1}[\bullet]^\sharp + \varepsilon \boldsymbol{\gamma}^{\sharp(k)} \otimes \boldsymbol{\gamma}^{\sharp(l)}$$

$$\mathbf{r}_\varepsilon^{\sharp(kl)} = \mathbf{r}^\sharp \left({}^{n+1}[\bullet]_\varepsilon^{\sharp(kl)}, \dots \right)$$

$$\mathbf{j}_\varepsilon^{ij(kl)} = \frac{1}{\varepsilon} \left[r_\varepsilon^{ij(kl)} - r^{ij} \right]$$

Numerical derivatives wrt $[\bullet]^b, \mathbf{j}^b \in \mathbb{L}^{3 \times 3} : T \mathcal{B}_t \times T \mathcal{B}_t \times T^* \mathcal{B}_t \times T^* \mathcal{B}_t \rightarrow \mathbb{R}$

$${}^{n+1}[\bullet]_\varepsilon^b(kl) = {}^{n+1}[\bullet]^b + \varepsilon \boldsymbol{\gamma}_{(k)}^b \otimes \boldsymbol{\gamma}_{(l)}^b$$

$$\mathbf{r}_\varepsilon^b(kl) = \mathbf{r}^b \left({}^{n+1}[\bullet]_\varepsilon^b(kl), \dots \right)$$

$$\mathbf{j}_\varepsilon^{ij(kl)} = \frac{1}{\varepsilon} \left[r_{\varepsilon ij(kl)} - r_{ij} \right]$$


Numerical derivatives wrt $[\bullet]^\sharp, \mathbf{J}^\sharp : [T \mathcal{B}_0 \rightarrow T \mathcal{B}_t] \rightarrow [T \mathcal{B}_0 \rightarrow T \mathcal{B}_t]$

$${}^{n+1}[\bullet]_\varepsilon^{\sharp(k)(l)} = {}^{n+1}[\bullet]^\sharp + \varepsilon \boldsymbol{\gamma}^{\sharp(k)} \otimes \boldsymbol{\Gamma}_{(l)}^{\sharp}$$

$$\mathbf{R}_\varepsilon^{\sharp(k)(l)} = \mathbf{R}^\sharp \left({}^{n+1}[\bullet]_\varepsilon^{\sharp(k)(l)}, \dots \right)$$

$$\mathbf{J}_\varepsilon^{ij(k)(l)} = \frac{1}{\varepsilon} \left[R_{\varepsilon ij(k)(l)} - R_{ij} \right]$$

Bibliography

ie Bücher erwecken die Toten nicht wieder zum Leben, machen einen Irren nicht zu einem vernünftigen Mann oder einen Dummkopf zu einem Gelehrten. Sie schärfen den Geist, rütteln ihn wach, verfeinern ihn und stillen den Wissensdurst. Will jemand alles wissen, sollte seine Familie sich seiner annehmen! Dieses Verlangen kann nur von einem seelischen Problem herrühren.

Denis Guedj

- [AB95] J.L. Alperin and R.B. Bell. *Groups and Representations*. Number 162 in Graduate Texts in Mathematics. Springer, 1995.
- [AB00] A. Acharya and J.L. Bassani. Lattice incompatibility and the gradient theory of crystal plasticity. *J. Mech. Phys. Solids*, 48(8):1565–1595, 2000.
- [Adk55] J.E. Adkins. Finite deformation of materials exhibiting curvilinear aeolotropy. *Proc. Roy. Soc. London A*, 229:119–134, 1955.
- [Alt86] S.L. Altmann. *Rotation, Quaternions and Double Groups*. Oxford University Press, 1986.
- [AM78] R. Abraham and J.E. Marsden. *Foundations of Mechanics*. The Benjamin/Cummings Publishing Company, 2nd edition, 1978.
- [AMMC00] Y.P. Arramon, M.M. Mehrabadi, D.W. Martin, and S.C. Cowin. A multidimensional anisotropic strength criterion based on Kelvin modes. *Int. J. Solids Struct.*, 37:2915–2935, 2000.
- [Ant95] S.S. Antman. *Nonlinear Problems of Elasticity*. Number 107 in Applied Mathematical Sciences. Springer, 1995.
- [AP98] U.M. Ascher and L.R. Petzold. *Computer Methods for Ordinary Differential Equations and Differential–Algebraic Equations*. SIAM, 1998.
- [Arn95] V.I. Arnold. *Ordinary Differential Equations*. The MIT Press, 9th edition, 1995.
- [AS98] E.S. Almeida and R.L. Spilker. Finite element formulations for hyperelastic transversely isotropic biphasic soft tissues. *Comput. Methods Appl. Mech. Engrg.*, 151:513–538, 1998.
- [Bac56] J.S. Bach. *Die Kunst der Fuge*. Number TP 26 in Study scores. Bärenreiter, edited from the autograph and the first print by H. Diener, 1956. BWV 1080.
- [Bal77] J.M. Ball. Convexity conditions and existence theorems in nonlinear elasticity. *Arch. Rational Mech. Anal.*, 63:337–403, 1977.
- [BB98] J. Bonet and A.J. Burton. A simple orthotropic, transversely isotropic hyperelastic constitutive equation for large strain computations. *Comput. Methods Appl. Mech. Engrg.*, 162:151–164, 1998.
- [BB01] T. Böhlke and C. Brüggemann. Graphical representation of the generalized Hooke’s law. *Technische Mechanik*, 21(2):145–158, 2001.
- [Ber98] A. Bertram. An alternative approach to finite plasticity based on material isomorphisms. *Int. J. Plasticity*, 52:353–374, 1998.
- [Bet76] J. Betten. Ein Beitrag zur Invariantentheorie in der Plastomechanik anisotroper Werkstoffe. *Z. Angew. Math. Mech.*, 56:557–559, 1976.

- [Bet82a] J. Betten. Integrity basis for a second-order and a fourth-order tensor. *Internat. J. Math. Math. Sci.*, 5(1):87–96, 1982.
- [Bet82b] J. Betten. Theory of invariants in creep mechanics of anisotropic materials. In J. P. Boehler, editor, *Mechanical Behaviour of Anisotropic Materials, EUROMECH Colloquium 115 in Grenoble 1979*, pages 65–80. Martinus Nijhoff Publishers, 1982.
- [Bet84] J. Betten. Interpolation methods for tensor functions. In X.J.R. Avula et al., editor, *Mathematical Modelling in Science and Technology*, pages 52–57. Pergamon, 1984.
- [Bet85] J. Betten. The classical plastic potential theory in comparison with the tensor function theory. *Engng. Fract. Mech.*, 21(4):641–652, 1985.
- [Bet91] J. Betten. Recent advances in applications of tensor functions in solid mechanics. *Adv. Mech.*, 14(1):79–109, 1991.
- [BFP99] G. Borino, P. Fuschi, and C. Polizzotto. A thermodynamic approach to nonlocal plasticity and related variational principles. *ASME J. Appl. Mech.*, 66:952–963, 1999.
- [BM95] M.W. Biegler and M.M. Mehrabadi. An energy-based constitutive model for anisotropic solids subject to damage. *Mechanics of Materials*, 19:151–164, 1995.
- [Boe77] J.P. Boehler. On irreducible representations for isotropic scalar functions. *Z. Angew. Math. Mech.*, 57:323–327, 1977.
- [Boe79] J.P. Boehler. A simple derivation of representations for non-polynomial constitutive equations in some cases of anisotropy. *Z. Angew. Math. Mech.*, 59:157–167, 1979.
- [Boe87] J.P. Boehler, editor. *Applications of Tensor Functions in Solid Mechanics*. Number 292 in CISM Courses and Lectures. Springer, 1987.
- [Bon01] J. Bonet. Large strain viscoelastic constitutive models. *Int. J. Solids Struct.*, 38:2953–2968, 2001.
- [Brü01] M. Brüning. A framework for large strain elastic-plastic damage mechanics based on metric transformation tensors. *Int. J. Engng. Sci.*, 39:1033–1056, 2001.
- [BS76] J.P. Boehler and A. Sawczuk. Application of representation theorems to describe yielding of transversely isotropic solids. *Mech. Res. Comm.*, 3:277–283, 1976.
- [BS77] J.P. Boehler and A. Sawczuk. On yielding of oriented solids. *Acta Mech.*, 27:185–206, 1977.
- [BSZ98] J. Betten, S. Sklepus, and A. Zolochovsky. A creep damage model for initially isotropic materials with different properties in tension and compression. *Engng. Fract. Mech.*, 59(5):623–641, 1998.
- [BXM99] O. Bruhns, H. Xiao, and A. Meyers. On representations of yield functions of crystals, quasicrystals and transversely isotropic solids. *Euro. J. Mech. A/Solids*, 18:47–67, 1999.
- [Cap89] G. Capriz. *Continua with Microstructure*, volume 35 of *Springer Tracts in Natural Philosophy*. Springer, 1989.
- [CG67] B.D. Coleman and M.E. Gurtin. Thermodynamics with internal state variables. *J. Chem. Phys.*, 47(2):597–613, 1967.
- [CH00] Y.-C. Chen and A. Hoger. Constitutive functions of elastic materials in finite growth and deformation. *J. Elasticity*, 59:175–193, 2000.
- [Cha93] J.-L. Chaboche. Development of continuum damage mechanics for elastic solids sustaining anisotropic and unilateral damage. *Int. J. Damage Mechanics*, 2:311–329, 1993.
- [Cia88] P.G. Ciarlet. *Mathematical Elasticity – Volume 1: Three Dimensional Elasticity*, volume 20 of *Studies in Mathematics and its Applications*. North-Holland, 1988.
- [CM95] S.C. Cowin and M.M. Mehrabadi. Anisotropic symmetries of linear elasticity. *ASME Appl. Mech. Rev.*, 48(5):247–285, 1995.
- [CN63] B.D. Coleman and W. Noll. The thermodynamics of elastic materials with heat conduction and viscosity. *Arch. Rational Mech. Anal.*, 13:167–178, 1963.
- [Com01] C. Comi. A non-local model with tension and compression damage mechanisms. *Euro. J. Mech. A/Solids*, 20:1–22, 2001.
- [Cor69] J.F. Cornwell. *Group Theory and Electronic Energy Bands in Solids*, volume 10 of *Selected Topics in Solid State Physics*. North-Holland, 1969.

- [Cow85] S.C. Cowin. The relationship between the elasticity tensor and the fabric tensor. *Mechanics of Materials*, 4:137–147, 1985.
- [CRW01] E. Carol, I. Rizzi, and K. Willam. On the formulation of anisotropic elastic degradation. Part I: Theory based on a pseudo–logarithmic damage tensor rate, Part II: Generalized pseudo–Rankine model for tensile damage. *Int. J. Solids Struct.*, 38:491–518, 519–546, 2001.
- [CT00] S. Cleja-Tigoiu. Nonlinear elasto–plastic deformations of transversely isotropic material and plastic spin. *Int. J. Engng. Sci.*, 38:737–763, 2000.
- [CTM00] S. Cleja-Tigoiu and G.A. Maugin. Eshelby’s stress tensors in finite elastoplasticity. *Acta Mech.*, 139:231–249, 2000.
- [CY97] S.C. Cowin and G Yang. Averaging anisotropic elastic constant data. *J. Elasticity*, 46:151–180, 1997.
- [Daf98] Y.F. Dafalias. Plastic spin: Necessity or redundancy? *Int. J. Plasticity*, 14(9):909–931, 1998.
- [dB00] R. de Boer. *Theory of Porous Media, Highlights in the Historical Development and Current State*. Springer, 2000.
- [DEE98] S. Diebels, P. Ellsiepen, and W. Ehlers. Error–controlled Runge–Kutta time integration of a viscoplastic hybrid two–phase model. *Technische Mechanik*, 19(1):19–27, 1998.
- [DJT00] E. Diegele, W. Jansohn, and Ch. Tsakmakis. Finite deformation plasticity and viscoplasticity laws exhibiting nonlinear hardening rules: Part I: Constitutive theory and numerical integration, Part II: Representative examples. *Comput. Mech.*, 25:1–12, 13–27, 2000.
- [DP91] C.T.J. Dodson and T. Poston. *Tensor Geometry*, volume 130 of *Graduated Texts in Mathematics*. Springer, 2nd edition, 1991.
- [DS84] C.S. Desai and H.J. Siriwardane. *Constitutive Laws for engineering materials – with emphasis on geologic materials*. Prentice–Hall, 1984.
- [DS96] J.E. Dennis, Jr. and R.B. Schnabel. *Numerical Methods for Unconstrained Optimization and Non-linear Equations*. Number 16 in Classics in Applied Mathematics. SIAM, 1996.
- [dSN01] E.A. de Souza Neto. The exact derivative of the exponential of an unsymmetric tensor. *Comput. Methods Appl. Mech. Engrg.*, 190:2377–2383, 2001.
- [EM90] M. Epstein and G.A. Maugin. The energy–momentum tensor and material uniformity in finite elasticity. *Acta Mech.*, 83:127–133, 1990.
- [EM96] M. Epstein and G.A. Maugin. On the geometrical material structure of anelasticity. *Acta Mech.*, 115:119–131, 1996.
- [EM00] M. Epstein and G.A. Maugin. Thermomechanics of volumetric growth in uniform bodies. *Int. J. Plasticity*, 16:951–978, 2000.
- [EMRS02] M. Ekh, A. Menzel, K. Runesson, and P. Steinmann. Anisotropic damage with the MCR effect coupled to plasticity. *Int. J. Engng. Sci.*, 2002. accepted for publication.
- [EMU96] G. Engeln-Müllges and F. Uhlig. *Numerical Algorithms with FORTRAN*. Springer, 1996.
- [ER54] J.L. Ericksen and R.S. Rivlin. Large elastic deformations of homogeneous anisotropic materials. *J. Rational Mech. Anal.*, 3:281–301, 1954.
- [ER94] D. Elata and M.B. Rubin. Isotropy of strain energy functions which depend only on a finite number of directional strain measures. *ASME J. Appl. Mech.*, 61:284–289, 1994.
- [ER01] M. Ekh and K. Runesson. Modelling and numerical issues in hyperelasto–plasticity with anisotropy. *Int. J. Solids Struct.*, 38(52):9461–9478, 2001.
- [Eri60] J.L. Ericksen. Tensor fields. In S. Flügge, editor, *Encyclopedia of Physics*, volume III/1, pages 794–858. Springer, 1960.
- [Eri62] A.C. Eringen. *Nonlinear Theory of Continuous Media*. Series in Engineering Science. McGraw–Hill, 1962.
- [Eri71] A.C. Eringen. Tensor analysis. In A.C. Eringen, editor, *Continuum Physics*, volume I – Mathematics, pages 1–155. Academic Press, 1971.
- [Eri00] J.L. Ericksen. On invariance groups for equilibrium theories. *J. Elasticity*, 59:9–22, 2000.
- [Fla89] H. Flanders. *Differential Forms with Applications to the Physical Science*. Dover, 1989.

- [GA70] A.E. Green and J.E. Adkins. *Large Elastic Deformations*. Oxford University Press, 2nd edition, 1970.
- [Gai79] B.K.D. Gairola. Nonlinear elastic problems. In F.R.N. Nabarro, editor, *Dislocations in Solids*, volume 1 (The Elastic Theory), chapter 4, pages 223–342. Elsevier North–Holland, 1979.
- [GN91] A.E. Green and P.M. Naghdi. A re–examination of the basic postulates of thermomechanics. *Proc. Roy. Soc. London A*, 432:171–194, 1991.
- [GN93] A.E. Green and P.M. Naghdi. Thermoelasticity without energy dissipation. *J. Elasticity*, 31:189–208, 1993.
- [GR97] S. Govindjee and S. Reese. A presentation and comparison of two large strain deformation viscoelasticity models. *ASME J. Eng. Mat. Tech.*, 119:251–255, 1997.
- [Gug77] H.W. Guggenheimer. *Differential Geometry*. Dover, 1977.
- [Gur64] G.B. Gurevich. *Foundations of the Theory of Algebraic Invariants*. Noordhoff Ltd., 1964.
- [Gur81] M.E. Gurtin. *An Introduction to Continuum Mechanics*, volume 158 of *Mathematics in Science and Engineering*. Academic Press, 1981.
- [Gur00] M.E. Gurtin. *Configurational Forces as Basic Concept in Continuum Physics*, volume 137 of *Applied Mathematical Sciences*. Springer, 2000.
- [GZ92] A.E. Green and W. Zerna. *Theoretical Elasticity*. Dover, 1992.
- [Hac98] K. Hackl. A survey on time–integration algorithms for convex and nonconvex elastoplasticity. In R.P. Gilbert, P.D. Panagiotopoulos, and P. Pardalos, editors, *From Convexity to Nonconvexity, Nonsmooth Optimization and its Applications*. Kluwer, 1998.
- [Hau00] P. Haupt. *Continuum Mechanics and Theory of Materials*. Advanced Texts in Physics. Springer, 2000.
- [HC83] R. Huiskes and E.Y.S. Chao. A survey of finite element analysis in orthopedic biomechanics: The first decade. *J. Biomechanics*, 16(6):385–409, 1983.
- [HC96] D. Hull and T.W. Clyne. *An Introduction to Composite Materials*. Cambridge Solid State Science Series. Cambridge University Press, 2nd edition, 1996.
- [HG01] G.A. Holzapfel and T.C. Gasser. A viscoelastic model for fibre–reinforced composites at finite strains: Continuum basis, computational aspects and applications. *Comput. Methods Appl. Mech. Engrg.*, 190:4379–4403, 2001.
- [Hil50] R. Hill. *The Mathematical Theory of Plasticity*. Oxford University Press, 1950.
- [Hil68] R. Hill. On constitutive inequalities for simple materials – I. *J. Mech. Phys. Solids*, 16:229–242, 1968.
- [Hil70] R. Hill. Constitutive inequalities for isotropic materials under finite strains. *Proc. Roy. Soc. London A*, 314:457–472, 1970.
- [Hil00] R. Hill. Plastic anisotropy and the geometry of yield surfaces in stress space. *J. Mech. Phys. Solids*, 48:1093–1106, 2000.
- [HN75] B. Halphen and Q.S. Nguyen. Sur les matériaux standards généralisés. *Journal de Mécanique*, 14:39–62, 1975.
- [HNW93] E. Hairer, S.P. Nørsett, and G. Wanner. *Solving Ordinary Differential Equations I – Nonstiff Problems*. Number 8 in Springer Series in Computational Mathematics. Springer, 2nd edition, 1993.
- [Hou75] A.S. Householder. *The Theory of Matrices in Numerical Analysis*. Dover, 1975.
- [HS94] N.R. Hansen and H.L. Schreyer. A thermodynamically consistent framework for theories of elastoplasticity coupled with damage. *Int. J. Solids Struct.*, 31(3):359–389, 1994.
- [HSB01] K. Hackl and M. Schmidt-Baldassari. Time integration algorithms for evolution equations in finite strain plasticity. In *Trends in Computational Structural Mechanics*, pages 128–139. CIMNE, 2001.
- [Hug00] T.J.R. Hughes. *The Finite Element Method*. Dover, 2000.
- [Ibr94] A. Ibrahimbegović. Equivalent spatial and material description of finite deformation elastoplasticity in principal axes. *Int. J. Solids Struct.*, 31(22):3027–3040, 1994.
- [JSBC97] C.R. Jacobs, J.C. Simo, G.S. Beaupré, and D.R. Carter. Adaptive bone remodelling incorporating simultaneous density and anisotropy considerations. *J. Biomechanics*, 30(6):603–613, 1997.

- [Jur74] H.J. Juretschke. *Crystal Physics – Macroscopic Physics of Anisotropic Solids*. Number 3 in Modern Physics Monograph Series. W.A. Benjamin, Inc., 1974.
- [Kal00] M. Kaliske. A formulation of elasticity and viscoelasticity for fibre reinforced material at small and finite strains. *Comput. Methods Appl. Mech. Engrg.*, 185:225–243, 2000.
- [Kau49] H. Kauderer. Über ein nichtlineares Elastizitätsgesetz. *Ingenieur-Archiv*, XVII:450–480, 1949.
- [KB93] A.P. Karafillis and M.C. Boyce. A general anisotropic yield criterion using bounds and a transformation weighting tensor. *J. Mech. Phys. Solids*, 41(12):1859–1886, 1993.
- [KE90] E. Kiral and A.C. Eringen. *Constitutive Equations of Nonlinear Electromagnetic-Elastic Crystals*. Springer, 1990.
- [KK99] E. Kirchner and F.G. Kollmann. Application of modern time integrators to Hart’s model. *Int. J. Plasticity*, 15(6):647–666, 1999.
- [KTW00] U.F. Kocks, C.N. Tomé, and H.-R. Wenk. *Texture and Anisotropy – Preferred Orientations in Polycrystals and their Effect on Material Properties*. Cambridge University Press, 2000.
- [Lam91] J.D. Lambert. *Numerical Methods for Ordinary Differential Systems: The Initial Value Problem*. Wiley, 1991.
- [Lav93] B.H. Lavenda. *Thermodynamics of Irreversible Processes*. Dover, 1993.
- [LC98] J. Lemaitre and J.-L. Chaboche. *Mechanics of Solid Materials*. Cambridge, 2nd edition, 1998.
- [Liu82] I.-S. Liu. On representations of anisotropic invariants. *Int. J. Engng. Sci.*, 20(10):1099–1109, 1982.
- [LO81] F.A. Leckie and E.T. Onat. Tensorial nature of damage measuring internal variables. In J. Hult and J. Lemaitre, editors, *Physical Non-Linearities in Structural Analysis*, pages 140–155. IUTAM Symposium Senlis/France 1980, Springer, 1981.
- [Lod51] A.S. Lodge. The compatibility conditions for large strains. *Quart. J. Mech. Appl. Math.*, IV(1):85–93, 1951.
- [Lod64] A.S. Lodge. *Elastic Liquids – An Introductory Vector Treatment of Finite-strain Polymer Rheology*. Academic Press, 1964.
- [Lod74] A.S. Lodge. *Body Tensor Fields in Continuum Mechanics – With Application to Polymer Rheology*. Academic Press, 1974.
- [Lov44] A.E.H. Love. *A Treatise on the Mathematical Theory of Elasticity*. Dover, 4th edition, 1944.
- [LP00] J. Lu and P. Papadopoulos. A covariant constitutive description of anisotropic non-linear elasticity. *Z. Angew. Math. Phys.*, 51:204–217, 2000.
- [LS81] A. Litewka and A. Sawczuk. A yield criterion for perforated sheets. *Ingenieur-Archiv*, 50:393–400, 1981.
- [LS84] D. Levine and P.J. Steinhardt. Quasicrystals: A new class of ordered structures. *Phys. Rev. Lett.*, 53(26):2477–2480, 1984.
- [LT00] H. Lämmer and Ch. Tsakmakis. Discussion of coupled elastoplasticity and damage constitutive equations for small and finite deformations. *Int. J. Plasticity*, 16:495–523, 2000.
- [Lub90] J. Lubliner. *Plasticity Theory*. MacMillan Publishing Company, 1990.
- [Mah02] R. Mahnen. Anisotropic creep modelling based on elastic projection operators with application to the superalloy CMSX-4. *Comput. Methods Appl. Mech. Engrg.*, 191(15):1611–1638, 2002.
- [Man74] J. Mandel. Thermodynamics and plasticity. In J.J. Delgado Domingos, M.N.R. Nina, and J.H. Whitelaw, editors, *Foundations of Continuum Thermodynamics*, pages 283–304. MacMillan, 1974.
- [Mar99] L.C. Martins. The representation theorem for linear, isotropic material revisited. *J. Elasticity*, 54:89–92, 1999.
- [Mau92] G.A. Maugin. *The Thermomechanics of Plasticity and Fracture*. Cambridge Texts in Applied Mathematics. Cambridge University Press, 1992.
- [Mau93] G.A. Maugin. *Material Inhomogeneities in Elasticity*, volume 3 of *Applied Mathematics and Mathematical Computation*. Chapman & Hall, 1993.
- [Mau94] G.A. Maugin. Eshelby stress in elastoplasticity and ductile fracture. *Int. J. Plasticity*, 10(4):393–408, 1994.

- [Mau99] G.A. Maugin. *The Thermodynamics of Nonlinear Irreversible Behaviors*, volume 27 of *World Scientific Series on Nonlinear Science: Series A*. World Scientific Publishing, 1999.
- [MC90] M.M. Mehrabadi and S.C. Cowin. Eigentensors of linear anisotropic elastic materials. *Quart. J. Mech. Appl. Math.*, 43(1):15–41, 1990.
- [MER01] L. Mähler, M. Ekh, and K. Runesson. A class of thermo–hyperelastic–viscoplastic models for porous materials: Theory and numerics. *Int. J. Plasticity*, 17, 2001.
- [MESR02] A. Menzel, M. Ekh, P. Steinmann, and K. Runesson. Anisotropic damage coupled to plasticity: Modelling based on the effective configuration concept. *Int. J. Numer. Methods Engng.*, 54(10):1409–1430, 2002.
- [MH94] J.E. Marsden and T.J.R. Hughes. *Mathematical Foundations of Elasticity*. Dover, 1994.
- [Mie94] C. Miehe. Aspects of the formulation and finite element implementation of large strain isotropic elasticity. *Int. J. Numer. Methods Engng.*, 37:1981–2004, 1994.
- [Mie95] C. Miehe. Algorithmic formulations of large–strain rate–independent multisurface thermoplasticity. In D.R. Owen and E. Oñate, editors, *Computational Plasticity – Fundamentals and Application – Proceedings of the 4th International Conference*, volume 1, pages 119–132. CIMNE Barcelona, Pineridge Press, 1995.
- [Mie96a] C. Miehe. Exponential map algorithm for stress updates in anisotropic multiplicative elastoplasticity for single crystals. *Int. J. Numer. Methods Engng.*, 39:3367–3390, 1996.
- [Mie96b] C. Miehe. Numerical computation of algorithmic (consistent) tangent moduli in large–strain computational inelasticity. *Comput. Methods Appl. Mech. Engrg.*, 134:223–240, 1996.
- [Mie98a] C. Miehe. A constitutive frame of elastoplasticity at large strains based on the notion of a plastic metric. *Int. J. Solids Struct.*, 35(30):3859–3897, 1998.
- [Mie98b] C. Miehe. A formulation of finite elastoplasticity based on dual co– and contra–variant eigenvector triads normalized with respect to a plastic metric. *Comput. Methods Appl. Mech. Engrg.*, 159:223–260, 1998.
- [ML01] C. Miehe and M. Lambrecht. Algorithms for computation of stresses and elasticity moduli in terms of Seth–Hill’s family of generalized strain tensors. *Commun. Numer. Methods Engng.*, 17:337–353, 2001.
- [MR76] Z. Mróz and B. Raniecki. On the uniqueness problem in coupled thermoplasticity. *Int. J. Engng. Sci.*, 14:211–221, 1976.
- [MS92] C. Miehe and E. Stein. A canonical model of multiplicative elasto–plasticity: Formulation and aspects of the numerical implementation. *Euro. J. Mech. A/Solids*, 11:25–43, 1992. Special issue.
- [MS94] A. Matzenmiller and J.L. Sackman. On damage induced anisotropy for fiber composites. *Int. J. Damage Mechanics*, 3:71–86, 1994.
- [MS98] A. Menzel and P. Steinmann. On the formulation of higher gradient single and polycrystal plasticity. *J. Phys. IV France*, 8:239–247, 1998.
- [MS99] A. Menzel and P. Steinmann. A theoretical and computational setting for geometrically nonlinear damage mechanics. In W. Wunderlich, editor, *Proceedings of the European Conference on Computational Mechanics, No. 329*. ECCM, 1999. Munich.
- [MS00] A. Menzel and P. Steinmann. On the continuum formulation of higher gradient plasticity for single and polycrystals. *J. Mech. Phys. Solids*, 48(8):1777–1796, 2000. Erratum 49(5):1179–1180, 2001.
- [MS01a] A. Menzel and P. Steinmann. Formulation and computation of geometrically nonlinear anisotropic inelasticity. Technical Report P 01–08, UKL/LTM, 2001. submitted for publication.
- [MS01b] A. Menzel and P. Steinmann. Geometrically nonlinear anisotropic inelasticity based on fictitious configurations: Application to the coupling of continuum damage and multiplicative elasto–plasticity. *Int. J. Numer. Methods Engng.*, 2001. accepted for publication.
- [MS01c] A. Menzel and P. Steinmann. On the comparison of two strategies to formulate orthotropic hyperelasticity. *J. Elasticity*, 62:171–201, 2001.
- [MS01d] A. Menzel and P. Steinmann. On the spatial formulation of anisotropic multiplicative elasto–plasticity. Technical Report J 01–07, UKL/LTM, 2001. submitted for publication.

- [MS01e] A. Menzel and P. Steinmann. On the theory and computation of anisotropic damage at large strains. *Revue européenne des éléments finis*, 10(2–4):369–283, 2001.
- [MS01f] A. Menzel and P. Steinmann. A theoretical and computational setting for anisotropic continuum damage mechanics at large strains. *Int. J. Solids Struct.*, 38(52):9505–9523, 2001.
- [MS01g] A. Menzel and P. Steinmann. A theoretical and computational framework for anisotropic inelasticity. In *Proceedings of the European Conference on Computational Mechanics*. ECCM, 2001. Cracow.
- [MS01h] A. Menzel and P. Steinmann. A view on anisotropic finite hyper-elasticity. *Euro. J. Mech. A/Solids*, 2001. accepted for publication.
- [MS02] F. Mollica and A.R. Srinivasa. A general framework for generating convex yield surfaces for anisotropic metals. *Acta Mech.*, 154:61–84, 2002.
- [Mur37] F.D. Murnaghan. Finite deformations of an elastic solid. *Am. J. Math.*, 59:235–260, 1937.
- [Mur51] F.D. Murnaghan. *Finite Deformations of an Elastic Solid*. Applied Mathematics Series. Wiley, 1951.
- [Mur87] S. Murakami. Anisotropic aspects of material damage and application of continuum damage mechanics. In D. Krajcinovic and J. Lemaitre, editors, *Continuum Damage Mechanics – Theory and Application*, number 295 in CISM Courses and Lectures, pages 91–133. Springer, 1987.
- [Mur88] S. Murakami. Mechanical modeling of material damage. *ASME J. Appl. Mech.*, 55:280–286, 1988.
- [Mur00] A.I. Murdoch. On objectivity and material symmetry for simple elastic solids. *J. Elasticity*, 60:233–242, 2000.
- [Nag90] P.M. Naghdi. A critical review of the state of finite plasticity. *Z. Angew. Math. Phys.*, 41:315–394, 1990.
- [Ned02] B. Nedjar. Frameworks for finite strain viscoelastic-plasticity based on multiplicative decompositions. Part I: Continuum formulations, Part II: Computational aspects. *Comput. Methods Appl. Mech. Engrg.*, 191(15–16):1541–1562, 1563–1593, 2002.
- [Nem97] E. Nembach. *Particle Strengthening of Metals and Alloys*. Wiley, 1997.
- [NNH93] S. Nemat-Nasser and M. Hori. *Micromechanics: Overall Properties of heterogeneous materials*. Applied Mathematics and Mechanics. Elsevier, 1993.
- [Nol58] W. Noll. A mathematical theory of the mechanical behavior of continuous media. *Arch. Rational Mech. Anal.*, 2:197–226, 1958.
- [NW93] M. Negahban and A.S. Wineman. The evolution of material symmetry in the elastic response of a fully strain space theory of plasticity. *ASME AMD*, 158:19–23, 1993.
- [OBMO95] S. Oller, S. Botello, J. Miquel, and E. Oñate. An anisotropic elastoplastic model based on an isotropic formulation. *Engng. Comput.*, 12:245–262, 1995.
- [Ode72] J.T. Oden. *Finite Elements of Nonlinear Continua*. Advanced Engineering Series. McGraw–Hill, 1972.
- [Ogd97] R.W. Ogden. *Non-Linear Elastic Deformations*. Dover, 1997.
- [Olv99] P.J. Olver. *Classical Invariant Theory*. Number 44 in London Mathematical Society Student Texts. Cambridge University Press, 1999.
- [PFRFH00] A. Pérez-Foguet, A. Rodriguez-Ferran, and A. Huerta. Numerical differentiation for local and global tangent operators in computational plasticity. *Comput. Methods Appl. Mech. Engrg.*, 189:277–296, 2000.
- [PG00] P. Podio-Guidugli. A primer in elasticity. *J. Elasticity*, 58(1):1–104, 2000.
- [Phi01] R. Phillips. *Crystals, Defects and Microstructures – Modeling Across Scales*. Cambridge University Press, 2001.
- [PL98] P. Papadopoulos and J. Lu. A general framework for the numerical solution of problems in finite elasto-plasticity. *Comput. Methods Appl. Mech. Engrg.*, 159:1–18, 1998.
- [PL01] P. Papadopoulos and J. Lu. On the formulation and numerical solution of problems in anisotropic finite plasticity. *Comput. Methods Appl. Mech. Engrg.*, 190:4889–4910, 2001.
- [PR59] A.C. Pipkin and R.S. Rivlin. The formulation of constitutive equations in continuum physics. I. *Arch. Rational Mech. Anal.*, 4:129–144, 1959.

- [PR92] J.E. Paulun and R.B. Reçherski. On the relation for plastic spin. *Arch. Appl. Mech.*, 62:376–385, 1992.
- [PSSS99] K.A. Pericak-Spector, J. Silvaloganathan, and S.J. Spector. The representation theorem for linear, isotropic tensor functions in even dimensions. *J. Elasticity*, 57:157–164, 1999.
- [PV98] T. Park and G.Z. Voyiadjis. Kinematic description of damage. *ASME J. Appl. Mech.*, 65:93–98, 1998.
- [PW63] A.C. Pipkin and A.S. Wineman. Material symmetry restrictions on non-polynomial constitutive equations. *Arch. Rational Mech. Anal.*, 12:420–426, 1963.
- [PY98] H.C. Park and S.-K. Youn. Finite element analysis and constitutive modelling of anisotropic non-linear hyperelastic bodies with convected frames. *Comput. Methods Appl. Mech. Engrg.*, 151:605–618, 1998.
- [QB99] W. Qi and A. Bertram. Anisotropic continuum damage modeling for single crystals at high temperatures. *Int. J. Plasticity*, 15:1197–1215, 1999.
- [QP97] G.Y. Qiu and T.J. Pence. Remarks on the behavior of simple directionally reinforced incompressible nonlinear elastic solids. *J. Elasticity*, 49(1):1–30, 1997.
- [RHM94] E.K. Rodriguez, A. Hoger, and D. McCulloch. Stress-dependent finite growth in soft elastic tissues. *J. Biomechanics*, 27(4):455–467, 1994.
- [Ric52] H. Richter. Zur Elastizitätstheorie endlicher Verformungen. *Math. Nachr.*, 8:65–73, 1952.
- [Riv66] R.S. Rivlin. The fundamental equations of nonlinear continuum mechanics. In S.I. Pai, editor, *Dynamics of Fluids and Plasmas*, pages 83–126. Academic Press, 1966.
- [Riv70] R.S. Rivlin. Red herrings and sundry unidentified fish in nonlinear continuum mechanics. In M.F. Kanninen, editor, *Inelastic behavior of solids*, Series in Materials Science and Engineering, pages 117–134. McGraw-Hill, 1970.
- [Riv73] R.S. Rivlin. On the principles of equipresence and unification. *Quart. Appl. Math.*, XXX:227–228, 1973.
- [Riv80] R.S. Rivlin. Material symmetry and constitutive equations. *Ingenieur-Archiv*, 49:325–336, 1980.
- [Riv91] R.S. Rivlin. Objectivity of the constitutive equation for a material with memory. *Int. J. Solids Struct.*, 27(3):395–397, 1991.
- [RRW01] S. Reese, T. Raible, and P. Wriggers. Finite element modelling of orthotropic material behaviour in pneumatic membranes. *Int. J. Solids Struct.*, 38(52):9525–9544, 2001.
- [RS87] R.S. Rivlin and G.F. Smith. A note on material frame indifference. *Int. J. Solids Struct.*, 23(12):1639–1643, 1987.
- [Ryc95] J. Rychlewski. Unconventional approach to linear elasticity. *Arch. Mech.*, 47(2):147–171, 1995.
- [SA92] J.C. Simo and F. Armero. Geometrically non-linear enhanced strain mixed methods and the method of incompatible modes. *Int. J. Numer. Methods Engrg.*, 33:1413–1449, 1992.
- [SAKS98] B. Svendsen, S. Arndt, D. Klingbeil, and R. Sievert. Hyperelastic models for elastoplasticity with non-linear isotropic and kinematic hardening at large deformation. *Int. J. Solids Struct.*, 35(25):3363–3389, 1998.
- [San93] D.E. Sands. *Introduction to Crystallography*. Dover, 1993.
- [San95] D.E. Sands. *Vectors and Tensors in Crystallography*. Dover, 1995.
- [SB99] B. Svendsen and A. Bertram. On frame-indifference and form-invariance in constitutive theory. *Acta Mech.*, 132:195–207, 1999.
- [SC98] P. Steinmann and I. Carol. A framework for geometrically nonlinear continuum damage mechanics. *Int. J. Engng. Sci.*, 36:1793–1814, 1998.
- [Sch89] J.A. Schouten. *Tensor Analysis for Physicists*. Dover, 2nd edition, 1989.
- [Sch95] H.L. Schreyer. Continuum damage based on elastic projection tensors. *Int. J. Damage Mechanics*, 4:171–195, 1995.
- [Set64] B.R. Seth. Generalized strain measure with application to physical problems. In M. Reiner and D. Abir, editors, *Second-Order Effects in Elasticity, Plasticity and Fluid Dynamics*, pages 162–172, 1964.

- [Sid81] F. Sidoroff. Description of anisotropic damage application to elasticity. In J. Hult and J. Lemaitre, editors, *Physical Non-Linearities in Structural Analysis*, pages 237–244, 1981. IUTAM Symposium Senlis/France, 27.–30.05.1980, Springer.
- [Šil97] M. Šilhavý. *The Mechanics and Thermomechanics of Continuous Media*. Texts and Monographs in Physics. Springer, 1997.
- [Sim98] J.C. Simo. Numerical analysis and simulation of plasticity. In P.G. Ciarlet and J.L. Lions, editors, *Numerical Methods for Solids (Part 3)*, volume VI of *Handbook of Numerical Analysis*. North-Holland, 1998.
- [SK01] C. Sansour and F.G. Kollmann. Anisotropic formulations for finite strain viscoplasticity. Applications to shells. In *Trends in Computational Structural Mechanics*, pages 198–207. CIMNE, 2001.
- [SLR97] P. Steinmann, R. Larsson, and K. Runesson. On the localization properties of multiplicative hyperelasto–plastic continua with strong discontinuities. *Int. J. Solids Struct.*, 34(8):969–990, 1997.
- [SM84] J.C. Simo and J.E. Marsden. On the rotated stress tensor and the material version of the Doyle–Eriksen formula. *Arch. Rational Mech. Anal.*, 86:213–231, 1984.
- [SM92] J.C. Simo and C. Miehe. Associated coupled thermoplasticity at finite strains: Formulation, numerical analysis and implementation. *Comput. Methods Appl. Mech. Engrg.*, 98:41–104, 1992.
- [Smi62] G.F. Smith. On the yield condition for anisotropic materials. *Q. Appl. Math.*, 20(3):241–247, 1962.
- [Smi71a] G.F. Smith. On isotropic functions of symmetric tensors, skew–symmetric tensors and vectors. *Int. J. Engng. Sci.*, 9:899–916, 1971.
- [Smi71b] J.R. Smith. Eigenvalues and eigenvectors of the rotation tensor. *The Matrix and Tensor Quarterly*, 22:35–37, 1971.
- [Smi94] G.F. Smith. *Constitutive Equations for Anisotropic and Isotropic Materials*, volume 3 of *Mechanics and Physics of Discrete Systems*. North Holland, 1994.
- [SMS94] P. Steinmann, C. Miehe, and E. Stein. Comparison of different finite deformation inelastic damage models within multiplicative elastoplasticity for ductile materials. *Comput. Mech.*, 13:458–474, 1994.
- [SMS96] P. Steinmann, C. Miehe, and E. Stein. Fast transient dynamic plane stress analysis of orthotropic Hill-type solids at finite elastoplastic strains. *Int. J. Solids Struct.*, 33:1543–1562, 1996.
- [Spe71] A.J.M. Spencer. Theory of invariants. In A.C. Eringen, editor, *Continuum Physics*, volume I – Mathematics, pages 239–353. Academic Press, 1971.
- [Spe72] A.J.M. Spencer. *Deformations of Fibre–reinforced Materials*. Oxford University Press, 1972.
- [Spe84] A.J.M. Spencer. Constitutive theory of strongly anisotropic solids. In A.J.M. Spencer, editor, *Continuum Theory of the Mechanics of Fibre–Reinforced Composites*, number 282 in CISM Courses and Lectures, pages 1–32. Springer, 1984.
- [Spe01] A.J.M. Spencer. A theory of viscoplasticity for fabric–reinforced composites. *J. Mech. Phys. Solids*, 49:2667–2687, 2001.
- [SR57] G.F. Smith and R.S. Rivlin. Stress–deformation relations for anisotropic solids. *Arch. Rational Mech. Anal.*, 1:107–112, 1957.
- [SR58] G.F. Smith and R.S. Rivlin. The strain–energy function for anisotropic elastic materials. *Trans. Amer. Math. Soc.*, 88:175–193, 1958.
- [ST82] J.C. Simo and R.L. Taylor. Penalty function formulations for compressible nonlinear elastostatics. *Comput. Methods Appl. Mech. Engrg.*, 35:107–118, 1982.
- [ST94] B. Svendsen and Ch. Tsakmakis. A local differential geometric formulation of dual stress–strain pairs and time derivatives. *Arch. Mech.*, 46(1–2):49–91, 1994.
- [Ste94] S. Sternberg. *Group Theory and Physics*. Cambridge University Press, 1994.
- [Ste96] P. Steinmann. Views on multiplicative elastoplasticity and the continuum theory of dislocations. *Int. J. Engng. Sci.*, 34(15):1717–1735, 1996.
- [Ste99] P. Steinmann. Formulation and computation of geometrically non–linear gradient damage. *Int. J. Numer. Methods Engrg.*, 46:757–779, 1999.
- [Ste00] P. Steinmann. Application of material forces to hyperelastostatic fracture mechanics. I. Continuum mechanical setting. *Int. J. Solids Struct.*, 37:7371–7391, 2000.

- [Ste01] P. Steinmann. On spatial and material settings of hyperelastodynamics. *Acta Mech.*, 2001. accepted for publication.
- [Şuh75] E.S. Şuhubi. Thermoelastic solids. In A.C. Eringen, editor, *Continuum Physics*, volume II – Continuum Mechanics of Single-Substance Bodies, pages 173–265. Academic Press, 1975.
- [Sut92] S. Sutcliffe. Spectral decomposition of the elasticity tensor. *ASME J. Appl. Mech.*, 59:762–773, 1992.
- [Sve98] B. Svendsen. A thermodynamic formulation of finite-deformation elastoplasticity with hardening based on the concept of material isomorphism. *Int. J. Plasticity*, 14(6):473–488, 1998.
- [Sve99] T. Svedberg. Gradient-regularized hyperelasto-plasticity coupled to damage – thermodynamics and numerical algorithm. *Int. J. Plasticity*, 1999. submitted.
- [Sve01a] B. Svendsen. Formulation of balance relations and configurational fields for continua with microstructure and moving point defects via invariance. *Int. J. Solids Struct.*, 38:1183–1200, 2001.
- [Sve01b] B. Svendsen. On the modeling of anisotropic elastic and inelastic material behaviour at large deformation. *Int. J. Solids Struct.*, 38(52):9579–9599, 2001.
- [SZ99] G. Sarma and T. Zacharia. Integration algorithm for modeling the elastoviscoplastic response of polycrystalline materials. *J. Mech. Phys. Solids*, 47:1219–1238, 1999.
- [Tab95] L.A. Taber. Biomechanics of growth, remodelling, and morphogenesis. *ASME Appl. Mech. Rev.*, 48(8):487–545, 1995.
- [Teo97] C. Teodosiu, editor. *Large Plastic Deformations of Crystalline Aggregates*. Number 376 in CISM Courses and Lectures. Springer, 1997.
- [Tho56] Lord Kelvin (W. Thomson). Elements of a mathematical theory of elasticity. *Phil. Trans. Roy. Soc. London*, 166:481–498, 1856.
- [TN92] C. Truesdell and W. Noll. *The Non-Linear Field Theories of Mechanics*. Springer, 2nd edition, 1992.
- [Tru66] C. Truesdell. *Continuum Mechanics I: The Mechanical Foundations of Elasticity and Fluid Dynamics*, volume 8 of *International Science Review Series*. Gordon and Beach, 1966.
- [Tru77] C. Truesdell. *A First Course in Rational Continuum Mechanics*, volume I General Concepts of *Pure and Applied Mathematics*. Academic Press, 1977.
- [Tsa00] Ch. Tsakmakis. Description of plastic anisotropy effects at large deformations. Part I: Restrictions imposed by the second law and the postulate of Il'iusin. *Int. J. Plasticity*, 2000. submitted.
- [TT60] C. Truesdell and R.A. Toupin. The classical field theories. In S. Flügge, editor, *Encyclopedia of Physics*, volume III/1, pages 226–793. Springer, 1960.
- [vdG89] E. van der Giessen. Continuum models of large deformation plasticity, Part I: Large deformation plasticity and the concept of a natural reference state, Part II: A kinematic hardening model and the concept of a plastically induced orientational structure. *Euro. J. Mech. A/Solids*, 8(1,2):15–34, 89–108, 1989.
- [WA90] G. Weber and L. Anand. Finite deformation constitutive equations and a time integration procedure for isotropic, hyperelastic-viscoplastic solids. *Comput. Methods Appl. Mech. Engrg.*, 79:173–202, 1990.
- [Wan70] C.C. Wang. A new representation theorem for isotropic functions: An answer to Professor G.F. Smith's criticism of my papers on representations for isotropic functions, Part 1. Scalar-valued isotropic functions Part 2. Vector-valued isotropic functions, symmetric tensor-valued isotropic functions and skew-symmetric tensor-valued isotropic functions. *Arch. Rational Mech. Anal.*, 36:166–197, 198–223, 1970. Corrigendum **43**:392–395, 1971.
- [Wan84] C.C. Wang. On the symmetry of the heat-conduction tensor. In C. Truesdell, editor, *Rational Thermodynamics*, chapter 7A, pages 396–401. Springer, 2nd edition, 1984.
- [WB74] C.C. Wang and F. Bloom. Material uniformity and inhomogeneity in anelastic bodies. *Arch. Rational Mech. Anal.*, 53:246–276, 1974.
- [Wen98] S. Weng. Ein anisotropes Knochenbaummodell und dessen Anwendung. *Technische Mechanik*, 18(3):173–180, 1998.
- [Wey52] H. Weyl. *Symmetry*. Princeton University Press, 1952.

- [Wey87] H. Weyl. *The Classical Groups – their Invariants and Representations*. Princeton University Press, 2nd edition, 1987.
- [WMG96] J.A. Weiss, B.N. Maker, and S. Govindjee. Finite element implementation of incompressible, transversely isotropic hyperelasticity. *Comput. Methods Appl. Mech. Engrg.*, 135:107–128, 1996.
- [WP64] A.S. Wineman and A.C. Pipkin. Material symmetry restrictions on constitutive equations. *Arch. Rational Mech. Anal.*, 17:184–214, 1964.
- [Xia97] H. Xiao. On isotropic invariants of the elasticity tensor. *J. Elasticity*, 46:115–149, 1997.
- [ZB94] Q.-S. Zheng and J.P. Boehler. The description, classification and reality of material and physical symmetries. *Acta Mech.*, 102:72–89, 1994.
- [ZC95] P.K. Zysset and A. Curnier. An alternative model for anisotropic elasticity based on fabric tensors. *Mechanics of Materials*, 21:243–250, 1995. see Technical Note by S.C. Cowin, *J. Biomechanics*, 31:759–762, 1998.
- [Zhe93a] Q.-S. Zheng. On the representations for isotropic vector-valued, symmetric tensor-valued and skewsymmetric tensor-valued functions. *Int. J. Engng. Sci.*, 31(7):1013–1024, 1993.
- [Zhe93b] Q.-S. Zheng. On transversely isotropic, orthotropic and relative isotropic functions of symmetric tensors, skew-symmetric tensors and vectors. Part I: Two dimensional orthotropic and relative isotropic functions and three dimensional relative isotropic functions, Part II: The representations for three dimensional transversely isotropic functions. *Int. J. Engng. Sci.*, 31(10):1399–1409, 1411–1423, 1993.
- [ZR90] J.M. Zhang and J. Rychlewsky. Structural tensors for anisotropic solids. *Arch. Mech.*, 42(3):267–277, 1990.
- [ZS93] Q.-S. Zheng and A.J.M. Spencer. Tensors which characterize anisotropies. *Int. J. Engng. Sci.*, 31(5):679–693, 1993.

Curriculum Vitae

Surname	Menzel
Forename	Andreas
Nationality	German
Date of Birth	23.04.1972, Hannover

08/1978 – 06/1982 Grundschule, Berenbostel

08/1982 – 06/1984 Orientierungsstufe, Berenbostel

08/1984 – 06/1991 Gymnasium, Berenbostel

07/1991 – 09/1992 Civilian Service, Garbsen

10/1992 – 03/1997 Civil Engineering, University of Hannover

06/1997 – 09/1997 Research Associate, University of Hannover
Institute for Structural and Computational Mechanics
(Prof. Dr.-Ing. Dr.-Ing. E.h. Dr. h.c. mult. E. Stein)

since 10/1997 Research Associate, University of Kaiserslautern
Chair of Applied Mechanics
(Prof. Dr.-Ing. P. Steinmann)

Axiomata sive Leges Motus

Lex I.

corpora perseverare in statu suo
et directum, nisi quatenus a-
moverentur.

perseverant in motibus suis
Lasciantur et in gravitate nisi
secundo profectus retrahuntur sed
non nisi quatenus ab aere et
visum et Comelavum corpora
removetur in statu suo nisi re-
sistat.

Lex II.

corpora motus proportionaliter effe-
rentur lineam rectam qua vis
sua motum generat generat
generabit, sive simul et sive
separata fuerit. Et tunc motus
in eum in generatorem deter-
minatur, motus sive vel cessat
et oblique oblique adhibetur et
compositionem componitur.

Lex III.

contrariam semper et aequalem
vim actiones in se mutuo per-
cipias dirigi

premit vel trahit alterum
trahitur. Sicut lapidem digito
et lapide. Si equus lapidem et
equum et equus aequaliter in la-
pide eodem relaxandi se conati
sunt, ac lapidem traxerit equus
et quatuor premit et pro,
in corpus aliud impingit.
mutaverit, idem quoque visus
actionem in partem contrariam
trahitur mutuo) trahitur. Hoc